1-1-2016

Selective Oxidative Homo- and Cross-Coupling of Phenols

Young Eun Lee
University of Pennsylvania, youngelhan@gmail.com

Selective Oxidative Homo- and Cross-Coupling of Phenols

Abstract

The efforts described in this dissertation initially focus on the asymmetric coupling of phenols. We have developed Schiff base vanadium catalyst for the oxidative coupling of phenols with high reactivity and enantioselectivity. To the best of our knowledge, this example constitutes the first highly selective asymmetric coupling of phenols. Several substrates were coupled with our vanadium catalyst with good enantioselectivity (72-89% ee).

The first simple catalystic system that uses atom-economical oxygen as the terminal oxidant to accomplish selective ortho–ortho, ortho–para, or para–para homo-couplings of phenols was developed. Chromium salen catalysts have been discovered and verified as uniquely effective in the cross-coupling of different phenols with high chemo- and regio-selectivity. A broad scope of phenol substrates was found for these reaction conditions giving cross-coupling products with good yield (up to 88%). In order to understand the mechanism of cross-coupling reaction, spectroscopic methods, additive experiments, SAR studies, and kinetic experiments were performed and a mechanism was postulated.

Finally, we established an efficient route for the total synthesis of honokiol by utilizing a novel disconnection that transits new structures. This five step (six chemical reactions) synthesis was initiated by oxidative cross-coupling of inexpensive commercial phenols with high yield (91%). Following retro Friedel-Crafts alkylation, a protection reaction proceeded smoothly with excellent yield (89% for three steps). The remaining steps of radical bromination, Kumada coupling and demethylation were each optimized. The total yield over five steps was 34% and gram-scale reactions were conducted for each step.

Degree Type
Dissertation

Degree Name
Doctor of Philosophy (PhD)

Graduate Group
Chemistry

First Advisor
Marisa C. Kozlowski

Subject Categories
Chemistry

SELECTIVE OXIDATIVE HOMO- AND CROSS-COUPLING OF PHENOLS

Young Eun Lee

A DISSERTATION

in

Chemistry

Presented to the Faculties of the University of Pennsylvania

in

Partial Fulfillment of the Requirements for the

Degree of Doctor of Philosophy

2016

Supervisor of Dissertation

_____

Dr. Marisa C. Kozlowski

Professor of Chemistry

Graduate Group Chairperson

_____

Dr. Gary A. Molander

Hirschmann-Makineni Professor of Chemistry

Dissertation Committee

Dr. Patrick J. Walsh, Professor of Chemistry

Dr. Madeleine M. Joullié, Professor of Chemistry

Dr. David M. Chenoweth, Assistant Professor of Chemistry

To my family, for all of their love and support

ACKNOWLEDGMENTS

This dissertation is the culmination of my whole graduate research, and there are numerous people to whom I owe sincere thanks.

I would like to thank my advisor, Marisa C. Kozlowski, for her guidance and suggestions. She is a great scientist and a mentor who I always yearn to be. I have always gained a certain degree of freedom to pursue my ideas and to help steer the projects into other directions. I am very grateful to have been a part of the Kozlowski group. Past and present, I could not ask for a better group of friends and coworkers to work with. I appreciate everyone's suggestions and input they have provided towards my research. My committee members, Professors Patrick Walsh, Madeleine Joullié, and David Chenoweth have provided much insight and suggestions for my projects not only during my annual committee meetings but also all the time.

I greatly acknowledge Pastor Ock Soo Park, my spiritual mentor. He guided me to become a true Christian. I am also thankful to my spiritual family in Good News Philadelphia Church. Finally, I would like to acknowledge all of my family, my parents, brother, my precious three children Mieun, Jinuk and Younguk, and especially my husband Heeoon Han, whose love and support helped me get through graduate school and complete my degree.

"The Lord is my shepherd; I shall not want." (Psalm 23:1)

ABSTRACT

SELECTIVE OXIDATIVE HOMO- AND CROSS-COUPLING OF PHENOLS

Young Eun Lee

Professor Marisa C. Kozlowski

The efforts described in this dissertation initially focus on the asymmetric coupling of phenols. We have developed Schiff base vanadium catalyst for the oxidative coupling of phenols with high reactivity and enantioselectivity. To the best of our knowledge, this example constitutes the first highly selective asymmetric coupling of phenols. Several substrates were coupled with our vanadium catalyst with good enantioselectivity (72-89% ee).

The first simple catalystic system that uses atom-economical oxygen as the terminal oxidant to accomplish selective *ortho−ortho*, *ortho−para*, or *para−para* homo-couplings of phenols was developed. Chromium salen catalysts have been discovered and verified as uniquely effective in the cross-coupling of different phenols with high chemo- and regio-selectivity. A broad scope of phenol substrates was found for these reaction conditions giving cross-coupling products with good yield (up to 88%). In order to understand the mechanism of cross-coupling reaction, spectroscopic methods, additive experiments, SAR studies, and kinetic experiments were performed and a mechanism was postulated.

Finally, we established an efficient route for the total synthesis of honokiol by utilizing a novel disconnection that transits new structures. This five step (six chemical reactions) synthesis was initiated by oxidative cross-coupling of inexpensive commercial phenols with high yield (91%). Following retro Friedel-Crafts alkylation, a protection reaction proceeded smoothly with excellent yield (89% for three steps). The remaining steps of radical bromination, Kumada coupling and demethylation were each optimized. The total yield over five steps was 34% and gram-scale reactions were conducted for each step.

TABLE OF CONTENTS

CHAPTER 1. Asymmetric Oxidative Coupling of Phenols

1.1. Background

Bisphenolic compounds represent an important class of natural products, the inherent reactivity of which causes them to be both important synthetic intermediates and components in biologically active molecules.[1] Many chiral bisphenolic natural products are known that also contain a stereogenic axis,[2] which is presumably generated biosynthetically via enantioselective oxidative coupling. Therefore, any methods to generate bisphenols in high yield and high enantioselectivity would be very valuable to the synthetic community.

Modern methods specific to the asymmetric synthesis of bisphenols include the dynamic kinetic resolution of biaryl lactones via the addition of chiral nucleophiles,[3] the

(1) Hassan, J.; Sevignon, M.; Gozzi, C.; Schulz, E.; Lemair, M. "Aryl-Aryl Bond Formation One Century after the Discovery of the Ullmann Reaction" *Chem. Rev.* **2002**, *102*, 1359-1470.

(2) (a) Pal, T.; Pal, A. "Oxidative Phenol Coupling: A Key Step for the Biomimetic Synthesis of Many Important Natural Products" *Curr. Sci.* **1996**, *71*, 106–109. (b) Quideau, S.; Feldman, K. S., Eds. [Tetrahedron Vol. 57, Issue 2.] *Tetrahedron* **2001**, *57*, 265–424. (c) Keseru, G. M.; Nogradi, M. "Natural Products by Oxidative Phenolic Coupling Phytochemistry, Biosynthesis and Synthesis" In *Studies in Natural Products Chemistry, Vol. 20: Structure and Chemistry (Part F)* (Atta-ur-Rahman, Editor) Elsevier Science **1998**, p 263. (d) Bringmann, G.; Gulder, T.; Gulder, T. M; Breuning, M. "Atroposelective Total Synthesis of Axially Chiral Biaryl Natural Products" *Chem. Rev.* **2011**, *111*, 563–639. (e) Quideau, S.; Deffieux, D.; Douat-Casassus, C.; Pouységu, L. "Plant Polyphenols: Chemical Properties, Biological Activities, and Synthesis" *Angew. Chem. Int. Ed.* **2011**, *50*, 586–621.

(3) (a) Bringmann, G.; Menche, D. "Stereoselective Total Synthesis of Axially Chiral Natural Products via Biaryl Lactones" *Acc. Chem. Res.* **2001**, *34*, 615–624. (b) Bringmann, G.; Scharl, H.; Maksimenka, K.;

catalytic kinetic resolution of axially chiral biaryldiols [4] direct metal-catalyzed asymmetric oxidative cross-coupling [5] diastereoselective Ullmann couplings [6] or asymmetric atroposelective bromination.[7] These methods, however, require either the activation of a phenol monomer or derivatization of the phenol prior to the coupling step. A single-step oxidative coupling step of two phenolic monomers would be a more efficient method for the construction of chiral biphenols. More recently, the first phosphoric acid-catalyzed asymmetric direct arylative reactions of 2-naphthols with quinone derivatives have been developed, giving chiral biaryldiols with excellent enantioselectivities.[8]

Radacki, K.; Braunschweig, H.; Wich, P.; Schmuck, C. "Atropodiastereoselective Cleavage of Configurationally Unstable Biaryl Lactones with Amino Acid Esters" *Eur. J. Org. Chem.* **2006**, 4349–4361.

(4) (a) Lu, S.; Poh, S. B.; Zhao, Y. "Kinetic Resolution of 1,1'-Biaryl-2,2'-Diols and Amino Alcoholsthrough NHC-Catalyzed Atroposelective Acylation" *Angew. Chem., Int. Ed.* **2014**, *53*, 11041–11045. (b) Ma, G.; Deng, J.; Sibi, M.P. "Fluxionally Chiral DMAP Catalysts: Kinetic Resolution of AxiallyChiral Biaryl Compounds" *Angew. Chem., Int. Ed.* **2014**, *53*, 11818–11821.

(5) (a) Yan, P.; Sugiyama, Y.; Takahashi, Y.; Kinemuchi, H.; Temma, T.; Habaue, S. "Lewis acid-assisted oxidative cross-coupling of 2-naphthol derivatives with copper catalysts" *Tetrahedron* **2008**, *64*, 4325–4331. (b) Guo. F.; Konkol, L. C.; Thomson, R. J. "Enantioselective Synthesis of Biphenols from 1,4-Diketones by Traceless Central-to-Axial Chirality Exchange" *J. Am. Chem. Soc.* **2011**, *133*, 18–20.

(6) (a) Degnan, A. P.; Meyers, A. I. "Total Syntheses of (–)-Herbertenediol, (–)-Mastigophorene A, and (–)-Mastigophorene B. Combined Utility of Chiral Bicyclic Lactams and Chiral Aryl Oxazolines" *J. Am. Chem. Soc.* **1999**, *121*, 2762–2769. (b) Li, Y.; Wang, Q.; Dong, L.; Guo, X.; Wang, W.; Xie, J.; Chang, J. "Asymmetric Synthesis of (+)- and (-)-Wuweizisu C Stereoisomers and Their Chemosensitizing Effects on Multidrug-Resistant Cancer Cells" *Synthesis* **2009**, *2009*, 3383–3390.

(7) Mori, K,; Ichikawa, Y.; Kobayashi, M.; Shibata, Y.; Yamanaka, M.; Akiyama, T. "Enantioselective Synthesis of Multisubstituted Biaryl Skeleton by Chiral Phosphoric Acid Catalyzed Desymmetrization/Kinetic Resolution Sequence" *J. Am. Chem. Soc.* **2013**, *135*, 3964–3970.

(8) Chen, Y.–H.; Cheng, D.–J.; Zhang, J.; Wang, Y.; Liu, X.–Y.; Tan, B. "Atroposelective Synthesis of Axially Chiral Biaryldiols via Organocatalytic Arylation of 2-Naphthols" *J. Am. Chem. Soc.* **2015**, *137*, 15062–15065.

Some examples of natural products are shown in **Figure 1.1** including isoschizandrin,[9] knipholone,[10] chaetoglobin A,[11] mastigophorene A,[12] and gossypol.[13] Notably, no synthesis of these natural products utilizes an asymmetric oxidative coupling. Rather, approaches rely on dynamic kinetic resolutions and diastereoselective biaryl bond formation. Further no synthesis, asymmetric or otherwise, of chaetoglobin A has been reported. Bisphenols have also been used in asymmetric catalysis. Schrock and Hoveyda have used the di-*tert*-butyl biphenol in asymmetric ring-opening and ring-closing metathesis.[14] The diphosphine ligands C3*-Tunephos[15] and (*S*)-HexaPHEMP, which can

(9) Ikeya, Y.; Taguchi, H.; Mitsuhashi, H.; Takeda, S.; Kase, Y.; Aburada, M. "A Lignan from Schizandra Chinesis" *Phytochemistry* **1988**, *27*, 569-573.

(10) Dagne, E.; Steglich, W. "Knipholone: a Unique Anthraquinone Derivative from *Kniphofia Foliosa*" *Phytochemistry* **1984**, *23*, 1729-1731.

(11) Ge, H. M.; Zhang, W. Y.; Ding, G.; Saparpakorn, P.; Song, Y. C.; Hannongbua, S.; Tan, R. X. "Chaetoglobin A and B, Two Unusual Alkaloids from Endophytic Chaetomium Globosum Culture" *Chem. Commun.* **2008**, 5978–5980.

(12) Fukuyama, Y.; Asakawa, Y. "Novel Neurotrophic Isocuparane-type Sesquiterpene Dimers, Mastigophorenes A, B, C, and D, Isolated from the Liverwort Mastigophora Diclados" *J. Chem. Soc., Perkin Trans.1* **1991**, 2737–2741.

(13) Adams, R.; Morris, R. C.; Butterbaugh, D. J.; Kirkpatrick, E. C. "Stucture of Gossypol" *J. Am. Chem. Soc.* **1938**, *60*, 2191–2193.

(14) (a) Alexander, J. B.; La, D. S.; Cefalo, D. R.; Hoveyda, A. H.; Schrock, R. R. "Catalytic Enantioselective Ring-Closing Metathesis by a Chiral Biphen-Mo Complex" *J. Am. Chem. Soc.* **1998**, *120*, 4041-4042. (b) Alexander, J. B.; Schrock, R. R.; Davis, W. M.; Hultzsch, K. C.; Hoveyda, A. H.; Houser, J. H. "Synthesis of Molybdenum Imido Alkylidene Complexes That Contain 3,3-Dialkyl-5,5,6,6-tetramethyl-1,1-biphenyl-2,2-diolates (Alkyl = *t*-Bu, Adamantyl). Catalysts for Enantioselective Olefin Metathesis Reactions" *Organometallics* **2000**, *19*, 3700-3715.

(15) Sun, X.; Li, W.; Hou, G.; Zhou, L.; Zhang, X. "Axial Chirality Control by 2,4-Pentanediol for the Alternative Synthesis of C3*-TunePhos Chiral Diphosphine Ligands and Their Applications in Highly Enantioselective Ruthenium-Catalyzed Hydrogenation of β-Keto Esters" *Adv. Synth. Catal.* **2009**, *351*, 2553-2557.

3

be generated from the corresponding biphenols,[16] have been employed in the asymmetric

hydrogenation of olefins.
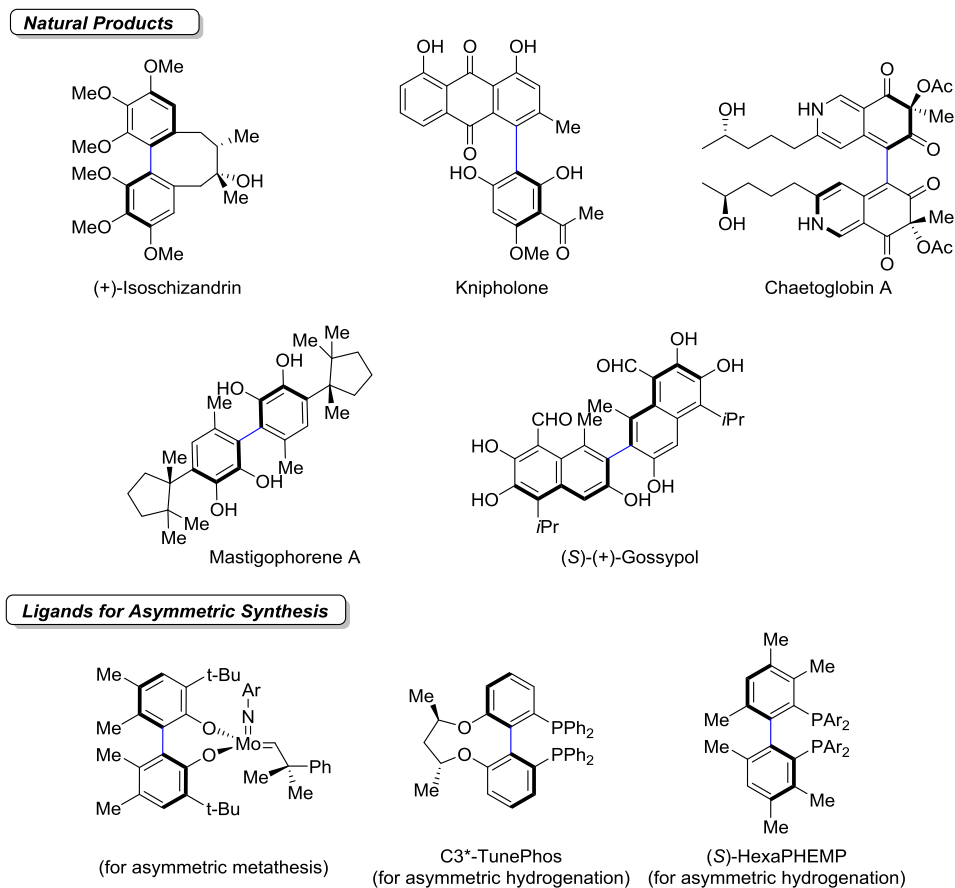
Figure 1.1 Natural Products and Ligands Containing the Biphenol Moeity

(16) Henschke, J. P.; Burk, M. J.; Malan, C. G.; Herzberg, D.; Peterson, J. A.; Wildsmith, A. J.; Cobley, C. J.; Casy, G. "Synthesis and Applications of HexaPHEMP, a Novel Biaryl Diphosphine Ligand" *Adv. Synth. Catal.* **2003**, *345*, 300-307.

1.2. Previous Developments of Vanadium Catalyst

In the past years, the Kozlowski group reported a catalytic protocol for the asymmetric synthesis of BINOLs by using Cu(I)-1,5-diaza-*cis*-decalin complexes.[17] Due to the presence of other reaction pathways when this copper catalyst was employed with oxidizable phenols (e.g. quinone formation), we became interested in using the milder vanadium catalysts for this transformation, which have been reported to convert 2-naphthol to BINOL with 90% ee.[18] These vanadium-catalyzed couplings proceed under mild reaction conditions, using dioxygen as the terminal oxidant, often with air being sufficient. Unfortunately, addition of electron-withdrawing groups to naphthols greatly slows reaction (trace coupling product after 10 d). Since phenols are less reactive than such naphthols, this result was of great concern. Furthermore, any substitution at C3 was found to be highly detrimental in naphthol coupling, which is problematic since our

(17) (a) Li, X.; Yang, J.; Kozlowski, M. C. "Enantioselective Oxidative Biaryl Coupling Reactions Catalyzed by 1,5-Diazadecalin Metal Complexes" *Org. Lett.* **2001**, *3*, 1137-1140. (b) Li, X.; Hewgley, J. B.; Mulrooney, C. A.; Yang, J.; Kozlowski, M. C. "Enantioselective Oxidative Biaryl Coupling Reactions Catalyzed by 1,5-Diazadecalin Metal Complexes: Efficient Formation of Chiral Functionalized BINOL Derivatives" *J. Org. Chem.* **2003**, *68*, 5500-5511.

(18) (a) Chu, C.-Y.; Hwang, D.-R.; Wang, S.-K.; Uang, B.-J. "Chiral Oxovanadium Complex Catalyzed Enantioselective Oxidative Coupling of 2-Naphthols" *Chem. Commun.* **2001**, 980-981. (b) Luo, Z.; Liu, Q.; Gong, L.; Cui, X.; Mi, A.; Jiang, Y. "The Rational Design of Novel Chiral Oxovanadium(IV) Complexes for Highly Enantioselective Oxidative Coupling of 2-Naphthols" *Chem. Commun.* **2002**, 914-915. (c) Luo, Z. B.; Liu, Q. Z.; Gong, L. Z.; Cui, X.; Mi, A. Q.; Jiang, Y. Z. "Novel Achiral Biphenol-Derived Diastereomeric Oxovanadium(IV) Complexes for Highly Enantioselective Oxidative Coupling of 2-Naphthols" *Angew. Chem., Int. Ed.* **2002**, *41*, 4532-4535. (d) Somei, H.; Asano, Y.; Yoshida, T.; Takizawa, S.; Yamataka, H.; Sasai, H. "Dual Activation in a Homolytic Coupling Reaction Promoted by an Enantioselective Dinuclear Vanadium(IV) Catalyst." *Tetrahedron Lett.* **2004,** *45*, 1841-1844. (e) Guo, Q-X.; Wu, Z-J.; Luo, Z-B.; Liu, Q-Z.; Ye, J-L.; Luo, S-W.; Cun, L-F.; Gong, L-Z. "Highly enantioselective oxidative couplings of 2-naphthols catalyzed by chiral bimetallic oxovanadium complexes with either oxygen or air as oxidant" *J. Am. Chem. Soc.* **2007**, 129, 13927-13938. (f) Takizawa, S.; Katayama, T.; Kameyama, C.; Onitsuka, K.; Suzuki, T.; Yanagida, T.; Kawai, T.; Sasai, H. "Chiral dinuclear vanadium(V) catalysts for oxidative coupling of 2-naphthols" *Chem. Commun.* **2008**, 1810-1812. (g) Takizawa, S.; Grçger, H.; Sasai, H. "Vanadium in Asymmetric Synthesis: Emerging Concepts in Catalyst Design and Applications" *Chem. Eur. J.* **2015**, *21*, 8992 – 8997.

initial plans centered on phenols with one *ortho*-position blocked so as to force coupling through the unsubstituted *ortho*-position. However, we were encouraged by a report that VO(acac)$_2$ catalyzed racemic phenol couplings in 62-66% yield after 48-120 h.[19] And a report with tetrahydronaphthol (12%, 26% ee) [20] provided further evidence of the potential of vanadium catalysts in phenol coupling.

Initial results with the optimal reported catalyst **V1** (**Figure 1.2**) in a test reaction were promising (37% ee). Screening of additives provided additional improvement (**V1 + HOAc**, 60% ee, 76% *ortho-ortho*).[21] After reviewing the mechanisms proposed for vanadium catalyzed naphthol couplings, we proposed that either ligand exchange or substrate oxidation were crucial to the outcome. To probe these possibilities, electron deficient ligands, which render the vanadium more Lewis acidic accelerating associative exchange processes *and/or* facilitate formation of the lower oxidation state vanadium(IV), as well as strained ligands, which facilitate ligand exchange, were generated. Both types of catalysts improved the selectivity and the best results were seen with **V2** (77% ee). Since further modification of this scaffold was not fruitful, a different linkage (**V3**) was examined with poor results (0% ee). Speculating that the dramatic drop

(19) Hwang, D.-R.; Chen, C.-P.; Uang, B.-J. "Aerobic Catalytic Oxidative Coupling of 2-Naphthols and Phenols by VO(acac)$_2$" *Chem. Commun.* **1999**, 1207-1208.

(20) Takizawa, S.; Katayama, T.; Somei, H.; Asano, Y.; Yoshida, T.; Kameyama, C.; Rajesh, D.; Onitsuka, K.; Suzuki, T.; Mikami, M.; Yamataka, H.; Jayaprakash, D.; Sasai, H. "Dual Activation in Oxidative Coupling of 2-Naphthols Catalyzed by Chiral Dinuclear Vanadium Complexes" *Tetrahedron* **2008**, 64, 3361-3371.

(21) Jon Ghergurovich and Sangeeta Dey are gratefully acknowledged for developing the vanadium catalyst **V1** and screening additives.

in selectivity with **V3** arose from loss of a sterically "large" group adjacent to the ligand phenoxide, catalyst **V4** was examined resulting in a great improvement (67% ee).[22]
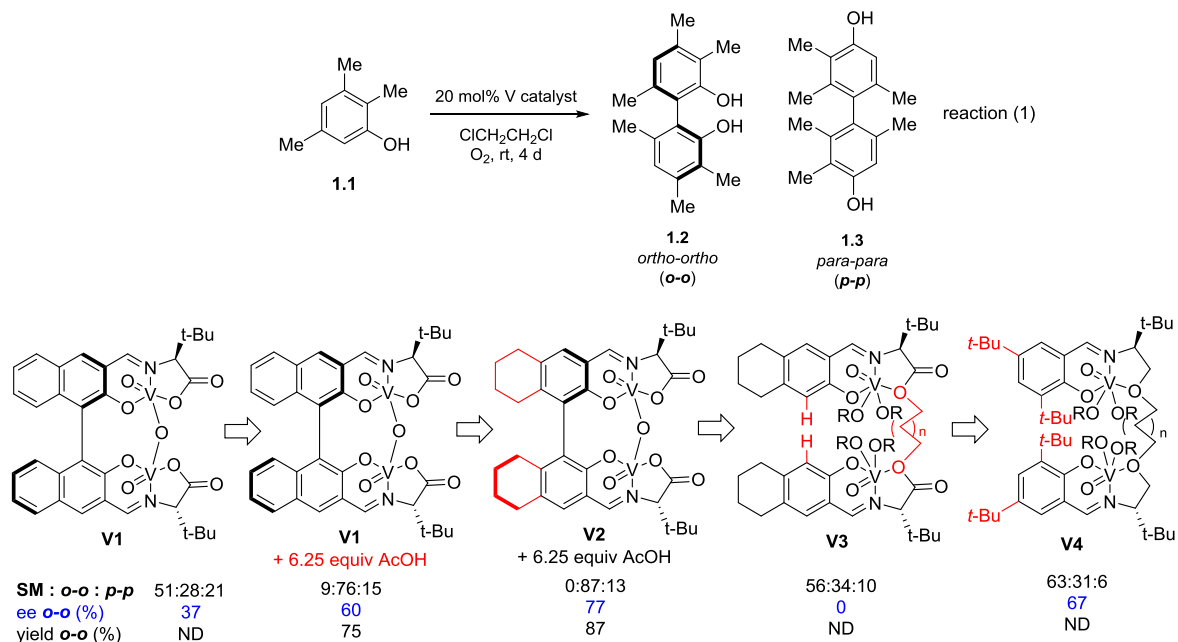
Figure 1.2 Developments of Dimeric Vanadium Catalysts

1.3. Monomeric Vanadium Catalysts

Early advances in the field included the development of monomeric Schiff base-derived vanadyl catalysts by the groups of Chen[23] and Uang.[24] After we discovered

(23) Barhate, N. B.; Chen, C.-T. "Catalytic Asymmetric Oxidative Couplings of 2-Naphthols by Tridentate *N*-Ketopinidene-Based Vanadyl Dicarboxylates" *Org. Lett.* **2002**, *4*, 2529-2532.

monomer **V5** gave similar results (63% ee) in reaction (1), the dimeric scaffold was abandoned even though it had shown superior results in naphthol coupling due to a second order dependence for 2-naphthol.[18c,20b] The monomeric catalyst **V5** was a very tunable and, thus, attractive scaffold. The next focus was to generate a structure-reactivity relationship for modification at every position.

Oxovanadium complex **V5** was prepared by condensation of the unnatural amino acid (*S*)-*tert*-leucine with the corresponding salicylaldehyde and oxovanadium(V) triethoxide, $VO(OEt)_3$ according to Gong's or Sasai's original protocol.[18c,18e,18h,20b] Different amino acid esters and salicaldehydes were incorporated into the vanadium complex. Examination of the resultant catalysts in the phenol coupling revealed that either R^2 = H (acid catalyst) or R^2 = Me or Bn (ester catalyst) was superior and that R^1 = *t*-Bu (entry **1**–**3**) was an absolute requirement (**Table 1.1**).

(24) Chu, C.-Y.; Uang, B.-J. "Catalytic Enatioselective Coupling of 2-Naphthols by New Chiral Oxovanadium Complexed Bearing a Self Accelerating Functional Group" *Tetrahedron:Asymmetry*, **2003**, *14*, 53-55.

Table 1.1 Ligand Developments: Amino Ester Screening
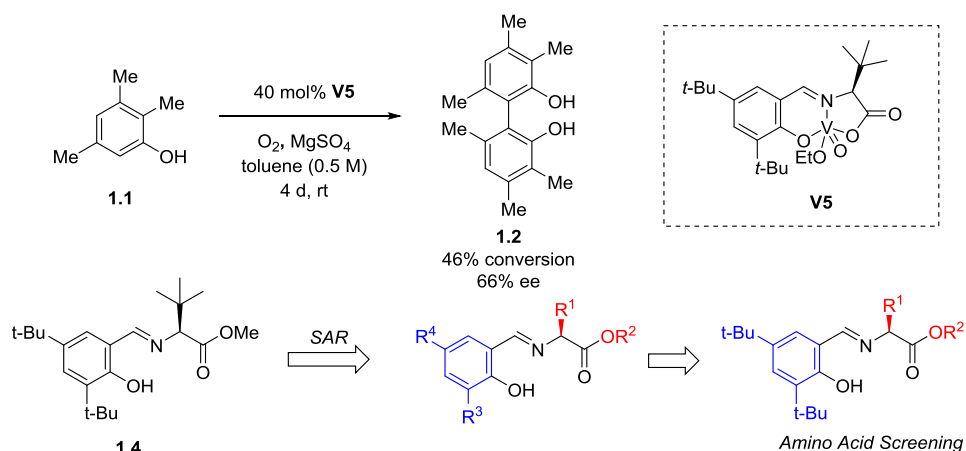
Entry	R^1	R^2	Conversion (%)	ee (%)
1	*t*-Bu	H	46	66
2	*t*-Bu	Me	40	66
3	*t*-Bu	Bn	37	70
4	*t*-Bu	*t*-Bu	35	65
5	2-methylpropyl	Me	67	50
6	2-methylprolyl	Bn	53	27
7	*i*-Bu	Me	65	5
8	*i*-Bu	*t*-Bu	18	0
9	Bn	Me	73	0
10	Bn	Bn	64	0

Analyzing prior data,[25] we hypothesized that a large group at R^3 would be superior. This hypothesis was borne out with better results with bulky groups such as *t*-Bu (entry **1**), silyl groups (entry **6–8**), and 1,1-dimethylbenzyl (entry **12**) as shown in the **Table 1.2**. Other very sterically demanding R^3 groups (i.e., 2,6-xylyl and adamantly etc.) result in further improvements in turnover, but at the cost of lower enantioselectivies. Further screening of the R^4 group revealed a dependence of the electron-withdrawing power of this group. We concluded that electron-withdrawing group destabilizes the

---

(25) Chen, C.-T.; Kao, J.-Q.; Salunke, S. B.; Lin, Y.-H. "Enantioselective Aerobic Oxidation of α-Hydroxy-Ketones Catalyzed by Oxovanadium(V) Methoxides Bearing Chiral, *N*-Salicylidene-*tert*-butylglycinates" *Org. Lett.*, **2011**, *13*, 26-29.

vanadium (V) oxidation state rendering it more reactive in the rate-limiting redox event and thereby accelerating the reaction. In line with this reasoning, $R^4 = NO_2$ (entry **15–16**) provided both high reactivity and high enantioselectivity (**Table 1.2**). Therefore, the best catalyst classes included 3-*tert*-butyl-5-nitro-, and 3-triethylsilyl-5-nitro-*N*-salicylidene-L-*tert*-butylglycine ligands.

Table 1.2 Ligand Developments: Salicylaldehyde Screening
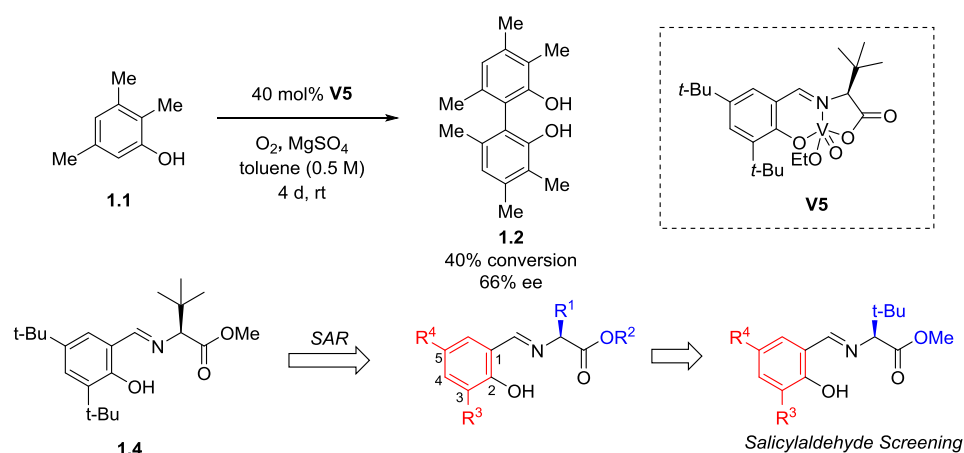
Entry	R^3	R^4	Conversion (%)	ee (%)
1	*t*-Bu	*t*-Bu	40	66
2	2-tolyl	*t*-Bu	78	49
3	2,6-xylyl	*t*-Bu	92	50
4	1-naphthyl	*t*-Bu	85	38
5	2-methoxy-1-naphthyl	*t*-Bu	81	57
6	$SiMe_3$	*t*-Bu	70	73
7	$SiEt_3$	*t*-Bu	58	75
8	SiiPr_3	*t*-Bu	35	76
9	$SiPh_2t$Bu	*t*-Bu	13	60
10	adamantyl	*t*-Bu	24	66
11	CPh_3	*t*-Bu	15	56
12	CMe_2Ph	*t*-Bu	37	76
13	*t*-Bu	OMe	47	65
14	*t*-Bu	OAc	43	62
15	*t*-Bu	NO_2	86	75
16	$SiEt_3$	NO_2	100	75

In the catalyst preparation, the salicylaldehyde **1.6** was prepared by *ortho*-formylation of commercial phenol **1.5**, followed by an introduction of the 5-nitro

substituent. [25] The aldehyde **1.6** was subjected to L-*tert*-leucine to generate a Schiff base, and then immediately treated with oxovanadium (V) triethoxide to yield a highly reactive (100% conversion), and selective (83% ee) vanadium complex **V6**. Complex **V6** obtained in this manner was dark-blue. The addition of acid to the coupling reaction increased both yield and enantioselction, most likely via protonation of the catalyst which would accelerated ligand exchange in analogy to transesterification. The improved reactivity of **V6** allowed lower catalyst loading (20 mol%) and shorter reaction time (2 days), and none of the *para-para* regioisomer **1.3** was observed.

Scheme 1.1 Preparation of catalyst and phenol coupling in the optimal condition
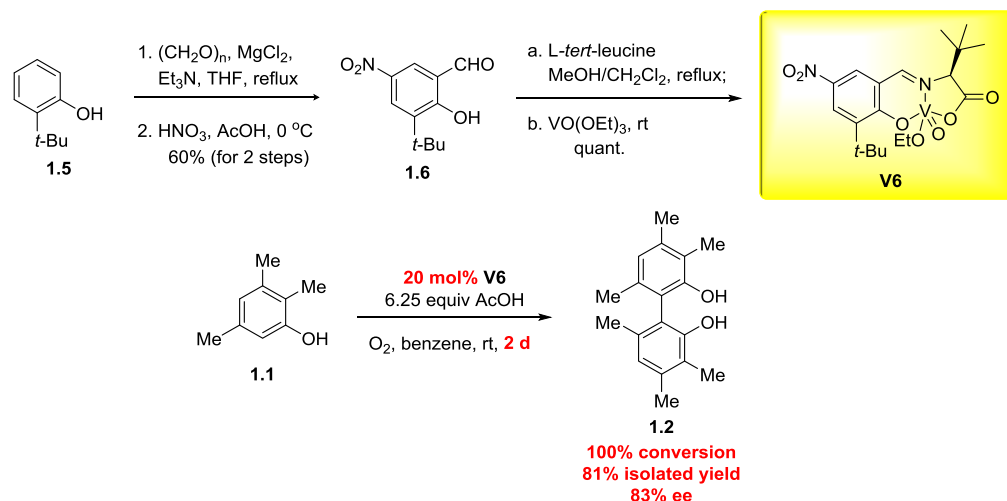
Encouraged by these results, additional phenol substrates were examined with this catalyst and the results are shown in the **Figure 1.3**. The results of this study pinpointed the structural features key to enantioselectivity. For example, the substrate **1.1** and **1.7** differed only in the position of one methyl group, but the latter resulted in no selectivity indicating that substitution at the *ortho*-position of the phenol was highly important. This

11

point was further reinforced by the results from **1.8** and **1.10**. Electron-withdrawing groups were expected to slow the oxidation, which was supported by the sluggish reactivity of bromo-substituted analogs (**1.12**, **1.14** and **1.16**). Among the substrate classes examined, better levels of asymmetric induction were observed in the coupling of 2,3,5-trisubstituted phenols, from 50% to 83% ee (**1.1**, **1.13** and **1.15**).
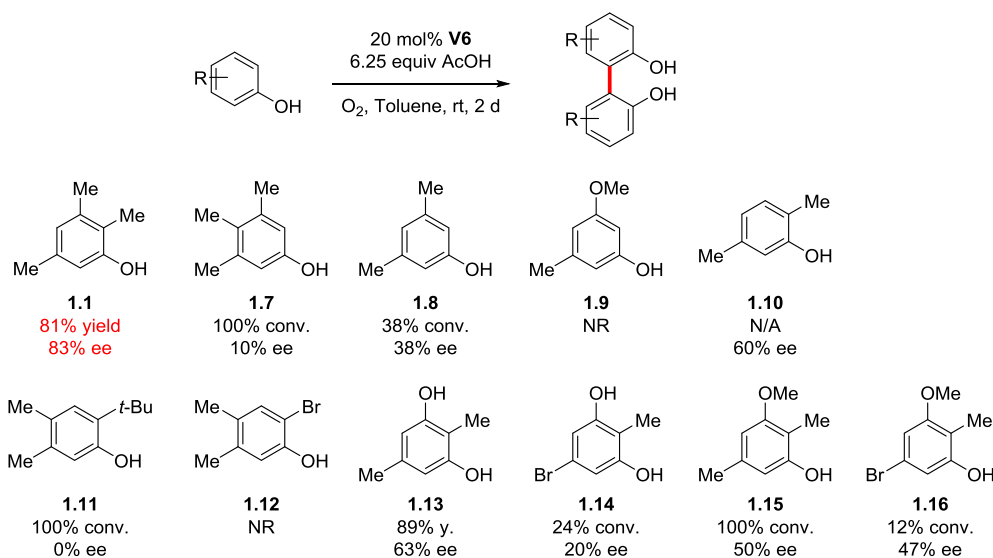
Figure 1.3 Substate Scope in Asymmetric Phenol Coupling

1.4. More Improvements

To improve the enantioselection in the coupling reaction, we further examined key factors such as temperature and additives. It was determined that enantioselectivity of the coupling product of 2,5-dimethyl resorcinol (**1.13**) improved up to 85% ee when the reaction temperature was lowered to –40 °C (**Table 1.3**), although reactivity suffered,

Table 1.3 Temperature Effect on Asymmetric Coupling of Phenol **1.13**

| Entry	temperature($^{\circ}$C)	conversion (%)[a]	ee (%)
1	25	72	50
2	0	53	63
3	-20	30	75
4	-40	15	85
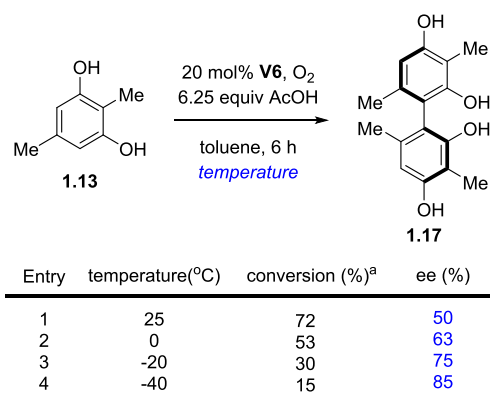
[a]Conversions were determined after 6 hours reactions at 0 $^{\circ}$C by ^{1}H-NMR.

Encouraged by these results, several additives were examined in place of acetic acid (**Table 1.4**). At this stage, a further exciting result was discovered. Namely, Lewis acids were found to improve enantio-selection relative to acetic acid although reactions were slightly slower (entries 2-5). Of the Lewis acids, LiCl, even though it was insoluble throughout the process of reaction, was superior resulting in 85% ee vs 52% without the additive (entry 1 and 2). To pinpoint the attribute of LiCl causing this improvement, a series of chloride salts was screened (entries 6-8); none were superior to LiCl, although results were very good for MgCl$_2$ (entry 7, 78% ee). Examination of various lithium salts (entries 9-14) revealed that lithium perchlorate was second best (entry 12, 73% ee). In a reported Diels-Alder reaction, LiCO$_4$·Et$_2$O enhanced both *endo* selectivity and reaction rate by retained solvent ordering[26] and it may operate here in a similar way. Water is formed during reaction from the reduction of dioxygen. To probe whether the

(26) Grieco, P. A.; Nunes, J. J.; Gaul, M. D. "Dramatic Rate Accelerations of Diels-Alder Reactions in 5 M Lithium Perchlorate-Diethyl Ether: The Cantharidin Problem Reexamined" *J. Am. Chem. Soc.* **1990**, *112*, 4595-4596.

improvements noted about arose from the desiccant properties of the additives, additional desiccants were screened (entries 15-16). Based on the improvements seen, it appears that LiCl acts as a Lewis acid and desiccant. Further experiments are needed to determine if the LiCl enhances the selectivity by coordinating and activating the catalyst or the substrate.

Table 1.4 Additives Screening.

20 mol% **V6**, O$_2$
0.4 equiv additives
toluene, 0 ^{o}C, 6 h

1.13 → **1.17**
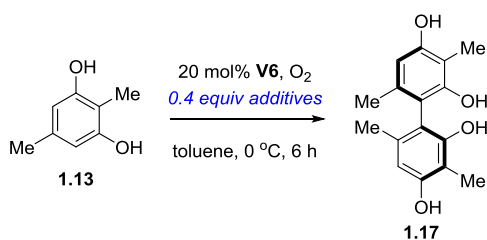
Entry	Additives		Conversion (%)^a	ee(%)
1	none		70	52
2	LiCl		46	85
3	Sc(OTf)$_3$	Lewis acids	43	67
4	Sn(OTf)$_2$		33	43
5	Yb(OTf)$_3$		48	69
6	NaCl		52	47
7	MgCl$_2$	Cl$^-$ salts	28	78
8	KCl		59	45
9	LiF		46	46
10	LiBr		100	63
11	LiI	Li$^+$ salts	12	57
12	LiClO$_4$		94	73
13	LiOAc		93	18
14	Li$_2$CO$_3$		52	27
15	4Å MS	Drying agents	-	68
16	MgSO$_4$		50	70

^{a}Conversions were determined after 6 hours reactions at 0 ^{o}C by ^{1}H-NMR.

Unfortunately, LiCl did not provide equal levels of improvement for all substrates. Excitingly, LiCl did give high enanioselectivity with 2,5-dimethyl-3-hydroxyphenol (**1.13**, 85% ee) and 2,5-dimethyl-3-methoxyphenol (**1.15**, 82% ee). Notably, the amount of LiCl did not change the enatioselectivity. The enantiopurity could

also be upgraded easily by trituration. For example, substrate **1.25** was enhanced to 95% ee following triturations using hexane.

Scheme 1.2 Optimized Oxidative Coupling of Phenols **1.13** and **1.15**
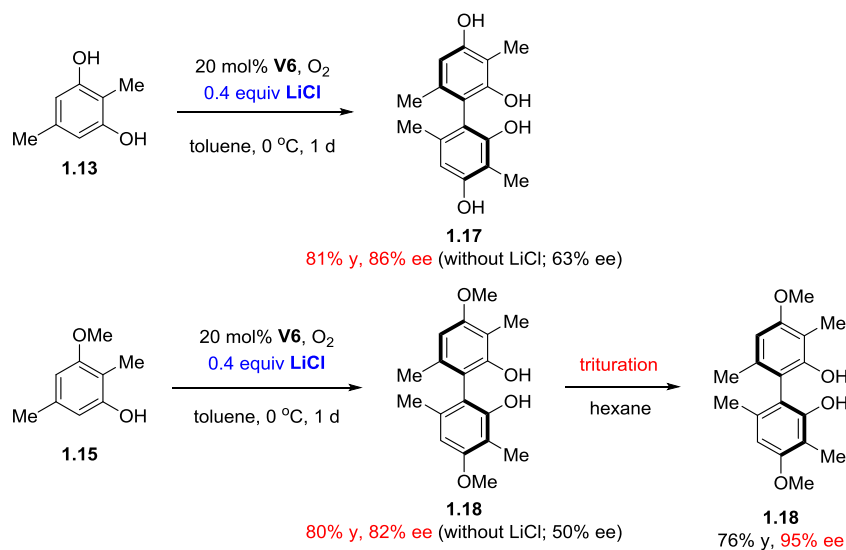
1.5. Stereochemistry

To determine the stereochemistry of the asymmetric coupling, efforts focused on obtaining a crystal structure. On larger scale, the coupling of 2,3,5-trimethylphenol (**1.1**) gives higher selectivity (85% ee compared to 83%). Our group has noted that racemic biaryl products have much poorer solubility than enantiopure biaryls in hexane. Exploiting this difference, one trituration was found to increase the enantiomeric excess of the filtrate to 89% ee. By sequential trituration, highly enantioenriched material (95% ee) was obtained in 72% yield (**Figure 1.4**). Crystallization from hexane and ethyl acetate

(10:1) afforded white crystals, and an (*S*) absolute axial configuration was assigned to compound **1.2** generated from catalyst **V6**.[27]
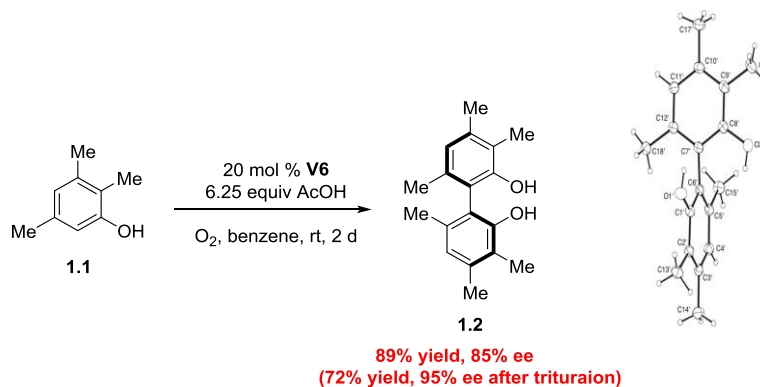
Figure 1.4 Absolute Configuration of Coupling Product **1.2**

1.6. Substrate Syntheses and Oxidative Coupling

The common feature of the substrates that give good enantioselecivity in the coupling reaction is a 2,3,5-trialkyl phenol. To access substrates with a bulkier group at the 2-position, allyation of the hydroxyl group of a 3,5-disubstituted phenols was undertaken followed by [3,3]-sigmatropic rearrangement. Kyle Niederer, an undergraduate student sponsored by LRSM REU program during summer 2014, and Houng Kang helped synthesizing a variety of 2,3,5-trisubstituted phenols via this approach.

(27) Bringmann, G.; Mortimer, A. J. P.; Keller, P. A.; Gresser M. J.; Garner, J.; Breuning, M. "Atroposelective Synthesis of Axially Chiral Biaryl Compounds" *Angew. Chem. Int. Ed.* **2005**, *44*, 5384–5427.

The synthesis of each substrate is shown in **Scheme 1.3**. 3,5-Disubstituted phenols were first allylated using allyl bromide. Lewis acid-mediated Claisen rearrangement on these allyl ethers afforded the 2-allylated phenols. Subsequent hydrogenation generated additional alkyl analogs for testing.

Scheme 1.3 Syntheses of 2,3,5-trisubstituted phenols
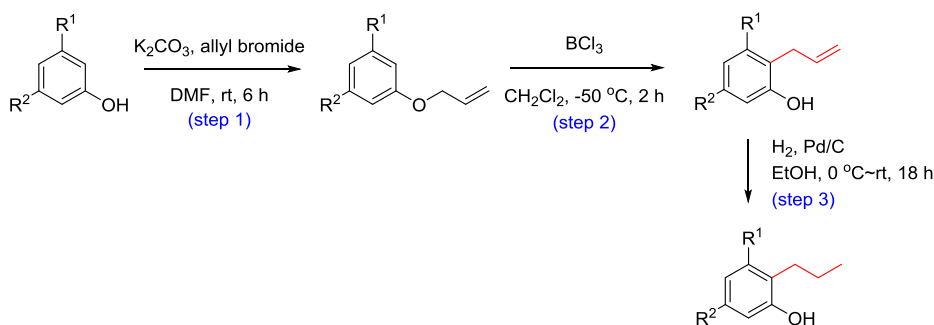
| Entry	R^1	R^2	Reaction Yield (%)		
			step 1	step 2	step 3
1	Me	Me	99	90	79
2*	Me	OMe	92	53	78
3*	OMe	Me	92	17	40
4	OMe	OMe	78	69	66

*entry 2 and 3 began from the same starting phenol substrate and separated after step 2.

Both the 2-allyl- and 2-propylphenols were used as coupling substrates. Among the eight substrates synthesized, only two substrates gave good enantioselectivity (**Scheme 1.4**). 2-Allyl-3,5-dimethylphenol (**1.20**) and 3,5-dimethyl-2-propylphenol (**1.21**) proceeded smoothly under the reaction conditions of **V6**/acetic acid to give the *ortho-ortho* coupling product with good selectivities (77% ee and 72% ee, respectively). Even though the allyl group in the substrate **1.20** decelerated reaction rate compared to the substrate **1.21**, the enantioselectivity remained high.

Scheme 1.4 Substrate Syntheses and Oxidative Coupling

(a) *Substrate Syntheses*

(b) *Oxidative Coupling Reactions*

1.22
56% y (99% brsm), 77% ee

1.23
80% y (98% brsm), 72% ee
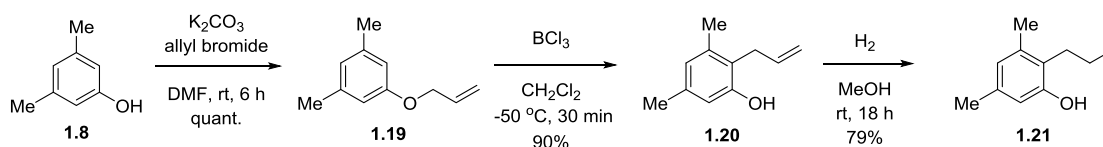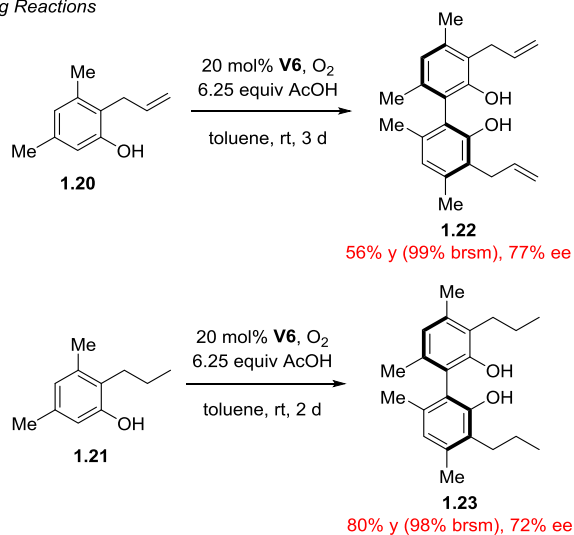
The 3-methoxy-5-methyl-phenol (**1.9**) produced two allylated substrates via the Claisen rearrangement, 2-allyl-3-methoxy-5-methylphenol (**1.24**), and 2-allyl-3-methyl-5-methoxyphenol (**1.26**), each of which was also hydrogenated. Unfortunately, however, those substrates coupled to give poor enantioselectivity (**Figure 1.5**).

18
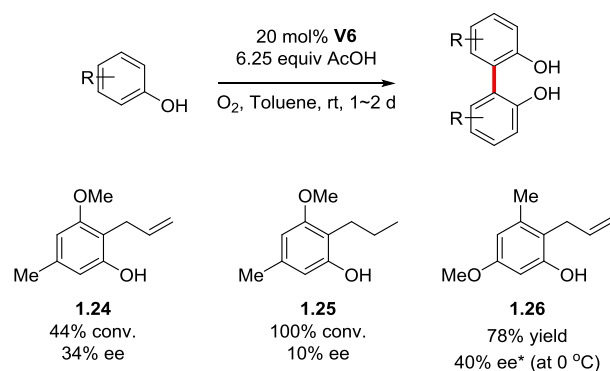
Figure 1.5 Oxidative Coupling of 2,3,5-trisubstituted phenols

In a different strategy, the effect of bulkier group adjacent to the formed biaryl bond was probed. Specifically, phenyl and silyl groups were introduced at 5-position of bromophenol **1.14** by conventional coupling reactions. Phenyl substituted phenol coupled smoothly to give the product with moderate selectivity (50% ee), and additives provided no improvement. The silyl substituted phenol was not stable in the oxidative conditions; after 16 h, all the starting material was consumed, but no desired product was observed (**Scheme 1.5**).

Scheme 1.5 Substrate with bulky group Syntheses and Oxidative Coupling
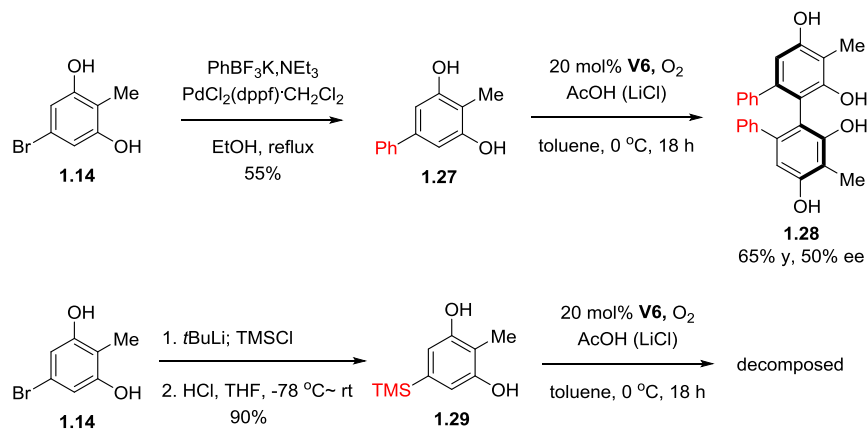
At this point, we became curious how catalyst **V6** compares to dimeric vanadium catalysts **V1** and **V2** in 2-naphthol coupling, where the latter are known to give high selectivity in 2-naphthol coupling. In contrast, our new monomeric **V6** catalysts showed poor performance in the 2-naphthol coupling reaction (**Figure 1.6**) indicating substantial different control factors are in play. In support of this hypothesis, 2-naphthol (**1.30**) gives the (*R*)-enantiomer, whereas the (*S*)-enantiomer is seen with the same catalyst in the phenol coupling.
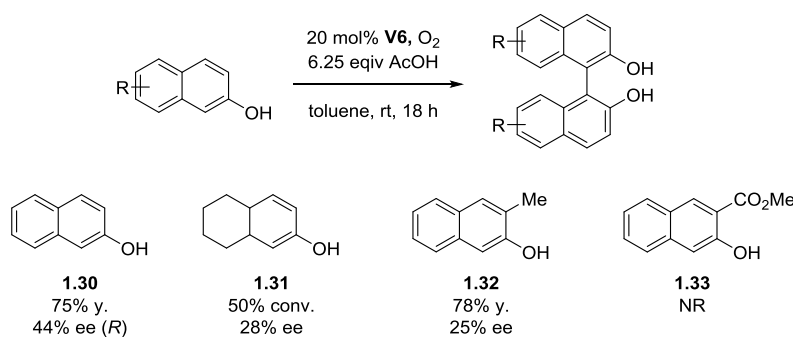
Figure 1.6 Oxidative Coupling Reaction of 2-Naphthol Derivatives with **V6**

1.7. Alkynyl Phenol Coupling and Application to Chaetoglobin A Synthesis
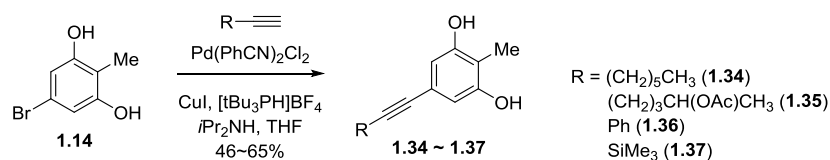
The chaetoglobins[10] are a structurally unique class of azaphilone alkaloid dimers with reported anticancer activity. Notably, this class of compounds has not been synthesized to date. The major challenge inherent to these structures lies in the enantioselective formation of the axial chiral bond between the two units. Therefore,

asymmetric oxidative phenol coupling would be a critical step for the enantioselective synthesis of chaetoglobin natural products.

Alkynyl phenol **1.34**, as a model substrate for chaetoglobin, was subjected to the oxidative phenol coupling reaction and it gave high enantioselectivity of 89% ee without any significant decomposition (67% conversion after 16 h, **Scheme 1.6**). Encouraged by this preliminary result, we decided to investigate the substrate scope with various alkynes. Substrates **1.34**–**1.37** were prepared via Sonogashira cross-coupling reaction between aryl bromide **1.14** and the corresponding alkyne. While the alkyl substituted alkynyl phenol (**1.34**, **1.35**) coupled with good enantioselectivity (89% ee and 94:6 dr, respectively), phenylalkynyl phenol **1.36** and silylalkynyl phenol **1.37** did not give any desired products.

Scheme1.6 Oxidative Coupling of Alkynyl Phenols

(a) *Sonogashira Coupling for Substrate Syntheses*

OH
Me
Br
OH
1.14

R⎯≡
Pd(PhCN)$_2$Cl$_2$

CuI, [tBu$_3$PH]BF$_4$
iPr$_2$NH, THF
46~65%

OH
Me
OH
R
1.34 ~ 1.37

R = (CH$_2$)$_5$CH$_3$ (**1.34**)
    (CH$_2$)$_3$CH(OAc)CH$_3$ (**1.35**)
    Ph (**1.36**)
    SiMe$_3$ (**1.37**)

(b) *Oxidative Coupling of Alkenyl Phenols*

OH
Me
OH
R

20 mol% **V4**, O$_2$
0.4 equiv LiCl

toluene, 0 °C

OH
Me
OH
R
R
OH
Me
OH

R = (CH$_2$)$_5$CH$_3$ (**1.38**)
    (CH$_2$)$_3$CH(OAc)CH$_3$ (**1.39**)

OH
Me
OH
1.34
66-74% y, 89% ee

OH
Me
OH
OAc
1.35
67% y, 94:6 dr

OH
Me
OH
Ph
1.36
decomp.

OH
Me
OH
TMS
1.37
decomp.

Recently, Houng Kang has finished the first total synthesis of chaetoglobin A utilizing asymmetric phenol coupling as a key step. He modified the catalyst **V6** into opposite enantiomer with (*R*)-*tert*-leucine to obtain the stereochemistry corresponding to that of the natural product.

22

Scheme 1.7 First Total Synthesis of Chaetoglobin A

1.39
67% y, 94:6 dr

Chaetoglobin A
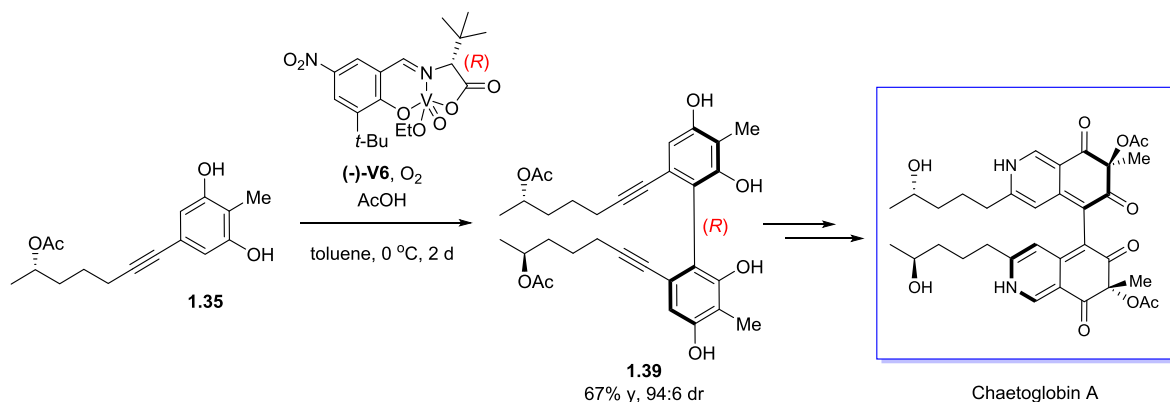
1.8. Mechanism

It has been reported that the oxidative coupling generally proceeds via three possible mechanisms: (1) the radical–radical coupling, (2) the radical–anion coupling, and (3) the heterolytic coupling of cationic species.[28] Compelling evidence supporting a radical–radical pathway has been reported for one vanadium-catalyzed oxidative coupling reactions of 2-naphthols.[19h]

A proposed catalytic cycle for phenol coupling built on these precedents is shown in **Figure 1.6**. First, the phenol coordinates to a vanadium complex and becomes oxidized to phenoxide **B** via electron transfer. The produced radical can give two possible products (*ortho–ortho* and *para-para*), but our studies have shown that the *ortho-ortho* product is

---

(28) (a) "Oxidative coupling of phenols and phenol ethers": D. A.Whiting in Comprehensive Organic Synthesis, Vol. 3. (Eds.:B. M. Trost, I. Fleming, G. Pattenden), Pergamon, Oxford, **1991**, pp. 659. (b) Waldvogel, S. R.; Mirk, D. Handbook of CH-Transformations, Vol. 1 (Ed.: G. Dyker), Wiley-VCH,Weinheim, **2005**, pp. 251.

favored in **C**. Dissociation and rearomatization provides the corresponding bisphenol. Finally, oxygen reoxidizes the vanadium catalyst.
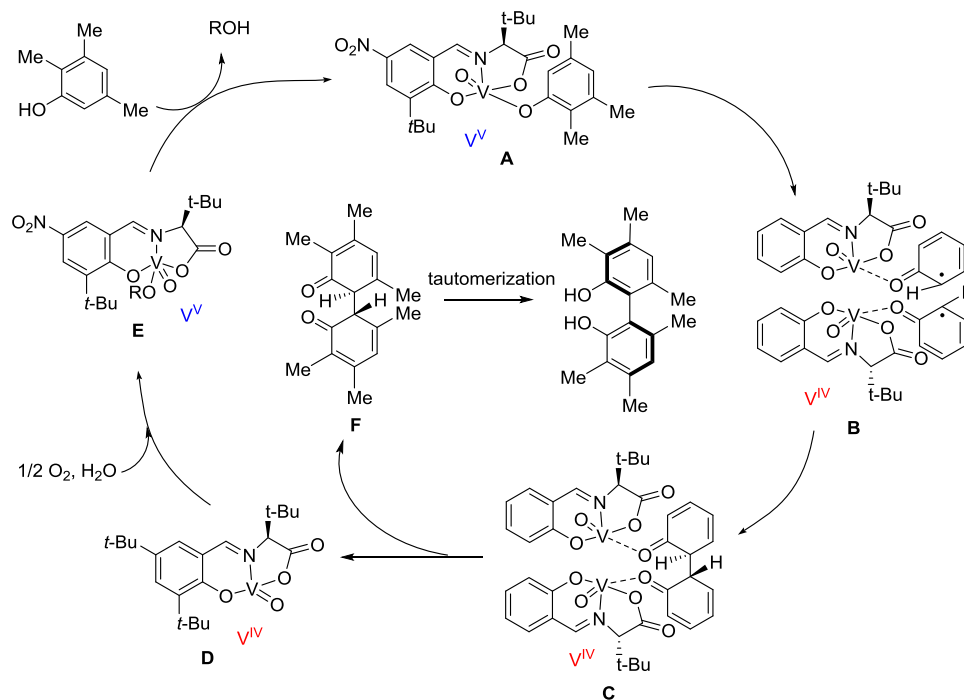
Figure 1.7 Proposed Mechanism of Asymmetric Oxidative Phenol Coupling

This proposed mechanism was supported by radical inhibitor experiments. With 20 mol% of **V6**, the oxidative coupling of 2,3,5-trimethyl phenol was completed within 2 days at ambient temperature under oxygen. However, with equimolar TEMPO relative to catalyst, the same reaction proceeded with only 35% conversion under the same conditions (**Scheme 1.8**). Moreover, under inert atmosphere, 9% and 26% conversions were observed with 20 and 50 mol% of catalyst loading, respectively. And it is consistent with the vanadium(V) species being the active oxidant and each vanadium

abstracting one electron as would be the case with vanadium(V) to vanadium(IV) redox event.

Scheme 1.8 Supporting Experiments of Oxidative Coupling Reaction

Entry	Condition	Conversion
1	control	100%
2	0.2 equiv TEMPO	35%
3	N_2 atmosphere	9% (3 days)
4	50 mol% **V6**, N_2 atmosphere	26% (3 days)
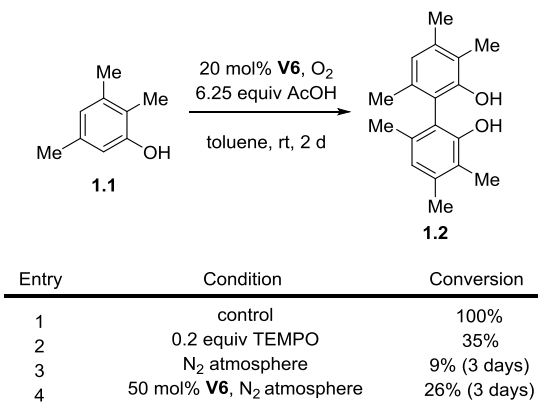
1.9. Summary

In summary, we have developed Schiff base catalyst **V6** for the oxidative coupling of phenols with high reactivity and enantioselectivity. To the best of our knowledge, this example constitutes the first highly selective asymmetric coupling of phenols. It was found that the chiral centers on the amino acid portion and the substituents on salicylaldehyde portion of the catalyst were both crucial to stereocontrol. Importantly, an electron-withdrawing group on the ligand destabilized the higher oxidation state of vanadium rendering the catalyst more reactive. Several substrates (**Figure 1.8**) were coupled with **V6** with good enantioselectivity (72-89% ee).

25
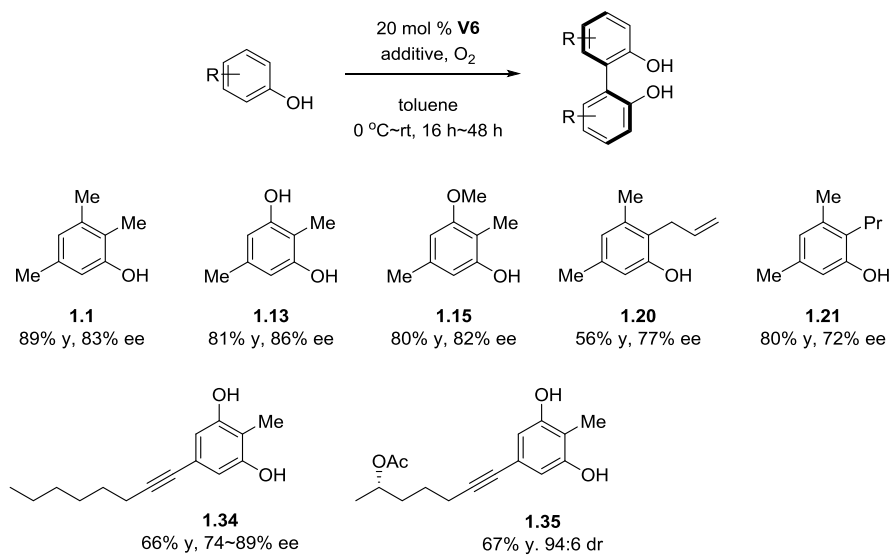
Figure 1.8 Substrate Scope in Asymmetric Phenol Coupling

1.10. Experimental

General Consideration

All reactions were carried out under an atmosphere of dry nitrogen or argon, unless otherwise noted. When necessary, solvents and reagents were dried prior to use. Methylene chloride, 1,2-dichloroethane, and acetonitrile were distilled from CaH_2, THF was distilled from sodium/benzophenone ketyl, toluene was distilled from sodium, and DMF was distilled from $MgSO_4$. Reactions were all monitored via analytical thin layer chromatography (TLC) using Silicycle glass backed TLC plates with 250 μm silica and F254 indicator. Visualization was accomplished with UV light and/or ceric ammonium

26

molybdate stain. Column chromatography was performed with Silicycle SiliaFlash P60 silica gel (40-63 μm particle size).

NMR spectra were recorded on 300 MHz, 360 MHz, and 500 MHz spectrometers. Multiplicities for ^{1}H NMR data are reported as follows: s = singlet, d = doublet, t = triplet, br = broad, m = multiplet. ^{1}H NMR spectra were referenced to the residual solvent peaks: $CDCl_3$ (7.26 ppm), DMSO-d_6 (2.50 ppm), acetone-d_6 (2.05 ppm), THF-d_8 (3.58 ppm), CD_3OD (3.31 ppm), or C_6D_6 (7.16 ppm). ^{13}C NMR spectra were referenced to: $CDCl_3$ (77.16 ppm), DMSO-d_6 (39.52 ppm), acetone-d_6 (29.84 ppm), or THF-d_8 (67.57 ppm). Infrared spectra were recorded on either a Jasco FT/IR-480 Plus spectrometer [29] or an Applied Systems ReactIR 1000. UV spectra were measured on a JASCO FT/IR-480 Plus spectrometer. High-resolution mass spectra were measured on a Waters LC-TOF mass spectrometer (model LCT-XE Premier) with ionization mode ESI+ or ESI–.[30] Enantiomeric excesses were determined using analytical HPLC on an Agilent 1100 Series HPLC with UV detection at 254 nm. An analytical Chiralpak IA column (4.6 mm x 250 mm, 5 μm) from Daicel was used. Optical rotations were measured on a Jasco polarimeter with a sodium lamp.[31]

---

(29) The Smith group is thanked for use of their UV and IR spectrometers.

(30) Dr. Rakesh Kohli at the Mass Spectrometry Laboratory at the University of Pennsylvania is gratefully acknowledged for obtaining high resolution mass spectra.

(31) The Smith group is thanked for use of their polarimeter.

O_2N —CHO —OH —t-Bu
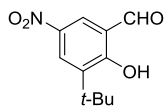
3-(*tert*-Butyl)-2-hydroxy-5-nitrobenzaldehyde (1.6). Dry formaldehyde (0.7 g, 23.3 mmol) was added in portions to a mixture of 4-*tert*-butylphenol (1.0 g, 6.66 mmol), triethylamine (2.6 mL, 18.8 mmol) and anhydrous $MgCl_2$ (2.0 g, 20.6 mmol) in 50 mL of THF. The mixture was refluxed for 8 h, cooled to room temperature, acidified with 3N HCl (70 mL), and extracted with diethyl ether (30 mL x 3). The ether layer was washed with water (50 mL), and brine (50 mL), and dried using $MgSO_4$. Removal of solvent and purification by column chromatography yielded 3-(*tert*-butyl)-2-hydroxy-benzaldehyde as yellow oil (710 mg, 61% yield). Spectral data matched those reported in the literature.[32]

In a 100 mL round-bottomed flask was placed 3-(*tert*-butyl)-2-hydroxy-benzaldehyde (710 mg, 4.0 mmol) in HOAc (12 mL). Nitric acid (4.0 mL, 96 mmol) was added dropwise at 0 °C and the mixture was stirred for 1 h at ambient temperature. The resulting mixture was poured into iced water (100 mL) with vigorous stirring. The orange precipitate formed was filtered through a sintered glass funnel, and then washed with water (10 mL). The product was recrystallized from ethanol to give 360 mg (65% yield) of **1.6** as a yellow solid: ^{1}H NMR (500 MHz, CDCl_3) δ 12.44 (s, 1H), 9.97 (s, 1H), 8.41 (s, 2H), 1.46 (s, 9H); ^{13}C NMR (500 MHz, CDCl3) δ 196.2, 165.8, 140.7, 140.1, 128.7, 127.0, 119.3, 31.4, 35.4. Spectral data matched that reported in the literature.[25]

---

(32) Gisch, N.; Balzarini, J.; Meier, C. "Enzymatically Activated *cyclo*Sal-d4T-monophosphates: The Third Generation of *cyclo*Sal-Pronucleotides" *J. Med. Chem.* ***2007***, *50, 1658-1667.*

Representative Procedure for Vanadium Catalyst V6.
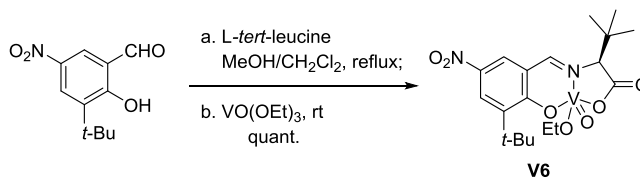
All glass ware was flame dried. A mixture of L-*tert*-leucine (45 mg, 0.34 mmol) and 3-*tert*-butyl-5-nitro-2-hydroxybenzaldehyde (**1.6**) (76 mg, 0.34 mmol) in MeOH:CH$_2$Cl$_2$ (2 mL, 1:1) was heated at reflux and monitored by TLC. The reaction mixture was cooled to room temperature and VO(OEt)$_3$ (69 mg, 0.34 mmol) was added. After 3 h under argon atmosphere, solvent was removed under reduced pressure to afford the catalyst (147 mg, 99%) as a deep blue solid.

(*S*)-**Vanadium Catalyst V6**. Dark blue solid; HRMS (ESI) *m/z* = 433.1180 calcd for C$_{18}$H$_{26}$N$_2$O$_7$V [M+H]$^+$, found 433.1179.

**General Procedure for Oxidative Coupling of Phenols.**

Racemic Coupling with VO(acac)₂.[20]
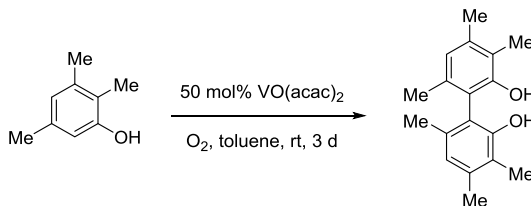
2,3,5-Trimethylphenol (30 mg, 0.22 mmol) and VO(acac)$_2$ (29 mg, 0.11 mmol) were dissolved in toluene (1 mL) at room temperature. The resulting deep green solution was stirred for 3 days. The solution was concentrated and purified by column chromatography (5% ethyl acetate in hexane) to yield racemic 3,3',4,4',6,6'-hexamethylbiphenyl-2,2'-diol (**1.2**) as a pale-yellow solid (19 mg, 63%). Spectral data matched that reported in the literature.[33]

Asymmetric Coupling with Catalyst V6: Method A
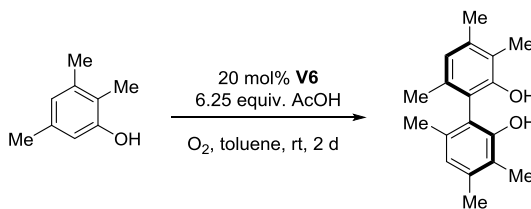
To a microwave vial was added 2,3,5-trimethylphenol (**1.1**) (180 mg, 1.31 mmol), 20 mol% oxovanadium catalyst **V6** (110 mg, 0.27 mmol), and acetic acid (0.47 mL, 8.26

---

(33) Armstrong, D. R.; Cameron, C.; Nonhebel, D. C.; Perkins, P. G. "Oxidative Coupling of Phenols. Part 10. The Role of Steric Effects in the Formation of C-O Coupled Products" *J. Chem. Soc.-Perkin Trans. 2* **1983**, 581-585.

mmol). The vial sealed and toluene (2.6 mL) was added. Oxygen was added via active purge. The deep blue reaction solution was stirred for 2 d at 25 °C, then concentrated *in vacuo*. The crude product was purified by flash column chromatography to yield **1.2** as a pale yellow solid (160 mg, 89%) in 83% ee. Crystallization from hexane and ethyl acetate (10:1) afforded white crystals with 95% ee. The absolute axial configuration of compound **1.2** was determined as *S*. See Appendix B for crystallographic data.

(*S*)-3,3',4,4',6,6'-Hexamethyl-[1,1'-biphenyl]-2,2'-diol (1.2). ^{1}H NMR (500 MHz, CDCl$_3$) δ 6.74 (s, 2H), 4.74 (s, 2H), 2.29 (s, 6H), 2.17 (s, 6H), 1.92 (s, 6H); ^{13}C NMR (500 MHz, CDCl$_3$) δ 15.9, 138.6, 135.2, 123.9, 120.4, 117.0, 20.1, 19.3, 11.9; IR (film) 3509, 3460, 2922, 2359, 1560, 1458, 1298, 1079 cm^{-1}; HRMS (ESI) *m/z* = 270.1620 calcd for C$_{18}$H$_{22}$O$_2$ [M]$^+$, found 270.1623; $[\alpha]_D^{23}$ −32.23 (*c* 0.15, 95% ee, CHCl$_3$); Enantiomeric excess was determined with Chiral HPLC: Chiralpak IA column (1% *i*-PrOH/hexanes, 1 mL/min) t$_r$(*R*) = 5.09 min, t$_r$(*S*) = 6.11 min.

**Asymmetric Coupling with Catalyst V6: Method B**
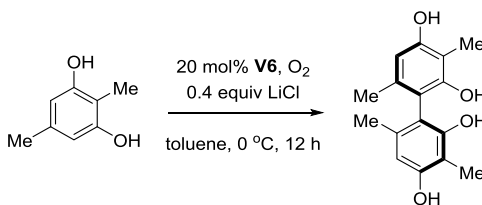
To a microwave vial was added 2,5-dimethylbenzene-1,3-diol (**1.13**) (180 mg, 1.30 mmol), 20 mol% oxovanadium catalyst **V6** (110 mg, 0.27 mmol), and LiCl (22 mg, 0.52 mmol). The vial sealed and toluene (2.6 mL) was added. Oxygen was added *via* active purge. The deep blue reaction solution was stirred for 12 h at 0 °C, and

concentrated *in vacuo*. The crude product was purified by flash column chromatography to yield **1.17** as a white solid (144 mg, 81%).

(*S*)-3,3',6,6'-Tetramethyl-[1,1'-biphenyl]-2,2',4,4'-tetraol (**1.17**). ^{1}H NMR (500 MHz, CDCl$_3$) δ 6.41 (s, 2H), 4.85 (s, 2H), 4.71 (s, 2H), 2.15 (s, 6H), 1.91 (s, 6H); ^{13}C NMR (500 MHz, CDCl$_3$) δ 155.2, 153.5, 137.0, 111.7, 109.4, 108.1, 19.5, 8.5; IR (film) 3459, 2925, 1592, 1326, 1078 cm^{-1}; HRMS (ESI) *m/z* = 273.1127 calcd for C$_{16}$H$_{17}$O$_4$ [M–H]$^-$, found 273.1139. $[\alpha]_D^{23}$ −52.39 (*c* 0.04, 86% ee, CH$_2$Cl$_2$); Enantiomeric excess was determined with Chiral HPLC: Chiralpak IA column (20% *i*-PrOH/hexanes, 1 mL/min) t$_r$(*S*) = 4.95 min, t$_r$(*R*) = 6.88 min.
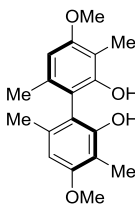
(*S*)-4,4'-Dimethoxy-3,3',6,6'-tetramethyl-[1,1'-biphenyl]-2,2'diol (**1.18**). Following the general procedure using method B at 0 °C for 18 h, the *ortho-ortho* product was obtained as a yellow solid in 80% yield: ^{1}H NMR (500 MHz, CDCl$_3$) δ 6.46 (s, 2H), 4.80 (s, 2H), 3.86 (s, 6H), 2.12 (s, 6H), 1.97 (s, 6H); ^{13}C NMR (500 MHz, CDCl3) δ 158.7, 152.9, 136.3, 111.9, 109.9, 104.7, 55.5, 19.7, 8.4; IR (film) 3513, 2921, 1577, 1466, 1326, 1104, 819, 739 cm^{-1}; HRMS (ESI) *m/z* = 325.1416 calcd for C$_{18}$H$_{22}$O$_4$Na [M+Na]$^+$, found 325.1414. $[\alpha]_D^{23}$ −19.68 (*c* 0.05, 86% ee, CHCl$_3$); Enantiomeric excess was determined with Chiral HPLC: Chiralpak IA column (1% *i*-PrOH/hexanes, 1 mL/min) t$_r$(*R*) = 7.99 min, t$_r$(*S*) = 15.11 min.

General Procedure for the Preparation of Allyl- and Propyl- Substrates: Various allyl- and propyl substrates were prepared from the corresponding phenol and allyl bromide with high yield in two (allyl) and three (propyl) steps according to the literature procedure.
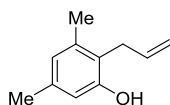

2-Allyl-3,5-dimethylphenol (1.20). Allyl bromide (0.2 mL, 2.2 mmol) was added to a solution of 3,5-dimethylphenol (244 mg, 2.0 mmol) and potassium carbonate (304 mg, 2.2 mmol) in DMF (4.0 mL). The reaction mixture was stirred 16 hours at room temperature, diluted with ether (15 mL) and quenched with water (10 mL). The organic layer was separated and the aqueous layer was extracted with ether (10 mL x 3). The combined organic layers were dried over Na_2SO_4. The crude product was used with purification for the next step.

To a solution of crude allyl aryl ether in dichloromethane (10 mL) was added boron trichloride (4.0 mL, 4 mmol) dropwise at −50 °C. After stirring for 2 h at −50 °C, the solution was quenched with water (10 mL), extracted with dichloromethane (15 mL x 3), dried over $MgSO_4$. The product was purified by flash chromatography (5% EtOAc/hexane) to give 2-allyl-3,5-dimethylphenol (292 mg, 0.18 mmol) as a white solid in 90% yield for 2 steps. ^{1}H NMR (500 MHz, $CDCl_3$) δ 6.61 (s, 1H), 6.50 (s, 1H), 5.99-5.91 (m, 1H), 5.05 (d, J = 10.5 Hz, 1H), 5.02 (d, J = 17 Hz, 1H), 4.73 (s, 1H), 3.39 (d, J = 4.5 Hz, 2H), 2.25 (s, 3H), 2.24 (s, 3H); ^{13}C NMR (500 MHz, CDCl3) δ 153.9, 137.8,

136.9, 135.8, 123.7, 120.6, 115.3, 114.1, 30.3, 20.9, 19.5; IR (film) 3466, 2921, 1623, 1584, 1458, 1308, 1207, 1138, 1110, 1039, 911, 837 cm^{-1}; HRMS (ESI) *m/z* = 161.0966 calcd for C$_{11}$H$_{13}$O [M–H]$^-$, found 161.0972.
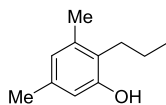
3,5-Dimethyl-2-propylphenol (1.21). To a stirring solution of allylated phenol (400 mg, 2.4 mmol) in dry methanol (4.0 mL) was added Pd/C (10 wt%, 40 mg). The reaction flask was evacuated and backfilled with H$_2$ (× 3 times). The reaction was stirred under H$_2$ atmosphere for 16 hours. The reaction mixture was then filtered through Celite™, concentrated by rotary evaporation. The product was purified by flash chromatography (5% EtOAc/hexane) to give the product (304 mg, 1.92 mmol) as a white solid in 79% yield: ^{1}H NMR (500 MHz, CDCl$_3$) δ 6.59 (s, 1H), 6.46 (s, 1H), 4.57 (s, 1H), 2.56 (t, *J* = 8.0 Hz, 2H), 2.26 (s, 3H), 2.23 (s, 3H), 1.54 (sextet, *J* = 8 Hz, 2H), 1.00 (t, *J* = 7.5 Hz, 3H); ^{13}C NMR (500 MHz, CDCl3) δ 153.4, 137.6, 136.0, 124.1, 123.6, 113.6, 28.1, 22.5, 20.8, 19.4, 14.4; IR (film) 3476, 2959, 1583, 1454, 1302, 1215, 1140, 1103, 1022, 949 cm^{-1}; HRMS (ESI) *m/z* = 163.1123 calcd for C$_{11}$H$_{15}$O [M–H]$^-$, found 163.1117.
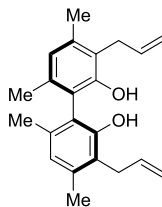
(*S*)-3,3'-Diallyl-4,4',6,6'-tetramethyl-[1,1'-biphenyl]-2,2'diol (1.22). Following the general procedure using method A at room temperature for 3 days, the *ortho-ortho* product was obtained as a white solid in 56% yield: ^{1}H NMR (500 MHz, CDCl$_3$) δ 6.76 (s, 2H), 5.99-5.92 (m, 2H), 5.00-4.93 (m, 4H), 4.76 (s, 2H), 3.43 (d, *J* = 3.5 Hz, 4H), 2.30 (s, 6H), 1.93 (s, 6H); ^{13}C NMR (500 MHz, CDCl$_3$) δ 151.8, 138.6, 136.0, 135.9, 124.2, 121.9, 117.2, 114.4, 30.6, 19.4, 19.2; IR (film) 3524, 3077, 2922, 1637, 1564, 1457, 1302, 1258, 1191, 1144, 1110, 1050, 995, 909, 851 cm^{-1}; HRMS (ESI) *m/z* = 323.2011 calcd for C$_{22}$H$_{27}$O$_2$ [M+H]$^{+}$, found 323.2020; $[\alpha]_D^{23}$ −21.88 (*c* 0.2, 77% ee, CHCl$_3$); Enantiomeric excess was determined with Chiral HPLC: Chiralpak IA column (1% *i*-PrOH/hexanes, 1 mL/min) t$_r$(*R*) = 5.63 min, t$_r$(*S*) = 7.19 min.
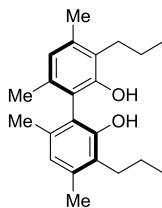

(*S*)-4,4',6,6'-Tetramethyl-3,3'-dipropyl-[1,1'-biphenyl]-2,2'diol (1.23). Following the general procedure using method A at room temperature for 3 d, the *ortho-ortho* product was obtained as a white solid in 80% yield: ^{1}H NMR (500 MHz, CDCl$_3$) δ 6.73 (s, 2H), 4.72 (s, 2H), 2.64-2.61 (m, 4H), 2.32 (s, 6H), 1.92 (s, 6H), 1.58-1.53 (m,

4H), 0.99-0.96 (m, 6H); 13C NMR (500 MHz, CDCl3) δ 151.8, 138.0, 135.2, 125.2, 124.0, 117.1, 28.5, 22.4, 19.4, 19.2, 14.3; IR (film) 3524, 2959, 2871, 1616, 1563, 1453, 1394, 1296, 1260, 1205, 1146, 1103, 1039, 954, 850 cm^{-1}; HRMS (ESI) m/z = 327.2324 calcd for $C_{22}H_{31}O_2$ [M+H]$^{+}$, found 327.2323; $[\alpha]_D^{23}$ −26.12 (c 0.2, 72% ee, CHCl$_3$); Enantiomeric excess was determined with Chiral HPLC: Chiralpak IA column (1% i-PrOH/hexanes, 1 mL/min) t$_r$(R) = 4.79 min, t$_r$(S) = 6.24 min.
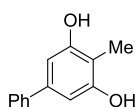
4-Methyl-[1,1'-biphenyl]-3,5-diol (1.27). Under a nitrogen atmosphere, a mixture of 5-bromo-2-methylbenzene-1,3-diol (203 mg, 1.0 mmol), potassium phenyltrifluoroborate (200 mg, 1.1 mmol), PdCl$_2$(dppf) ·CH$_2$Cl$_2$ (4 mg, 0.5 mol %), and triethylamine (0.4 mL, 3.0 mmol) in EtOH (4.0 mL) was stirred at 80 °C for 12 hours. After completion of the reaction as indicated by TLC, the reaction mixture was cooled to room temperature. The solvent was removed under reduced pressure, and the residue was diluted with EtOAc (15 mL) and washed with water (15 mL). Evaporation of the solvent followed by purification on silica gel (20% ethyl acetate in hexane) afforded the corresponding product **1.27** (110 mg, 0.55 mmol) as a yellow solid with 55% yield: ^{1}H NMR (500 MHz, CDCl$_3$) δ 7.52 (d, J = 8.0 Hz, 2H), 7.41 (t, J = 7.0 Hz, 2H), 7.33 (t, J = 7.0 Hz, 1H), 6.65 (s, 2H), 4.84 (s, 2H), 2.18 (s, 3H); ^{13}C NMR (125 MHz, CDCl$_3$) δ 154.9, 140.4, 140.1, 128.7, 127.4, 126.8, 109.4, 106.6, 7.8; IR (film) 3331, 2919, 1590, 1572, 1410, 1076, 848, 762, 694 cm^{-1}; HRMS (ESI) m/z = 201.0916 calcd for $C_{13}H_{13}O_2$ [M+H]$^{+}$, found 201.0914.
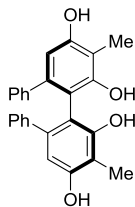
(*S*)-4',5''-Dimethyl-[1,1':2',1'':2'',1'''-quaterphenyl]-3',4'',5',6''-tetraol (1.28).

Following the general procedure using method A or B at 0 °C for 18 h, the *ortho-ortho*

product was obtained as a yellow solid in 65% yield: ^{1}H NMR (500 MHz, CDCl$_3$) δ 7.10

(t, *J* = 7.0 Hz, 2H), 7.02 (t, *J* = 8.0 Hz, 4H), 6.57 (d, *J* = 7.0 Hz, 4H), 6.31 (s, 2H), 5.32 (s,

2H), 4.87 (s, 2H), 2.23 (s, 6H); ^{13}C NMR (125 MHz, CDCl$_3$) δ 155.0, 153.7, 141.9, 140.0,

128.5, 127.4, 126.5, 110.7, 109.6, 109.4, 8.5; IR (film) 3437, 2920, 1620, 1395, 1342,

1077, 790, 760, 738, 700 cm^{-1}; HRMS (ESI) *m/z* = 399.1596 calcd for C$_{26}$H$_{23}$O$_4$

[M+H]$^+$, found 399.1591; Enantiomeric excess was determined with Chiral HPLC:

Chiralpak IA column (25% *i*-PrOH/hexanes, 1 mL/min) t$_r$(*S*) = 14.27 min, t$_r$(*R*) = 16.97

min.
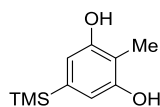
2-Methyl-5-(trimethylsilyl)benzene-1,3-diol (1.29). To a stirred solution of 5-

bromo-2-methylbenzene-1,3-diol (185 mg, 0.9 mmol) in anhydrous THF (5 mL) at −78

°C was added dropwise *t*-BuLi (3.5 mL, 1.6 M solution in pentane). The resulting

yellows solution was stirred at −78 °C for 1 hour, then TMSCl (0.58 mL, 4.5 mmol) was

added dropwise at −78 °C and the resulting colorless suspension was stirred at −78 °C

for 1 h and then allowed to warm to room temperature. 1N HCl (2 mL) solution was

added and after 2 h, extracted with diethyl ether (3 x 10 mL), and the combined organic extract was washed with water (15 mL) and brine (15 mL), dried over anhydrous MgSO$_4$. The crude product was purified by column chromatography on silica gel with eluent 10 % of ethyl acetate in hexanes. 160 mg of a white solid in 90% yield was obtained: ^{1}H NMR (500 MHz, CDCl$_3$) δ 6.53 (s, 2H), 4.72 (s, 2H), 2.14 (s, 3H), 0.22 (s, 9H); ^{13}C NMR (125 MHz, CDCl$_3$) δ 154.4, 139.2, 112.2, 111.1, 7.9, −1.2; IR (film) 3293, 2953, 1616, 1579, 1452, 1396, 1284, 1250, 1069, 917, 830, 755 cm^{-1}; HRMS (ESI) *m/z* = 195.0841 calcd for C$_{10}$H$_{15}$O$_2$Si [M–H]$^-$, found 195.0834.

General Procedure for Sonogashira Cross-Coupling: All solvent and reagents were deoxygenated. Pd(PhCN)$_2$Cl$_2$ (6 mol%), CuI (4 mol%), [*t*Bu$_3$PH]BF$_4$ (12 mol%) were weighed and transferred into a flame-dried flask. The system was evacuated and refilled with argon. 1,4-Dioxane (0.5 M) and *i*Pr$_2$NH (1.5 equiv) were added to the flask under argon, then a solution of 5-bromo-2-methylbenzene-1,3-diol and alkyne (1.2 equiv) in a 0.5 mL of dioxane were added to the mixture. After stirring at room temperature for 18 h, the reaction mixture was filtered through a silica pad which was washed with ethyl acetate. The combined eluents were concentrated and purified on silica gel.
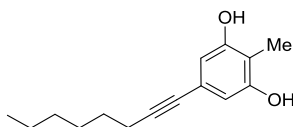
2-Methyl-5-(oct-1-yn-1-yl)benzene-1,3-diol (1.34). The product was purified via column chromatography with 15% ethyl acetate in hexane to give a desired product in 80% yield as a pale yellow solid: ^{1}H NMR (500 MHz, acetone-*d*$_6$) δ 8.20 (s, 2H), 6.44 (s,

2H), 2.86 (s, 3H), 2.35 (t, J = 7.0 Hz, 2H), 1.55 (m, 2H), 1.44 (m, 2H), 1.30 (m, 4H), 0.89

(t, J = 2.0 Hz, 3H); ^{13}C NMR (125 MHz, acetone-d_6) δ 157.0, 122.4, 112.3, 110.5, 89.0,

81.7, 32.1, 28.6, 28.5, 22.5, 19.6, 14.3, 8.5; IR (film) 3435, 3053, 2931, 2857, 2232,

1772, 1735, 1618, 1583, 1322, 1080, 737 cm^{-1}; HRMS (ESI) m/z = 232.1463 calcd for

$C_{15}H_{20}O_2$ [M]$^+$, found 232.1457.
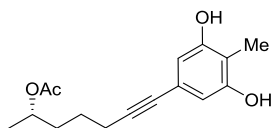
(*S*)-7-(3,5-Dihydroxy-4-methylphenyl)hept-6-yn-2-yl acetate (1.35). The

product was purified via column chromatography with 15% ethyl acetate in hexane to

give a desired product in 80% yield as a pale yellow solid: ^{1}H NMR (500 MHz, CDCl$_3$) δ

6.45 (s, 2H), 5.99 (brs, 2H), 4.99 (sextet, J = 6.0 Hz, 1H), 2.38 (t, J = 7.0 Hz, 2H), 2.11

(s, 3H), 2.06 (s, 3H), 1.73-1.66 (m, 2H), 1.64-1.57 (m, 2H), 1.24 (d, J = 6.5 Hz, 3H); [13]C

NMR (125 MHz, CDCl$_3$) δ 172.2, 154.8, 121.6, 111.7, 111.0, 88.7, 81.0, 71.4, 35.0, 24.6,

21.6, 20.0, 19.3, 8.2; IR (film) 3387, 2924, 1708, 1586, 1415, 1380, 1264, 1089, 843,

739, 702 cm^{-1}; HRMS (ESI) m/z = 275.1283 calcd for $C_{16}H_{19}O_4$ [M–H]$^-$, found 275.1288.
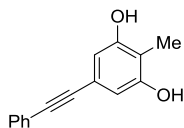

2-Methyl-5-(phenylethynyl)benzene-1,3-diol (1.36). The product was purified

via column chromatography with 20% ethyl acetate in hexane to give a desired product in

60% yield as a pale yellow solid: ^{1}H NMR (500 MHz, acetone-d_6) δ 8.38 (s, 2H), 7.50-

7.49 (m, 2H), 7.40-7.38 (m, 3H), 6.60 (s, 2H), 2.10 (s, 3H); ^{13}C NMR (125 MHz, acetone-d_6) δ 157.2, 132.2, 129.4, 129.1, 124.3, 121.2, 113.5, 110.5, 90.6, 88.3, 8.7; IR (film) 3328, 2918, 1629, 1503, 1383, 1088, 846, 754 cm^{-1}; HRMS (ESI) m/z = 225.0916 calcd for $C_{15}H_{13}O_2$ [M+H]$^+$, found 225.0918.
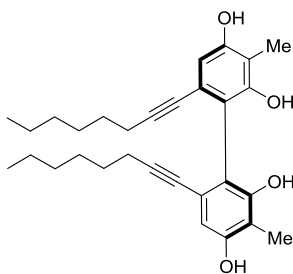
(S)-3,3'-Dimethyl-6,6'-di(oct-1-yn-1-yl)-[1,1'-biphenyl]-2,2',4,4'-tetraol (1.38).

Following the general procedure using method B at 0 °C for 18 h, the *ortho-ortho* product was obtained as a yellow solid in 69% yield: ^{1}H NMR (500 MHz, CDCl$_3$) δ 6.57 (s, 2H), 5.01 (s, 2H), 4.84 (s, 2H), 2.16 (s, 6H), 2.16-2.15 (m, 4H), 1.34-1.20 (m, 10H), 1.18-1.12 (m, 6H), 0.87 (t, J = 8 Hz, 6H); ^{13}C NMR (125 MHz, CDCl$_3$) δ 154.6, 153.5, 123.1, 115.3, 111.2, 110.9, 93.1, 78.3, 31.4, 28.4, 28.1, 22.5, 19.3, 14.1, 8.5; IR (film) 3443, 3304, 3054, 2930, 2306, 1606, 1584, 1395, 1265, 1077, 739 cm^{-1}; HRMS (ESI) m/z = 463.2848 calcd for $C_{30}H_{39}O_4$ [M+H]$^+$, found 463.2841; $[\alpha]_D^{23}$ −50.96 (c 0.05, 89% ee, CHCl$_3$); Enantiomeric excess was determined with Chiral HPLC: Chiralpak IA column (20% i-PrOH/hexanes, 1 mL/min) t_r(S) = 6.76 min, t_r(R) = 15.98 min.
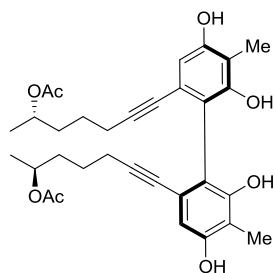
(2S,2'S)-((R)-4,4',6,6'-Tetrahydroxy-5,5'-dimethyl-[1,1'-biphenyl]-2,2'-diyl)bis(hept-6-yne-7,2-diyl) diacetate (1.39). Following the general procedure with 20 mol% (–)-**V6** using method B at 0 °C for 2 d, the *ortho-ortho* product was obtained as a yellow oil in 67% yield: ^{1}H NMR (500 MHz, CDCl$_3$) δ 6.60 (s, 2H), 6.27 (brs, 2H), 5.13 (s, 2H), 4.79 (sextet, *J* = 6.0 Hz, 2H), 2.24-2.17 (m, 4H), 2.16 (s, 6H), 2.03 (s, 6H), 1.41-1.37 (m, 6H), 1.28-1.24 (m, 2H), 1.18 (d, *J* = 6.5 Hz, 6H); ^{13}C NMR (125 MHz, CDCl$_3$) δ 171.6, 155.1, 153.5, 122.8, 115.2, 111.8, 111.0, 91.8, 79.2, 71.3, 34.5, 24.3, 21.4, 19.9, 19.1, 8.6; IR (film) 3409, 2936, 1707, 1585, 1515, 1415, 1377, 1269, 1165, 1134, 1085, 737 cm^{-1}; HRMS (ESI) *m/z* = 573.2464 calcd for C$_{32}$H$_{38}$O$_8$Na [M+Na]$^+$, found 573.2460.

41

Chapter 2. Selective Oxidative Homo- and Cross-Coupling of Phenols

2.1. Background

Bisphenolic compounds represent an important class of natural products the inherent reactivity of which makes them both important synthetic intermediates and components in biologically active molecules. Many natural products[34] and materials[35] can be constructed by oxidative phenol couplings including homo- and cross-coupling of phenols (**Figure 2.1**). The examples include those requiring regioselectivity in homo-coupling (euphorbetin vs isoeuphorbetin) or in cross-coupling of two different monomers (honokiol, ZD6126, riccardin C, vingramine). Methods that install the bisphenol bonds can give access to these complex molecules and can provide efficient synthetic routes to new classes of achiral and chiral ligands as well. Therefore, any methods to generate these bisphenols in high yield and high selectivity would be very valuable to the synthetic community. Although many stoichiometric phenolic oxidations have been reported,[36] the

(34) (a) Weiss, U.; Merlini, L.; Nasini, G. "Naturally Occurring Perylenequinones" *Prog. Chem. Org. Nat. Prod.* **1987**, *52*, 1–71. (b) Bringmann, G.; Günther, C.; Ochse, M.; Schupp, O.; Tasler, S. "Biaryls in Nautre: A Multi-Facetted Class of Stereochemically, Biosynthetically, and Pharmacologically Intriguing Secondary Metaobolites" *Prog. Chem. Org. Nat. Prod.* **2001**, *82*, 1–249.

(35) Kobayashi, S.; Higashimura, H. "Oxidative polymerization of phenols revisited" *Prog. Polym. Sci.* **2003**, *28*, 1015–1048.

(36) (a) Armstrong, D. R.; Cameron, C; Nonhebel, D. C.; Perkins, P. G. "Oxidative Coupling of Phenols. Part 6. A Study of the Role of Spin Density Factors on the Product Composition in the Oxidations of 3,5-Dimethylphenol and Phenol" *J. Chem. Soc. Perk. Trans. 2* **1983**, 563–568. (b) Noshino, H.; Itoh, N.; Nagashima, M.; Kurosawa, K. "Choice of Manganese(III) Complexes for the Synthesis of 4,4′-Biphenyldiols and 4,4′-Diphenoquiones" *Bull. Chem. Soc. Jpn*. **1992**, *65*, 620–622. (c) Morimoto, K.; Sakamoto, K.; Ohnishi, Y.; Miyamoto, T.; Ito, M.; Dohi, T. Kita, Y. "Metal-Free Oxidative para Cross-Coupling of Phenols" *Chem. Eur. J.* **2013**, *19*, 8726–8731.

coupling selectivities are typically low when multiple coupling sites are available (red arrows in **Figure 2.1**). Furthermore, the reactions are often stoichiometric and require the use of hazardous and expensive materials and the products are difficult to remove from the reaction mixtures.[37]
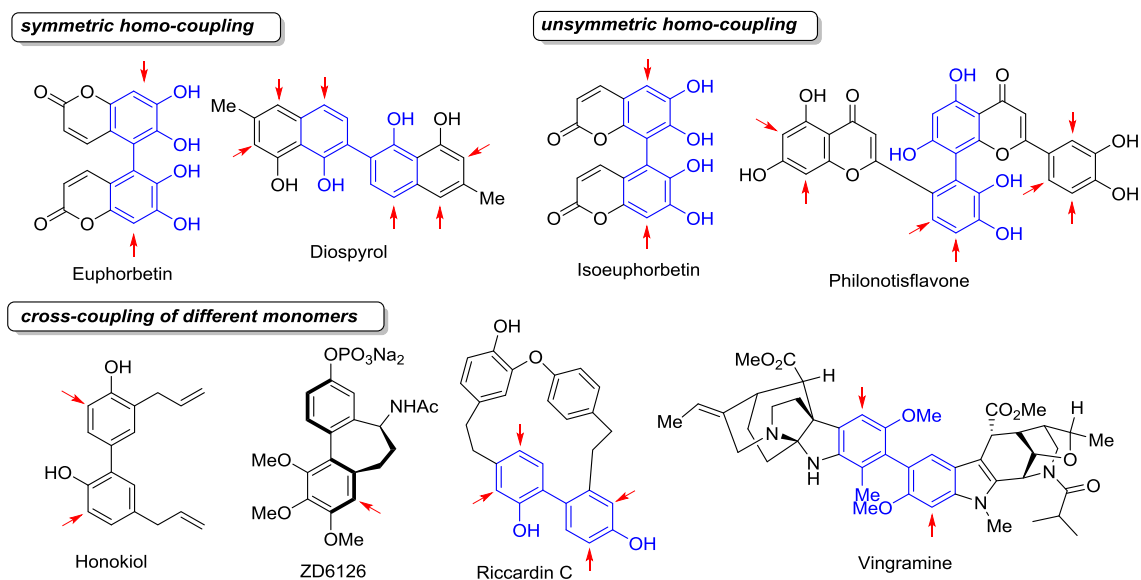
Figure 2.9 Natural Products Derived from Oxidative Phenolic Coupling

Figure 2.2 illustrates some of the difficulties underlying oxidative coupling of phenols. First, the oxidation potential is quite high, especially compared to substrates that are readily oxidized, such as 2-naphthol (**Figure 2.2a**).[38] Second, significant radical

---

(37) (a) Jiang, Q.; Sheng, W.; Tian, M.; Tang, J.; Guo, C. "Cobalt(II)–Porphyrin-Catalyzed Aerobic Oxidation: Oxidative Coupling of Phenols" *Eur. J. Org. Chem.* **2013**, 1861–1866. (b) Feng, J.; Yang, X.-B.; Liang, S.; Zhang, J.; Yu, X.-Q. "An efficient oxidative coupling method for synthesis of novel diastereomeric biaryl diols derived from estrone" *Tetrahedron Lett.* **2013**, *54*, 355–357.

(38) Bordwell, F. G.; Cheng, J. P. "Substituent Effects on the Stabilities of Phenoxyl Radicals and the Acidities of Phenoxyl Radical Cations" *J. Am. Chem. Soc.* **1991**, *113*, 1736–1743.

character is present at more than one position in a phenol radical (**Figure 2.2b**), leading to multiple products. Again, the situation is quite different for 2-naphthol, where the benzylic 1-radical is highly stabilized.[39] Also, the direct oxygenation of the aromatic ring to quinones and further adducts can become competitive. Methods to affect selective couplings are limited and **Figure 2.2c** outlines a typical example. Only the *ortho-ortho* isomer (*o-o*) can be produced high selectivity (85%), and the use of superstoichiometric di-*tert*-butyl peroxide at >120 °C is not ideal. Thus, our goal is to identify catalysts that allow regioselective homo-couplings and cross-couplings.
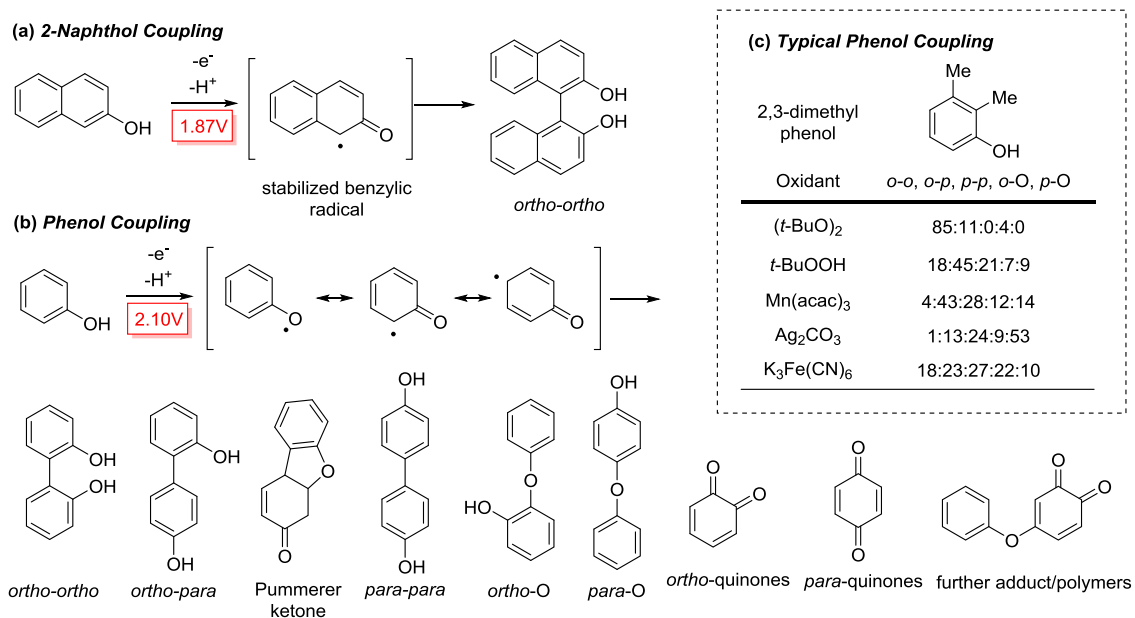
Figure 2.10 Oxidation Products of Phenols

(39) Kozlowski, M. C.; Morgan, B. J.; Linton, E. C.; "Total Synthesis of Chiral Biaryl Natural Products by Asymmetric Biaryl Coupling" *Chem. Soc. Rev.* **2009**, 38, 3193–3207.

We selected metals with sufficiently high redox potentials (Cr, Cu, Fe, Mn, Ru, V) to oxidize phenols and that, in turn, can be reoxidized by O_2.[40] Further, ligands that solubilize the metal, allow tuning of the redox potential, and are oxidatively stable were selected. Both the salen and salan scaffolds were studied (**Figure 2.3**). Due to the large number of variables, parallel microscale screening was used.[41]
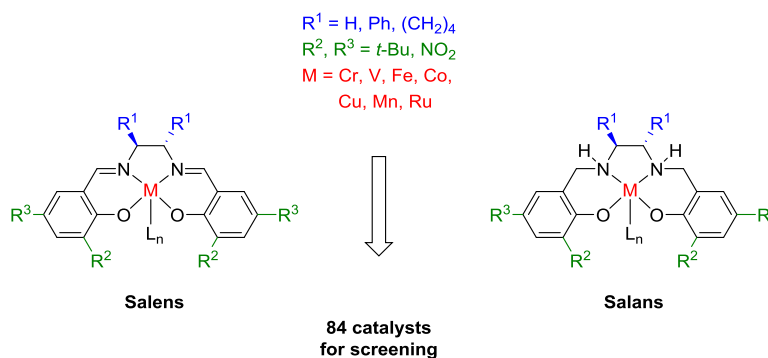
Figure 2.11 Catalysts for Exploration in Oxidative Chemistry

Screens by Dr. Trung Cao revealed that all the salens/salans were effective with O_2 for easily oxidized substrates such as 2-naphthol. Screening of phenol substrates that give rise to mixtures with conventional oxidants and optimization of the best leads identified catalysts for a remarkably broad range of couplings with control of *ortho-*

(40) (a) Hon, S.-W.; Li, C.-H.; Kuo, J.-H.; Barhate, N. B.; Liu, Y.-H.; Wang, Y.; Chen, C.-T. "Catalytic Asymmetric Coupling of 2-Naphthols by Chiral Tridentate Oxovanadium(IV) Complexes" *Org. Lett.* **2001**, *3,* 869–872. (b) Takizawa, S.; Rajesh, D.; Katayama, T.; Sasai, H. "One-Pot Preparation of Chiral Dinuclear Vanadium(V) Complex" *Synlett*, **2009**, *10*, 1667–1669.

(41) (a) Dreher, S. D.; Dormer, P. G.; Sandrock, D. L.; Molander, G. A. "Efficient Cross-Coupling of Secondary Alkyltrifluoroborates with Aryl Chlorides – Reaction Discovery Using Parallel Microscale Experimentation" *J. Am. Chem. Soc.* **2008***, 130,* 9257–9259. (b) Schmink, J. R.; Bellomo, A.; Berritt, S. "Scientist-Led High-Throughput Experimentation (HTE) and Its Utility in Academia and Industry" *Aldrichimica Acta* **2013**, *46*, 71–80.

ortho, *ortho-para* selectivity (**Figure 2.4**).[42] Notably, a rapid increase in complexity was observed in the *ortho-para* manifold (**Figure 2.4b**) giving rise to the Pummerer ketone, found in biologically active natural products such as the galanthamines and usnic acids.[43]
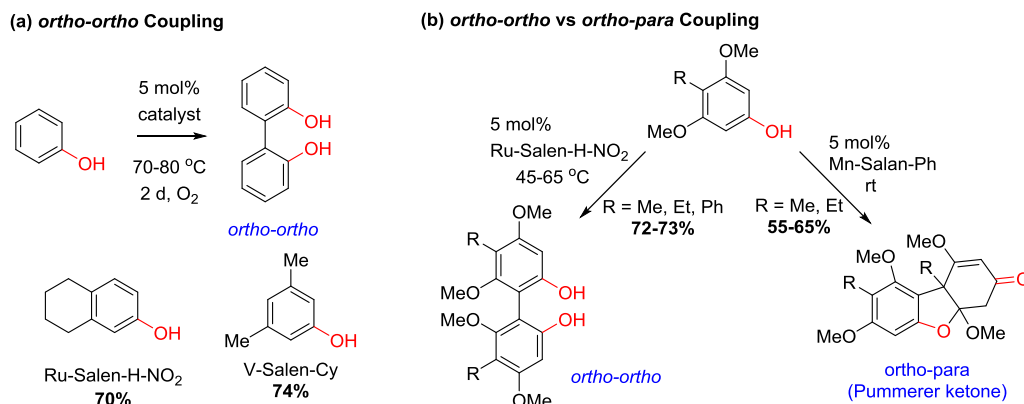
Figure 2.12 Regioselective Phenol Coupling

2.2. *ortho-ortho* Coupling by Ru-Salen Catalyst

In screening phenol substrates for the oxidative coupling, we have come across a number of limitations.[44] There were some substrates, for which the catalysts provided

(42) Lee, Y. E.; Cao, T.; Torruellas, C.; Kozlowski, M. C. "Selective Oxidative Homo- and Cross-Coupling of Phenols with Aerobic Catalysts" *J. Am. Chem. Soc.* **2014**, *136*, 6782–6785.

(43) (a) Pelish, H. E.; Westwood, N. J.; Feng, Y.; Kirchhausen, T.; Shair, M. D. "Use of Biomimetic Diversity-Oriented Synthesis to Discover Galanthamine-Like Molecules with Biological Properties beyond Those of the Natural Product" *J. Am. Chem. Soc.* **2001**, *123*, 6740–6741. (b) Cocchietto, M.; Skert, N.; Nimis, P. L.; Sava, G. "A review on usnic acid, an interesting natural compound" *Naturwissenschaften* **2002**, *89*, 137–146. (c) Elo, H.; Matikainen, J.; Pelttari, E. "Potent activity of the lichen antibiotic (+)-usnic acid against clinical isolates of vancomycin-resistant enterococci and methicillin-resistant Staphylococcus aureus" *Naturwissenschaften* **2007**, *94*, 465–468. (d) Arkley, V.; Dean, F. M.; Robertson, A.; Sidisunthorn, P. "451. Usnic Acid. Part XII. Pummerer's Ketone" *J. Chem. Soc.* **1956**, 2322–2328.

poor control over regioselectivity. With electron-withdrawing groups, phenol substrates were resistant to oxidation even when temperature was elevated. On the other hand, electron-rich phenols were easily oxidized to quinones or gave multiple products. For example, when 3,5-dimethoxy-4-*iso*-propylphenol (**2.1**, **Scheme 2.1**) was screened with our oxidation catalyst library, the hydroxyl hexadienone **2.2** and quinone **2.3** were observed as major products, whereas phenoxy hexadienone **2.4**, which could undergo further thermal rearrangement to generate the *ortho-ortho* coupling product, was found only as minor product. Furthermore, substrate **2.1** was found to oxidize spontaneously under air to give hydroxyl hexadienone **2.2** in 33% conversion after 30 days.

Scheme 2.9 Products from Catalyst Screening of 3,5-Dimethoxy-4-*iso*-propylphenol
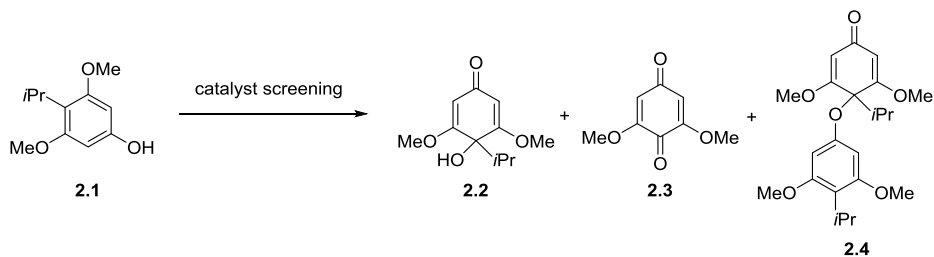
In screening other electron-rich phenol substrates (**Scheme 2.2**), the Ru-Salen-Ph catalyst was found to readily give coupling products for 3,4,5-trimethylphenol (**2.5**) and 2-*tert*-butyl-4,5-dimethylphenol (**2.7**). After 2 days reactions at 80 °C, this Ru catalyst gave 50% and 85% of the *ortho-ortho* coupling products, respectively.

---

(44) Cao, T. "Part B: The Regioselective Oxidative Coupling of Phenols" *Dissertation.* **2013**, University of Pennsylvania

Scheme 2.10 *ortho-ortho* Coupling Reaction

2.5 → **2.6** *ortho-ortho,* 50%

5 mol%
Rh-Salen-Ph, O₂

DCE, 80 °C, 2 d

2.7 → **2.8** *ortho-ortho,* 85%

5 mol%
Rh-Salen-Ph, O₂

DCE, 80 °C, 2 d
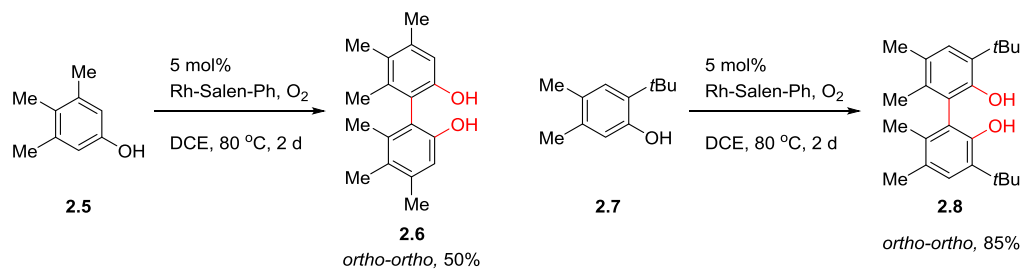
2.3. Regioselective Coupling of 2,3,5-Trimethylphenol

Interestingly, 2,3,5-trimethylphenol (**2.9**) gave all possible coupling products, *ortho-ortho*, *ortho-para* and *para-para* bisphenol, with the catalyst library in HTE (High Throughput Experimentation). These screening results are shown in **Figure 2.5**.

2.9

5 mol% catalyst
O₂

DCE
50 °C, 1 d

2.10 *ortho-ortho*

2.11 *ortho-para*

2.12 *para-para*
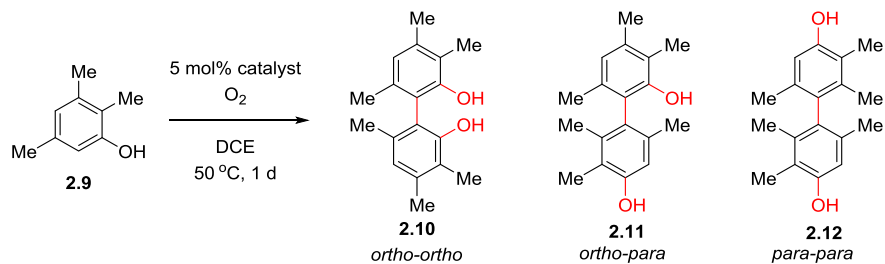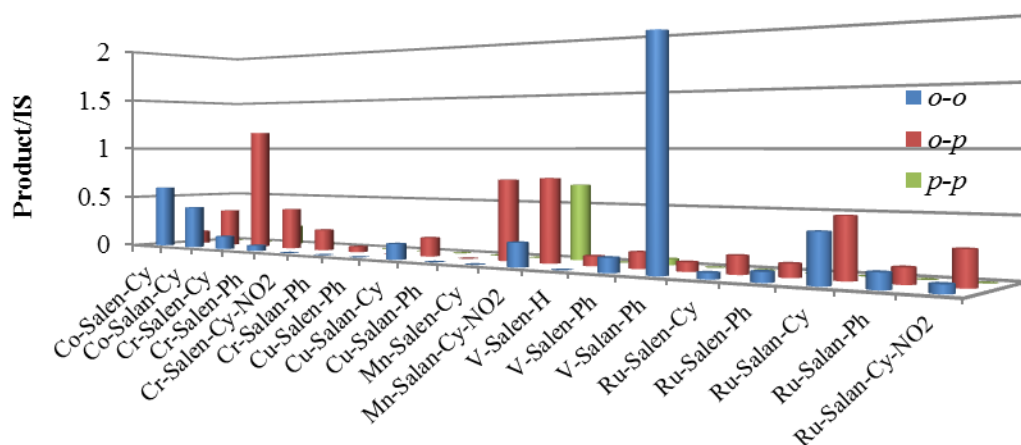
Figure 2.13 HTE Screening: Oxidative Coupling of 2,3,5-Trimethylphenol

However, the *ortho-ortho* product could not be reproduced on bench scale (0.2 mmol) with the V-Salen-Ph catalyst even though this lead gave the highest conversion in the HTE screen. Turning to the *ortho-para* coupling, a 12-membered expanded library focused on chromium catalysts [Cr-(Salen/Salan)-(H/Cy/Ph)-(tBu/NO$_2$)] was screened to find the best conversion. With Cr-Salen-H, a mixture of *ortho-para* and *para-para* coupling products was obtained (**Figure 2.6**). Only Cr-Salen-Cy gave the *ortho-para* coupling product exclusively, and the other Cr(III) complexes were either not as selective or as reactive.

49

(a) *Design of Cr-Salen(Salan) Catalyst*

Cr-Salen(Salan)-H-(NO$_2$)

Cr-Salen(Salan)-Cy-(NO$_2$)

Cr-Salen(Salan)-Ph-(NO$_2$)

(b) *Screening Results*

2.9

Cr-catalysts Screening

O$_2$

2.10
ortho-ortho

2.11
ortho-para

2.12
para-para
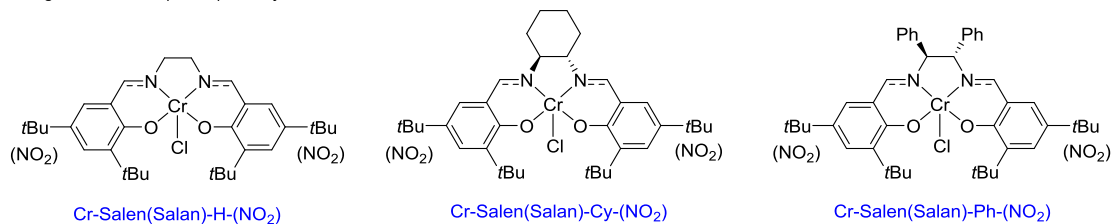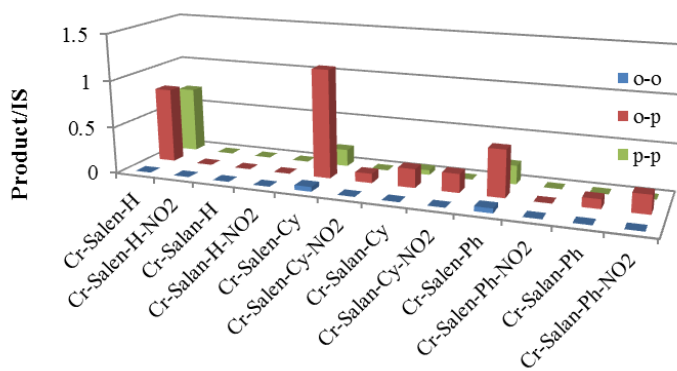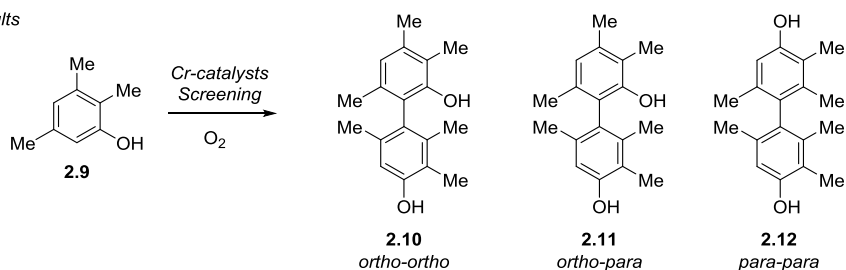
Figure 2.14 Screening of Cr-Salen/Salan Catalysts

A survey of different reaction conditions (temperature, concentration, catalyst loading etc.) led to optimal conditions (50 °C, 0.05 M in CH$_2$Cl$_2$, 5 mol%, **Scheme 2.3**). This reaction mixture was quenched after 2 days when the conversion reached to 55%; there was no side product, but starting material remained. If the reaction was permitted to proceed longer than 2 days, there was significant decomposition.

Scheme 2.11 Optimized Conditions for Homo-Coupling of 2,3,5-Trimethylphenol
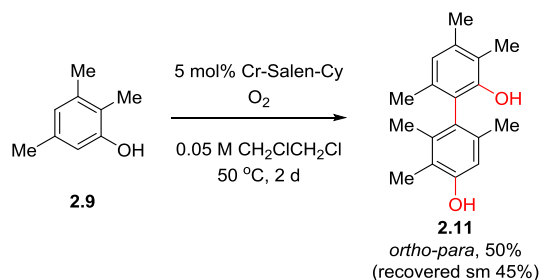
2.4. Expansion of Chromium (III) Catalyst to Oxidative Phenol Coupling

In the screening of several different substrates, the reactivity of Cr-Salen-Cy catalyst was unusual even though Cr salens have not been reported previously in oxidative phenolic coupling. For example, for 2-*tert*-butyl-5-methylphenol, both Cr salens and Ru salens gave the *para-para* product, whereas V-Salen-Cy gave the *ortho-ortho* product (not verified on bench scale).

The Cr-Salen-Cy gave *para-para* product for 2,5- and 2,6-disubstituted phenol. The *para-para* products were formed from the 2,5-disubstituted phenols at the less-hindered *para*-site flanked by a single substituent (**Scheme 2.4a**). When there was competition between *ortho-* and *para*-sites, steric factors appeared to control the selectivity with the Cr-Salen-Cy. Yields were modest (38-44%) due to low reactivity, a challenge to be addressed.

When both *ortho*-positions were blocked, the expected *para-para* product was obtained with Cr-Salen-Cy catalyst. For the more electron-rich phenol substrates,

overoxidation of the *para-para* bisphenol to the diphenoquinone dimer was seen. However, the diphenoquinone was reduced readily back to *para-para* bisphenol coupling product (**Scheme 2.4b**). Interestingly, even though 2,3,6-trimethylphenol has more electron density than 2,6-dimethylphenol, it showed less conversion for *para-para* coupling. This result again points to steric interactions dominating, in this case from the 3-methyl group adjacent to the coupling site.

Scheme 2.12 *para-para* Coupling with Cr-Salen-Cy
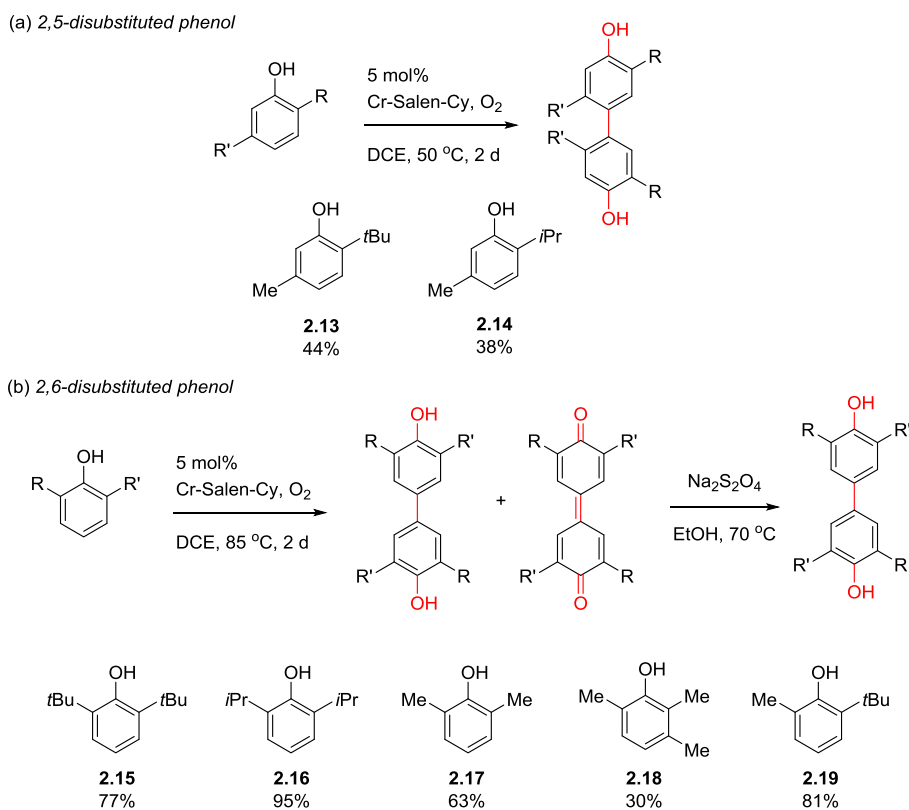
Kobayashi and coworkers have broadly studied and published Fe-Salen catalysts as effective in oxidative coupling of 2,6-disubstituted phenols using hydrogen peroxide as

a terminal oxidant.[45] For example, 2,6-di*iso*propyl- and 2,6-dimethoxyphenol yielded biphenyl dimer. The addition of small amount of pyridine with this catalyst suppressed the formation of the diphenoquinone byproduct.

On the other hand, Cr-Salen-Cy gave the *ortho-para* product not only for 2,3,5-trimethylphenol (**2.9**) but for 3,5-dimethylphenol (**2.20**) even though the conversion was very low (8%) (**Scheme 2.5**). The elements controlling selectivity for the *ortho-para* products with Cr-Salen-Cy are less clear with these substrates than for the *para-para* products. One possible model to explain this outcome is that one phenol partner is bound to the catalyst via the phenol, rendering the *ortho*-site more hindered such that reaction occurs at the *para*-site for this monomer. A second unbound substrate then approaches and reacts at the less hindered *ortho*-site.

Scheme 2.13 *ortho-para* Coupling with Cr-Salen-Cy

(a) *Examples of ortho-para Homo-coupling*

(b) *Tentative Binding mode*
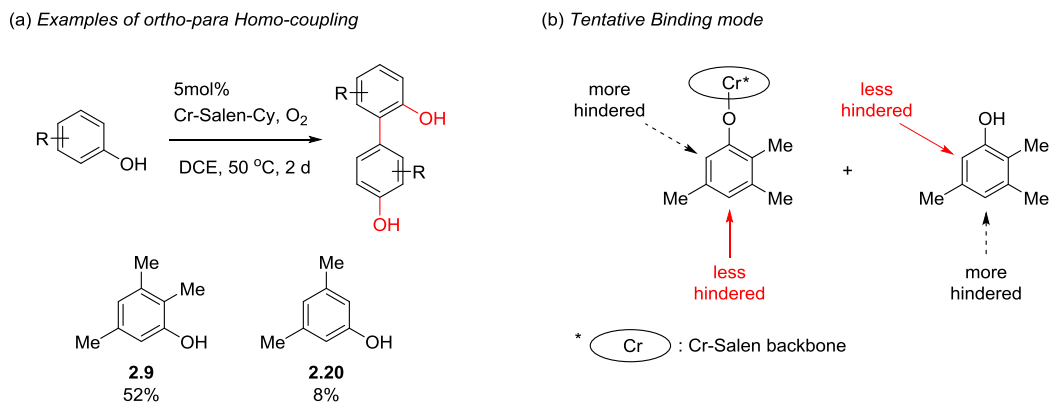
(45) Tonami, H.; Uyama, H.; Kobayashi, S.; Higashimura, H.; Oguchi, T. "Oxidative Polymerization of 2,6-Disubstituted Phenols Catalyzed by Iron-Salen Complex" *J. Macromol. Sci., Pure Appl. Chem.* **1999**, *A36*, 719-730.

2.5. Cross-Coupling Reaction of Phenols

At this point, the question of cross-coupling between different phenols arose, and this was regarded as a very difficult venture since any catalyst must promote the cross-coupling much faster than either of the corresponding homo-couplings.

Many groups attempted oxidative cross-coupling reaction between different two naphthols or phenols.[46] After Katsuki and coworkers discovered that ruthenium salen complexes could be used for aerobic oxidative homo-coupling of 2-naphthol,[47] they found bis-μ-hydroxo dimeric iron salan complex to be an excellent catalyst for not only for homo-coupling of 2-naphthols but also for the cross-coupling of 2-naphthols.[48] In 2014, the Waldvogel group revealed the electrochemical methods for cross-coupling of phenols.[14a] Employing electrolytes with a high capacity for hydrogen bonding, a direct electrolysis in an undivided cell provided mixed 2,2'-biphenols with high selectivity. And, more recently, Doron Pappo and coworkers developed an iron-catalyzed oxidative unsymmetrical biphenol coupling in 1,1,1,3,3,3-hexafluoro-2-propanol and postulated a

(46) For an alternate cross-coupling after our publication in 2014: (a) Elsler, B.; Schollmeyer, D.; Dyballa, K. M.; Franke, R.; Waldvogel, S. R. "Metal- and Reagent-Free Highly Selective Anodic Cross-Coupling Reaction of Phenols" *Angew. Chem., Int. Ed.* **2014**, *53*, 5210-5213. (b) Libman, A.; Shalit, H.; Vainer, Y.; Narute, S.; Kozuch, S.; Pappo, D. "Synthetic and Predictive Approach to Unsymmetrical Biphenols by Iron-Catalyzed Chelated Radical−Anion Oxidative Coupling" *J. Am. Chem. Soc.* **2015**, *137*, 11453-11460. (c) More, N. Y.; Jeganmohan, M. "Oxidative Cross-Coupling of Two Different Phenols: An Efficient Route to Unsymmetrical Biphenols" *Org. Lett.* **2015**, *17*, 3042−3045.

(47) Iried, R.; Masutani, K.; Katsuki, T. "Asymmetric Aerobic Oxidative Coupling of 2-Naphthol Derivatives Catalyzed by Photo-Activated Chiral (NO)Ru(II)-Salen Complex" *Synlett* **2000**, 1433-1436.

(48) (a) Egami, H.; Matsumoto, K.; Oguma, T.; Kunisu, T.; Katsuki, T. "Enantioenriched Synthesis of C-1-Symmetric Binols: Iron-Catalyzed Cross-Coupling of 2-Naphthols and Some Mechanistic Insight" *J. Am. Chem. Soc.* **2010**, *132*, 13633-13635. (b) Matsumoto, K.; Egami, H.; Oguma, T.; Katsuki, T. "What Factors Influence the Catalytic Activity of Iron-Salan Complexes for Aerobic Oxidative Coupling of 2-Naphthols?" *Chem. Commun.* **2012**, *48*, 5823-5825.

chelated radical−anion coupling mechanism.[14b] They determined oxidation potential (E_{ox}) and the theoretical global nucleophilicity (N) parameters of various phenols to support their mechanism.

The intriguing finding that the Cr-Salen-Cy catalyst permits coupling at two different sites of a monomer stimulated us to study its behavior with different monomers especially if were possible to selectively coordinate one monomer to the catalyst in line with our putative model (**Scheme 2.5**). Initial studies showed a significant amount of cross-coupling when two different phenol substrates were employed in a 1:1 ratio (**Scheme 2.6**). More excitingly, as we switched to different coupling partners, the homo-coupling reactions were suppressed.

<div align="center">Scheme 2.14 Initial Trials of Cross-Coupling Reaction</div>
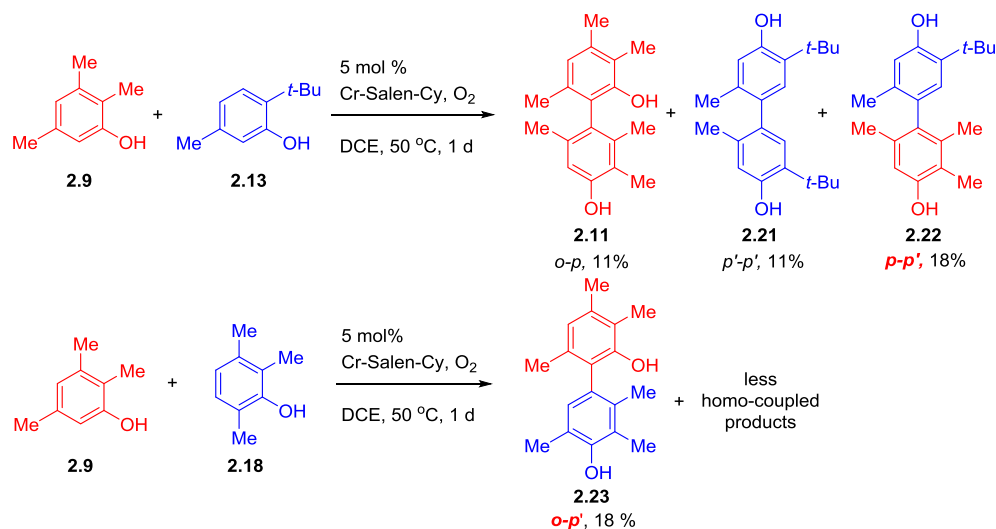
Changing the coupling partner to 2,6-di-*tert*-butylphenol (**2.15**) gave more cross-coupling product with higher selectivity. With 2,3,5-trimethylphenol (**2.9**), 2,6-di-*tert*-

butylphenol gave 50% of the *para-ortho* coupling product after 1 day at 50 °C. In a similar fashion, several other phenol substrates gave cross-coupling product selectively with moderate yield (**Scheme 2.7**). The same reaction conditions for the homo-coupling (50 °C, 0.05 M, 5 mol%) were used for the cross-coupling reaction. There was no side product, but the both phenol substrates remained unreacted. Reaction times longer than 2 days caused decomposition of both the starting phenols and the product.

With 2,6-di-*tert*-butylphenol (**2.15**), coupling partners with open *ortho-* and *para-* sites underwent reaction at the less sterically hindered position in a similar fashion in homo-coupling (**Scheme 2.7**). For example, 2,3,5-trisubstituted phenols and 3,5-disubstituted phenols coupled in the *ortho* position and gave *ortho-para* product (**2.24**, **2.25**), whereas 2,5-disubstituted phenols coupled in *para* position to give the corresponding *para-para* bisphenols (**2.26**-**2.29**).

Scheme 2.15 Cross-Coupling Reaction with 2,6-Di-*tert*-butylphenol

(a) *ortho-para Cross-Coupling*

2.24
55% *o-p*
(89%)[a]

2.25
56% *o-p*
(91%)[a]

(b) *para-para Cross-Coupling*

2.26
57% *p-p*
(90%)[a]

2.27
44% *p-p*
(95%)[a]

2.28
45% *p-p*
(94%)[a]

2.29
20% *p-p*

2.30
25% *p-p*

[a]Parenthetical yields: based on recovered substrate.
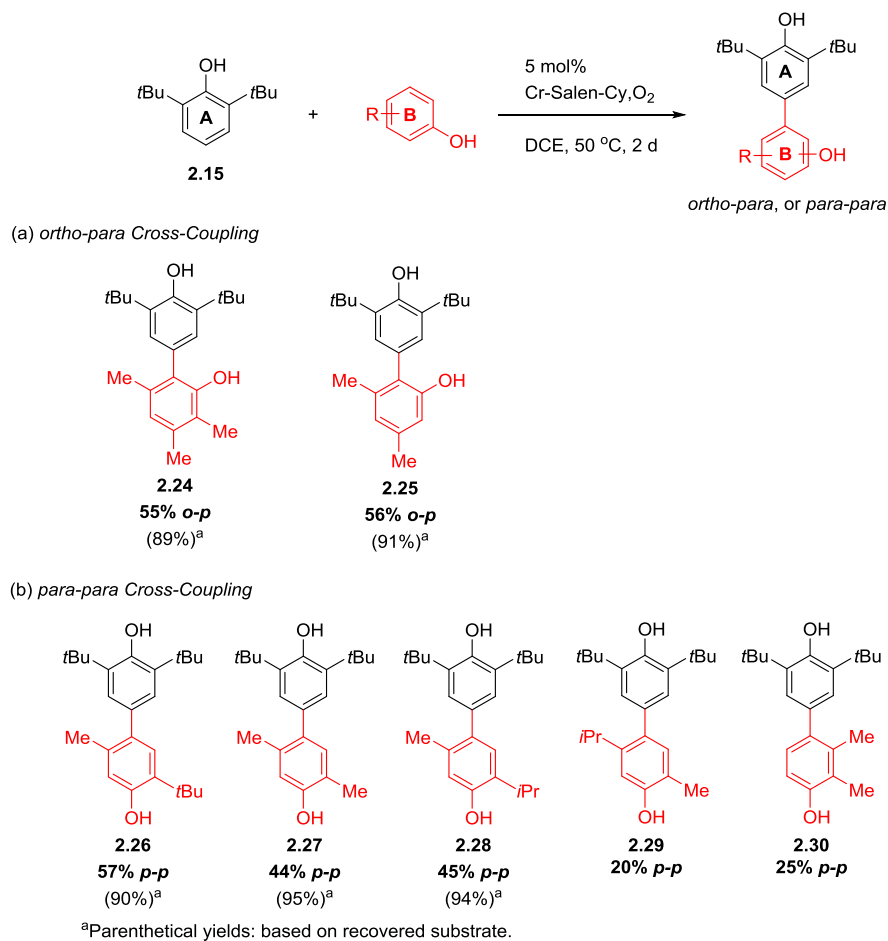
Additional screening of 2,6-disubstituted phenols revealed similar trends. 2,6-Dimethylphenol (**2.31** and **2.32**), 2,6-di*iso*propylphenol (**2.33**), and even unsymmetrical 2-methyl-6-*tert*-butylphenol (**2.34**–**2.37**) coupled in same way with various partners (**Scheme 2.8**). Notably, 2-methyl-6-*tert*-butylphenol gave high conversion, up to 77% at 70 °C; the other substrates either decomposed or coupled twice to form trimers with 2,6-di-*tert*-butylphenol at this temperature.

Scheme 2.16 Cross-Coupling Reaction with 2,6-Disubstituted Phenols

2.31	2.32	2.33	2.34	2.35	2.36	2.37
51%, *o-p*	40%, *p-p*	47%, *p-p*	77%, *p-p*	74%, *p-p*	52%, *p-p*	30%, *p-p*
(89%)[a]		(90%)[a]	(at 70 °C)	(at 70 °C)	(at 70 °C)	(at 70 °C)

[a]Parenthetical yields: based on recovered substrate.
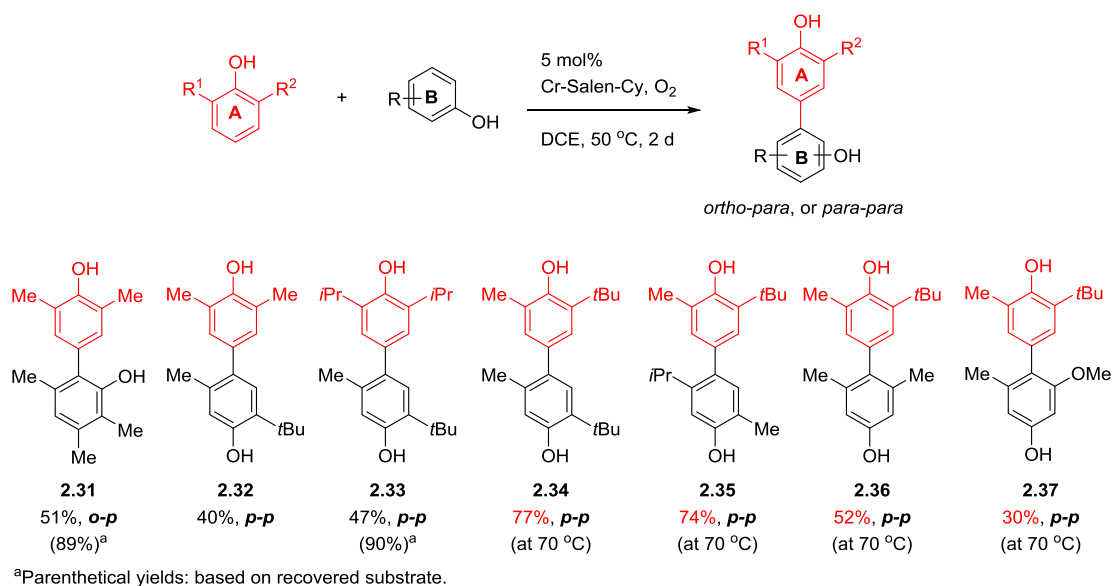
For less reactive substrates, coupling could be induced at higher temperature (70 °C). However, the resultant dimeric product was more reactive in these cases than the original monomer leading to trimers (**Scheme 2.9**) with negligible amounts of dimer (less than 5%) in these cases. The second cross-coupling proceeded successively, and trimers were observed in fair yield (44–46%) along with unreacted starting materials after 2 days.

Scheme 2.17 Trimer Formation in Cross-Coupling

2.15

2.38
46%

2.39
44%

2.40
45%
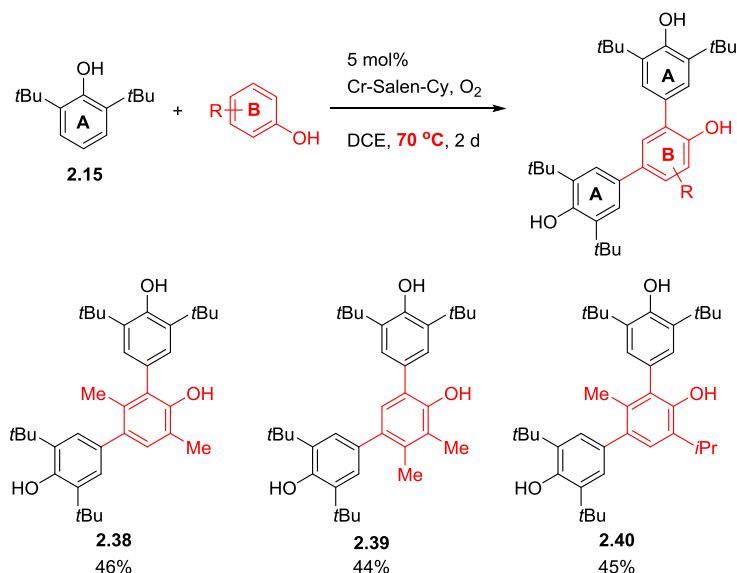
There were some substrates where both dimer and trimer were observed indicating that the dimer product was not more reactive than the monomers. For example, *para*-alkylphenol gave a mixture of dimer and trimer with 2,6-disubsituted phenols. Symmetric resorcinol also gave a mixture (**Table 2.1**). It was reasoned that if the reactivities of dimer and monomer were similar to each other, both products were observable. Since these formations of dimer and trimer were competitive, reactions were uncontrollable. Repeated trials to influence the outcome by adjusting the ratio between two products did not succeed. For example, slow addition of 2,6-di-*tert*-butylphenol during the reaction course did not suppress trimer formation, and excess addition of 2,6-di-*tert*-butylphenol also did not expedite trimer formation; in both case, dimer and trimer were observed forming at similar rates.

Table 2.5 Dimer vs. Trimer

Entry	Phenol B	Dimer	Trimer	A	B
1	**2.41** (Me)	42%	53%	-	-
2	**2.42** (iPr)	35%	33%	9% A=A*	29%
3	**2.43** (tBu)	31%	14%	29% A=A*	26%
4	**2.44** (Me, Me)	38%	29%	8% A=A*	-

*A=A diphenoquinone

2,6-Disubstituted phenols (**A**, **Scheme 2.10**) were combined with phenols with only one open *ortho*-coupling site (**B**, **Scheme 2.10**) to render the *ortho-para* coupling products stable and prevent trimer formation by limiting the outcome to three coupling products: two homo-coupling products and one cross-coupling product (**Scheme 2.10**). The yields were excellent (up to 88%) due to the stability of the coupled product. However, in our system, there were examples that was inconsistent with Pappo's postulation.[14b] For example, in product **2.46**, 2,4-dimehtylphenol is both more nucleophilic and more oxidizable than 2,6-di-*tert*-butylphenol.

A range of naphthols was also effective in dimer formation with 2,6-disubstituted phenol providing products in good yield. Notably, even though there were two identical

coupling sites, 2,7-dihydroxynaphthalene did not form any trimer, but only dimer was observed with good yield (**2.54**, 82%).

Scheme 2.18 Cross-Coupling Reaction

(a) *ortho-para Cross-Coupling*

(b) *Cross-Coupling with 2-Naphthol*
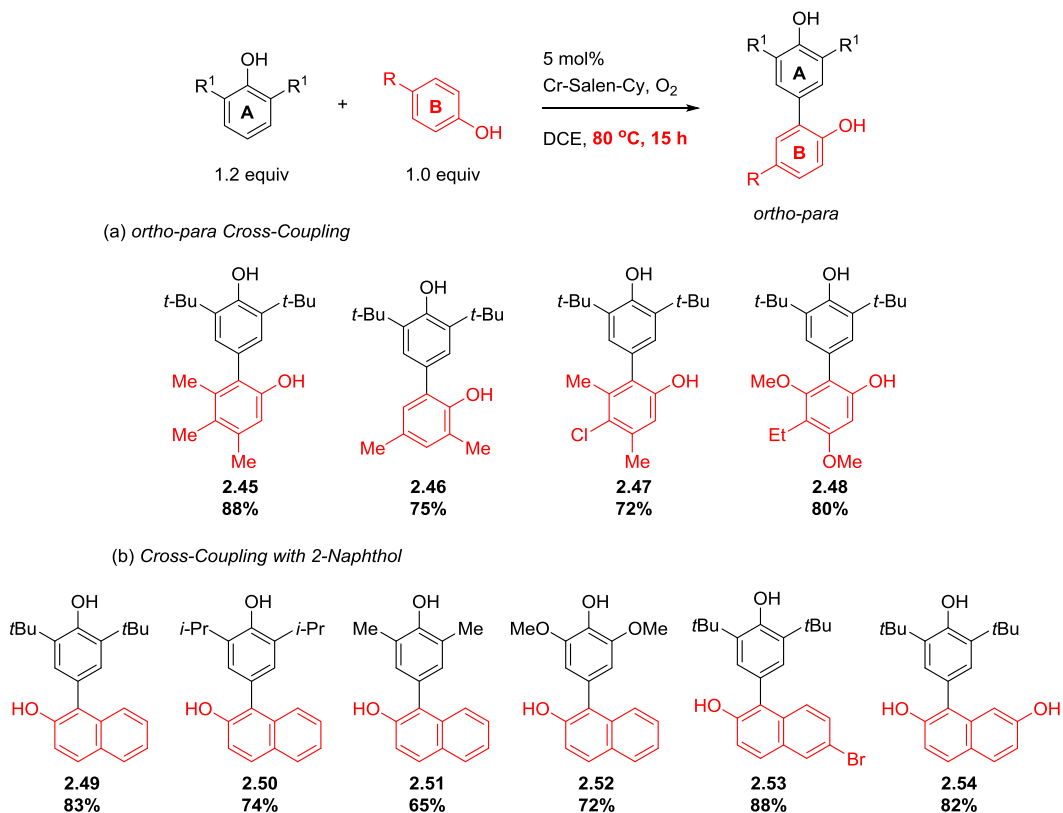
On the other hand, there were many challenging substrates in the cross-coupling reaction (**Scheme 2.11**). Electronic effects of phenol B played an important role in the reactivity of the cross-coupling. For example, amines (**2.55** and **2.57**) or vinyl groups (**2.58**) were not compatible with the cross-coupling reaction condition; no starting materials remained after overnight reaction and only decomposition was observed. 1-Naphthols (**2.63** and **2.64**) also failed to couple with 2,6-di-*tert*-butylphenol due to the oxygenation of substrates to naphthoquinones.

On the other hand, electron-withdrawing groups, such as formyl group (**2.59**), halide groups (**2.60–2.62**), or ester group (**2.65**), suppressed cross-coupling reaction with 2,6-di-*tert*-butylphenol. Only the diphenoquinone of 2,6-di-*tert*-butylphenol was observed along with the starting phenol substrates.

Unlike phenols with open sites in *ortho* position, phenols with open sites in the *para* position were not as prone to oxidative coupling reaction with the chromium catalyst. After three days reaction at 80 °C, only 10% conversion was observed between 2,6-di-*tert*-butylphenol (**2.15**) and 2,6-dimethylphenol (**2.17**, **Scheme 2.11**). Again, when the cross-coupling did not happen for the substrates **2.66** and **2.67**, the diphenoquinone of 2,6-di-*tert*-butylphenol and both unreacted substrates were observed.

Scheme 2.19 Challenging Substrates in Cross-Coupling
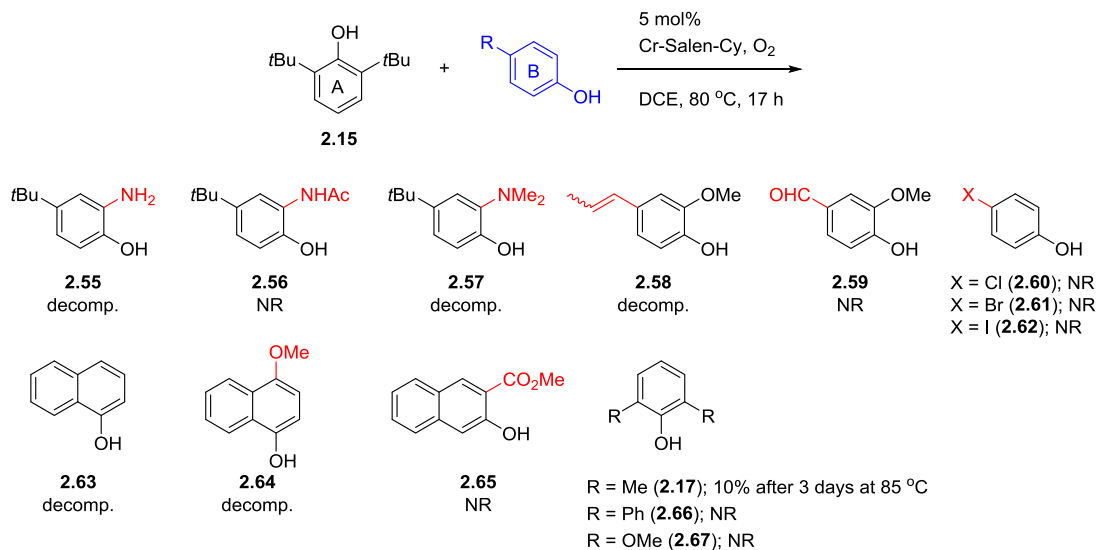
The evidence from the present study that the scope of the cross-coupling reaction is different from that of the homo-coupling is noteworthy. For example, 2,6-disubstituted

phenol which also couples itself to give homo-coupling product is essential in the cross-coupling, whereas the coupling partner which cannot undergo a homo-coupling reaction under the present aerobic oxidation conditions, can undergo a cross-coupling reaction.

2.6. Intramolecular Coupling of Phenols

Tyrosine derivatives (**Figure 2.6**) are another challenging substrate class. Cross-linked tyrosine residues are common in biologically active cyclic peptides, including the cycloisodityrosine-containing bouvardins, [49] RA-series compounds, [50] and the neurotensin antagonist RP-66453, [51] which contains a pulcherosine moiety. The functionalized tyrosine derivatives in these complex peptides are believed to be of critical importance to their three dimensional structure and biological activity. Even though an oxygen-driven process has been implicated in the biosynthesis of these natural products, no successful oxidative couplings have been reported. Instead, synthetic routes to these materials have relied on Suzuki and related couplings[52] which require additional functionalization. A

(49) Boger, D. L.; Patane, M. A.; Zhou, J. C. "Total Synthesis of Bouvardin, *O*-Methylbouvardin, and *O*-Methyl-N^9-desmethylbouvardin" *J. Am. Chem. Soc.* **1994**, *116*, 8544-8556.

(50) Bigot, A.; Dau, M. E. T. H.; Zhu, J. "Total Synthesis of an Antitumor Agent RA-VII via an Efficient Preparation of Cycloisodityrosine" *J. Org. Chem.* **1999**, *64*, 6283-6296.

(51) (a) Bios-Choussy, M.; Cristau, P.; Zhu, J. "Total Synthesis of an Atropdiastereomer of RP-66453 and Determination of Its Absolute Configuration" *Angew. Chem., Int. Ed.* **2003**, *42*, 4238-4241. (b) Krenitsky, P. J.; Boger, D. L. "Synthesis of the (*S,S,S*)-diastereomer of the 15-membered biaryl ring system of RP 66453" *Tetrahedron Lett.* **2003**, *44*, 4019-4022.

(52) Decicco, C. P.; Song, Y.; Evans, D. A. "Intramolecular *O*-Arylation of Phenols with Phenylboronic Acids: Application to the Synthesis of Macrocyclic Metalloproteinase Inhibitors" *Org. Lett.* **2001**, *3*, 1029-1032.

direct route to such materials would increase efficiency and permit facile synthesis of a broader array of analogs for study.
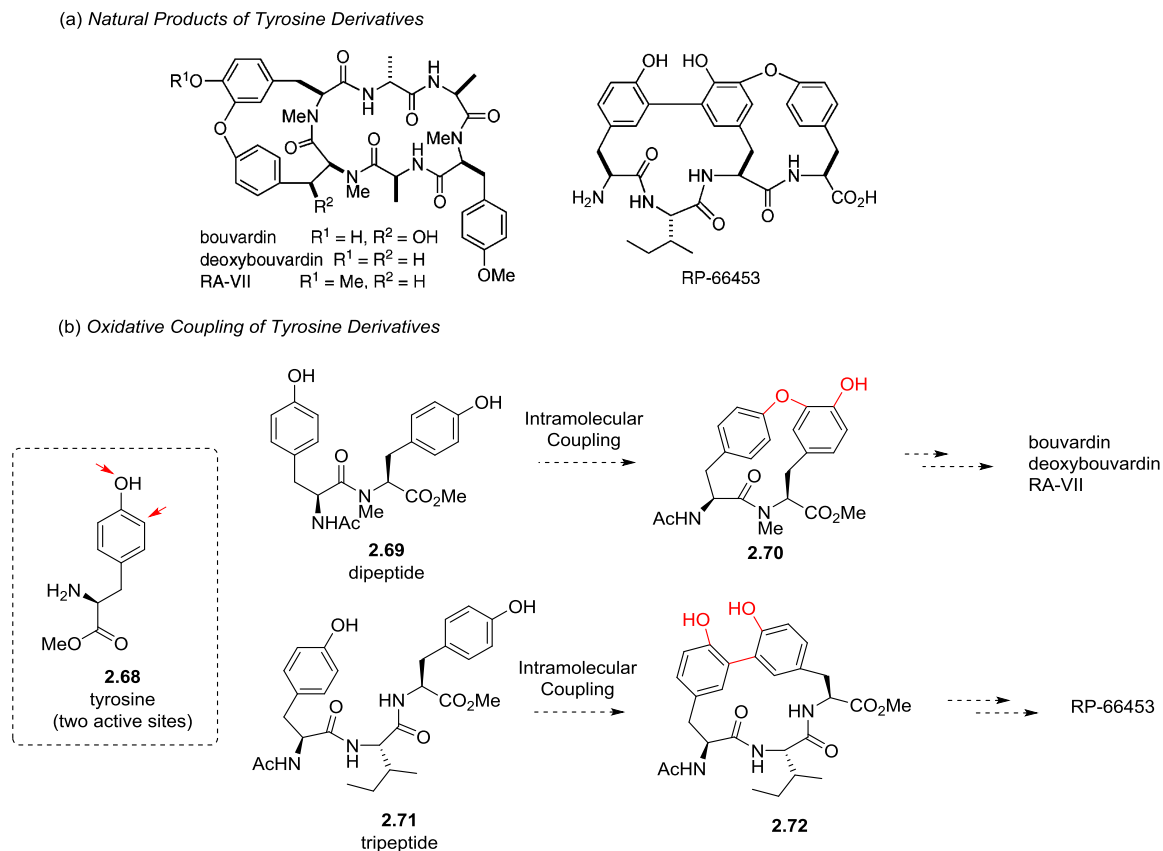
Figure 2.15 Intramolecular Oxidative Coupling in Di- and Tripeptide

Dityrosine (**2.69**) and trityrosine (**2.71**) obtained by peptide coupling between tyrosine methyl ester and *N*-protected tyrosine[53] failed to give any type of coupling product with our catalyst library. Under oxygen atmosphere, these substrates were too stable and no conversion was observed. In collaboration with Allison Metz, we pursued

---

(53) Ray, S.; Das, A. K.; Banerjee, A. "Smart oligopeptide gels: *in situ* formation and stabilization of gold andsilver nanoparticles within supramolecular organogel networks" *Chem.Commun.* **2006**, *26*, 2816-2818.

further screening using several oxidants and catalysts, but only side products were observed. With *tert*-butyl hydroperoxide, **V6** catalyst from **Chapter 1** produced a *tert*-butyl peroxy group adduct and a dimer of starting material via intermolecular coupling; there was no intramolecular coupling product found (**Scheme 2.12**).

Scheme 2.20 Oxidative Coupling of Dityrosine
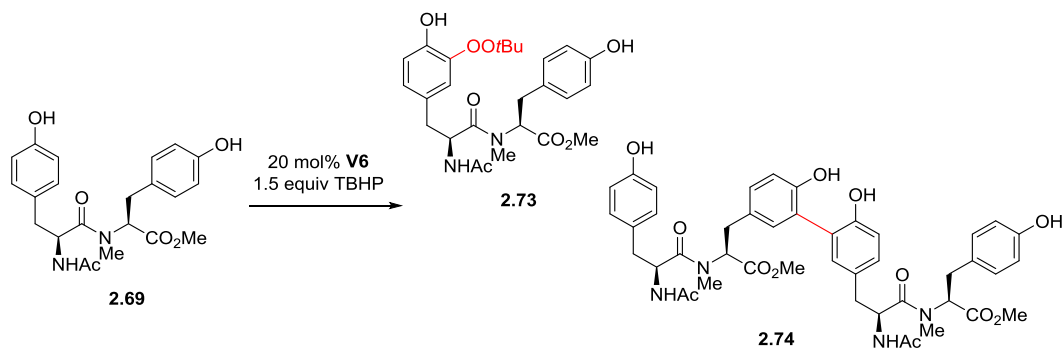
To simplify this coupling, different phenols linked with simple alkyl tethers were synthesized. Staring from 3-hydroxybenzaldehyde (**2.75**) and *m*-anisaldehyde (**2.79**) respectively, multi-step syntheses led to the substrates for the coupling reaction (**Scheme 2.13**). [54] After each benzaldehyde was linked through alkyl chains by the conventional coupling reactions, substrates were further designed to incorporate *tert*-butyl groups in order to increase electron density on the phenyl ring and thereby enhance reactivity.

---

(54) Vonlanthen, D.; Rotzler, J.; Neuburger, M.; Mayor, M. "Synthesis of Rotationally Restricted and Modular Biphenyl Building Blocks" *Eur. J. Org. Chem.* **2010,** 120–133.

Scheme 2.21 Syntheses of Bisphenols for Intramolecular Coupling
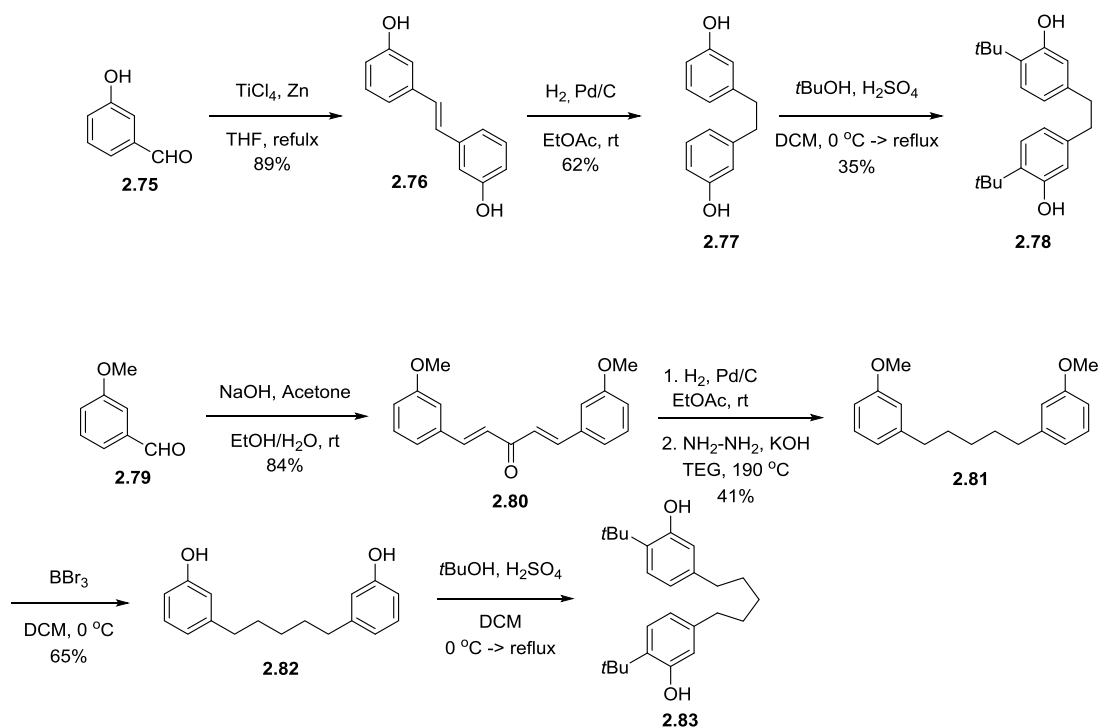
Intramolecular coupling reactions of the synthesized bisphenols were attempted by the catalyst screening. Nevertheless, oxidative coupling was not feasible except with a few substrates which gave small amounts of *ortho-para* products. For example, with Co-Salen-H catalyst, substrate **2.77** gave *ortho-para* product and the Cr-Salen-Cy catalyst yielded *ortho-para* coupling product for the substrate **2.78** (**Scheme 2.14**). Even though we were unable to obtain good conversion in any intramolecular couplings, the result from these substrates were intriguing in that coupling occurred at the more hindered *ortho*-position.

Scheme 2.22 Intramolecular Coupling of Bisphenol
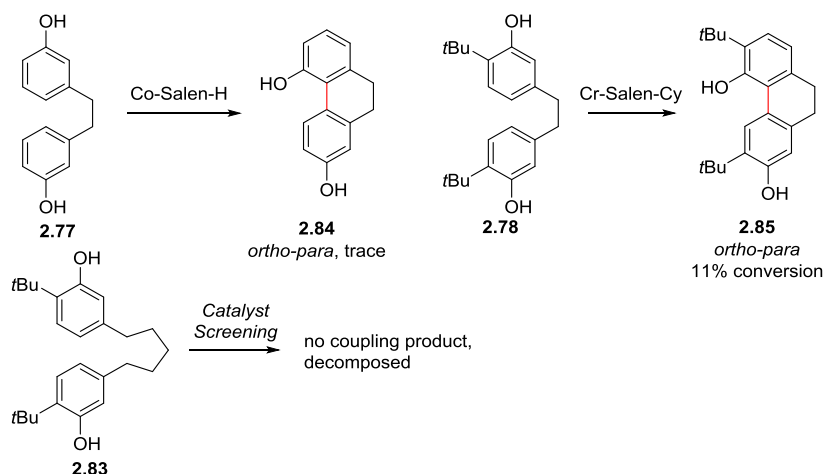
2.7. Mechanism Studies

2.7.1. Radical Inhibitors

In order for the cross-coupling reaction to occur, any catalyst must promote the cross-coupling much faster than either of the corresponding homo-couplings. It was discovered that Cr-Salen-Cy was broadly effective for the cross-coupling of phenols, not only for the homo-coupling, and many substrates were well tolerated. Even though Cr salens have been known for decades,[55] there have been no prior reports in phenol coupling. In order to develop this method further, especially with respect to less electron rich substrates, there is an urgent need to understand this mechanism.

(55) McGarrigle, E. M.; Gilheany, D. G. "Chromium− and Manganese−salen Promoted Epoxidation of Alkenes" *Chem. Rev.* **2005**, *105*, 1563–1602.

Control experiments of the cross-coupling reaction between 2,6-di-*tert*-butylphenol (**2.15**) and 3,4,5-trimethylphenol (**2.5**) revealed an excellent yield (88%) of product **2.45** within 3 hours. The results from **Table 2.2** clearly show that not only the Cr-Salen-Cy catalyst, but oxygen and heat are necessary for the cross-coupling reaction to proceed.

Table 2.6 Control Experiments in the Cross-Coupling

Entry	Condition	Conversion
1	5 mol% Cr-Salen-Cy, O_2	100%
2	100 mol% Cr-Salen-Cy, N_2	7.4%
3	O_2 only	NR
4	TEMPO, O_2	NR
5	5 mol% Cr-Salen-Cy, O_2, rt	NR
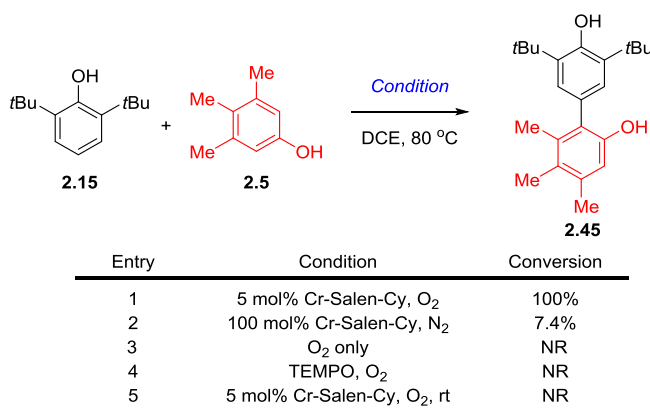
In order to determine whether this cross-coupling reaction involved a radical mechanism, several radical scavengers (diphenylethylene, 2,2,6,6-tetramethyl-piperidinyloxy, butylated hydroxytoluene and galvinoxyl) were tested (**Table 2.3**). One half equivalent radical scavenger was added to each cross-coupling reaction. Only TEMPO (2,2,6,6-tetramethylpiperidinyloxyl) was found to inhibit the cross-coupling pathway, reducing the yield by about half compared to the control reaction. Instead, TEMPO promoted the formation of diphenoquinone up to 42%. Doubling the amount of TEMPO suppressed the reaction to approximately same extent as half equivalent did, but

did cause the formation of more diphenoquinone (up to 62%). The other radical scavengers had no effect.

Table 2.7 Radical Scavengers in Cross-Coupling
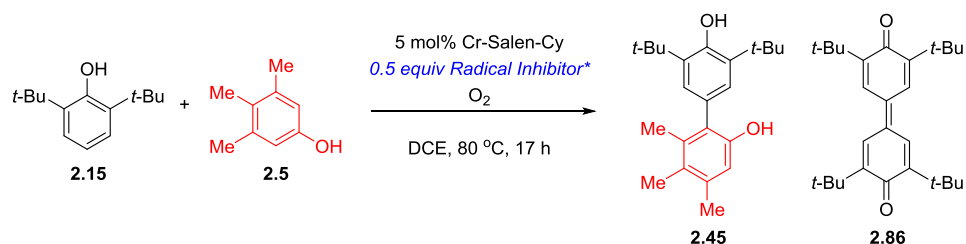
Entry	Radical Inhibitor	^{1}H NMR Yield (**2.45**, **2.86**)
1	None	78%, 0%
2	Diphenylethylene	80%, 0%
3	TEMPO	35%, 42%
4	100 mol% TEMPO	38%, 62%
5	BHT	71%, 0%
6	Galvinoxyl	74%, 0%
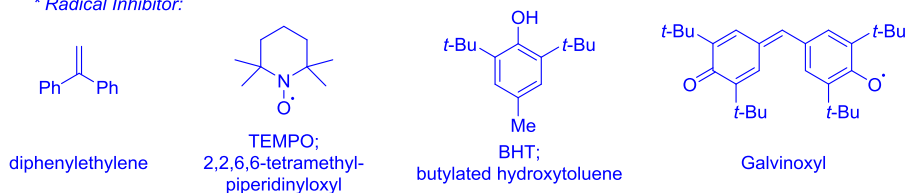
On the other hand, experiments with radical scavengers in the homo-coupling reactions did reveal perturbations with more than one radical inhibitor (highlighted with blue), which is strongly supportive of radical character in the homo-couplings (**Table 2.4**). It was noteworthy that TEMPO functioned as an oxidant for the homo-coupling reaction of the substrate **2.15**. It gave more *para-para* coupling product by more than double. This was consistent with the result in cross-coupling reaction in **Table 2.3** and revealed that catalyzed cross-coupling reaction was more rapid than the homo-coupling reaction.

Table 2.8 Radical Scavengers in Homo-Coupling Reactions

		2.7 Ru-Salen-Ph; *ortho-ortho*	2.15 Cr-Salen-Cy; *para-para*	2.13 Cr-Salen-Cy; *para-para*	2.87 Cr-Salen-H; *Pummerer ketone, ortho-ortho*
Entry	Radical Inhibitor		^{1}H NMR Yield		PK, *o-o*
1	None	74%	40%	55%	13%, 19%
2	Diphenylethylene	76%	43%	54%	12%, 11%
3	TEMPO	43%	100%	NR	10%, 0%
4	BHT	37%	19%	12%	0%, 0%
5	Galvinoxyl	73%	23%	35%	7%, 0%
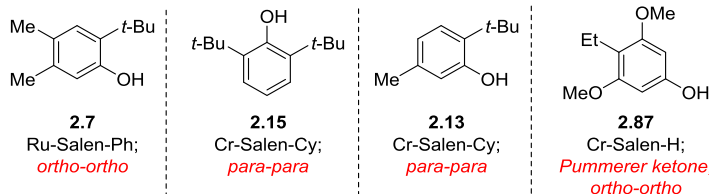
2.7.2. UV-Vis Spectroscopy

UV-Vis spectroscopy was used to monitor oxidation state change of the metal complexes (**Figure 2.8**). The Ru catalyst did not change upon treatment with TEMPO under the reaction conditions as judged by UV-Vis. For the Cr catalyst, a Cr(III) complex was found to be present at the onset (see crystal structure below) with a band at 430 nm and was ineffective in the coupling without O_2. Spectroscopic studies revealed that O_2 at high temperatures caused the disappearance of the 430 nm band and generation of a new species with a band at 480 nm, which is consistent with a Cr(IV).[56] This species did not form in the presence of TEMPO, which accounts for the reaction inhibition by TEMPO as shown in **Table 2.3**.

---

(56) Brown, C.;Krzystek, J.; Achey, R; Lita, A.; Fu, R.; Meulenberg, R. W.; Polinski, M.; Peek, N.; Wang, Y.; van de Burgt, L. J.; Profeta, Jr. S.; Stiegman, A. E.; Scott, S. L. "Mechanism of Initiation in the Phillips Ethylene Polymerization Catalyst: Redox Processes Leading to the Active Site" *ACS. Catal.* **2015**, *5*, 5574–5583.

(a) *Ru-Salen-Ph Oxidation State Change:*

Ru-Salen-Ph, O$_2$, rt

Ru-Salen-Ph, O$_2$, 80 ^{o}C

Ru-Salen-Ph, O$_2$, 80 ^{o}C, TEMPO
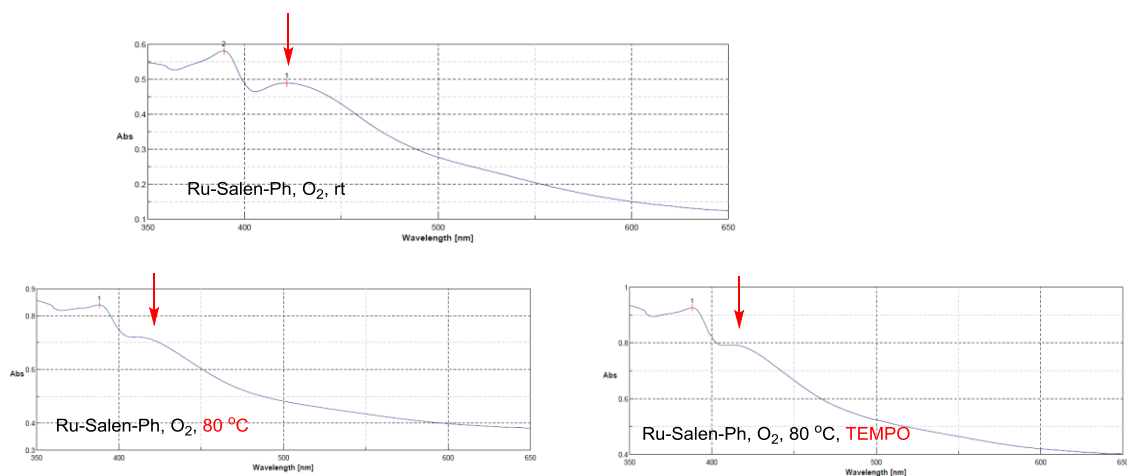
(b) *Cr-Salen-Cy Oxidation State Change:*

Cr-Salen-Cy, O$_2$, rt

Cr-Salen-Cy, O$_2$, 80 ^{o}C

Cr-Salen-Cy, O$_2$, 80 ^{o}C, TEMPO
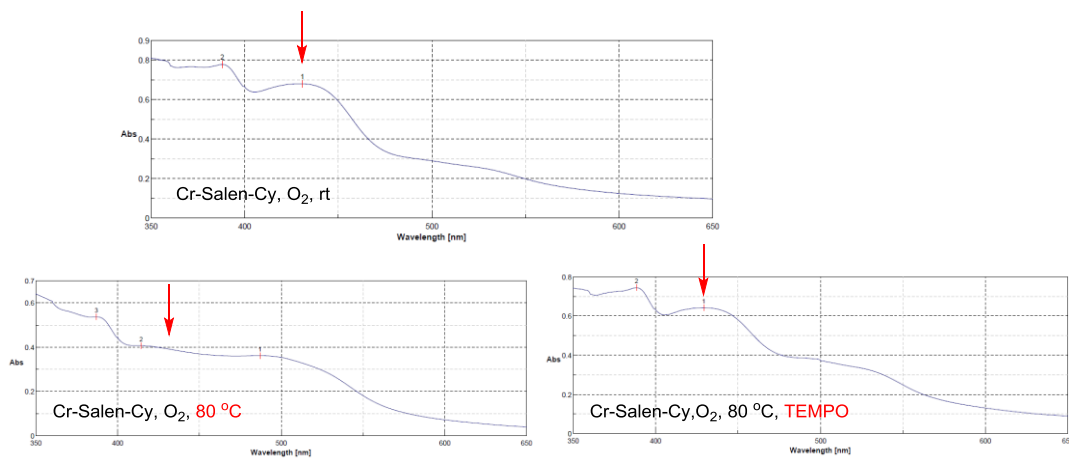
Figure 2.16 UV-Vis Spectra of Ru-Salen-Ph vs. Cr-Salen-Cy

71

2.7.3. Reactivity of Cr(III) Complexes

The Jacobsen group has reported the Cr-Salen-Cy complex as a highly effective catalyst for enantioselective epoxide ring opening reactions.[57] They also discovered it induced hetero Diels-Alder reaction with high e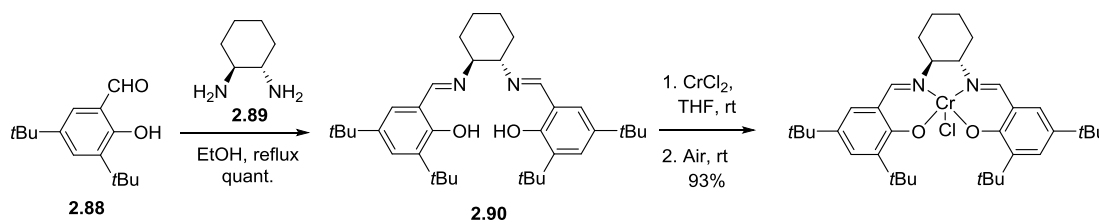nantioselectivity.[58] The chromium(III) salen complex was prepared from commercially available salicylaldehyde **2.88** (**Scheme 2.15**). Schiff base formation with *trans*-1,2-diaminocyclohexane (**2.89**) followed by metal ion complexation and oxidation afforded the Cr(III) complex in good yield.

Scheme 2.23 Representative Scheme for Cr-Salen-Cy Synthesis

The same procedure with different salicylaldehydes and diamines produced various Cr(III) salen complexes.[10, 59] Further reduction of imine moiety using LiAlH$_4$ gave the Cr(III) salan complexes. Counterion metatheses were accomplished with AgSbF$_6$ and AgBF$_4$ in *tert*-butyl methyl ether (TBME) to yield the corresponding hexafluoroantimonate and tetrafluoroborate complexes, respectively. With these Cr(III)

(57) Martinez, L. E.; Leighton, J. L.; Carsten, D. H.; Jacobsen, E. N. "Highly Enantioselective Ring Opening of Epoxides Catalyzed by (salen)Cr(III) Complexes" *J. Am. Chem. Soc.* **1995***, 117*, 5897-589.

(58) Schaus, S. E.; Brånalt, J. E.; Jacobsen, E. N. "Asymmetric Hetero-Diels–Alder Reactions Catalyzed by Chiral (salen)Chromium(III) Complexes" *J. Org. Chem.* **1998***, 63*, 403-405.

(59) Cozzi, P. G. "Metal–Salen Schiff base complexes in catalysis: practical aspects" *Chem. Soc. Rev.* **2004***, 33,* 410–421.

complexes synthesized, one of the challenging cross-coupling reactions was tested (**Table 2.5**).

Table 2.9 Reactivity of Cr(III) Catalyst

Entry	R^1	R^2	R^{3*}	A^-	salen/salan	Conversion
1	tBu	tBu	*trans* $(CH_2)_4$	Cl	salen	55%
2	tBu	tBu	*cis* $(CH_2)_4$	Cl	salen	20%
3	tBu	tBu	Ph	Cl	salen	15%
4	tBu	tBu	H	Cl	salen	40%
5	tBu	tBu	*trans* $(CH_2)_4$	Cl	salan	NR
6	tBu	tBu	H	Cl	salan	NR
7	H	H	*trans* $(CH_2)_4$	Cl	salen	NR
8	$SiEt_3$	tBu	*trans* $(CH_2)_4$	Cl	salen	NR
9	tBu	OMe	*trans* $(CH_2)_4$	Cl	salen	62%
10	tBu	NO_2	*trans* $(CH_2)_4$	Cl	salen	NR
11	tBu	tBu	*trans* $(CH_2)_4$	SF_6	salen	20%
12	tBu	tBu	*trans* $(CH_2)_4$	BF_4	salen	25%

*1,2-diaminobenzene was used to make salen and tested: 30% conversion

The salen series (entries 1-4) was superior to the salan series (entries 5-6) likely due to their greater donor properties. Within the salen series, the *trans*-cyclohexanediamine backbone was superior (entry 1) than the other groups probably due to structural geometry and solubility. The salen ligand without any substituent on the phenyl ring (entry 7) was poorly soluble, which hampered reactivity. A *tert*-butyl group was needed *ortho* to the phenolic group, and even a similarly sized silyl group did not function similarly (entries 8 vs entry 1).

Notably, an electron-donating group on the ligand of the chromium catalyst accelerated the cross-coupling reaction (entry 9), whereas an electron withdrawing group

73

suppressed it (entry 10). This result indicates that the rate determining step is likely oxidation of the catalyst. An electron withdrawing group on the salen destabilizes higher oxidation states of the chromium and makes oxidation to a reactive Cr(IV) or Cr(V) more difficult. Once generated, such a species would be a stronger oxidant and would be expect to cause a more rapid reaction if substrate oxidation was rate-determining, which is the opposite of what was observed. The converse holds true for the salen with the electron donating methoxy group, which facilitates catalyst oxidation and did result in a more reactive catalyst.

The use of more labile counterions in place of chloride was deleterious (entries 11, 12 in **Table 2.5**) indicating that a more cationic complex is not more reactive. Cationic tetradentate Cr(Salen)SF$_6$ and Cr(Salen)BF$_4$ complexes catalyzed the cross-coupling reaction, but to a lesser extent than neutral complex Cr(Salen)Cl (entry 1).

Some additives known as co-oxidant and sacrificial catalyst in oxidation reactions were tried in the cross-coupling reaction. However, triphenylphosphine oxide and *N*-methylmorpholine *N*-oxide did not give any corresponding cross-coupling product (**Scheme 2.16**).

Scheme 2.16 Additive Test in the Cross-Coupling Reaction

| Entry	Additive	Conversion
1	Ph_3PO	no reaction
2	NMO	diphenoquinone (**2.15**) only
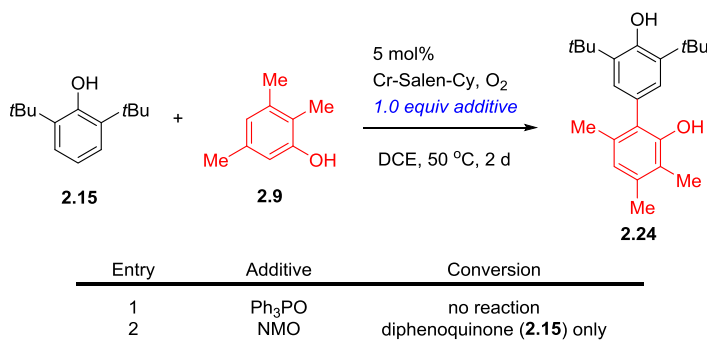
2.7.4. X-Ray Crystal Structure

Chromium(III) salen complex is a brown solid insoluble in all non-coordinating solvents but slightly soluble in donor solvents such as THF, CH_3CN, Et_2O, etc. Under our cross-coupling conditions, the Cr-Salen-Cy catalyst was not soluble in toluene. However, as the reaction proceeded, the reaction mixture became homogeneous. An X-ray structure of this precatalyst was obtained by the crystals grown from CH_3CN (**Figure 2.9**), which confirmed the starting state as Cr(III).[60] The octahedral chromium(III) complex has a d^3 configuration and half-filled t_{2g} orbital in the central metal ion, so that the Cr(III) ion is paramagnetic and redox innocent in the classical potential range.[61] The observed axial coordination of the solvent to the catalyst suggested that phenolic substrates could

---

(60) Hansen, K. B.; Leighton, J. L.; Jacobsen, E. N. "On the Mechanism of Asymmetric Nucleophilic Ring-Opening of Epoxides Catalyzed by (Salen)Cr(III) Complexes" *J. Am. Chem. Soc.* **1996**, *118*, 10924-10925.

(61) Shimazaki, Y. "Recent Advances in X-Ray Structures of Metal-Phenoxyl Radical Complexes" *Advances in Materials Physics and Chemistry* **2013**, *3*, 60-71.

coordinate in this position, which would be consistent with substrate inhibition results (see below). However, we were unable to obtain a crystal structure of this complex bound to a phenol. The crystal structure of Cr(III)-phenoxyl radical complex having a three phenolate moieties connected with the triazacyclononane backbone has been reported.[62] However, no X-ray crystal structures of the other metal complexes having this ligand and its analogues have been reported yet.
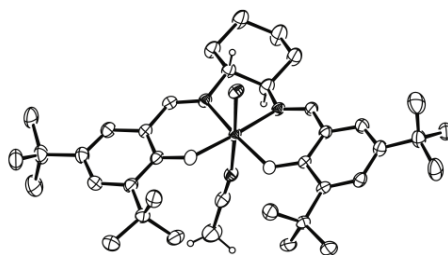
Figure 2.9 X-Ray Structure of **Cr-Salen-Cy** complex

(Thermal ellipsoids represent 50% electron probability, and hydrogen atoms are omitted for clarity.)

2.7.5. Kinetic Experiments

In order to provide further evidence to delineate the mechanism, a study of the reaction kinetics was undertaken. ^{1}H NMR spectroscopy was found to be the optimal

---

(62) Sokolowski, A.; Bothe, E.; Bill, E.; Weyhermüller, T.; Wieghardt, K. "Phenoxyl radical complexes of Chromium(III)" *Chem. Commun.,* **1996**, 1671-1672.

method to monitor the cross-coupling reaction of 2,6-di-*tert*-butylphenol with 3,4,5-trimethylphenol (**Scheme 2.17**).

Scheme 2.17 Design for Kinetic Experiments
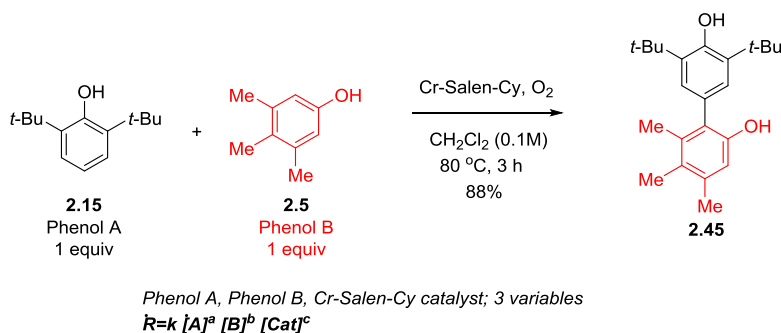
1,1'-Biphenyl (0.05 M) was used as an internal standard. The integration ratios of the peak at 6.83 ppm for 2,6-di-*tert*-butylphenol, 6.52 ppm for 3,4,5-trimethylphenol, 7.36 ppm for 1,1'-biphenyl, and 6.74 ppm for product were used to establish the concentration of each of the components. Detailed procedures are described in the experimental section. A representative stacked ^{2}H NMR time lapse spectrum and corresponding reaction profile using Cr-Salen-Cy catalyst (5 mol%) are shown in **Figure 2.10** and **Figure 2.11**, respectively.
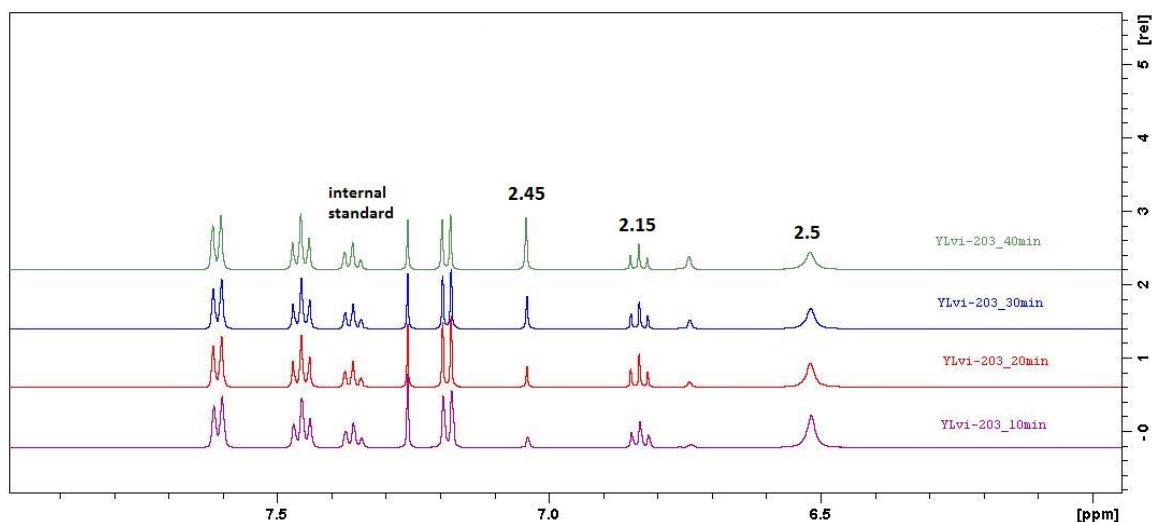
Figure 2.17 ^{2}H NMR Time-lapse for the Cross-Coupling Reaction
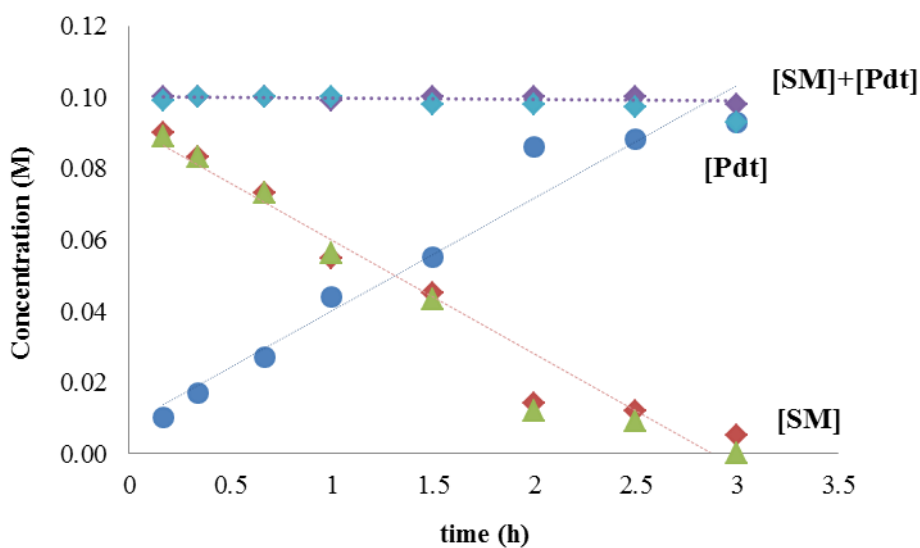
Figure 2.18 Reaction Profile for the Cross-Coupling Reaction

The analysis was performed by varying the substrate and catalyst concentrations independently in a series of cross-coupling reactions and measuring the initial rates of disappearance of the substrates and formation of the product. The initial reaction rates for

each experiment were obtained by analyzing the concentration vs time profile from the linear portion (<15% starting materials consumption).

For the catalyst order measurement, a set of five reactions was carried out with the substrates **2.15** and **2.5** (0.1 M, each substrate) and Cr-Salen-Cy catalyst (0.002, 0.003, 0.005, 0.007, 0.010 M; [cat]/[SM]$_o$ = 0.02, 0.03, 0.05, 0.07, 0.1, respectively) using a 5 mL reaction volume. The reaction profiles are illustrated in **Figure 2.12**. The initial linear portion from the graph was used to obtain initial rates R$_o$ (**Table 2.6**).
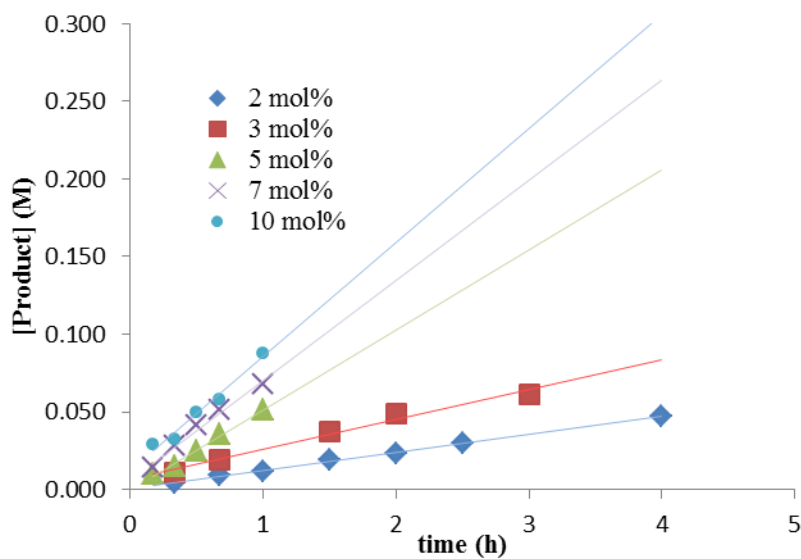
Figure 2.19 Reaction Profiles at Various Catalyst Concentrations
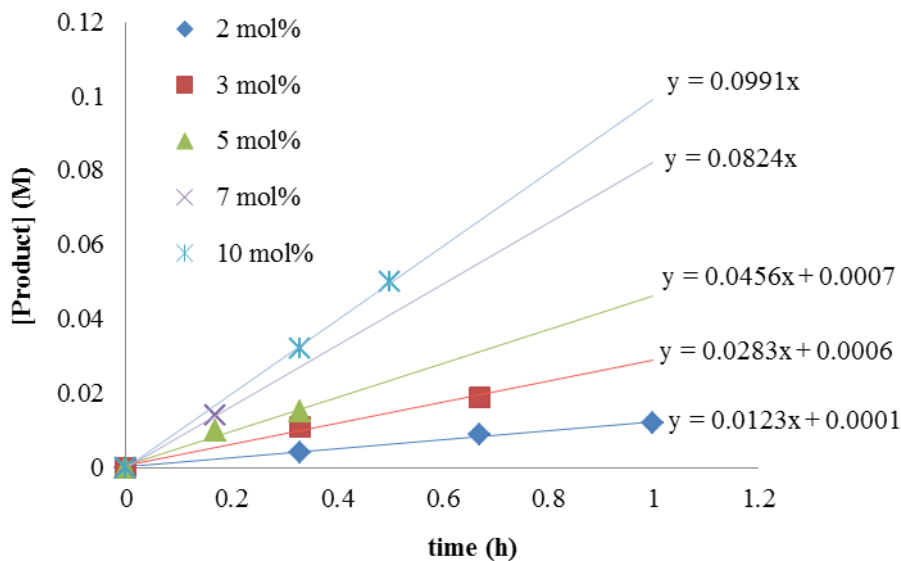
Figure 2.20 Initial Rates at Various Catalyst Concentrations

Table 2.6 Initial Rates at Each Catalyst Concentration

Concentration (M)	Initial Rate (M/s)
0.002	3.41667E-06
0.003	7.86111E-06
0.005	1.26667E-05
0.007	2.28889E-05
0.010	2.75278E-05

A log/log plot of R_o vs catalyst concentration revealed a slope of 1.29 consistent with a first order catalyst dependence (**Figure 2.14**). In recent kinetics studies by Poppo group[14b] on cross-coupling reaction of phenols using $FeCl_3$ as catalyst, the reactions were also found to be first order in a multicoordinated iron catalyst.
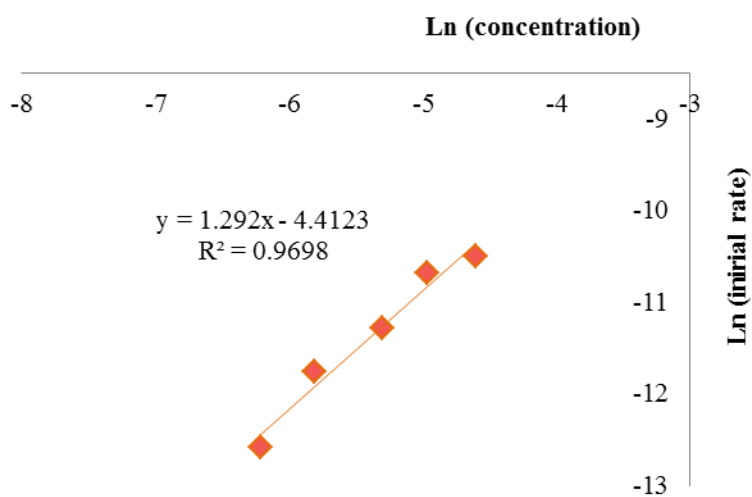
Figure 2.21 Plot of $\log(R_o)$ vs. $\log[\text{cat}]$

This result was supported by additional kinetic experiments. In the same way, different coupling partner with 2,6-di-*tert*-butylphenol, 2-naphthol substrate also showed same order in Cr-catalyst. The log/log plot of R_o vs catalyst concentration resulted in first order from its slop (**Figure 2.15**)

81
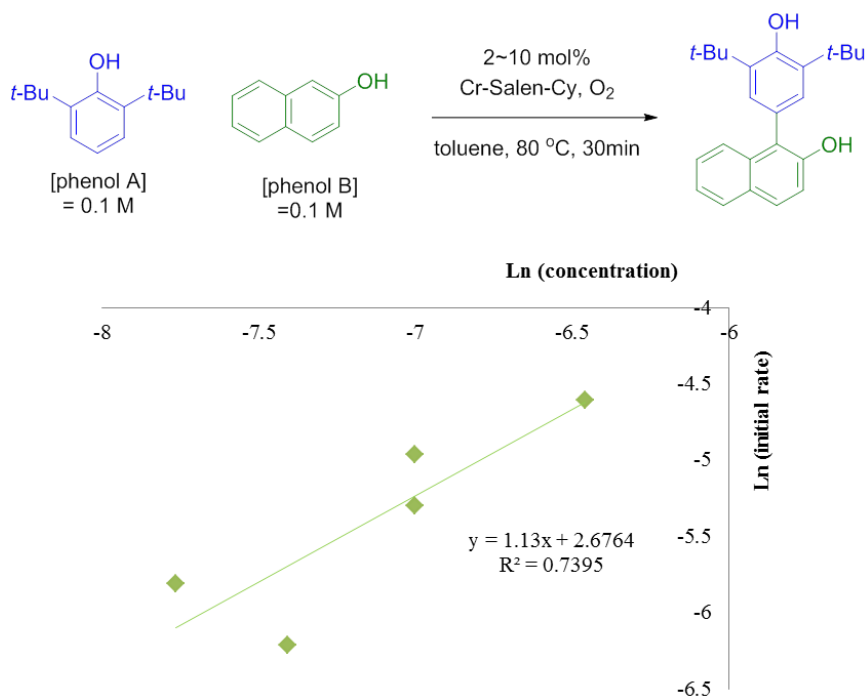
Figure 2.15 Catalyst Order in Cross-Coupling Reaction with 2-Naphthol

For the measurements of each substrate orders, two sets of four reactions were carried out with the same catalyst concentration (0.005 M). The concentrations of phenol A (**2.15**) and phenol B (**2.5**) were varied over a 10-fold range (0.1, 0.2, 0.5, 1.0 M) while the concentrations of the other phenol and catalyst were held constant at 0.1 M and 0.005 M.

While the concentration of phenol B was held constant and the concentration of phenol A was changed, the four reaction profiles overlapped (**Figure 2.16**) indicating that this coupling is not affected by the concentration of 2,6-disubstituted phenol (phenol A). From this result, we conclude that the reaction order for phenol A is zero, which a plot of phenol A concentration vs R_o (**Figure 2.17**) confirms.
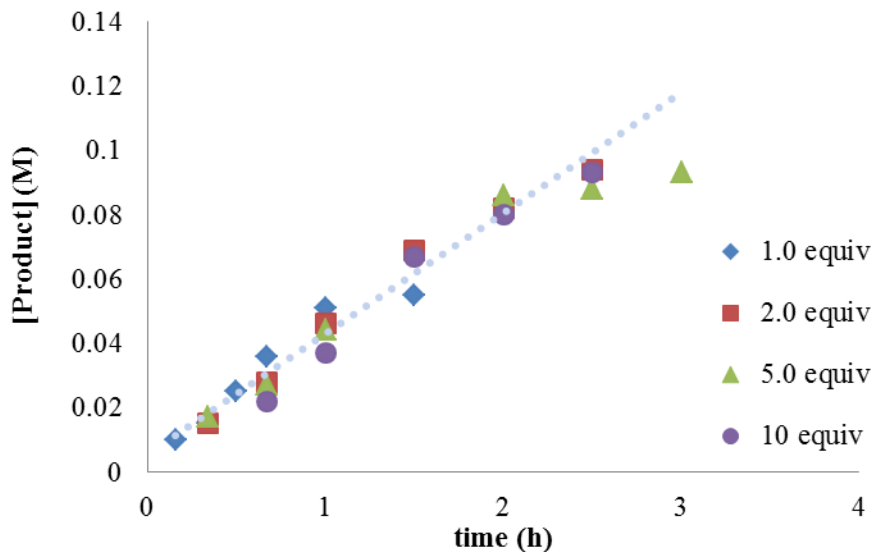
Figure 2.16 Reaction Profiles at Various Concentrations of Phenol A
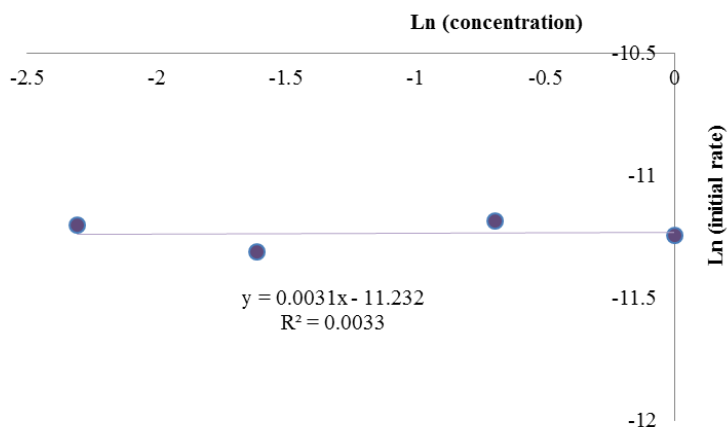
Figure 2.17 Plot of log(R_o) vs. log[Phenol A]

When reversed, the reaction profile for the phenol B was obtained and shown in
Figure 2.18. Notably, these reaction profiles indicate that the reaction slows when higher
concentrations of phenol B are employed. The linear portion was used to obtain initial
rate (R_o, **Figure 2.19**) and a log/log plot (**Figure 2.20**) revealed a slope of –0.979

consistent with negative first order dependence. In addition, a plot of concentration vs R_o clearly indicates that the reaction slows at higher concentrations of phenol B consistent with phenol B inhibiting the rate determining step.
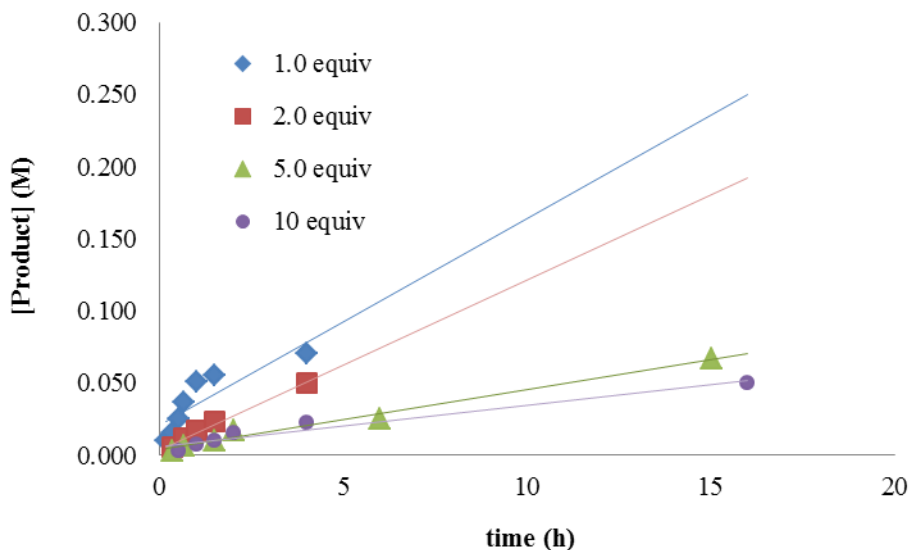
Figure 2.18 Reaction Profiles at Different Phenol B Concentrations
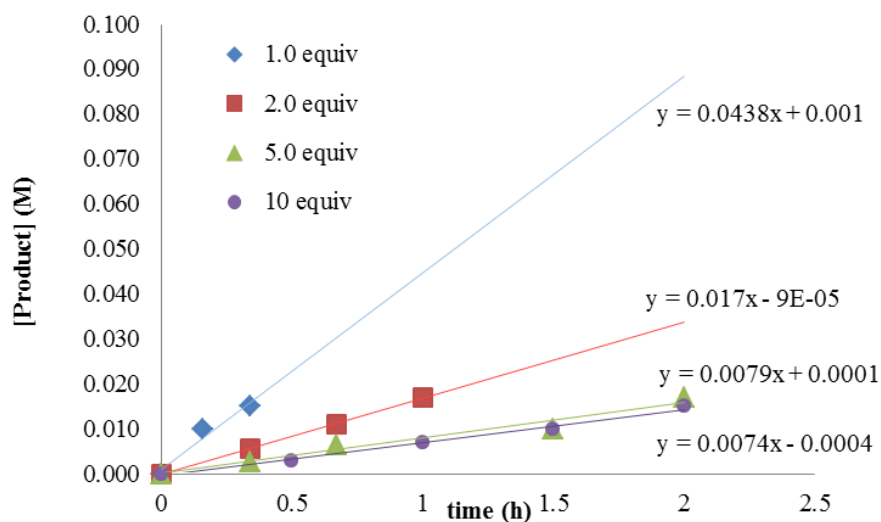
Figure 2.19 Initial Rates at Different Phenol B Concentrations

84

Table 2.7 Initial Rates at Each Catalyst Concentration

Concentration (M)	Initial Rate (M/s)
0.10	1.21667E-05
0.20	4.72222E-06
0.50	2.19444E-06
1.00	2.05556E-06
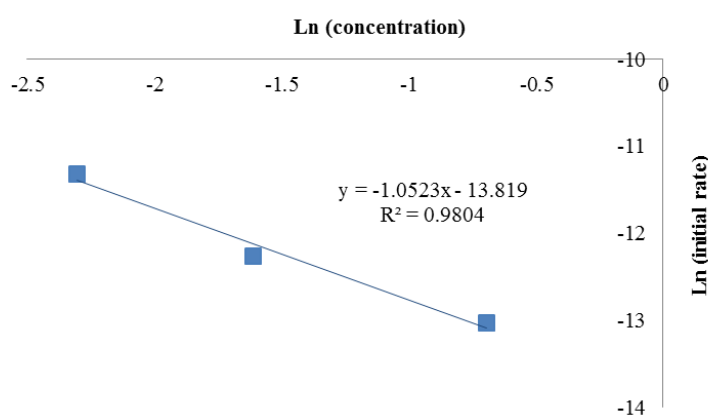
Figure 2.20 Plot of $\log(R_o)$ vs. $\log$[Phenol B]

In order to understand oxidant dependence in the cross-coupling reaction, the reaction flask was put into a Parr bomb reactor and oxygen was added *via* active purge. The reactor was closed and oxygen pressure was maintained at 10 atm and left to stir at 80 °C. The reaction profile was overlapped to the one under ambient pressure (**Figure 2.21**). It tells that either this cross-coupling is independent to the oxidant or the cross-coupling is already saturated in the ambient oxygen pressure. So we will try this coupling reaction in partial pressure of oxygen atmosphere to conclude the oxygen effect.
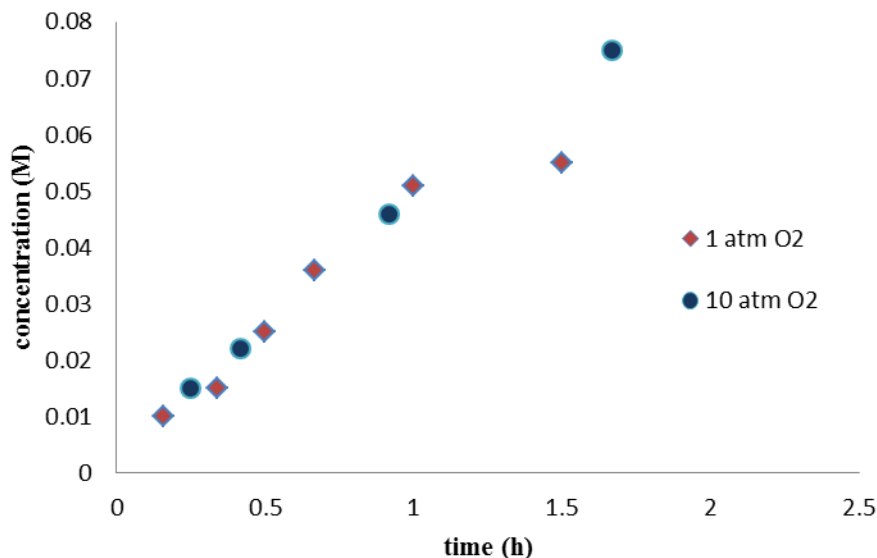
Figure 2.21 Oxygen Dependence in Cross-Coupling Reaction

There are many independent researches published regarding of cross-coupling reaction of phenols and they try to manifest its mechanism.[36, 63] For example, the Lumb group explained that the selectivity of cross-coupling reaction was achieved by change to ligand, metal counterion and temperature. Kita *et al*. proposed a cationic phenoxenium intermediate reacted with another arene to form cross-coupling adduct. Finally, the Pappo group proposed a chelated radical-anion coupling mechanism. Among those, Pappo's proposal is most consistent to our system to explain the mechanism. However, still there are limitations to meet every reaction condition with Cr-catalyzed cross-coupling reaction.

(63) Esguerra, K. V. N.; Fall, Y.;Petitjean, L.; Lumb, J.−P. "Controlling the Catalytic Aerobic Oxidation of Phenols" *J. Am. Chem. Soc.* **2014**, *136*, 7662−7668.

Future catalysts and conditions will thus be designed based on these results. For example, even more electron deficient chromioum salen will give rise to more potent oxidizing catalysts but will also require stronger stoichiometric terminal oxidants or a cocatalyst to be able to utilized dioxygen directly. Facial salen geometries will be probed to see if *cis* substrate coordination is advantageous.[64] Further experiments will include linked salens/pairs[65] to probe molecularity, isolation of intermediates, and computation of possible pathways.

2.7.6. Proposed Mechanism

Cr salens are well known to form Cr(V) oxo-speices, which equilibrate with Cr(III) to form μ-oxo-Cr(IV) complexes (**Scheme 2.18**).[66] Cr(V) oxo-species are typically generated with peroxide, PhIO, etc. On the other hand, oxygen does not rapidly form Cr(V) oxo-species, but is known to generate a Cr(IV) superoxide.[67] A Cr(IV) superoxide would be expected cause hydrogen atom abstraction, which was not

(64) Katsuki, T. "Unique asymmetric catalysis of cis-β metal complexes of salen and its related Schiff-base ligands" *Chem. Soc. Rev.* **2004**, *33*, 437–444.

(65) (a) Konsler, R. G.; Karl, J.; Jacobsen, E. N. "Cooperative Asymmetric Catalysis Using Dimeric Salen Complexes" *J. Am. Chem. Soc*. **1998**, *120*, 10780–10781. (b) Mazet, C.; Jacobsen, E. N. "Dimeric (salen)Al Complexes Display Expanded Scope in the Conjugate Cyanation of α, β-Unsaturated Imides" *Angew. Chem. Int. Ed.* **2008**, *47*, 1762–1765.

(66) Ruminski, R. R.; Healy, M. H.; Coleman, W. F. "Photoredox Processes in 254–nm Photochemistry of Chromium(III) Ammine" *Inorg. Chem.* **1989**, *28*, 1666–1669.

(67) Cho, J.; Woo, J.; Han, J. E.; Kubo, M.; Ogura, T.; Nam, W. "Chromium(V)-oxo and Chromium(III)-superoxo Complexes Bearing a Macrocyclic TMC Ligand in Hydrogen Atom Abstraction Reactions" *Chem. Sci.* **2011**, *2*, 2057.

consistent with the radical inhibition experiments with BHT and galvinoxyl (**Table 2.3**). Such a Cr(IV) superoxide might undergo exchange to form a μ-oxo-Cr(IV) or might slowly decompose to Cr(V) oxo which could recombine with remaining Cr(III) to form the same μ-oxo-Cr(IV). Similar coupling results were observed at lower temperatures with *t*-BuOOH, which is known to generate Cr(V) oxo-speices more readily than O_2. [68]

Scheme 2.18 Formation of μ-Oxo-Cr(IV) Species
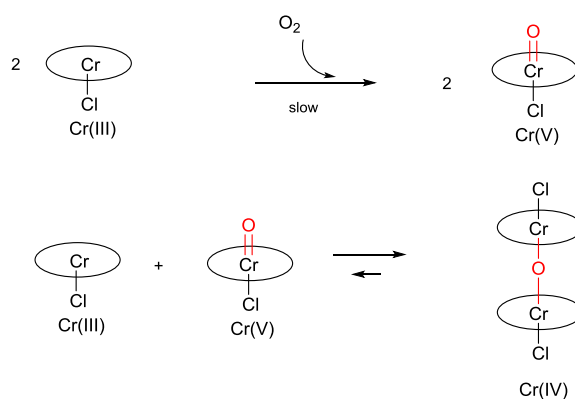
Ligand exchange of the less hindered phenol component (**Component B**) with the μ-oxo-Cr(IV) followed by electron transfer would give rise to the Cr(III) species shown in **Figure 2.20**. We speculate that **component A** is too hindered to coordinate to the salen metal center, but could hydrogen bond to the salen via one of the oxygens. The *para*-site of **component A** is less hindered, and perhaps more nucleophilic,[14b] relative to the open sites of **component B** and is best able to capture the keto radical. Chromium pophyrins could be utilized to interrogate this hydrogen bonding; they had very similar oxidation

(68) Kotani, H.; Kaida, S.; Ishizuka, T.; Sakaguchi, M.; Ogura, T.; Shiota, Y.; Yoshizawa, K.; Kojima, T. "Formation and Characterization of a Reactive Chromium(V)–Oxo Complex: Mechanistic Insight into Hydrogen-Atom Transfer reactions" *Chem. Sci.* **2015**, *6*, 945–955.

potentials relative the salens[69] but were poorer in hydrogen bonding. The mechanism in

Figure 2.22 was the most consistent with all of the observations to date, but alternative

possibilities cannot be discounted at this stage. Most importantly, experiments need to be

devised to establish the order of oxidation. Since the only homo-coupling product

observed arises from the more hindered **component A**, it seems likely that this

component either oxidizes more quickly than **component B** or that the hydrogen bonded

portion of **A** may be prone to dissociation subsequent to oxidation allowing trapping of

additional molecules of **component A**.
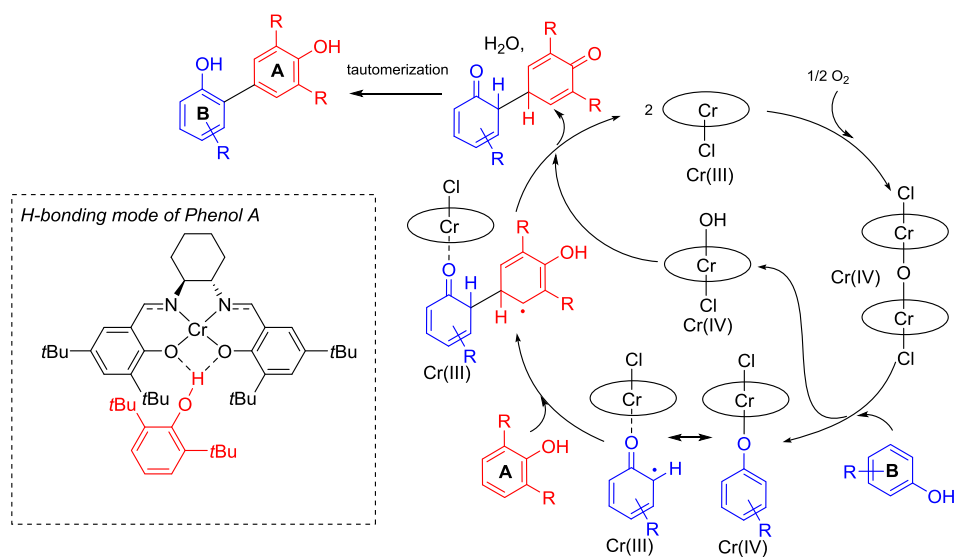
Figure 2.22 Preliminary Cross-Coupling Mechanism

(69) (a) Garrison, J. M.; Ostovic, D.; Bruice, T. C. "Is a Linear Relationship Between the Free Energies of Activation and One-Electron Oxidation Potential Evidence for One-Electron Transfer Being Rate Determining? Intermediates in the Epoxidation of Alkenes by Cytochrome P-450 Models. 4. Epoxidation of a Series of Alkenes by Oxo(meso-tetrakis(2,6-dibromophenyl)porphinato)chromium(V)" *J. Am. Chem. Soc.* **1989**, *111*, 4960–4966. (b) Premsingh, S.; Venkataramanan, N. S.; Rajagopal, S.; Mirza, S. P.; Vairamani, M.; Rao, P. S.; Velavan, K. "Electron Transfer Reaction of Oxo(salen)chromium(V) Ion with Anilines" *Inorg. Chem.* **2004**, *43*, 5744–5753. (c) Venkataramanan, N. S.; Kuppuraj, G.; Rajagopal, S. "Metal–salen Complexes as Efficient Catalysts for the Oxygenation of Heteroatom Containing Organic Compounds—Synthetic and Mechanistic Aspects" *Coord. Chem. Rev.* **2005**, *249*, 1249–1268.

From our prior experience with mechanisms of catalytic oxidations,[70] the most urgent experiments were determining the catalyst oxidation state, molecularity, and kinetic order. The Cr(V) oxo-complex is a stable species, which was easily synthesized in a stoichiometric manner, and can be combined with Cr(III) to yield the Cr(IV)-μ-oxo (**Scheme 2.18**).[27] Both species were subjected to single turnover experiments in the absence of O_2 to determine whether they reproduce the catalytic profile. Anion exchange followed by oxidation led to Cr(V)-oxo complex (**Scheme 2.19**).[71] A slight excess of iodosylbenzene was added to Cr(III)-Salen complex **2.91** dissolved in CH_3CN. The reaction mixture turned from orange to dark green. This slurry was stirred for 20 min and then filtered to remove the unreacted iodosylbenzene. Ether was slowly added to the dark filtrate in order to precipitate crystals of oxochromium(V) salts (**2.92**) as a black solid.

Scheme 2.19 Preparation of Cr(V)-Oxo Complex
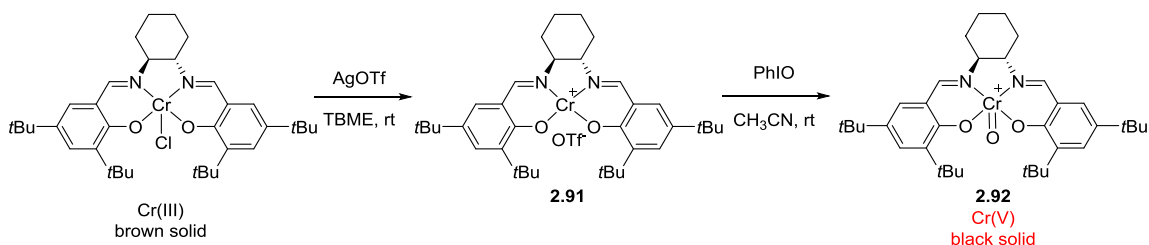
(70) Hewgley, J. B.; Stahl, S. S.; Kozlowski, M. C. "Mechanistic Study of Asymmetric Oxidative Biaryl Coupling: Evidence for Self-Processing of the Copper Catalyst to Achieve Control of Oxidase vs. Oxygenase Activity" *J. Am. Chem. Soc.* **2008**, *130*, 12232–12233.

(71) Sevvel, R.; Rajagopal, S.; Srinivasan, C.; Alhaji, N. I.; Chellamani, A. "Mechanism of Selective Oxidation of Organic Sulfides with Oxo(salen)chromium(V) Complexes" *J. Org. Chem.* **2000**, *65*, 3334-3340.

The Cr(IV)-μ-oxo complex was obtained from disproportionating the Cr(III) and Cr(V)-oxo species. The The Cr(IV)-μ-oxo complex in the reaction solution was dark brown, consistent with the reaction color during the general cross-coupling reaction with Cr(III) complex. However, the Cr(IV)-μ-oxo did not provide the coupling product with stoichiometric yield (**Table 2.8**). In the reaction between 2,6-di-*tert*-butylphenol and 3,4,5-trimethylphenol, stoichiometric amount of either the Cr(V) and Cr(IV) species did not give the corresponding coupling product with reasonable yield. 1.0 equiv of Cr(IV)-μ-oxo complex gave only 12% yield of the coupling product in the absence of O_2 (Entry 6). Future work will focus on generation of the Cr(V)-oxo complex in pure form for this experiment by recrystallization.

Table 2.8 Cross-Coupling using Cr-Complexes with Various Oxidation States
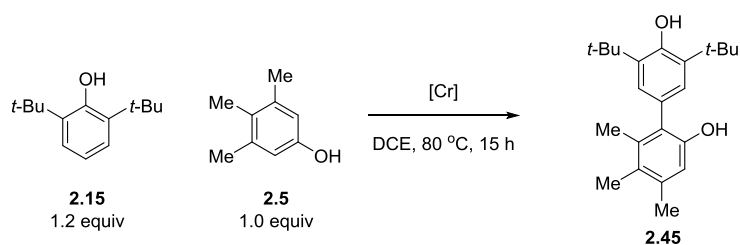
Entry	[Cr]	^{1}H NMR Yield
1	0.1 equiv Cr(III), O_2 (control)	78%
2	0.1 equiv Cr(V), N_2	2.7%
3	0.5 equiv Cr(V), N_2	18%
4	0.1 equiv Cr(IV), N_2	5.1%
5	0.5 equiv Cr(IV), N_2	13%
6	1.0 equiv Cr(IV), N_2	12%

2.8. Selective Coupling of Alkenyl Phenols

In spite of considerable study on the reaction of alkenyl phenols, the control elements are poorly understood and many outcomes are possible upon oxidation. [72] Nonetheless, control over such processes would permit access to a large number of biologically active natural products. The prevailing view is that these transformations are largely free radical in nature and that the substrates dictate the product unless dirigent proteins are present to bias the outcome.[73] As such, the mechanistic principles are similar to those at the inception of our phenol coupling studies, except that reactivity is delocalized to the distal β-position. Based on our results that salen/salan catalysts intimately interact with phenols to control coupling selectivity, we posited a similar outcome for alkenyl phenols.

As a first step to develop a catalytic and enantioselective coupling of *para*-alkenyl phenols, we undertook an assessment of isoeugenol (**2.93**) with achiral salen/salan catalysts (**Figure 2.23**) and found that racemic licarin A could be produced in good yields

(72) (a) Lindsley, C. W.; Chan, L. K.; Goess, B. C.; Joseph, R.; Shair, M. D. "Solid-Phase Biomimetic Synthesis of Carpanone-like Molecules" *J. Am. Chem. Soc.* **2000**, *122*, 422–423. (b) Daniels, R. N.; Fadeyi, O. O.; Lindsley, C. W. "A New Catalytic Cu(II)/Sparteine Oxidant System for β,β-Phenolic Couplings of Styrenyl Phenols: Synthesis of Carpanone and Unnatural Analogs" *Org. Lett.* **2008**, *10*, 4097–4100. (c) Zhang, Y.; Sigman, M. S. "Palladium(II)-Catalyzed Enantioselective Aerobic Dialkoxylation of 2-Propenyl Phenols: A Pronounced Effect of Copper Additives on Enantioselectivity" *J. Am. Chem. Soc.* **2007**, *129*, 3076–3077.

(73) (a) Pickel, B.; Constantin, M.-A.; Pfannstiel, J.; Conrad, J.; Beifuss, U.; Schaller, A. "An Enantiocomplementary Dirigent Protein for the Enantioselective Laccase-Catalyzed Oxidative Coupling of Phenols" *Angew. Chem. Int. Ed.* **2010**, *49*, 202 –204. (b) Davin, L. B.; Lewis, N. G. "Dirigent phenoxy radical coupling: advances and challenges" *Current Opinion in Biotechnology* **2005**, *16*, 398–406. (c) Davin, L. B.; Lewis, N. G. "Dirigent Proteins and Dirigent Sites Explain the Mystery of Specificity of Radical Precursor Coupling in Lignan and Lignin Biosynthesis" *Plant Physiology* **2000**, *123*, 453–461.

relative to stoichiometric[74] or enzymatic[75] oxidants. Specifically, an achiral Ru-salen-H catalyst generated racemic licarin A in 52% yield in presence of 3 Å molecular sieves as an additive.
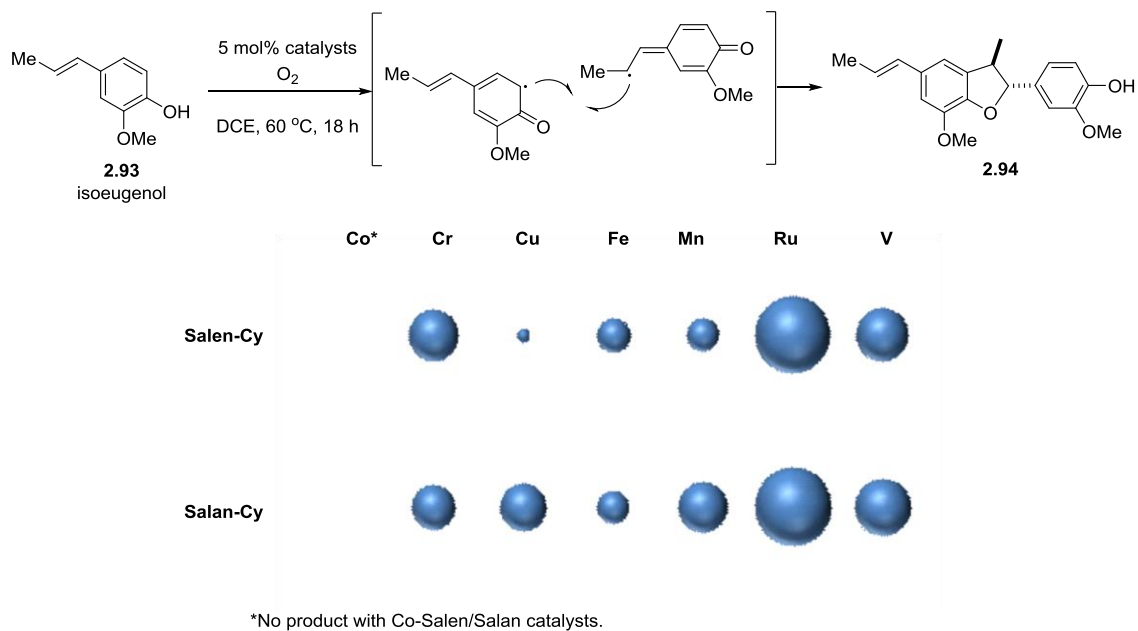
Figure 2.23 Bubble Chart of HTE Screening for Oxidative Coupling of Isoeugenol

To achieve an enantioselective phenolic coupling, future work will focus on assessment of the most encouraging Ru leads which would then permit design more selective catalysts following the approach discussed in the previous chapter. An alternate approach is to use the V catalyst in **Chapter 1** as a lead. If successful, such catalysts

(74) Liu, S.-Y.; Wang, G.-Q.; Liang, Z.-Y.; Wang, Q.-A. "Synthesis of Dihydrobenzofuran Neoligans Licarin A and Dihydrocarinatin as Well as Related Triazolylglycosides" *Chemical Research in Chinese Universities* **2013**, *29*, 1119–1124.

(75) Chioccara, F.; Poli, S.; Rindone, B.; Pilati, T.; Brunow, G.; Pietikäinen, P.; Setälä, H. "Regio- and Diastereo-selective Synthesis of Dimeric Lignans Using Oxidative Coupling." *Acta Chem. Scand.* **1993**, *47*, 610–616.

would be useful in generate analogs of licarin A (**Figure 2.23**), a compound with promising activity against leishmaniosis, [76] schistosomiasis and Chagas disease. [77] Notably, (–)-licarin A is 2-6 times more effective than the racemate and the (+)-enantiomer is considerably less effective.[78]
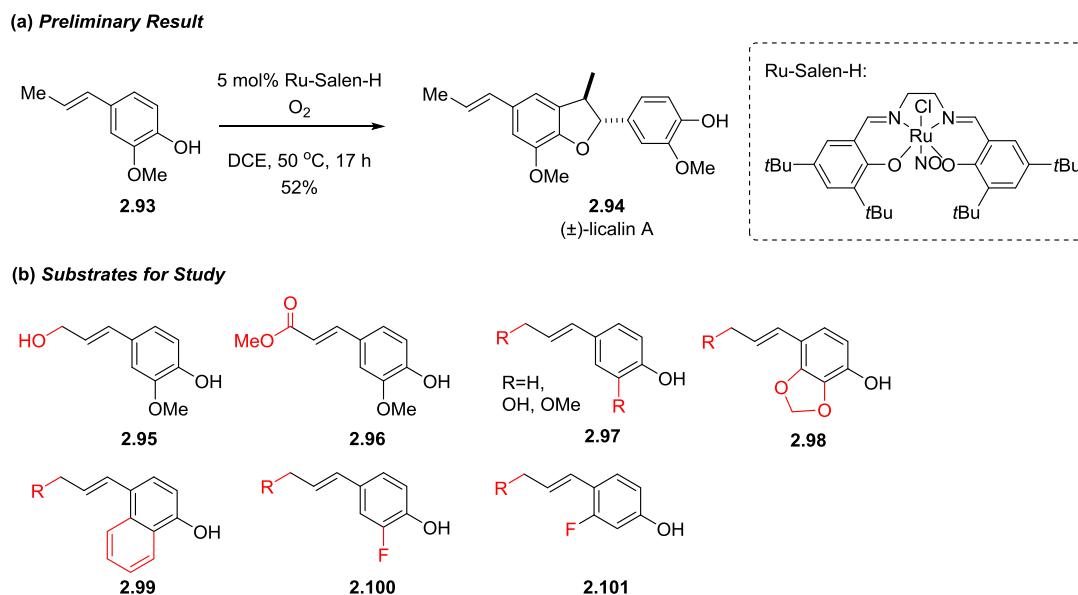
Figure 2.24 *para*-Alkenylphenol Coupling

(76) Aveniente, M.; Pinto, E. F.; Santos, L. S.; Rossi-Bergmann, B.; Barata, L. E. S. "Structure–Activity Relationship of Antileishmanials Neolignan Analogues" *Bioorg. Med. Chem.* **2007**, *15*, 7337–7343.

(77) Pereira, A. C.; Magalhães, L. G.; Gonçalves, U. O.; Luz, P. P.; Moraes, A. C. G.; Rodrigues, V.; da Matta Guedes, P. M.; da Silva Filho, A. A.; Cunha, W. R.; Bastos, J. K.; Nanayakkara, N. P. D.; e Silva, M. L. A. "Schistosomicidal and trypanocidal structure–activity relationships for (±)-licarin A and its (–)- and (+)-enantiomers" *Phytochemistry* **2011**, *72*, 1424–1430.

(78) (a) Wang, E.-C.; Wein, Y.-S.; Kuo, Y.-H.; "A Concise and Efficient Synthesis of Salvinal From Isoeugenol Via a Phenoxenium Ion Intermediate" *Tetrahedron Lett.* **2006**, *47*, 9195–9197. (b) Chen, P.-Y.; Wu, Y.-H.; Hsu, M.-H.; Wang, T.-P.; Wang, E.-C. "Cerium Ammonium Nitrate-Mediated the Oxidative Dimerization of p-alkenylphenols: A New Synthesis of Substituted (±)-*trans*-dihydrobenzofurans" *Tetrahedron* 2013, *69*, 653–657.

2.9. Summary

In summary, the first simple catalytic system that uses atom-economical oxygen as the terminal oxidant to accomplish selective *ortho−ortho*, *ortho−para*, or *para−para* homo-couplings of phenols was developed. Chromium salen catalysts have been discovered and verified as uniquely effective in the cross-coupling of different phenols with high chemo- and regio-selectivity. A broad scope of phenol substrates could be employed in this reaction condition and gave cross-coupling products with good yield (up to 88%). In order to understand the mechanism of cross-coupling reaction, spectroscopic methods, additive experiments, SAR studies and kinetic experiments were performed and tentative mechanism was postulated.

2.10. Experimental

General Procedure for High Throughput Experimentation (HTE)

The following procedure is a representative of the HTE screening. The solutions of catalysts (2 μmol, 50 μL) in DCE and the solutions of phenol (10 μmol, 50 μL) in DCE were dosed into the 24-well plate reactor vials. The reaction plate was then purged and continuously back-filled with oxygen using a desiccator fixed with a T-valve for 3-5 min. The plate was sealed and stirred at 50 °C for 24 h. After cooling to ambient temperature, the vials were diluted with a solution of biphenyl (1 μmol, 500 μL) in MeCN and then sealed. The contents were shaken for 15 min. To a separate 96-well LC

plate with 1 mL vials were added 700 μL of MeCN, and then 25 μL of the diluted

reaction mixtures. The mixture was then analyzed using Agilent Chemstation on an

HPLC modified with a 96-well plate auto-sampler. Assay conditions: Supelco Ascentis

Express C18 100 mm x 4.6 mm or ZORBAX Eclipse XDB-C8, 4.6 x 50 mm, 1.8 μm.

MeCN with H_2O + 0.1 % H_3PO_4. 1.8 mL/min; 10 % in MeCN to 95 % MeCN in 6 min,

hold for 2 min. Post time 2 min. Column at 40 °C; 210 nm.

HTE of 2,3,5-trimethylphenol (Figure 2.5)
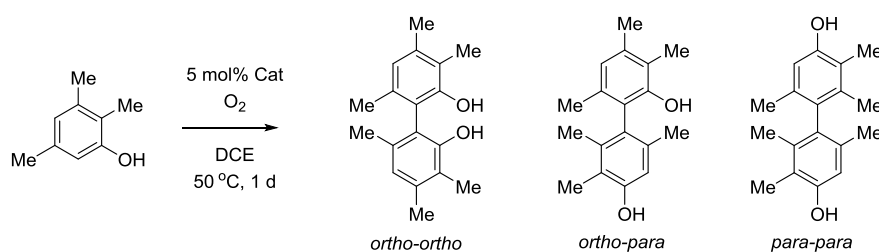
Table 2.9 Results from HTE Screening (product vs internal standard)

catalyst	*o-o*/IS	*o-p*/IS	*p-p*/IS
Co-Salen-Cy	0.59	0.12	0.00
Co-Salan-Cy	0.40	0.35	0.00
Cr-Salen-Cy	0.12	1.16	0.18
Cr-Salen-Ph	0.05	0.39	0.04
Cr-Salen-Cy-	0.00	0.20	0.00
Cr-Salan-Ph	0.00	0.05	0.00
Cu-Salen-Ph	0.00	0.00	0.00
Cu-Salan-Cy	0.14	0.17	0.00
Cu-Salan-Ph	0.00	0.00	0.00
Mn-Salen-Cy	0.00	0.72	0.00
Mn-Salan-	0.21	0.74	0.67
V-Salen-H	0.00	0.09	0.00
V-Salen-Ph	0.12	0.14	0.05
V-Salan-Ph	1.93	0.08	0.00
Ru-Salen-Cy	0.05	0.15	0.00
Ru-Salen-Ph	0.08	0.11	0.00

Ru-Salan-Cy	0.40	0.49	0.00
Ru-Salan-Ph	0.13	0.13	0.00
Ru-Salan-Cy-	0.07	0.28	0.00

General Procedure for the Regioselective Oxidative Coupling of Phenols

To a 5 mL microwave vial was added phenol (0.1 mmol) and catalyst (0.005 mmol). The vial was sealed with a septum and solvent (1 mL) was added. Oxygen was added *via* active purge. The septum was replaced with a crimping cap and the vessel was sealed and stirred for the indicated time at the indicated temperature. After the reaction mixture was filtered through a plug of silica and concentrated *in* vacuo, the resultant mixture was chromatographed using ethyl acetate/hexane to afford the product.
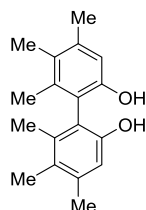
4,4',5,5',6,6'-Hexamethyl-[1,1'-biphenyl]-2,2'diol (2.6). Following the general procedure, using Ru-Salen-Ph catalyst in dichloroethane at 80 °C for 2 days, the *ortho-ortho* product was obtained as a yellow solid in 50% yield: ^{1}H NMR (500 MHz, CDCl$_3$) δ 6.75 (s, 2H), 4.46 (s, 2H), 2.31 (s, 6H), 2.16 (s, 6H), 1.92 (s, 6H). Spectral data matched that reported in the literature.[16]
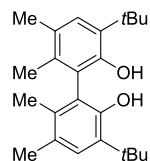
3,3'-Di-*tert*-butyl-5,5',6,6'-tetramethyl-[1,1'-biphenyl]-2,2'diol (2.8). Following

the general procedure, using Ru-Salen-H catalyst in dichloroethane at 80 °C for 3 d, the
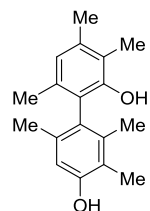
ortho-ortho product was obtained as a colorless resin in 85% yield: ^{1}H NMR (500 MHz,

CDCl$_3$) δ 7.14 (s, 2H), 4.80 (s, 2H), 2.27 (s, 6H), 1.83 (s, 6H), 1.41 (s, 18H); ^{13}C NMR

(125 MHz, CDCl$_3$) δ 150.4, 134.1, 133.4, 128.8, 128.1, 121.0, 34.5, 29.6, 20.0, 15.9; IR

(film) 3493, 2959, 1388, 1277, 1183, 1041, 892 cm^{-1}; HRMS (ESI) *m/z* = 354.2559 calcd

for C$_{24}$H$_{34}$O$_2$ [M]$^+$, found 354.2559. Spectral data matched that reported in the

literature.[79]

2',3,3',4,6,6'-Hexamethyl-[1,1'-biphenyl]-2,4'-diol (2.11). Following the general

procedure, using Cr-Salen-Cy catalyst in dichloroethane at 50 °C for 2 d, the *ortho-para*

product was obtained in 52% yield: ^{1}H NMR (500 MHz, CDCl$_3$) δ 6.68 (s, 1H), 6.65 (s,

1H), 4.65 (s, 1H), 4.53 (s, 1H), 2.82 (s, 3H), 2.19 (s, 3H), 2.17 (s, 3H), 1.90 (s, 3H), 1.89

(s, 3H), 1.83 (s, 3H); ^{13}C NMR (125 MHz, CDCl$_3$) δ 153.3, 150.5, 138.4, 136.5, 136.3,

(79) Malkowsky, I. M.; Rommel, C. E.; Fröhlich, R.; Griesbach, U.; Pütter, H.; Waldvogel, S. R. *Chem. Eur. J.* **2006**, *12*, 7482-7488.

133.5, 126.4, 123.7, 123.0, 120.6 119.3, 114.7, 19.9, 19.8, 19.2, 16.6, 11.9, 11.8; IR (film) 3435, 2920, 1590, 1453, 1299, 1088, 910, 848 cm^{-1}; HRMS (ESI) m/z = 271.1698 calcd for $C_{18}H_{23}O_2$ [M+H]$^+$, found 271.1700. Spectral data matched that reported in the literature.[6]

5,5'-Di-*tert*-butyl-2,2'-dimethyl-[1,1'-biphenyl]-4,4'-diol (2.21). Following the general procedure, using Cr-Salen-Cy catalyst in dichloroethane at 50 °C for 2 d, the *para-para* product was obtained in 44% yield: ^{1}H NMR (500 MHz, CDCl$_3$) δ 7.00 (s, 2H), 6.58 (s, 2H), 4.67 (s, 2H), 1.98 (s, 6H), 1.41 (s, 18H); ^{13}C NMR (125 MHz, CDCl$_3$) δ 152.7, 134.9, 133.8, 133.0, 128.9, 117.7, 34.3, 29.9, 19.3; IR (film) 3324, 2917, 1611, 1383, 1093 cm^{-1}; HRMS (ESI) m/z = 325.2168 calcd for $C_{22}H_{29}O_2$ [M–H]$^-$, found 325.2170.

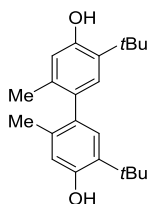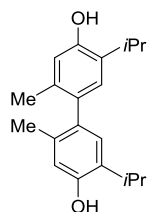**5,5'-Di*iso*propyl-2,2'-dimethyl-[1,1'-biphenyl]-4,4'-diol**. Following the general procedure, using Cr-Salen-Cy catalyst in dichloroethane at 50 °C for 2 d, the *para-para* product was obtained in 38% yield: ^{1}H NMR (500 MHz, CDCl$_3$) δ 6.93 (s, 2H), 6.66 (s,

2H), 4.61 (s, 2H), 3.18 (sept, J = 6.9 Hz, 2H), 1.25 (d, J = 6.9 Hz, 6H), 1.24 (d, J = 6.9

Hz, 6H); ^{13}C NMR (125 MHz, CDCl$_3$) δ 151.4, 134.7, 134.1, 131.2, 128.0, 116.4, 26.8,

22.8, 22.7, 19.5; IR (film) 3328, 2920, 1616, 1405, 1335, 1097, 899, 735 cm^{-1}; HRMS

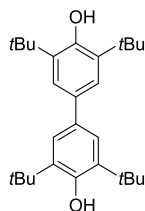(ESI) m/z = 297.1855 calcd for C$_{20}$H$_{25}$O$_2$ [M–H]$^-$, found 297.1872.

3,3',5,5'-Tetra-*tert*-butyl-[1,1'-biphenyl]-4,4'-diol. Following the general

procedure, using Cr-Salen-Cy catalyst in dichloroethane at 85 °C for 2 d, a mixture of the

para-para bisphenol and the *para-para* diphenoquinone was obtained, which was

concentrated *in vacuo* and directly subjected to sodium dithonite (0.3 mmol) in EtOH

(0.2 M) heated to reflux for 5 h. The resultant precipitate was removed and the filtrate

was concentrated *in vacuo* and chromatographed with EtOAc/hexanes to provide the

para-para product in 77% yield: ^{1}H NMR (500 MHz, CDCl$_3$) δ 7.31 (s, 4H), 5.18 (s,

2H), 1.50 (s, 36H); ^{13}C NMR (125 MHz, CDCl$_3$) δ 152.8, 136.0, 133.9, 124.1, 34.4, 30.4;

IR (film) 3622, 3304, 2917, 1649, 1424, 1098 cm^{-1}; HRMS (ESI) m/z = 410.3185 calcd

for C$_{28}$H$_{42}$O$_2$ [M]$^+$, found 410.3166.

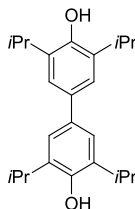**3,3',5,5'-Tetra*iso*propyl-[1,1'-biphenyl]-4,4'-diol**. Following the general procedure, using Cr-Salen-Cy catalyst in dichloroethane at 85 °C for 1 d, a mixture of the *para-para* bisphenol and the *para-para* diphenoquinone was obtained, which was concentrated *in vacuo* and directly subjected to sodium dithonite (0.3 mmol) in EtOH (0.2 M) heated to reflux for 5 h. The resultant precipitate was removed and the filtrate was concentrated *in vacuo* and chromatographed with EtOAc/hexanes to provide the *para-para* product in 95% yield: ^{1}H NMR (500 MHz, CDCl$_3$) δ 7.20 (s, 4H), 4.78 (s, 2H), 3.22 (septet, J = 6.5Hz, 4H), 1.34 (d, J = 6.5Hz, 24H); ^{13}C NMR (125 MHz, CDCl$_3$) δ 149.1, 134.7, 133.8, 122.4, 27.4, 22.8; IR (film) 3568, 2960, 1723, 1442, 1304, 1197, 1147 cm$^{-1;}$ HRMS (ESI) m/z = 353.2481 calcd for C$_{24}$H$_{33}$O$_2$ [M–H]$^-$, found 353.2481.
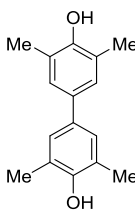
3,3',5,5'-Tetramethyl-[1,1'-biphenyl]-4,4'-diol. Following the general procedure, using Cr-Salen-Cy catalyst in dichloroethane at 85 °C for 2 d, a mixture of the *para-para* bisphenol and the *para-para* diphenoquinone was obtained, which was concentrated *in vacuo* and directly subjected to sodium dithonite (0.3 mmol) in EtOH (0.2 M) heated to reflux for 5 h. The resultant precipitate was removed and the filtrate was concentrated *in*

101

vacuo and chromatographed with EtOAc/hexanes to provide the *para-para* product in 63%

yield: ^{1}H NMR (500 MHz, CDCl$_3$) δ 7.15 (s, 4H), 4.56 (s, 2H), 2.30 (s, 12H); ^{13}C NMR

(125 MHz, CDCl$_3$) δ 151.2, 133.4, 127.0, 123.1, 16.0; IR (film) 3339, 2919, 1650, 1385,

1094 cm^{-1}; HRMS (ESI) *m/z* = 242.1307 calcd for C$_{16}$H$_{18}$O$_2$ [M]$^+$, found 242.1305.

General Procedure for the Oxidative Cross-coupling Reaction of Phenols using Cr-Salen-Cy catalyst
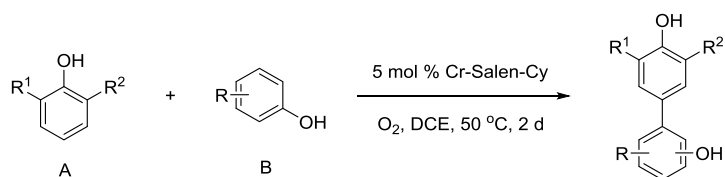
To a 5 mL microwave vial was added phenol A (0.3 mmol), phenol B (0.25 mmol)

and Cr-Salen-Cy catalyst (0.025 mmol). The vial was sealed with a septum and 1,2-

dichloroethane (2.5 mL) was added. Oxygen was added *via* active purge. The septum was

replaced with a crimping cap and the vessel was sealed and stirred for 3–48 h at 50–80 °C.

The reaction mixture was filtered through a plug of silica and the resultant material was

concentrated *in vacuo* and chromatographed using 10% ethyl acetate/hexane to afford the

ortho-para or *para-para* biphenol.
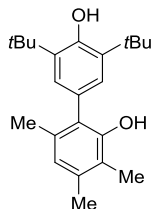
3',5'-Di-*tert*-butyl-3,4,6-trimethyl-[1,1'-biphenyl]-2,4'-diol **(2.24)**. Following the general procedure (reaction for 2 d at 50 °C), the *ortho-para* product was obtained in 55% yield (89% based on recovered starting material): ^{1}H NMR (500 MHz, CDCl$_3$) δ 7.05 (s, 2H), 6.69 (s, 1H), 5.29 (s, 1H), 5.03 (s, 1H), 2.29 (s, 3H), 2.19 (s, 3H), 2.03 (s, 3H), 1.45 (s, 18H); ^{13}C NMR (125 MHz, CDCl$_3$) δ 153.5, 151.0, 37.0, 136.6, 133.8, 126.9, 126.2, 126.2, 122.9, 119.6, 34.5, 30.4, 20.1, 19.8, 11.7; IR (film) 3640, 3536, 2918, 1654, 1436, 1084, 890 cm^{-1}; HRMS (ESI) *m/z* = 339.2324 calcd for C$_{23}$H$_{31}$O$_2$ [M–H]$^-$, found 339.2319.
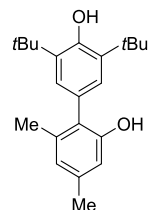
3',5'-Di-*tert*-butyl-4,6-dimethyl-[1,1'-biphenyl]-2,4'-diol **(2.25)**. Following the general procedure (reaction for 2 d at 50 °C), the *ortho-para* product was obtained in 56% yield (91% based on recovered starting material): ^{1}H NMR (500 MHz, CDCl$_3$) δ 7.05 (s, 2H), 6.69 (s, 2H), 5.29 (s, 1H), 4.92 (s, 1H), 2.32 (s, 3H), 2.06 (s, 3H), 1.45 (s, 18H); ^{13}C NMR (125 MHz, CDCl$_3$) δ 153.6, 153.1, 138.1, 137.3, 136.9, 126.9, 126.1, 125.6, 122.7,

112.9, 34.5, 30.4, 21.2, 20.4; IR (film) 3531, 2957, 1625, 1560, 1434, 1154 cm^{-1}; HRMS

(ESI) m/z = 325.2168 calcd for $C_{22}H_{29}O_2$ [M–H]$^-$, found 325.2167.

3',5,5'-Tri-*tert*-butyl-2-methyl-[1,1'-biphenyl]-4,4'-diol (**2.26**). Following the

general procedure (reaction for 2 d at 50 °C), the *para-para* product was obtained in 57%

yield (90% based on recovered starting material): ^{1}H NMR (500 MHz, CDCl$_3$) δ 7.16 (s,

1H), 7.12 (s, 2H), 6.59 (s, 1H), 5.18 (s, 1H), 4.71 (s, 1H), 2.21 (s, 3H), 1.47 (s, 18H), 1.42

(s, 9H); ^{13}C NMR (125 MHz, CDCl$_3$) δ 152.8, 152.4, 135.2, 135.0, 134.2, 133.3, 132.9,

129.0, 126.1, 118.2, 34.4, 34.3, 30.4, 29.8, 20.0; IR (film) 3637, 3514, 2957, 1611, 1386,

1323, 1230, 1154 cm^{-1}; HRMS (ESI) m/z = 367.2637 calcd for $C_{25}H_{35}O_2$ [M–H]$^-$, found

367.2639.

3',5'-Di-*tert*-butyl-2,5-dimethyl-[1,1'-biphenyl]-2,4'-diol (**2.27**). Following the

general procedure (reaction for 2 d at 50 °C), the *para-para* product was obtained in 44%

yield (95% based on recovered starting material): ^{1}H NMR (500 MHz, CDCl$_3$) δ 7.08 (s,

2H), 7.01 (s, 1H), 6.69 (s, 1H), 5.16 (s, 1H), 4.60 (s, 1H), 2.25 (s, 3H), 2.22 (s, 3H), 1.46

(s, 18H); ^{13}C NMR (125 MHz, CDCl$_3$) δ 152.4, 135.3, 134.3, 132.6, 132.5, 126.0, 120.7, 116.6, 34.4, 30.4, 20.3, 15.2; IR (film) 3640, 3419, 2957, 1618, 1506, 1437, 1393, 1311, 1221, 1155, 1040, 883, 739 cm^{-1}; HRMS (ESI) m/z = 325.2168 calcd for C$_{22}$H$_{29}$O$_2$ [M–H]$^-$, found 325.2155.
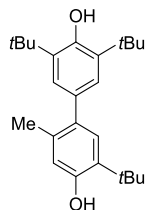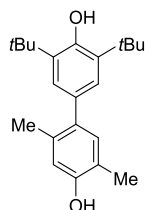

3',5'-Di-*tert*-butyl-5-isopropyl-2-methyl-[1,1'-biphenyl]-2,4'-diol **(2.28)**.

Following the general procedure (reaction for 2 d at 50 °C), the *para-para* product was obtained in 44% yield (95% based on recovered starting material): ^{1}H NMR (500 MHz, CDCl$_3$) δ 7.12 (s, 2H), 7.11 (s, 1H), 6.67 (s, 1H), 5.19 (s, 1H), 4.67 (s, 1H), 3.20 (septet, J = 7.0 Hz, 1H), 2.22 (s, 3H), 1.48 (s, 18H), 1.28 (d, J = 7.0 Hz, 6H); ^{13}C NMR (125 MHz, CDCl$_3$) δ 152.4, 151.4, 135.6, 135.2, 133.9, 132.8, 131.5, 128.2, 126.1, 116.9, 34.4, 30.4, 26.9, 22.7, 20.2; IR (film) 3642, 3529, 2959, 1614, 1509, 1437, 1321, 1221, 1156, 1121, 1028, 885, 739 cm^{-1}; HRMS (ESI) m/z = 353.2481 calcd for C$_{24}$H$_{33}$O$_2$ [M–H]$^-$, found 353.2466.
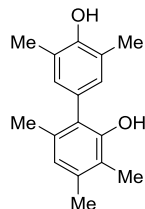
3,3',4,5',6-Pentamethyl-[1,1'-biphenyl]-2,4'-diol (2.31). Following the general procedure (reaction for 2 d at 50 °C), the *ortho-para* product was obtained in 51% yield (89% based on recovered starting material): ^{1}H NMR (500 MHz, CDCl$_3$) δ 6.88 (s, 2H), 6.66 (s, 1H), 4.90 (s, 1H), 4.69 (s, 1H), 2.28 (s, 6H), 2.27 (s, 3H), 2.17 (s, 3H), 2.02 (s, 3H); ^{13}C NMR (125 MHz, CDCl$_3$) δ 152.0, 150.9, 136.6, 133.6, 130.6, 127.2, 125.2, 124.1, 122.9, 119.5, 20.0, 19.9, 15.9, 11.7; IR (film) 3533, 2921, 1568, 1455, 1300, 1192, 1082 cm^{-1}; HRMS (ESI) *m/z* = 255.1385 calcd for C$_{17}$H$_{19}$O$_2$ [M–H]$^-$, found 255.1392.
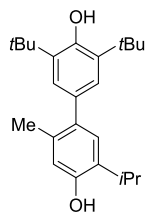

5-(*tert*-Butyl)-2,3', 5'-trimethyl-[1,1'-biphenyl]-4,4'-diol (2.32). Following the general procedure (reaction for 2 d at 50 °C), the *ortho-para* product was obtained in 40% yield: ^{1}H NMR (500 MHz, CDCl$_3$) δ 7.08 (s, 1H), 6.92 (s, 2H), 6.56 (s, 1H), 4.73 (s, 1H), 4.60 (s, 1H), 2.29 (s, 6H), 2.18 (s, 3H), 1.41 (s, 9H); ^{13}C NMR (125 MHz, CDCl$_3$) δ 152.8, 150.8, 134.1, 134.0, 133.3, 129.6, 128.8, 122.5, 118.1, 34.2, 29.7, 19.8, 16.0; IR (film) 3453, 2958, 1635, 1485, 1415, 1386, 1188, 1034, 876, 737 cm^{-1}; HRMS (ESI) *m/z* = 283.1698 calcd for C$_{19}$H$_{23}$O$_2$ [M–H]$^-$, found 283.1701.

5-(*tert*-Butyl)-3',5'-diisopropyl-2-methyl-[1,1'-biphenyl]-4,4'-diol **(2.33)**.

Following the general procedure (reaction for 2 d at 50 °C), the *para-para* product was

obtained in 47% yield (90% based on recovered starting material): ^{1}H NMR (500 MHz,

CDCl$_3$) δ 7.14 (s, 1H), 7.00 (s, 2H), 6.59 (s, 1H), 4.76 (s, 1H), 4.69 (s, 1H), 3.20 (septet, *J*

= 7.0 Hz, 2H), 2.19 (s, 3H), 1.42 (s, 9H), 1.29 (d, *J* = 7.0 Hz, 12H); ^{13}C NMR (125 MHz,

CDCl$_3$) δ 152.8, 148.6, 134.8, 134.2, 133.4, 133.1, 128.8, 124.7, 118.2, 34.2, 29.8, 27.2,

22.8, 19.9; IR (film) 3409, 2919, 1611, 1466, 1385, 1096 cm^{-1}; HRMS (ESI) *m/z* =

339.2324 calcd for C$_{23}$H$_{31}$O$_2$ [M–H]⁻, found 339.2326.
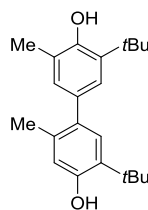
3',5-Di-*tert*-butyl-2,5'-dimethyl-[1,1'-biphenyl]-4,4'-diol **(2.34)**. Following the

general procedure (reaction for 1 d at 70 °C), the *para-para* product was obtained in 77%

yield: ^{1}H NMR (500 MHz, CDCl$_3$) δ 7.12 (s, 1H), 7.09 (d, *J* = 2.0 Hz, 1H), 6.95 (d, *J* =

2.0 Hz, 1H), 6.58 (s, 1H), 4.75 (s, 1H), 4.69 (s, 1H), 2.93 (s, 3H), 2.20 (s, 3H), 1.44 (s,

9H), 1.42 (s, 9H); ^{13}C NMR (125 MHz, CDCl$_3$) δ 152.8, 151.3, 135.0, 134.5, 134.1,

133.6, 133.4, 129.4, 128.9, 126.5, 122.6, 118.2, 34.6, 34.2, 29.9, 29.8, 19.9, 16.1; IR

107

(film) 3513, 2956, 1610, 1387, 1327, 1263, 1192, 1034 cm^{-1}; HRMS (ESI) m/z = 325.2168 calcd for C$_{22}$H$_{29}$O$_2$ [M–H]$^-$, found 325.2168.
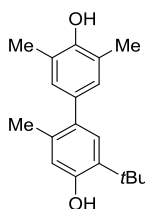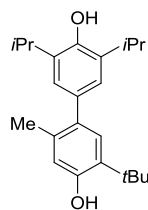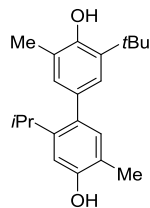

3'-(*tert*-Butyl)-2-isopropyl-5,5'-dimethyl-[1,1'-biphenyl]-4,4'-diol (**2.35**).

Following the general procedure (reaction for 1 d at 70 °C), the *para-para* product was obtained in 74% yield: ^{1}H NMR (500 MHz, CDCl$_3$) δ 7.04 (d, J = 2.0 Hz, 1H), 6.95 (s, 1H), 6.91 (d, J = 2.0 Hz, 1H), 6.78 (s, 1H), 4.76 (s, 1H), 4.70 (brs, 1H), 3.03 (ddd, J = 7.0 Hz, 1H), 2.29 (s, 3H), 2.24 (s, 3H), 1.44 (s, 9H), 1.14 (d, 6H, J = 7.0 Hz); IR (film) 3387, 2918, 1616, 1434, 1141 cm^{-1}; HRMS (ESI) m/z = 311.2011 calcd for C$_{21}$H$_{27}$O$_2$ [M–H]$^-$, found 311.2011.
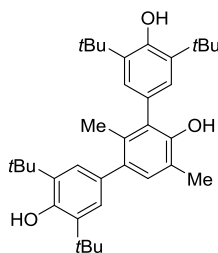
3,3'',5,5''-Tetra-*tert*-butyl-2',5'-dimethyl-[1,1':3',1''-terphenyl]-4,4',4''-triol

(**2.38**). Following the general procedure (reaction for 1 d at 70 °C), the trimer was obtained in 46% yield: ^{1}H NMR (500 MHz, CDCl$_3$) δ 7.13 (s, 2H), 7.12 (s, 2H), 7.06 (s, 1H), 5.31 (s, 1H), 5.16 (s, 1H), 4.99 (s, 1H), 2.30 (s, 3H), 1.94 (s, 3H), 1.47 (s, 18H), 1.46 (s, 18H); ^{13}C NMR (125 MHz, CDCl$_3$) δ 153.6, 152.4, 150.2, 137.1, 135.2, 135.0, 133.4,

108

132.2, 131.4, 128.8, 126.9, 126.5, 126.3, 120.9, 34.5, 34.4, 30.5, 30.4, 18.7, 15.9; IR (film) 3530, 2959, 1639, 1436, 1233, 1154, 879, 740 cm^{-1}; HRMS (ESI) m/z = 529.3682 calcd for $C_{36}H_{49}O_3$ [M–H]$^-$, found 529.3674.
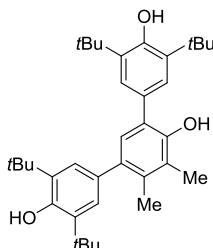
3,3'',5,5''-Tetra-tert-butyl-5',6'-dimethyl-[1,1':3',1''-terphenyl]-4,4',4''-triol (2.39). Following the general procedure (reaction for 1 d at 70 °C), the trimer was obtained in 44% yield: ^{1}H NMR (500 MHz, CDCl$_3$) δ 7.27 (s, 2H), 7.13 (s, 2H), 7.04 (s, 1H), 5.42 (s, 1H), 5.31 (s, 1H), 5.17 (s, 1H), 2.31 (s, 3H), 2.24 (s, 3H), 1.46 (s, 36H); ^{13}C NMR (125 MHz, CDCl$_3$) δ 149.5, 137.1, 135.4, 133.5, 128.7, 126.6, 126.1, 34.7, 34.6, 30.6, 30.5, 17.9, 12.8; IR (film) 3443, 2960, 2101, 1635, 1428, 1232, 1154, 1119, 1077, 739 cm^{-1}; HRMS (ESI) m/z = 529.3682 calcd for $C_{36}H_{49}O_3$ [M–H]$^-$, found 529.3670.
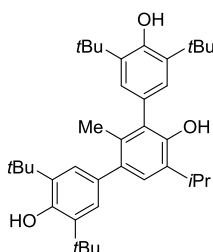
3,3'',5,5''-Tetra-tert-butyl-5'-isopropyl-2'-methyl-[1,1':3',1''-terphenyl]-4,4',4''-triol (2.40). Following the general procedure (reaction for 1 d at 70 °C), the trimer was obtained in 45% yield: ^{1}H NMR (500 MHz, CDCl$_3$) δ 7.16 (s, 2H), 7.15 (s,

1H), 7.14 (s, 2H), 5.31 (s, 1H), 5.17 (s, 1H), 5.02 (s, 1H), 3.34 (sept, J = 7.0 Hz, 1H), 1.93 (s, 3H), 1.48 (s, 18H), 1.46 (s, 18H), 1.30 (d, J = 7.0 Hz, 6H); ^{13}C NMR (125 MHz, CDCl$_3$) δ 153.6, 152.4, 149.3, 137.1, 135.2, 135.0, 133.8, 132.2, 131.3, 129.0, 127.0, 126.6, 126.4, 34.6, 34.5, 30.5, 30.4, 27.3, 22.7, 18.7; IR (film) 3465, 2100, 1636, 1385, 1234, 1156, 1096, 679 cm^{-1}; HRMS (ESI) m/z = 557.3995 calcd for C$_{38}$H$_{53}$O$_3$ [M–H]$^-$, found 557.3976.
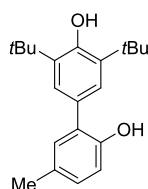

3',5'-Di-*tert*-butyl-5-methyl-[1,1'-biphenyl]-2,4'-diol (2.41dimer). Following the general procedure (reaction for 18 hours at 80 °C), the dimer was separated from trimer and obtained in 42% yield: ^{1}H NMR (500 MHz, CDCl$_3$) δ 7.23 (s, 2H), 7.04 (d, J = 8.5 Hz, 2H), 6.89 (d, J = 7.5 Hz, 1H), 5.31 (s, 1H), 5.15 (s, 1H), 2.32 (s, 3H), 1.47 (s, 18H); ^{13}C NMR (125 MHz, CDCl$_3$) δ 153.6, 150.4, 136.9, 130.7, 129.7, 129.0, 128.7, 127.9, 125.7, 115.2, 34.5, 30.3, 20.5; IR (film) 3635, 3541, 2958, 1632, 1438, 1235, 1156, 909, 734 cm^{-1}; HRMS (ESI) m/z = 311.2011 calcd for C$_{21}$H$_{27}$O$_2$ [M–H]$^-$, found 311.2002.

3,3'',5,5''-Tetra-tert-butyl-5'-methyl-[1,1':3',1''-terphenyl]-2',4,4''-triol (**2.41 trimer**). Following the general procedure (reaction for 18 hours at 80 °C), the trimer was separated from dimer and obtained in 53% yield: ^{1}H NMR (500 MHz, CDCl$_3$) δ 7.35 (s, 4H), 7.05 (s, 2H), 5.38 (s, 1H), 5.28 (s, 2H), 2.36 (s, 3H), 1.48 (s, 36H); ^{13}C NMR (125 MHz, CDCl$_3$) δ 153.4, 147.2, 136.1, 129.9, 129.1, 128.7, 127.2, 126.1, 34.5, 30.3, 20.6; IR (film) 3442, 2960, 2100, 1642, 1437, 1398, 1233, 1155, 1120, 739 cm^{-1}; HRMS (ESI) m/z = 517.3682 calcd for C$_{35}$H$_{49}$O$_3$ [M+H]$^+$, found 517.3682.
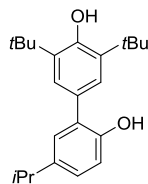
3',5'-Di-*tert*-butyl-5-isopropyl-[1,1'-biphenyl]-2,4'-diol (2.42dimer). Following the general procedure (reaction for 18 hours at 80 °C), the dimer was separated from trimer and obtained in 35% yield: ^{1}H NMR (500 MHz, CDCl$_3$) δ 7.24 (s, 2H), 7.11 (dd, J = 8.2 Hz, 2.2 Hz, 1H), 7.08 (d, J = 2.2 Hz, 1H), 6.92 (d, J = 8.2 Hz, 1H), 5.32 (s, 1H), 5.16 (s, 1H), 2.89 (quint, J = 6.9 Hz, 1H), 1.48 (s, 18H), 1.27 (d, J = 6.9 Hz, 6H); ^{13}C NMR (125 MHz, CDCl$_3$) δ 153.6, 150.6, 141.0, 136.9, 128.6, 128.2, 128.1, 126.4, 125.8,

115.2, 34.5, 33.4, 30.3, 24.2; IR (film) 3637, 3546, 2958, 1497, 1437, 1234, 1156, 883, 734 cm^{-1}; HRMS (ESI) m/z = 363.2300 calcd for $C_{23}H_{32}O_2Na$ [M+Na]$^+$, found 363.2301.
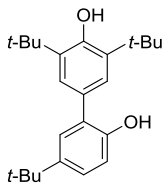
3',5,5'-Tri-*tert*-butyl-[1,1'-biphenyl]-2,4'-diol (2.43dimer). Following the general procedure (reaction for 18 hours at 80 °C), the dimer was separated from trimer and obtained in 31% yield: ^{1}H NMR (500 MHz, CDCl$_3$) δ 7.27 (dd, J = 8.0 Hz, 2.0 Hz, 1H), 7.25 (s, 2H), 7.23 (d, J = 2.0 Hz, 1H), 6.93 (d, J = 8.0 Hz, 1H), 5.33 (s, 1H), 5.16 (s, 1H), 1.48 (s, 18H), 1.33 (s, 9H); ^{13}C NMR (125 MHz, CDCl$_3$) δ 153.6, 150.3, 143.2, 136.9, 128.3, 127.1, 125.9, 125.5, 114.8, 34.5, 34.2, 31.6, 30.3; IR (film) 3638, 3544, 2958, 1437, 1393, 1156, 884, 821, 740 cm^{-1}; HRMS (ESI) m/z = 353.2481 calcd for $C_{24}H_{33}O_2$ [M–H]$^-$, found 353.2478.

3,3'',5,5',5''-Penta-tert-butyl-[1,1':3',1''-terphenyl]-2',4,4''-triol (2.43trimer). Following the general procedure (reaction for 18 hours at 80 °C), the trimer was separated from dimer and obtained in 14% yield: ^{1}H NMR (500 MHz, CDCl$_3$) δ 7.35 (s, 4H), 7.26 (s, 2H), 5.36 (s, 1H), 5.28 (s, 1H), 1.48 (s, 36H), 1.36 (s, 9H); ^{13}C NMR (125

MHz, CDCl$_3$) δ 153.4, 147.2, 142.8, 136.1, 129.1, 128.7, 126.6, 126.2, 34.5, 31.6, 30.3, 29.4; IR (film) 3530, 2959, 1654, 1438, 1395, 1362, 1232, 1155, 879, 739 cm^{-1}; HRMS (ESI) m/z = 559.4151 calcd for C$_{38}$H$_{55}$O$_3$ [M+H]$^+$, found 559.4152.
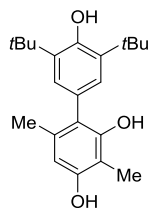
3',5'-Di-*tert*-butyl-3,6-dimethyl-[1,1'-biphenyl]-2,4,4'-triol **(2.44dimer)**. Following the general procedure (reaction for 18 hours at 80 °C), the dimer was separated from trimer and obtained in 38% yield: ^{1}H NMR (500 MHz, CDCl$_3$) δ 7.03 (s, 2H), 6.34 (s, 1H), 5.29 (s, 1H), 5.08 (s, 1H), 4.63 (s, 1H), 2.16 (s, 3H), 2.01 (s, 3H), 1.45 (s, 18H); ^{13}C NMR (125 MHz, CDCl$_3$) δ 153.5, 153.3, 152.0, 136.9, 134.8, 127.2, 126.0, 121.5, 108.2, 107.1, 34.5, 30.4, 20.2, 8.2; IR (film) 3536, 3525, 2959, 1627, 1416, 1234, 1080, 908, 734 cm^{-1}; HRMS (ESI) m/z = 341.2117 calcd for C$_{24}$H$_{29}$O$_3$ [M–H]$^-$, found 341.2115.
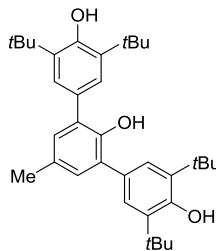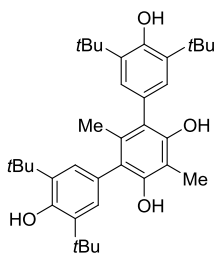

3,3'',5,5''-Tetra-*tert*-butyl-2',5'-dimethyl-[1,1':3',1''-terphenyl]-4,4',4'',6'-tetraol (2.44trimer). Following the general procedure (reaction for 18 hours at 80 °C), the trimer was separated from dimer and obtained in 29% yield: ^{1}H NMR (500 MHz, CDCl$_3$) δ 7.10 (s, 4H), 5.28 (s, 2H), 5.06 (s, 2H), 2.22 (s, 3H), 1.76 (s, 3H), 1.45 (s, 38H);

^{13}C NMR (125 MHz, CDCl$_3$) δ 153.4, 151.2, 136.9, 132.7, 127.4, 126.5, 121.0, 107.1, 34.5, 30.4, 18.4, 8.7; IR (film) 3638, 3531, 2959, 1616, 1438, 1415, 1234, 1085, 909, 734 cm^{-1}; HRMS (ESI) *m/z* = 547.3787 calcd for C$_{36}$H$_{51}$O$_4$ [M+H]$^+$, found 547.3803.
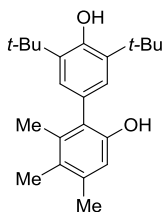
3',5'-Di-*tert*-butyl-4,5,6-trimethyl-[1,1'-biphenyl]-2,4'-diol (2.45). Following the general procedure (reaction for 3 h at 80 °C), the *ortho-para* product was obtained in 85% yield: ^{1}H NMR (500 MHz, CDCl$_3$) δ 7.04 (s, 2H), 6.73 (s, 1H), 5.29 (s, 1H), 4.75 (s, 1H), 2.31 (s, 3H), 2.17 (s, 3H), 2.02 (s, 3H), 1.45 (s, 18H); ^{13}C NMR (125 MHz, CDCl$_3$) δ 153.5, 150.7, 136.9, 136.6, 135.6, 127.1, 126.9, 126.5, 113.6, 34.5, 30.4, 20.8, 17.9, 15.3; IR (film) 3538, 2959, 1576, 1431, 1301, 1142, 1040 cm^{-1}; HRMS (ESI) *m/z* = 363.2300 calcd for C$_{23}$H$_{32}$O$_2$ Na [M+Na]$^+$, found 363.2310.
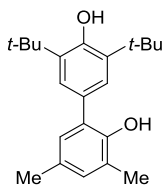
3',5'-Di-*tert*-butyl-3,5-dimethyl-[1,1'-biphenyl]-2,4'-diol (2.46). Following the general procedure (reaction for 15 h at 80 °C), the *ortho-para* product was obtained in 75% yield: ^{1}H NMR (500 MHz, CDCl$_3$) δ 7.22 (s, 2H), 6.93 (s, 1H), 6.87 (s, 1H), 5.30 (s, 1H), 5.22 (s, 1H), 2.29 (s, 3H), 2.28 (s, 3H), 1.47 (s, 18H); ^{13}C NMR (125 MHz, CDCl$_3$) δ

154.6, 148.5, 136.9, 130.6, 129.0, 128.3, 128.2, 128.1, 125.8, 124.1, 34.5, 30.3, 20.5, 16.1;

IR (film) 3623, 2444, 2917, 1436, 1314, 1118 cm^{-1}; HRMS (ESI) m/z = 325.2168 calcd

for C$_{22}$H$_{29}$O$_2$ [M–H]$^-$, found 325.2154.
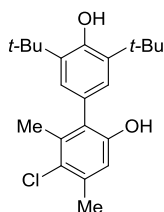
3',5'-Di-*tert*-butyl-5-chloro-4,6-dimethyl-[1,1'-biphenyl]-2,4'-diol **(2.47)**.

Following the general procedure (reaction for 1 d at 80 °C), the *ortho-para* product was

obtained in 72% yield: ^{1}H NMR (500 MHz, CDCl$_3$) δ 7.00 (s, 2H), 6.78 (s, 1H), 5.34 (s,

1H), 4.85 (s, 1H), 2.38 (s, 3H), 2.13 (s, 3H), 1.45 (s, 18H); ^{13}C NMR (125 MHz, CDCl$_3$)

δ 153.8, 151.2, 137.1, 136.2, 135.3, 127.9, 126.8, 126.3, 125.5, 114.5, 34.5, 30.3, 20.9,

18.7; IR (film) 3524, 2961, 1635, 1432, 1308, 1236, 1174, 1048, 889, 854, 741 cm^{-1};

HRMS (ESI) m/z = 359.1778 calcd for C$_{22}$H$_{28}$O$_2$Cl [M–H]$^-$, found 359.1779.
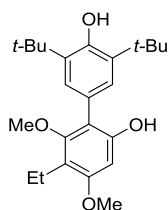
3',5'-Di-*tert*-butyl-5-ethyl-4,6-dimethoxy-[1,1'-biphenyl]-2,4'-diol **(2.48)**.

Following the general procedure (reaction for 1 d at 80 °C), the *ortho-para* product was

obtained in 80% yield: ^{1}H NMR (500 MHz, CDCl$_3$) δ 7.17 (s, 2H), 6.39 (s, 1H), 5.30 (s,

1H), 5.15 (s, 1H), 3.83 (s, 3H), 3.33 (s, 3H), 2.63 (q, J = 7.5 Hz, 2H), 1.45 (s, 18H), 1.15

(t, J = 7.5 Hz, 3H); ^{13}C NMR (125 MHz, CDCl$_3$) δ 158.2, 156.7, 153.5, 152.1, 136.8,

127.3, 123.3, 117.8, 114.9, 94.3, 61.0, 55.6, 34.4, 30.4, 17.0, 14.9; IR (film) 3436, 2960,

1620, 1434, 1233, 1119, 738 cm^{-1}; HRMS (ESI) m/z = 387.2535 calcd for C$_{24}$H$_{35}$O$_4$

[M+H]$^+$, found 387.2530.

1-(3,5-Di-*tert*-butyl-4-hydroxyphenyl)naphthalen-2-ol **(2.49)**. Following the

general procedure (reaction for 1 d at 80 °C), the *ortho-para* product was obtained in 83%

yield: ^{1}H NMR (500 MHz, CDCl$_3$) δ 7.81 (d, J = 8.0 Hz, 1H), 7.79 (d, J = 8.5 Hz, 1H),

7.47 (d, J = 8.0 Hz, 1H), 7.37-7.32 (m, 3H), 7.19 (s, 2H), 5.39 (s, 1H), 5.32 (s, 1H), 1.48

(s, 18H); ^{13}C NMR (125 MHz, CDCl$_3$) δ 154.0, 150.4, 137.2, 133.7, 129.0, 128.9, 128.0,

127.6, 126.3, 124.9, 124.4, 123.1, 121.9, 117.2, 34.6, 30.4; IR (film) 3629, 3525, 2959,

1610, 1441, 1389, 1149, 889, 819, 742 cm^{-1}; HRMS (ESI) m/z = 348.2089 calcd for

C$_{24}$H$_{28}$O$_2$ [M]$^+$, found 348.2098.
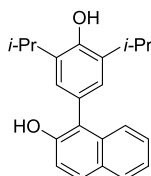
1-(4-Hydroxy-3,5-diisopropylphenyl)naphthalen-2-ol **(2.50)**. Following the

general procedure (reaction for 1 d at 80 °C), the *ortho-para* product was obtained in 74%

yield: ^{1}H NMR (500 MHz, CDCl$_3$) δ 7.81 (d, J = 8.5 Hz, 1H), 7.80 (d, J = 9.5 Hz, 1H),

7.46 (d, J = 8.0 Hz, 1H), 7.37-7.32 (m, 2H), 7.27 (d, J = 9.0 Hz, 1H), 7.10 (s, 2H), 5.30

(s, 1H), 4.98 (s, 1H), 3.24 (septet, J = 7.0 Hz, 2H), 1.30 (dd, J = 4.0 Hz, 6.0 Hz, 12H);

^{13}C NMR (125 MHz, CDCl$_3$) δ 150.3, 150.1, 135.0, 133.6, 129.1, 128.9, 128.0, 126.3,

126.2, 125.5, 124.8, 123.1, 121.6, 117.1, 27.3, 22.8, 22.7; HRMS (ESI) m/z = 320.1776

calcd for C$_{22}$H$_{24}$O$_2$ [M]$^+$, found 320.1780.
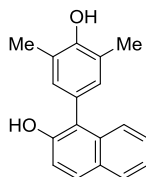
1-(4-Hydroxy-3,5-dimethylphenyl)naphthalen-2-ol **(2.51)**. Following the

general procedure (reaction for 1 d at 80 °C), the *ortho-para* product was obtained in 65%

yield: ^{1}H NMR (500 MHz, CDCl$_3$) δ 7.80 (d, J = 7.5 Hz, 1H), 7.79 (d, J = 9.0 Hz, 1H),

7.46 (d, J = 8.0 Hz, 1H), 7.34-7.31 (m, 2H), 7.25 (d, J = 9.0 Hz, 1H), 7.03 (s, 2H), 5.24

(s, 1H), 4.79 (s, 1H), 2.33 (s, 6H); ^{13}C NMR (125 MHz, CDCl$_3$) δ 152.4, 150.3, 133.6,

131.2, 129.1, 128.9, 128.0, 127.0, 126.3, 124.8, 124.3, 123.1, 121.9, 117.2, 16.0; HRMS

(ESI) m/z = 264.1150 calcd for C$_{18}$H$_{16}$O$_2$ [M]$^+$, found 264.1148.
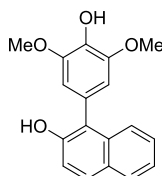
1-(4-Hydroxy-3,5-dimethoxyphenyl)naphthalen-2-ol **(2.52)**. Following the

general procedure (reaction for 2 d at 80 °C), the *ortho-para* product was obtained in 72%

yield: ^{1}H NMR (500 MHz, CDCl$_3$) δ 7.82 (d, J = 5.0 Hz, 1H), 7.80 (d, J = 6.5 Hz, 1H),

7.47 (d, *J* = 8.5 Hz, 1H), 7.39-7.34 (m, 2H), 7.27 (d, *J* = 9.0 Hz, 1H), 6.64 (s, 2H), 5.70 (s, 1H), 5.30 (s, 1H), 3.90 (s, 6H); ^{13}C NMR (125 MHz, CDCl$_3$) δ 150.3, 148.0, 134.7, 133.5, 129.4, 128.8, 128.0, 126.5, 124.6, 124.5, 123.3, 121.0, 117.2, 107.4, 56.4; IR (film) 3466, 1620, 1518, 1465, 1393, 1335, 1212, 1114, 817, 735, 634 cm^{-1}; HRMS (ESI) *m/z* = 297.1127 calcd for C$_{18}$H$_{17}$O$_4$ [M+H]$^+$, found 297.1132.
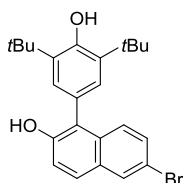
6-Bromo-1-(3,5-di-*tert*-butyl-4-hydroxyphenyl)naphthalen-2-ol **(2.53)**.

Following the general procedure (reaction for 1 d at 80 °C), the *ortho-para* product was obtained in 88% yield: ^{1}H NMR (500 MHz, CDCl$_3$) δ 7.95 (d, *J* = 1.5 Hz, 1H), 7.69 (d, *J* = 9.0 Hz, 1H), 7.41 (dd, *J* = 9.0 Hz, 2.0 Hz, 1H), 7.34 (d, *J* = 9.0 Hz, 1H), 7.28 (d, *J* = 9.0 Hz, 1H), 7.15 (s, 2H), 5.42 (s, 1H), 5.35 (s, 1H), 1.47 (s, 18H); ^{13}C NMR (125 MHz, CDCl$_3$) δ 154.1, 150.7, 137.3, 132.2, 130.0, 129.8, 129.5, 128.0, 127.5, 126.8, 123.8, 122.1, 118.3, 116.9, 34.5, 30.3; IR (film) 3498, 2962, 2102, 1638, 1502, 1437, 1362, 1236, 883, 738 cm^{-1}; HRMS (ESI) *m/z* = 425.1116 calcd for C$_{24}$H$_{26}$O$_2$Br [M–H]$^-$, found 425.1113.

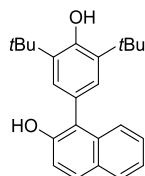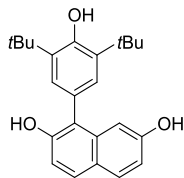**1-(3,5-Di-*tert*-butyl-4-hydroxyphenyl)naphthalene-2,7-diol** **(2.54)**. Following the general procedure (reaction for 1 d at 80 °C), the *ortho-para* product was obtained in 88% yield: ^{1}H NMR (500 MHz, CDCl$_3$) δ 7.71 (d, J = 2.5 Hz, 1H), 7.70 (d, J = 3.0 Hz, 1H), 7.16 (s, 2H), 7.16 (s, 2H), 7.11 (d, J = 9.0 Hz, 1H), 6.93 (dd, J = 9.0 Hz, 2.0 Hz, 1H), 6.74 (d, J = 2.0 Hz, 1H), 5.39 (s, 1H), 5.26 (s, 1H), 4.88 (s, 1H), 1.47 (s, 18H); ^{13}C NMR (125 MHz, CDCl$_3$) δ 154.0, 151.1, 137.3, 135.2, 130.0, 128.9, 127.5, 124.5, 124.3, 120.7, 114.8, 114.6, 107.1, 34.5, 30.4; IR (film) 3498, 2959, 1625, 1516, 1434, 1172, 831, 738 cm^{-1}; HRMS (ESI) m/z = 363.1960 calcd for C$_{24}$H$_{27}$O$_3$ [M–H]$^-$, found 363.1946.
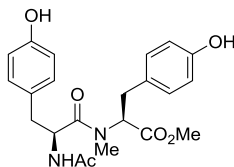
Methyl *N*-(acetyl-*L*-tyrosyl)-*N*-methyl-*L*-tyrosinate **(2.69)**. Ac-Tyr-OH (460 mg, 2 mmol) was dissolved in DMF (2 mL, 1.0 M) in an ice-water bath. H-Tyr-OMe (280 mg, 1 mmol) was added to the reaction mixture, followed immediately by di-chlorohexylcarbodiimide (206 mg, 1.0 equiv) and hydroxybenzotriazole (135 mg, 1.0 equiv). The reaction mixture was allowed to come to room temperature and stirred for 24 h. Dicyclohexylurea was filtered off. The organic layer was washed with 2 N HCl (5 mL), brine (5 mL), 1 N Na$_2$CO$_3$ (5 mL), respectively. Then dried over anhydrous sodium

sulfate, and evaporated in vacuo to yield dipeptide (250 mg, 0.55 mmol) as a white solid. Spectral data matched that reported in the literature.[53]
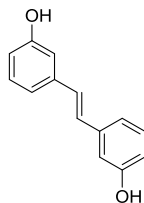
(*E*)-3,3'-(Ethene-1,2-diyl)diphenol (2.76). To a solution of zinc (dust, 2.1 g, 8.0 equiv) in dry THF (15 mL) was added $TiCl_4$ (1.3 mL, 3.0 equiv) dropwise at 0 °C under argon atmosphere. After addition was complete, reaction mixture was refluxed for 2 h and then cooled back to 0 °C. A solution of 3-hydroxybenzaldehyde (488 mg, 4.0 mmol) in dry THF (5 mL) was added to this ice cooled reaction mixture slowly portion wise over 20 minutes and then reaction mixture was allowed to reflux for 6 h. The reaction mixture was then concentrated using rotary evaporator and residue was dissolved in ethyl acetate (15 mL). To this solution saturated K_2CO_3 solution (15 mL) was added and allowed to stir for another 7 h. To remove the undissolved salts, the mixture was filtered and the residue was washed with ethyl acetate (7 mL). The ethyl acetate layer was collected and the aqueous layer was further extracted with ethyl acetate (5 mL). The combined ethyl acetate layers were washed sequentially with brine (10 mL) and water (10 mL), dried over anhydrous Na_2SO_4 and concentrated in vacuo. The crude product was purified by flash chromatography (hexane/EtOAc, 5:1) to give (*E*)-3,3'-(ethene-1,2-

diyl)diphenol (376 mg, 1.77 mmol) as a light brown solid in 89% yield. Spectral data

matched that reported in the literature.[80]
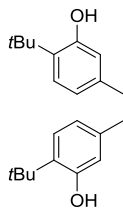
5,5'-(Ethane-1,2-diyl)bis(2-(*tert*-butyl)phenol) (2.78). To a solution of 3,3'-

(ethane-1,2-diyl)diphenol (166 mg, 0.77 mmol) in CH_2Cl_2 (4 mL, 0.2 M) at 0 °C was

added *tert*-butanol (62 mg, 2.4 equiv) and conc. H_2SO_4 (80 mg, 2.4 equiv). The reaction

was allowed to warm to room temperature and stirred for 24 h. It was quenched with

$NaHCO_3$ (5 mL) and the organic layer was separated. The aqueous layer was extracted

with CH_2Cl_2 (3 x 5 mL) and the combined organic fractions were dried over $MgSO_4$,

concentrated and purified by column chromatography (hexane/EtOAc, 8:1). The product

was obtained in 50% yield as a white solid. ^1H NMR (500 MHz, $CDCl_3$) δ 7.19 (d, J =

8.0 Hz, 2H), 6.74 (dd, J = 8.0 Hz, 1.5 Hz, 2H), 6.52 (d, J = 1.5 Hz, 2H), 4.71 (s, 2H),

2.81 (s, 4H), 1.41 (s, 18H).

(80) Baskin, R.; Gali, M.; Park, S. O.; Zhao, Z, J.; Keseru, G. M.; Bisht, K. S.; Sayeski, P. P. "Identification of novel SAR properties of the Jak2 small molecule inhibitor G6: Significance of the *para*-hydroxyl orientation" *Bioorg. Med. Chem. Lett.* **2012**, *22*, 1402-1407.
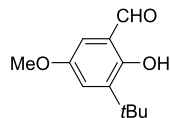
3-(*tert*-Butyl)-2-hydroxy-5-methoxybenzaldehyde. A mixture of 3-*tert*-butyl-4-hydroxyanisole (736 mg, 4.0 mmol) and hexamethylenetetramine (1.13 g, 8.0 mmol) dissolved in glacial acetic acid (4 mL) was heated at 110 °C for 2h. After disappearance of 3-*tert*-butyl-4-hydroxyanisole was confirmed, aqueous H_2SO_4 solution (33 %, 4 mL) was added at 75 °C. The resulting mixture was heated at 110 °C for 3 h. The mixture was extracted with diethyl ether (10 mL), and the extract was washed with water (2×10 mL), saturated Na_2CO_3 solution (2×10 mL) and saturated NaCl solution (10 mL). The organic layer was dried over $MgSO_4$, and then the solvent was removed by evaporation under reduced pressure. The crude mixture was purified by flash chromatography (hexane/EtOAc, 20:1) to give clear liquid of product (616 mg, 2.96 mmol) in 74% yield: ^{1}H NMR (500 MHz, CDCl3) δ 11.50 (s, 1H), 9.84 (s, 1H), 7.17 (d, *J* = 3.0 Hz, 1H), 6.82 (d, *J* = 3.0 Hz, 1H), 3.81 (s, 3H), 1.41 (s, 9H). Spectral data matched that reported in the literature.[81]

---

(81) Kurahashi, T.; Fujii, H. "One-Electron Oxidation of Electronically Diverse Manganese(III) and Nickel(II) Salen Complexes: Transition from Localized to Delocalized Mixed-Valence Ligand Radicals" *J. Am. Chem. Soc.* **2011***, 133,* 8307–8316.

Representative Procedure for the Preparation of Salen Ligands
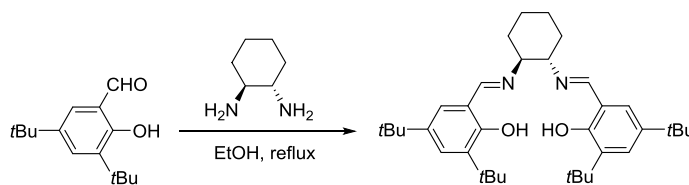
The salicylaldehyde **2.86** (4.1 g, 1.75 mol) was added as a solid to a solution to the diamine **2.87** (1.0 g, 0.88 mol) in absolute ethanol (43 mL, 0.2 M). The mixture was heated to reflux for 1 h under an Ar atmosphere. And then, water (10 mL) was added dropwise to the cooled bright yellow solution. The resulting yellow crystalline solid was collected by filtration and washed with a small portion of 95% ethanol. The resultant material was recrystallized using a 1:1 mixture of methanol and ethyl acetate to yield the salen ligand **2.88** as a yellow solid (4.3 g, 90% yield). Spectral data matched that reported in the literature.[82]

General Procedure for the Reduction of Salens to Salans

To a solution of the salen in THF:MeOH (1:1), sodium borohydride (10 equiv) was slowly added. The mixture was stirred at room temperature for 2 h (with a change of the solution color from yellow to colorless, except in the cases of nitro derivatives). The mixture was quenched with water and extracted with dichloromethane. The combined organic layers were washed with brine, dried over Na_2SO_4, filtered and concentrated to yield the salan ligand as a solid.

---

(82) Bergbreiter, D.; Hobbs, C.; Hongfa, C. "Polyolefin-Supported Recoverable/Reusable Cr(III)-Salen Catalysts" *J. Org. Chem.* **2011**, *76*, 523–533.

Representative Procedure for Preparation of Chromium Catalyst
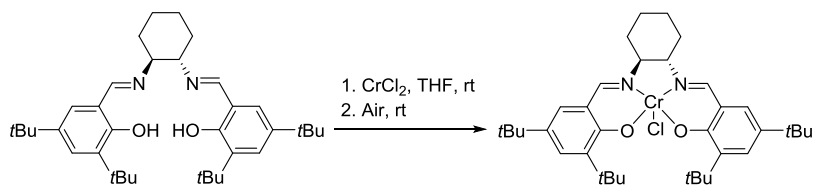
The salen ligand **2.88** (500 mg, 0.91 mmol) and CrCl$_2$ (123 mg, 1.0 mmol, 1.1 equiv) were dissolved in THF (18 mL, 0.05 M). The mixture was stirred under argon at ambient temperature for 3 h. Then the reaction mixture was exposed to air and stirred for an additional 3 h. The reaction mixture was poured into TBME (15 mL), washed with aqueous saturated NH$_4$Cl (3 × 30 mL) and brine (3 × 30 mL), followed by drying with Na$_2$SO$_4$. After filtration, the mixture was concentrated *in vacuo* to yield the chromium catalyst (535 mg, 93% yield). The Cr-Salen-Cy catalyst was further recrystallized from CH$_3$CN.

Cr-Salen-Cy. Dark brown solid; HRMS (ESI) *m/z* = 596.3434 calcd for C$_{38}$H$_{64}$N$_2$O$_4$Cr [M–Cl]$^+$, found 596.2793.
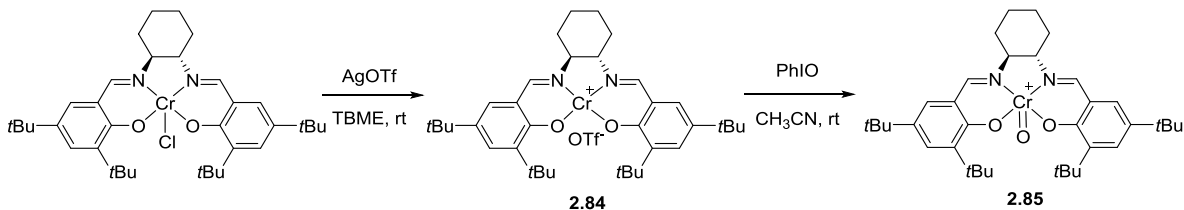
The Cr-Salen-Cy catalyst (100 mg, 0.16 mmol) was dissolved in TBME (1.7 mL, 0.1 M) and treated with solid AgOTf (40 mg, 0.16 mmol). The reaction flask was wrapped with aluminum foil and stirred at rt for 5 h. The resulting mixture was filtered

through Celite. Solvent removal by rotary evaporation afforded 106 mg (0.14 mmol, 90% yield) of **2.84** as a brown solid which was used without further purification: The oxochromium(V) salt **2.85** was prepared from **2.84** in acetonitrile (2.84 mL, 0.05 M) with 37 mg (0.17 mmol, 1.2 equiv) of iodosylbenzene. The suspension was stirred for 30 min, and the dark brown-black solution was filtered to remove unreacted iodosylbenzene. Anhydrous ether (7 mL) was slowly added to the dark filtrate in order to precipitate crystals, and the oxochromium(V) complex **2.85** (80 mg, 0.13 mmol) was isolated as a flaky black solid by filtration.

Kinetic Analysis of Cross-Coupling

General Procedure. For accessing the order of species X, three to five reactions of varying [X] were set up in parallel. For each reaction, in an oven dried 25 mL round bottomed flask equipped with a stir bar and reflux condenser was added Cr-Salen-Cy catalyst, 2,6-di-*tert*-butylphenol, 3,4,5-trimethylphenol, and biphenyl (internal standard) in the amounts illustrated in the tables below. To this mixture was subsequently added chloroform-d (0.1 M). Oxygen was added *via* active purge and the reaction mixture was heated to reflux under oxygen atmosphere. For each of the parallel reactions, aliquots of 50 µL were taken every 10~30 minutes over the course. The 50 µL aliquot was immediately diluted with additional 500 µL of chloroform-d and analyzed by ^{1}H NMR. A graph of [product] vs. time was plotted for the different concentration of reaction component X. A linear trend representing the first 15% conversion was fitted to determine the initial rate of the reaction component X. Theses initial rate values vs. [X] in order to determine the order of the reaction in component X.

Order in Cr-Salen-Cy catalyst. In each oven dried 25 mL round bottomed flask equipped with a stir bar and reflux condenser was added 2,6-di-*tert*-butylphenol (103.2 mg, 0.5 mmol, 1.0 equiv), 3,4,5-trimethylphenol (68.1 mg, 0.5 mmol, 1.0 equiv), and biphenyl (38.6 mg, 0.25 mmol, 0.5 equiv). To this mixture was subsequently added chloroform-*d* (5.0 mL, 0.1 M). Finally, 6.3 mg (0.01 mmol, 2 mol%), 9.5 mg (0.015 mmol, 3 mol%), 15.8 mg (0.025 mmol, 5 mol%), 22.1 mg (0.035 mmol, 7 mol%), 31.6 mg (0.05 mmol, 10 mol%) of Cr-Salen-Cy catalyst was added, respectively, in each of the flasks. The reaction flasks were left to stir at 80 °C and aliquots were taken and the data analyzed according to the general procedure described above.
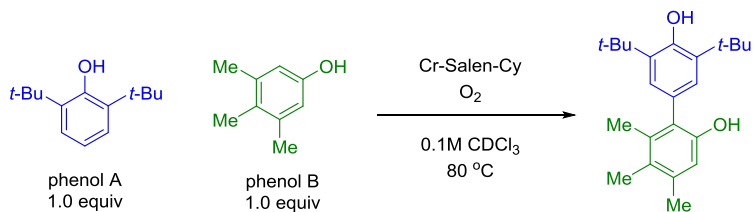
Table 2.10 Concentration of Components in the Cross-Coupling Reaction in Catalyst

1. 2 mol% Cr-Salen-Cy

time (min)	[Product] (M)	[phenol A] (M)	[phenol B] (M)
20	0.00400	0.09600	0.09700
40	0.00900	0.09100	0.09100
60	0.01200	0.08700	0.08600
90	0.01900	0.08000	0.07900
120	0.02300	0.07700	0.07600
150	0.03000	0.06900	0.06600

time (min)			
240	0.04700	0.05300	0.05000

2. 3 mol% Cr-Salen-Cy

time (min)	[Product] (M)	[phenol A] (M)	[phenol B] (M)
20	0.01100	0.08900	0.08800
40	0.01900	0.08200	0.07800
60	0.03400	0.06700	0.06300
90	0.03700	0.06400	0.05800
120	0.04900	0.05100	0.04700
180	0.06100	0.03800	0.03400

3. 5 mol% Cr-Salen-Cy

time (min)	[Product] (M)	[phenol A] (M)	[phenol B] (M)
10	0.01000	0.09000	0.08900
20	0.01500	0.08500	0.08400
30	0.02500	0.07500	0.07100
40	0.03600	0.06400	0.06000
60	0.05100	0.04900	0.04500
90	0.05500	0.04500	0.04300
120	0.06800	0.02600	0.01900
240	0.07000	0.00000	0.00000

4. 7 mol% Cr-Salen-Cy

time (min)	[Product] (M)	[phenol A] (M)	[phenol B] (M)

10	0.01400	0.08600	0.08400
20	0.02800	0.07100	0.06700
30	0.04100	0.05700	0.05100
40	0.05100	0.04800	0.04300
60	0.06800	0.03200	0.02500
90	0.08800	0.00600	0.00500
120	0.07900	0.00000	0.00000

5. 10 mol% Cr-Salen-Cy

time (min)	[Product] (M)	[phenol A] (M)	[phenol B] (M)
10	0.02900	0.07200	0.07000
20	0.03200	0.06700	0.06200
30	0.05000	0.04900	0.04300
40	0.05800	0.04300	0.03200
60	0.08800	0.01100	0.00600
90	0.08800	0.00800	0.00300
240	0.02600	0.00000	0.00000

Table 2.11 Initial Rates for Order in Catalyst

Concentration (M)	Initial Rate (M/s)
0.002	3.48333E-06
0.003	8.98333E-06
0.005	1.43833E-05
0.007	2.30000E-05
0.01	2.50000E-05

Order in Cr-Salen-Cy catalyst.with 2-Naphthol The reaction flasks were set up in the same way above and left to stir for 30 min at 80 °C and aliquots were taken and the data analyzed according to the general procedure described above.

Table 2.12 Initial Rate in Cross-Coupling with 2-Naphthol
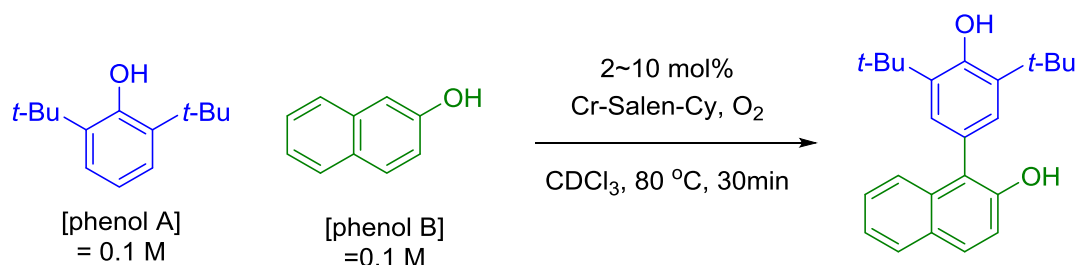
[Cr-Salen-Cy] (M)	Initial Rate (mol/Ls)	Ln[Cr-Salen-Cy]	Ln(initial rate Product)
0.002	0.000606061	-6.214608098	-7.408530567
0.003	0.000424242	-5.80914299	-7.765205511
0.005	0.000909091	-5.298317367	-7.003065459
0.007	0.000909091	-4.96184513	-7.003065459
0.01	0.001565657	-4.605170186	-6.459450012

Order in 2,6-di-tert-butylphenol. In each oven dried 25 mL round bottomed flask equipped with a stir bar and reflux condenser was added Cr-Salen-Cy catalyst (9.5 mg, 0.015 mmol, 0.05 equiv), 3,4,5-trimethylphenol (40.9 mg, 0.3 mmol, 1.0 equiv), and biphenyl (23.1 mg, 0.15 mmol, 0.5 equiv). To this mixture was subsequently added chloroform-*d* (3.0 mL, 0.1 M). Finally, 61.9 mg (0.3 mmol, 1 equiv), 123.8 mg (0.6 mmol, 2 equiv), 310 mg (1.5 mmol, 5 equiv), 619 mg (3.0 mmol, 10 equiv) of 2,6-di-*tert*-butylphenol was added, respectively, in each of the flasks. The reaction flasks were left to

stir at 80 °C and aliquots were taken and the data analyzed according to the general procedure described above.

Table 2.13 Concentration of Components in the Cross-Coupling Reaction

1. 1 equiv 2,6-di-*tert*-butylphenol

time (min)	Product (M)	phenolA (M)	phenolB (M)
10	0.01000	0.09000	0.08900
20	0.01500	0.08500	0.08400
30	0.02500	0.07500	0.07100
40	0.03600	0.06400	0.06000
60	0.05100	0.04900	0.04500
90	0.05500	0.04500	0.04300
240	0.07000	0.00000	0.00000

2. 2 equiv of 2,6-di-*tert*-butylphenol

time (min)	Product (M)	Phenol A (M)	Phenol B (M)
20	0.01500	0.18000	0.08600
40	0.02800	0.17000	0.07500
60	0.04600	0.15600	0.05600
90	0.06900	0.12700	0.03400
120	0.08200	0.11400	0.01900
150	0.09400	0.08500	0.00000
180	0.07800	0.06600	0.00000

3. 5 equiv of 2,6-di-*tert*-butylphenol

time (min)	Product (M)	Phenol A (M)	Phenol B (M)
20	0.01700	0.46600	0.08300
40	0.02700	0.45400	0.07300
60	0.04400	0.44800	0.05600
120	0.08600	0.39500	0.01200
150	0.08800	0.39100	0.00900
180	0.09300	0.31500	0.00000

4. 10 equiv of 2,6-di-*tert*-butylphenol

time (min)	Product (M)	Phenol A (M)	Phenol B (M)
20	0.11000	0.99000	0.08400
40	0.02200	1.00500	0.07200
60	0.03700	0.97400	0.05000
90	0.06700	0.91700	0.02500
120	0.08000	0.88500	0.01200
210	0.09300	0.83800	0.00000

Order in 3,4,5-trimethylphenol. In each oven dried 25 mL round bottomed flask equipped with a stir bar and reflux condenser was added Cr-Salen-Cy catalyst (9.5 mg, 0.015 mmol, 0.05 equiv), 2,6-di-*tert*-butylphenol (61.9 mg, 0.3 mmol, 1.0 equiv), and biphenyl (23.1 mg, 0.15 mmol, 0.5 equiv). To this mixture was subsequently added chloroform-*d* (3.0 mL, 0.1 M). Finally, 40.9 mg (0.3 mmol, 1 equiv), 81.7 mg (0.6 mmol, 2 equiv), 204 mg (1.5 mmol, 5 equiv), 408 mg (3.0 mmol, 10 equiv) of 3,4,5-

131

trimethylphenol was added, respectively, in each of the flasks. The reaction flasks were left to stir at 80 °C and aliquots were taken and the data analyzed according to the general procedure described above.

Table 2.14 Concentration of Components in the Cross-Coupling Reaction

1. 1 equiv 3,4,5-trimethylphenol

time (min)	Product (M)	PhenolA (M)	PhenolB (M)
10	0.01000	0.09000	0.08900
20	0.01500	0.08500	0.08400
30	0.02500	0.07500	0.07100
40	0.03600	0.06400	0.06000
60	0.05100	0.04900	0.04500
90	0.05500	0.04500	0.04300
240	0.07000	0.00000	0.00000

2. 2 equiv 3,4,5-trimethylphenol

time (min)	Product (M)	phenol A (M)	phenol B (M)
20	0.00560	0.09300	0.17100
40	0.01120	0.08700	0.16600
60	0.01700	0.08300	0.16200
90	0.02300	0.07600	0.15100
120	0.04000	0.06000	0.13400
240	0.05000	0.05100	0.12000

3. 5 equiv 3,4,5-trimethylphenol

time (min)	Product (M)	phenol A (M)	phenol B (M)
20	0.00270	0.09500	0.44000
40	0.00650	0.09400	0.43500
90	0.01000	0.08800	0.44200
120	0.01700	0.08400	0.42300
360	0.02500	0.07500	0.43000
900	0.06700	0.03300	0.00000

4. 10 equiv 3,4,5-trimethylphenol

time (min)	Product (M)	phenolA (M)	phenolB (M)
30	0.00300	0.09700	1.01000
60	0.00700	0.09400	1.00900
90	0.01000	0.08900	0.99300
120	0.01500	0.08400	0.99000
240	0.02200	0.07500	0.98700
960	0.05000	0.04900	0.93000

Table 2.15 Initial Rates for Order in 3,4,5-Trimethylphenol

Concentration (M)	Initial Rate (M/s)
0.1	1.46700E-05
0.2	4.75000E-06
0.5	2.15000E-06
1	1.48000E-06

Order in Oxygen Pressure. In oven dried 25 mL round bottomed flask equipped with a stir bar was added Cr-Salen-Cy catalyst (9.5 mg, 0.015 mmol, 0.05 equiv), 2,6-di-*tert*-butylphenol (61.9 mg, 0.3 mmol, 1.0 equiv), 3,4,5-trimethylpenol (40.9 mg, 0.3 mmol, 1.0 equiv) and biphenyl (23.1 mg, 0.15 mmol, 0.5 equiv). To this mixture was subsequently added chloroform-*d* (3.0 mL, 0.1 M). The reaction flask was put into a Parr bomb reactor and oxygen was added *via* active purge. The reactor was closed and oxygen pressure was maintained at 10 atm and left to stir at 80 °C and aliquots were taken and the data analyzed according to the general procedure described above.

Table 2.16 Concentration of Components in the Cross-Coupling Reaction

time (min)	[Product] (M)	[phenol A] (M)	[phenol B] (M)
15	0.01500	0.07500	0.07400
25	0.02200	0.06500	0.06700
55	0.04600	0.04100	0.04200
100	0.07500	0.00000	0.00000

CHAPTER 3. Honokiol Synthesis

3.1. Background

Honokiol (**3.1**) is an unsymmetrical biphenyl compound isolated from *Magnolia* plants such as *Melilotus officinalis*, [83] *Magnolia obovate*, [84] and *Magnolia garretti*. [85] In spite of its simple biphenyl structure having two hydroxyl and two allyl groups, honokiol exhibits various biological activities[86] such as anxiolytic, antithrombotic, anti-depressant, antiemetic, antibacterial, antiviral, anticancer, and anti-inflammatory effects.

Honokiol contains a biphenyl ring system with *para*-allyl phenol and *ortho*-allyl phenol coupling together at the *ortho-* and *para*-positions, respectively. A structure-activity relationship (SAR) study revealed that 4'-hydroxy and 5-allyl groups of honokiol

(83) Fujita, M.; Itokawa, H.; Sashida, Y. "Honokiol, a new phenolic compound isolated from the bark of *Magnolia obovata Thunb*" *Chem. Pharm. Bull.* **1972**, *20*, 212–213.

(84) Fukuyama, Y.; Otoshi, Y.; Miyoshi, K.; Nakamura, K.; Kodama, M.; Nagasawa, M.; Hasegawa, T.; Okazaki, H.; Sugawara, M. "Neurotrophic sesquiterpene-neolignans from *magnoliaobovata*: structure and neurotrophic activity" *Tetrahedron* **1992**, *48*, 377–392.

(85) Schuehly, W.; Voith, W.; Teppner, H.; Kunert, O. "Substituted Dineolignans from *Magnolia garrettii*" *J. Nat. Prod.* **2010**, *73*, 1381–1384.

(86) (a) Kong, Z.; Tzeng, S.; Liu, Y. Bioorg. "Cytotoxic neolignans: an SAR study" *Med. Chem. Lett.* **2005**, *15*, 163-166. (b) Amblard, F.; Govindarajan, B.; Lefkove, B.; Rapp, K. L.; Detorio, M.; Arbiser, J. L.; Schinazi, R. F. "Synthesis, cytotoxicity, and antiviral activities of new neolignans related to honokiol and magnolol" *Bioorg. Med. Chem. Lett.* **2007**, *17*, 4428-4431. (c) Fukuyama, Y.; Nakade, K.; Minoshima, Y.; Yokoyama, R.; Zhai, H.; Mitsumoto, Y. "Neurotrophic activity of honokiol on the cultures of fetal rat cortical neurons" *Bioorg. Med. Chem. Lett.* **2002**, *12*, 1163-1166. (d) Matsuda, H.; Kageura, T.; Oda, M.; Morikawa, T.; Sakamoto, Y.; Yoshikawa, M. "Effects of Constituents from the Bark of Magnolia obovata on Nitric Oxide Production in Lipopolysaccharide-Activated Macrophages" *Chem. Pharm. Bull.* **2001**, *49*, 716-720.

were crucial for neurotrophic activity.[87] Honokiol was obtained through natural sources, but its isolation has been quite inefficient because of the presence of its other constitutional isomer, magnolol.[88]
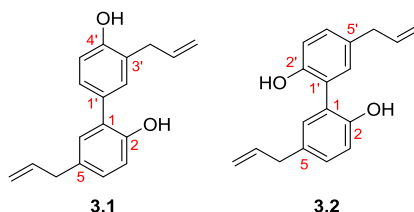
Figure 3.1 Honokiol (**3.1**) and Magnolol (**3.2**)

3.2. Reported Synthetic Approaches to Honokiol

Owing to its excellent biological activity and natural scarcity, various synthetic approaches have been reported for total synthesis of honokiol. Recently, there has been increased interest in devising a simple, scalable synthesis as evidenced by the three publications reported in 2014 alone. In 1986, Tobinaga and co-workers finished the first total synthesis of honokiol (**3.1**).[89] In 2004, the Fukuyama group reported the second synthesis of honokiol with a Suzuki-Miyaura reaction to connect two aryl substrates as a

(87) Esumi, T.; Makado, G.; Zhai, H.; Shimizu, Y.; Mitsumoto, Y.; Fukuyama, Y. "Efficient synthesis and structure–activity relationship of honokiol, a neurotrophic biphenyl-type neolignan" *Bioorg. Med. Chem. Lett.* **2004**, *14*, 2621-2625.

(88) Liu, L.; Wu, X.; Fan, L.; Chen, X.; Hu, Z. "Separation and determination of honokiol and magnolol in herbal medicines by flow injection-capillary electrophoresis" *Anal. Bioanal. Chem.* **2006**, *384*, 1533-1539.

(89) Takeya, T.; Okubo, T.; Tobinaga, S. "Synthesis of unsymmetrical biphenyl lignans, honokiol and related coumpounds, utilizing quinol-acetates as reactive intermediates" *Chem. Pharm. Bull.* **1986**, *34*, 2066-2075.

key step.[5] Short syntheses have been followed by Liu,[90] Denton,[91] and Chen.[92] In 2014, Reddy et al. disclosed a 6-step synthetic method starting from cyclohexane-1,4-dione monoethylene ketal that yields a 2:3 mixture of honokiol and isohonokiol.[93] This synthetic route involved the Grignard reaction, iodine mediated aromatization, and Claisen rearrangement as key steps.

Scheme 3.24 Honokiol synthesis by Reddy et al.

---
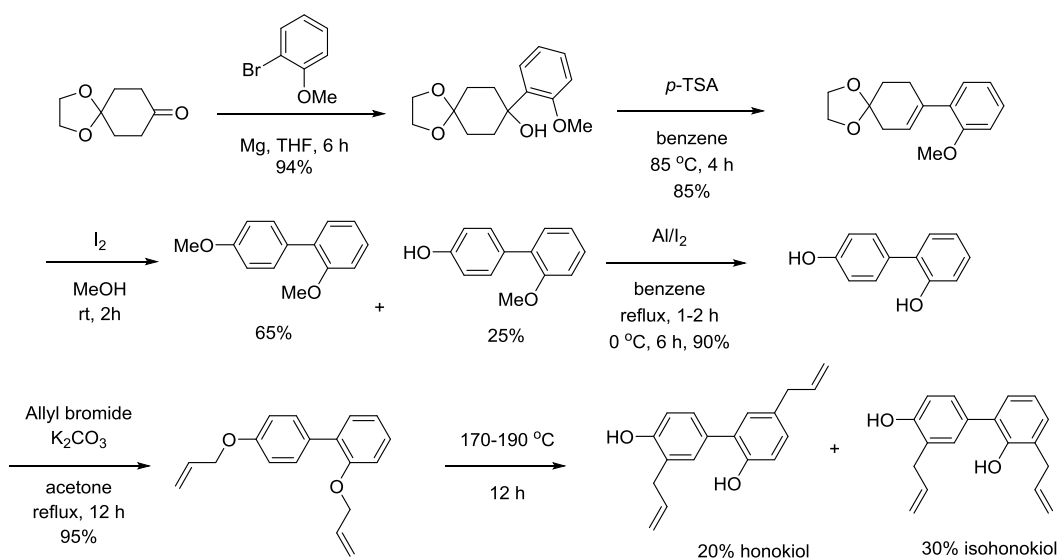
(90) Chen, C.-M.; Liu, Y.-C. "A Concise Synthesis of Honokiol" *Tetrahedron Lett.* **2009**, *50*, 1151-1152.

(91) Denton, R. M.; Scragg, J. T.; Galofre, A. M.; Gui, X.; Lewis, W. "A Concise Synthesis of Honokiol" *Tetrahedron* **2010**, *66*, 8029-8035.

(92) Tripathi, S.; Chan, M.-H.; Chen, C. "An Expedient Synthesis of Honokiol and Its Analogues as Potential Neuropreventive Agents" *Bioorg. Med. Chem. Lett.* **2012**, *22*, 216-221.

(93) Reddy, B. V. S.; Rao, R. N.; Reddy, N. S. S.; Yadav, J. S.; Subramanyam, R. "A Short and Efficient Synthesis of Honokiol via Claisen Rearrangement" *Tetrahedron Lett.* **2014**, *55*, 1049-1051.

The Kumar group published a four-step synthesis of honokiol (**3.1**) with 68% overall yield. [94] The present method involved tetrakis(triphenylphosphine)palladium catalyzed Kumada coupling in two key steps. Palladium catalyzed reactions are not desirable on production scale because of the high cost of palladium reagents and the difficulty of removing palladium impurities from the final product. In addition, the high mass and cost associated with the iodinated anisole precursor is undesirable.

Scheme 3.25 Honokiol Synthesis by Kumar et al.
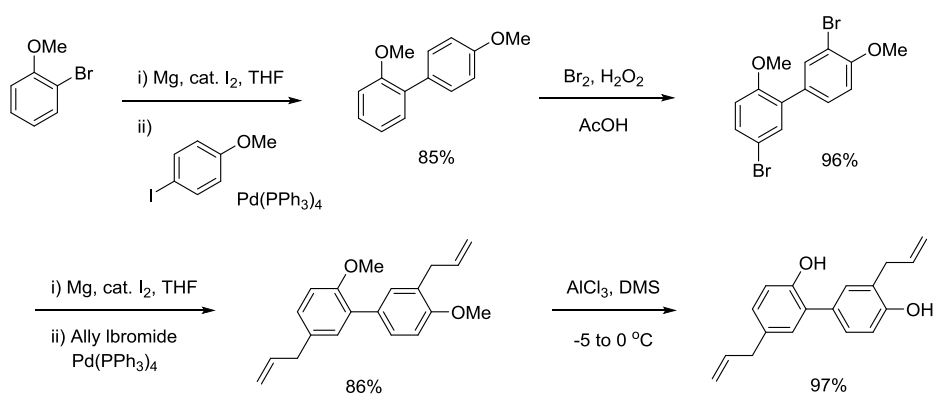
The Fukuyama group reported their second honokiol synthesis after 2004. [95] This route utilized two separate Suzuki-Miyaura reactions. The first Suzuki-Miyaura reaction was employed to couple 2-bromophenol with 4-hydroxyphenylboronic acid, giving rise to 2,4'-dihydroxybiphenyl. The second coupling was used to introduce allyl groups at the 5- and 3'-positions of honokiol. The total synthesis of honokiol was completed in 74%

(94) Srinivas, J.; Singh, P. P.; Varma, Y. K.; Hyder, I.; Kumar, H. M. S. "Concise Total Synthesis of Honokiol via Kumada Cross Coupling" *Tetrahedron Lett.* **2014**, *55*, 4295-4297.

(95) Harada, K.; Arioka, C.; Miyakita, A.; Kubo, M.; Fukuyama, Y. "Efficient Synthesis of Neurotrophic Honokiol Using Suzuki-Miyaura Reactions" *Tetrahedron Lett.* **2014**, *55*, 6001-6003.

yield over five steps from the starting material, 2-bromophenol (**Scheme 3.3**). Here, the

high costs of the boronic acids, coupled with their instability, limit large scale application.

Scheme 3.26 Honokiol Synthesis by Fukuyama et al.
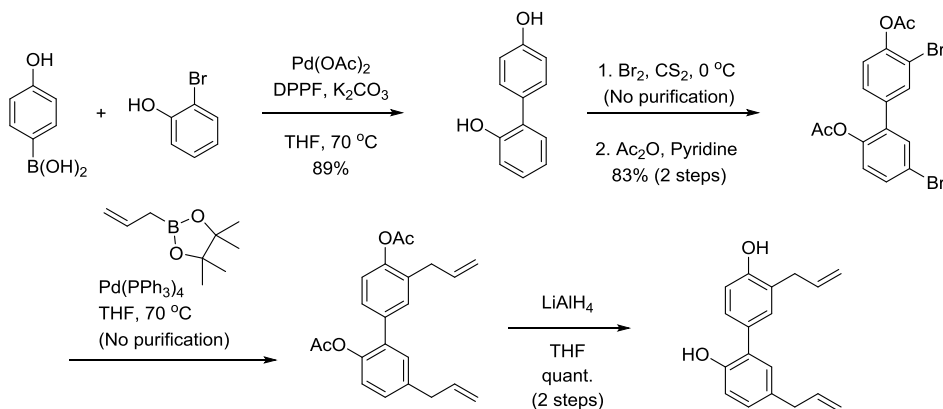
3.3. First Route to Honokiol Synthesis

The structure of honokiol (**3.1**) arises from union of an *ortho*-allylphenol (**3.3**) and

a *para*-allylphenol (**3.4**). Formation of the biaryl bond selectively from the monomers is

the crux in any synthesis of honokiol. To determine the limits of our cross-coupling

method, these two phenolic monomers were subjected to the Cr-Salen-Cy catalyst.

Unfortunately, no product formed; only decomposition of the substrates was observed.

Scheme 3.27 Direct Cross-coupling of Honokiol Phenol Monomers

139
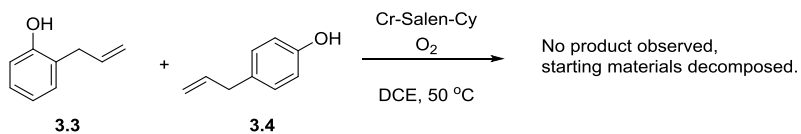
In **Chapter 2**, I described a method for coupling 2,6-disubstituted phenols with 4-substituted phenols using a chromium(III) catalyst to give selectively the *para-ortho-*coupled bisphenol. Based on this discovery, it was reasoned that an additional substituent was necessary at the *ortho*-posotion of 2-allyl phenol (**3.3**) to achieve a selective coupling with 4-allylphenol (**3.4**) using our method. The retrosynthetic analysis in **Scheme 3.5** described a simple and direct method for the synthesis of honokiol based on this premise. Specifically, honokiol (**3.1**) would be obtained in two steps, cross-coupling reaction and removal of X group (tertiary alkly, silyl group etc), from the corresponding monomers.

Scheme 3.28 Retrosynthetic Analysis of Honokiol: First Route.
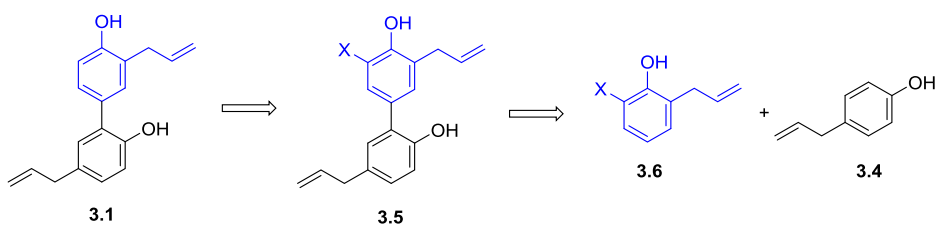
O-Allyation of commercial 2-*tert*-butylphenol (**3.7**) followed by thermal Claisen rearrangement gave monomer **3.9** for the cross-coupling reaction in 81% yield for two steps. The other monomer **3.4** is a natural isolate,[96] also known as chavicol, of which the methyl ether derivative is commercially available. The routes to the two monomers are shown in **Scheme 3.6**. Excitingly, the first trial of the cross-coupling reaction between **3.9** and **3.4** gave the desired product **3.11** in 31% yield even though byproducts such as diphenoquinone and trimer were seen. Unfortunately, several attempts at the deprotection

(96) Lide, D. R. *CRC Handbook of Chemistry and Physics* (86th Ed) **2005**

of *tert*-butyl group to get to the target, honokiol, were unsuccessful. Under several acidic conditions, the retro-Friedel-Crafts reaction did not occur; rather compound **3.11** decomposed or no reaction was seen (**Scheme 3.7**).

Scheme 3.6 Syntheses of Monomers
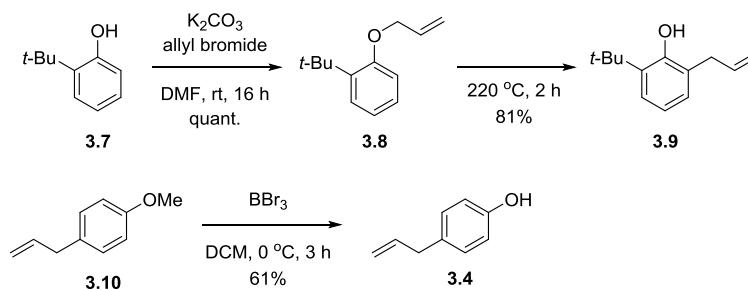
Scheme 3.29 Cross-Coupling of *tert*-Butyl Allyl Phenol and Deprotection
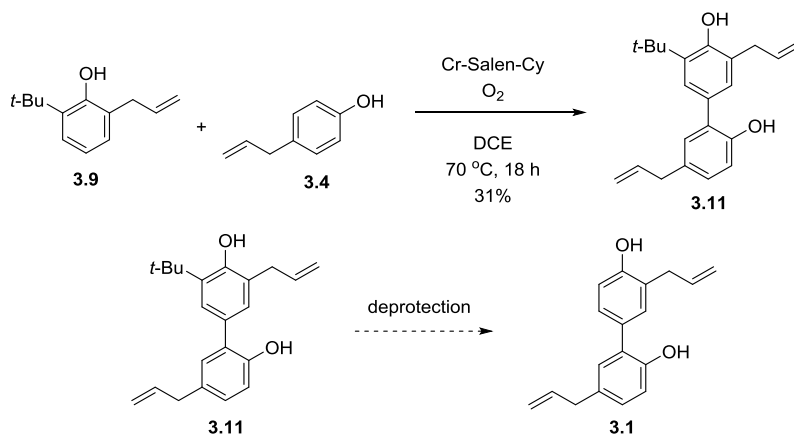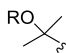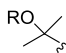
Entry	Acid	Conversion
1	AlCl$_3$	decomposed
2	AlMe$_3$	NR
3	CH$_3$C$_6$H$_4$SO$_3$H	NR
4	CH$_3$SO$_3$H	decomposed
5	CF$_3$SO$_3$H	decomposed

Along with *tert*-butyl group, several other blocking groups for the *ortho*-position were tested. As expected, electron-withdrawing blocking groups, such as halides, have a detrimental effect on reaction (**Table 3.1**, entries 4-6).

Table 3.1 Substituent Effects on the Oxidative Cross-Coupling Reaction
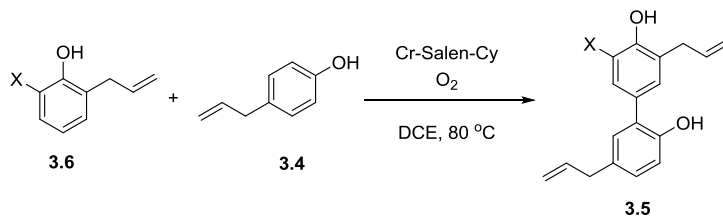
Entry	X	Conversion
1	*t*-Bu	31%
2	TMS	NR
3	TBS	24%
4	Cl	NR
5	Br	NR
6	I	NR
7	R=H	NR
8	R=Me	NR

In addition, a lack of reactivity was seen with trimethylsilyl (**Table 3.1**, entry 2). However, the phenol with a *tert*-butyldimethylsilyl group gave desired cross-coupling product **3.17** in 24% conversion (**Table 3.1**, entry 3). The remainder of the starting material was decomposed after 18 hours at 80 ^{o}C. Deprotection of the silyl group with HF·pyridine proceeded smoothly to give the final product (**Scheme 3.9**). These two steps were not optimized further because the costs of materials were not amenable to large scale production. Specifically, four steps were required to synthesize 2-allyl-6-*tert*-butyldimethylsilyl phenol (**3.16**) from 2-bromophenol (**3.12**) (**Sheme 3.8**). Also, the other starting material 4-allyl anisole (**3.10**) was prohibitively expensive ($73.07/100 g, Acros).

142

Nonetheless, this synthesis is meaningful as it constitutes the first honokiol synthesis based on an oxidative phenol cross-coupling.

Scheme 3.30 Synthesis of Substrate **3.15**
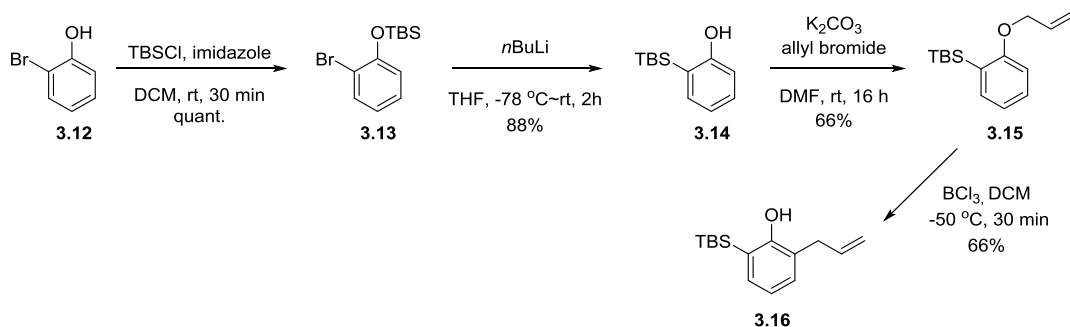
Scheme 3.31 First Honkiol Synthsis Utilizing Oxidative Cross-Coupling
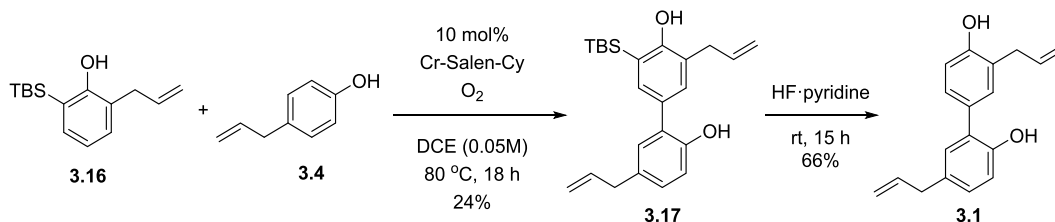
3.4. Second Route to Honokiol Synthesis

Aryl-aryl bond formation represents a key step in the total synthesis of honokiol and the initial route showed that our strategy of oxidative cross-coupling of electron-rich phenol substrates is sound. Since cross-coupling reaction between phenols with allyl substituents suffered limitations due to substrate stability, we redesigned the starting phenols with the goal of installing the allyl groups after oxidative coupling.

143

One retrosynthetic analysis of honokiol utilizing this approach is depicted in **Scheme 3.10**. This plan was inspired by Reddy's synthesis in 2014[11] which involved Claisen rearrangement of bis-*O*-allylbiphenyl **3.18**.

Scheme 3.32 Retrosynthetic Analysis of Honokiol: Second Route
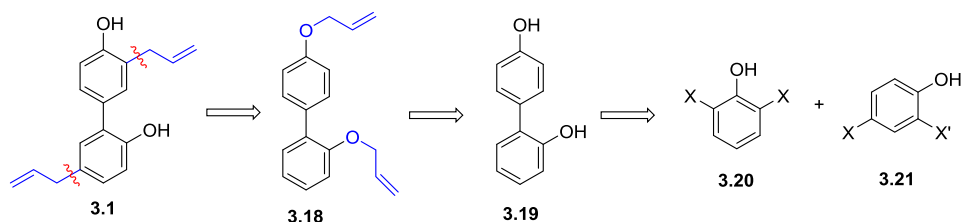
The synthesis of honokiol commenced with the preparation of 2,4'-biphenyl (**3.19**). There is a limited literature for the preparation of this compounds with most cases requiring Suzuki-Miyaura cross-coupling between a halophenol and phenol boronic acid.[97] While high-yielding, such a protocol requires additional steps to prepare the substrates. On the other hand, phenol can be subjected to oxidative coupling to obtain **3.19** with conventional oxidant, such as $(t\text{-BuO})_2$[98], VCl_3,[99] or gold nano-particle catalyst,[100] however, none of those examples give the *ortho-para* coupling product with high regioselectivity. For example, regioselective oxidative coupling method of simple

(97) Schmidt, B.; Riemer, M. "Suzuki-Miyaura Coupling of Halophenols and Phenol Boronic Acids: Systematic Investigation of Positional Isomer Effects and Conclusions for the Synthesis of Phytoalexins from Pyrinae" *J. Org. Chem.* **2014**, *79*, 4104-4118.

(98) Amstrong D. R.; Breckenridge, R. J.; Cameron C.; Nonhebel, D. C.; Pauson, P. L.; Perkins, P. G. "The Role of Stereoelectronic Factors in the Oxidation of Phenols" *Tetrahedron Lett.* **1983**, *24*, 1071-1074.

(99) O'Brien, M. K.; Vanasse, B. *e-EROS Encyclopedia of Reagents for Organic Synthesis*, **2001**.

(100) Serna, P.; Corma, A. "A Residue-free Production of Biaryls Using Supported Gold Nanoparticles" *J. Catal.* **2014**, *315*, 41-47.

phenol with CuCl(OH)·TMEDA was reported,[101] however, we failed to reproduce their result even after several trials. Direct *ortho-para* coupling of phenol was also unsuccessful with our chromium catalyst. As such, phenols with blocking groups to enforce regioselection were examined.

When 2,6-di-*tert*-butylphenol and 4-*tert*-butylphenol were subjected to the coupling reaction, a mixture of oxidative coupling products including diphenoquinone, dimer, and trimer were observed. Trials to suppress the byproducts by modifying the ratio of substrates, reaction time, temperature, and catalyst loading did not result in much improvement.

Scheme 3.33 Cross-Coupling between 2,6-Di-*tert*-butylphenol and 4-*tert*-Butylphenol
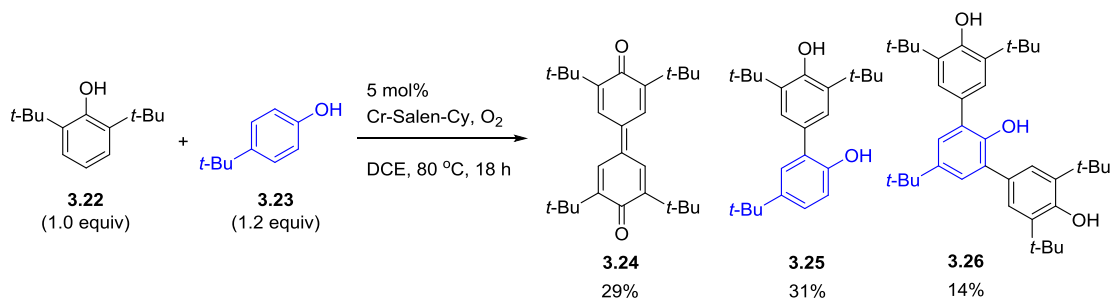
At this point, it was reasoned that modification of the second phenol substrate was needed to reduce the amount of trimer formation. Addition of a substituent at the *ortho-*position would prevent trimer formation and, moreover, would permit a selective

(101) Majumder, P. L.; Chakraborty, S.; Roychowdhury, M. "Catalytic aerobic oxidative coupling of some simple phenols and natural phenanthrols with CuCl(OH)·TMEDA" *J. Indian Chem. Soc.* **2000**, *77*, 389-393.

rearrangement in the final step. For this role, bromide, which would be removed after Claisen-Cope rearrangement reaction, was considered. 2-Bromo-4-*tert*-butylphenol (**3.27**), obtained readily by aromatic substitution reaction on **3.23**, was subjected to oxidative coupling reaction with **3.22**. The electron-withdrawing property of bromide affected the reactivity of the cross-coupling under normal condition using O_2. Specifically, only a trace amount of desired product was observed. With a stronger oxidant (*tert*-butylhydroxyperoxide) and higher reaction temperature (up to 140 °C), the coupling yield improved to 52%, at which point the reaction seemed to stop. Longer reaction times did not yield more product, and both starting phenols remained unreacted.

Scheme 3.34 Cross-Coupling Reaction of 2-Bromo-4-*tert*-butylphenol with TBHP
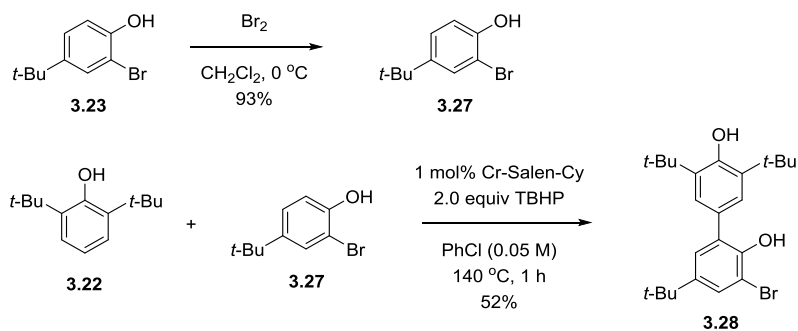
Retro Friedel-Crafts reaction for the removal of the *tert*-butyl group required further optimization with various acids because of the bromide substitution of the lower ring, which attenuated electron-density and, hence the ability of the aromatic ring to protonate. Four dealkylation products were observed (**Scheme 3.13**). Using the previously identified AlCl$_3$, either incomplete dealkylation was observed (entry 1) or, when sealed, dealkylation accompanied by dehalogenation (entry 2). Reasoning that

146

chloride anion might induce reductive removal of the bromide substitutent, attention turned to protic acids. Screening of several protic acid sources identified methanesulfonic acid with heat as suitable for target molecule **3.31**. After removal of three *tert*-butyl groups, allylation of both hydroxyl groups was performed quantitatively (**Scheme 3.14**).

Scheme 3.35 Acid Screening in the Retro Friedel-Craft Reaction

Entry	Acid (condition)	Product
1	AlCl$_3$ (under argon, rt)	**3.29 + 3.30**
2	AlCl$_3$ (closed, rt)	**3.32**
3	12 N HCl (90 $^{\circ}$C)	**3.29 + 3.30**
4	*p*-TsOH (90 $^{\circ}$C)	**3.30**
5	CF$_3$SO$_3$H (rt)	**3.30 + 3.31**
6	MeSO$_3$H (90 $^{\circ}$C)	**3.31**
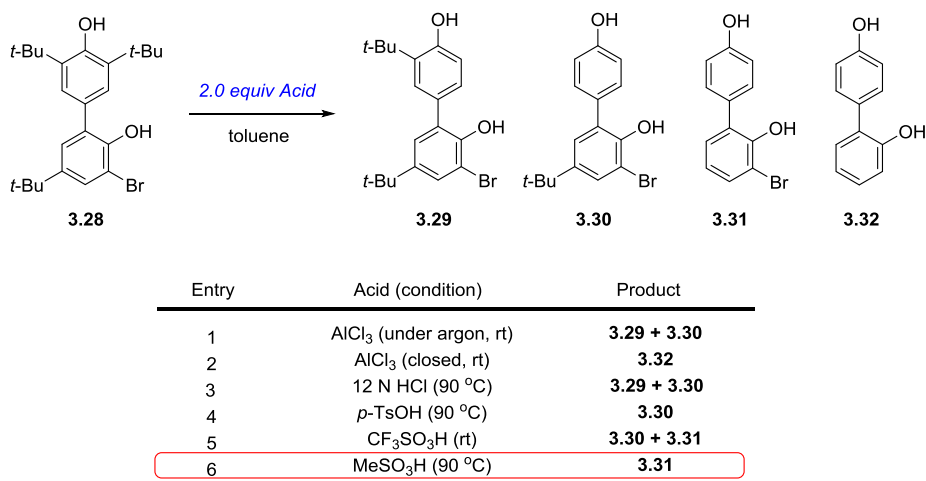
Scheme 3.36 Dealkylation and *O*-Allylation Reaction
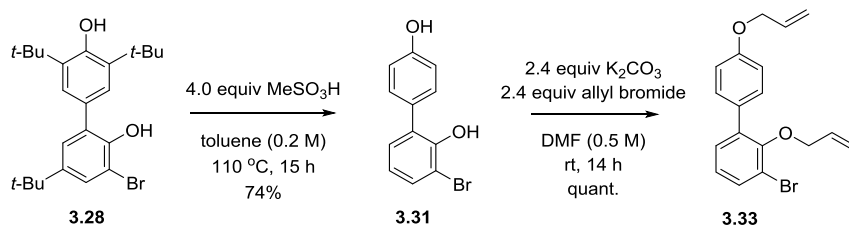
Our next goal was to effect a tandem rearrangement to obtain bromo-honokiol, **3.34** (**Scheme 3.15**). Since the *ortho*-site in the lower ring is blocked from aromatization by a bromine atom, a second [3,3]-rearrangement would happen readily after Claisen

rearrangement and give the product **3.34**.[102] Subsequent debromination would give the final product **3.1**. However, the Claisen-Cope rearrangement with several Lewis acids was unsuccessful and gave different undesirable products. For example, BCl_3 deprived the lower ring of one allyl group. On the other hand, bulkier and milder aluminum Lewis acid, MAD [methylaluminium bis(2,6-di-*tert*-butyl-4-methylphenoxide)],[103] gave a single product with only one allyl group in the upper ring rearranged; the other allyl group in the lower ring was left unaffected.

Thermally, when the substrate **3.33** was heated to 180 ^{o}C in the solvent of *N,N*-diethylaniline, a mixture of isohonokiol (**3.35**) and honokiol (**3.1**) was obtained in a 1.3:1 ratio. Sigmatropic rearrangement of substrate **3.18** also gave same mixture but with different ratios (c.f. 1.5:1 ration obtained by Reddy et al.).[11] Even though honokiol was obtained in higher yields with substrate **3.33** than with **3.18** (see **Scheme 3.1**), the undesired isohonokiol was still a major product.

(102) O'Brien, E. M.; Li, J.; Carroll, P. J.; Kozlowski, M. C. "Synthesis of the Cores of Hypocrellin and Shiraiachrome: Diastereoselective 1,8-Diketone Aldol Cyclization" *J. Org. Chem.* **2010**, *75*, 69-73.

(103) Saito, S.; Yamamoto, H. "Designer Lewis Acid Catalysts-Bulky Aluminium Reagents for Selective Organic Synthesis" *Chem. Comm.* **1997**, 1585-1592.

Scheme 3.37 Sigmatropic Rearrangement for Honokiol Synthesis
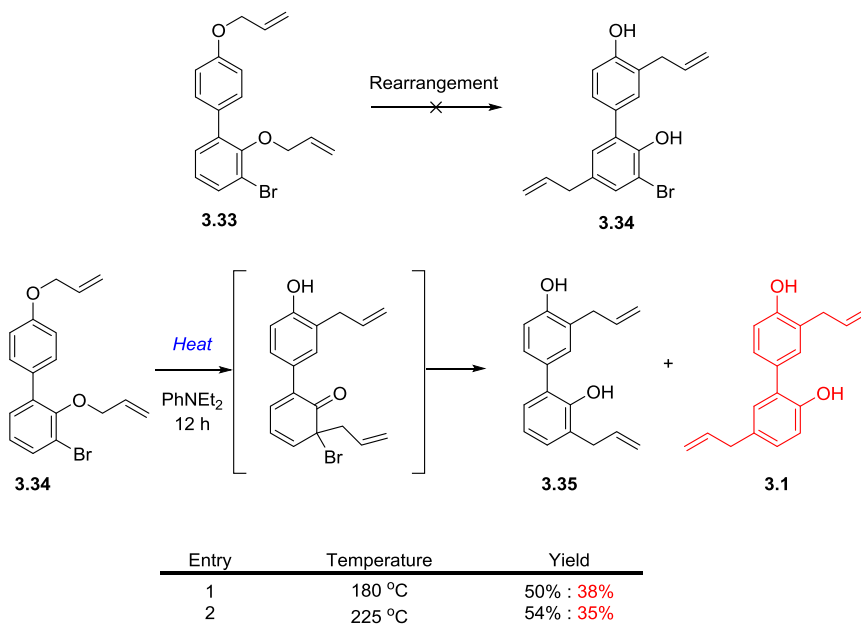
Additional thermal reaction experiments for both honokiol and isohonokiol were performed. For both substrates, nothing occurred even after extended heating. These results reveal that the rearrangement reaction to **3.1** does not transit **3.35**.

Scheme 3.38 Thermal Reaction on Isohonokiol (**3.35**) and Honokiol (**3.1**)
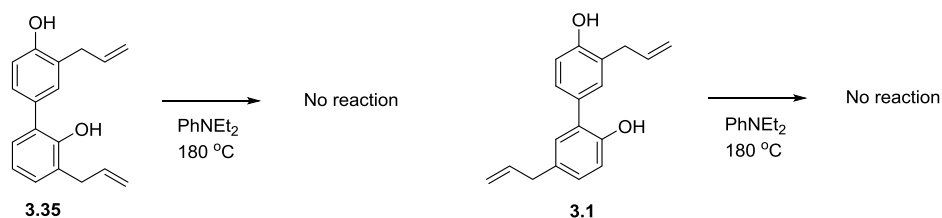
3.5. Third Route to Honokiol Synthesis

The above experiments indicate that any route to honokiol involving Claisen reaction of the lower ring is not tenable. Since installation of the allyl functionality was always problematic, we decided to defer this step to later in the synthesis (**Scheme 3.17**). Furthermore, allyl installation by vinyl addition to a benzylic bromide by substitution reaction appears more feasible and involves a novel disconnection for this target. In order to obtain bisbromomethylbiphenyl **3.36**, radical bromination would be performed on bistoluene derivative **3.37**. 3,5'-Dimethyl-2,4'-bisphenol (**3.37**) would be an equivalent to the fully protected cross-coupling product **3.38** between 2-*tert*-butyl-6-methylphenol (**3.39**) and 2-*tert*-butyl-4-methylphenol (**3.40**). This route is also appealing because these two starting phenols are commercially available at reasonable costs ($147.60/500 g for **3.39**; TCI, $39.02/500 g for **3.40**; Acros), which is beneficial for mass production.

Scheme 3.39 Retrosynthetic Analysis of Honokiol: Third Route
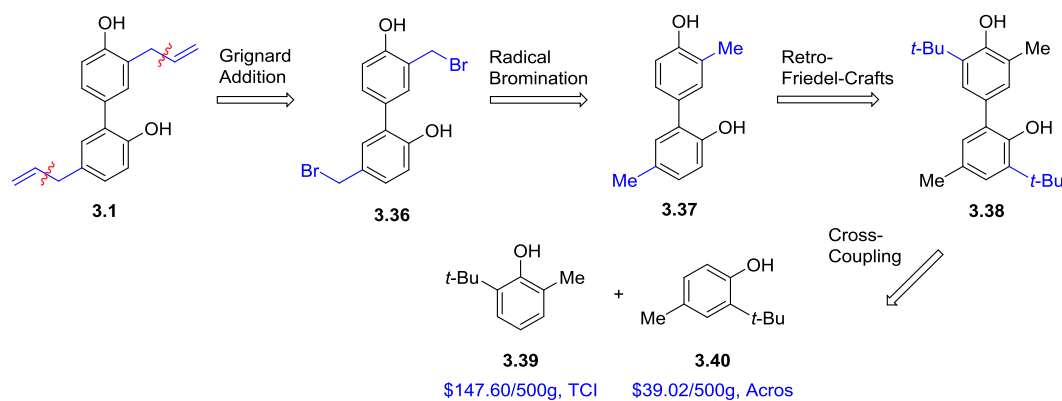
Substrates **3.39** and **3.40** coupled readily with our previously identified conditions and the optimal conditions for their cross-coupling were obtained in short order (**Scheme**

3.18). During this process, a reduced catalyst loading was discovered to be viable at higher concentrations. With 2.5 mol% Cr-Salen-Cy in 0.2 M toluene, (entry 6, **Scheme 3.18**) more cross-coupling product (92% conversion) was obtained since homo-coupling of phenol **3.38** to form diphenoquinone was suppressed to less than 5%.

Scheme 3.40 Optimization of Cr (III) catalyzed Cross-Coupling Reaction

Entry	Condition	Conversion
1	2.0 equiv TBHP	51%
2	O_2	66%
3	DCE	68%
4	toluene	89%
5	5 mol%, 0.1 M toluene	89%
6	2.5 mol%, 0.2 M toluene	92%
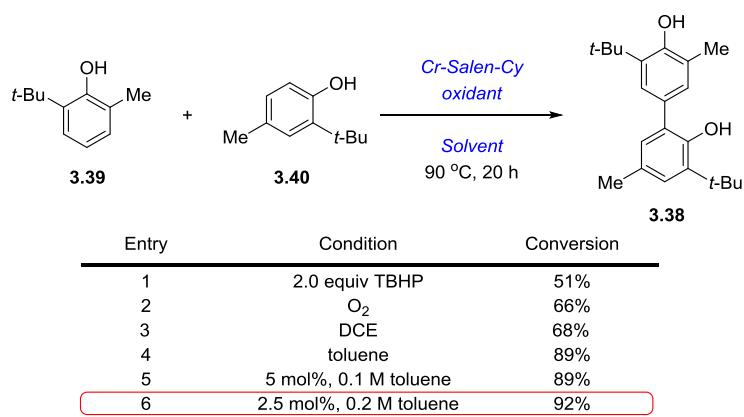
At the same time, a screen of conventional oxidants was performed to determine if this particular substrate pair was predisposed to cross-coupling. Surprisingly, a stoichiometric manganese oxidant gave a reasonable yield (56% conversion) after 15 hours (entry 8, **Scheme 3.19**).

151

Scheme 3.41 Oxidant Screening for Cross-Coupling Reaction
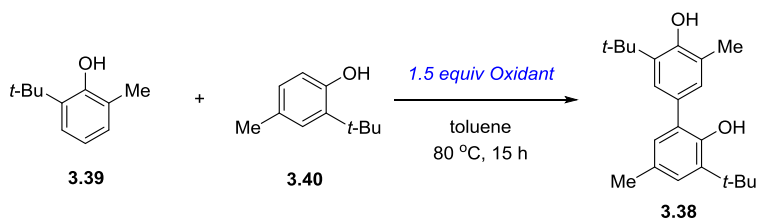
Entry	Oxidant	Conversion
1	H_2O_2	NR
2	t-BuOOH	24% pdt, 32% quinone
3	$(t$-BuO$)_2$ [a]	decomp.
4	PhIO	15% pdt, decomp.
5	NaOCl	<3% pdt, decomp.
6	$K_3Fe(CN)_6$	decomp.
7	$VO(OEt)_3$	decomp.
8	$Mn(OAc)_3 \cdot 2H_2O$	56% pdt, 41%A, 35%B
9	Ag_2CO_3	14% pdt, decomp.
10	$CuCl_2$	NR
11	$CuCl_2/TMEDA/O_2$	decomp.
12	$FeCl_3$	NR
13	$FeCl_3/O_2$	NR
14	O_2	NR

[a] run at 130 °C in dichlorobenzene

It has been reported in 1992, that Mn(acac)$_3$ oxidized 2,6-di-*tert*-butylphenol to corresponding 4,4'-biphenyldiol and Mn(OAc)$_3$ oxidized the same substrate to give corresponding 4,4'-diphenoquinone.[104] Thus, a further screening of manganese reagents was undertaken, which revealed that cross-coupling product was a major product (**Scheme 3.18**). Manganese(III) acetylacetonate showed better conversion than manganese (III) acetate for the cross-coupling reaction and also worked well with catalytic amounts (10 mol%) under oxygen atmosphere to give the product **3.38** with 74% isolated yield after 15 hours (**Scheme 3.20**). However, conversion did not seem to increase even after longer times.

(104) Nishino, H.; Itoh, N.; Nagashima, M.; Kurosawa, K. "Choice of Manganese(III) Complexes for the Synthesis of 4,4'-Biphenyldiols and 4,4'-Diphenoquinones" *Bull. Chem. Soc. Jpn.* **1992**, *65*, 620-622.

Scheme 3.20 Manganese Oxidant Screening for Cross-Coupling Reaction
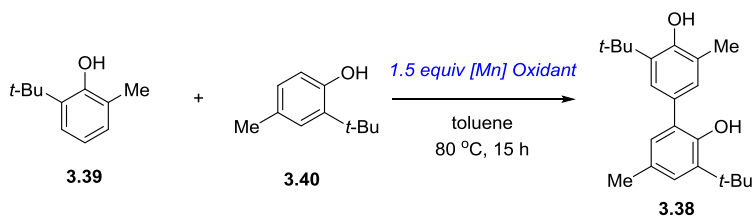
Entry	Manganese Oxidant	Converison
1	$Mn(OAc)_3$ $2H_2O$	56%
2	$Mn(OAc)_3$ $2H_2O^a$	>10%, incompleted
3	MnO_2	7.5% pdt, decomp
4	$Mn(acac)_3$	67%
5	$Mn(acac)_3{}^a$	75%
6	$KMnO_4$	decomp, no pdt

[a] catalytic (10 mol%) loading under oxygen atmosphere

Because the Cr(III) catalyzed cross-coupling reaction proceeded in excellent yield with few byproducts, a purification process did not seem necessary. After completion of the reaction, the reaction mixture was filtered through a silica plug to remove the Cr(III)-Salen complex, and then it was subjected to dealkylation reaction immediately. After two hours at ambient temperature, 3,5'-dimethyl-2,4'-bisphenol (**3.30**) was obtained with 82% yield over the two steps. Later, it was also found that even without filtration process, cross-coupling reaction and retro Fridel-Craft alkylation could be performed in single reaction vessel in excellent yield (85%). It was notable that water, a major byproduct of oxidation process, did not decrease the reacitivity of the Lewis acid in dealkylation step.

Scheme 3.42 One-pot Cross-Coupling and Retro Friedel-Craft Reaction
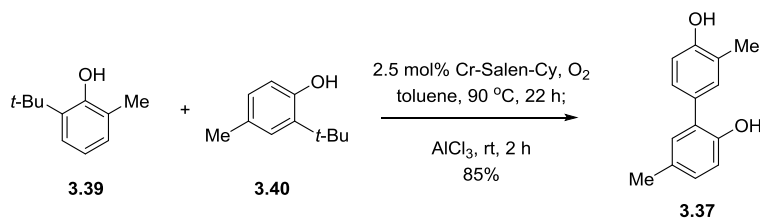
After protection of the hydroxyl groups in substrate **3.36** as the methyl ethers, radical bromination reaction was performed. Exploration of with several conditions including different solvents, bromide radical sources (*N*-bromosuccinimide, Br$_2$), reaction temperature etc. gave rise to a mixture of mono-bromide and over brominated products along with desired product in every case. The optimal conditions utilized NBS as a bromide source in presence of radical initiator azobis*iso*butyronitrile (AIBN) in carbon tetrachloride; even so, yields did not exceed 57%.

Scheme 3.43 Protection and Radical Bromination Reaction
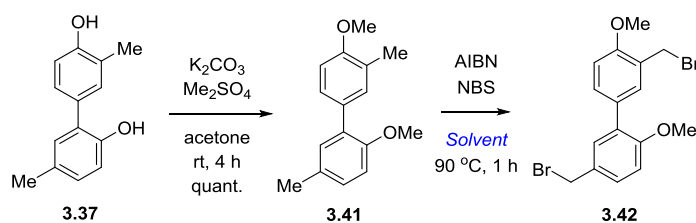
Solvent Screening in Radical Bromination Reaction

Entry	Solvent	Conversion[a]
1	THF	NR
2	CH$_3$CN	NR
3	dioxane	decomposed
4	DCE	many side pdts
5	CCl$_4$	57%
6	cyclohexane	47%
7	benzene	44%
8	PhCl	40%
9	EtOAc	38%
10	CF$_3$Ph	25%

[a]Conversions were determined by ^{1}H-NMR.

154

At this point, different protecting groups were tested to improve reaction yield in the radical bromination step. Tetrahydropyranyl acetal compound (**3.43**) gave rise to decomposition rather than the desired brominated. The acetate **3.44** gave the desired product with good yield (85%) in bromination step; however, the subsequent Kumada coupling did not work, giving rise to much decomposition instead.

Scheme 3.44 Protecting Groups in Radical Bromination Reaction
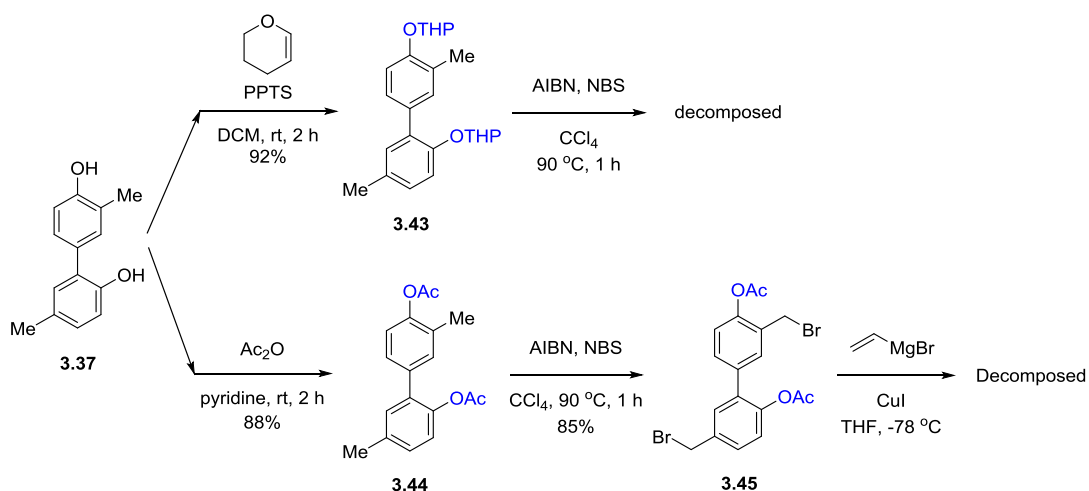
Given the success of bromination of the bisacetate derivative, several alternatives were considered at this stage. A deprotonative cross-coupling reaction[105] of **3.41**, which would reduce the sequence by one step, was attempted but failed. A series of studies on the corresponding monomers revealed that the coupling to the *ortho*-methyl was highly effective but coupling to the *para*-methyl did not occur. Reductive cross-coupling

(105) Sha, S.–C. "New Strategy in C-H Functionalizations with Bismetallic Catalysts" *Dissertation*, **2015**, University of Pennsylvania, Philadelphia, PA.

reactions[106] were tried, but did not give rise to the desired product. A model study with monomeric *para*-methyl anisole gave rise to decomposition pinpointing the *para* methyl as the problematic reaction partner.

Scheme 3.45 Deprotonative and Reductive Cross-Coupling Reaction
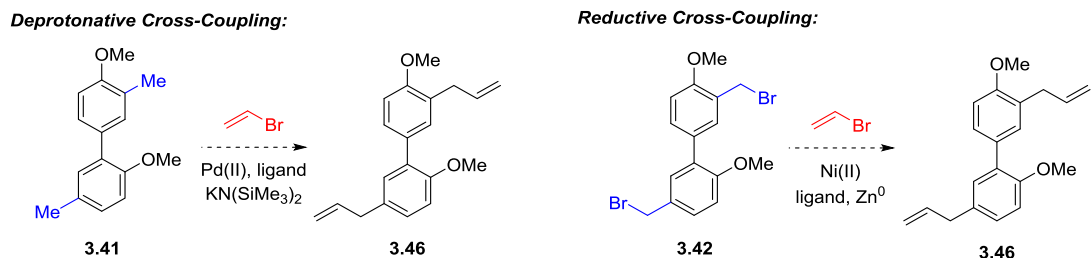
On the other hand, Kumada coupling with substrate **3.42** was successful. It was performed with the best yield when a 1.0 M solution of vinylmagnesium bromide was added slowly (3 mL/min) using a syringe pump in the presence of copper (I) iodide catalyst. With 3 mmol of starting substrate **3.42**, 760 mg of the desired product **3.46** was obtained in 75% isolated yield.

---

(106) (a) Reisman, S. E.; Cherney, A. H. "Nickel-Catalyzed Asymmetric Reductive Cross-Coupling Between Vinyl and Benzly Electrophile" *J. Am. Chem. Soc.* **2014**, *136*, 14365-14368. (b) Amatore, M.; Gosmini, C. "Direct Method for Carbon-Carbon Bond Formation: The Functional Group Tolerant Cobalt-Catalyzed Alkylation of Aryl Halides" *Chem. Eur. J.* **2010**, *16*, 5848-5852. (c) Durandetti, M.; Nedelec, J.-Y.; Perichon, J. "Nickel-Catalyzed Direct Electrochemical Cross-Coupling between Aryl Halides and Activated Aryl Halides" *J. Org. Chem.* **1996**, *61*, 1748-1755. (d) Wang, S.; Qian, Q.; Gong, H. "Nickel-Catalyzed Reductive Cross-Coupling of Aryl Halides with Secondary Alkyl Bromides and Allylic Acetate" *Org. Lett.,* **2012**, *14*, 3352-3355. (e) Yan, C.–S.; Peng, Y.; Xu, X.–B.; Wang, Y.–W. "Nickel-Mediated Inter- and Intramolecular Reductive Cross-Coupling of Unactivated Alkyl Bromides and Aryl Iodide at Room Temperature" *Chem. Eur. J.* **2012**, *18*, 6039-6048.

Scheme 3.46 Optimized Kumada Coupling Reaction
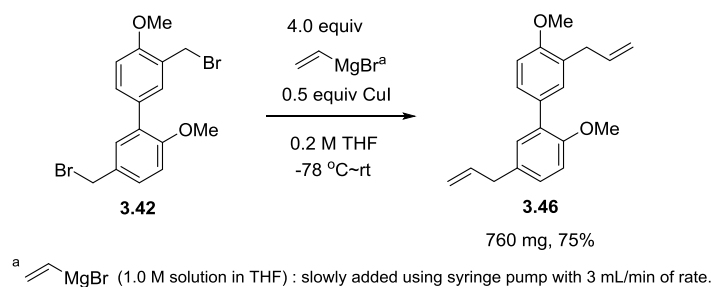
Finally, the demethyation step was optimized. First, we attempted to utilize the AlCl$_3$/dimethyl sulfide conditions reported by Kumar et al. for compound **3.46** that gave honokiol (**3.1**) in 97% yield.[11] However, we failed to reproduce their result even after several trials. Based upon descriptions communicated to us by Kumar, the reaction requires yellow granular AlCl$_3$ in order to succeed. All current sources of AlCl$_3$ that we have been able to obtain are white, free-flowing powders. Apparently, contamination with iron gives rise to yellow-colored AlCl$_3$. Unable to secure a source and uncertain about the exact type/amount of iron contaminant, we chose to explore alternate Lewis acids. There was no reaction with BCl$_3$ at ambient temperature and substrate **3.46** started to decompose at 70 ^{o}C. Even though BBr$_3$ gave honokiol in moderate yield (68% isolated yield), an inseparable impurity was seen due to the reaction at one of the allyl groups. Fortunately, we found that BBr$_3$·DMS complex gave the final product in excellent yield. Apparently, DMS attenuates the reactivity of BBr$_3$ and may also serve to quench any Br$_2$ formed.

Scheme 3.47 Lewis Acids Screening in the Final Reaction
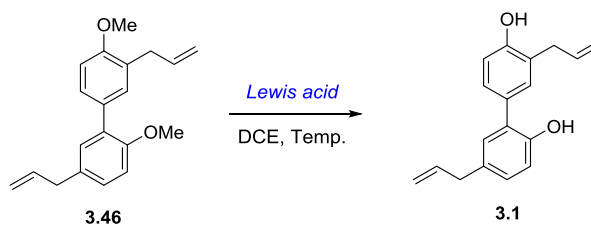
Entry	Lewis acid	Condition	Conversion
1	AlCl$_3$·DMS	-5 ^{o}C, 1 h rt, 3 h	NR NR
2	BCl$_3$	-5 ^{o}C, 1 h rt, 3 h reflux	NR NR SM + decomp.
3	BBr$_3$	-78 ^{o}C ~ 0 ^{o}C, 6 h	68% + byproduct 4%
4	BBr$_3$·DMS	-78 ^{o}C ~ 0 ^{o}C, 4 h reflux, 2 h	NR 95% + byproduct 5%

The final conditions with 2.4 equiv of BBr$_3$·DMS in a closed system gave honokiol with excellent yield (90%) (**Scheme 3.27**). Notably, reaction under an atmosphere of air or argon require more reagent (up to 6 equiv). There was some impurity from the side reaction caused by Br$_2$ (typically less than 5%). The byproduct was identified by ^{1}H NMR and mass spectrum as a bromocyclized adduct in the upper ring (**Scheme 3.28**). However, it was not separable through silica column chromatography and needs to be removed through other purification process such as trituration.

Scheme 3.48 Final Deprotection

2.4 equiv BBr₃·DMS

DCE (0.2 M)
70 °C, 3 h

3.46

3.1
350 mg, 90%
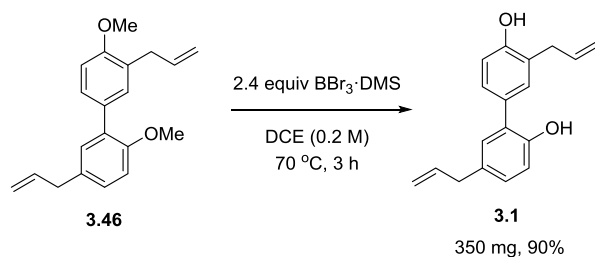
Scheme 3.28 Side Reaction at the Final Step

Br₂ in BBr₃

3.46

3.47
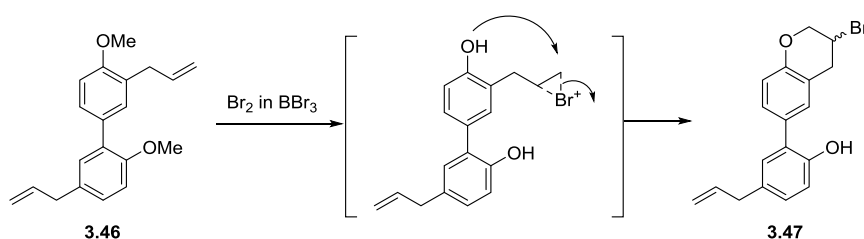
3.6. Conclusion

In conclusion, we have developed three different routes for the total synthesis of honokiol starting from commercial phenols. These three routes each include a Cr(III)-catalyzed oxidative cross-coupling of phenols as a key step.

In the first route, a direct cross-coupling between allyl substituted phenols gave the desired coupling product. A further deprotection then led to honokiol. However, conversion was limited due to the stability of the allyl-substituted substrates under the oxidave coupling conditions.

In the second route, oxidative coupling gave rise to a simple bisphenol. Subsequent allylation gave rise to a substrate for a tandem Claisen-Cope rearrangement reaction. While the rearrangement did precede, contamination of the final product with an isomeric rearrangement product, isohonokiol, could not be suppressed.

Finally, we established an efficient route for the total synthesis of honokiol by utilizing a novel disconnection that transits new structures (**3.37**, **3.38**, **3.46**) not previously indexed in CAS or Reaxys. This five step (six chemical reactions) synthesis was initiated by oxidative cross-coupling of inexpensive commercial phenols with high yield (91%). Following retro Friedel-Crafts alkylation, a protection reaction proceeded smoothly with excellent yield (89% for three steps). The remaining steps of radical bromination, Kumada coupling and demethylation were each optimized. The total yield over five steps was 34% and gram-scale reactions were conducted for each step. This process is the subject of a patent application.[107]

3.7. Experimental
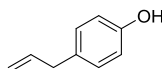
4-Allylphenol (3.4). A solution of 4-allylanisole (770 mg, 5.0 mmol) in dry CH_2Cl_2 (25 mL) was cooled to 0 ºC. Then, BBr_3 (0.6 mL, 1.2 equiv) was added slowly.

(107) Lee, Y. E.; Kozlowski, M. C. *et al*. "Improved Synthesis of Honokiol" *Provisional Patent*.

After stirring 3 h at room temperature, the reaction mixture was cooled to 0 °C and quenched with water (20 mL). Extraction with CH_2Cl_2 (15 mL x 3) afforded an organic layer, which was washed with brine (30 mL), dried over Na_2SO_4, and concentrated. The residue was chromatographed (30% EtOAc/hexanes) to afford 4-allylphenol (410 mg, 61%) as colourless oil: ^{1}H NMR (500 MHz, CDCl$_3$) δ 7.05 (d, J = 11.5 Hz, 2H), 6.76 (d, J = 11.5 Hz, 2H), 5.99-5.91 (m, 1H), 5.08-5.05 (m, 1H), 5.04 (t, J = 1.5 Hz, 1H), 4.61 (s, 1H), 3.32 (d, J = 7.0 Hz, 2H); ^{13}C NMR (125 MHz, CDCl$_3$) δ 153.8, 137.8, 132.3, 129.7, 115.5, 115.2, 39.3; IR (film) 3341, 3078, 2978, 2901, 2833, 1889, 1639, 1612, 1512, 1444, 1233, 1109, 994, 915, 824 cm^{-1}; HRMS (ESI) m/z = 133.0653 calcd for C_9H_9O [M–H]$^-$, found 133.0657.
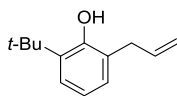
2-Allyl-6-*tert*-butylphenol (3.9). 2-*tert*-butylphenol (4.0 g, 26.6 mmol, Acros) was dissolved in DMF (15 mL) and kept stirring at room temperature. To this solution was added potassium carbonate (4.0 g, 1.1 equiv) followed by the dropwise addition of allyl bromide (2.5 mL, 1.1 equiv). The reaction mixture was then stirred for 15 hours at room temperature. Water (20 mL) was then added and the mixture was extracted with diethyl ether (20 mL x 3). The combined organic extracts were washed with water (30 mL), dried over $MgSO_4$. The crude product was purified by flash chromatography (hexane/EtOAc, 20:1) to give 1-allyloxy-2-*tert*-butylbenzene quantitatively. The crude product was used with purification for the next step.

1-Allyloxy-2-*tert*-butylbenzene (500 mg, 2.63 mmol) was heated to 220 °C in sealed tube. It was stirred for 2 h. Purification by flash chromatography (hexane/EtOAc, 15:1) gave **3.7** (405 mg, 81%) as colourless oil: ^{1}H NMR (500 MHz, CDCl$_3$) δ 7.20 (dd, *J* = 8.0 Hz, 1.5 Hz, 1H), 6.98 (dd, *J* = 8.0 Hz, 1.5 Hz, 1H), 6.83 (t, *J* = 7.5 Hz, 1H), 6.07-5.99 (m, 1H), 5.26-5.24 (m, 1H), 5.22 (t, *J* = 2.0 Hz, 1H), 5.19 (s, 1H), 3.43 (d, *J* = 6.5 Hz, 2H), 1.41 (s, 9H); ^{13}C NMR (125 MHz, CDCl$_3$) δ 153.5, 136.8, 136.3, 128.3, 125.7, 124.9, 120.2, 117.2, 36.2, 34.6, 29.7; IR (film) 3542, 2957, 1635, 1589, 1434, 1205, 1088, 1000, 922, 748 cm^{-1}; HRMS (ESI) *m/z* = 189.1279 calcd for C$_{13}$H$_{17}$O [M–H]$^-$, found 189.1274.
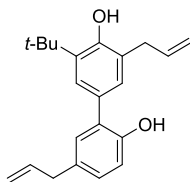
3',5-Diallyl-5'-(*tert*-butyl)-[1,1'-biphenyl]-2,4'-diol **(3.11).** Following the general cross-coupling procedure in **Chapter 2**, after a reaction for 15 h at 80 °C, the *ortho-para* product was obtained in 31% yield: ^{1}H NMR (500 MHz, CDCl$_3$) δ 7.25 (d, *J* = 8.0 Hz, 1H), 7.06 (d, *J* = 2.0 Hz, 1H), 7.04 (d, *J* = 2.0 Hz, 1H), 7.03 (d, *J* = 2.0 Hz, 1H), 6.91 (d, *J* = 8.0 Hz, 1H), 6.08-5.95 (m, 2H), 5.35 (s, 1H), 5.32-5.26 (m, 2H), 5.17 (s, 1H), 5.09 (dd, *J* = 17.0 Hz, 2.0 Hz, 1H), 5.05 (dd, *J* = 9.5 Hz, 1.0 Hz, 1H), 3.47 (d, *J* = 6.0 Hz, 2H), 3.36 (d, *J* = 6.5 Hz, 2H), 1.43 (s, 9H); ^{13}C NMR (125 MHz, CDCl$_3$) δ 153.4, 150.8, 137.9, 137.8, 135.9, 132.1, 130.2, 128.8, 128.7, 128.6, 128.2, 126.5, 125.9, 117.7, 115.5, 115.4, 39.4, 36.3, 34.9, 29.7; IR (film) 3436, 2957, 1638, 1471, 1362, 1202, 997, 918, 739 cm^{-1}; HRMS (ESI) *m/z* = 321.1855 calcd for C$_{22}$H$_{25}$O$_2$ [M–H]$^-$, found 321.1855.
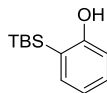
2-(*tert*-Butyldimethylsilyl)phenol (3.14). A solution of 2-bromophenol (520 mg, 3.0 mmol, Acros) in CH_2Cl_2 (6 mL) was added to imidazole (408 mg, 6.0 mmol) and TBSCl (543 mg, 3.6 mmol) in CH_2Cl_2 (3 mL) was added at 0 °C and the mixture was stirred for 30 min at ambient temperature. The reaction was quenched by the addition of water (10 mL) and the aqueous layer extracted with CH_2Cl_2 (10 mL x 3). The organic layer was separated, washed (water, 2 x 10 mL), dried (Na_2SO_4) and concentrated in vacuo to afford the crude product. Column chromatography of the residue (5% ethyl acetate in hexane) afforded silylether **3.13** as a pale pink oil (960 mg, quant.). Spectral data matched that reported in the literature.[108]

n-BuLi (1.8 mL, 4.0 mmol) was added dropwise to a stirred solution of the silylether **3.13** (0.96 g, 3.33 mmol) in THF (7 mL) at -78 °C under argon. The mixture was allowed to warm up to room temperature and stirred for 2 h. Water (1 mL) was added and after stirring for 5 min, ether (10 mL) was added. The organic layer was washed with water (3 x 10 mL), dried over $MgSO_4$ and concentrated in vacuo to afford the crude product as a yellow solid. Purification by flash column chromatography (hexane/ethyl acetate, 15:1) afforded 2-(*tert*-butyldimethylsilyl)phenol (**3.14**) as a pale orange solid (0.61 g, 88 %).

(108) Manley, D. W.; McBurney, R. T.; Miller, P.; Walton, J. C. "Titania-Promoted Carboxylic Acid Alkylations of Alkenes and Cascade Addition−Cyclizations" *J. Org. Chem.* **2014**, *79*, 1386−1398.
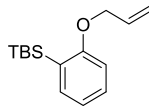
(2-(Allyloxy)phenyl)(tert-butyl)dimethylsilane **(3.15)**. 2-(*tert*-butyldimethylsilyl)phenol (608 mg, 2.92 mmol) was dissolved in DMF (6 mL). To this solution was added potassium carbonate (445 mg, 3.21 mmol) followed by the dropwise addition of allyl bromide (0.28 mL, 3.21 mmol). The reaction mixture was then stirred for 16 hours at room temperature. Water (10 mL) was then added and the mixture was extracted with diethyl ether (3 x 10 mL). The combined organic extracts were washed with water (20 mL), dried over MgSO$_4$. The crude product was purified by flash chromatography (hexane/EtOAc, 20:1) to give clear liquid of compound (480 mg, 1.93 mmol) in 66% yield: : ^{1}H NMR (500 MHz, CDCl$_3$) δ 7.38 (dd, J = 7.0 Hz, 1.5 Hz, 1H), 7.33-7.29 (m, 1H), 6.94 (t, J = 7.0 Hz, 1H), 6.81 (d, J = 8.0 Hz, 1H), 6.11-6.03 (m, 1H), 5.37 (d, J = 17.5 Hz, 1H), 5.26 (d, J = 10.5 Hz, 1H), 4.51 (d, J = 5.5 Hz, 2H), 0.88 (s, 9H), 0.28 (s, 6H); ^{13}C NMR (125 MHz, CDCl$_3$) δ 163.3, 136.6, 133.6, 130.5, 125.7, 120.2, 117.5, 110.5, 68.8, 27.1, 17.6, -4.51; IR (film) 3475, 3064, 2928, 2856, 1681, 1586, 1470, 1437, 1388, 1254, 1092, 835, 757, 661 cm^{-1}; HRMS (ESI) m/z = 247.1518 calcd for C$_{15}$H$_{23}$OSi [M–H]$^-$, found 247.1513.
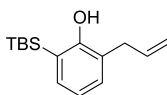
2-Allyl-6-(*tert*-butyldimethylsilyl)phenol (3.16). To a solution of allyl aryl ether (240 mg, 0.96 mmol) in dichloromethane (5 mL) was added boron trichloride (2.7 mL, 2.7 mmol) dropwise at -50 °C. After stirring for 30 min at -50 °C, the solution was

quenched with water (8 mL), extracted with dichloromethane (8 mL x 3), dried over MgSO$_4$. The crude product was purified by flash chromatography (hexane/EtOAc, 20:1) to give 2-Allyl-6-(*tert*-butyldimethylsilyl)phenol (**3.16**) (168 mg, 0.67 mmol) as a white solid in 70% yield: ^{1}H NMR (500 MHz, CDCl$_3$) δ 7.26 (dd, *J* = 7.5 Hz, 2.0 Hz, 1H), 7.12 (dd, *J* = 7.5 Hz, 2.0 Hz, 1H), 6.88 (t, *J* = 7.5 Hz, 1H), 6.06-5.98 (m, 1H), 5.21 (t, *J* = 1.5 Hz, 1H), 5.19-5.17 (m, 1H), 5.13 (s, 1H), 3.40 (d, *J* = 6.0 Hz, 2H), 0.90 (s, 9H), 0.32 (s, 6H); ^{13}C NMR (125 MHz, CDCl$_3$) δ 159.5, 136.2, 135.3, 131.7, 123.9, 123.4, 120.4, 116.9, 36.0, 26.9, 17.6, -4.6; IR (film) 3541, 2953, 2855, 1635, 1596, 1422, 1260, 1207, 831, 770 cm^{-1}; HRMS (ESI) *m/z* = 247.1518 calcd for C$_{15}$H$_{23}$OSi [M–H]$^-$, found 247.1518.
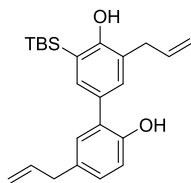
3',5-Diallyl-5'-(tert-butyldimethylsilyl)-[1,1'-biphenyl]-2,4'-diol   (**3.17**).

Following the general cross-coupling procedure in **Chapter 2**, after a reaction for 15 h at 80 °C, the *ortho-para* product was obtained in 31% yield: ^{1}H NMR (500 MHz, CDCl$_3$) δ 7.31 (s, 1H), 7.19 (s, 1H), 7.06 (d, *J* = 8.0 Hz, 1H), 7.02 (s, 1H), 6.91 (d, *J* = 8.0 Hz, 1H), 6.08-5.94 (m, 2H), 5.29 (s, 1H), 5.26 (d, *J* = 8.0 Hz, 1H), 5.24 (d, *J* = 1.4 Hz, 1H), 5.11-5.04 (m, 2H), 5.10 (s, 1H), 3.45 (d, *J* = 6.0 Hz, 2H), 3.36 (d, *J* = 6.5 Hz, 2H), 0.92 (s, 9H), 0.33 (s, 6H); ^{13}C NMR (125 MHz, CDCl$_3$) δ 159.4, 150.8, 137.8, 135.8, 135.6, 132.4, 132.2, 130.2, 128.8, 128.7, 128.0, 124.9, 124.7, 117.5, 115.6, 115.5, 39.4, 36.0,

26.9, 17.6, -4.6; IR (film) 3390, 2927, 2855, 1659, 1593, 1496, 1461, 1255, 917, 835, 740

cm^{-1}; HRMS (ESI) m/z = 379.2093 calcd for $C_{24}H_{31}O_2Si$ [M–H]$^-$, found 379.2102.
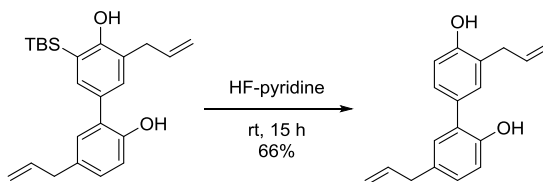
Honokiol (5,3'-diallyl-[1,1'-biphenyl]-2,4'-diol). A cold solution of 4% HF:pyridine (2 mL) was slowly added to a mixture of coupling product **3.17** (38 mg, 0.1 mmol) in pyridine (1 mL) at 0–5°C while stirring. The reaction mixture was stirred at ambient temperature for 1–2 hours. The reaction progress was monitored using TLC. After completion of the reaction, the solution was cooled and the reaction mixture was neutralized with saturated sodium bicarbonate solution. The organic layer was thoroughly washed with saturated sodium bicarbonate solution and dried over anhydrous sodium sulfate. Solvent was removed under reduced pressure. The respective residues were loaded onto a silica gel column and the column was eluted with a 20% ethyl acetate in hexanes to afford the desired honokiol (18 mg, 0.066 mmol) in 66% yield.
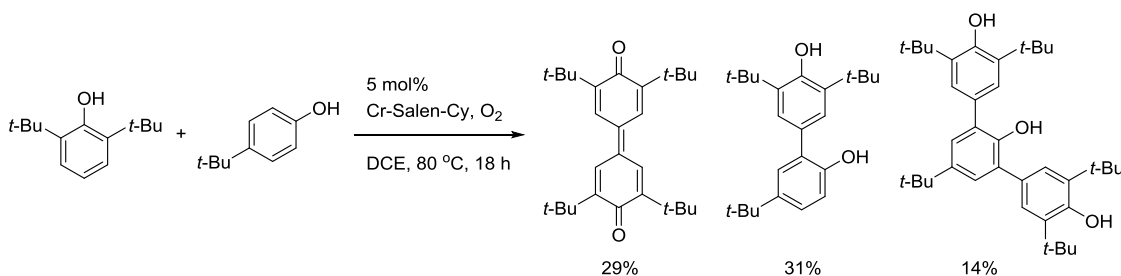
To a 5 mL microwave vial was added 2,6-di-*tert*-butylphenol (41 mg, 0.2 mmol), 4-*tert*-butylphenol (30 mg, 0.2 mmol) and Cr-Salen-Cy catalyst (13 mg, 0.02 mmol). The

166

vial was sealed with a septum and 1,2-dichloroethane (2.0 mL) was added. Oxygen was added *via* active purge. The septum was replaced with a crimping cap and the vessel was sealed and stirred for 18 h at 80 °C. The reaction mixture was filtered through a plug of silica and the resultant material was concentrated *in vacuo* and chromatographed using 10% ethyl acetate/hexane to afford a mixture of products in 29% of diphenoquinone, 31% of dimer and 14% of trimer.
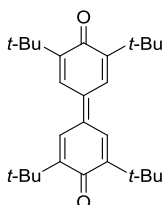
3,3',5,5'-Tetra-tert-butyl-[1,1'-bi(cyclohexylidene)]-2,2',5,5'-tetraene-4,4'-dione (3.24). ^{1}H NMR (500 MHz, CDCl$_3$) δ 7.71 (s, 4H), 1.36 (s, 36H); ^{13}C NMR (125 MHz, CDCl$_3$) δ 186.5, 150.4, 136.1, 126.0, 36.0, 29.6; IR (film) 2957, 1604, 1455, 1385, 1361, 1262, 1091, 1041, 898, 743 cm^{-1}; HRMS (ESI) *m/z* = 409.3107 calcd for C$_{28}$H$_{41}$O$_2$ [M+H]$^+$, found 409.3097.
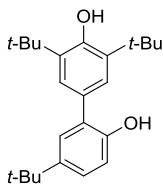
3',5,5'-Tri-*tert*-butyl-[1,1'-biphenyl]-2,4'-diol (3.25). ^{1}H NMR (500 MHz, CDCl$_3$) δ 7.27 (dd, *J* = 8.0 Hz, 2.0 Hz, 1H), 7.25 (s, 2H), 7.23 (d, *J* = 2.0 Hz, 1H), 6.93 (d, *J* = 8.0 Hz, 1H), 5.33 (s, 1H), 5.16 (s, 1H), 1.48 (s, 18H), 1.33 (s, 9H); ^{13}C NMR (125 MHz, CDCl$_3$) δ 153.6, 150.3, 143.2, 136.9, 128.3, 127.1, 125.9, 125.5, 114.8, 34.5, 34.2,

31.6, 30.3; IR (film) 3638, 3544, 2958, 1437, 1393, 1156, 884, 821, 740 cm^{-1}; HRMS (ESI) m/z = 353.2481 calcd for C$_{24}$H$_{33}$O$_2$ [M–H]$^{-}$, found 353.2478.
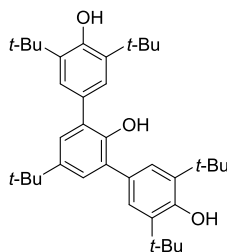
3,3'',5,5',5''-Penta-tert-butyl-[1,1':3',1''-terphenyl]-2',4,4''-triol (3.26). ^{1}H NMR (500 MHz, CDCl$_3$) δ 7.35 (s, 4H), 7.26 (s, 2H), 5.36 (s, 1H), 5.28 (s, 2H), 1.48 (s, 36H), 1.36 (s, 9H); ^{13}C NMR (125 MHz, CDCl$_3$) δ 153.4, 147.2, 142.8, 136.1, 129.1, 128.7, 126.6, 126.2, 34.5, 31.6, 30.3, 29.4; IR (film) 3530, 2959, 1654, 1438, 1395, 1362, 1232, 1155, 879, 739 cm^{-1}; HRMS (ESI) m/z = 559.4151 calcd for C$_{38}$H$_{55}$O$_3$ [M+H]$^{+}$, found 559.4152.
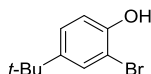
2-Bromo-4-(*tert*-butyl)phenol (3.27). A 250 mL round-bottom flask, equipped with a stir bar was charged with 4-*tert*-butyl-phenol (15 g, 100 mmol, 1.0 equiv) and CH$_2$Cl$_2$ (100 mL, 1.0 M). The resulting solution was cooled to 0 °C in an ice bath, and the temperature was allowed to equilibrate for 20 min. A homogenous solution of bromine (15.95 g, 5.15 mL, 100 mmol, 1.0 equiv) in CH$_2$Cl$_2$ (10 mL) was added dropwise via syringe over the course of 10 min to afford an orange heterogeneous mixture, which was stirred for 30 min. The resulting solution was allowed warm to 23 °C and stirred overnight. Distilled water (100 mL) was added to quench the reaction, and the

resulting biphasic mixture was diluted with EtOAc (200 mL). Phases were separated, and

the organic layer was washed with 10% aq. $Na_2S_2O_3$ (3 x 100 mL), dried over $MgSO_4$

and concentrated in vacuo to yield a yellow liquid that was purified by silica gel column

chromatography (EtOAc : hexanes, 1 : 9). 2-Bromo-4-*tert*-butylphenol (21.3 g) was

obtained as a clear liquid in 93% isolated yield: ^{1}H NMR (500 MHz, CDCl$_3$) δ 7.45 (d, *J*

= 2.5 Hz, 1H), 7.24 (dd, *J* = 8.5 Hz, 2.5 Hz, 1H), 6.95 (s, *J* = 8.5 Hz, 1H), 5.35 (s, 1H),

1.29 (s, 9H); ^{13}C NMR (125 MHz, CDCl$_3$) δ 149.9, 145.1, 128.8, 126.2, 115.5, 109.9,

34.2, 31.4; IR (film) 3512, 2962, 1604, 1499, 1405, 1364, 1269, 1183, 1040, 821, 703

cm^{-1}; HRMS (ESI) *m/z* = 227.0072 calcd for $C_{10}H_{12}OBr$ [M–H]$^-$, found 227.0071.
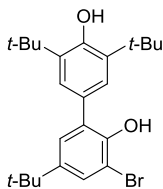
3-Bromo-3',5,5'-tri-*tert*-butyl-[1,1'-biphenyl]-2,4'-diol **(3.28).** A typical

procedure for the cross-coupling of phenols with Cr-Salen-Cy catalyst and TBHP as an

oxidant was as follow. To a 100 mL flask equipped with a reflux condenser was added

2,6-di-*tert*-butylphenol (206mg, 1.0 mmol), 2-bromo-4-*tert*-butylphenol (229 mg, 1.0

mmol), Cr-Salen-Cy (6.3 mg, 1 mol%), TBHP (0.36 mL, 5.5 M in decane) and

chlorobenzene (20 mL, 0.05 M). The reaction mixture was refluxed under air for 1 h.

After cooling to room temperature, the reaction mixture was filtered through Celite, and

the filtrate was concentrated under vacuum to afford an oily substance. The crude product

was purified by flash chromatography (hexane/EtOAc, 30:1) to give clear liquid of

compound (225 mg, 0.52 mmol) in 52% yield: ^{1}H NMR (500 MHz, CDCl$_3$) δ 7.44 (d, *J* =

2.5 Hz, 1H), 7.30 (s, 2H), 7.22 (d, J = 2.0 Hz, 1H), 5.55 (s, 1H), 5.33 (s, 1H), 1.32 (s, 9H), 1.28 (s, 19H); IR (film) 3636, 3512, 2960, 1653, 1481, 1363, 1235, 1155, 1076, 878, 739 cm^{-1}; HRMS (ESI) m/z = 455.1562 calcd for $C_{24}H_{33}O_2BrNa$ [M+Na]$^+$, found 455.1563.
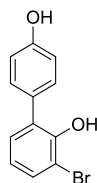
3-Bromo-[1,1'-biphenyl]-2,4'-diol (3.31). A mixture of the 3-bromo-3',5,5'-tri-*tert*-butyl-[1,1'-biphenyl]-2,4'-diol (380 mg, 0.88 mmol) and methansulfonic acid (0.23 mL, 3.5 mmol) in toluene (4.5 mL, 0.2 M) was heated at 110 °C for 15 h. The reaction mixture allowed to cool to room temperature, and poured into water (10 mL). The mixture was made slightly alkaline with sodium carbonate and extracted with dichloromethane (3 × 10 mL). The extract was dried with sodium sulfate and evaporated in vacuo to leave crude product that was purified by silica gel column chromatography (EtOAc : hexanes, 1 : 4). 3-Bromo-[1,1'-biphenyl]-2,4'-diol (196 mg, 0.65 mml) was obtained as pale yellow liquid in 74% isolated yield: ^{1}H NMR (500 MHz, CDCl$_3$) δ 7.44 (dd, J = 8.0 Hz, 1.5 Hz, 1H), 7.42 (d, J = 8.5 Hz, 2H), 7.21 (dd, J = 8.0 Hz, 1.5 Hz, 1H), 6.91 (d, J = 8.5 Hz, 2H), 6.86 (t, J = 7.5 Hz, 1H), 5.66 (s, 1H), 4.92 (s, 1H).
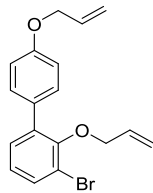
2,4'-Bis(allyloxy)-3-bromo-1,1'-biphenyl (3.33). 3-Bromo-[1,1'-biphenyl]-2,4'-diol (110 mg, 0.42 mmol) was dissolved in DMF (1 mL). To this solution was added potassium carbonate (138 mg, 1.00 mmol) followed by the dropwise addition of allyl bromide (86 µL, 1.00 mmol). The reaction mixture was then stirred for 16 hours at room temperature. Water (5 mL) was then added and the mixture was extracted with diethyl ether (3 x 10 mL). The combined organic extracts were washed with water (10 mL), dried over MgSO$_4$. The crude product was purified by flash chromatography (hexane/EtOAc, 20:1) to give clear liquid of compound (140 mg, 0.41 mmol) in 98% yield: ^{1}H NMR (500 MHz, CDCl$_3$) δ 7.52-7.49 (m, 1H), 7.50 (d, J = 8.5 Hz, 2H), 7.27 (d, J = 8.0 Hz, 1H), 7.02 (t, J = 8.0 Hz, 1H), 6.97 (d, J = 8.5 Hz, 2H), 6.12-6.06 (m, 1H), 5.86-5.80 (m, 1H), 5.45 (d, J = 17.0 Hz, 1H), 5.31 (d, J = 10.5 Hz, 1H), 5.15 (d, J = 17.0 Hz, 1H), 5.09 (d, J = 11.5 Hz, 1H), 4.59 (d, J = 4.0 Hz, 2H), 4.06 (d, J = 7.0 Hz, 2H).
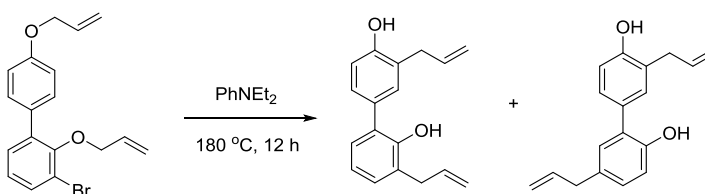
A solution of bis-*O*-allylbiphenyl ether **3.33** (75 mg, 0.22 mmol), in *N,N*-diethylaniline (0.5 mL) was stirred at 190 °C for 12 h in a sealed tube. After completion, the solvent was evaporated under reduced pressure and the residue was diluted with water

(5 mL) and extracted with EtOAc (3 x 10 mL). The combined organic layers were washed with brine solution, dried over anhydrous Na$_2$SO$_4$, and concentrated under reduced pressure to give the crude residue, which was purified by silica gel column chromatography (EtOAc/hexanes, 1:8) to afford the honokiol (22 mg, 0.083 mmol) in 38% yield and isohonokiol (30 mg, 0.11 mmol) in 50% yield. Spectral data from the two products are in agreement with those reported.[87]
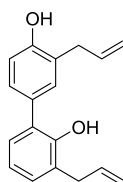
3,3'-Diallyl-[1,1'-biphenyl]-2,4'-diol (3.35, isohonokiol) ^{1}H NMR (500 MHz, CDCl$_3$) δ 7.24-7.22 (m, 2H), 7.12-7.08 (m, 2H), 6.93-6.90 (m, 2H), 6.10-6.00 (m, 2H), 5.32 (s, 1H), 5.22 (dd, J = 13.5 Hz, 1.5 Hz, 1H), 5.19 (dd, J = 6.5 Hz, 1.5 Hz, 1H), 5.15 (dd, J = 17.0 Hz, 1.5 Hz, 1H), 5.11 (dd, J = 10.0 Hz, 1.0 Hz, 1H), 5.06 (s, 1H), 3.46 (d, J = 6.5 Hz, 4H); ^{13}C NMR (125 MHz, CDCl$_3$) δ 153.9, 150.5, 136.7, 135.9, 131.3, 129.7, 129.4, 128.7, 128.3, 127.8, 126.3, 120.4, 117.0, 116.6, 115.8, 35.2, 34.8; IR (film) 3526, 2975, 1638, 1607, 1506, 1455, 1223, 1113, 997, 915, 748 cm^{-1}; HRMS (ESI) *m/z* = 265.1229 calcd for C$_{18}$H$_{17}$O$_2$ [M–H]$^-$, found 265.1230.
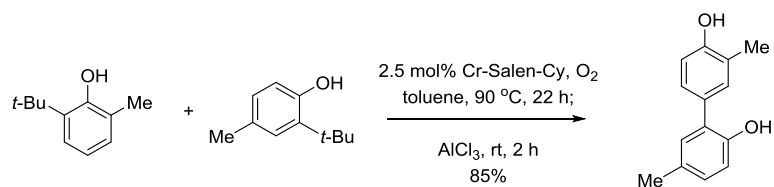
5,3'-Dimethyl-[1,1'-biphenyl]-2,4'-diol (3.37). To a 100 mL flask equipped with a reflux condenser was added 2-*tert*-butyl-6-methylphenol (657 mg, 4.0 mmol), 2-*tert*-butyl-4-methylphenol (788 mg, 4.8 mmol), Cr-Salen-Cy catalyst[109] (63 mg, 0.1 mmol) and distilled toluene (20 mL, 0.2 M). The reaction mixture was purged with oxygen and heated to 90 °C under an oxygen atmosphere for 20 h. The mixture was cooled to 0 °C for the next step.

To the resultant solution was added aluminum chloride (1.1 g, 8.8 mmol, Sigma Aldrich) slowly over 5 minutes at 0 °C, and the mixture was allowed to warm over 30 minutes to ambient temperature. After being stirred at room temperature for 2 h, the reaction mixture was quenched by addition of 30 mL of 1 N HCl solution at 0 °C. The mixture was thoroughly extracted with CH_2Cl_2 (20 mL × 2). The combined organic layers were concentrated by rotary evaporation. The resultant residue was purified by chromatography (silica) using 10% ethyl acetate/hexane as the eluent to afford 5,3'-dimethyl-[1,1'-biphenyl]-2,4'-diol (728 mg, 3.4 mmol, 85% yield) as a white crystalline solid: ^{1}H NMR (500 MHz, CDCl$_3$) δ 7.21 (d, *J* = 2.0 Hz, 1H), 7.16 (dd, *J* = 8.5, 2.0 Hz,

(109) Martinez, L. E.; Leighton, J. L.; Carsten, D. H.; Jacobsen, E. N. *J. Am. Chem. Soc.* **1995**, *117*, 5897-5898.

1H), 7.03 (dd, J = 8.5 Hz, 2.0 Hz, 1H), 7.01 (d, J = 2.0 Hz, 1H), 6.87 (d, J = 8.0 Hz, 2H), 5.07(s, 1H), 4.91 (s, 1H), 2.30 (s, 6H); ^{13}C NMR (125 MHz, CDCl$_3$) δ 153.6, 150.2, 131.7, 130.6, 129.8, 129.5, 129.2, 127.8, 127.6, 124.8, 115.6, 115.4, 20.5, 15.8; IR (film) 3402, 3026, 2922, 1611, 1496, 1456, 1384, 1118, 818 cm^{-1}; HRMS (ESI) m/z = 213.0916 calcd for C$_{14}$H$_{13}$O$_2$ [M–H]$^-$, found 213.0924.
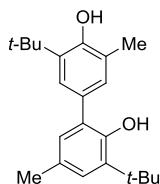
3,3'-Di-*tert*-butyl-5,5'-dimethyl-[1,1'-biphenyl]-2,4'-diol **(3.38).** A typical procedure for the cross-coupling of phenols with Mn(acac)$_3$ was as follow. To a 100 mL flask equipped with a reflux condenser was added 2-*tert*-butyl-6-methylphenol (490 mg, 3.0 mmol), 2-*tert*-butyl-4-methylphenol (590 mg, 3.6 mmol), Mn(acac)$_3$ (100 mg, 0.3 mmol) and distilled toluene (15 mL, 0.2 M). The reaction mixture was purged with oxygen and heated to 90 °C under an oxygen atmosphere for 20 h. The solvent was removed in vacuo, and the residue was purified by column chromatography using 5% ethyl acetate in hexane eluent to give 3,3'-Di-*tert*-butyl-5,5'-Dimethyl-[1,1'-biphenyl]-2,4'-diol (725 mg, 2.2 mmol, 74% yield) as a yellow solid : ^{1}H NMR (500 MHz, CDCl$_3$) δ 7.19 (d, J = 2.0 Hz, 1H), 7.07 (s, 2H), 6.88 (d, J = 2.0 Hz, 1H), 5.40 (s, 1H), 4.88 (s, 1H), 2.30 (s, 6H), 1.44 (s, 9H), 1.44 (s, 9H) ; ^{13}C NMR (125 MHz, CDCl$_3$) δ 152.5, 148.9, 136.8, 135.6, 129.4, 128.9, 128.6, 128.4, 128.3, 126.8, 126.4, 124.0, 34.8, 34.7, 29.7, 29.7, 20.8, 16.0; IR (film) 3532, 2956, 1636, 1483, 1443, 1315, 1199, 1179, 864,

779, 740 cm^{-1}; HRMS (ESI) m/z = 349.2144 calcd for $C_{22}H_{30}O_2Br$ [M+Na]$^+$, found 349.2129.
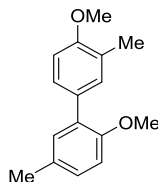
2,4'-Dimethoxy-5,3'-dimethylbiphenyl (3.41). To a stirred solution of 2,2'-dihydroxybiphenyl (728 mg, 3.4 mmol) in acetone (17 mL, 0.2 M) was added anhydrous K$_2$CO$_3$ (1.4 g, 10.2 mmol, 3.0 equiv). After stirring at ambient temperature for 10 min, dimethylsulfate (0.81 mL, 8.5 mmol, 2.5 equiv) was added and the reaction mixture stirred for 5 hours at ambient temperature. The reaction was quenched with deionized water (50 mL) and the acetone was removed by rotary evaporation. EtOAc (20 mL) was added and the organic layer separated. The aqueous layer was extracted with EtOAc (2 × 20 mL). The combined organic layers were washed with water and brine, dried (Na$_2$SO$_4$), and concentrated by rotary evaporation. The residue was purified by column chromatography (silica) using hexane/EtOAc (20:1) as the eluent to afford 2,4'-dimethoxy-5,3'-dimethylbiphenyl (758 mg, 3.13 mmol, 92%) as white solid: ^{1}H NMR (500 MHz, CDCl$_3$) δ 7.37 (dd, J = 8.0 Hz, 2.0 Hz, 1H), 7.29 (d, J = 2.0 Hz, 1H), 7.10 (d, J = 2.0 Hz, 1H), 7.07 (dd, J = 8.0 Hz, 2.0 Hz, 1H), 6.87 (d, J = 1.5 Hz, 1H), 6.86 (d, J = 1.5 Hz, 1H), 3.89 (s, 3H), 3.81 (s, 3H), 2.36 (s, 3H), 2.30 (s, 3H) ; ^{13}C NMR (125 MHz, CDCl$_3$) δ 157.0, 154.6, 132.0, 131.6, 130.8, 130.5, 130.1, 128.4, 128.0, 126.2, 111.4, 109.7, 55.9, 55.5, 20.7, 16.5; IR (film) 3437, 2949, 2834, 1609, 1495, 1463, 1242, 1135,

1033, 810, 741 cm^{-1}; HRMS (ESI) m/z = 243.1385 calcd for C$_{16}$H$_{19}$O$_2$ [M+H]$^+$, found 243.1384.
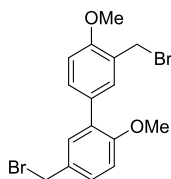
5,3'-Bis(bromomethyl)-2,4'-dimethoxybiphenyl (3.42). 2,4'-Dimethoxy-5,3'-dimethylbiphenyl (758 mg, 3.13 mmol), azobis-*iso*butyronitrile (26 mg, 0.16 mmol) and *N*-bromosuccinimide (1.11 g, 6.26 mmol, recrystallized from water) were dissolved in carbon tetrachloride (15 mL, 0.2 M). The reaction mixture was heated to 85 °C and stirred for 2 h under an argon atmosphere. The solution was filtered through Celite and the solvent was removed by rotary evaporation. The residue was purified by column chromatography (silica) using 5% ethyl acetate/hexane as the eluent to afford 5,3'-bis(bromomethyl)-2,4'-dimethoxybiphenyl (720 mg, 1.8 mmol, 57% yield) as a yellow solid: ^{1}H NMR (500 MHz, CDCl$_3$) δ 7.50 (d, J = 2.3 Hz, 1H), 7.47 (dd, J = 8.5 Hz, 2.3 Hz, 1H), 7.34-7.32 (m, 2H), 6.94 (d, J = 8.5 Hz, 1H), 6.92 (d, J = 8.5 Hz, 1H), 4.62 (s, 2H), 4.54 (s, 2H), 3.94 (s, 3H), 3.82 (s, 3H) ; ^{13}C NMR (125 MHz, CDCl$_3$) δ 156.7, 156.5, 132.0, 131.5, 131.2, 130.2, 130.1, 130.0, 129.2, 125.6, 111.3, 110.6, 55.7, 33.9, 29.1; IR (film) 3437, 2959, 1608, 1495, 1462, 1251, 1216, 1147, 1027, 818, 738 cm^{-1}.
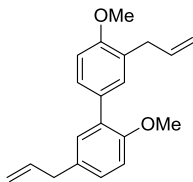
5,3'-Diallyl-2,4'-dimethoxybiphenyl (3.46). To a solution of CuI (286 mg, 1.5 mmol,) and 5,3'-bis(bromomethyl)-2,4'-dimethoxybiphenyl (1.2 g, 3.0 mmol) in dry THF (15 mL) at −78 °C, a solution of vinylmagnesium bromide (12 mL, 1.0 M in THF) was slowly added with a rate of 3 mL/min using syringe pump under an argon atmosphere. The resulting mixture was allowed to warm to ambient and was stirred for 8 hours. The reaction was then quenched by addition of 15 mL of saturated NH$_4$Cl solution. The mixture was extracted with diethyl ether (15 mL × 2). The combined organic layers were dried with anhydrous Na$_2$SO$_4$ and filtered. After removal of the solvent by rotary evaporation, the residue was purified by column chromatography (silcia) using 5% ethyl acetate/hexane as the eluent to give 5,3'-diallyl-2,4'-dimethoxybiphenyl (665 mg, 2.25 mmol, 75% yield) as a clear oil: ^{1}H NMR (500 MHz, CDCl$_3$) δ 7.39 (dd, J = 8.4 Hz, 2.2 Hz, 1H), 7.33 (d, J = 2.3 Hz, 1H), 7.14 (d, J = 2.2 Hz, 1H), 7.09 (dd, J = 8.4 Hz, 2.0 Hz, 1H), 6.91 (d, J = 8.4 Hz, 2H), 6.01-5.96 (m, 2H), 5.03-5.11 (m, 4H), 3.86 (s, 3H), 3.78 (s, 3H), 3.43 (d, J = 6.5 Hz, 2H), 3.37 (d, J = 6.5 Hz, 2H) ; ^{13}C NMR (125 MHz, CDCl$_3$) δ 156.4, 154.9, 137.8, 137.0, 132.2, 131.0, 130.9, 130.7, 130.5, 128.3, 128.1, 127.9, 115.5, 115.3, 111.3, 109.9, 55.7, 55.4, 39.4, 34.3; IR (film) 3435, 2938, 2836, 1638, 1606, 1493, 1463, 1245, 1134, 1029, 914, 815 cm^{-1}; HRMS (ESI) m/z = 295.1698 calcd for C$_{20}$H$_{23}$O$_2$ [M+H]$^+$, found 295.1705.
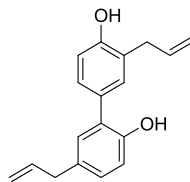
Honokiol (5,3'-diallyl-[1,1'-biphenyl]-2,4'-diol). To a solution of 5,3'-diallyl-2,4'-dimethoxybiphenyl (400 mg, 1.36 mmol) in distilled 1,2-dichloroethane (7 mL) was slowly added $BBr_3 \cdot DMS$ complex (1.0 g, 3.26 mmol). The reaction flask was sealed and heated to 65 °C for 15 h. The reaction was quenched with saturated $NaHCO_3$ solution (15 mL) and extracted with dichloromethane (15 mL × 3). The combined organic layers were washed with brine (15 mL), dried over Na_2SO_4, and filtered. The solvent was concentrated by rotary evaporation and the residue was purified by column chromatography (silica) with 20% ethyl acetate/hexane as eluent to give honokiol (345 mg, 1.29 mmol, 95% yield) as a white solid; ^{1}H NMR (500 MHz, $CDCl_3$) δ 7.23 (dd, J = 8.0 Hz, 2.0 Hz, 1H), 7.21 (d, J = 2.1 Hz, 1H), 7.05 (dd, J = 8.0 Hz, 2.0 Hz, 1H), 7.02 (d, J = 2.1 Hz, 1H), 6.93 (d, J = 8.2 Hz, 1H), 6.90 (d, J = 8.2 Hz, 1H), 5.93–6.08 (m, 2H), 5.17–5.24 (m, 3H), 5.03–5.11 (m, 3H) 3.46 (d, J = 6.5 Hz, 2H), 3.35 (d, J = 6.7 Hz, 2H) ; ^{13}C NMR (125 MHz, $CDCl_3$) δ 153.9, 150.7, 137.8, 136.0, 132.2, 131.1, 130.2, 129.6, 128.8, 128.6, 127.7, 126.4, 116.9, 116.6, 115.6, 115.5, 39.4, 35.1; HRMS (ESI) m/z = 265.1229 calcd for $C_{18}H_{17}O_2$ [M–H]⁻, found 265.1223. The above spectral data are in agreement with those reported for the natural product honokiol.[87]

APPENDIX A: SPECTROSCOPIC DATA

A.1 Chapter 1
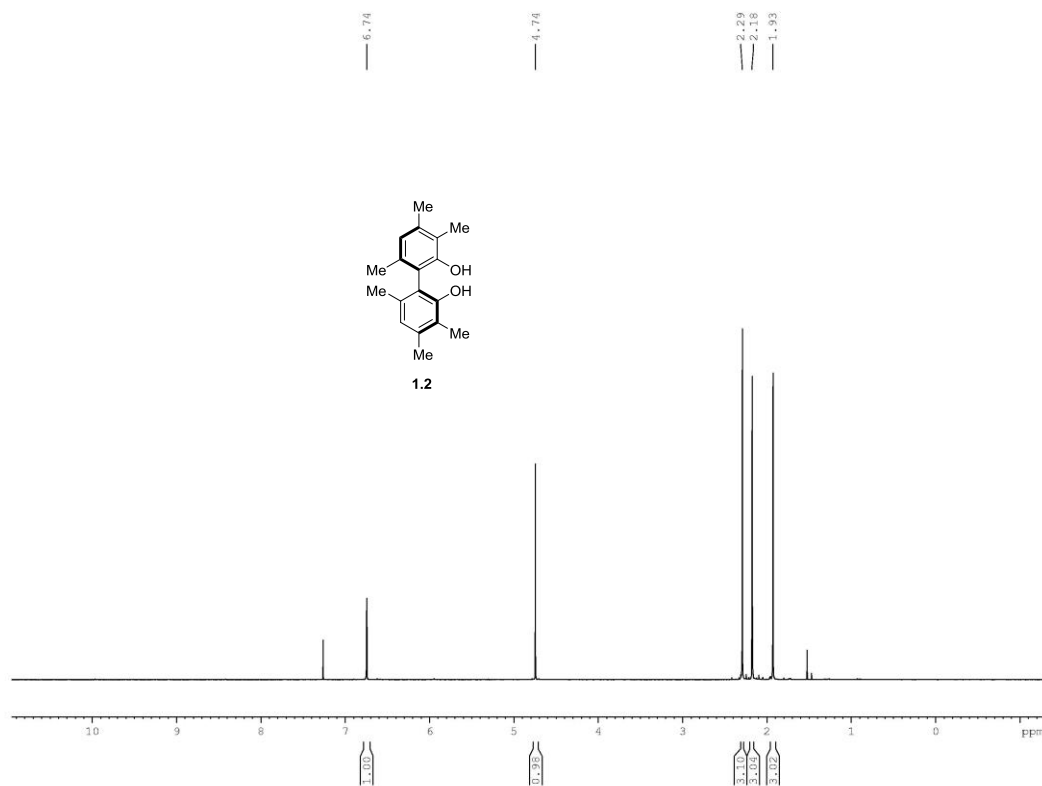
Figure A1.1 ^{1}H NMR spectrum of compound **1.2** (500 MHz, CDCl$_3$)
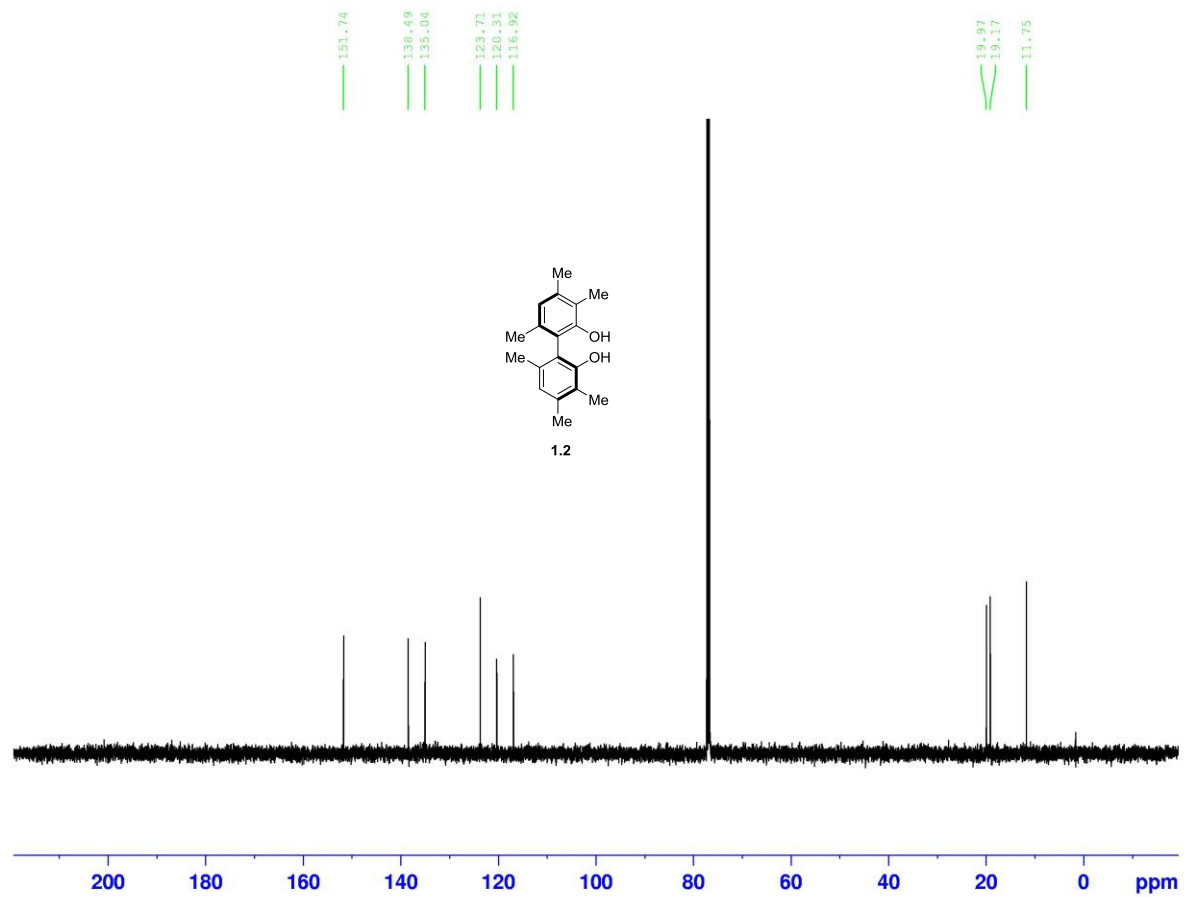
Figure A1.2 ^{13}C NMR spectrum of compound **1.2** (125 MHz, CDCl$_3$)
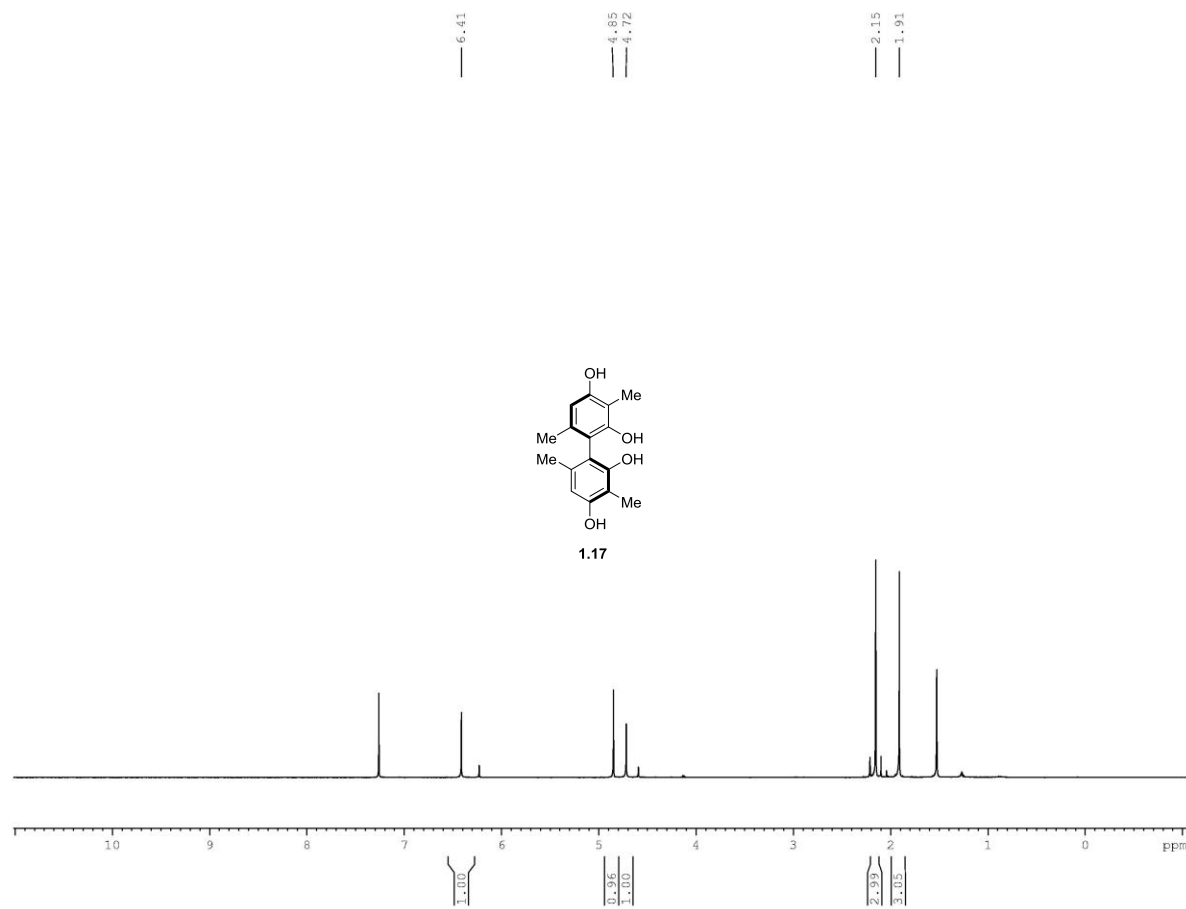
Figure A1.3 ^{1}H NMR spectrum of compound **1.17** (500 MHz, CDCl$_3$)

Figure A1.4 ^{13}C NMR spectrum of compound **1.17** (125 MHz, CDCl$_3$)

Figure A1.5 ^{1}H NMR spectrum of compound **1.18** (500 MHz, CDCl₃)

Figure A1.6 ^{13}C NMR spectrum of compound **1.18** (125 MHz, CDCl$_3$)

Figure A1.7 ^{1}H NMR spectrum of compound **1.20** (500 MHz, CDCl$_3$)

185

Figure A1.8 ^{13}C NMR spectrum of compound **1.20** (125 MHz, CDCl$_3$)

186

6.605
6.468

4.625

2.600
2.584
2.568
2.284
2.249
1.598
1.583
1.568
1.552
1.537
1.522
1.032
1.017
1.002

Me

Me OH

1.21

1.00
1.01

1.01

2.06
3.02
3.07

2.14

3.14

10   9   8   7   6   5   4   3   2   1   0   ppm

Figure A1.9 ^{1}H NMR spectrum of compound **1.21** (500 MHz, CDCl$_3$)

Figure A1.10 ^{13}C NMR spectrum of compound **1.21** (125 MHz, CDCl$_3$)

Figure A1.11 ^{1}H NMR spectrum of compound **1.22** (500 MHz, CDCl$_3$)

Figure A1.12 ^{13}C NMR spectrum of compound **1.22** (125 MHz, CDCl$_3$)

Figure A1.13 ^{1}H NMR spectrum of compound **1.23** (500 MHz, CDCl$_3$

Figure A1.14 ^{13}C NMR spectrum of compound **1.23** (125 MHz, CDCl$_3$)
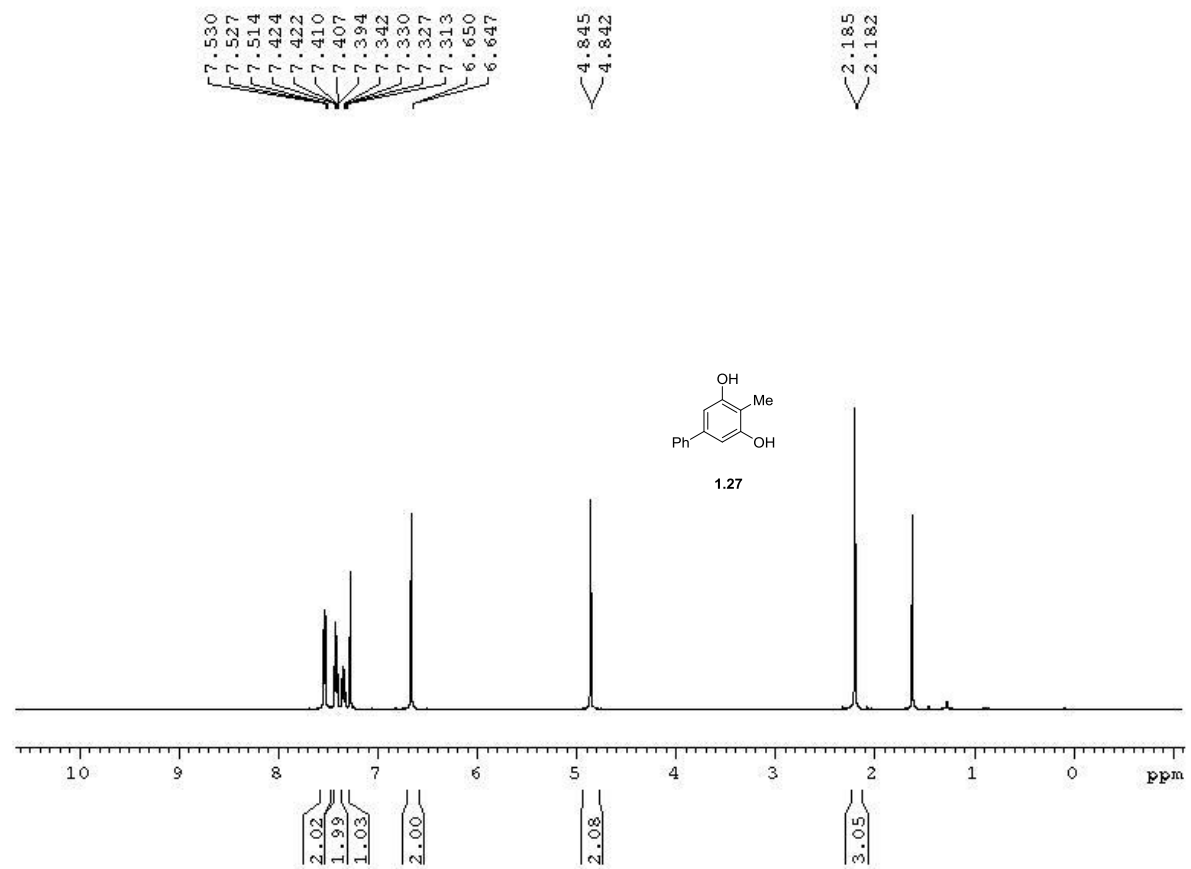
Figure A1.15 ^{1}H NMR spectrum of compound **1.27** (500 MHz, CDCl$_3$)
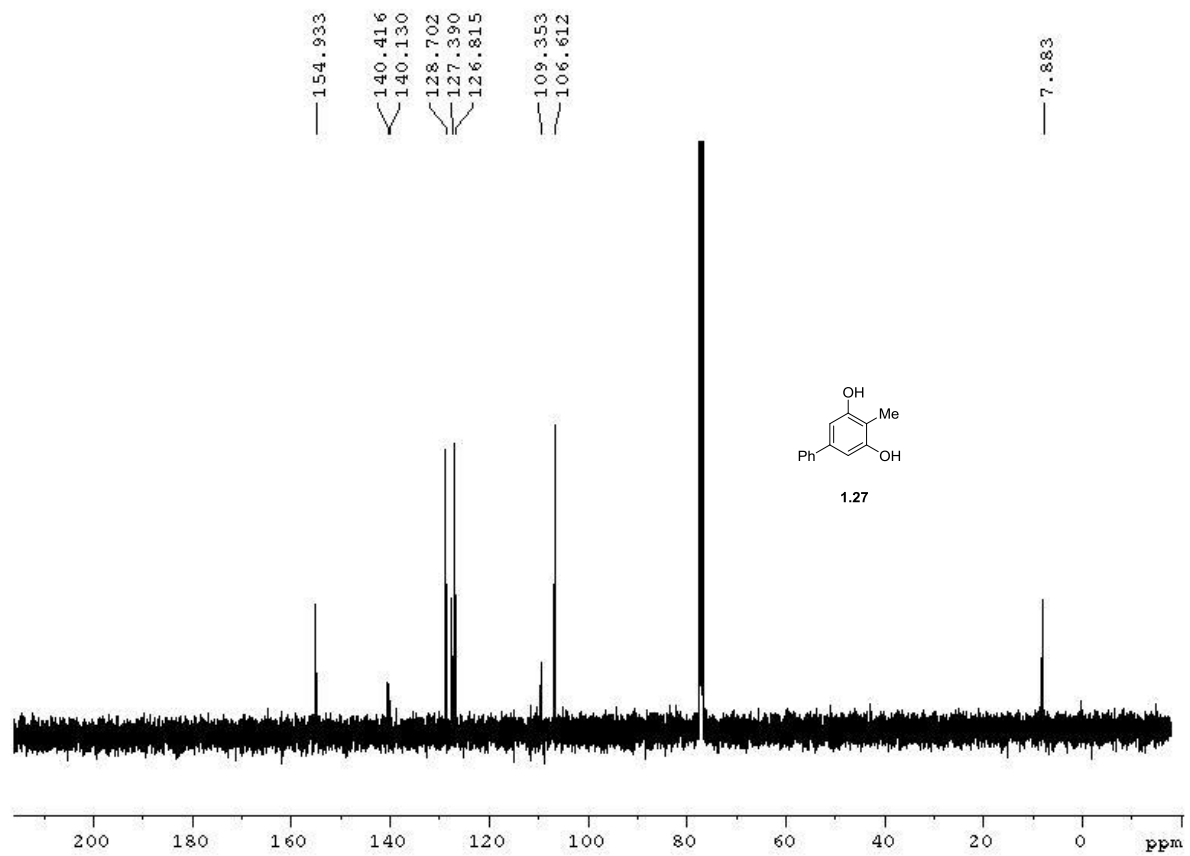
Figure A1.16 ^{13}C NMR spectrum of compound **1.27** (125 MHz, CDCl$_3$)
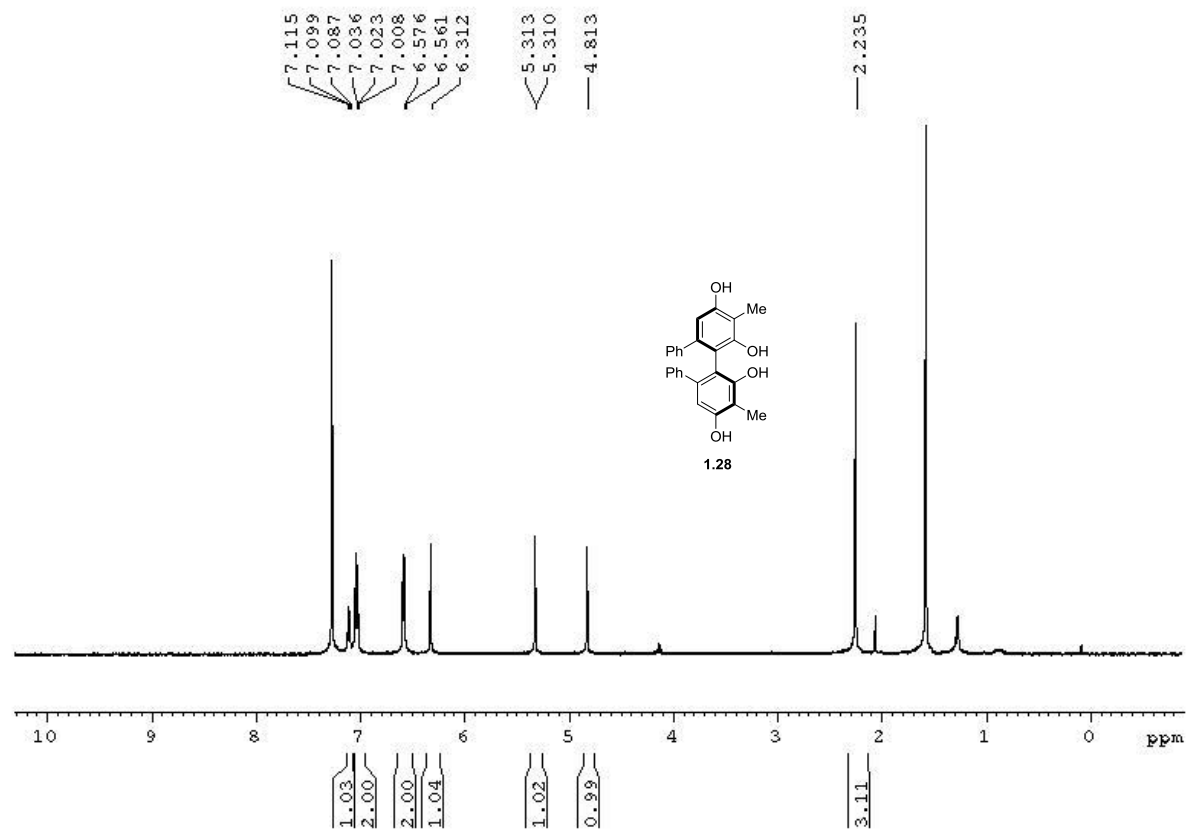
Figure A1.17 ^{1}H NMR spectrum of compound **1.28** (500 MHz, CDCl$_3$)
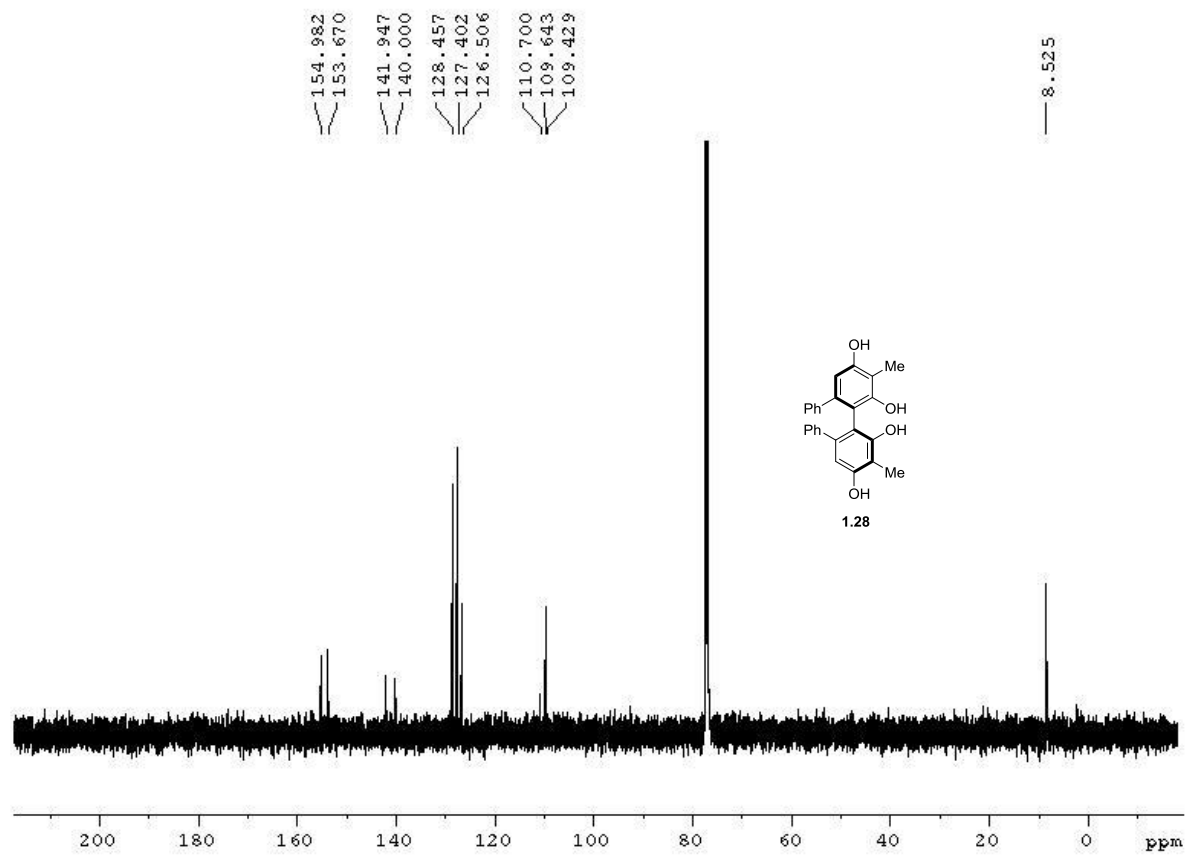
Figure A1.18 ^{13}C NMR spectrum of compound **1.28** (125 MHz, CDCl$_3$)
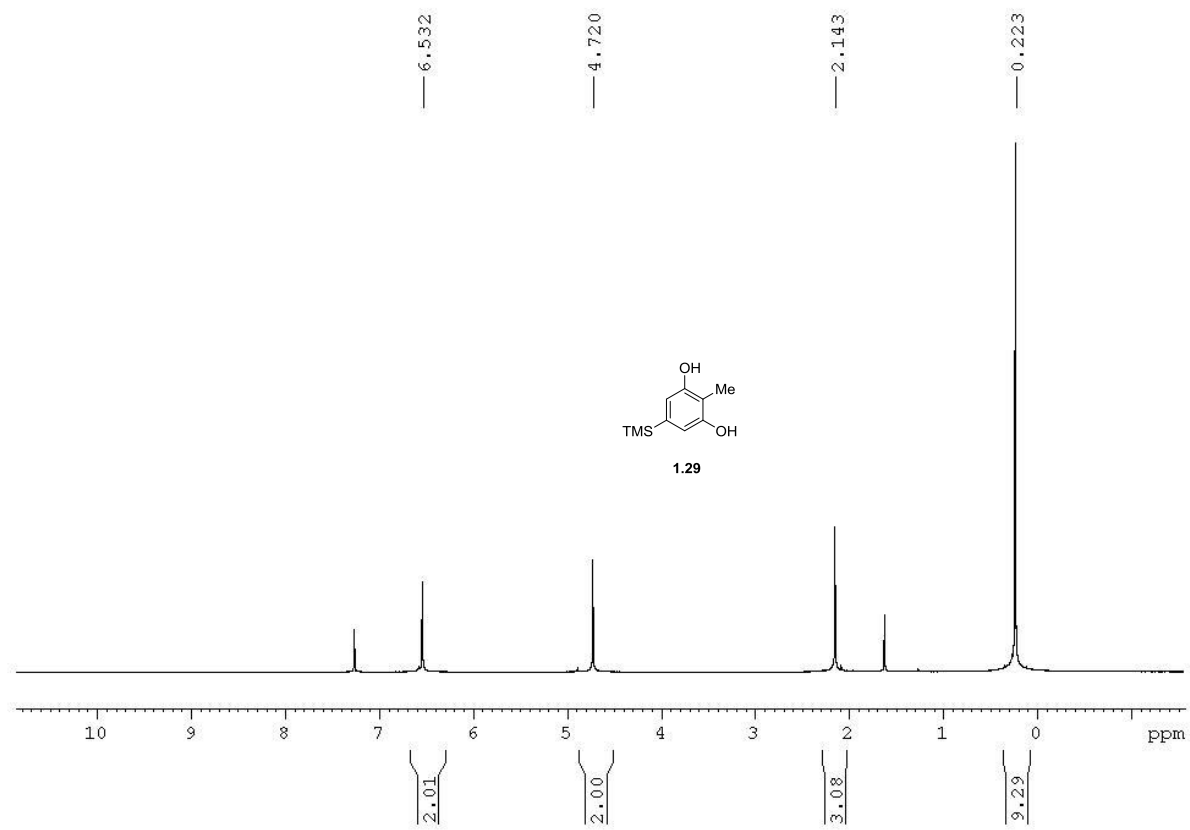
Figure A1.19 ^{1}H NMR spectrum of compound **1.29** (500 MHz, CDCl$_3$)

197
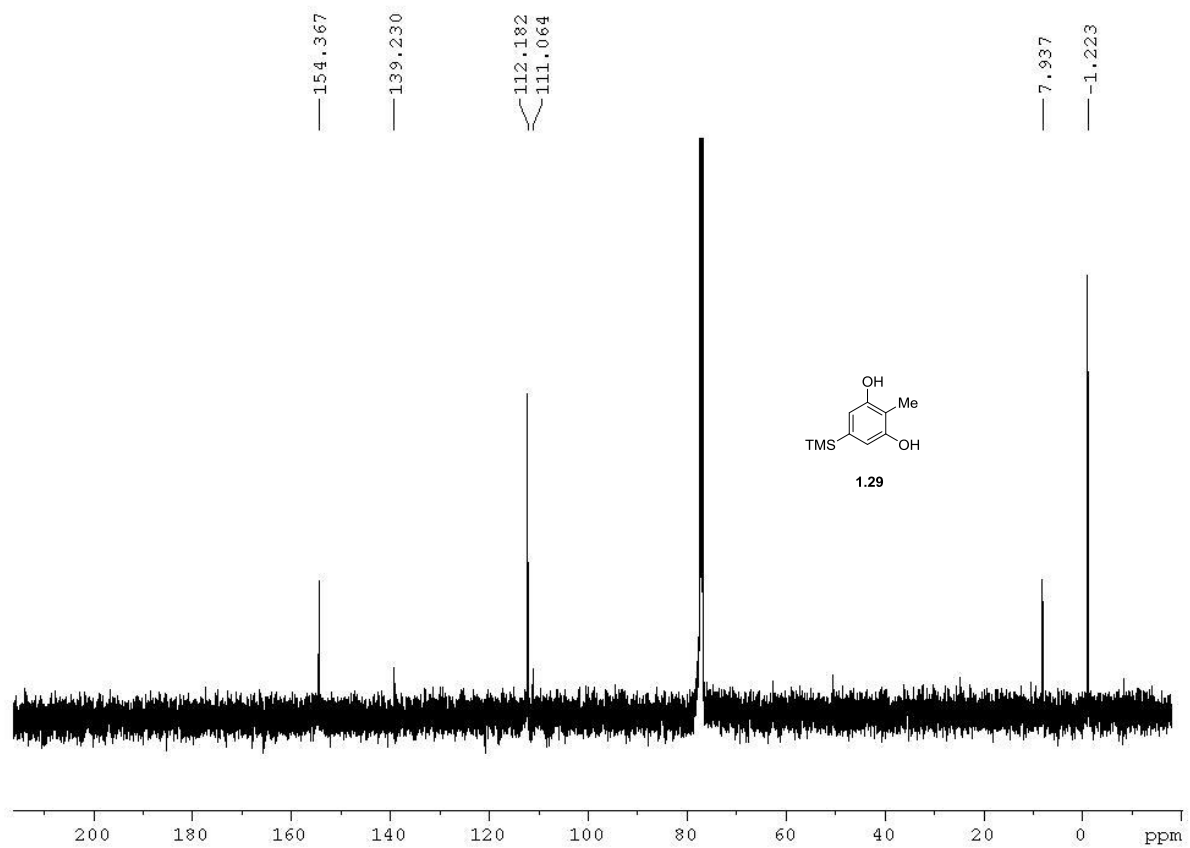
Figure A1.20 ^{13}C NMR spectrum of compound **1.29** (125 MHz, CDCl$_3$)
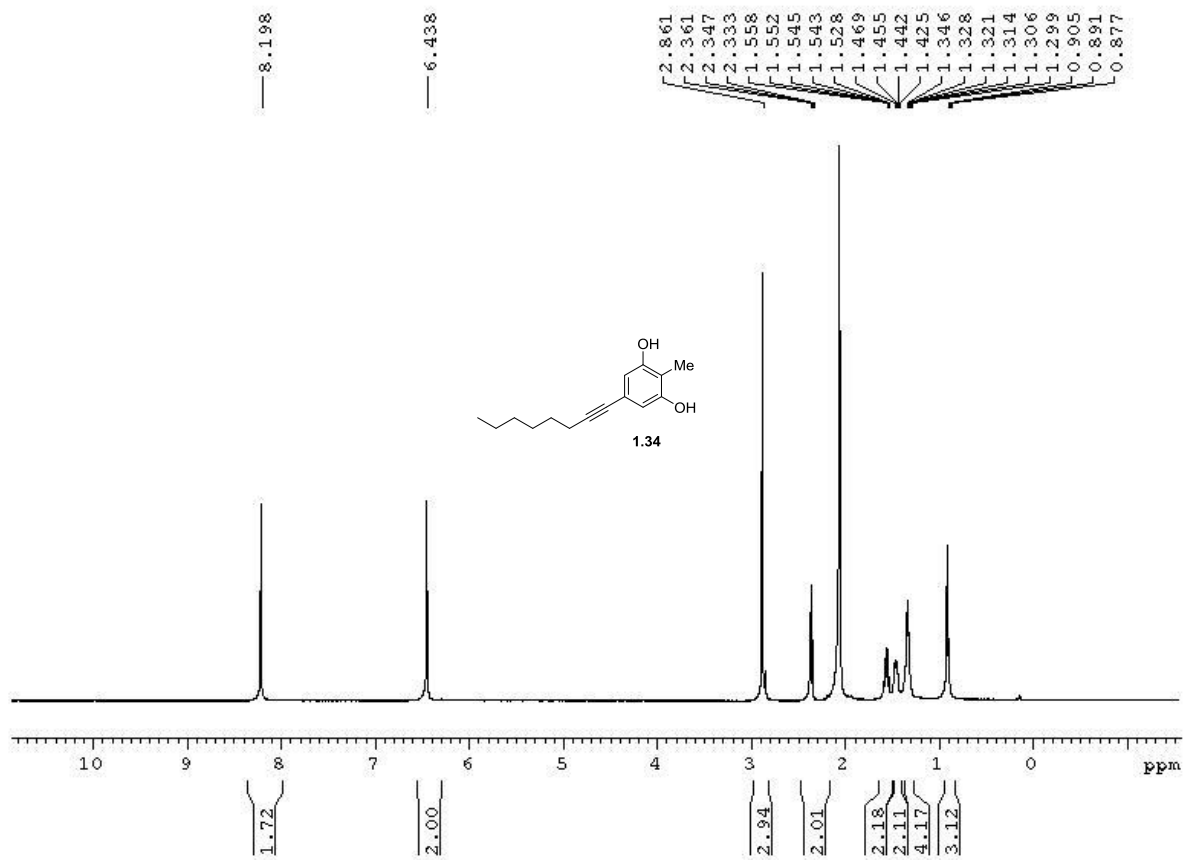
Figure A1.21 ^{1}H NMR spectrum of compound **1.34** (500 MHz, Acetone-d_6)
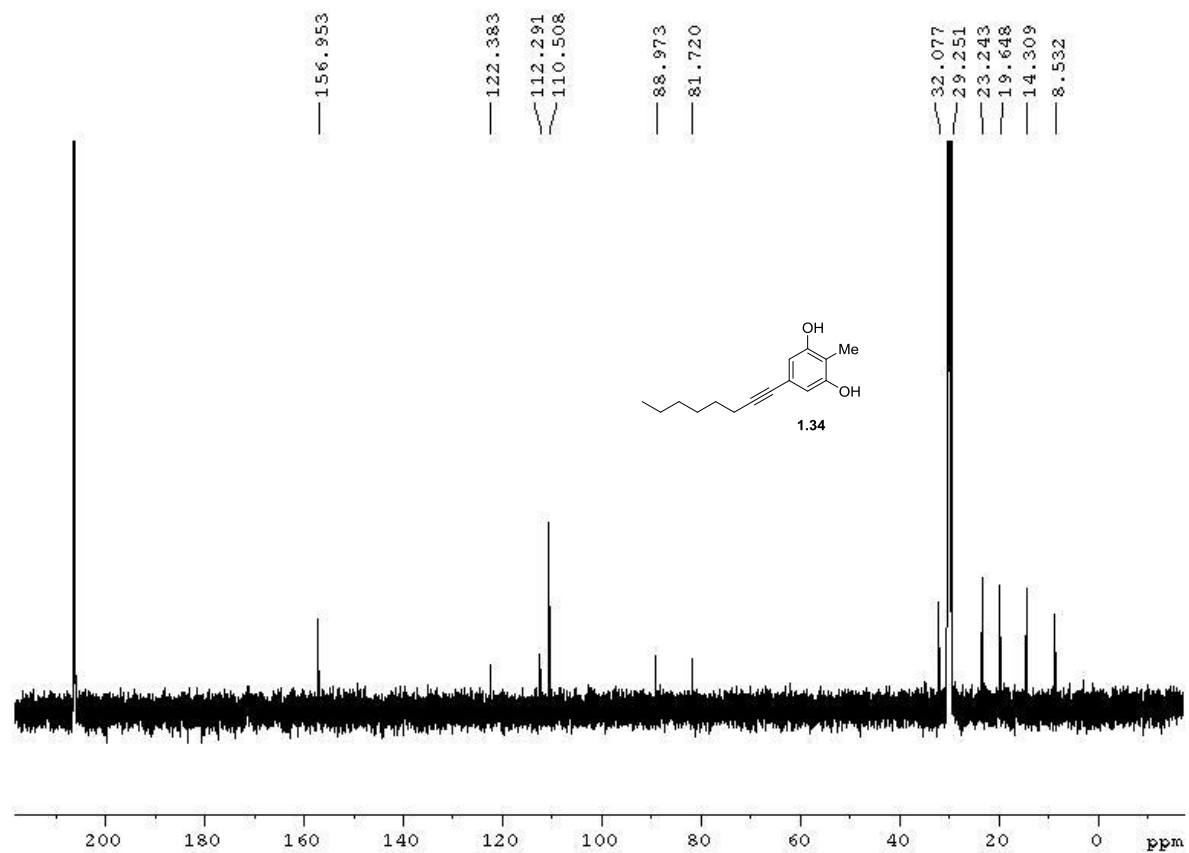
Figure A1.22 ^{13}C NMR spectrum of compound **1.34** (125 MHz, Acetone-d_6)
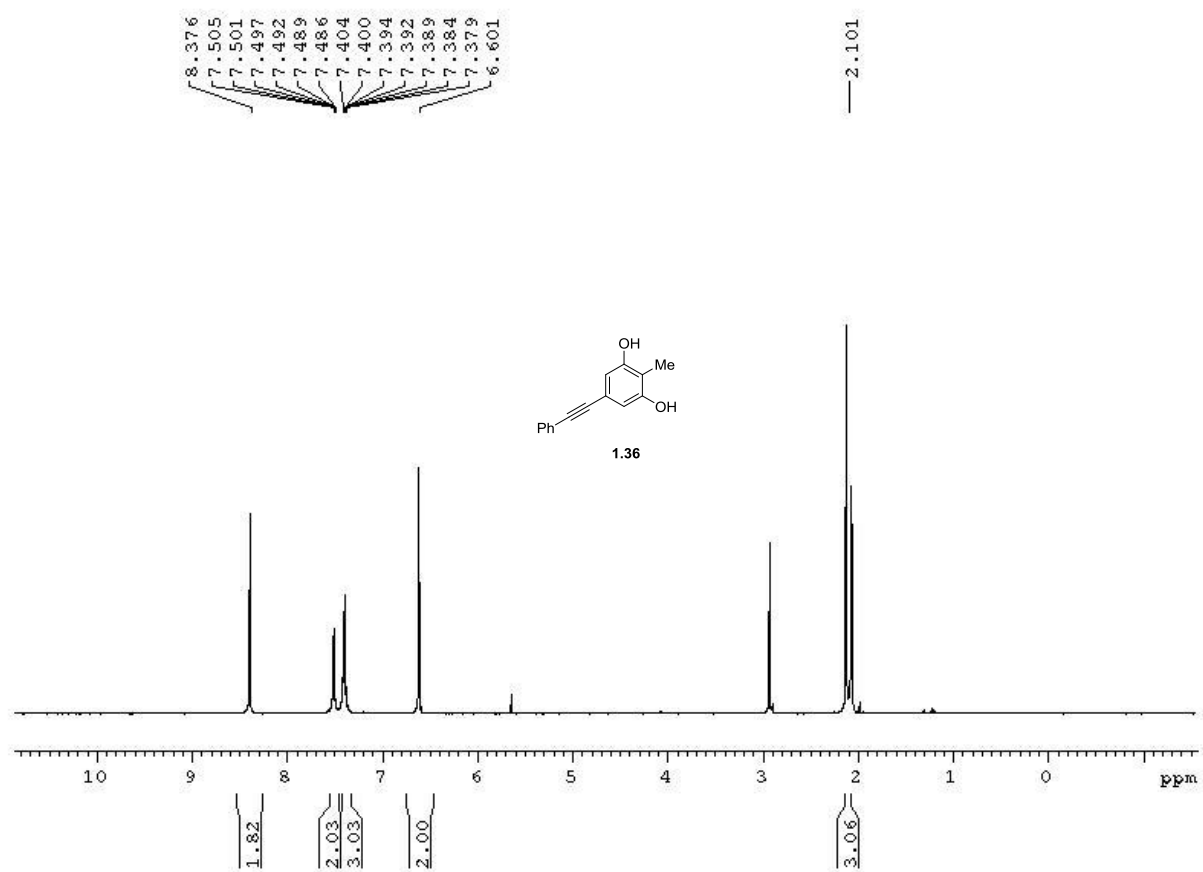
Figure A1.23 ^{1}H NMR spectrum of compound **1.36** (500 MHz, Acetone-d_6)
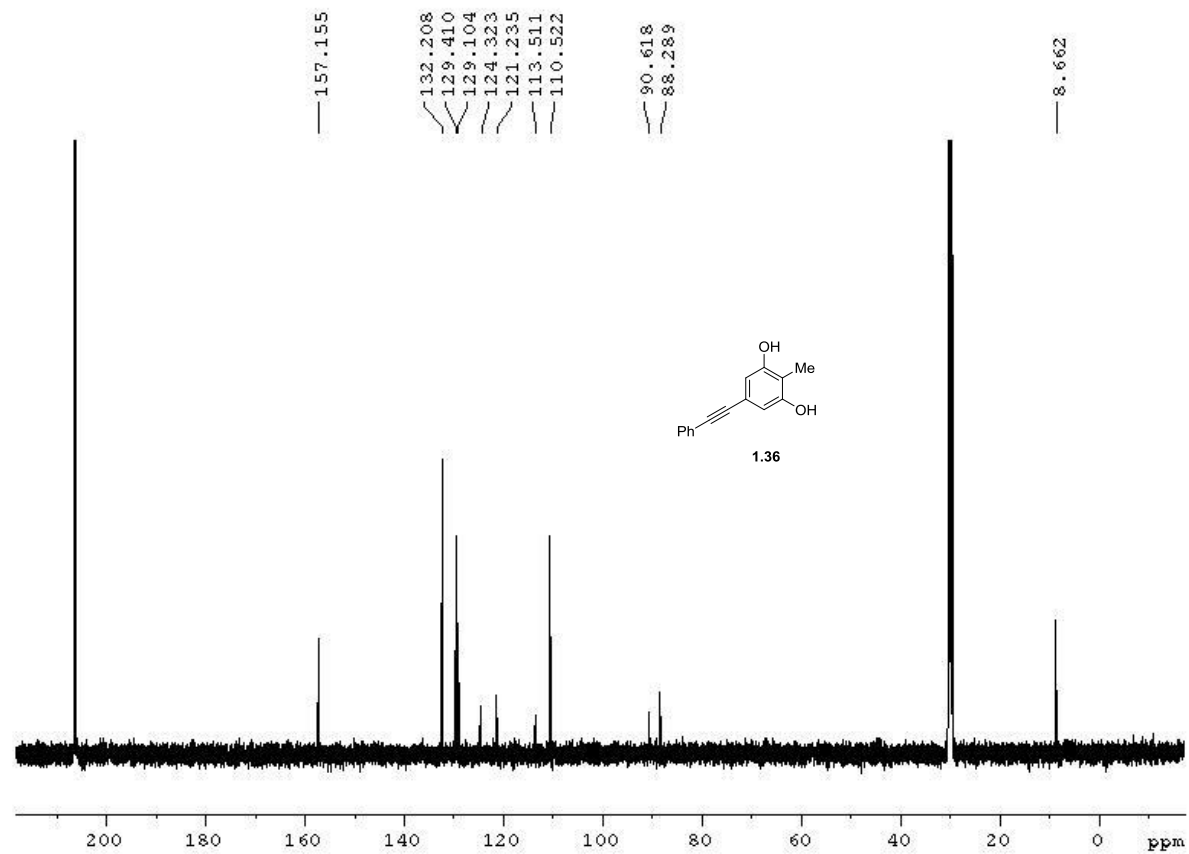
Figure A1.24 ^{13}C NMR spectrum of compound **1.36** (125 MHz, Acetone-d_6)
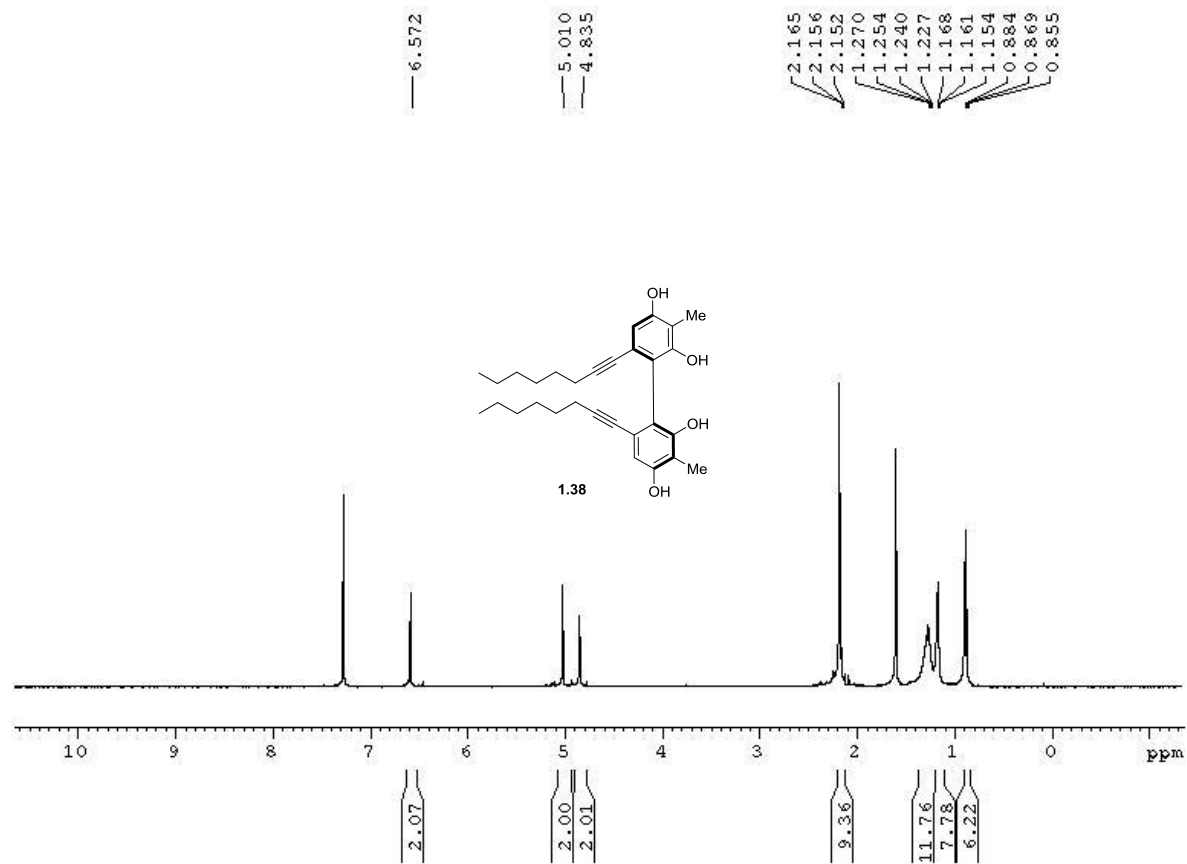
Figure A1.25 ^{1}H NMR spectrum of compound **1.38** (500 MHz, CDCl$_3$)
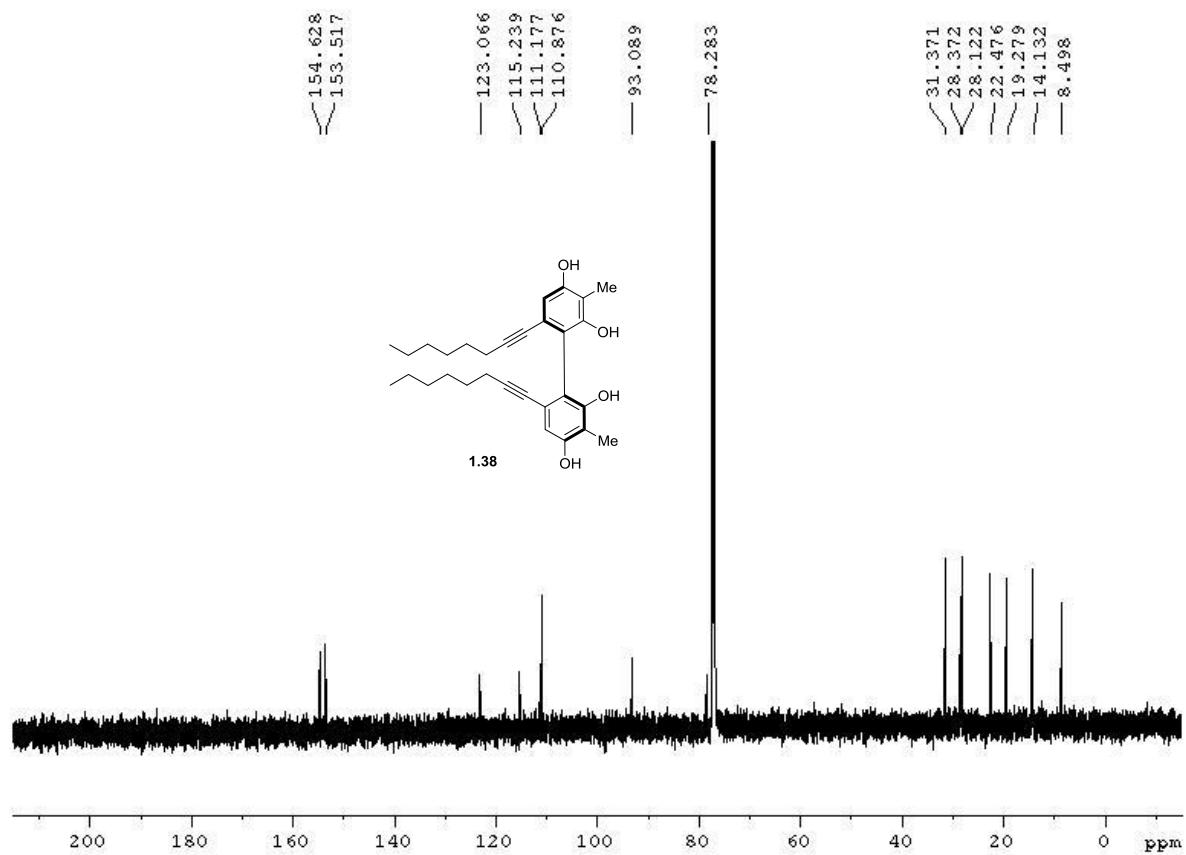
Figure A1.26 ^{13}C NMR spectrum of compound **1.38** (125 MHz, CDCl$_3$)
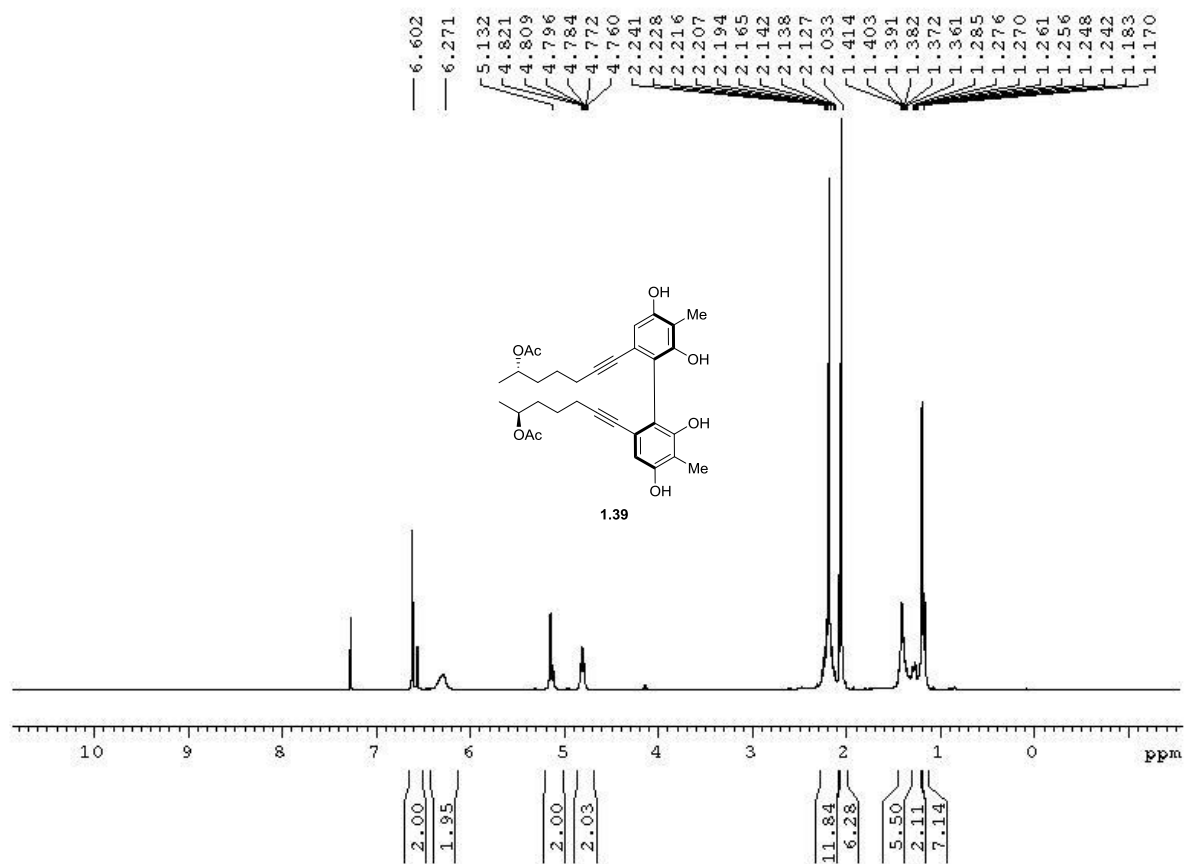
Figure A1.27 ^{1}H NMR spectrum of compound **1.39** (500 MHz, CDCl$_3$)
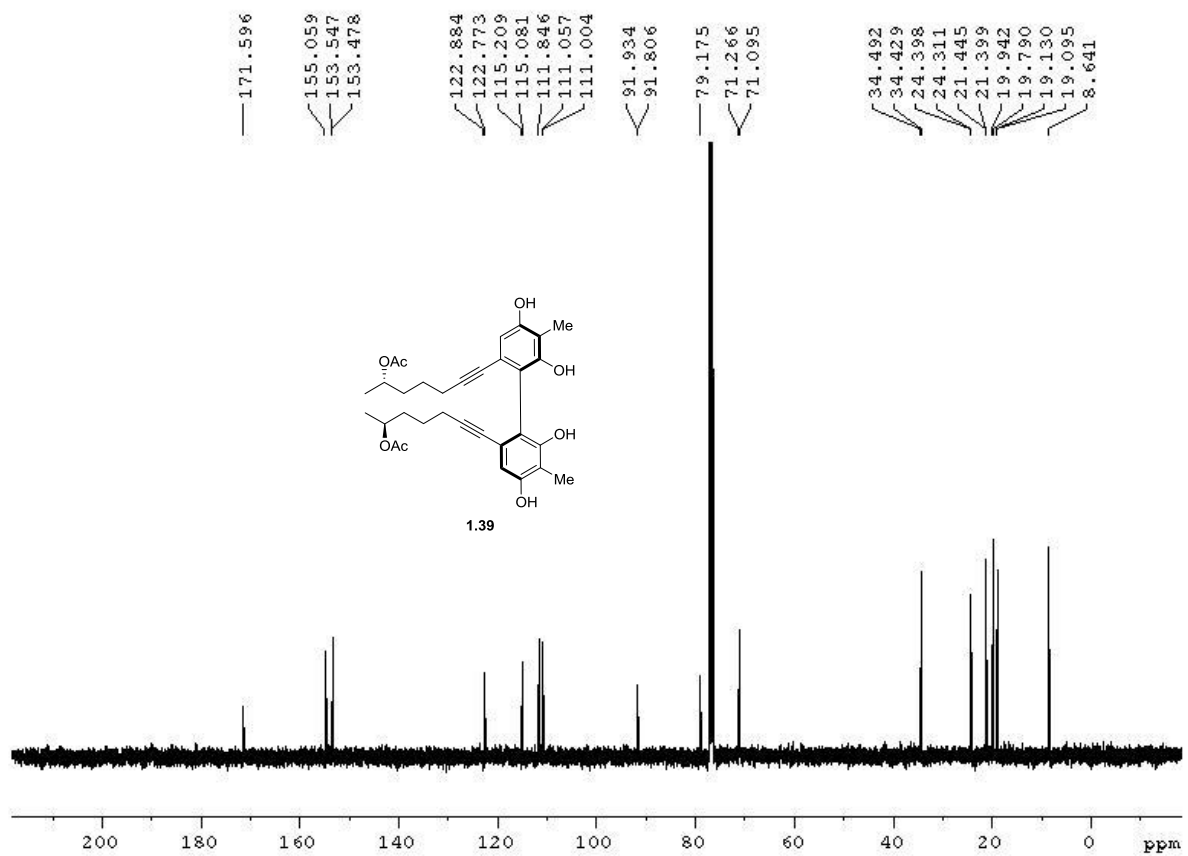
Figure A1.28 ^{13}C NMR spectrum of compound **1.39** (125 MHz, CDCl$_3$)
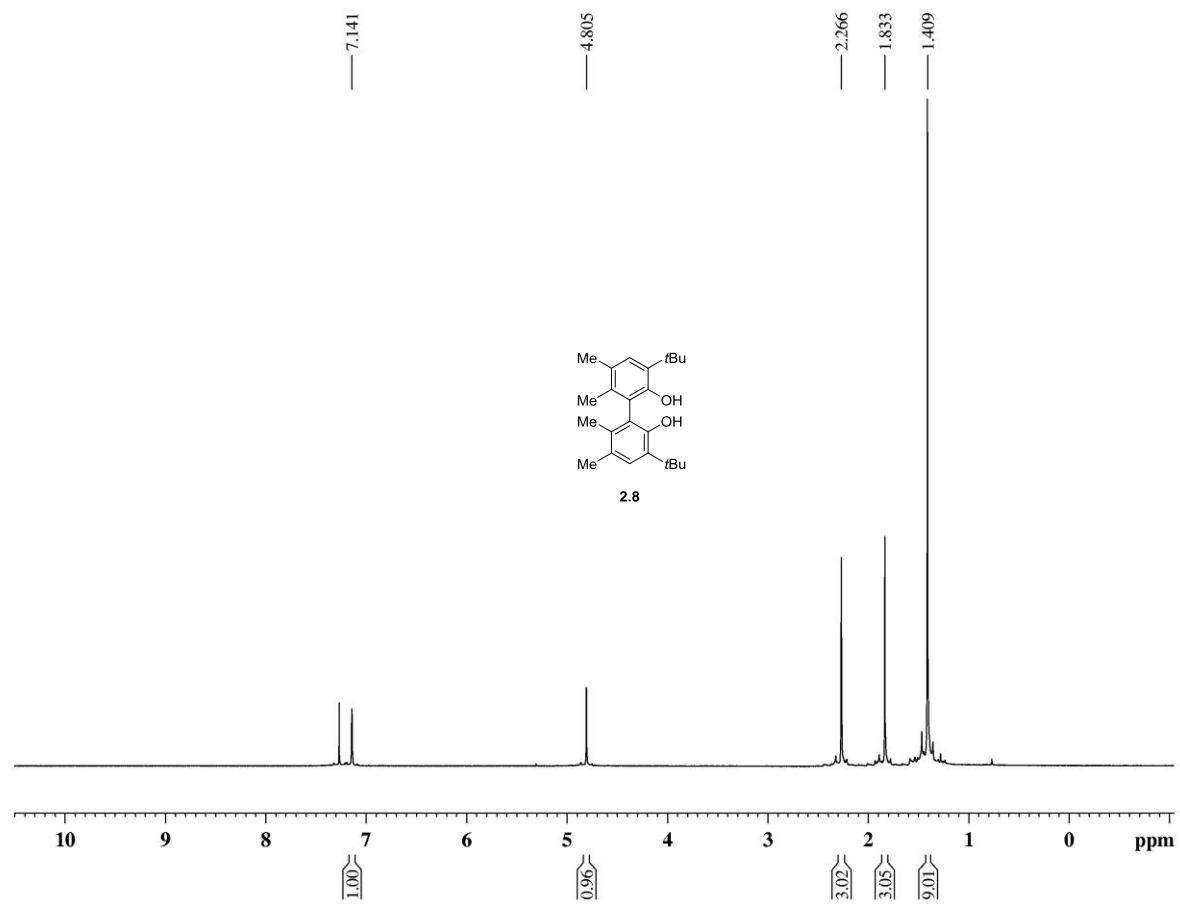
Figure A2.1 ¹H NMR spectrum of compound **2.8** (500 MHz, CDCl₃)
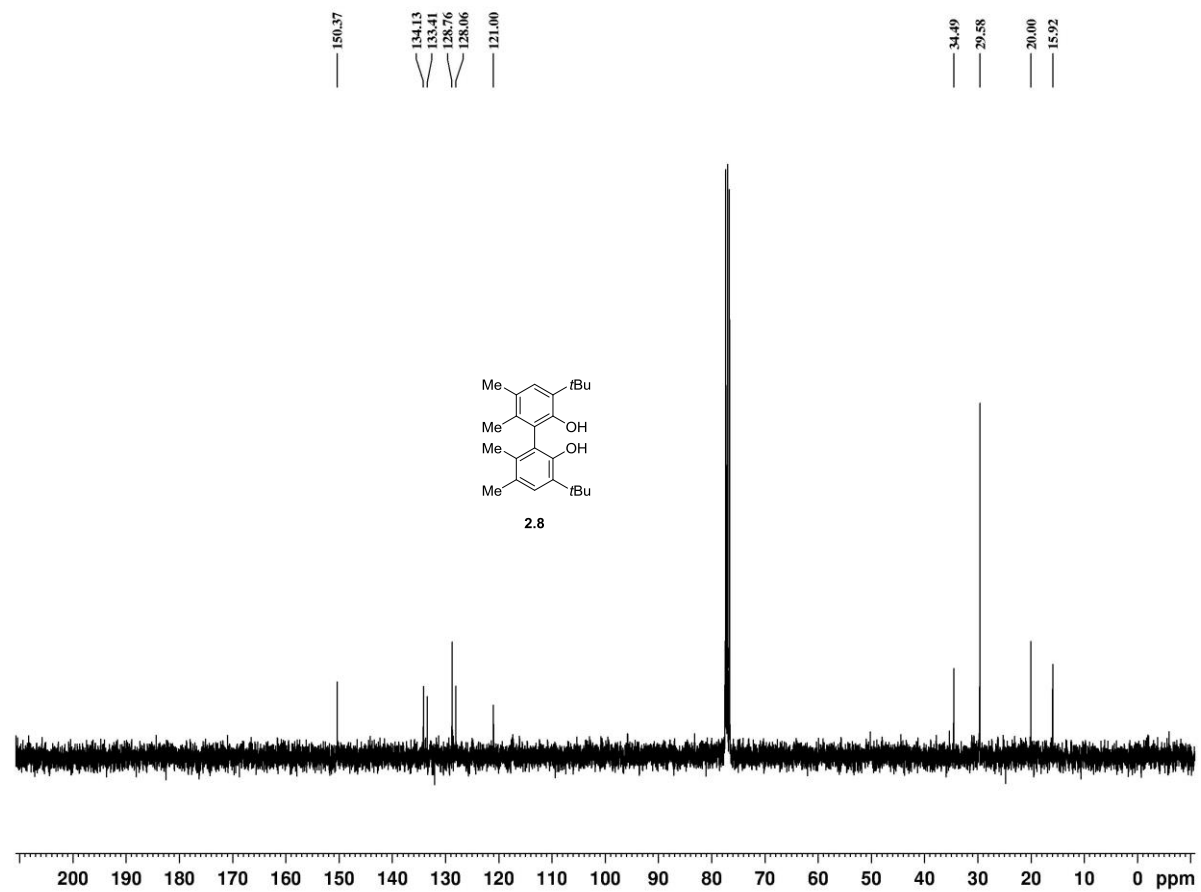
Figure A2.2 ^{13}C NMR spectrum of compound **2.8** (125 MHz, CDCl$_3$)
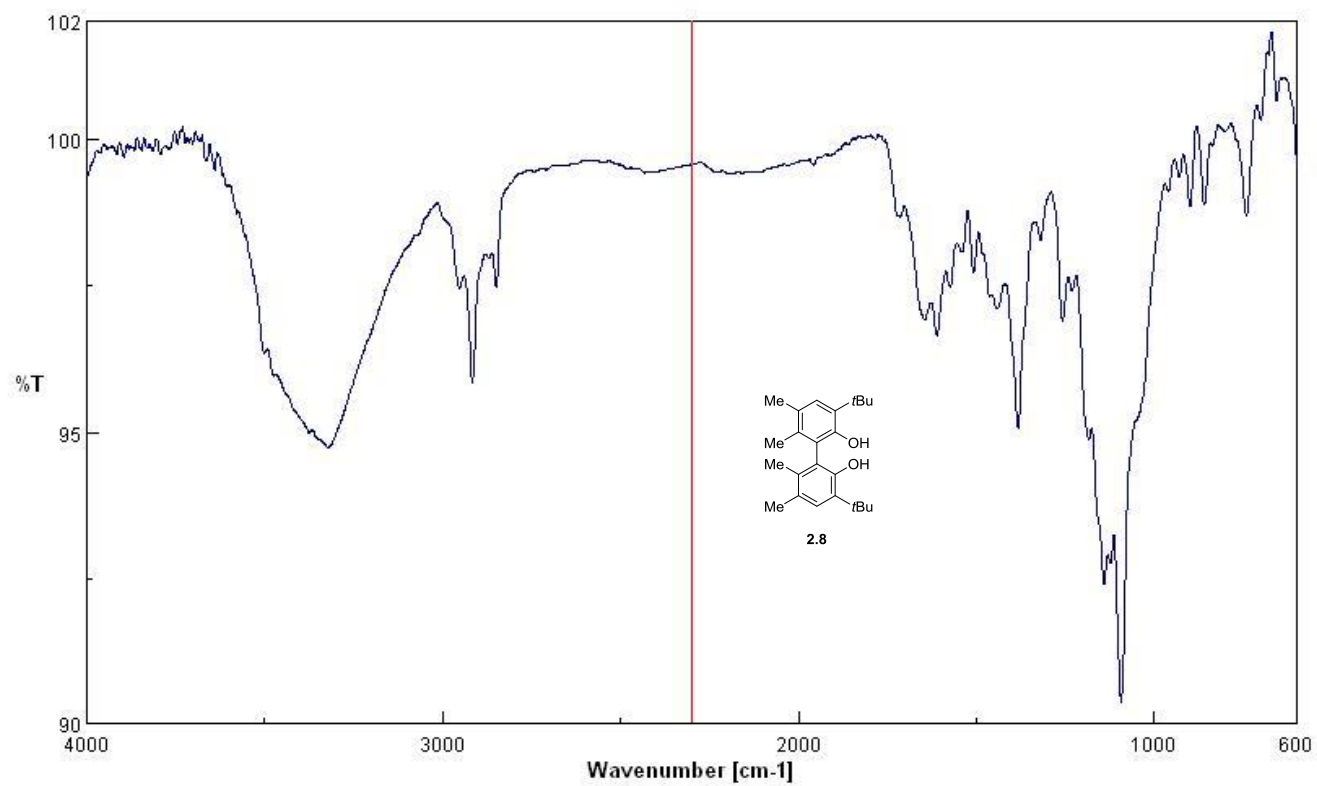
Figure A2.3 IR Spectrum of compound **2.8**
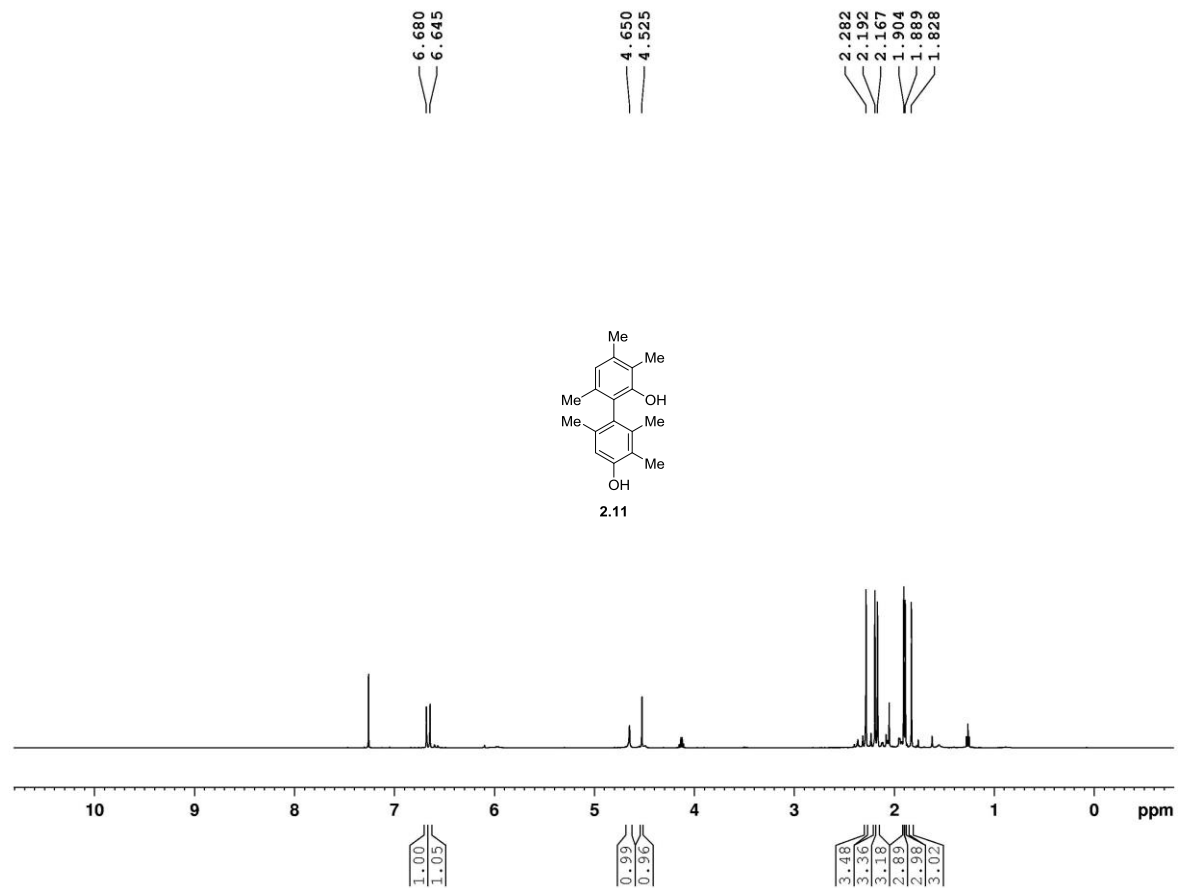
Figure A2.4 ^{1}H NMR spectrum of compound **2.11** (500 MHz, CDCl$_3$)
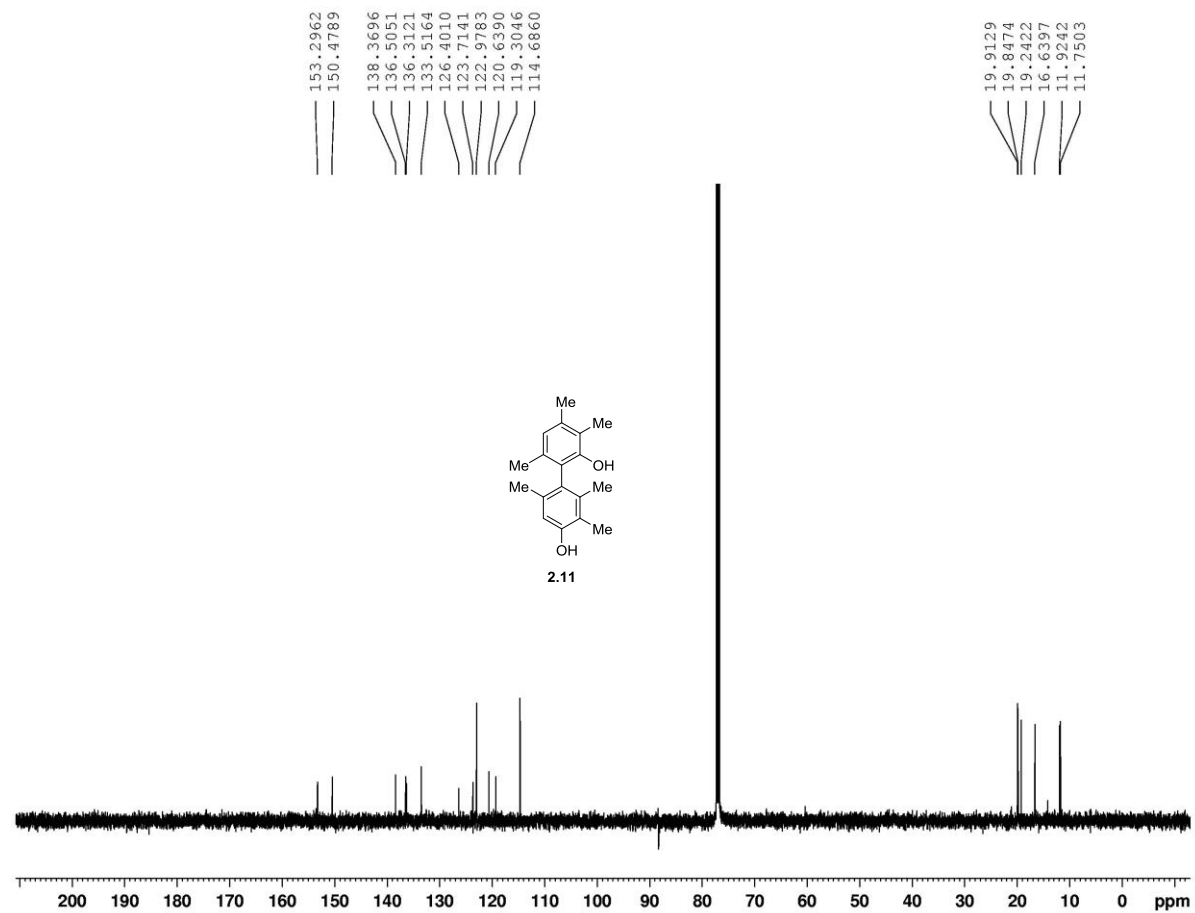
Figure A2.5 ^{13}C NMR spectrum of compound **2.11** (125 MHz, CDCl$_3$)
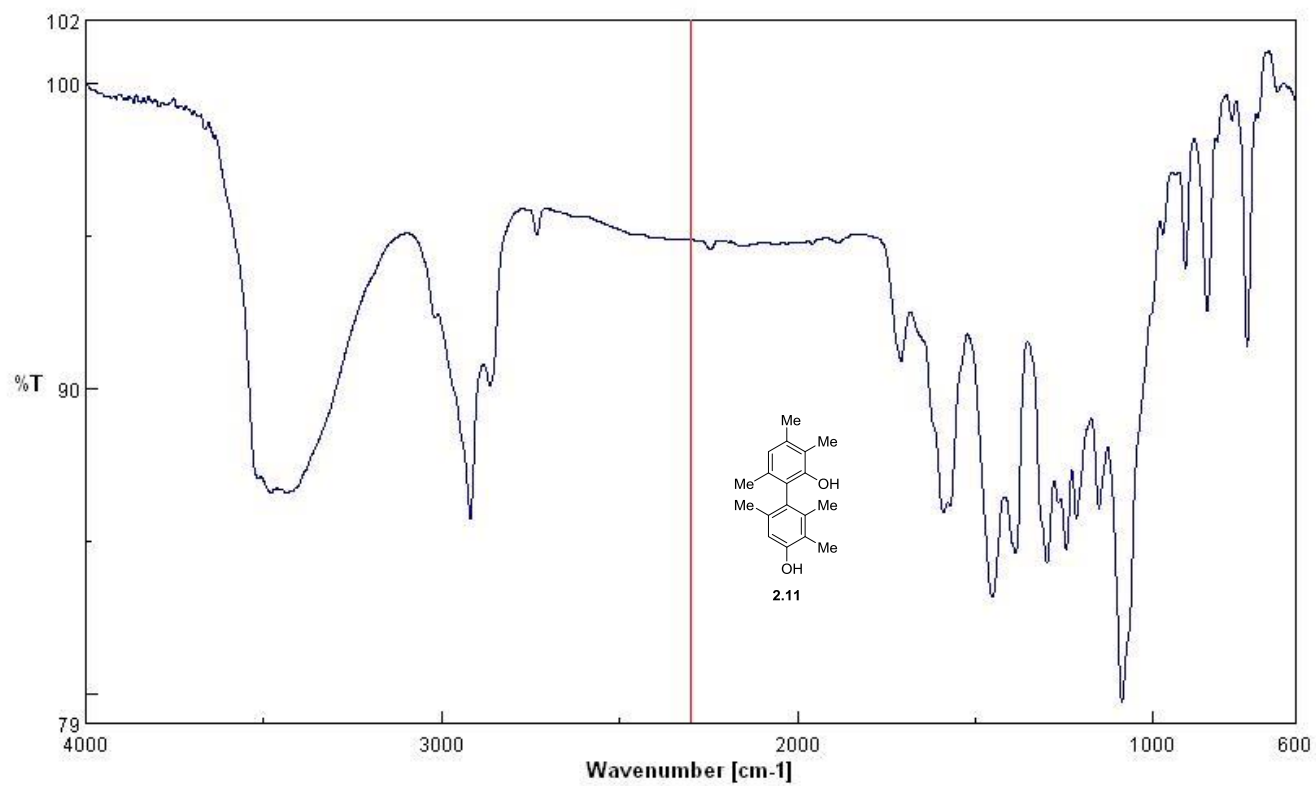
Figure A2.6 IR Spectrum of compound **2.11**
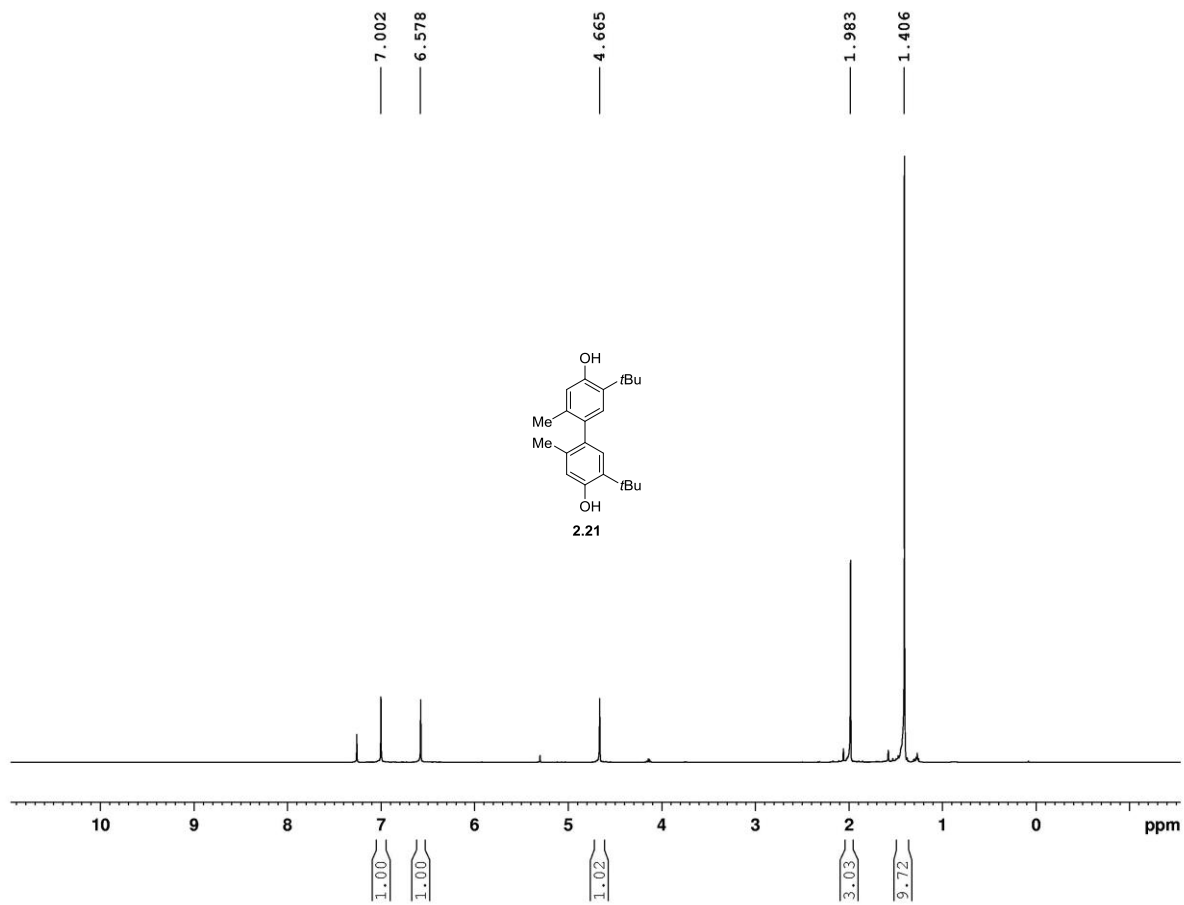
Figure A2.7 ^{1}H NMR spectrum of compound **2.21** (500 MHz, CDCl$_3$)
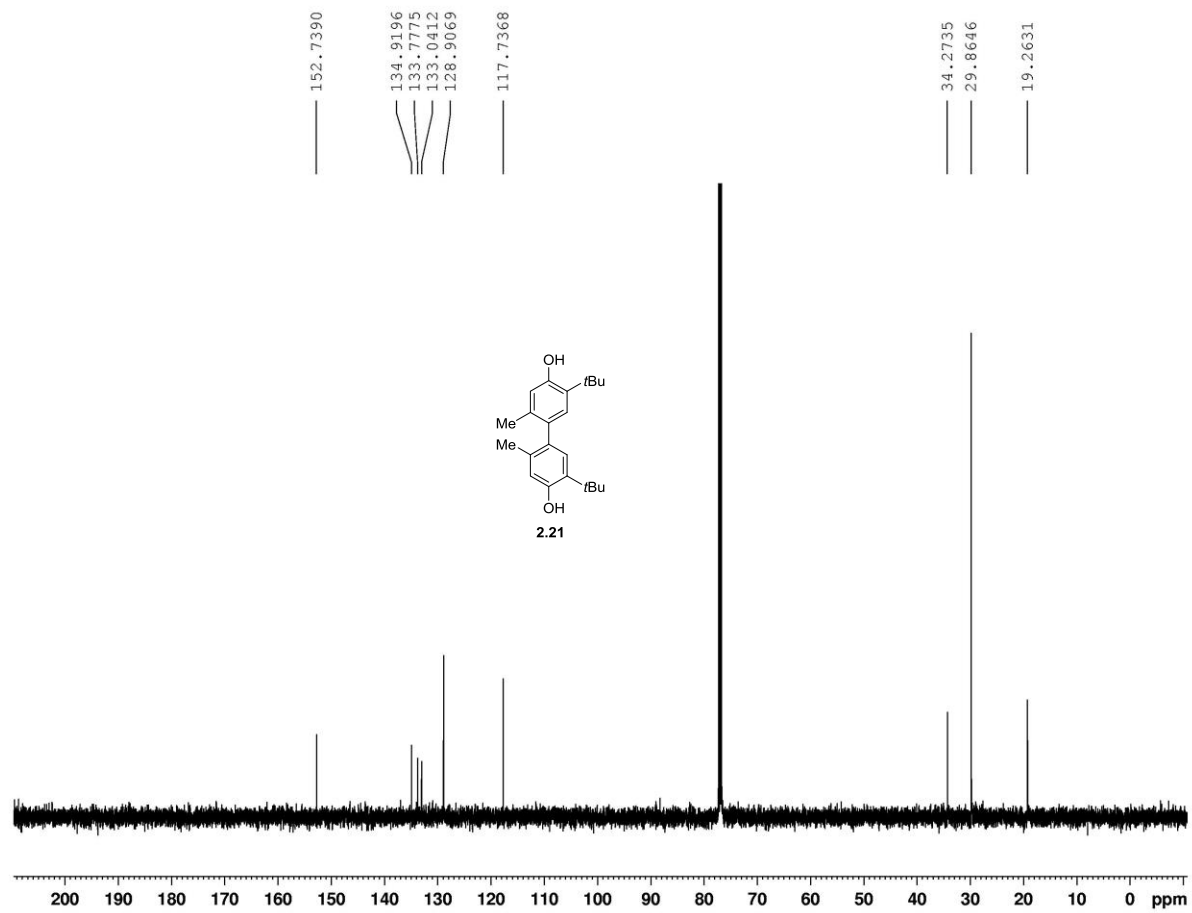
Figure A2.8 ^{13}C NMR spectrum of compound **2.21** (125 MHz, CDCl$_3$)
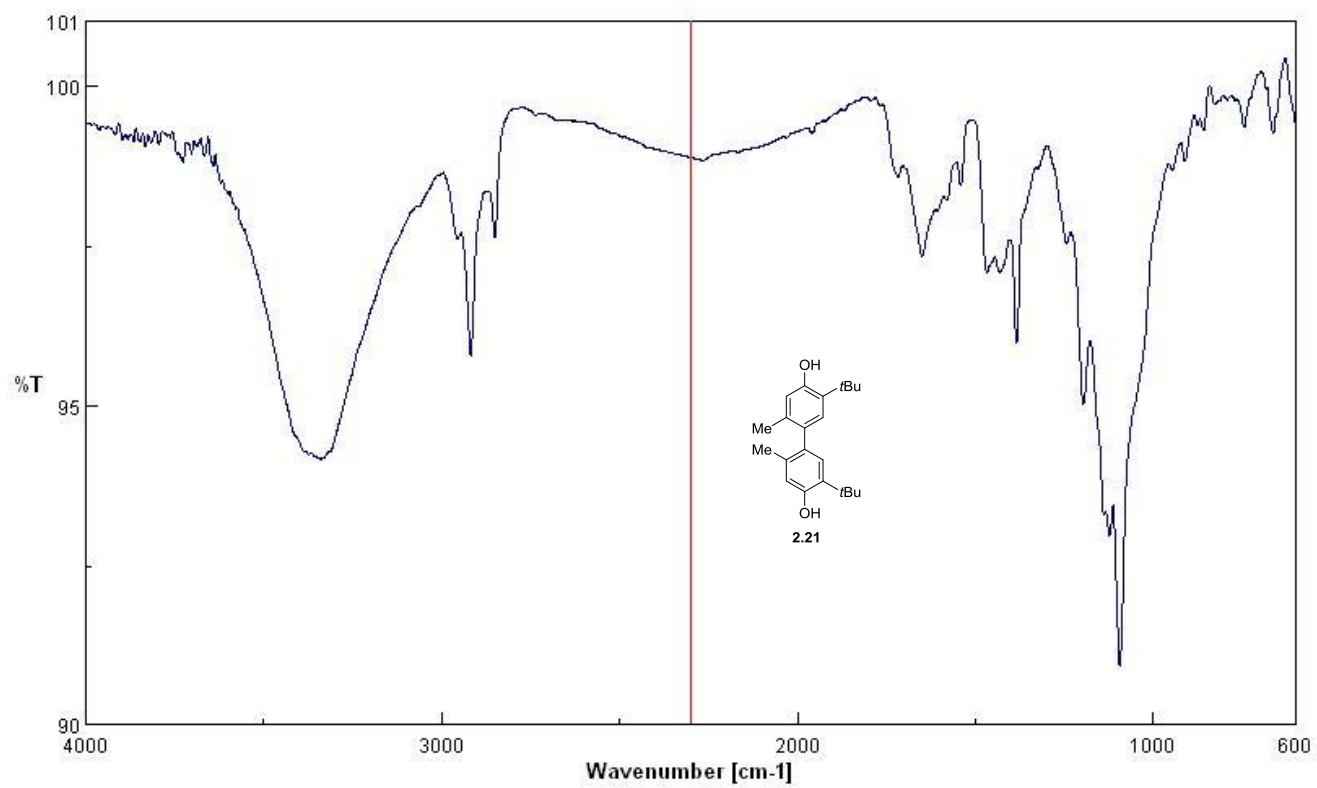
Figure A2.9 IR Spectrum of compound **2.21**
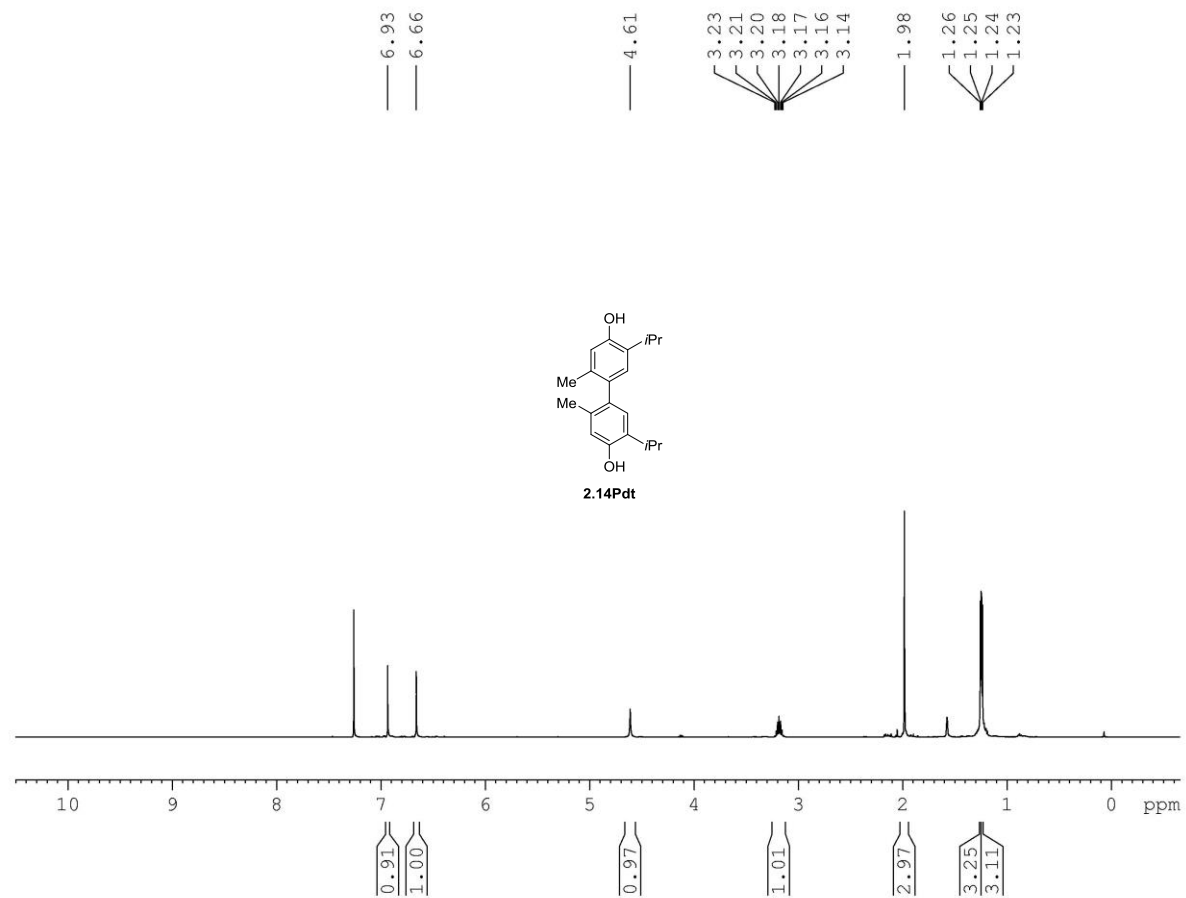
Figure A2.10 ^{1}H NMR spectrum of compound 2.14Pdt (500 MHz, CDCl$_3$)
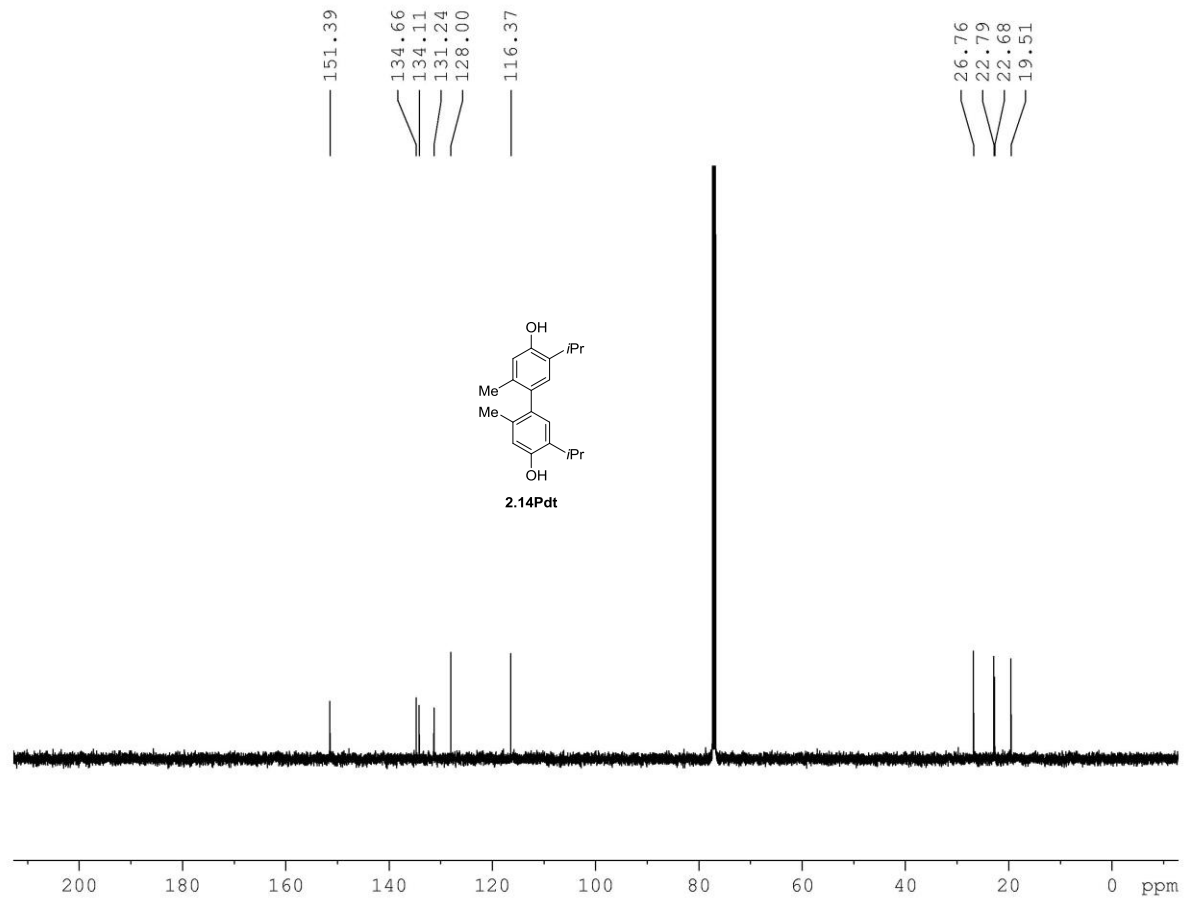
Figure A2.11 ^{13}C NMR spectrum of compound **2.14Pdt** (125 MHz, CDCl$_3$)
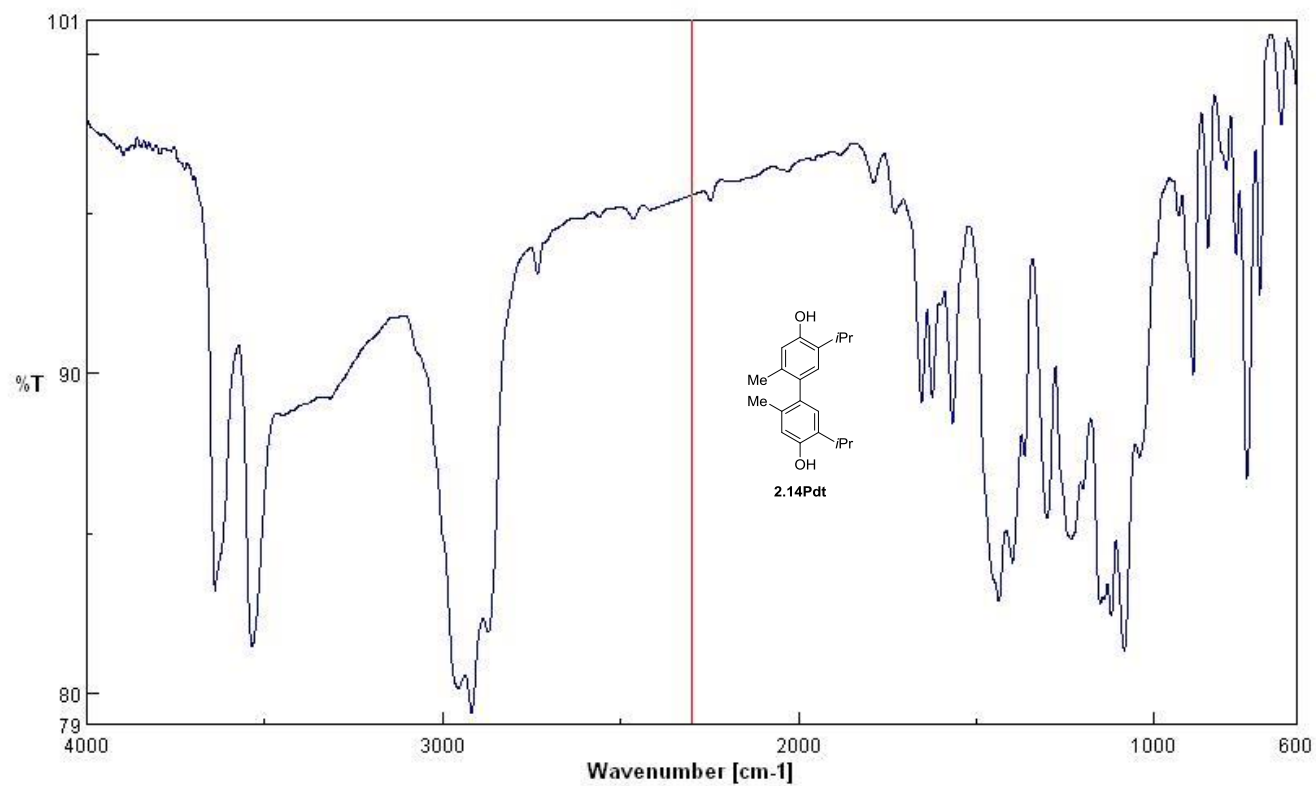
Figure A2.12 IR Spectrum of compound **2.14Pdt**
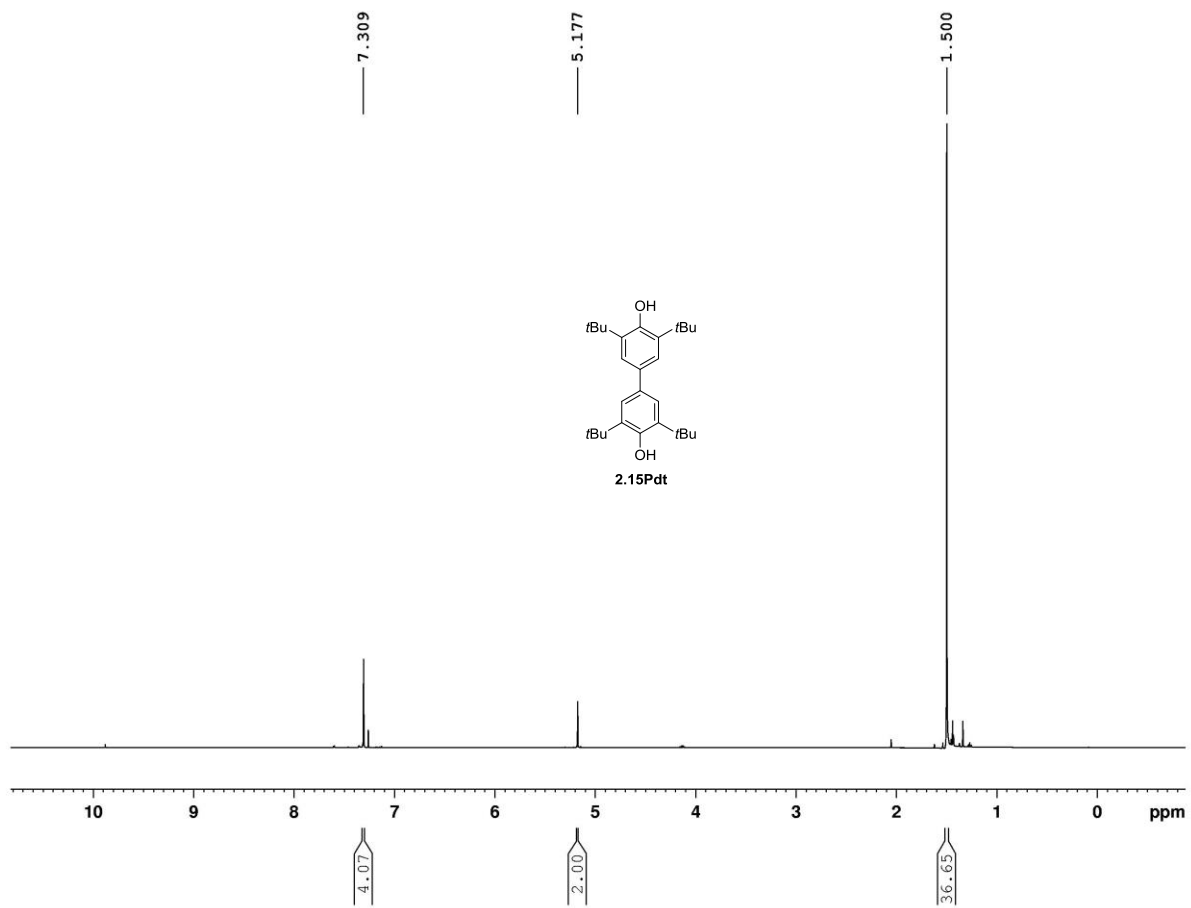
Figure A2.13 ^{1}H NMR spectrum of compound **2.15Pdt** (500 MHz, CDCl$_3$)
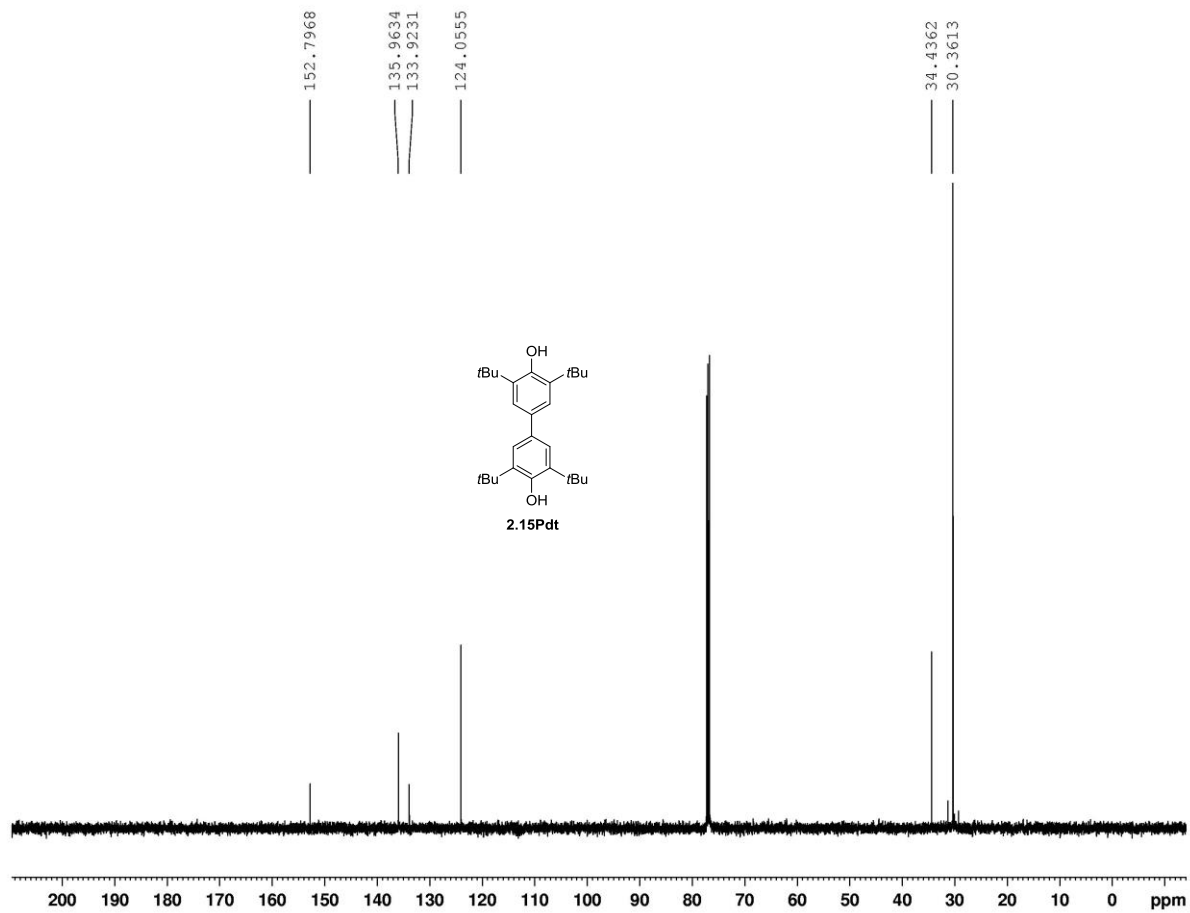
Figure A2.14 ¹³C NMR spectrum of compound **2.15Pdt** (125 MHz, CDCl₃)
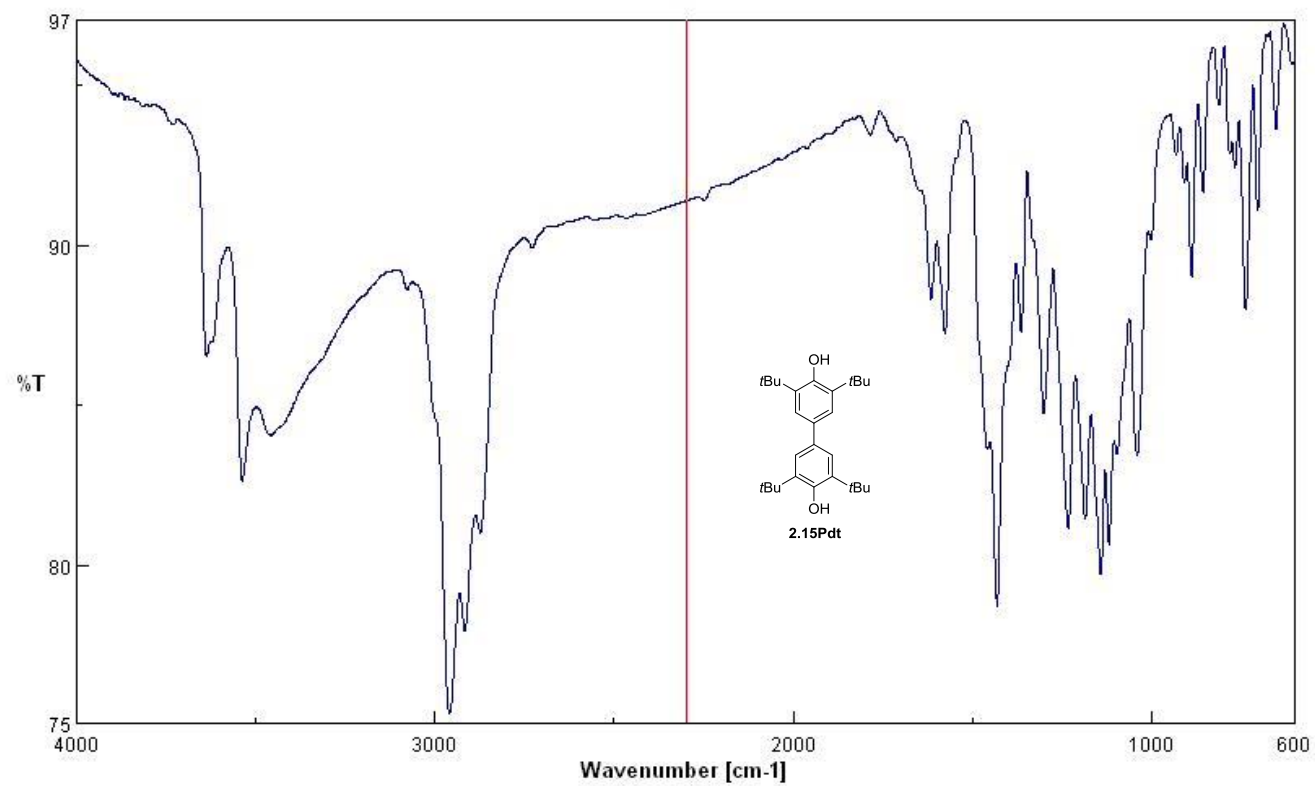
Figure A2.15 IR Spectrum of compound **2.15Pdt**

7.202
4.776
3.261
3.247
3.233
3.220
3.206
3.192
3.179
1.348
1.335

OH
*i*Pr   *i*Pr

*i*Pr   *i*Pr
OH

2.16Pdt

4.03   2.00   4.08   12.47 11.84
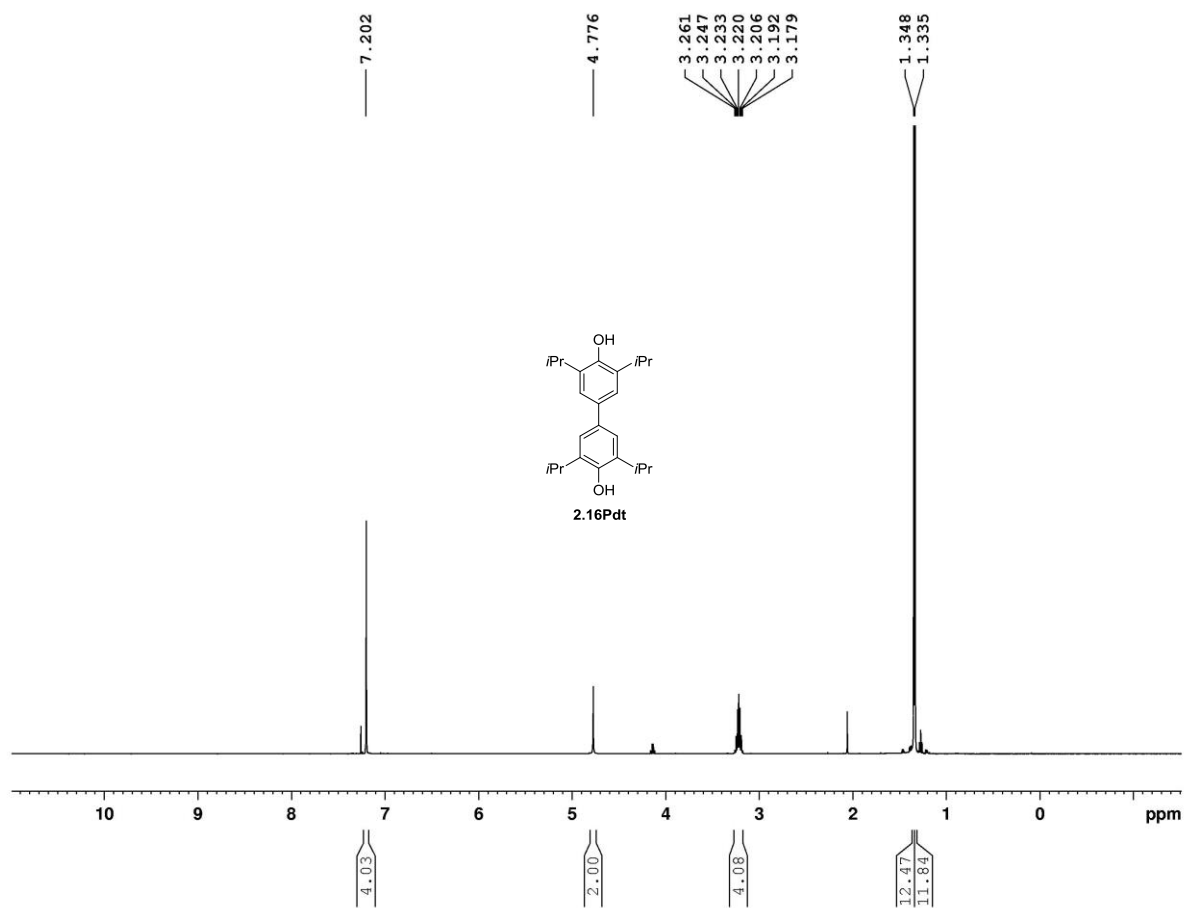
Figure A2.16 ^{1}H NMR spectrum of compound **2.16Pdt** (500 MHz, CDCl$_3$)
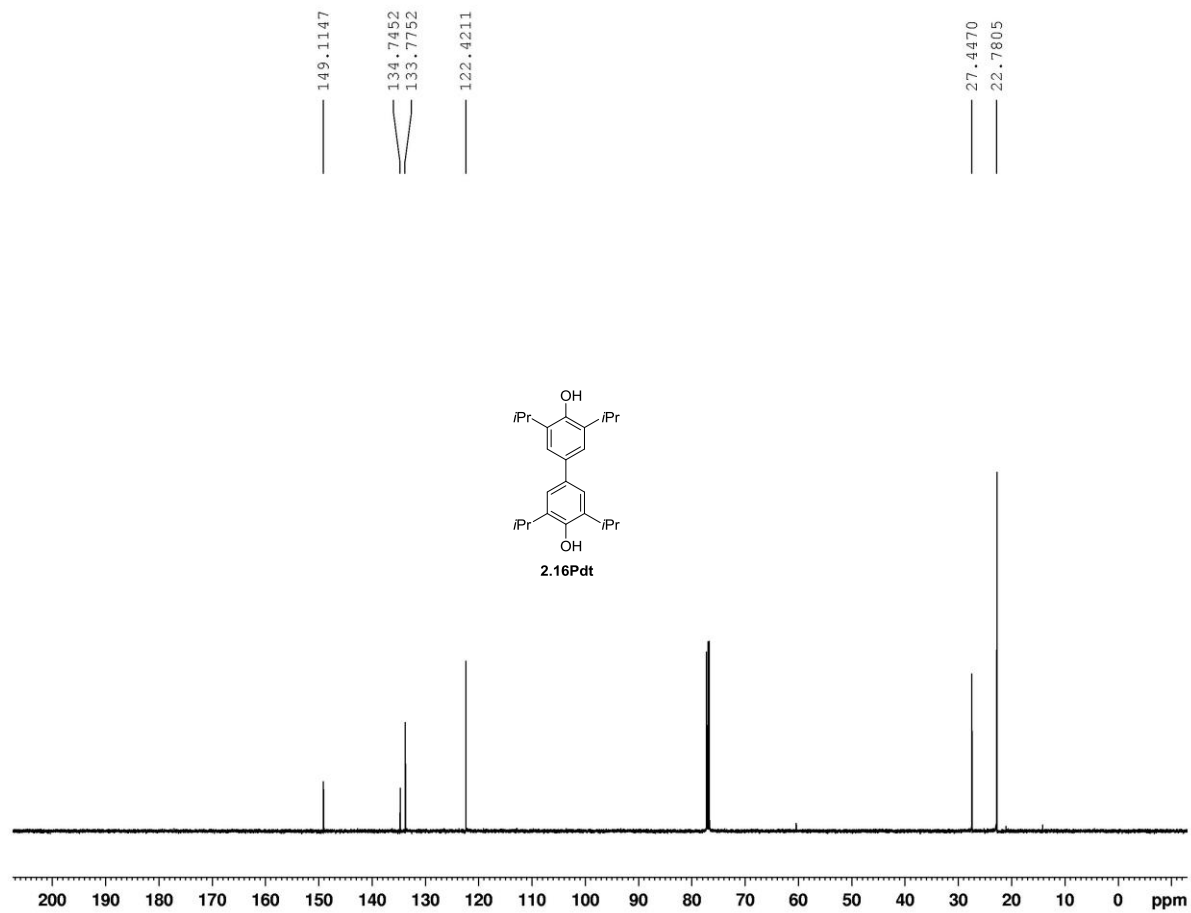
Figure A2.17 ^{13}C NMR spectrum of compound **2.16Pdt** (125 MHz, CDCl$_3$)
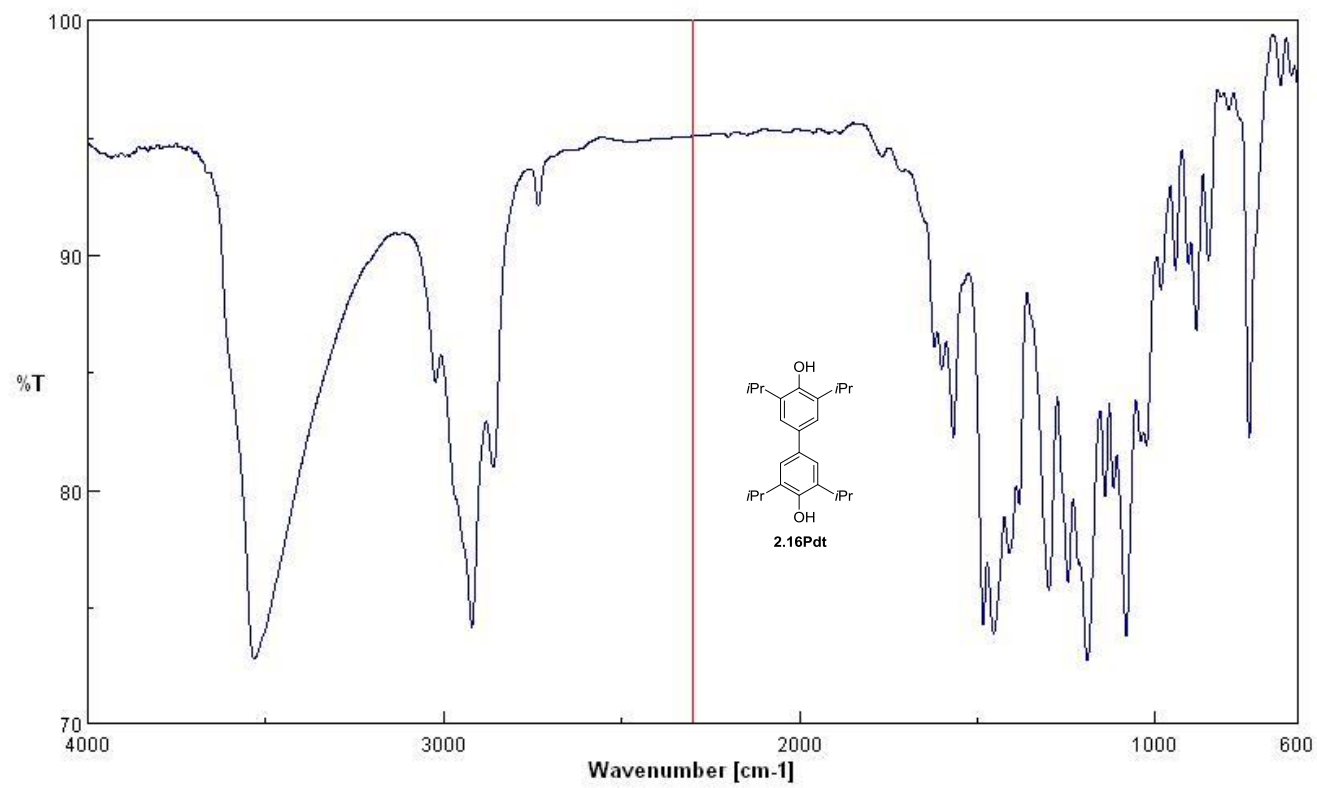
Figure A2.18 IR Spectrum of compound **2.16Pdt**
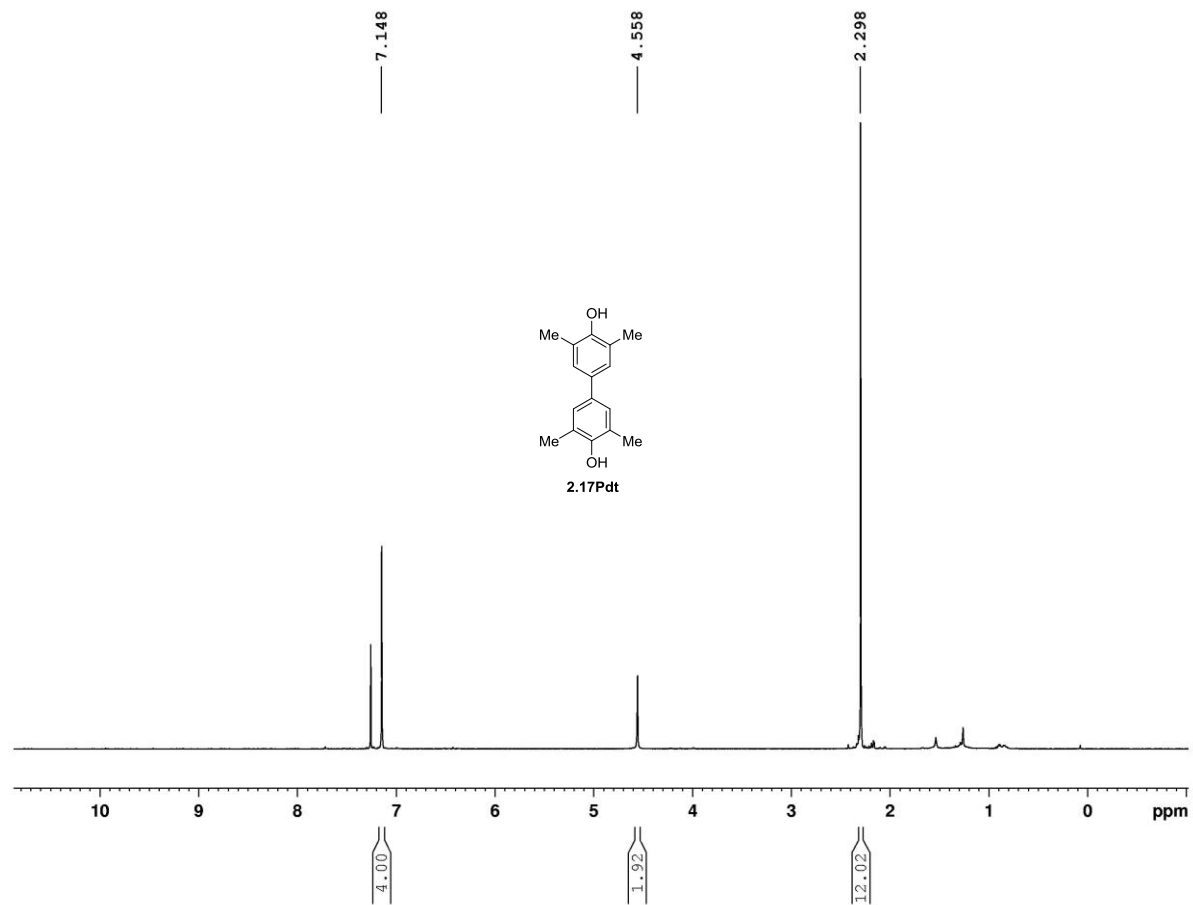
Figure A2.19 ^{1}H NMR spectrum of compound **2.17Pdt** (500 MHz, CDCl$_3$)
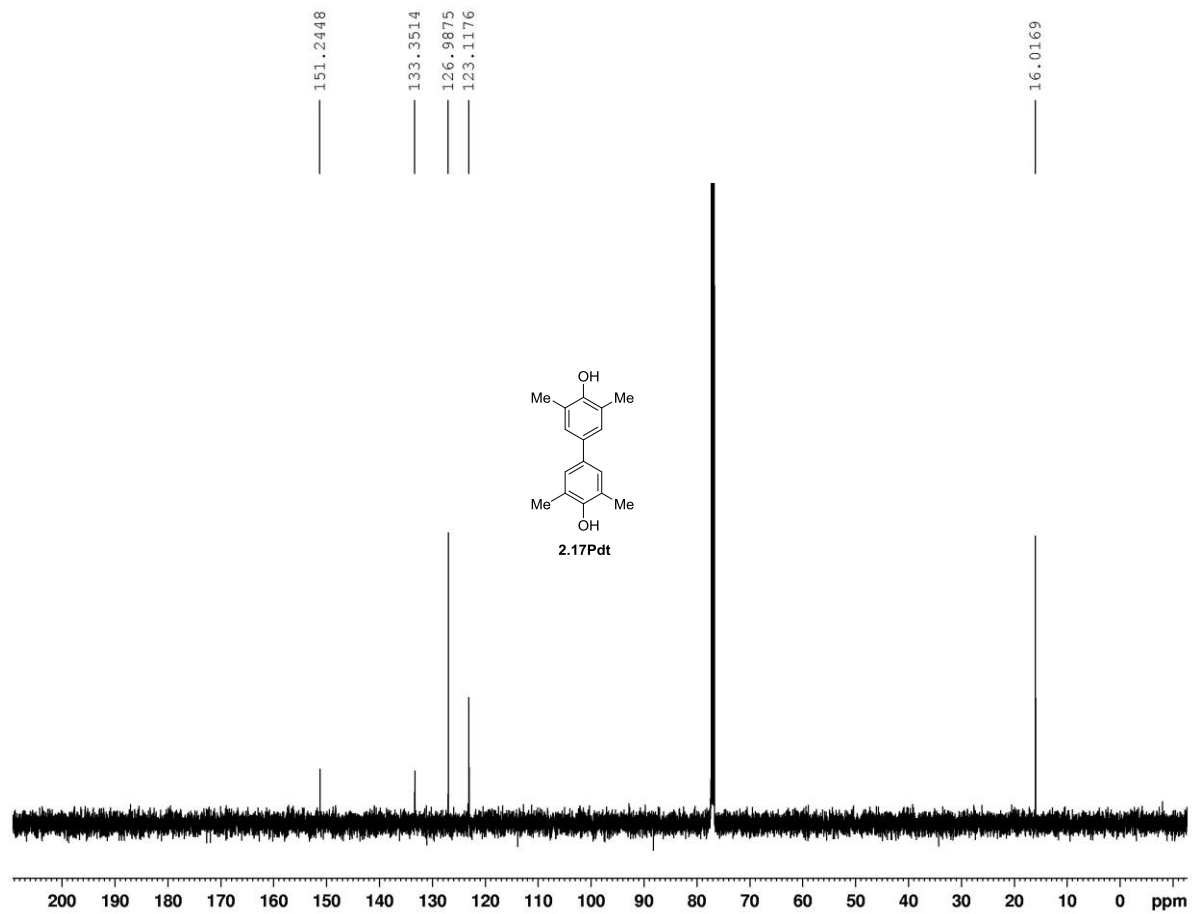
Figure A2.20 ^{13}C NMR spectrum of compound **2.17Pdt** (125 MHz, CDCl$_3$)
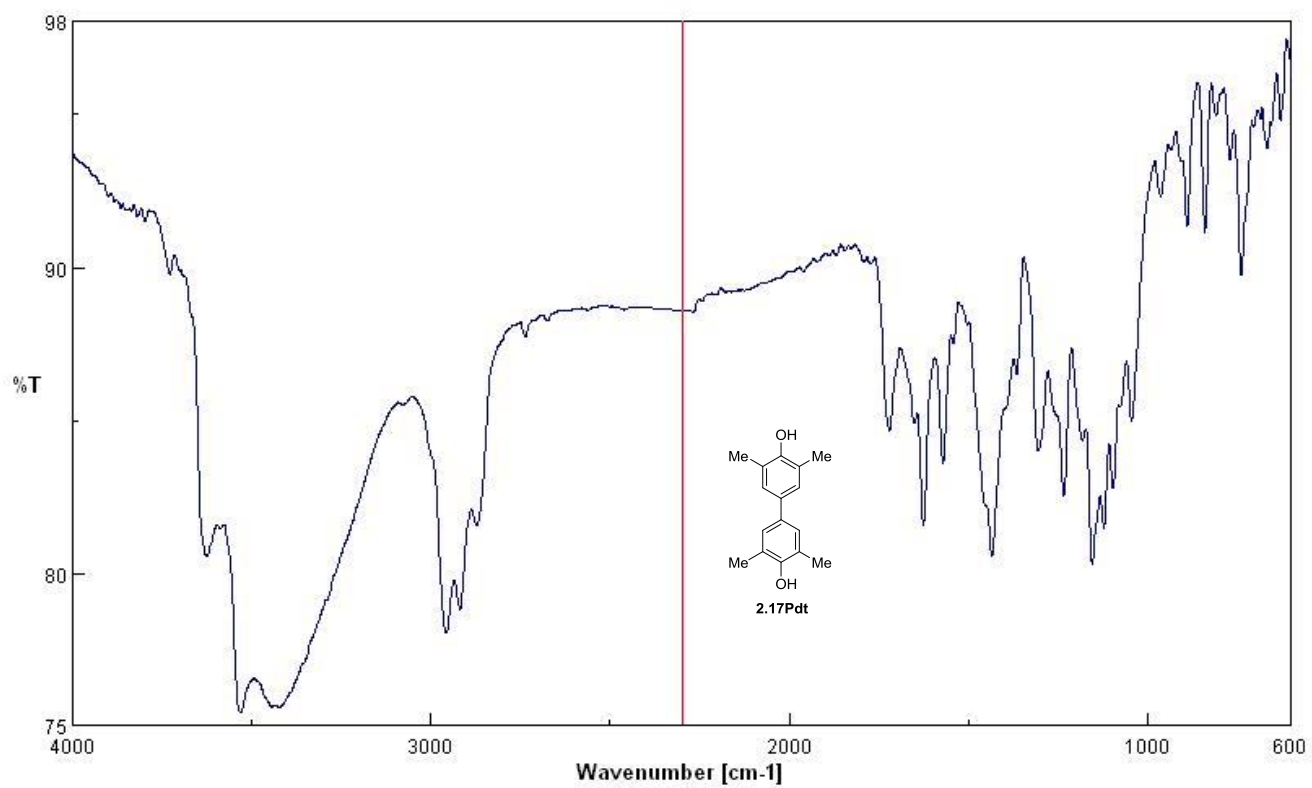
Figure A2.21 IR Spectrum of compound **2.17Pdt**
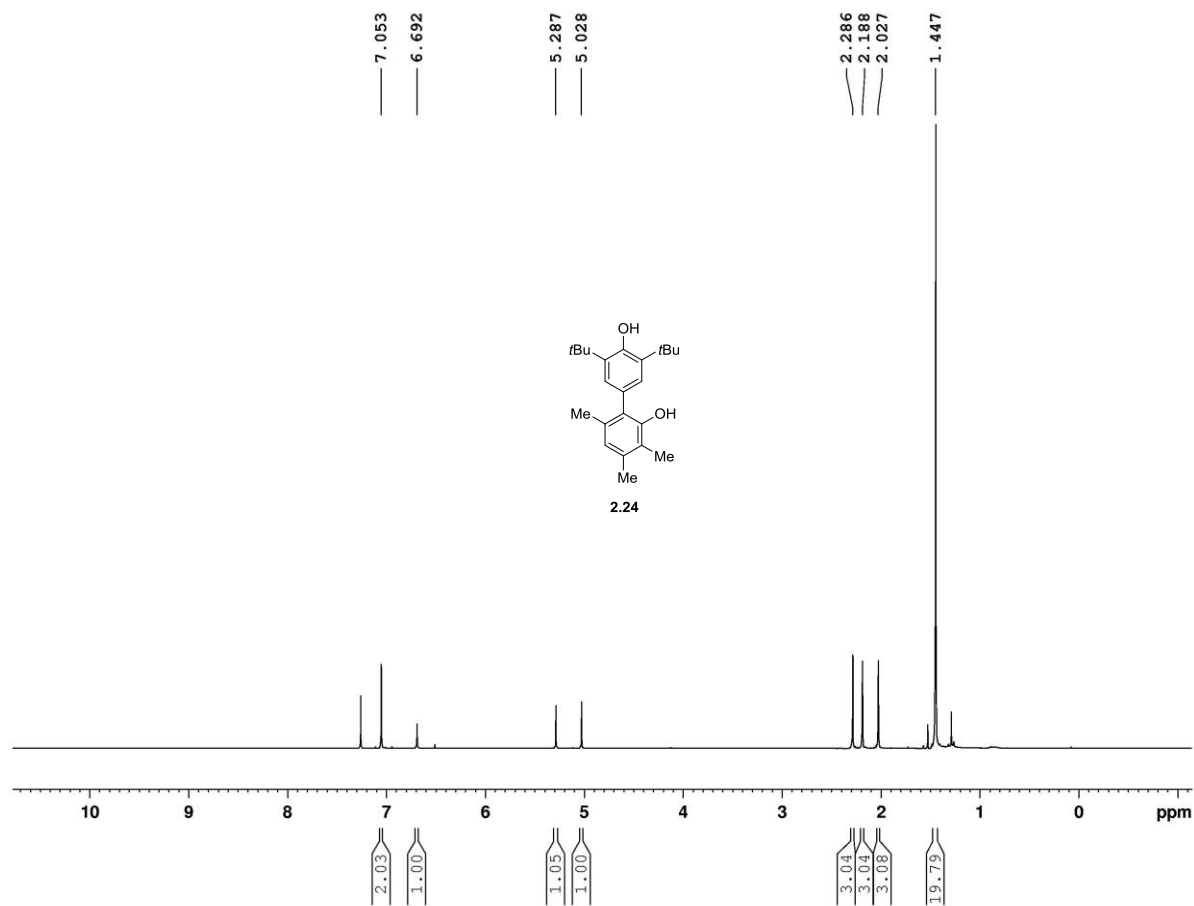
Figure A2.22 ^{1}H NMR spectrum of compound **2.24** (500 MHz, CDCl$_3$)

228
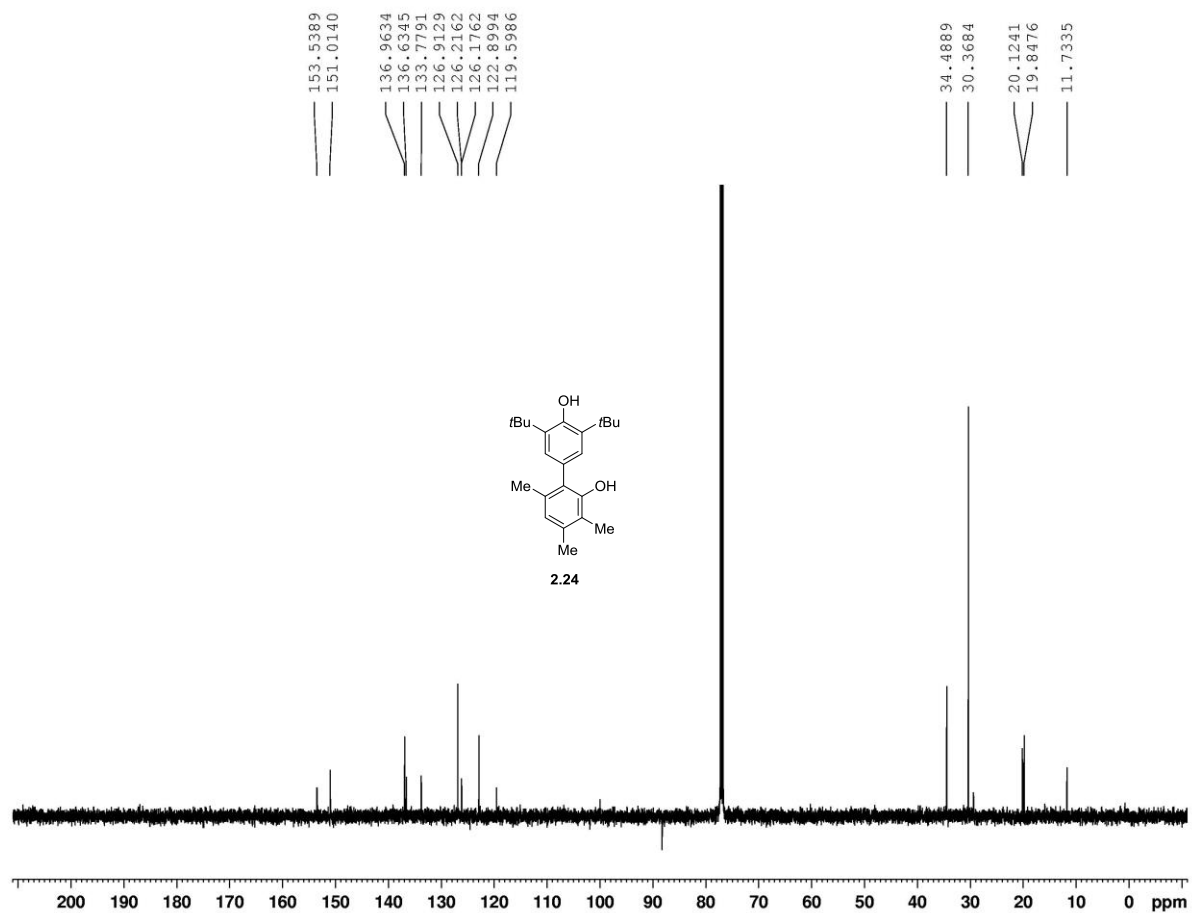
Figure A2.23 ¹³C NMR spectrum of compound **2.24** (125 MHz, CDCl₃)
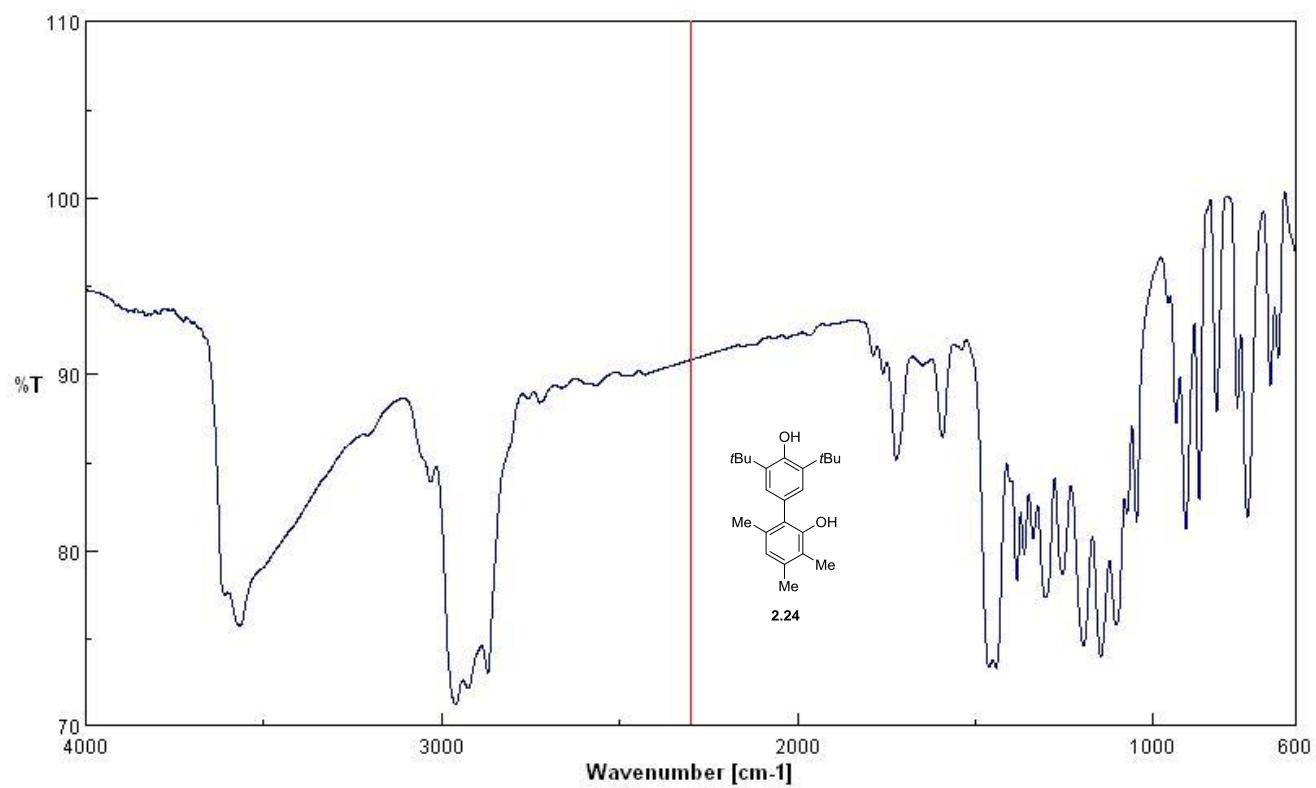
Figure A2.24 IR Spectrum of compound **2.24**
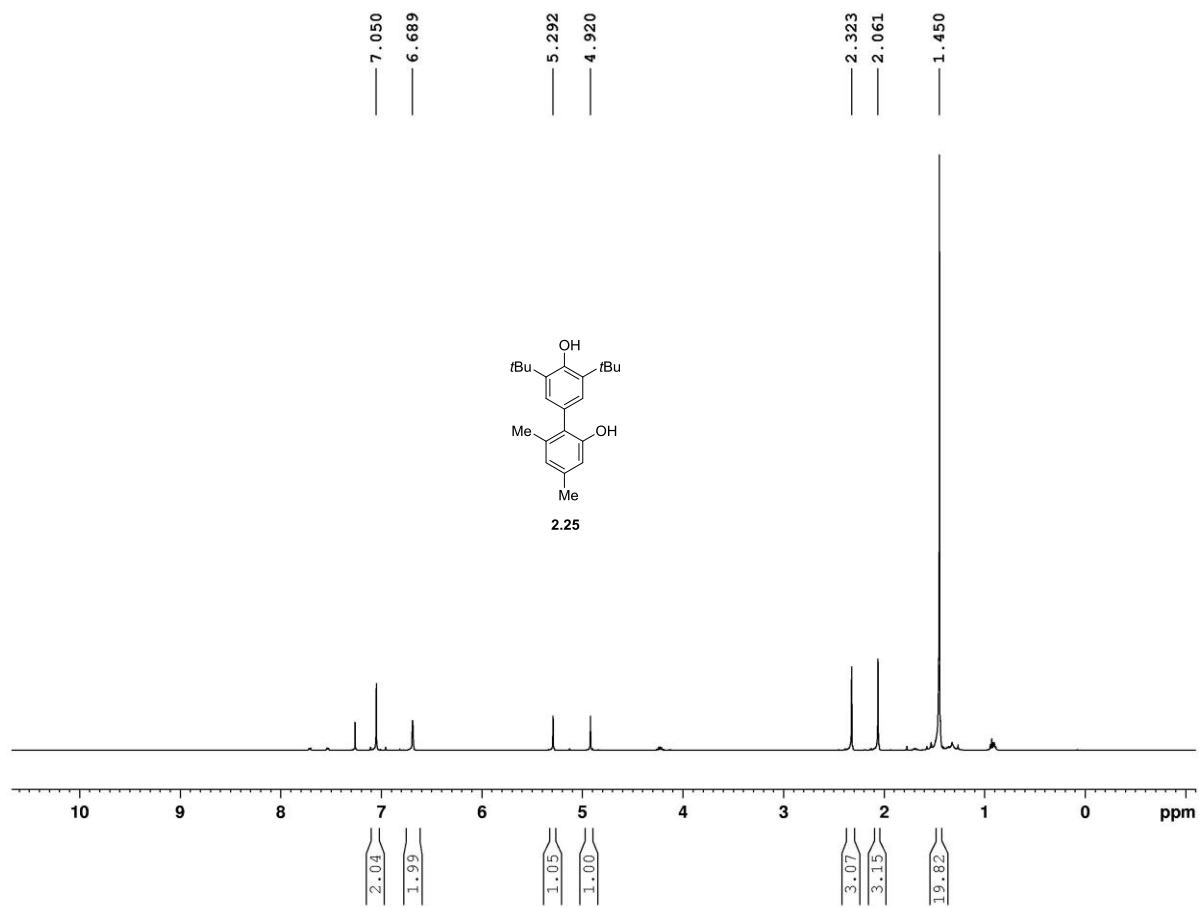
Figure A2.25 ^{1}H NMR spectrum of compound **2.25** (500 MHz, CDCl$_3$)
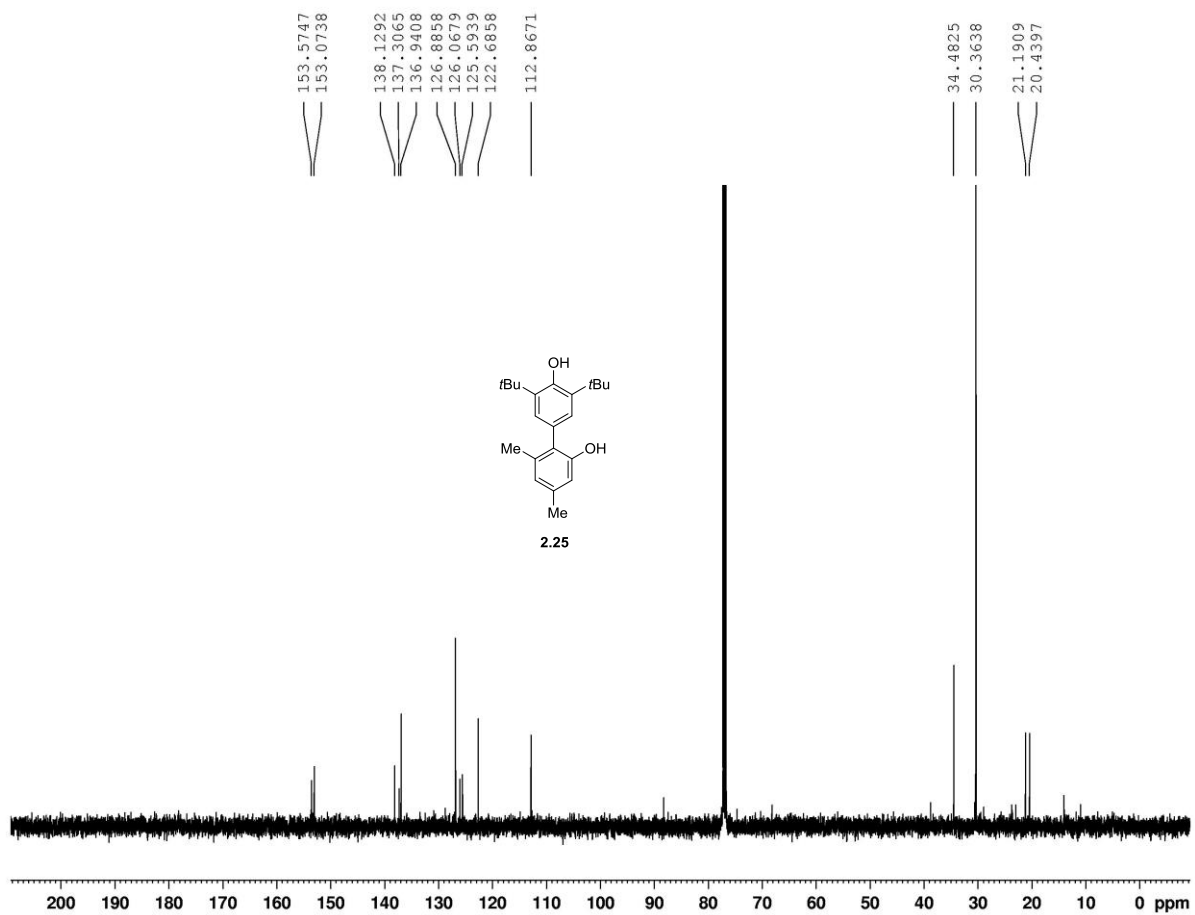
Figure A2.26 ^{13}C NMR spectrum of compound **2.25** (125 MHz, CDCl$_3$)
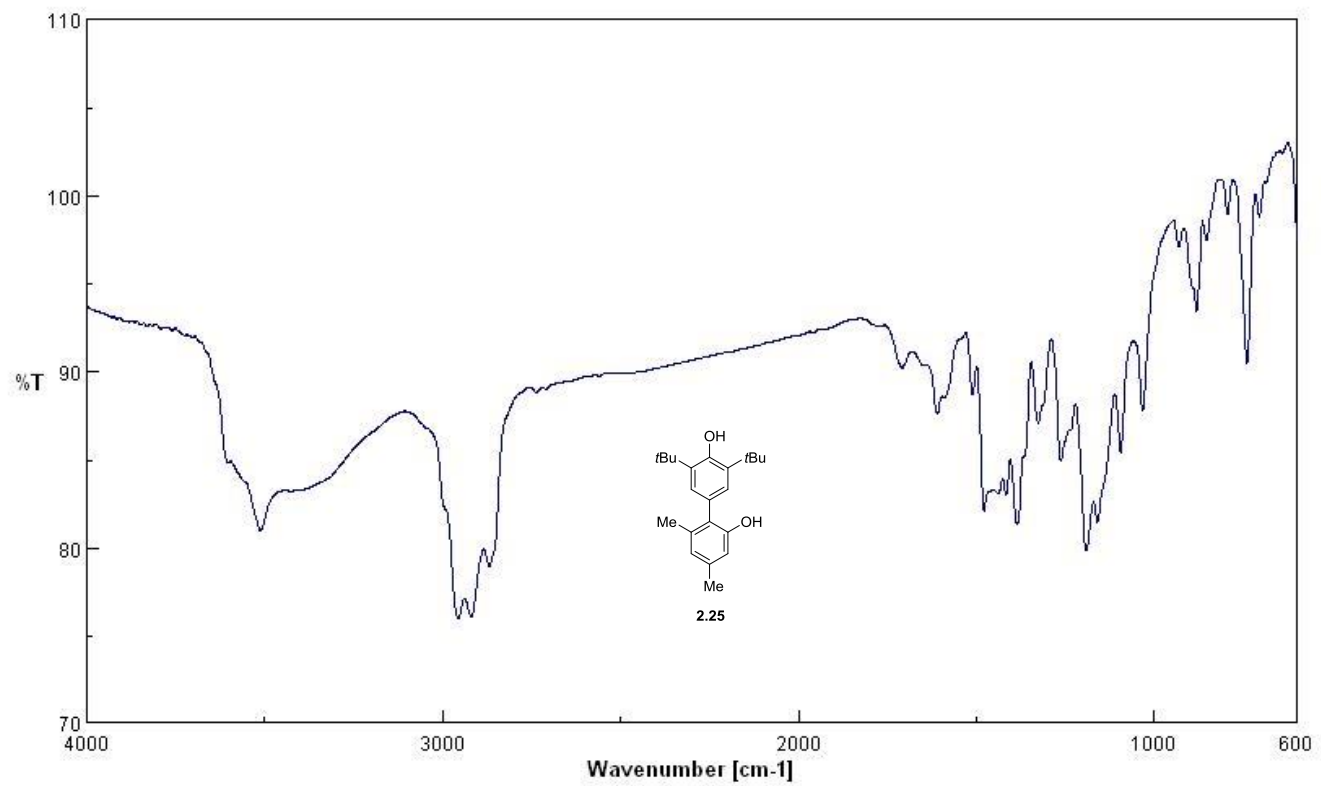
Figure A2.27 IR Spectrum of compound **2.25**
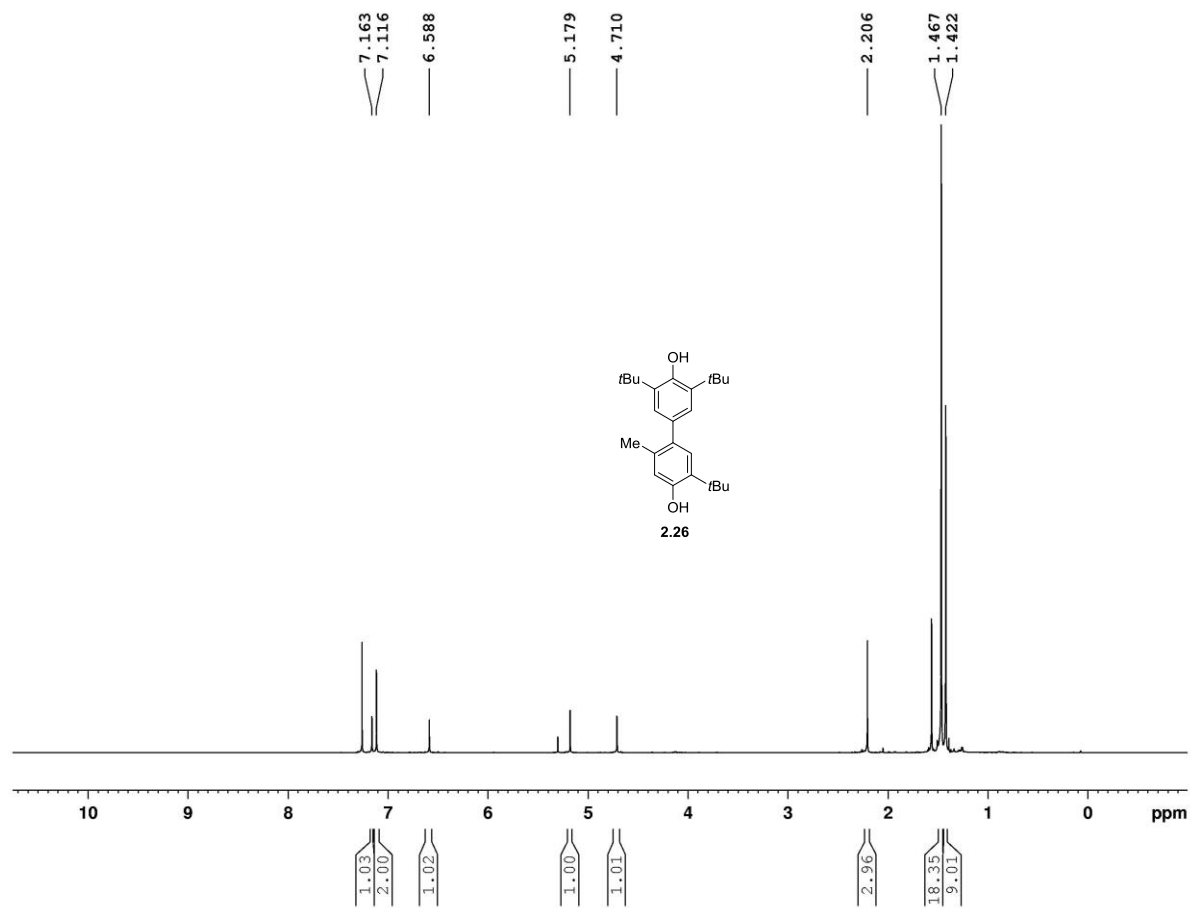
Figure A2.28 ^{1}H NMR spectrum of compound **2.26** (500 MHz, CDCl$_3$)
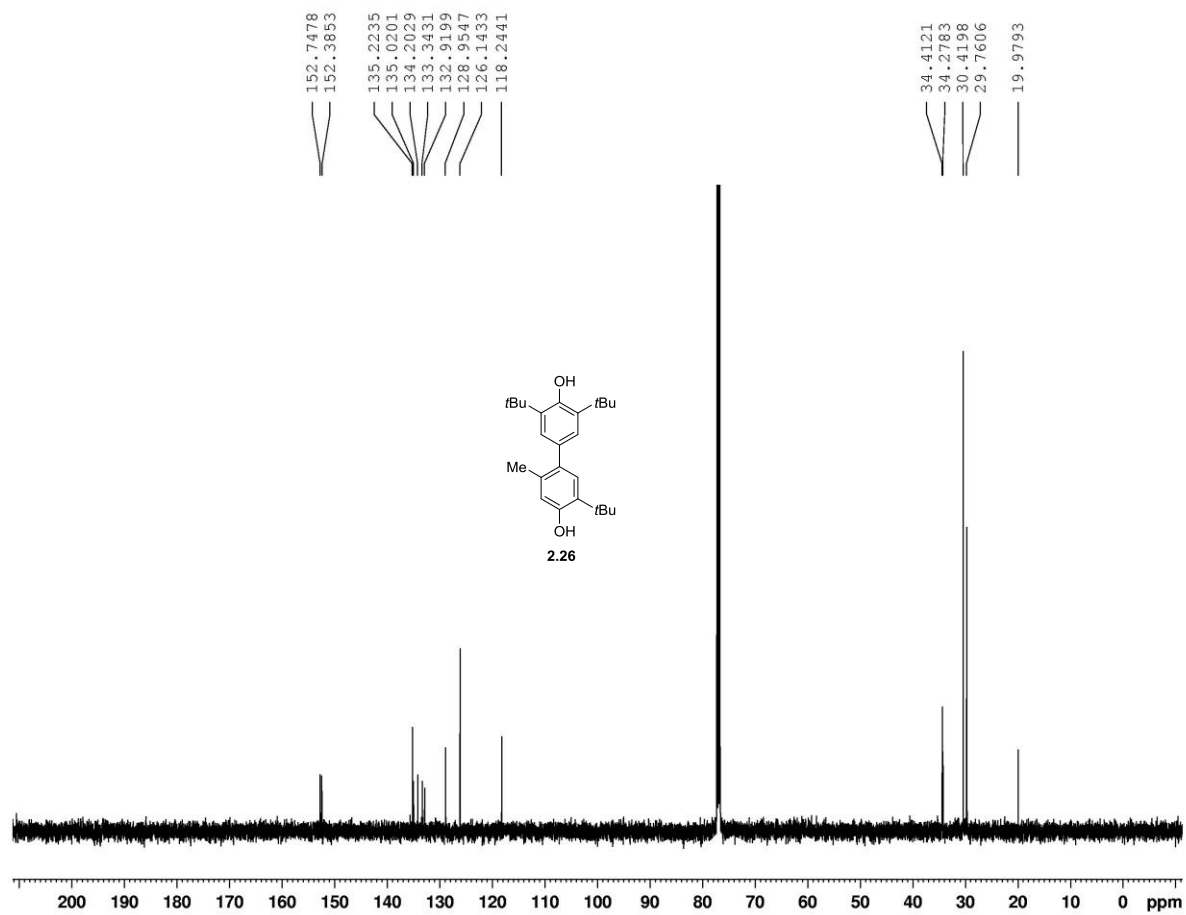
Figure A2.29 ^{13}C NMR spectrum of compound **2.26** (125 MHz, CDCl$_3$)
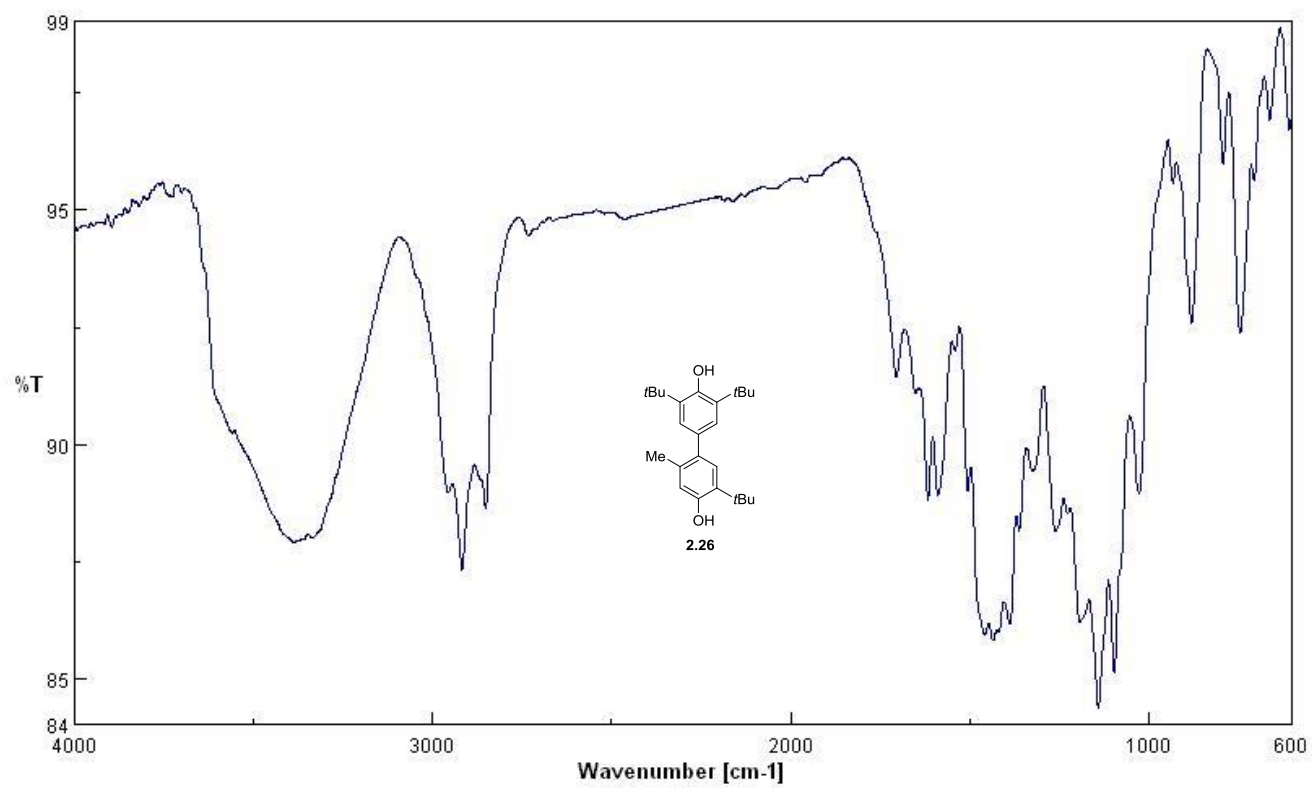
Figure A2.30 IR Spectrum of compound **2.26**
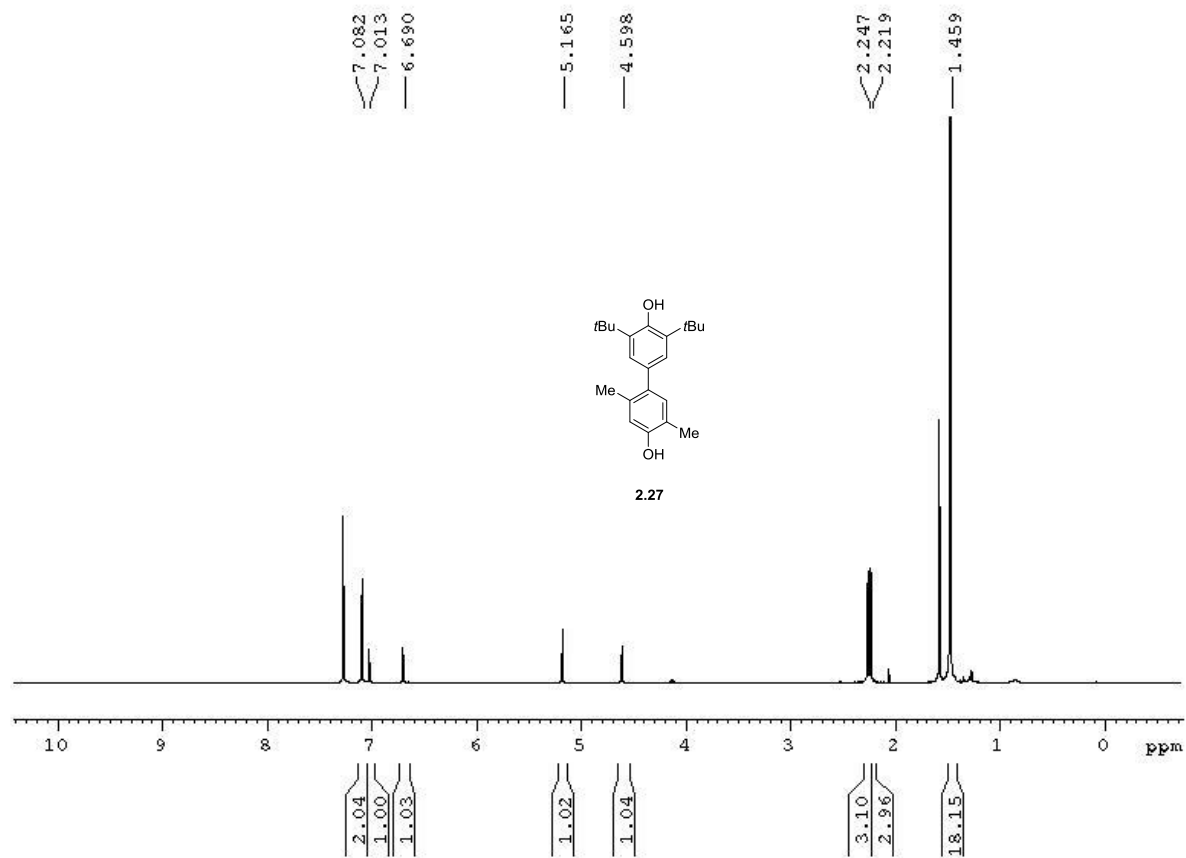
Figure A2.31 ^{1}H NMR spectrum of compound **2.27** (500 MHz, CDCl$_3$)
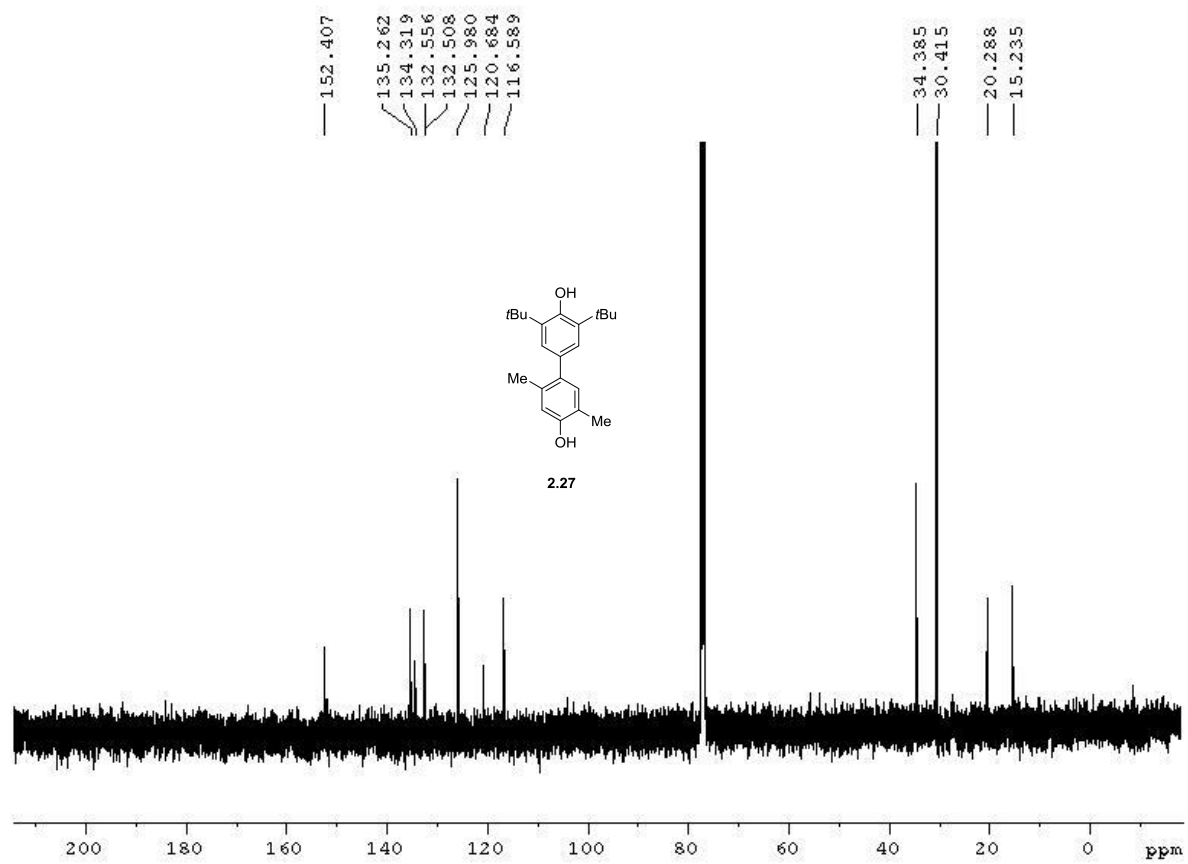
Figure A2.32 ^{13}C NMR spectrum of compound **2.27** (125 MHz, CDCl$_3$)
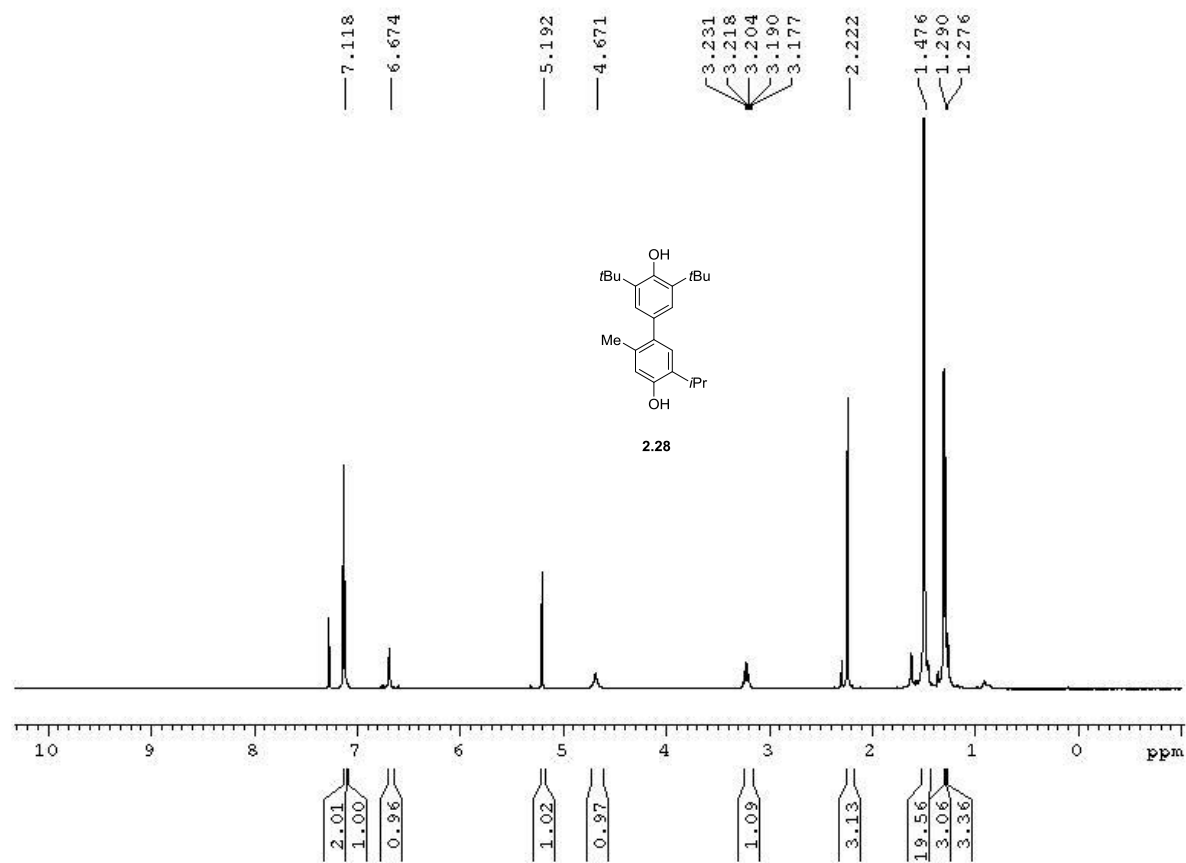
Figure A2.33 ^{1}H NMR spectrum of compound **2.28** (500 MHz, CDCl$_3$)
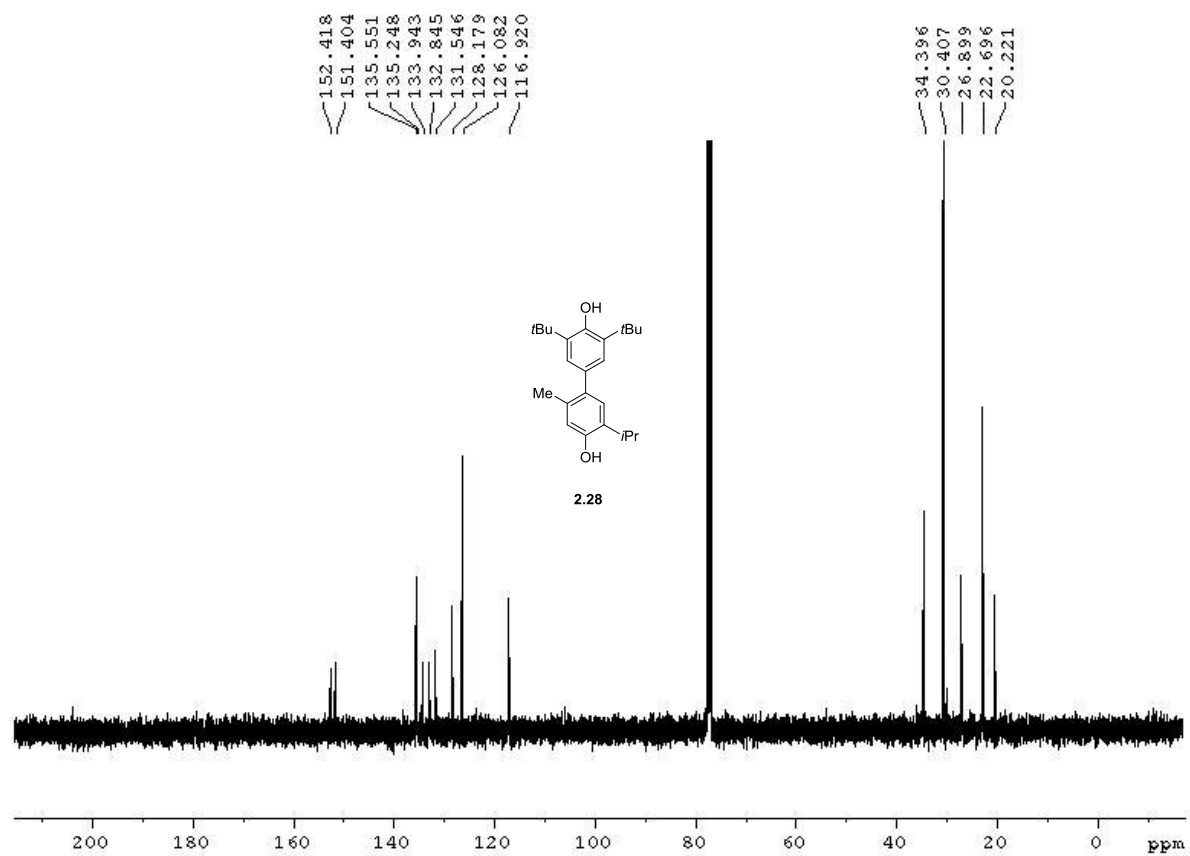
Figure A2.34 ^{13}C NMR spectrum of compound **2.28** (125 MHz, CDCl$_3$)

240
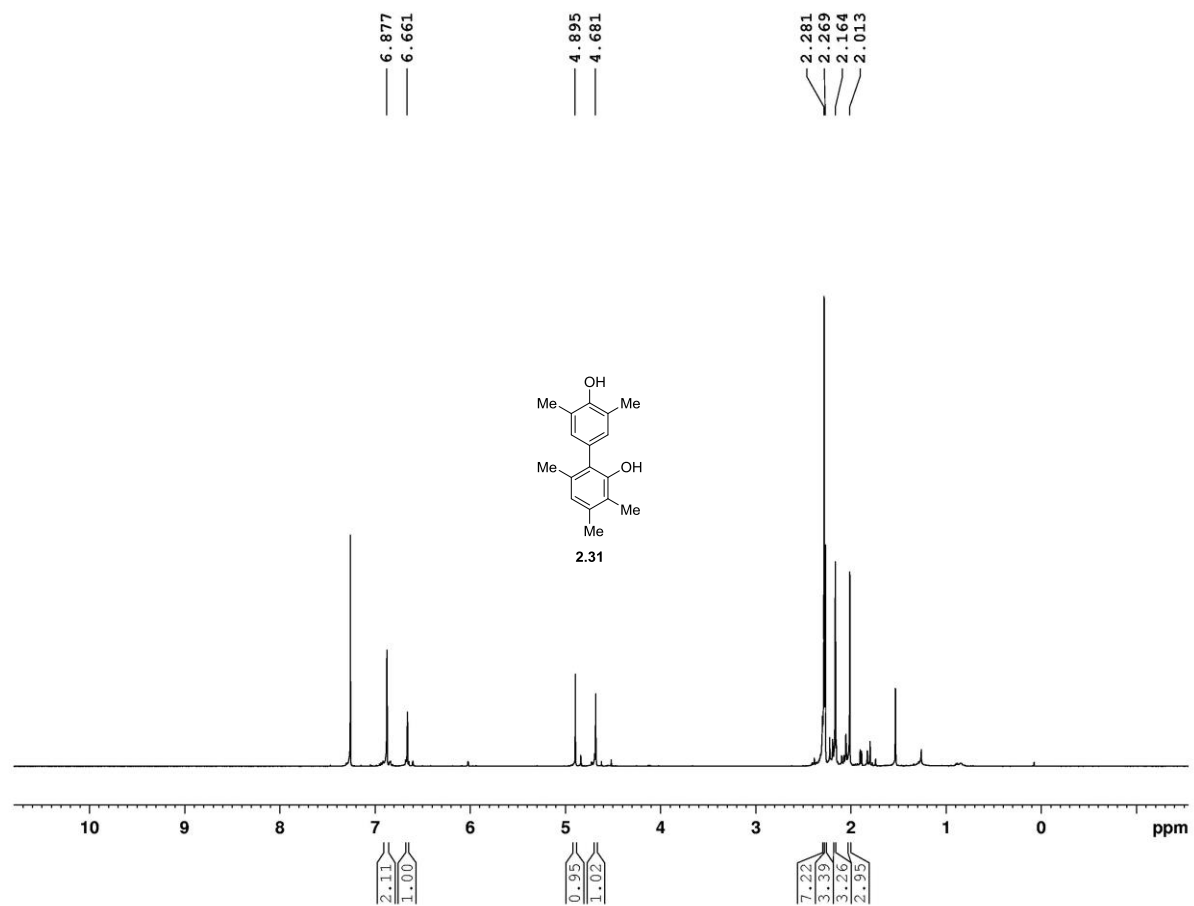
Figure A2.35 ^{1}H NMR spectrum of compound **2.31** (500 MHz, CDCl₃)

241
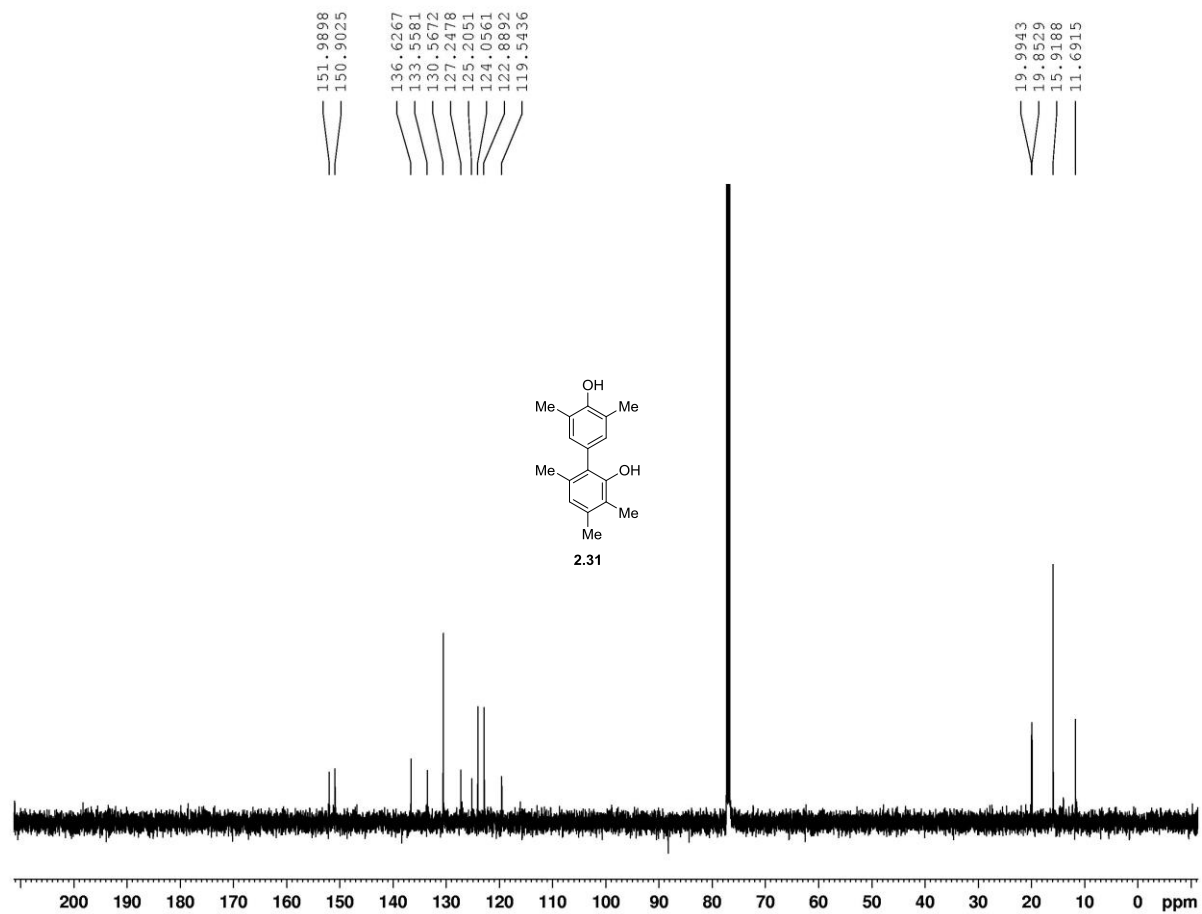
Figure A2.36 ^{13}C NMR spectrum of compound **2.31** (125 MHz, CDCl$_3$)
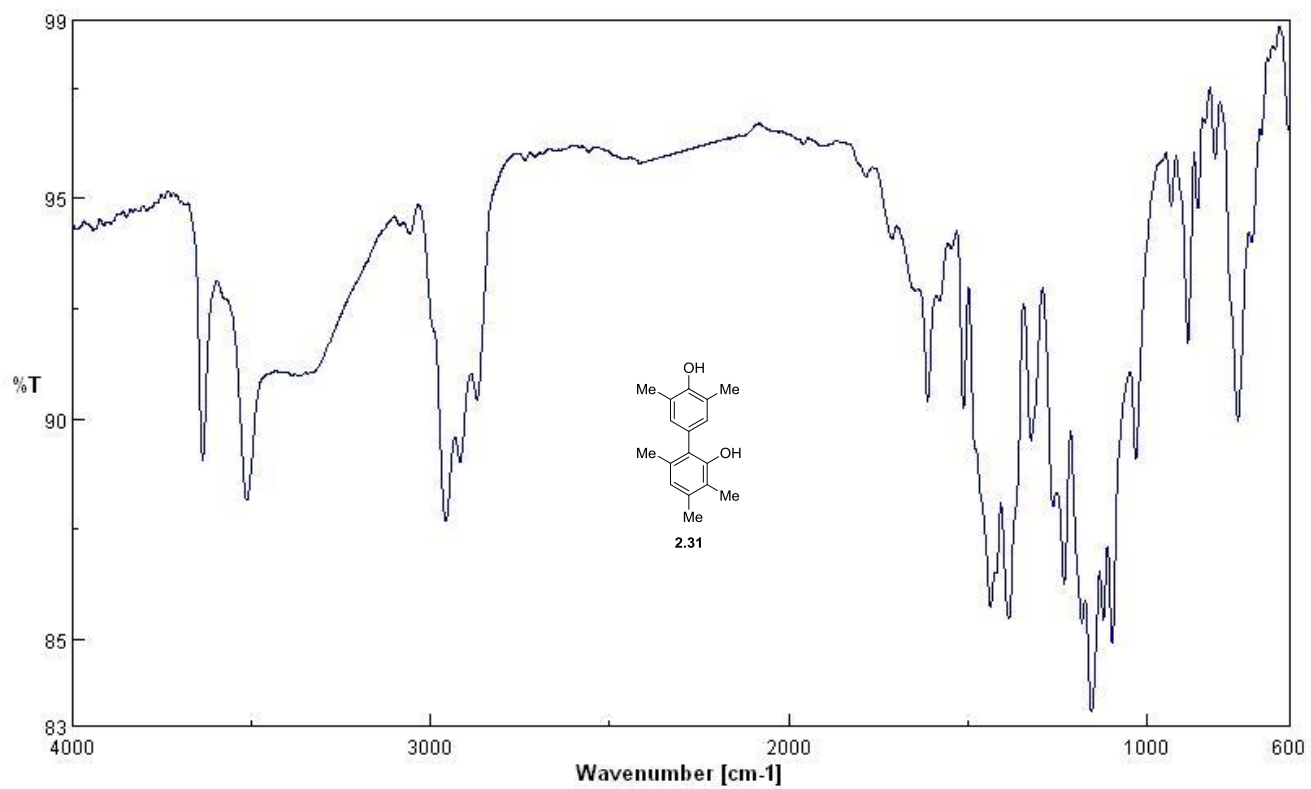
Figure A2.37 IR Spectrum of compound **2.31**
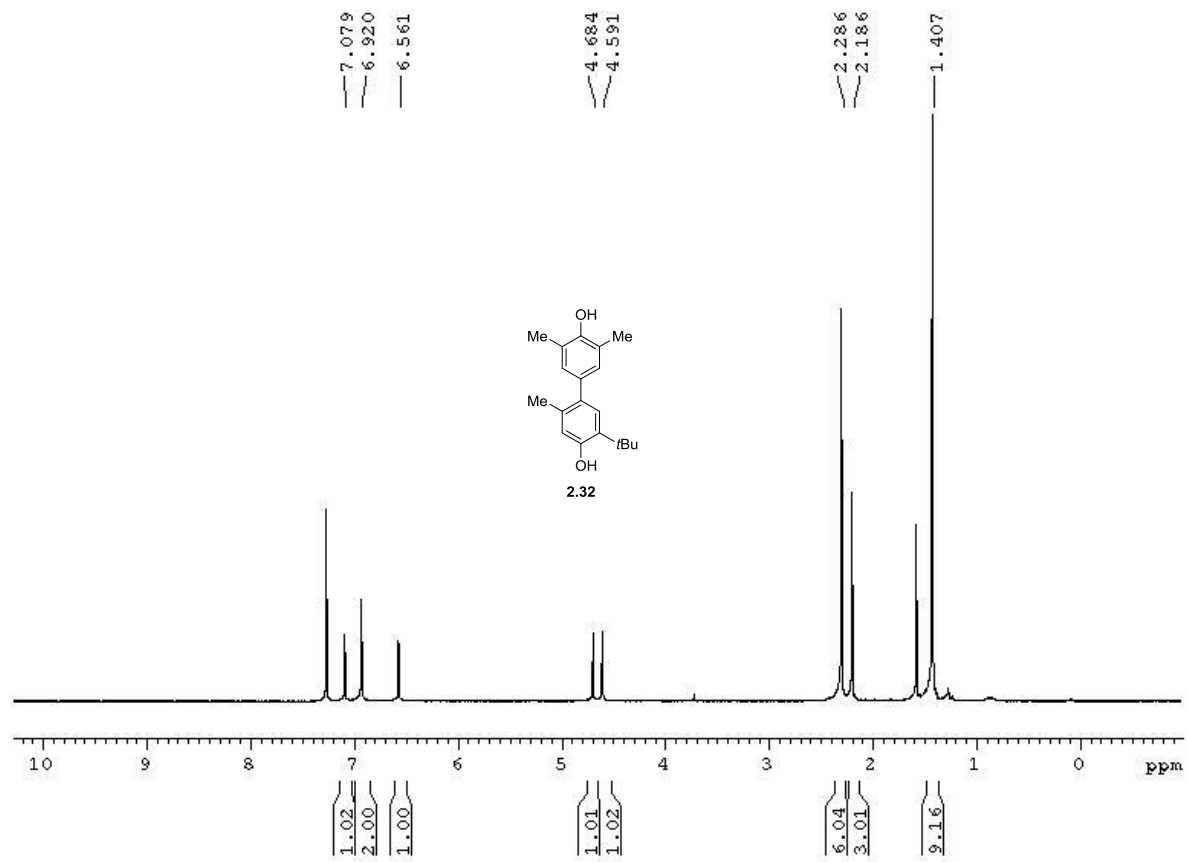
Figure A2.38 ^{1}H NMR spectrum of compound **2.32** (500 MHz, CDCl$_3$)
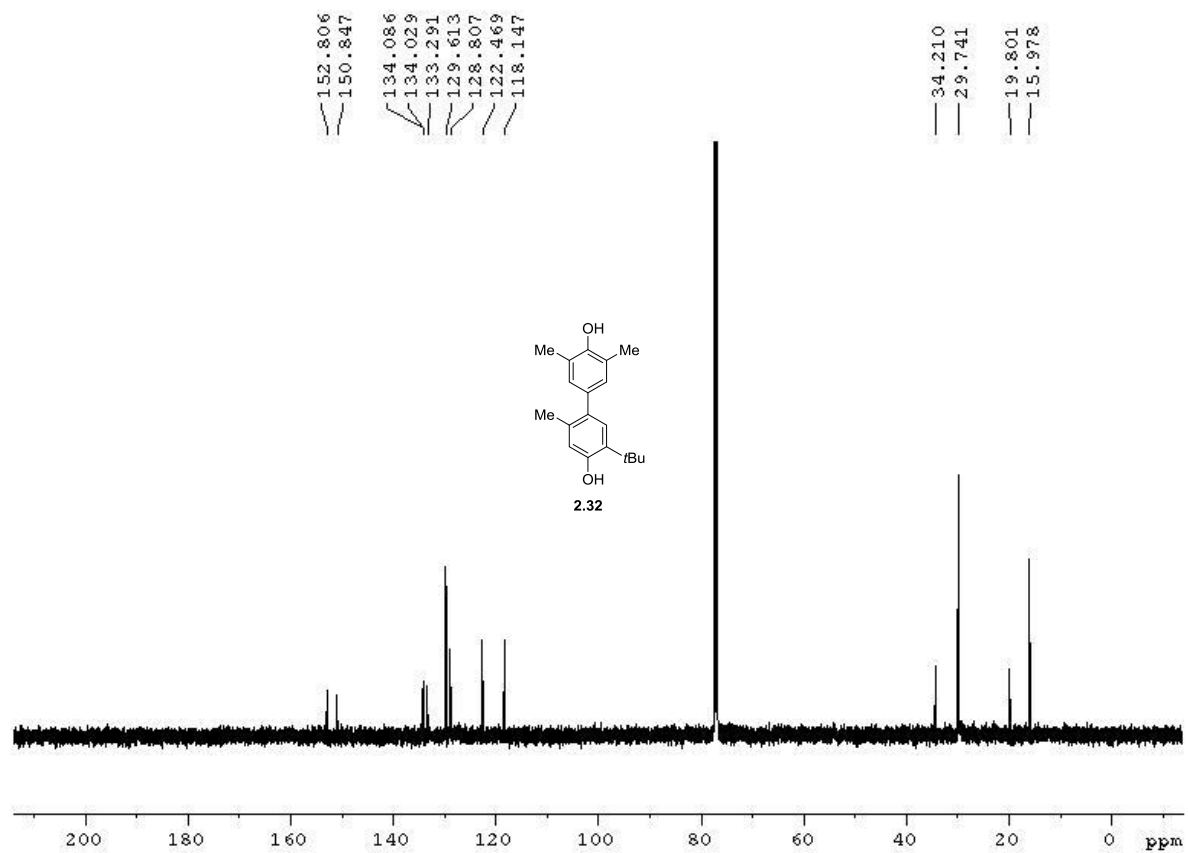
Figure A2.39 ^{13}C NMR spectrum of compound **2.32** (125 MHz, CDCl$_3$)
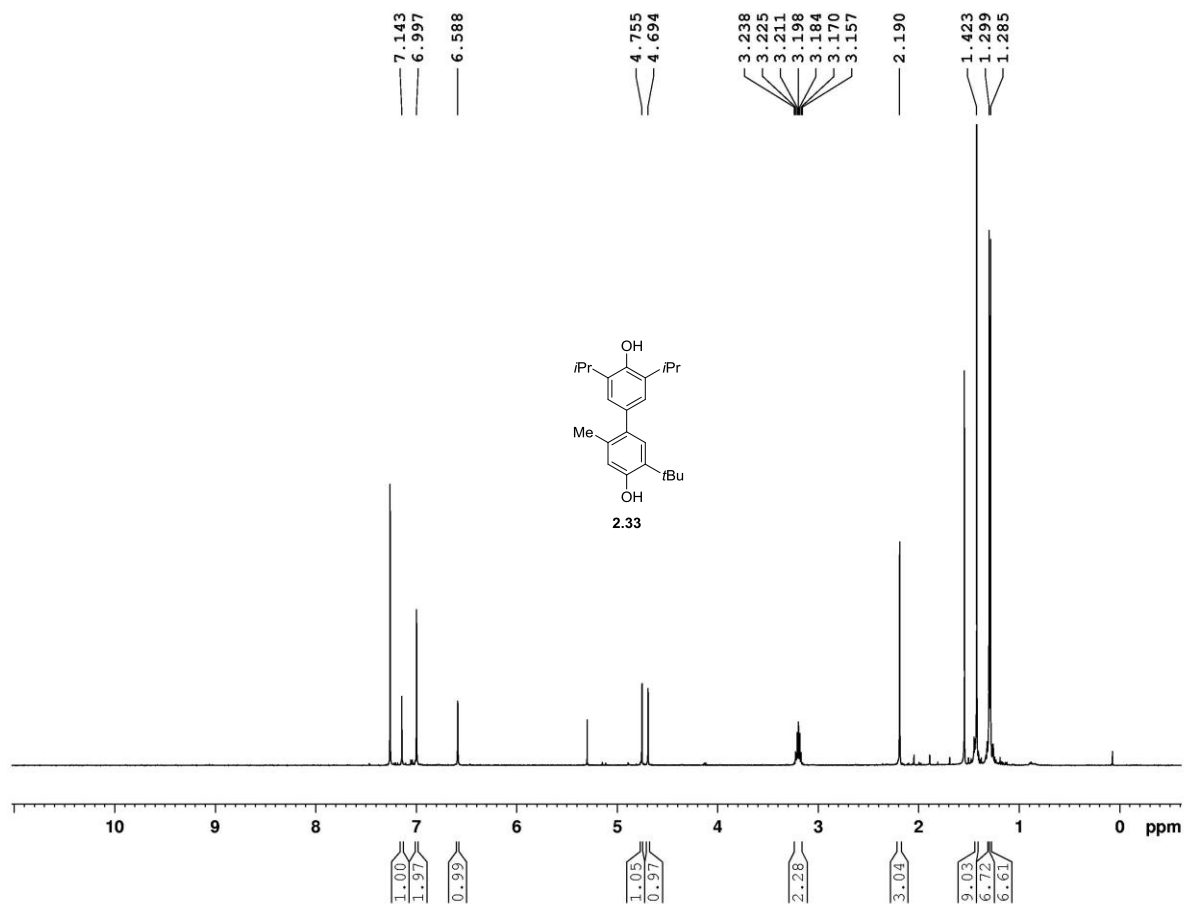
Figure A2.40 ^{1}H NMR spectrum of compound **2.33** (500 MHz, CDCl$_3$)
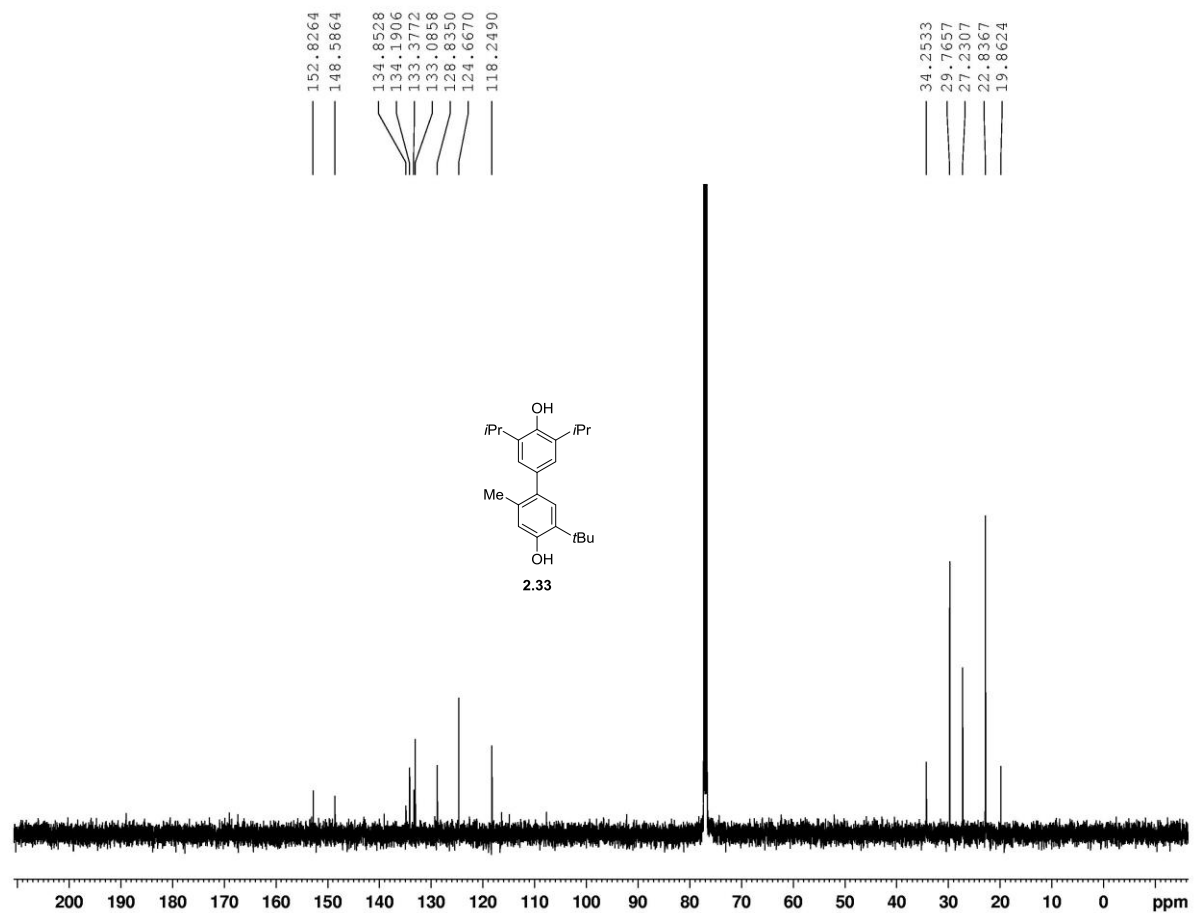
Figure A2.41 ^{13}C NMR spectrum of compound **2.33** (125 MHz, CDCl$_3$)
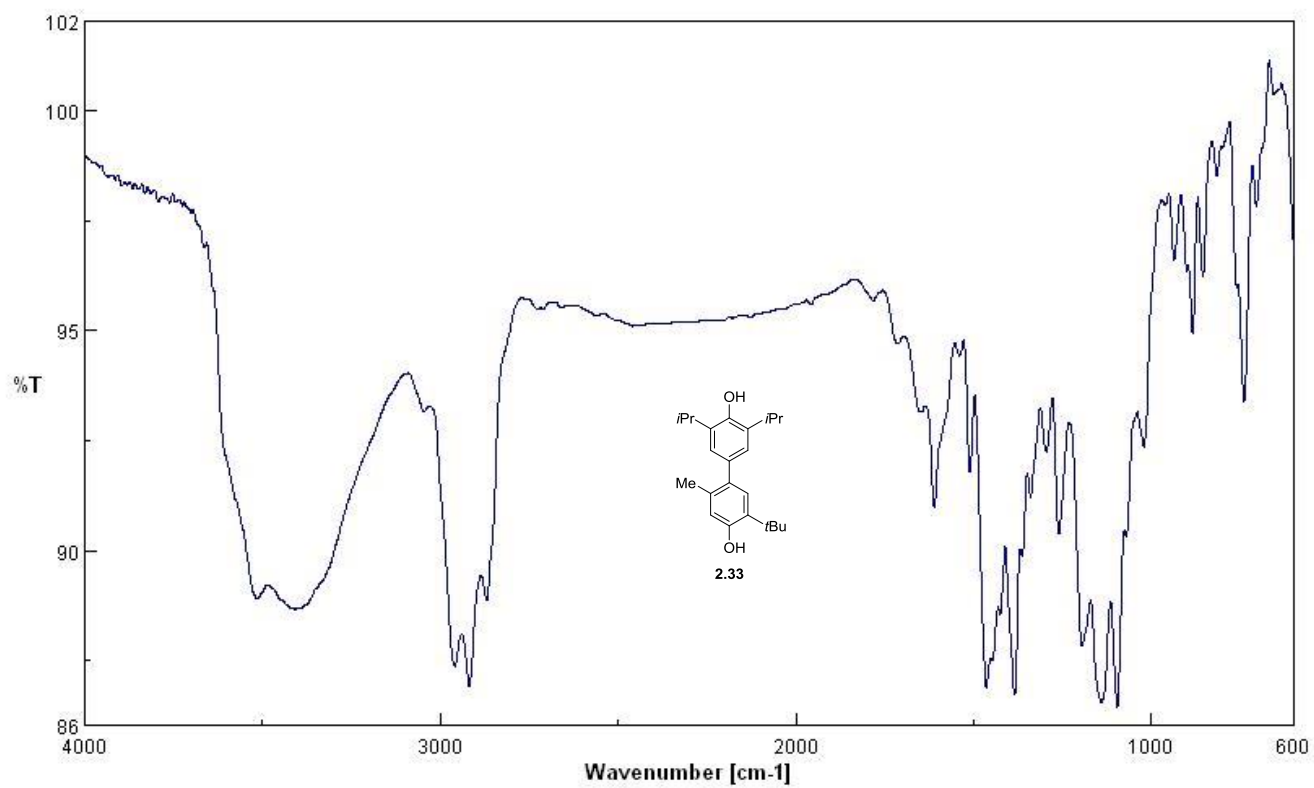
Figure A2.42 IR Spectrum of compound **2.33**
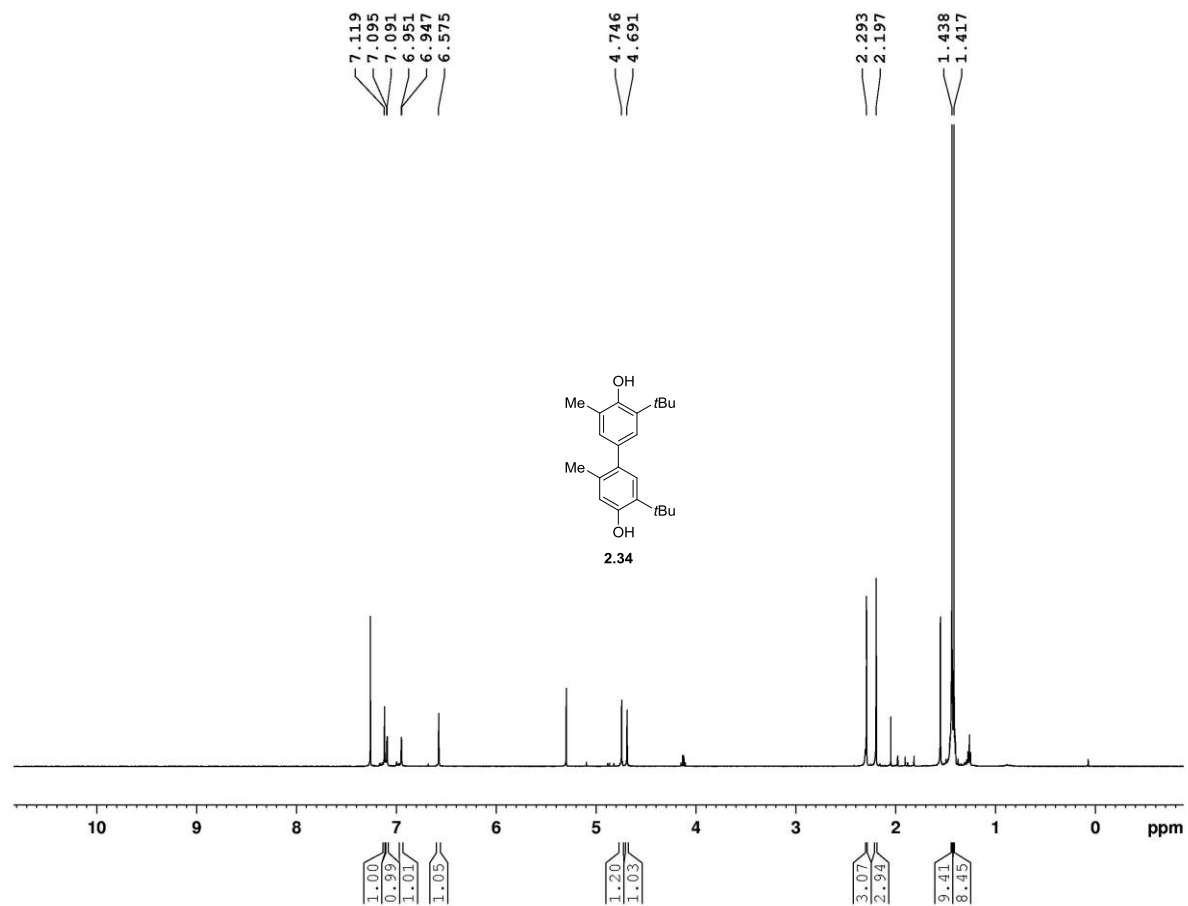
Figure A2.43 ^{1}H NMR spectrum of compound **2.34** (500 MHz, CDCl$_3$)
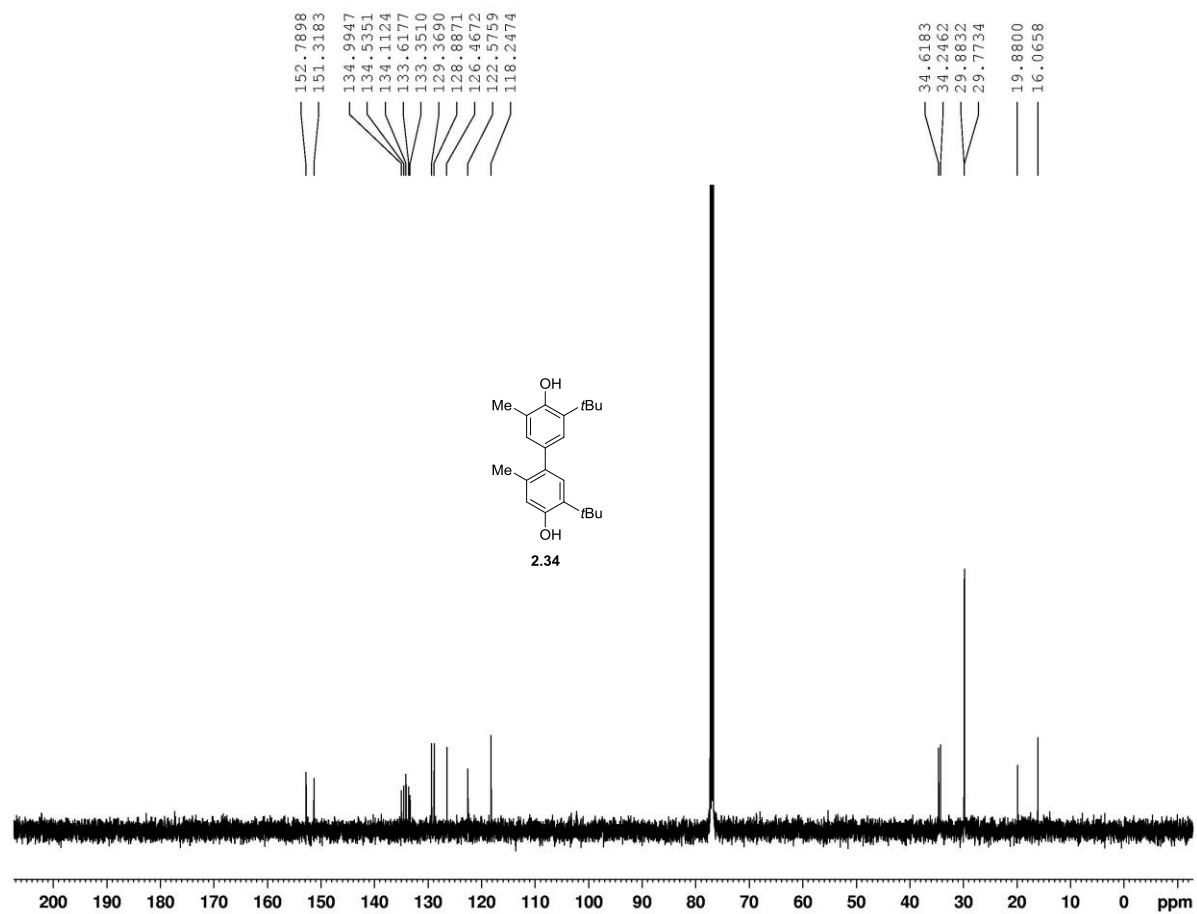
Figure A2.44 ^{13}C NMR spectrum of compound **2.34** (125 MHz, CDCl$_3$)
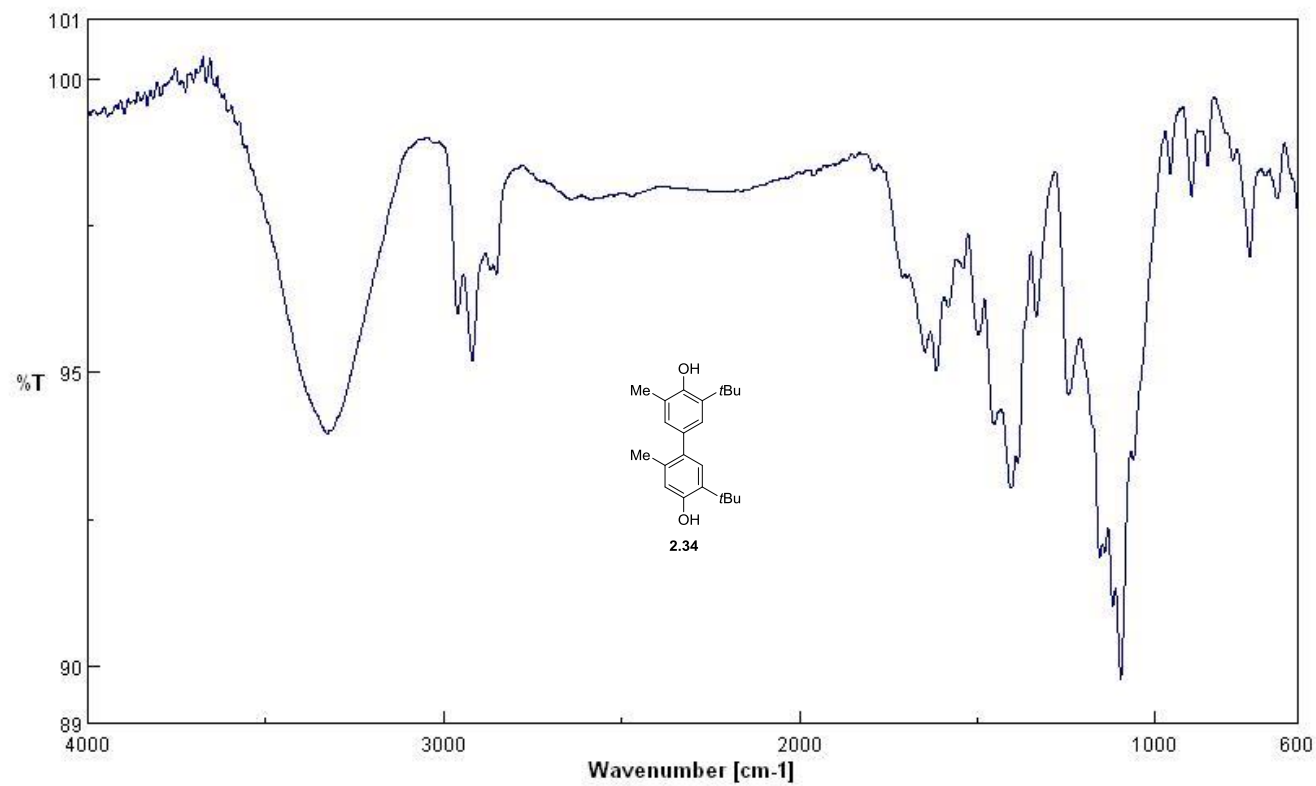
Figure A2.45 IR Spectrum of compound **2.34**
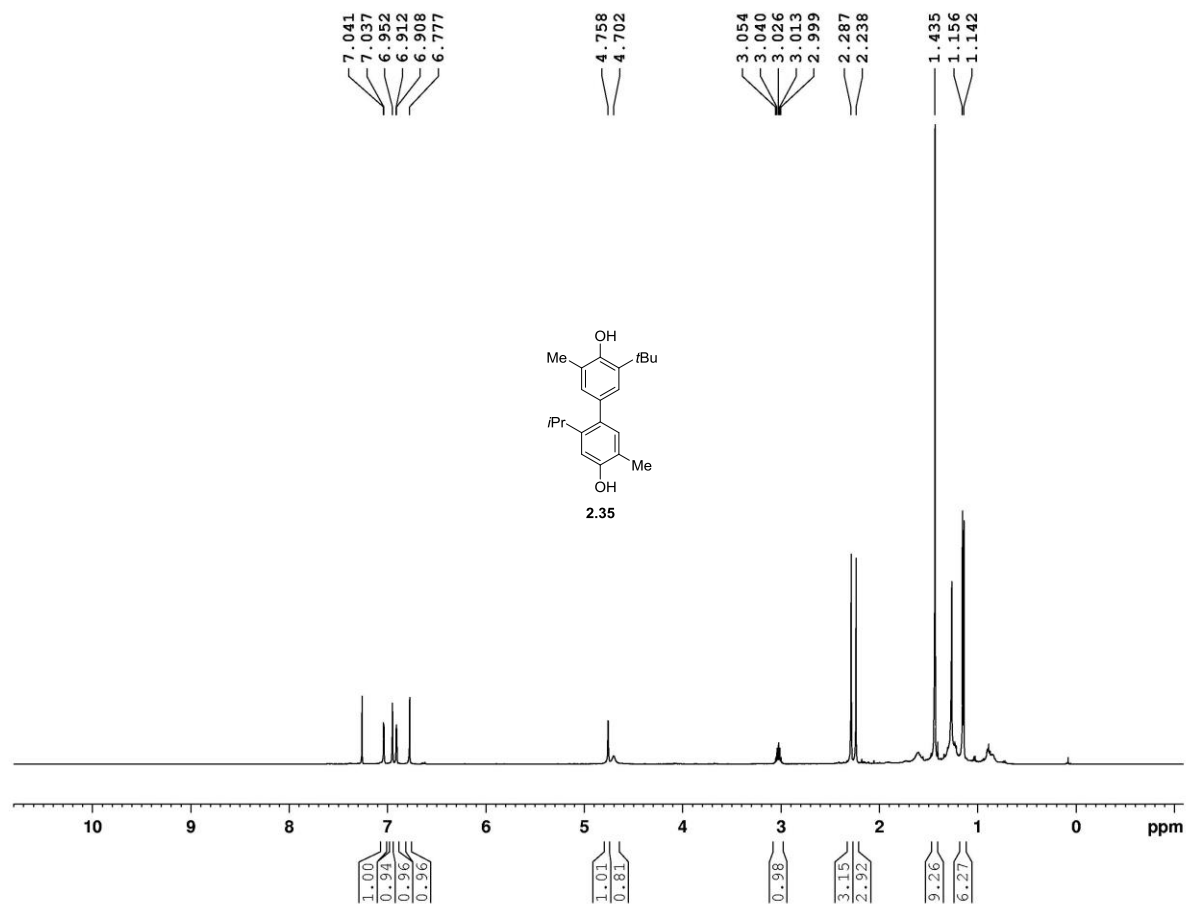
Figure A2.46 ^{1}H NMR spectrum of compound **2.35** (500 MHz, CDCl$_3$)
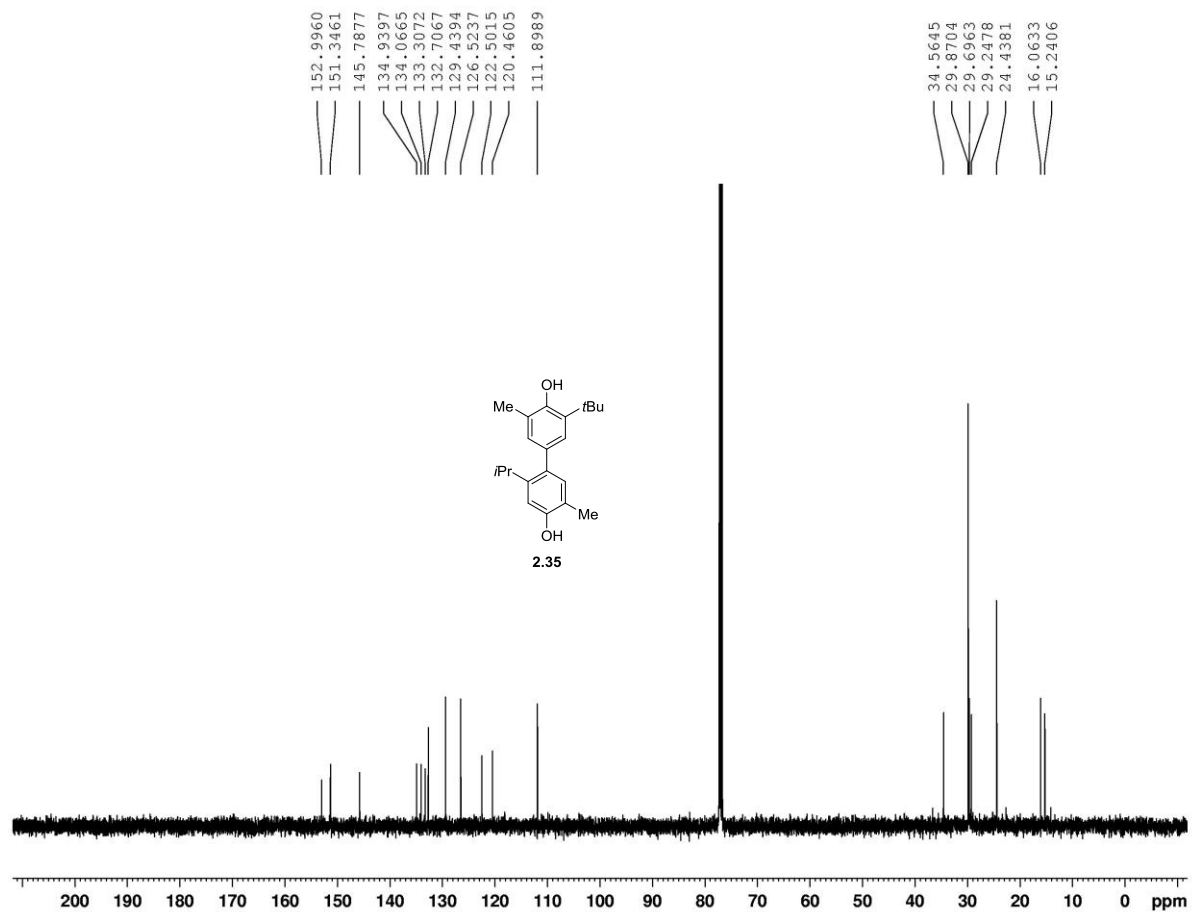
Figure A2.47 ^{13}C NMR spectrum of compound **2.35** (125 MHz, CDCl$_3$)
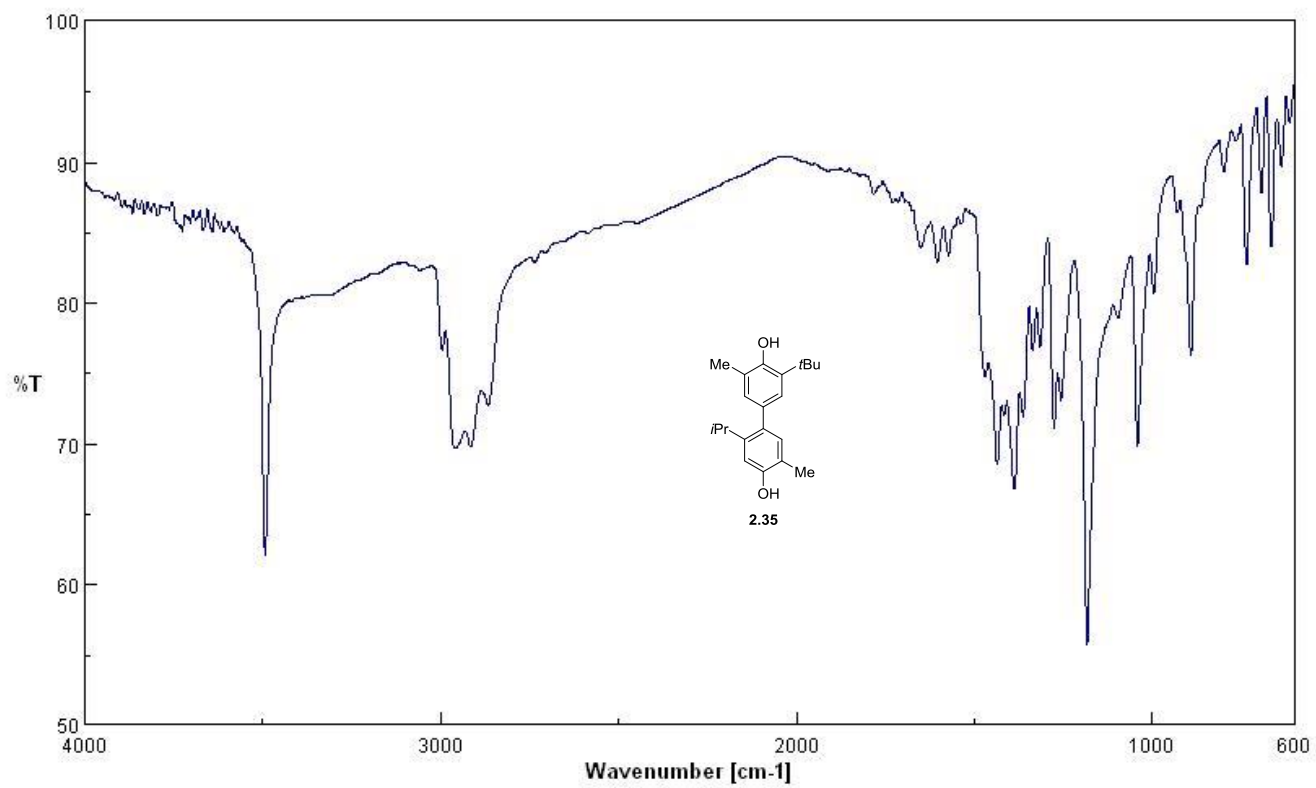
Figure A2.48 IR Spectrum of compound **2.35**
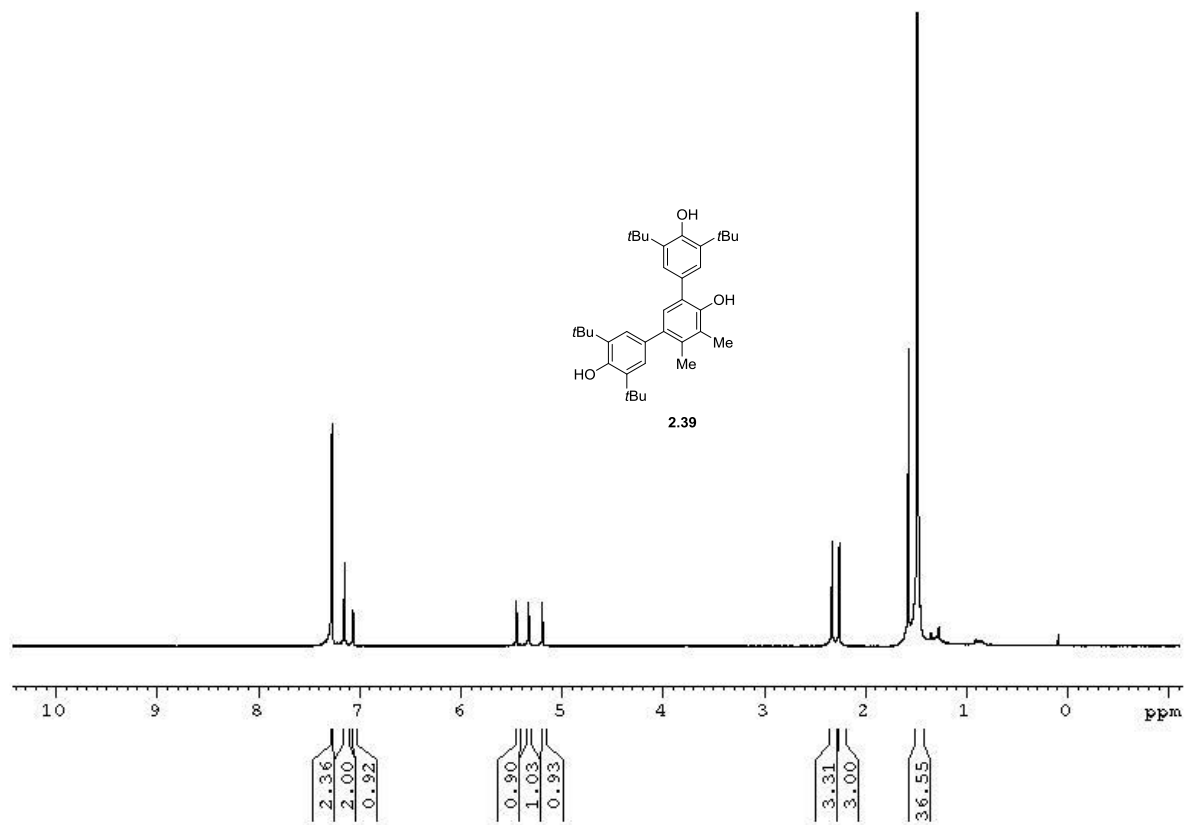
Figure A2.49 ^{1}H NMR spectrum of compound **2.39** (500 MHz, CDCl$_3$)
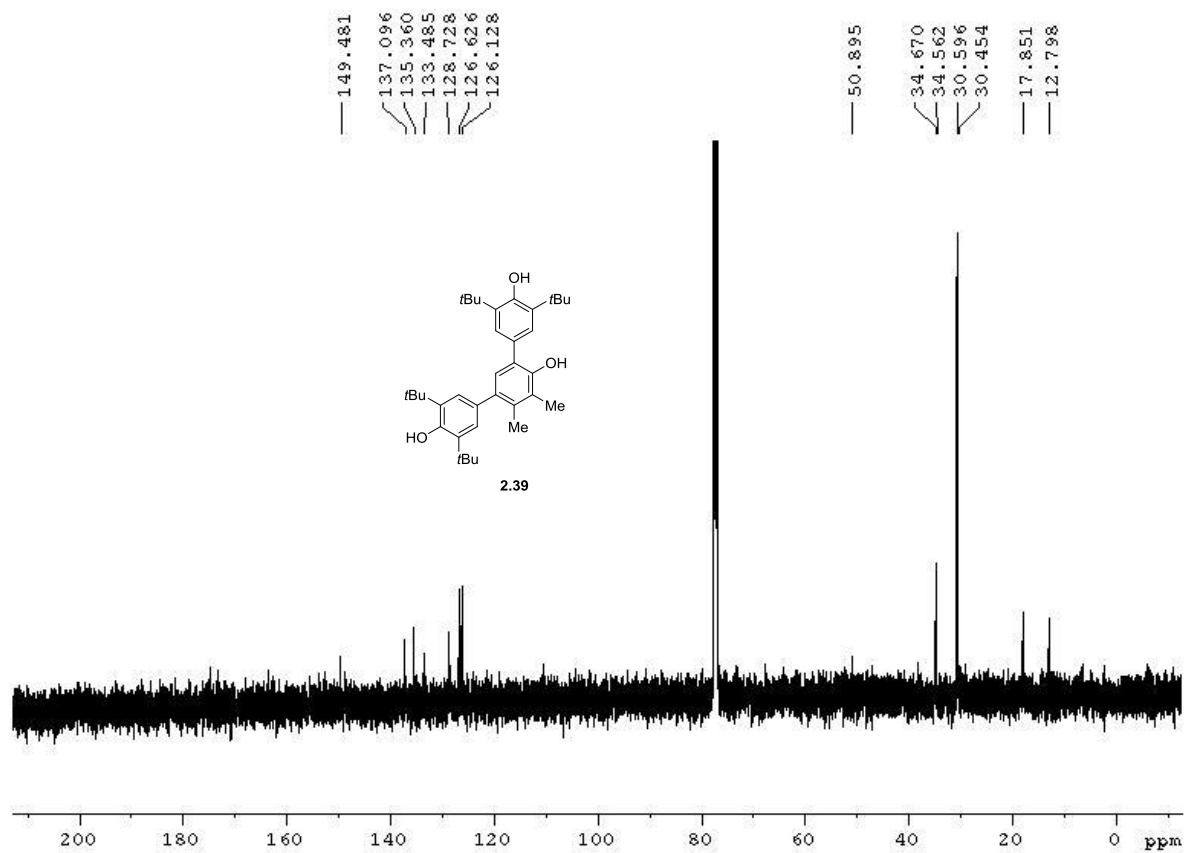
Figure A2.50 ^{13}C NMR spectrum of compound **2.39** (125 MHz, CDCl$_3$)
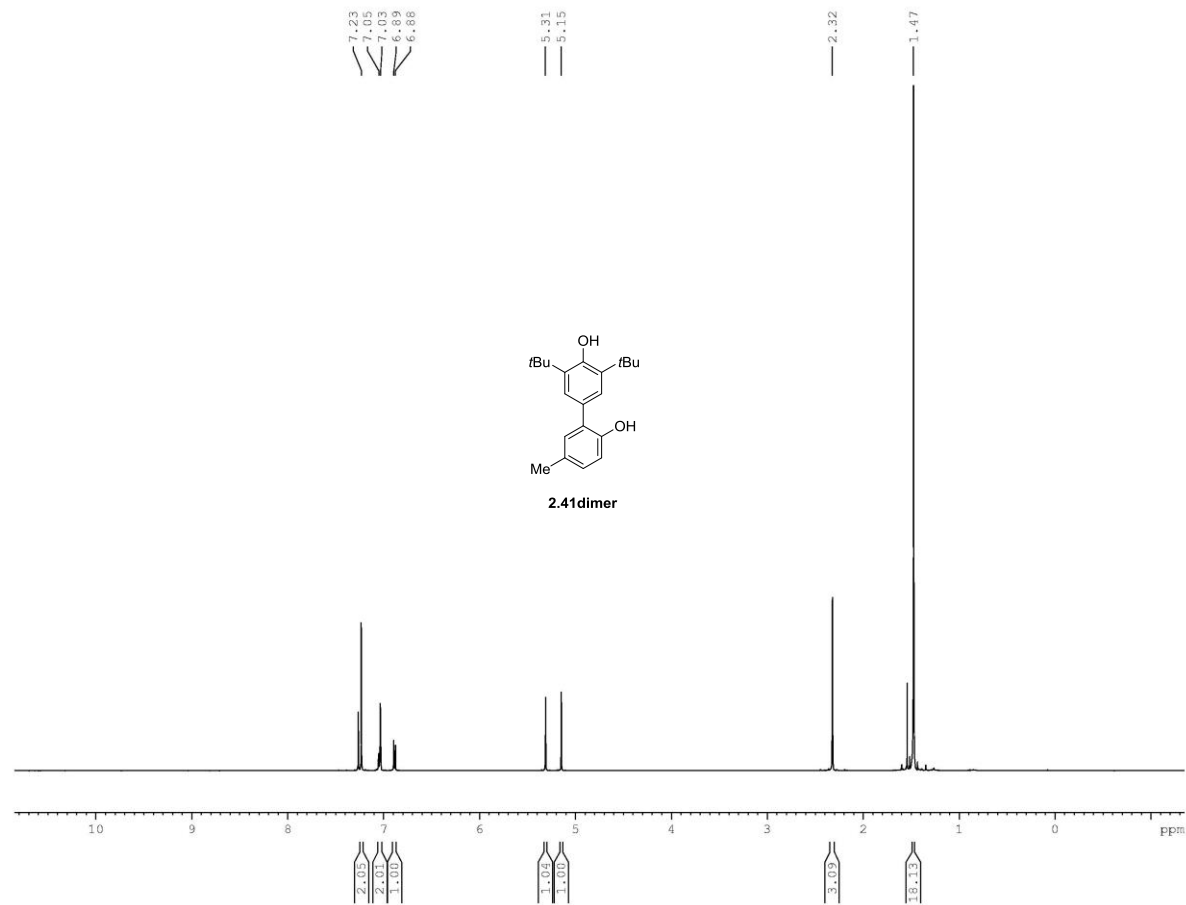
Figure A2.51 ^{1}H NMR spectrum of compound **2.41dimer** (500 MHz, CDCl$_3$)
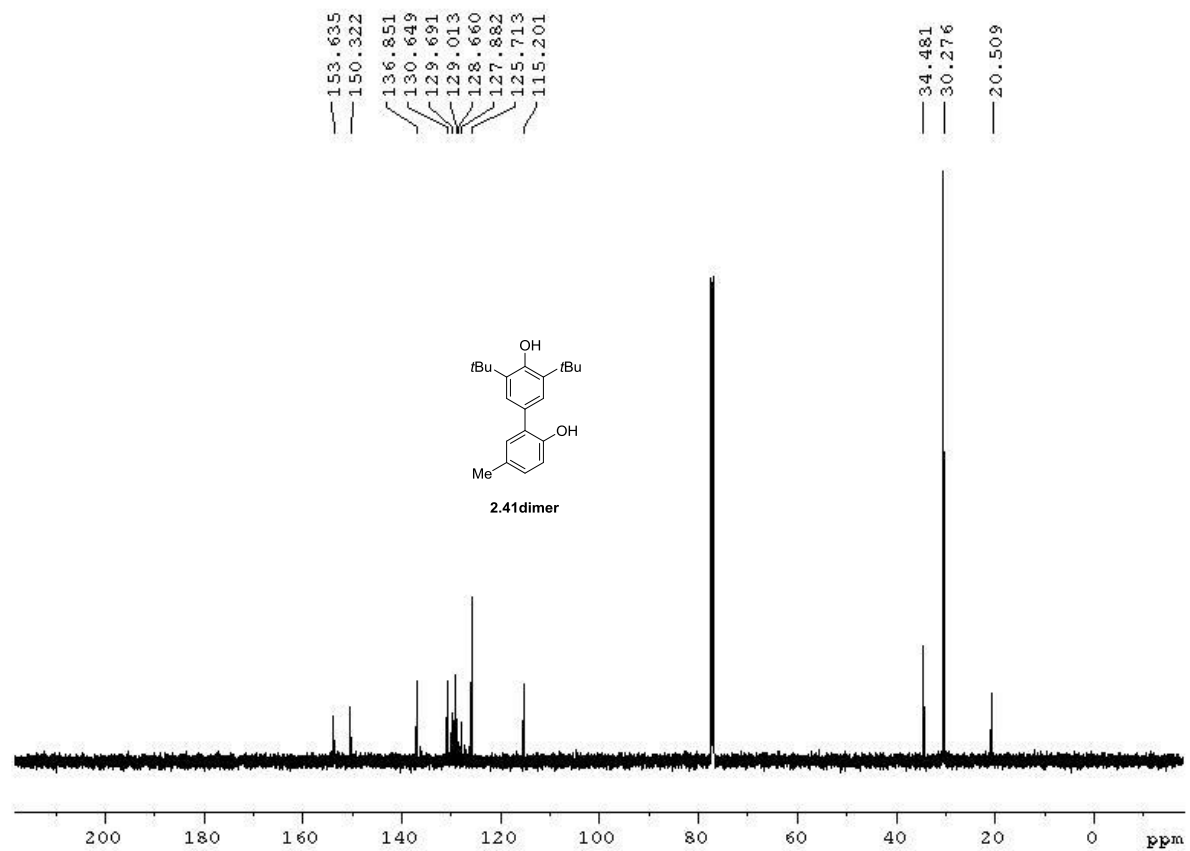
Figure A2.52 ^{13}C NMR spectrum of compound **2.41dimer** (125 MHz, CDCl$_3$)
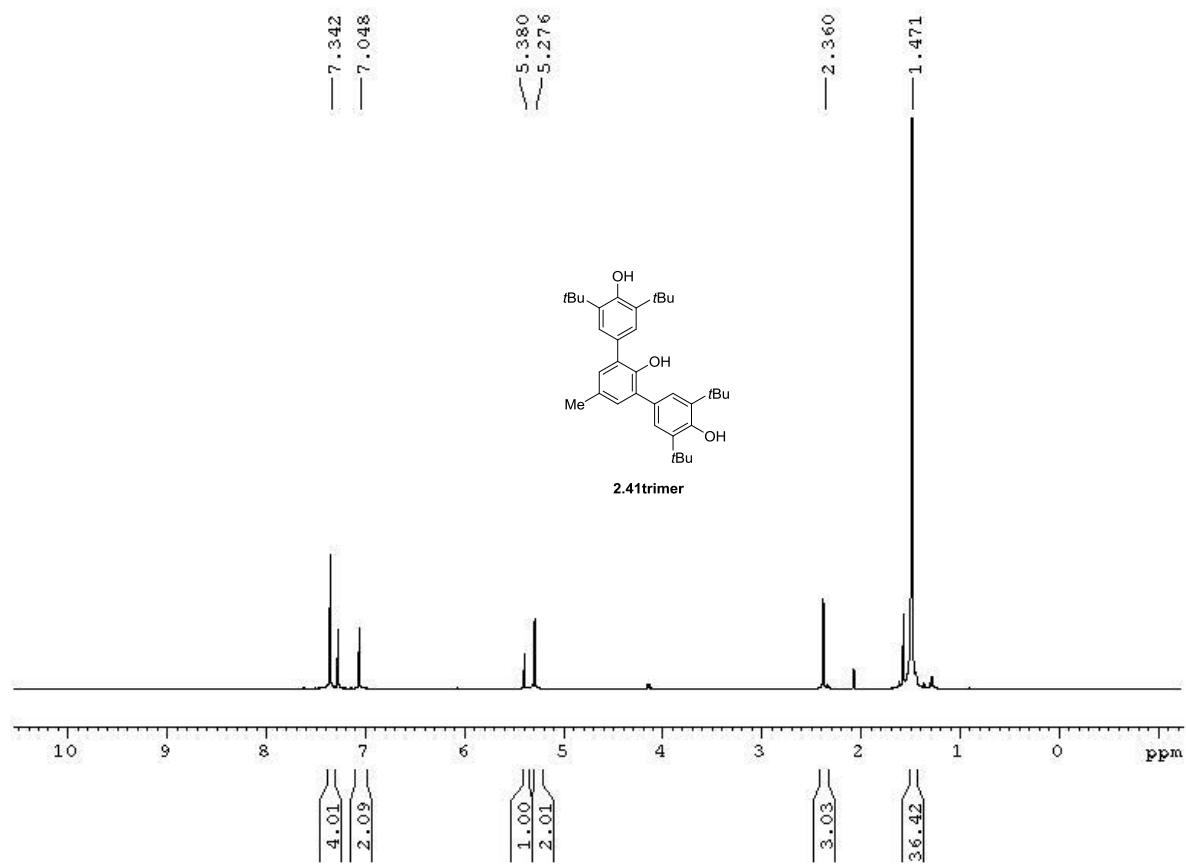
Figure A2.53 ^{1}H NMR spectrum of compound **2.41trimer** (500 MHz, CDCl$_3$)

259
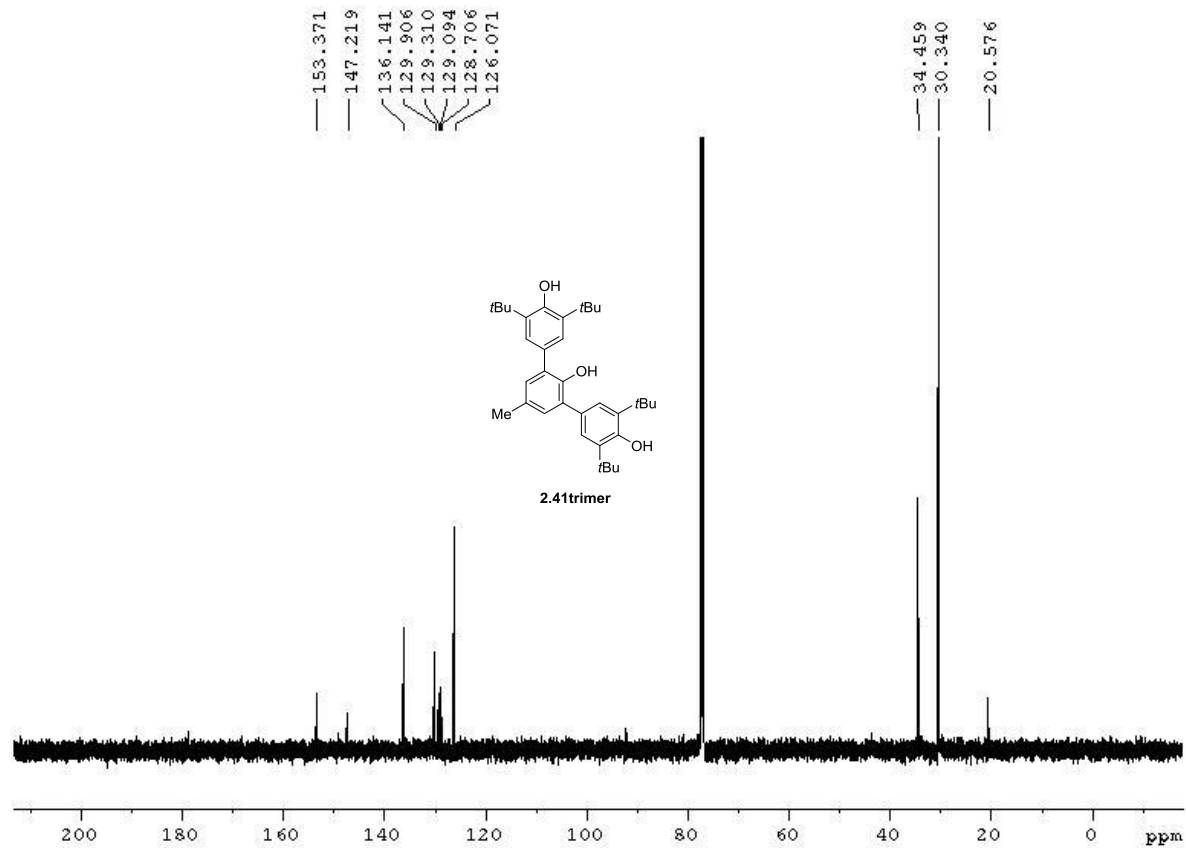
Figure A2.54 ^{13}C NMR spectrum of compound **2.41trimer** (125 MHz, CDCl$_3$)
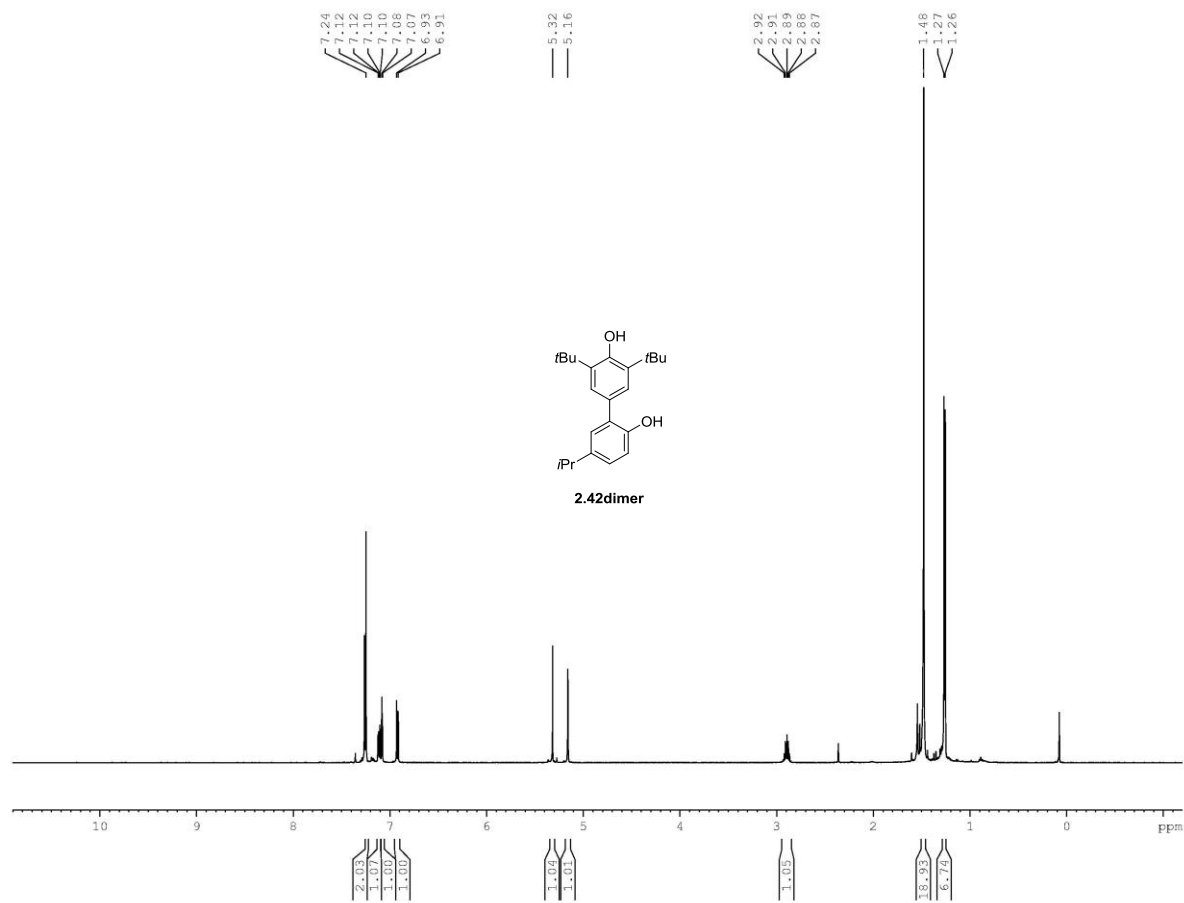
Figure A2.55 ^{1}H NMR spectrum of compound **2.42dimer** (500 MHz, CDCl$_3$)

261
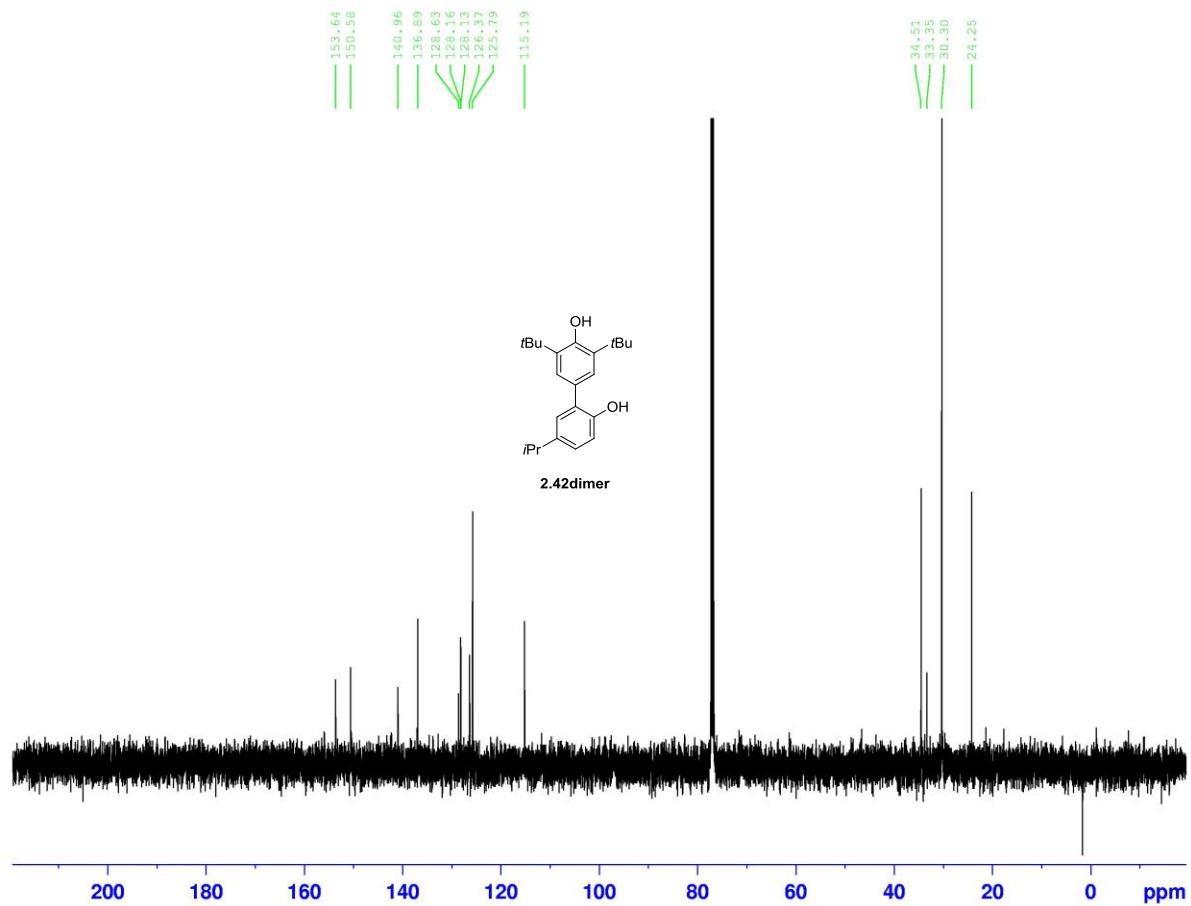
Figure A2.56 ^{13}C NMR spectrum of compound **2.42dimer** (125 MHz, CDCl$_3$)
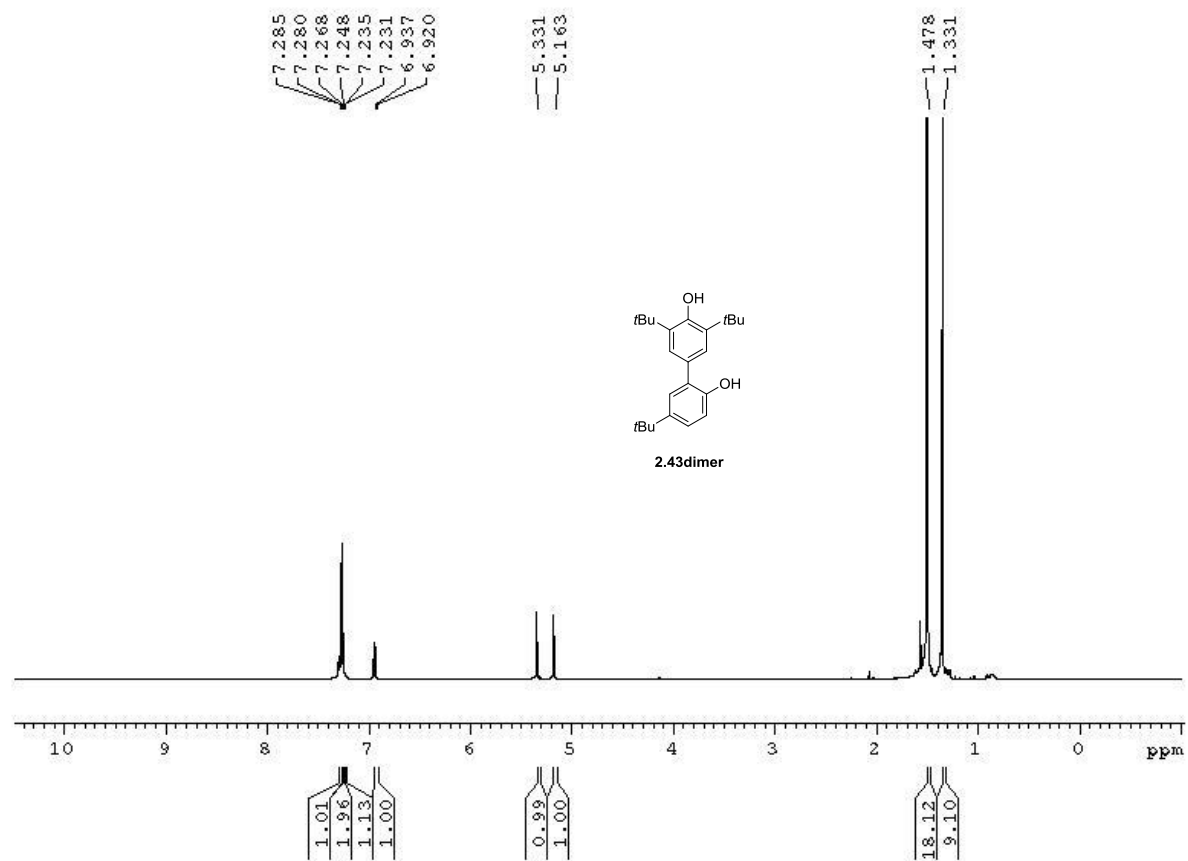
Figure A2.57 ^{1}H NMR spectrum of compound **2.43dimer** (500 MHz, CDCl$_3$)
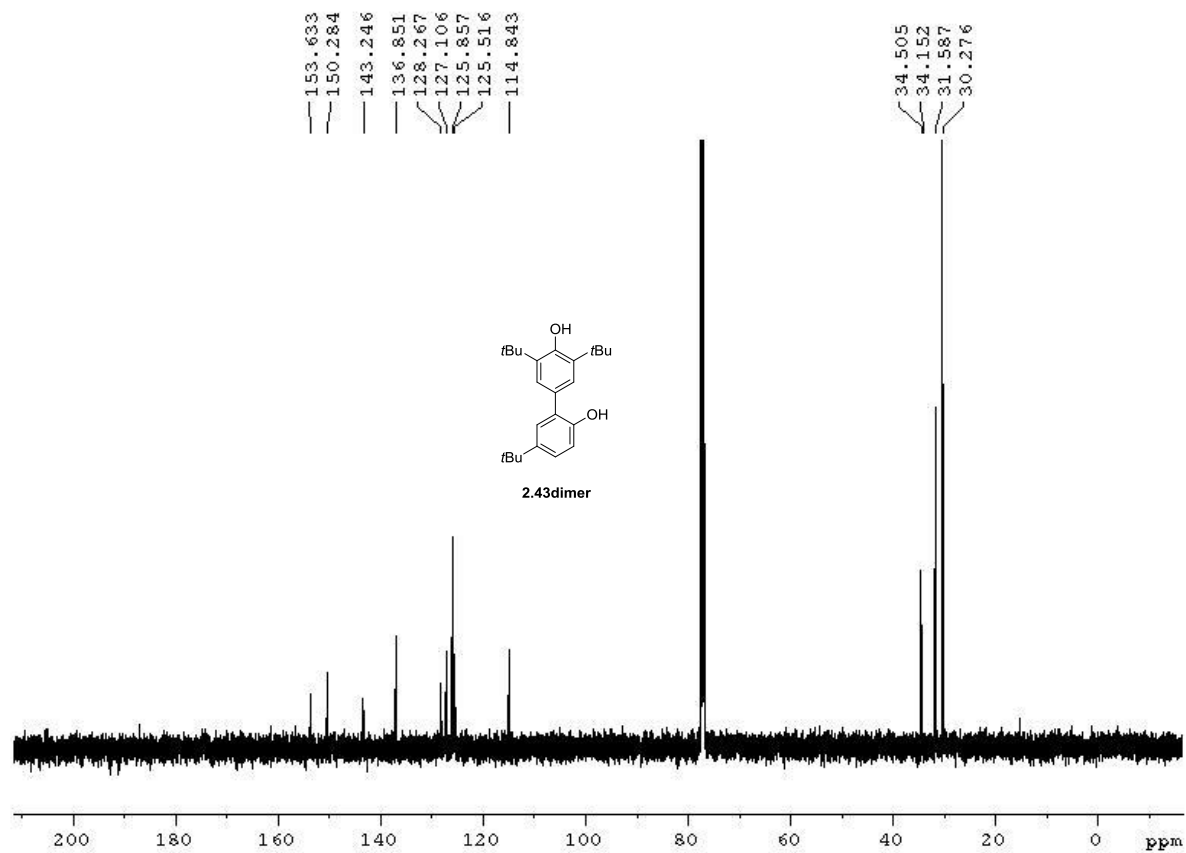
Figure A2.57 ^{13}C NMR spectrum of compound **2.43dimer** (125 MHz, CDCl$_3$)
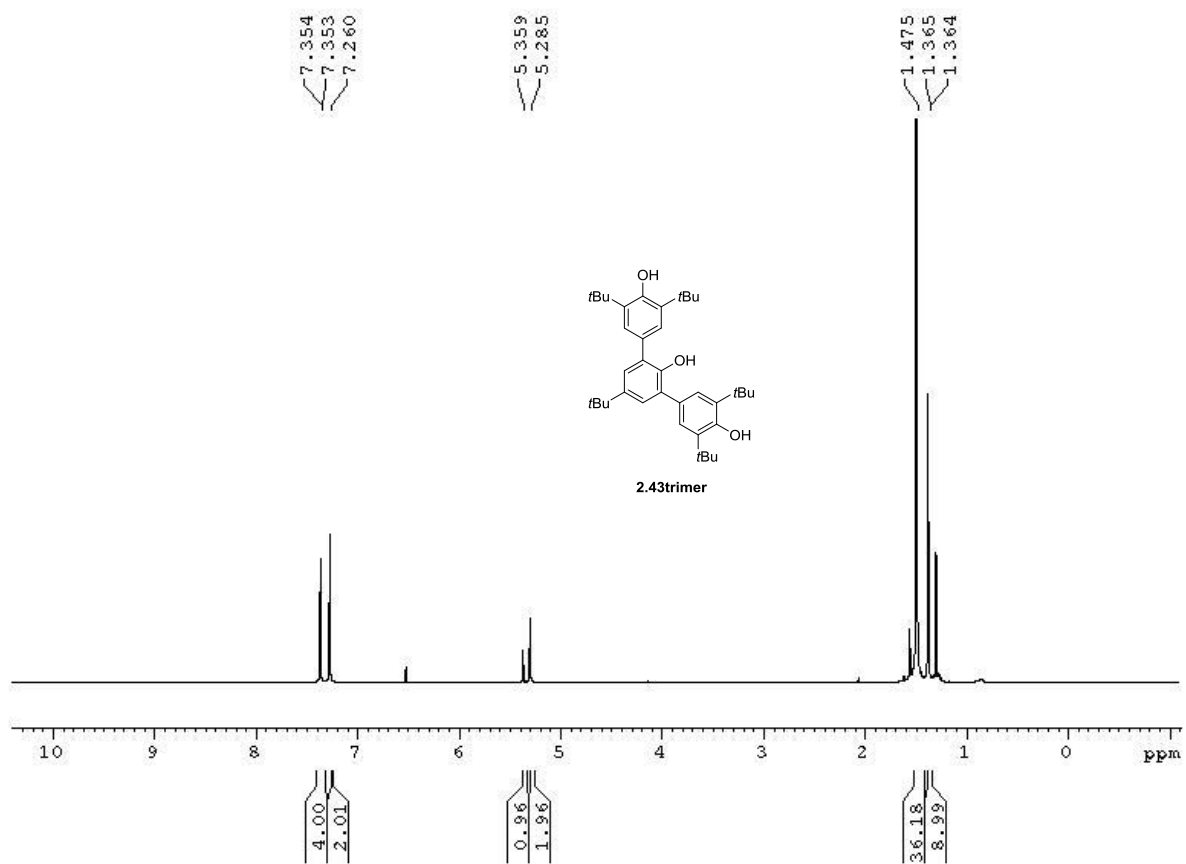
Figure A2.58 ¹H NMR spectrum of compound **2.43trimer** (500 MHz, CDCl₃)
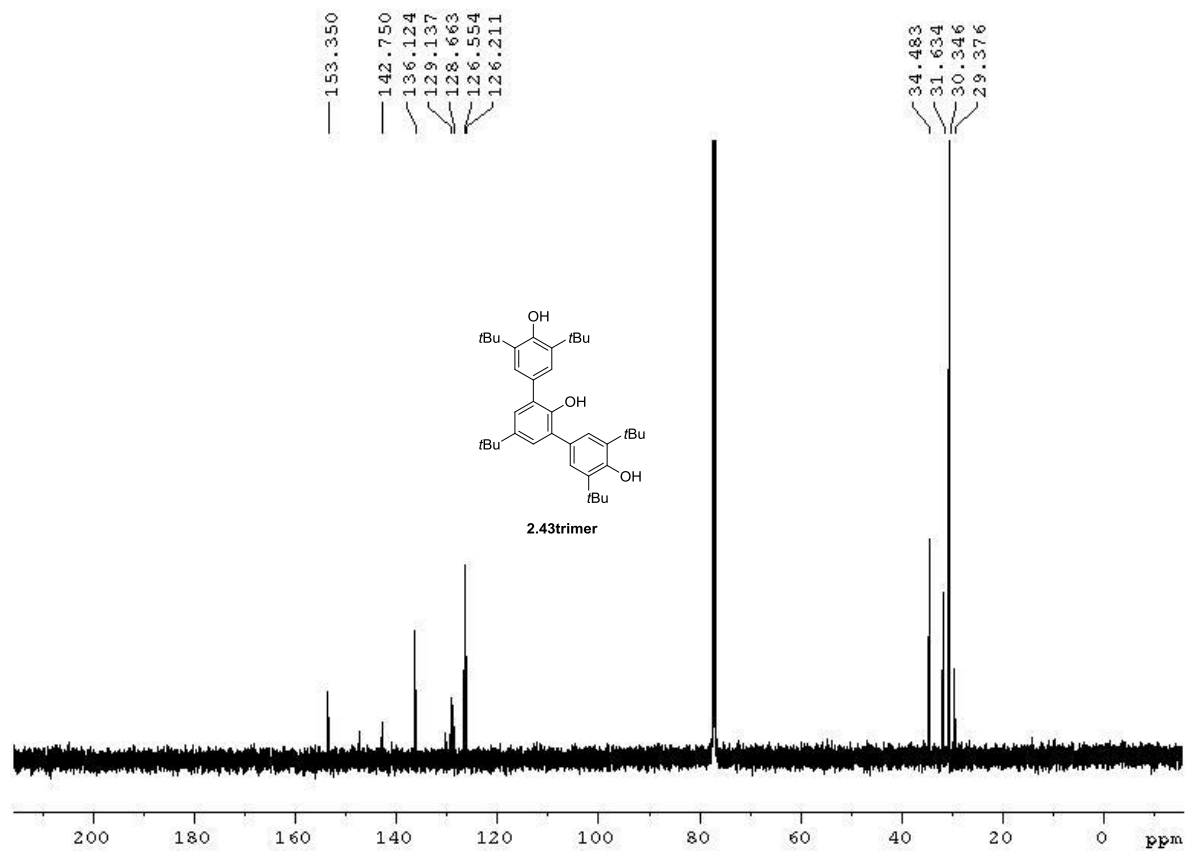
Figure A2.59 ^{13}C NMR spectrum of compound **2.43trimer** (125 MHz, CDCl$_3$)
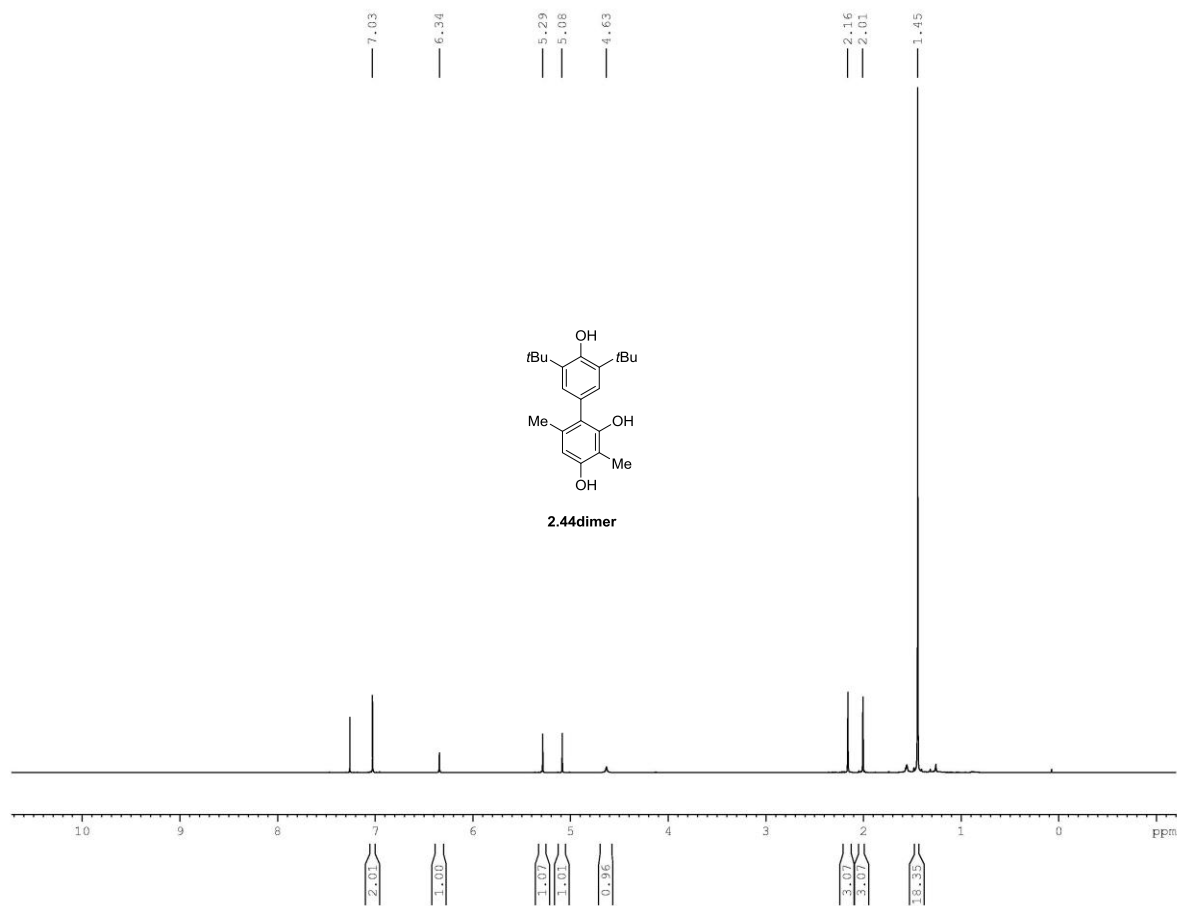
Figure A2.60 ^{1}H NMR spectrum of compound **2.44dimer** (500 MHz, CDCl$_3$)
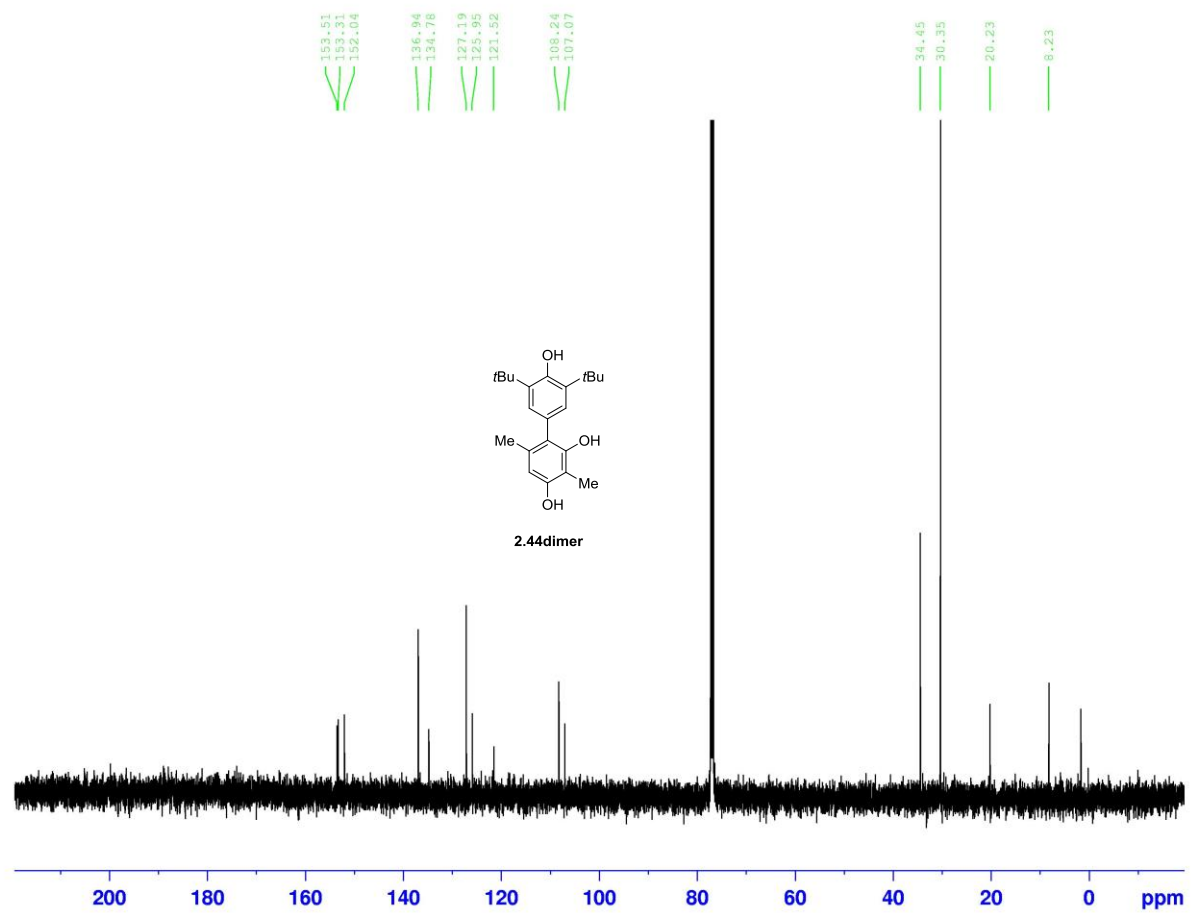
Figure A2.61 ^{13}C NMR spectrum of compound **2.44dimer** (125 MHz, CDCl$_3$)
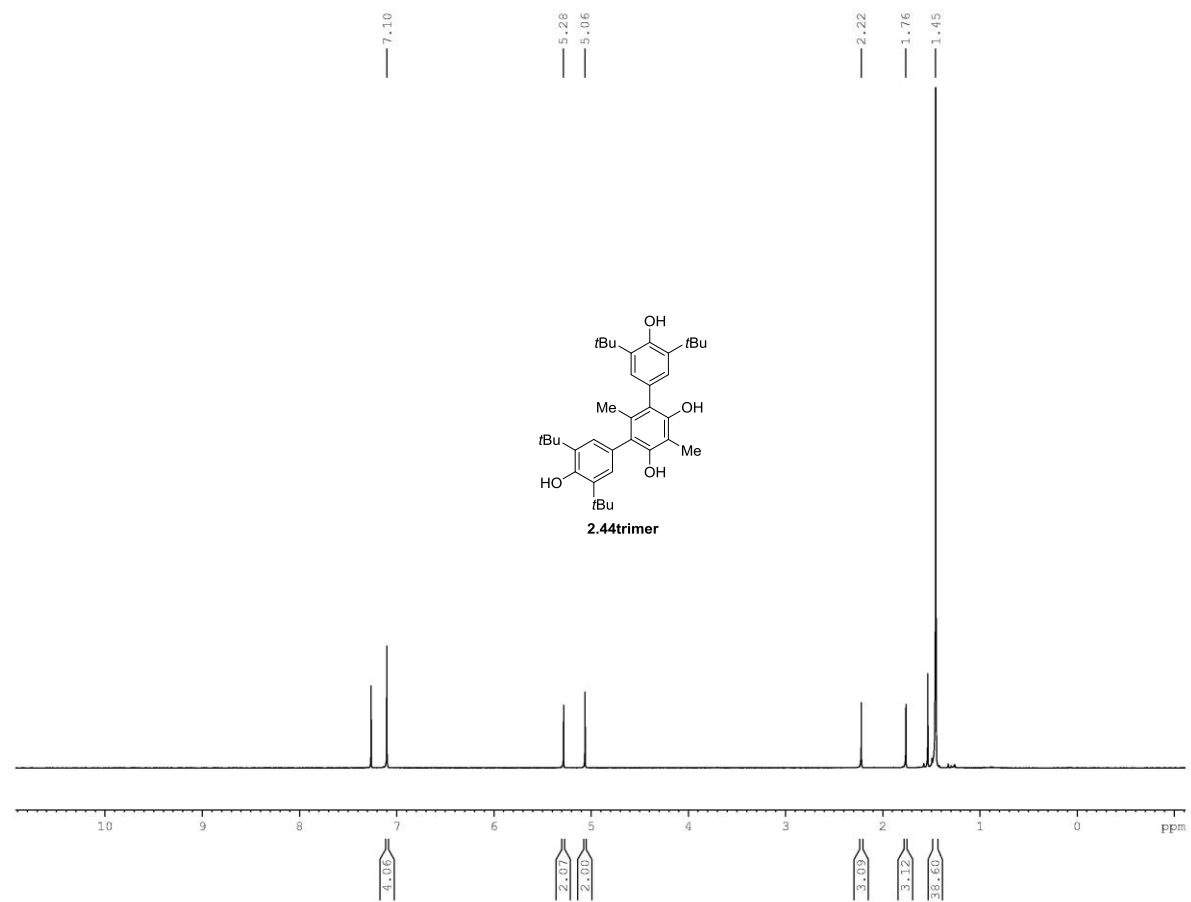
Figure A2.62 ^{1}H NMR spectrum of compound **2.44trimer** (500 MHz, CDCl$_3$)
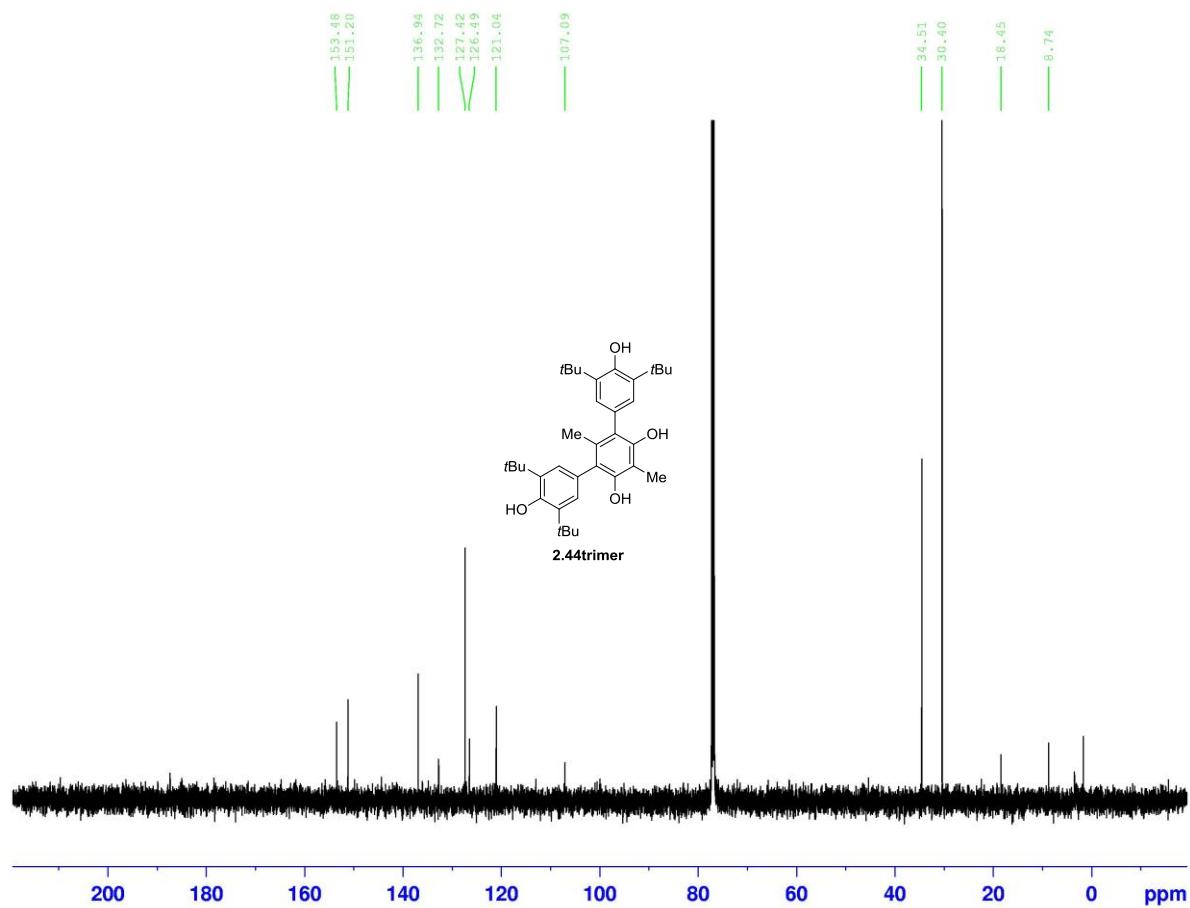
Figure A2.63 ^{13}C NMR spectrum of compound **2.44trimer** (125 MHz, CDCl$_3$)
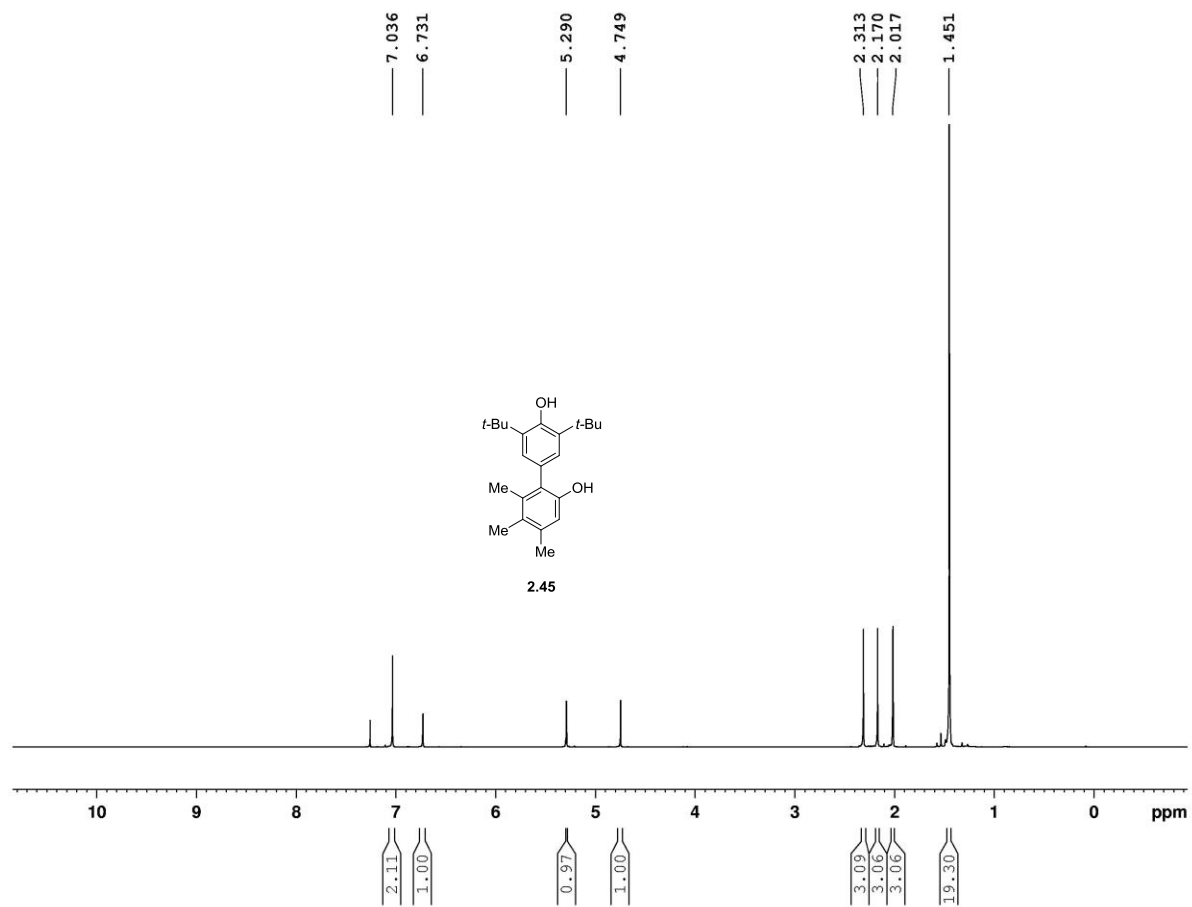
Figure A2.64 ^{1}H NMR spectrum of compound **2.45** (500 MHz, CDCl$_3$)

271
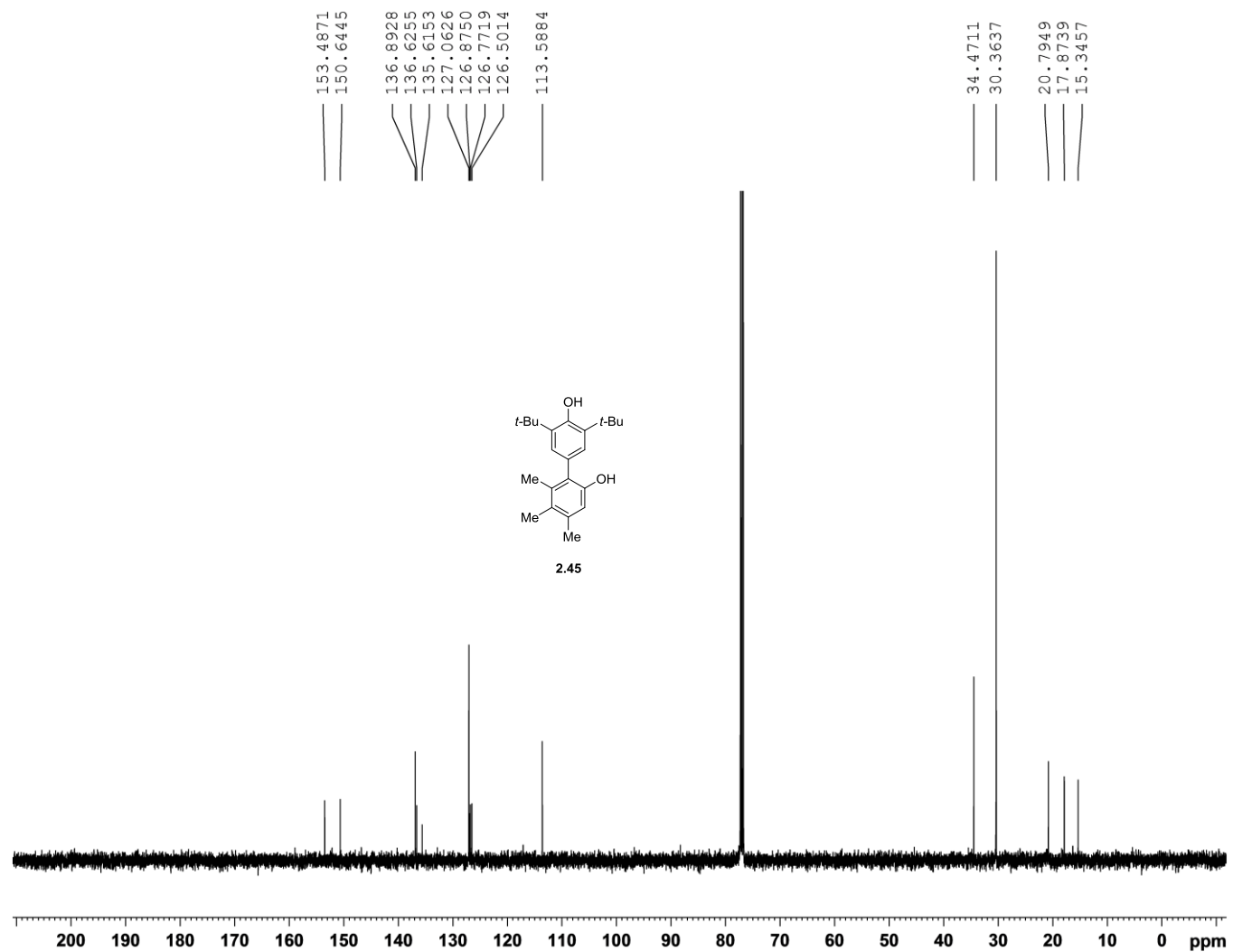
Figure A2.65 ^{13}C NMR spectrum of compound **2.45** (125 MHz, CDCl$_3$)
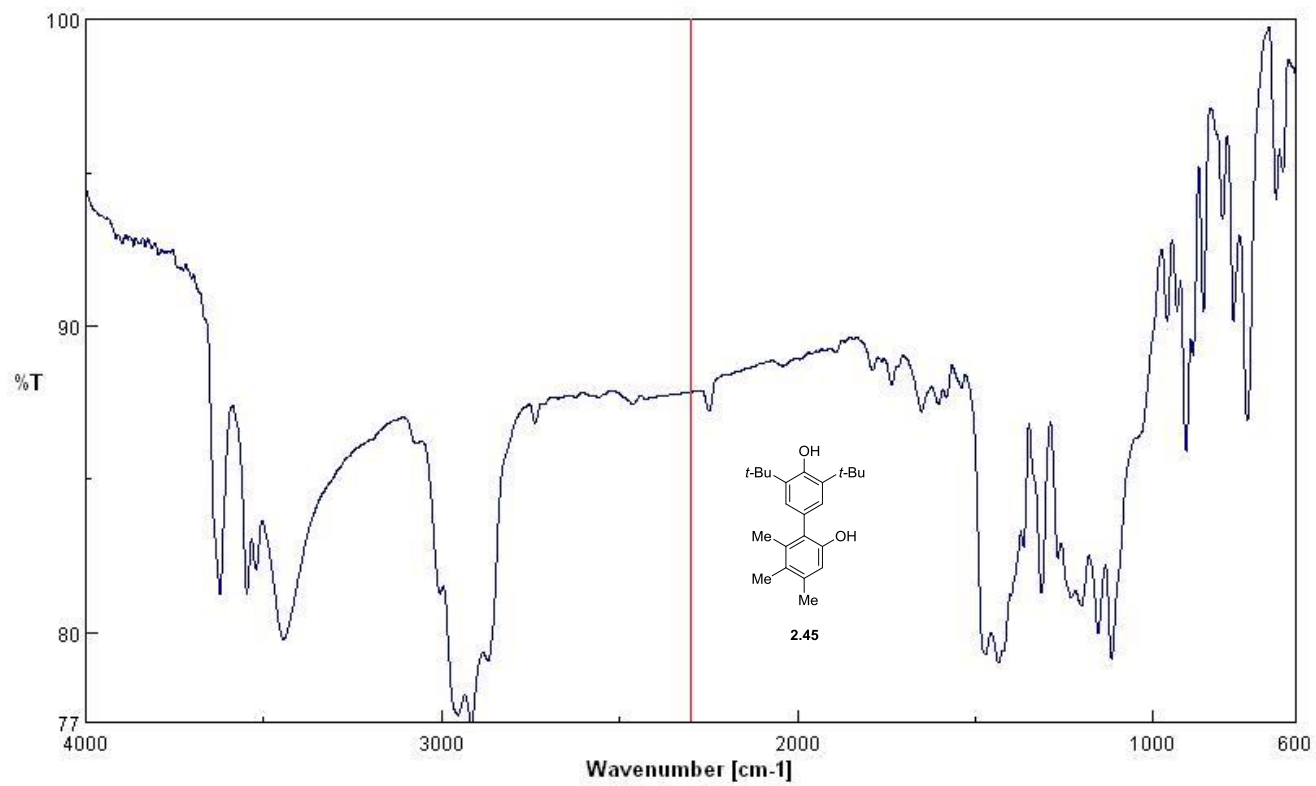
Figure A2.66 IR Spectrum of compound **2.45**
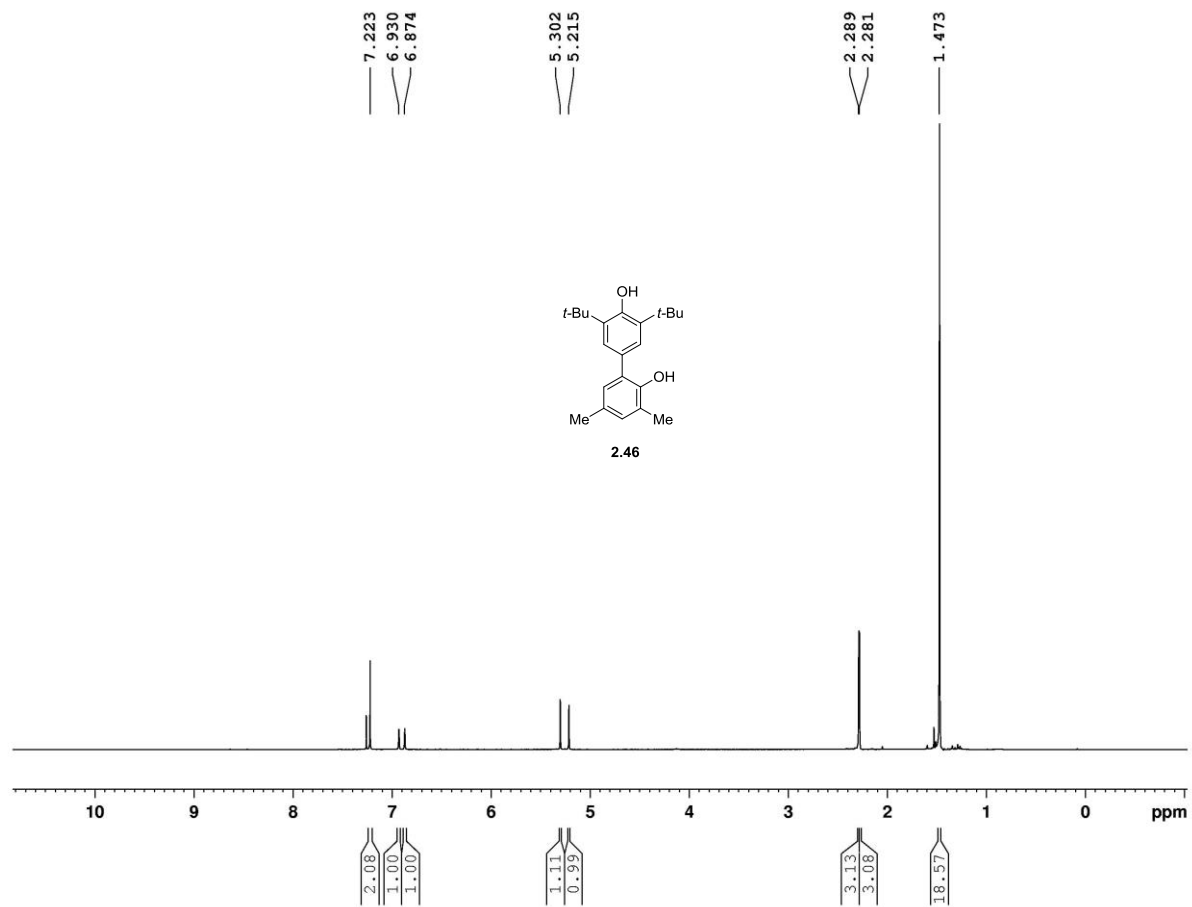
Figure A2.67 ^{1}H NMR spectrum of compound **2.46** (500 MHz, CDCl$_3$)

274
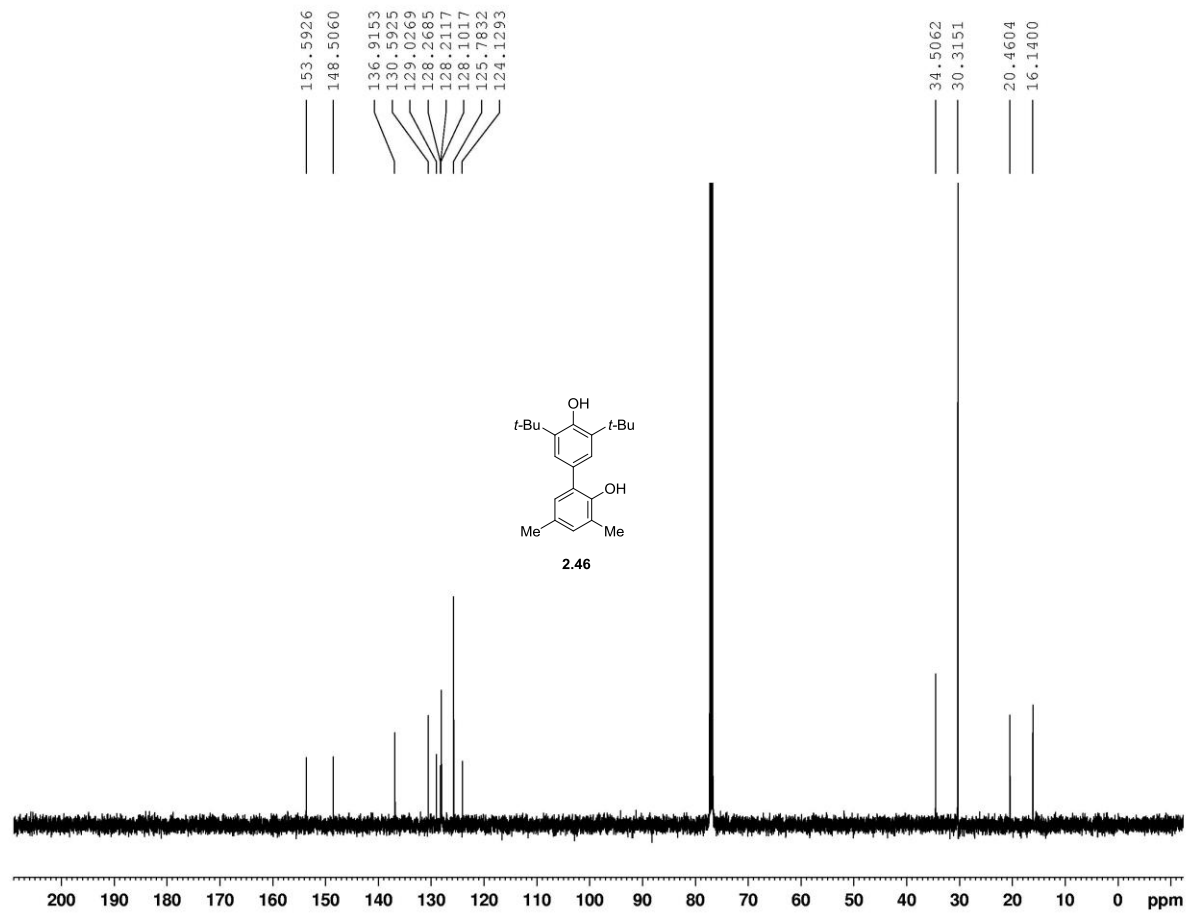
Figure A2.68 ^{13}C NMR spectrum of compound **2.46** (125 MHz, CDCl$_3$)
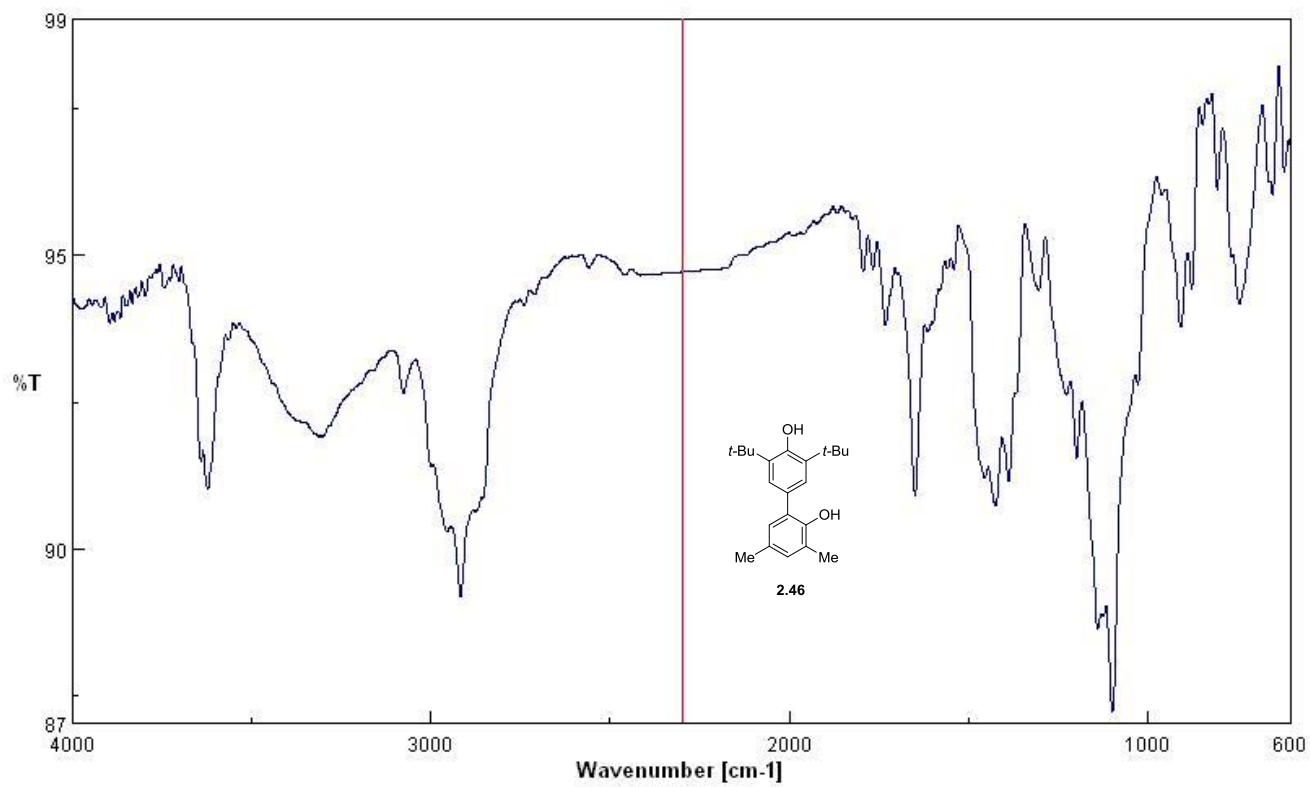
Figure A2.69 IR Spectrum of compound **2.46**
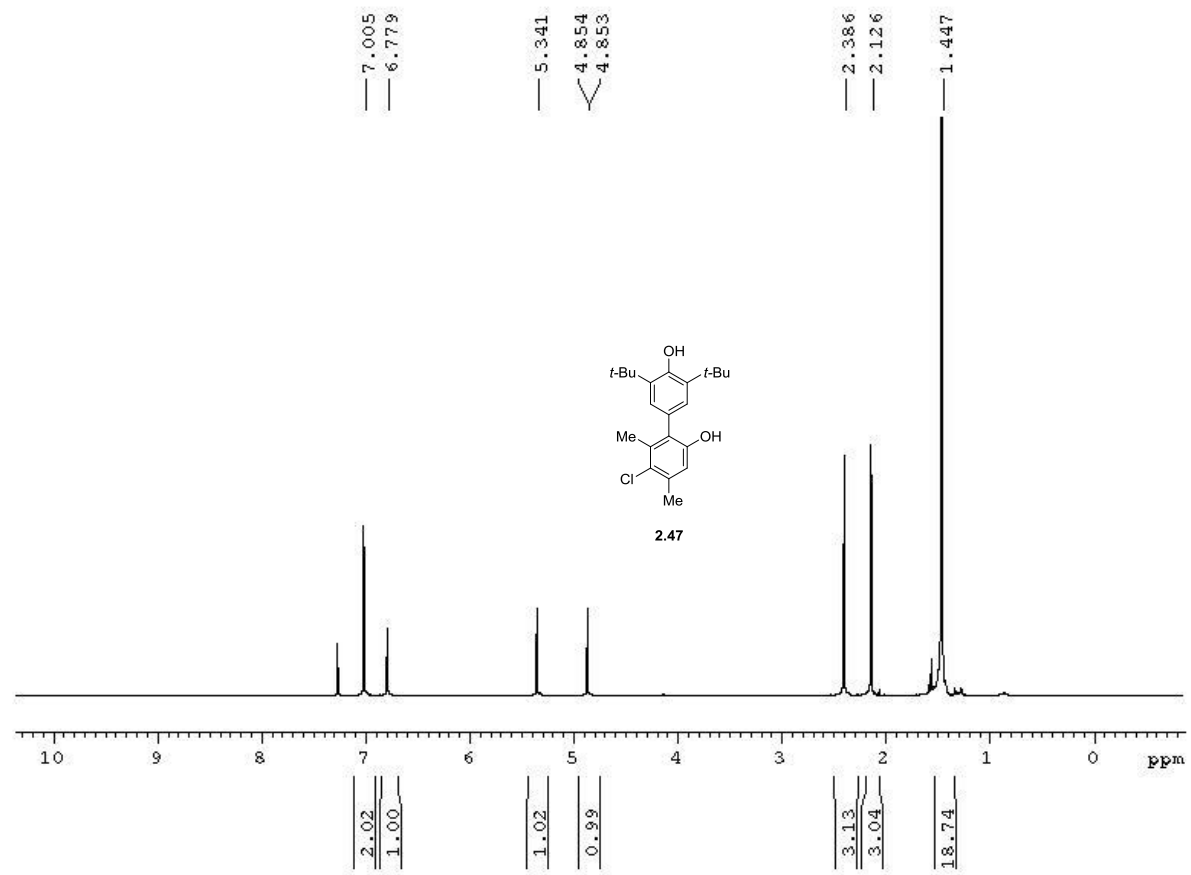
Figure A2.70 ^{1}H NMR spectrum of compound **2.47** (500 MHz, CDCl$_3$)
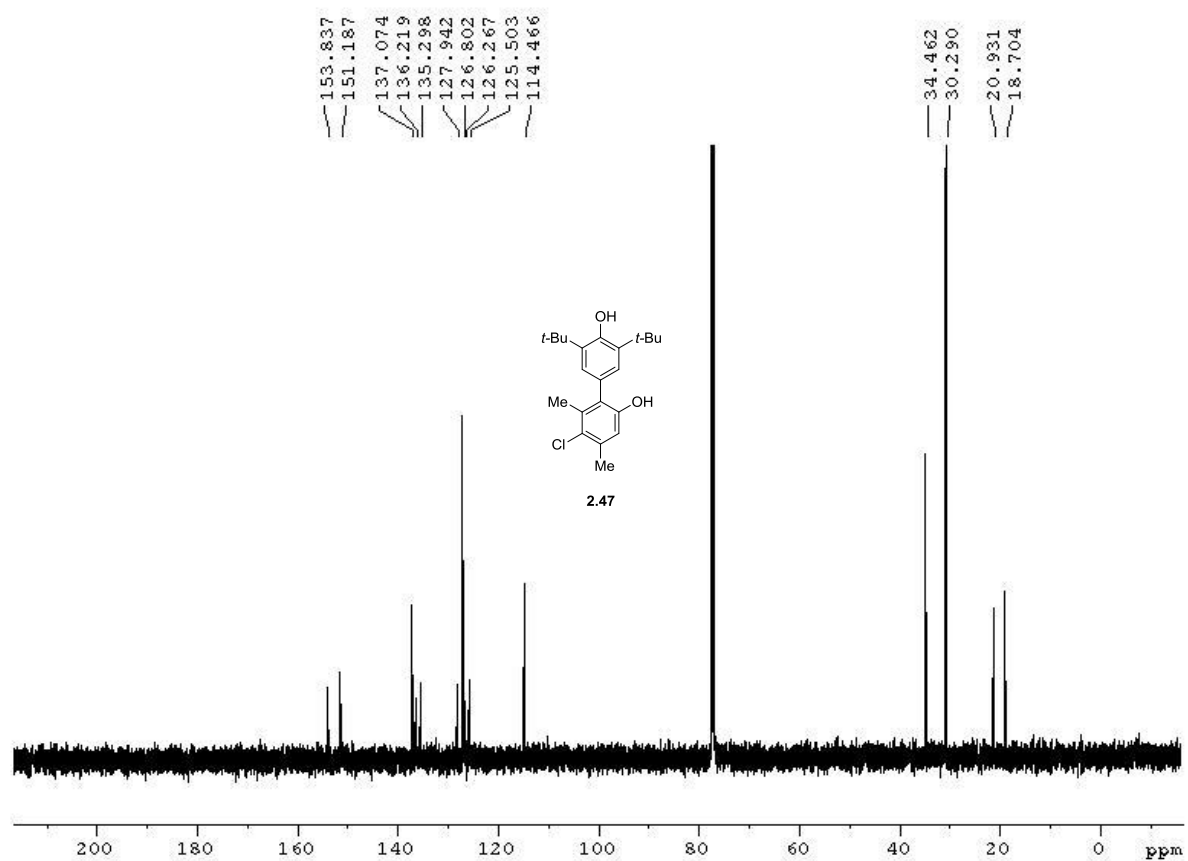
Figure A2.71 ^{13}C NMR spectrum of compound **2.47** (125 MHz, CDCl$_3$)
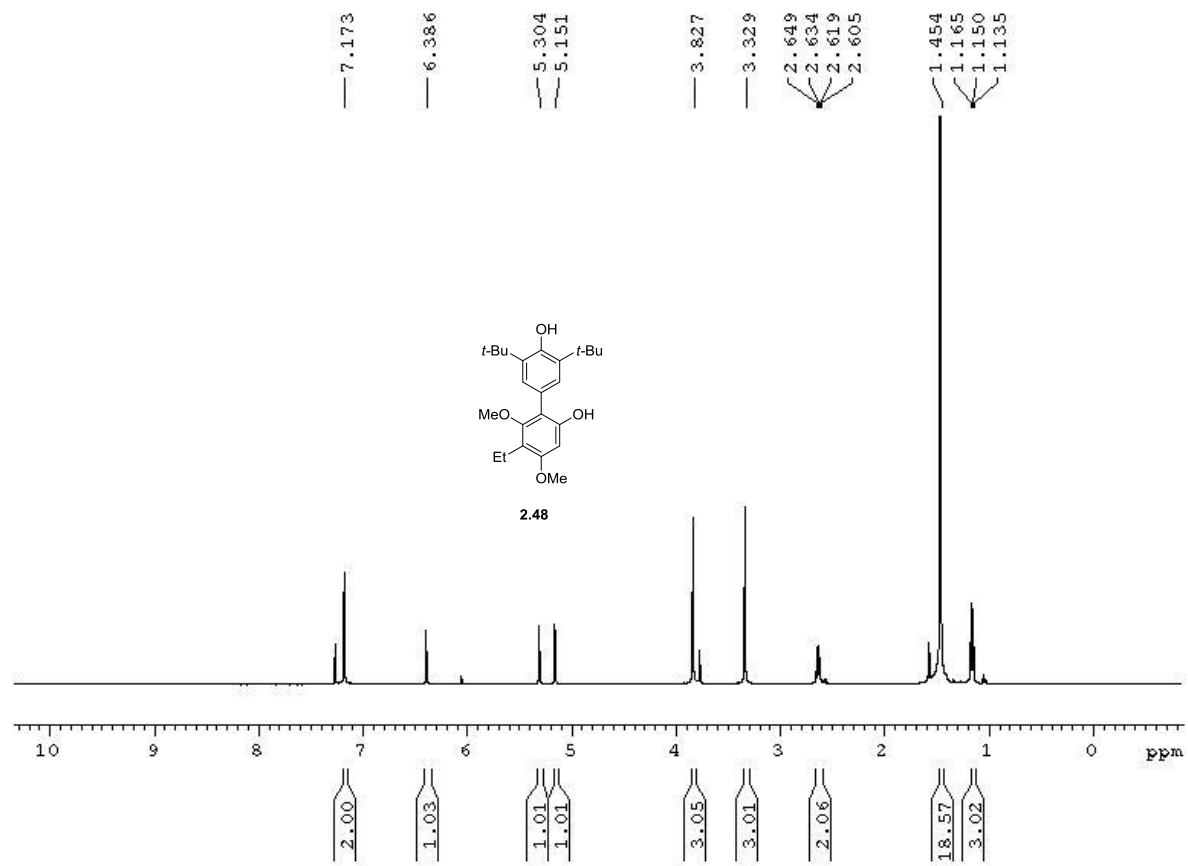
Figure A2.72 ^{13}C NMR spectrum of compound **2.48** (125 MHz, CDCl$_3$)
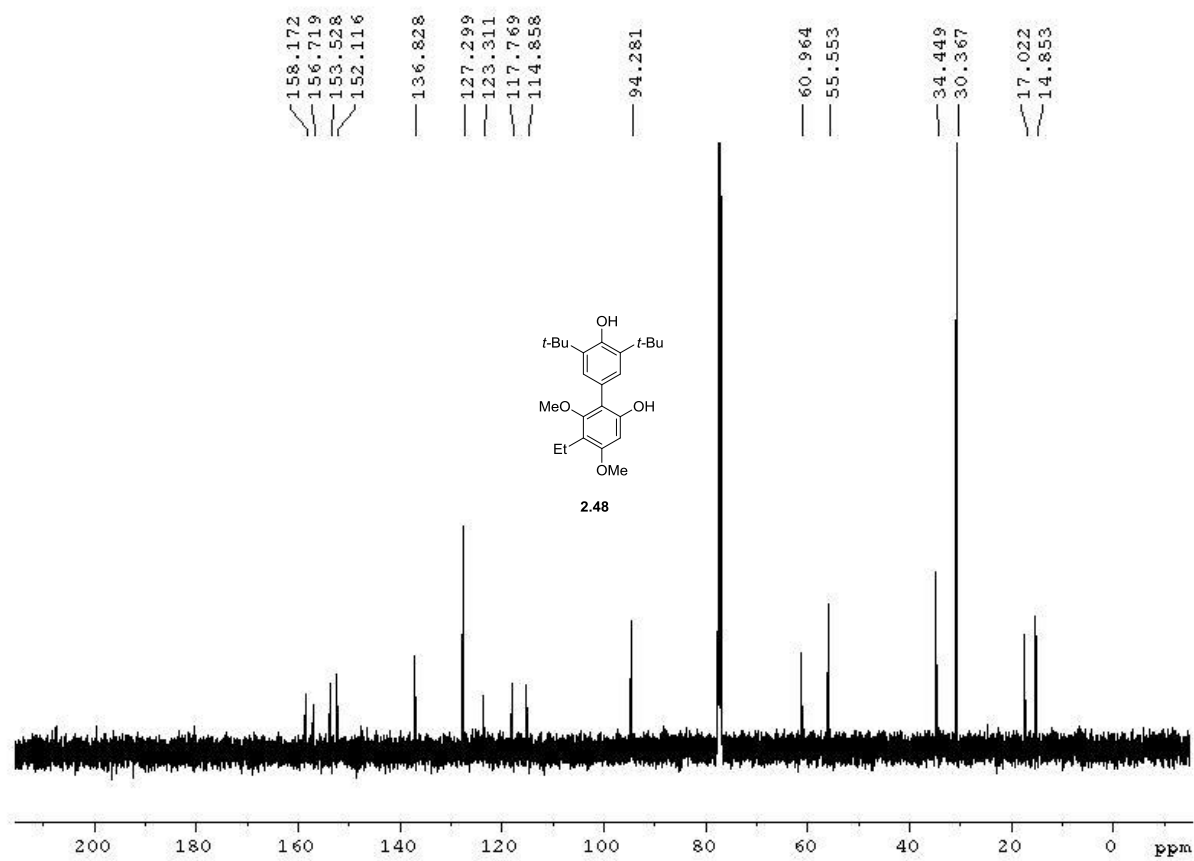
Figure A2.73 ^{13}C NMR spectrum of compound **2.48** (125 MHz, CDCl$_3$)
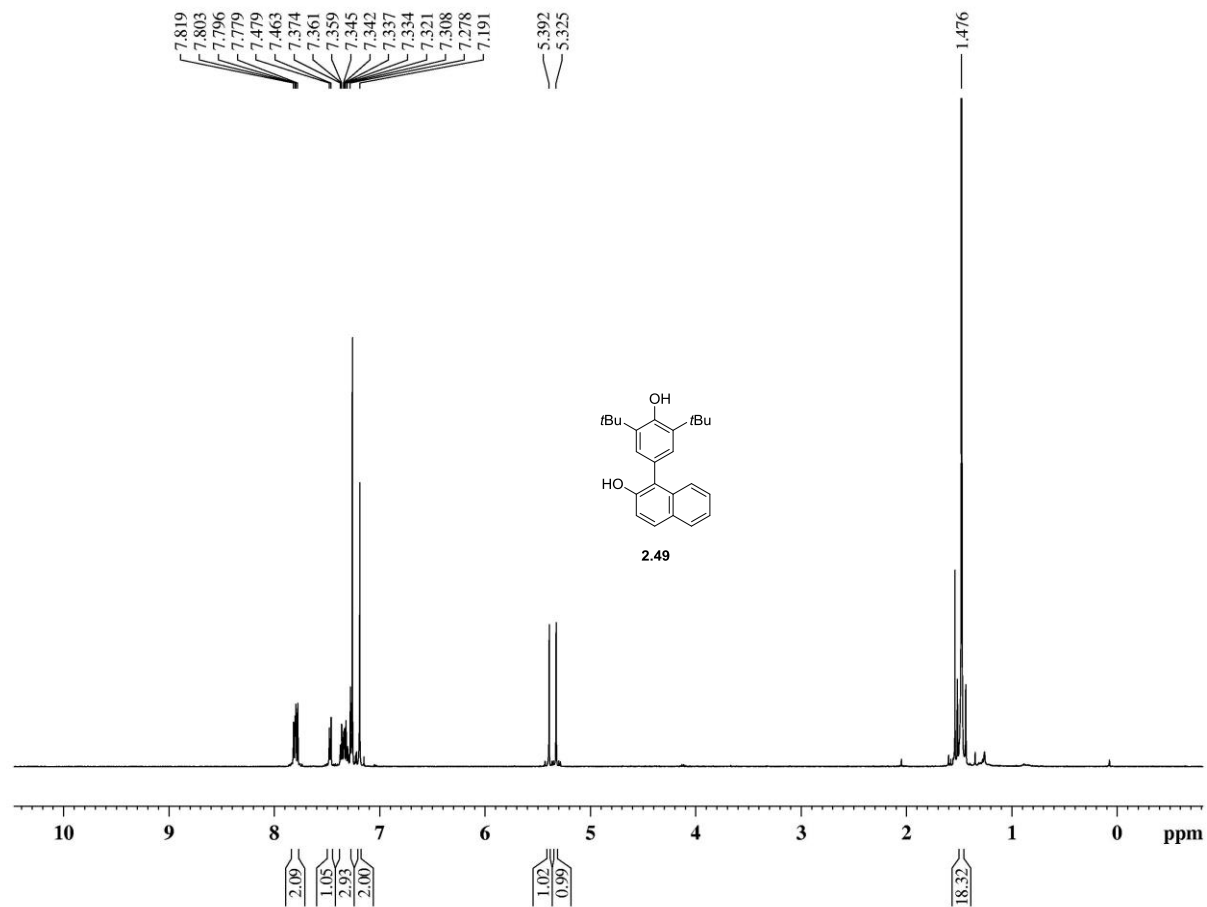
Figure A2.74 ^{1}H NMR spectrum of compound **2.49** (500 MHz, CDCl$_3$)
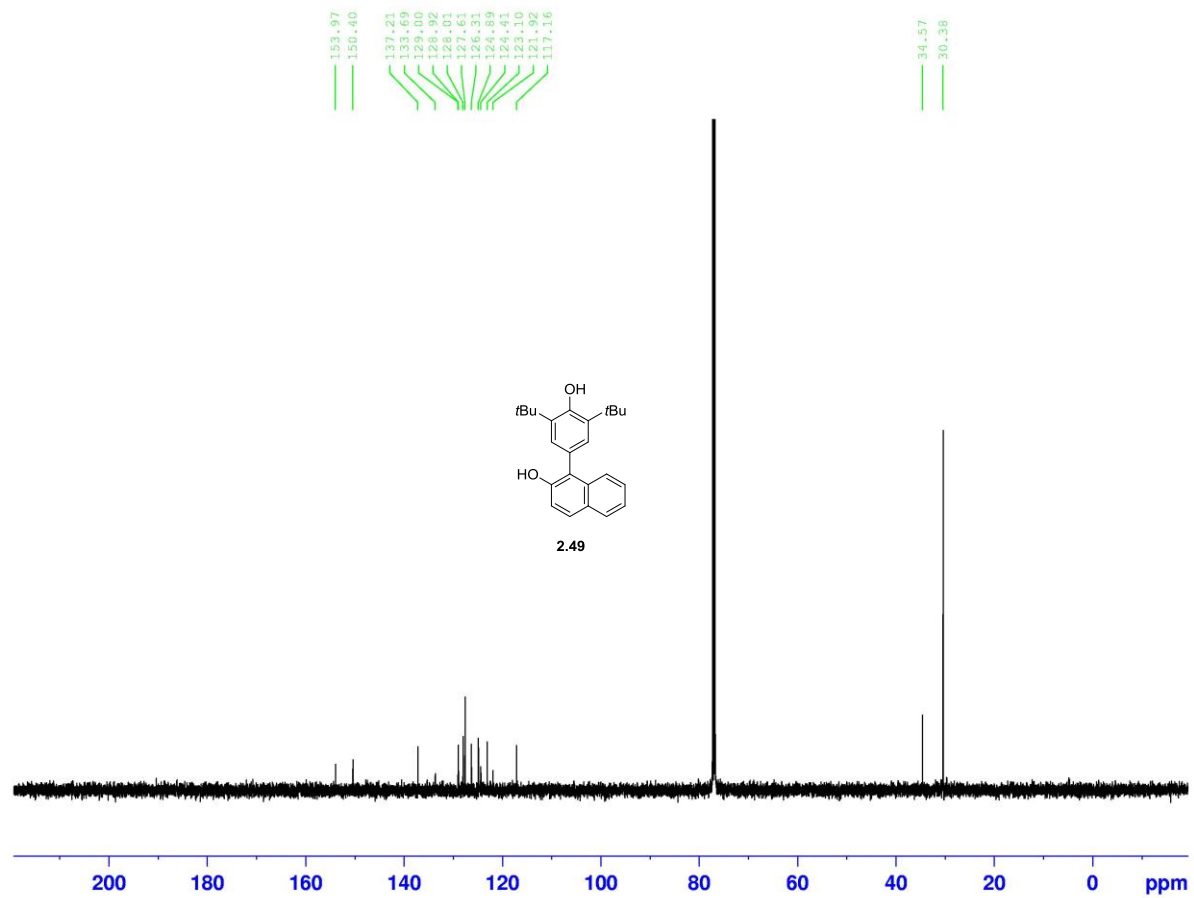
Figure A2.75 ^{13}C NMR spectrum of compound **2.49** (125 MHz, CDCl$_3$)
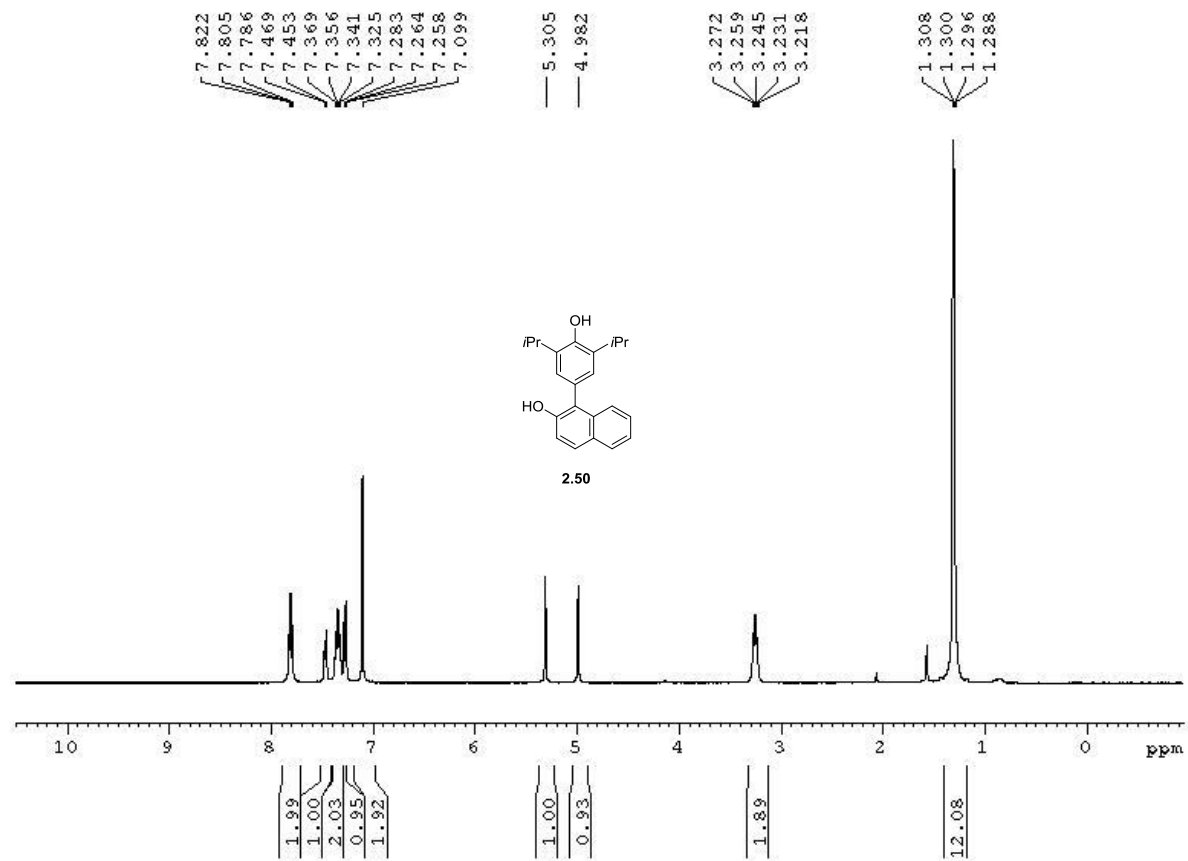
Figure A2.76 ^{1}H NMR spectrum of compound **2.50** (500 MHz, CDCl₃)
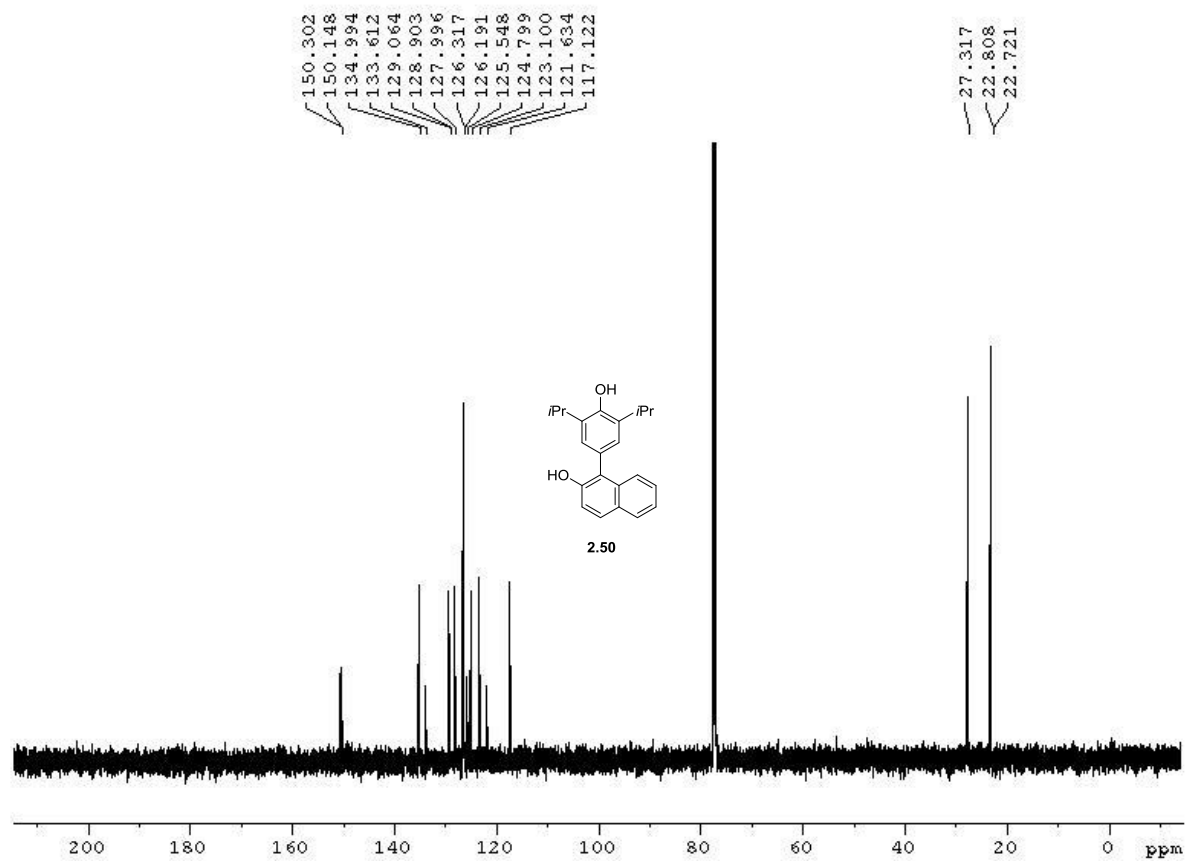
Figure A2.77 ^{13}C NMR spectrum of compound **2.50** (125 MHz, CDCl$_3$)
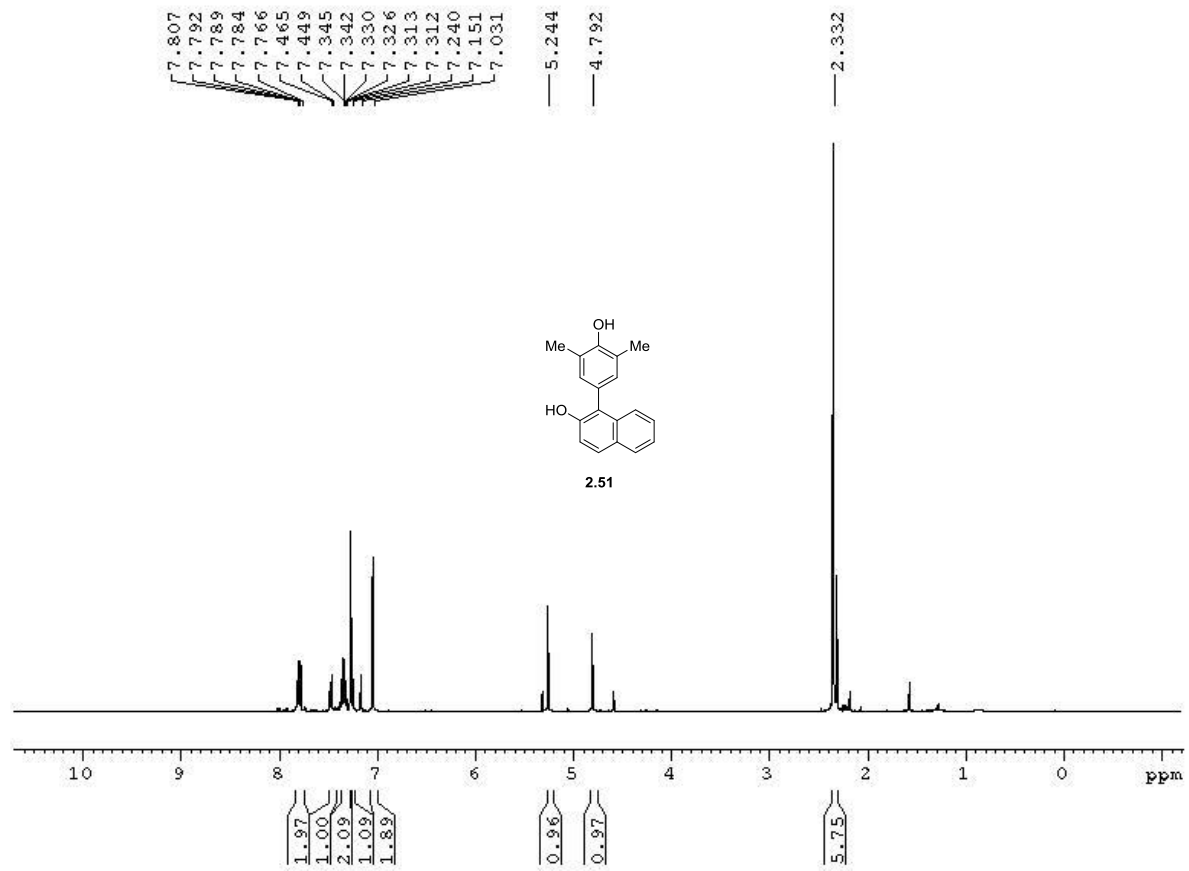
Figure A2.78 ^{1}H NMR spectrum of compound **2.51** (500 MHz, CDCl$_3$)
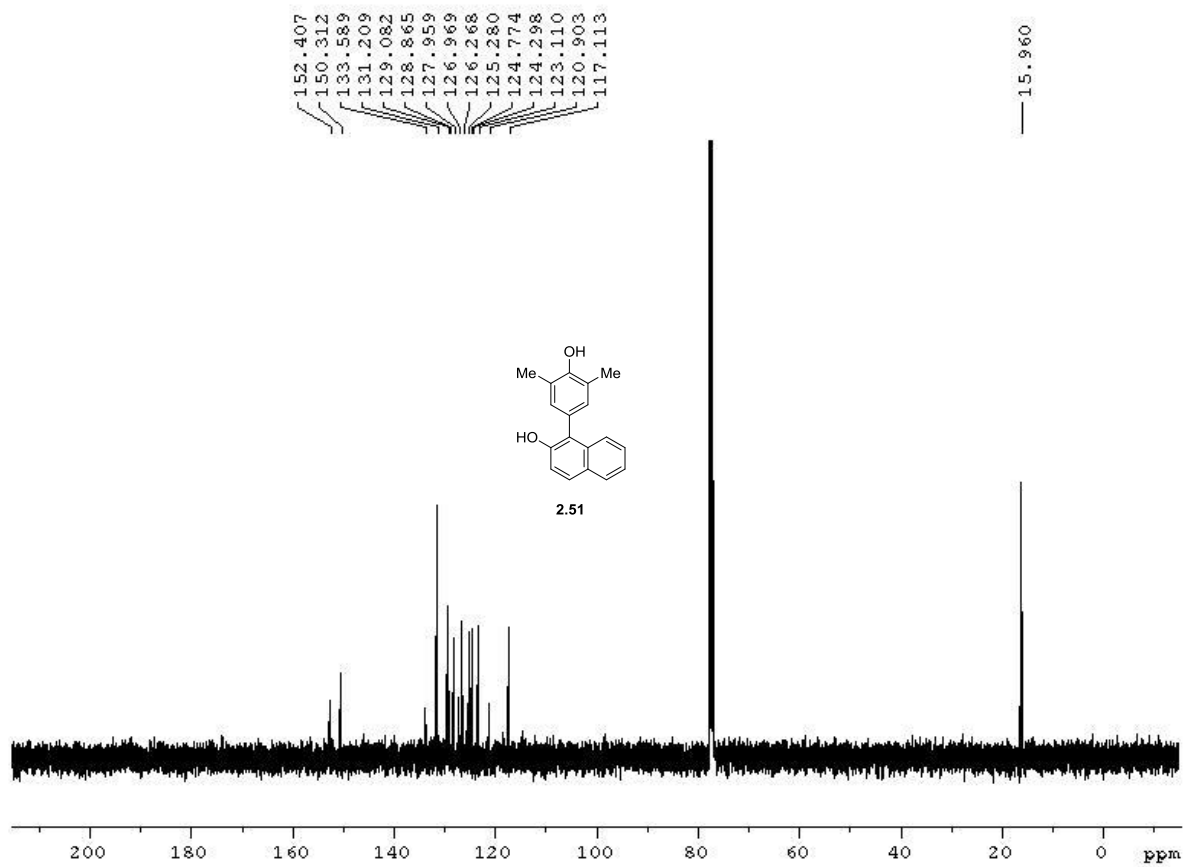
Figure A2.79 ^{13}C NMR spectrum of compound **2.51** (125 MHz, CDCl$_3$)
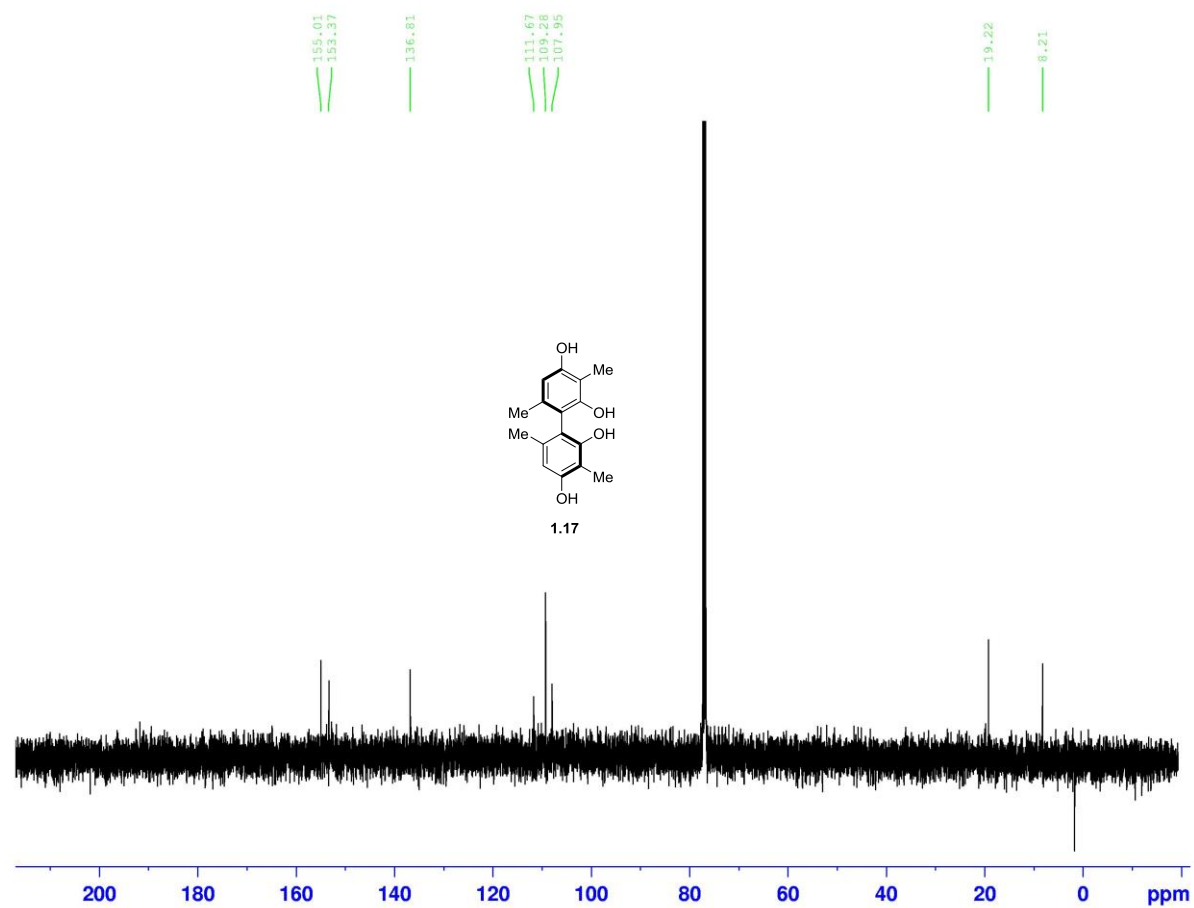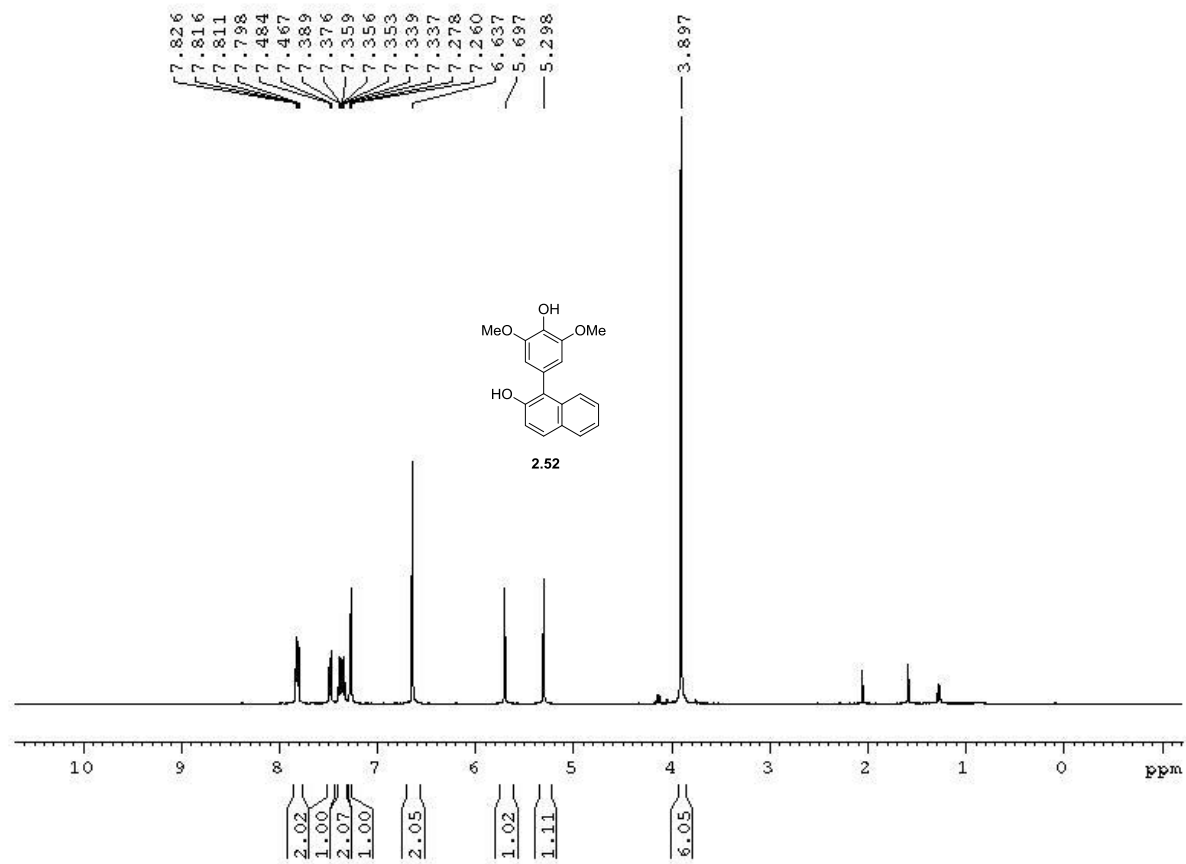
Figure A2.80 ^{1}H NMR spectrum of compound **2.52** (500 MHz, CDCl$_3$)
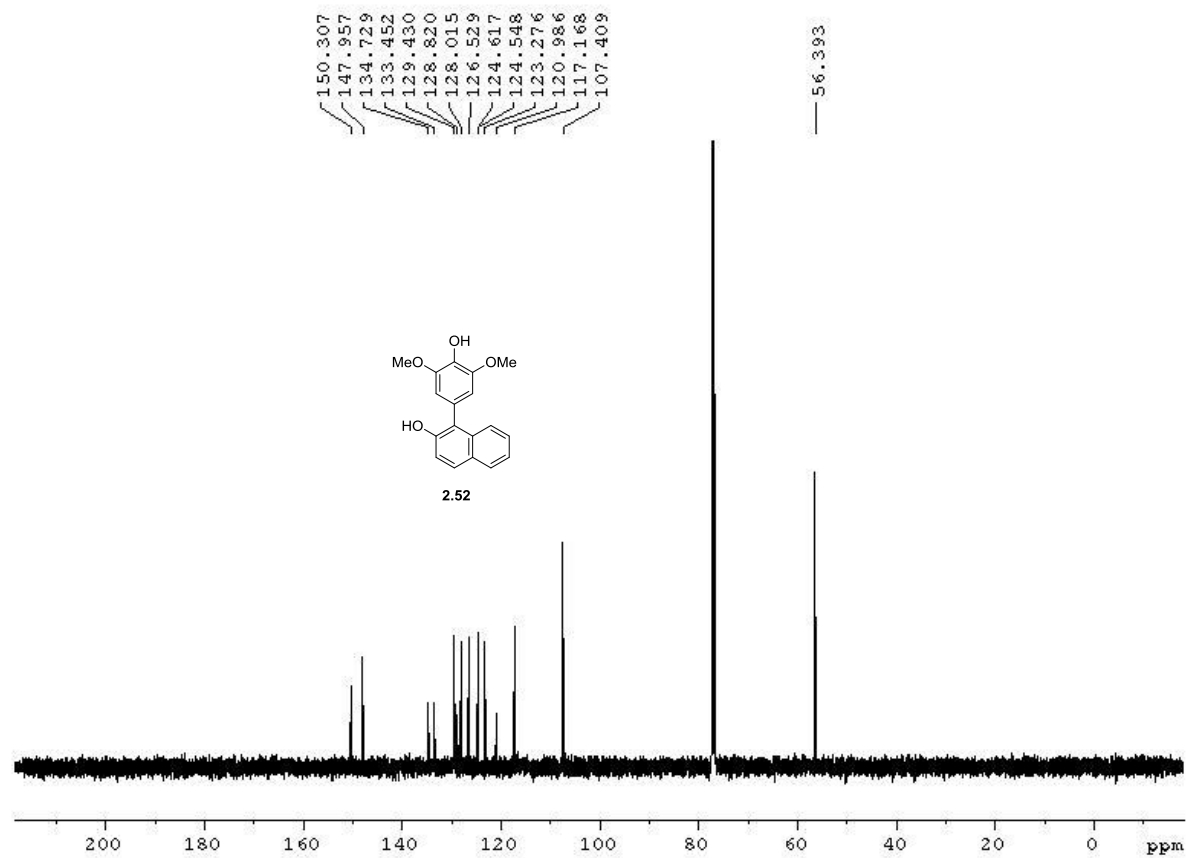
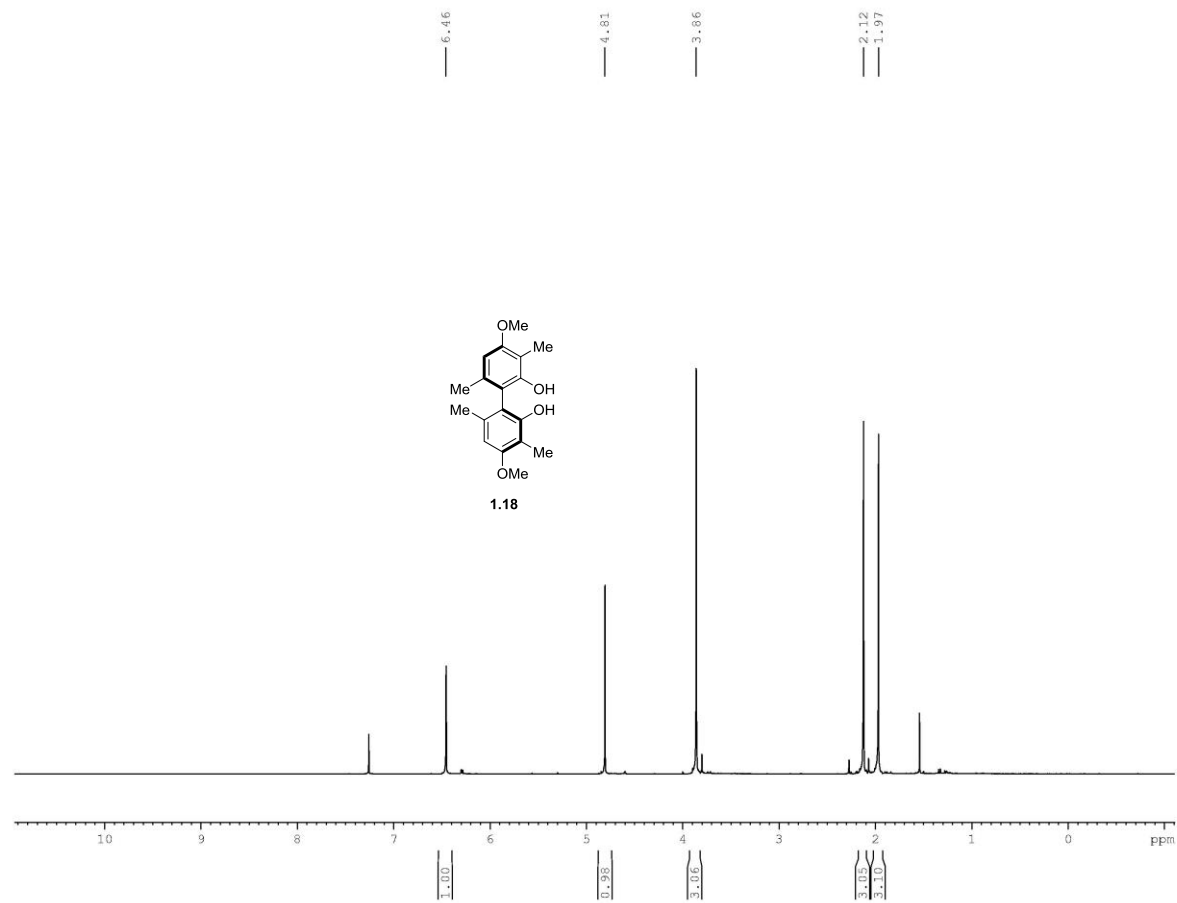**Figure A2.81** ^{13}C NMR spectrum of compound **2.52** (125 MHz, CDCl$_3$)
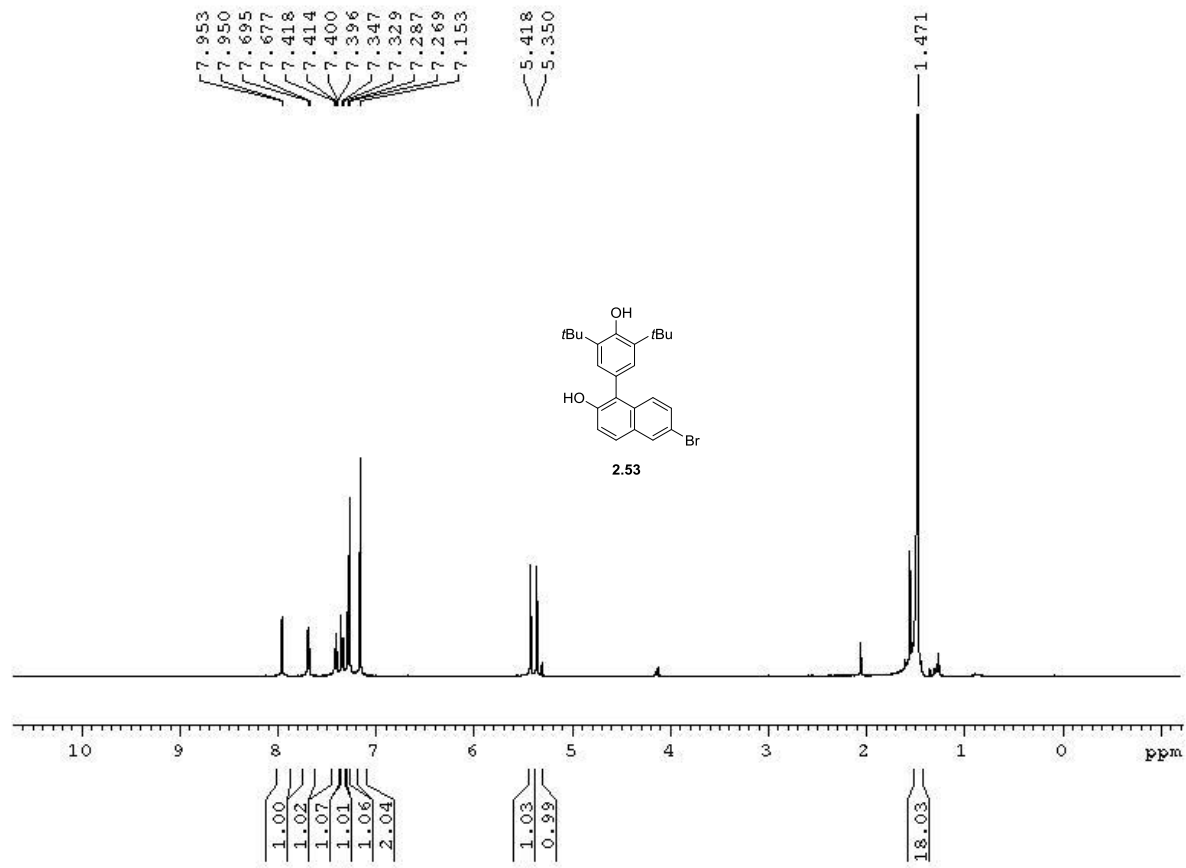
Figure A2.82 ^{1}H NMR spectrum of compound **2.53** (500 MHz, CDCl$_3$)
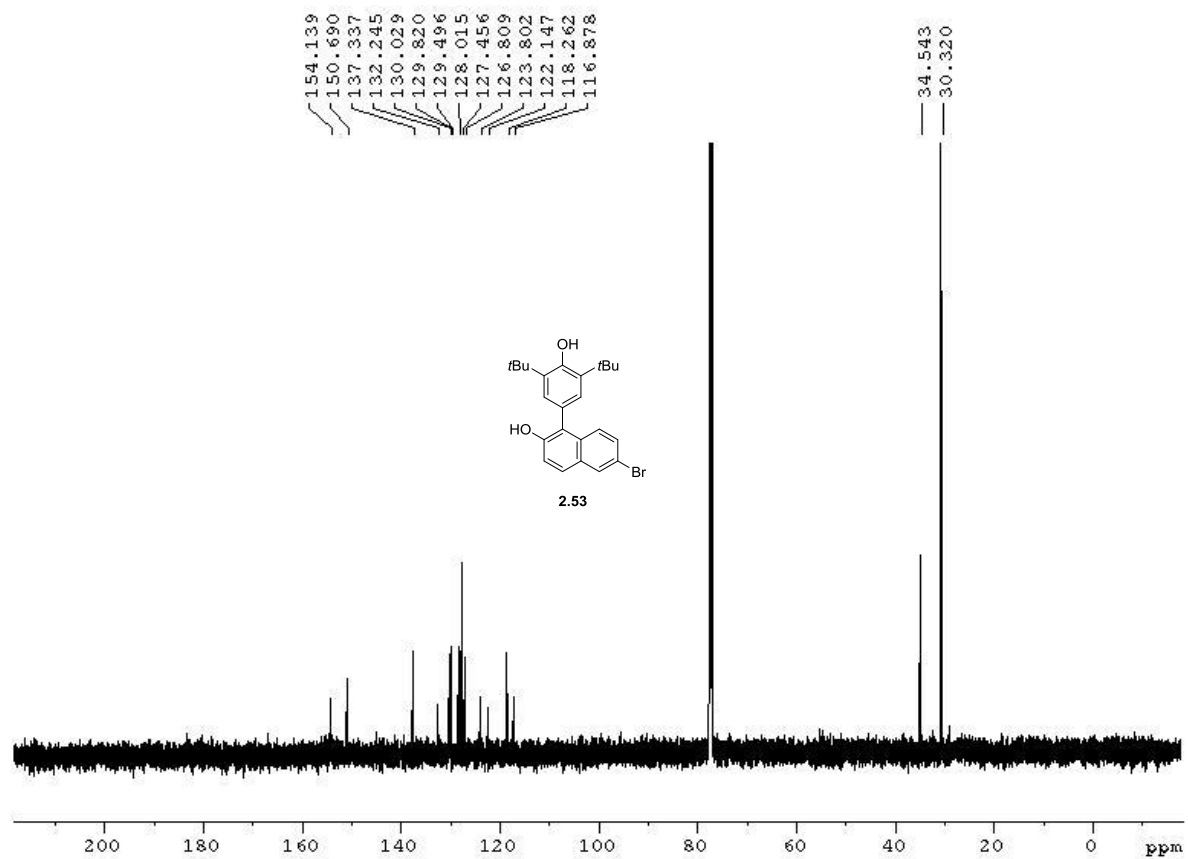
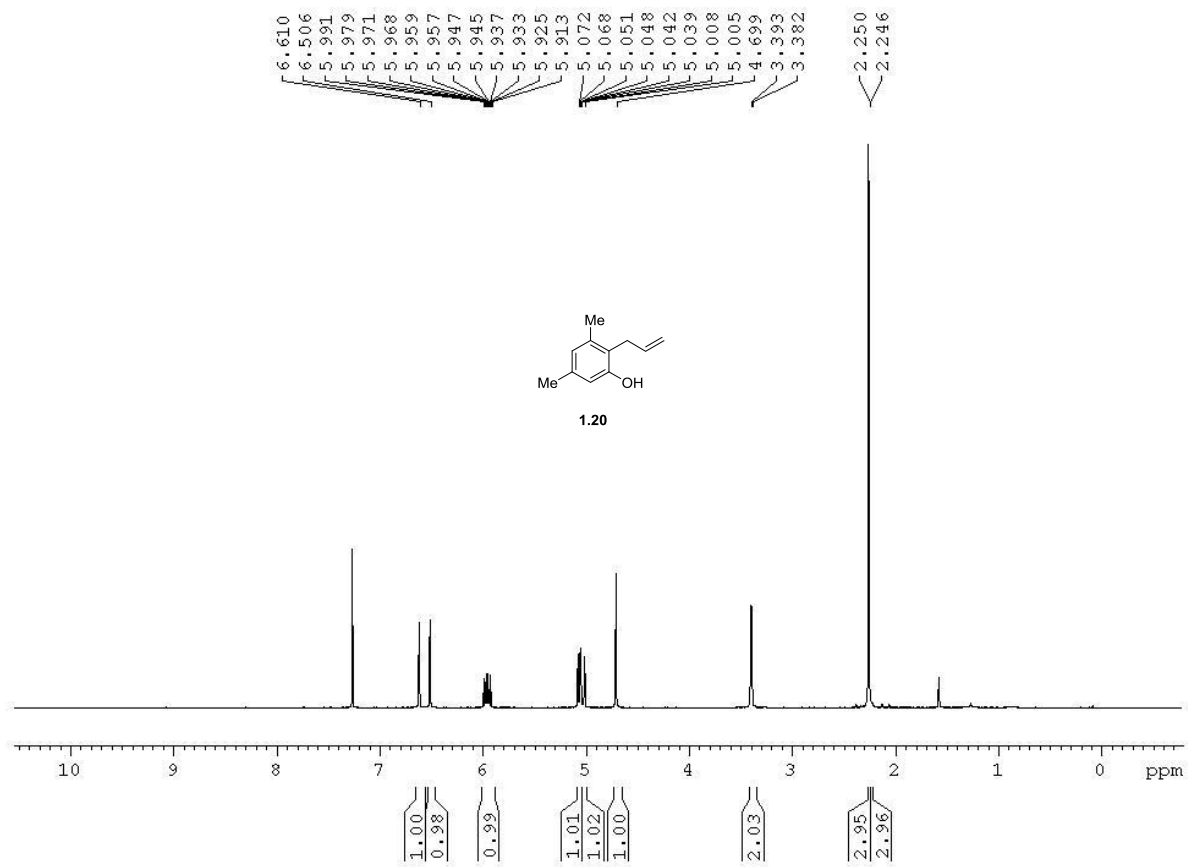**Figure A2.83** ^{13}C NMR spectrum of compound **2.53** (125 MHz, CDCl₃)
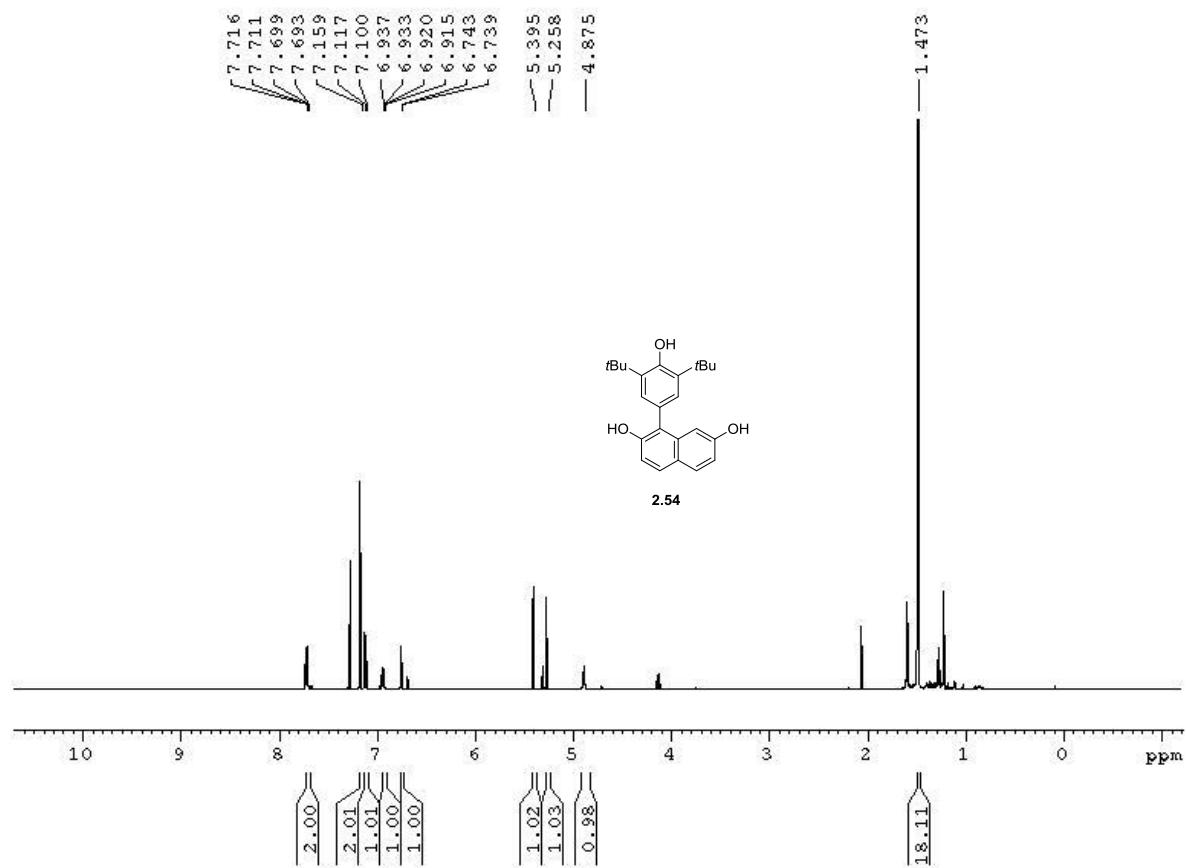
Figure A2.84 ^{1}H NMR spectrum of compound **2.54** (500 MHz, CDCl$_3$)

153.975
151.109
137.278
135.181
130.001
128.879
127.545
124.451
124.343
120.725
114.776
114.647
107.104

34.535
30.357

2.54

200   180   160   140   120   100   80   60   40   20   0   ppm
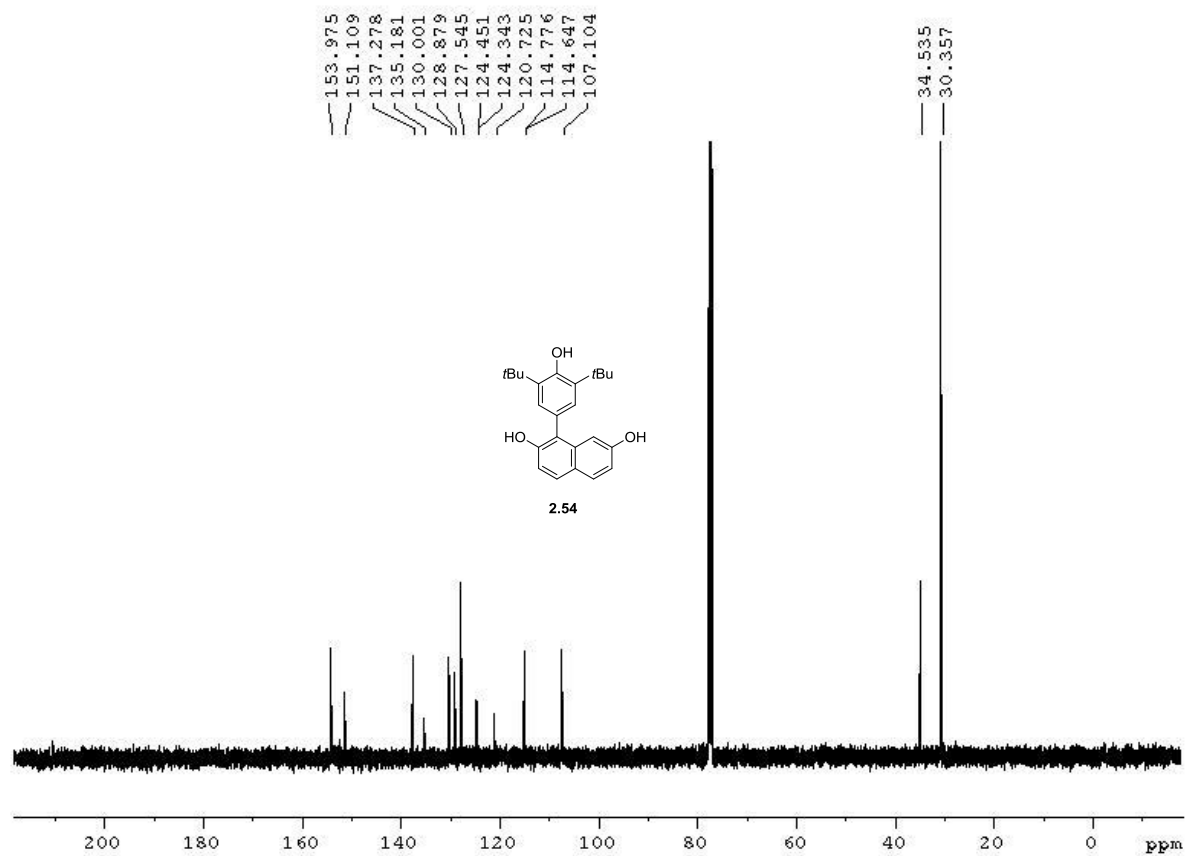
Figure A2.85 ^{13}C NMR spectrum of compound **2.54** (125 MHz, CDCl$_3$)
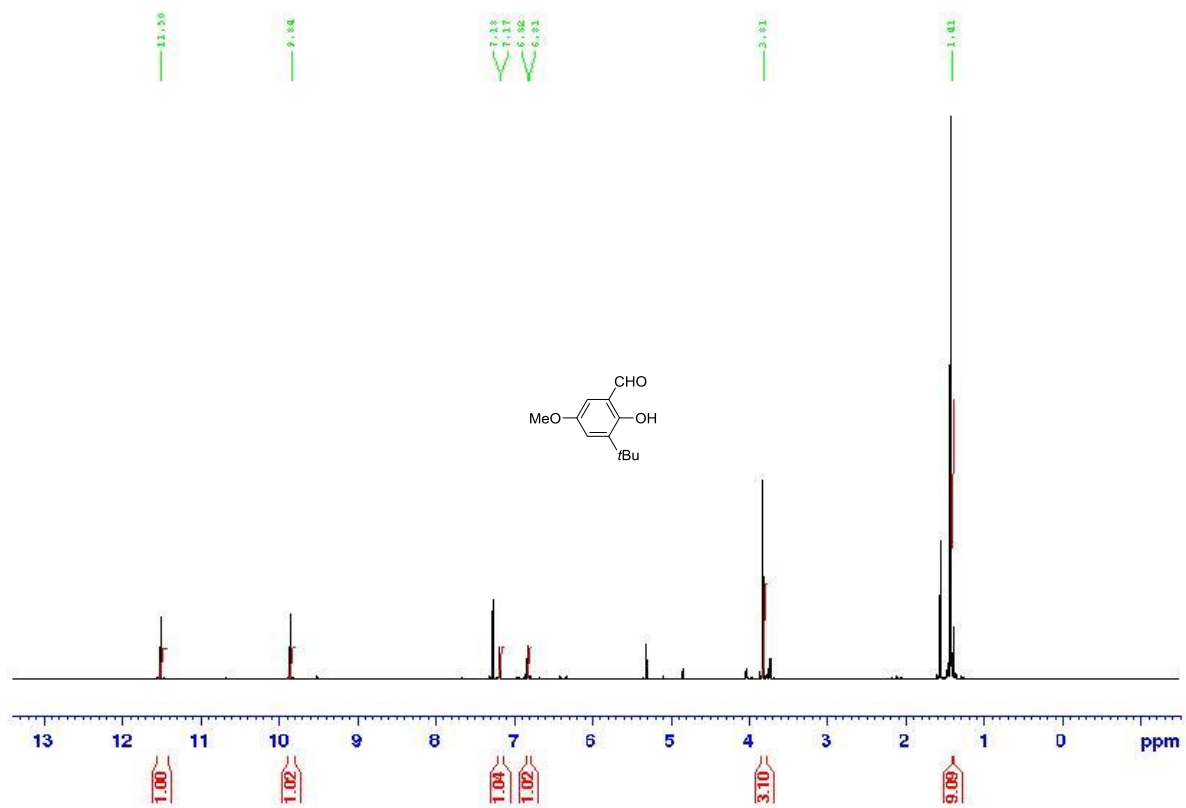
Figure A2.86 ^{1}H NMR spectrum of compound **3-(*tert*-butyl)-2-hydroxy-5-methoxyaldehyde** (500 MHz, CDCl$_3$)

Figure A3.1 ^{1}H NMR spectrum of compound **3.1** (500 MHz, CDCl3)
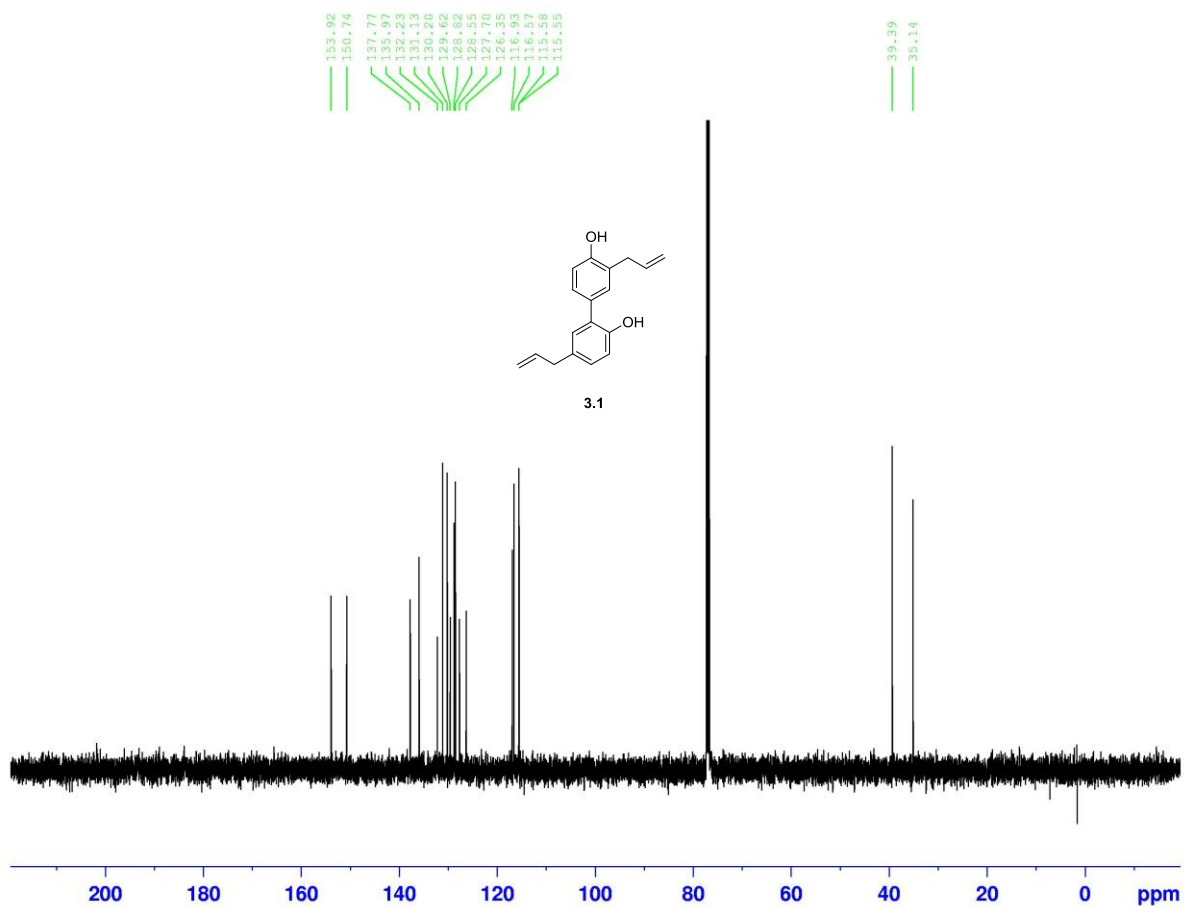
Figure A3.2 ^{13}C NMR spectrum of compound **3.1** (125 MHz, CDCl$_3$)
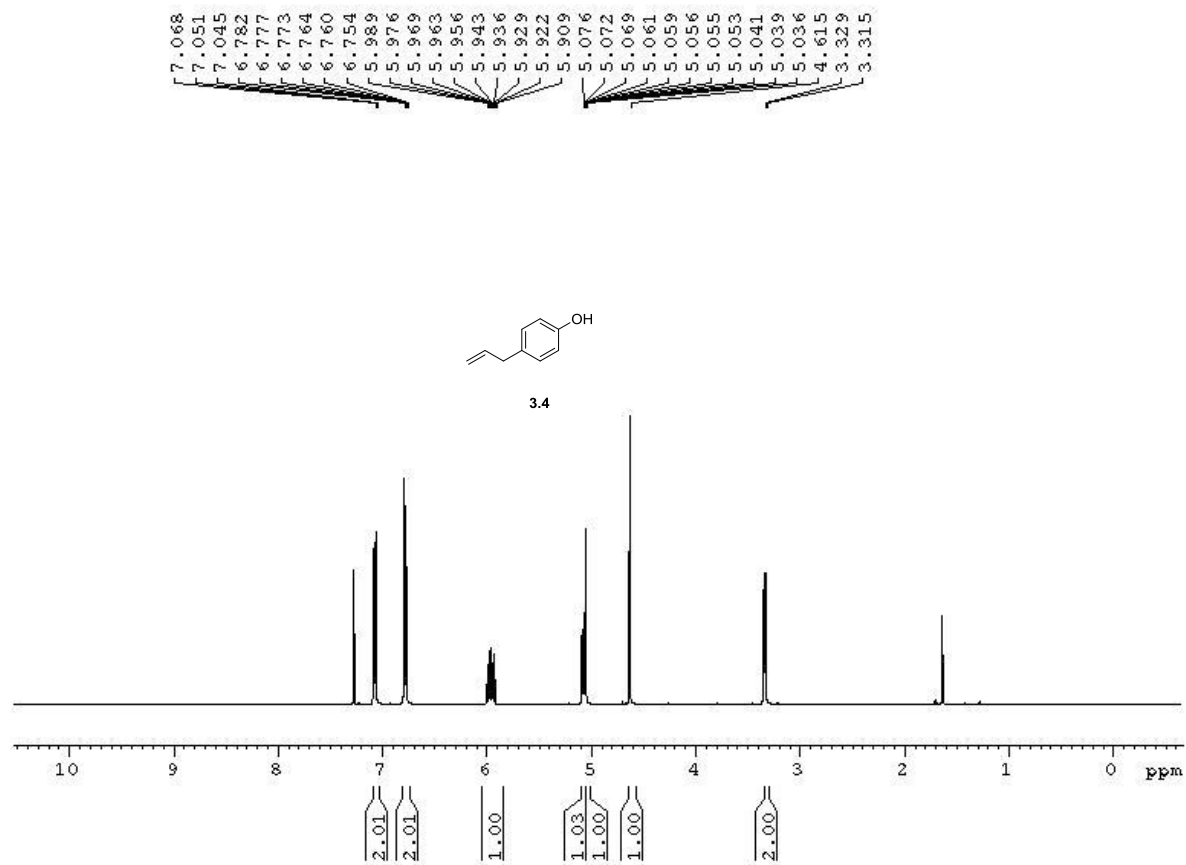
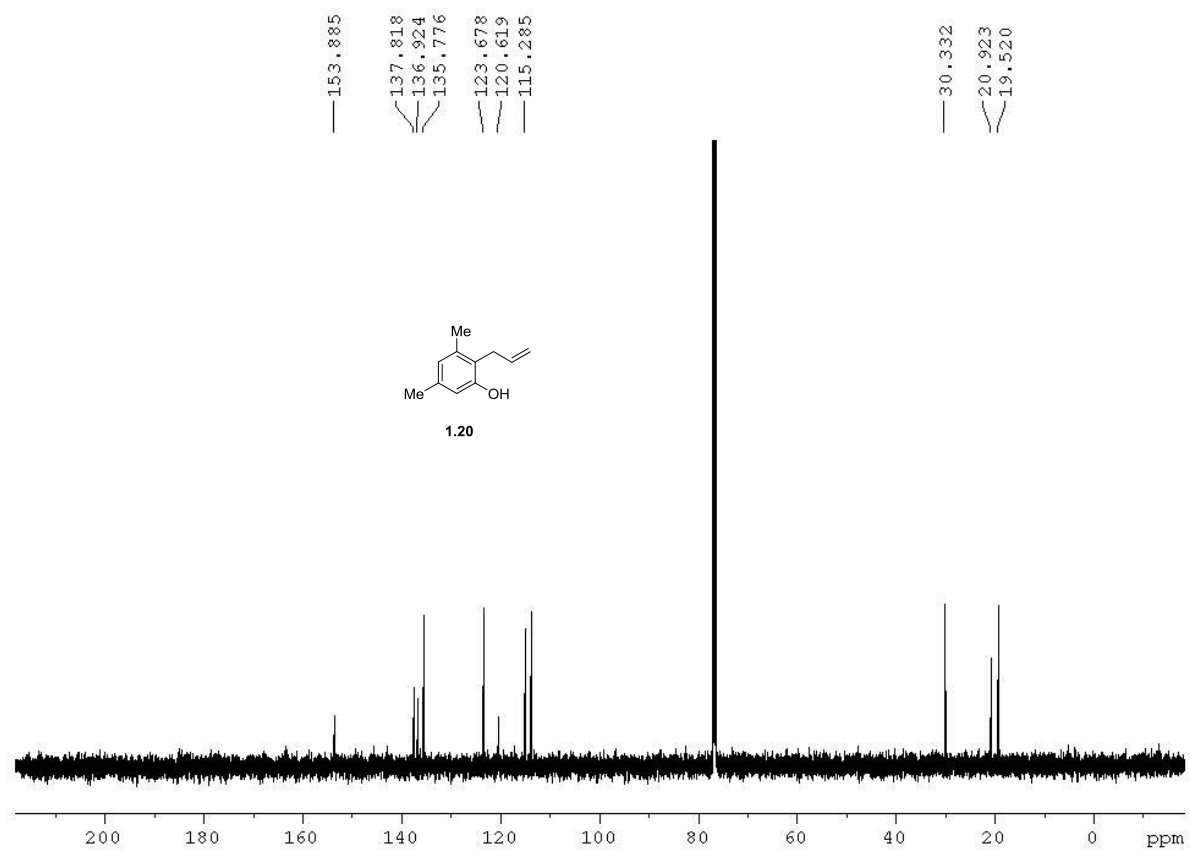**Figure A3.3** ^{1}H NMR spectrum of compound **3.4** (500 MHz, CDCl$_3$)

296
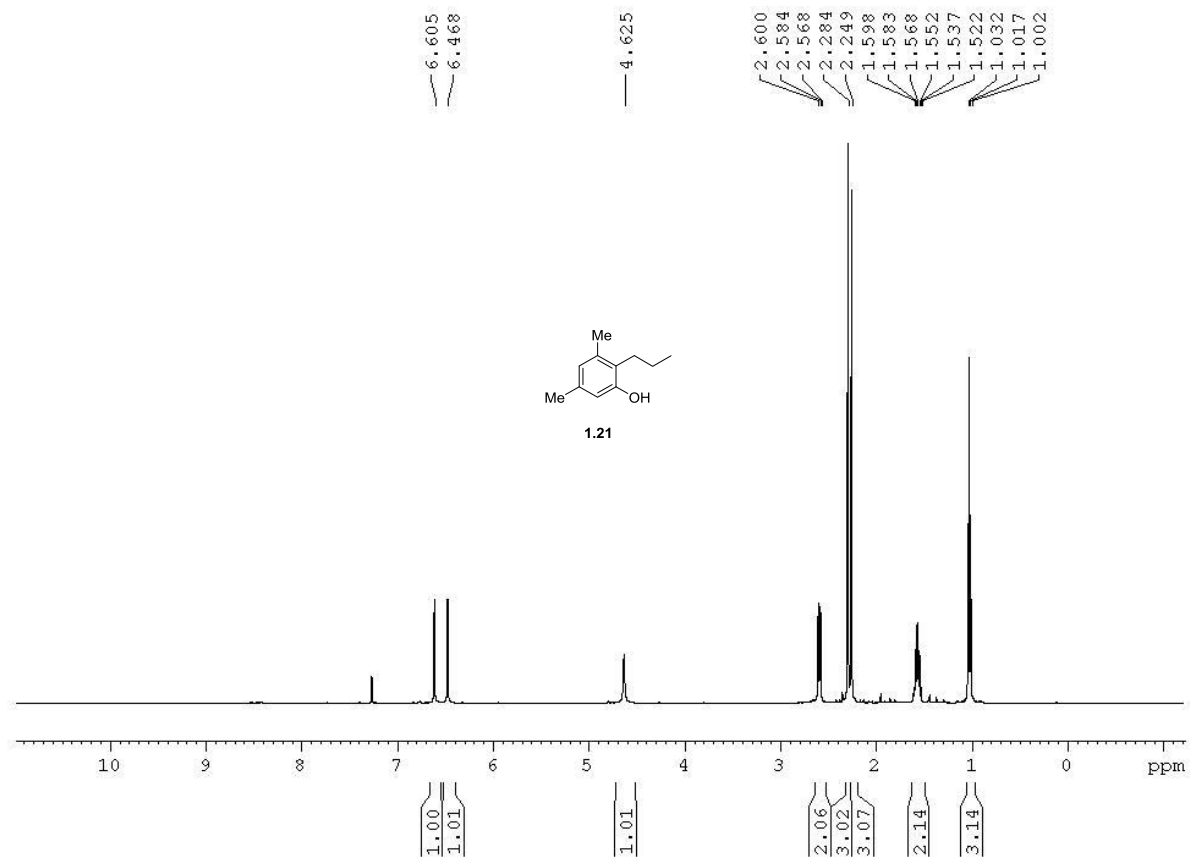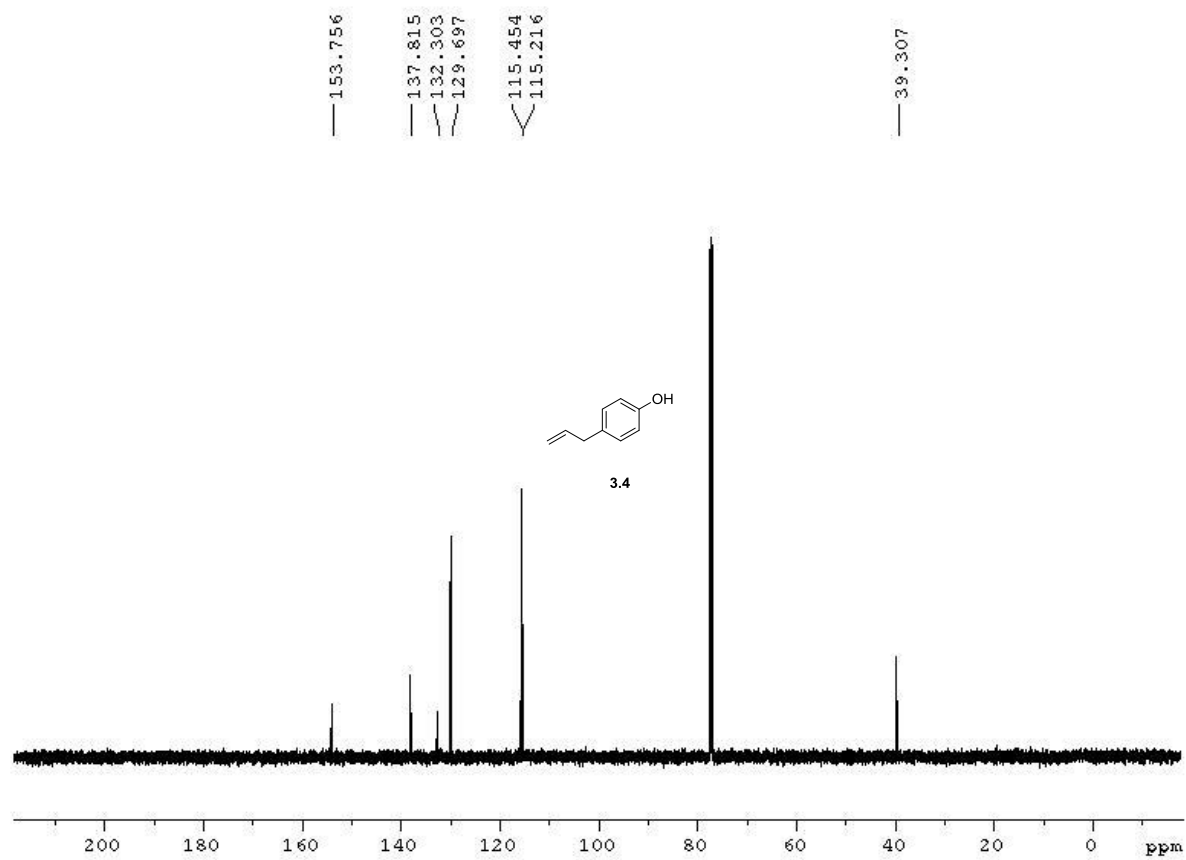
Figure A3.4 ^{13}C NMR spectrum of compound **3.4** (125 MHz, CDCl$_3$)
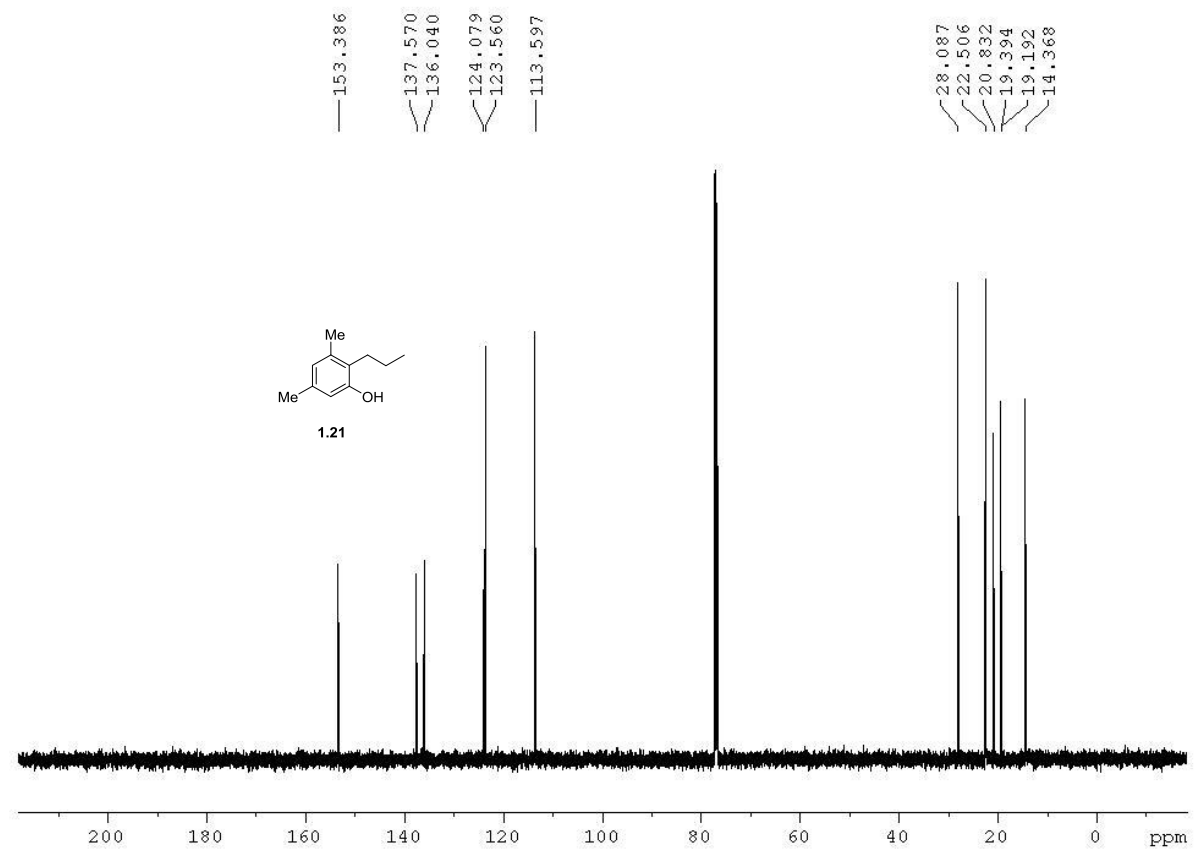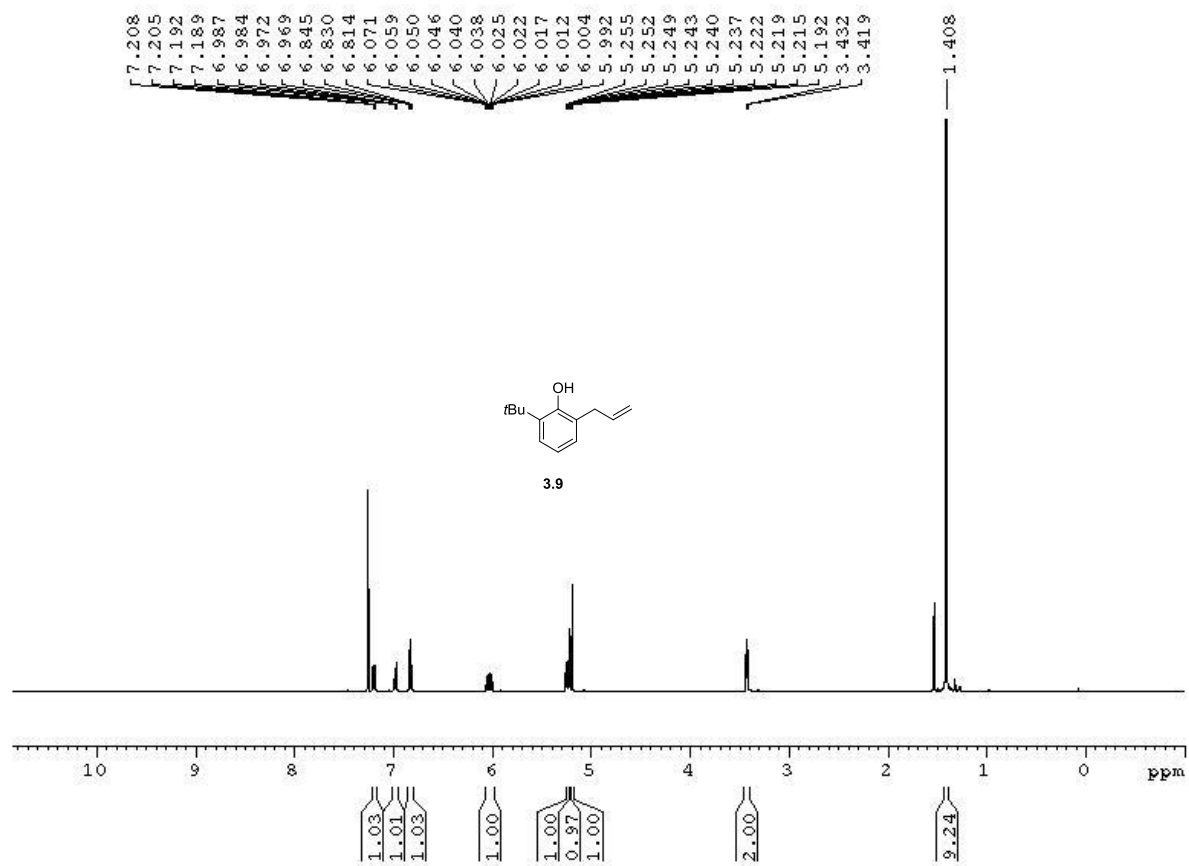
Figure A3.5 ^{1}H NMR spectrum of compound **3.9** (500 MHz, CDCl$_3$)
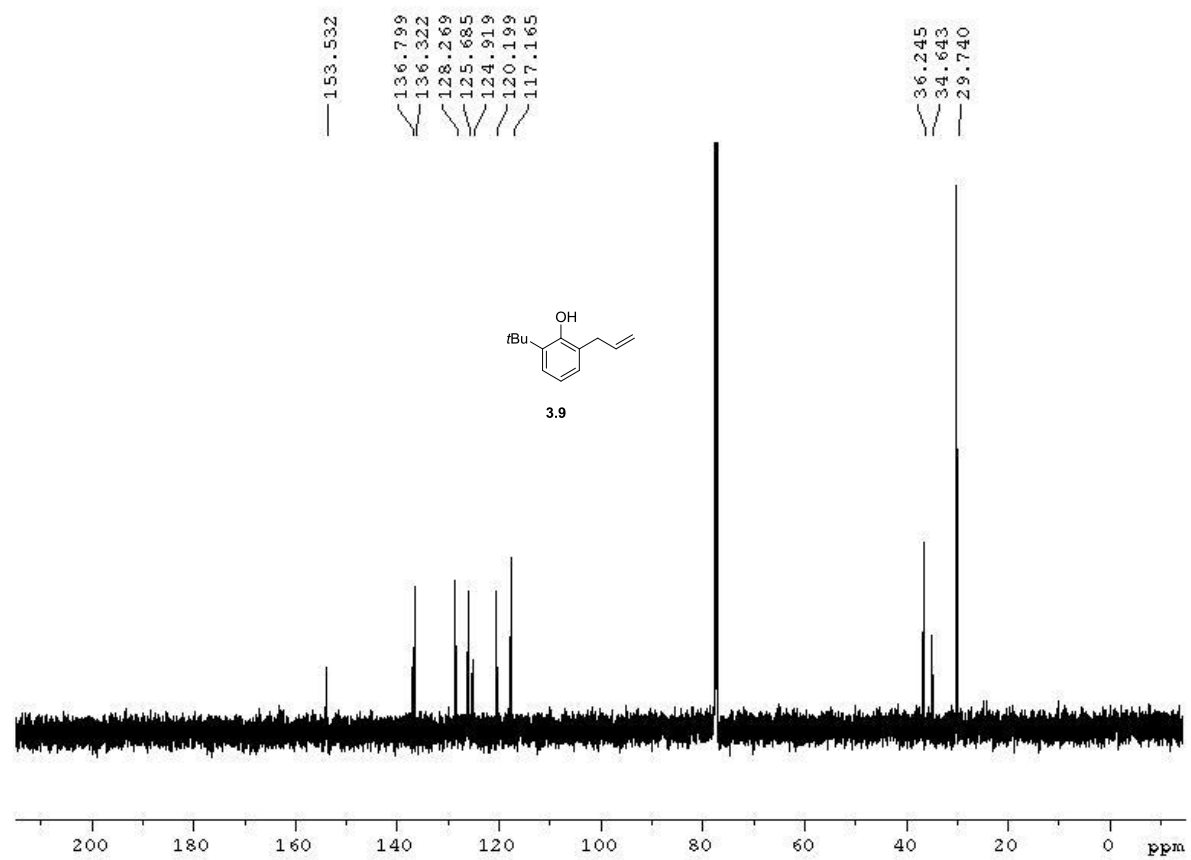
Figure A3.6 ^{13}C NMR spectrum of compound **3.9** (125 MHz, CDCl$_3$)
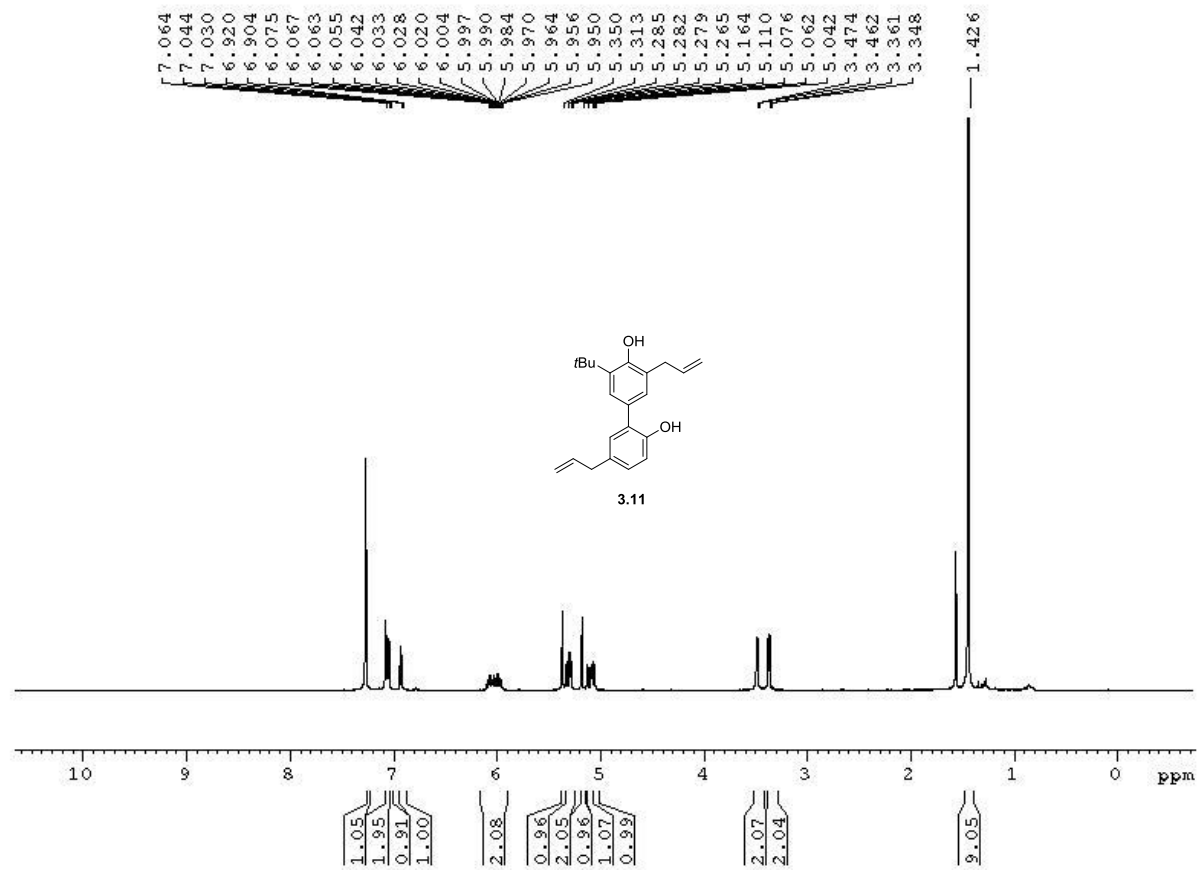
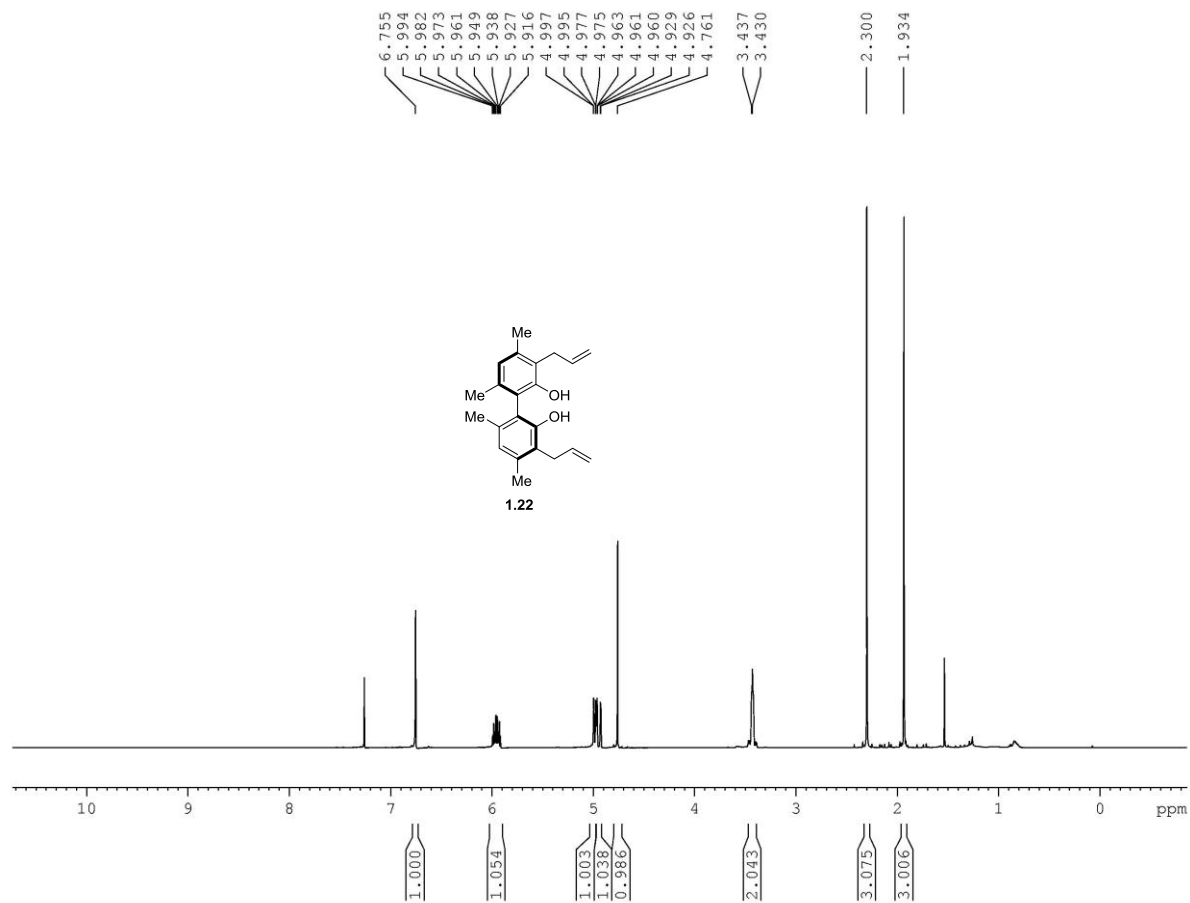**Figure A3.7** ^{1}H NMR spectrum of compound **3.11** (500 MHz, CDCl$_3$)
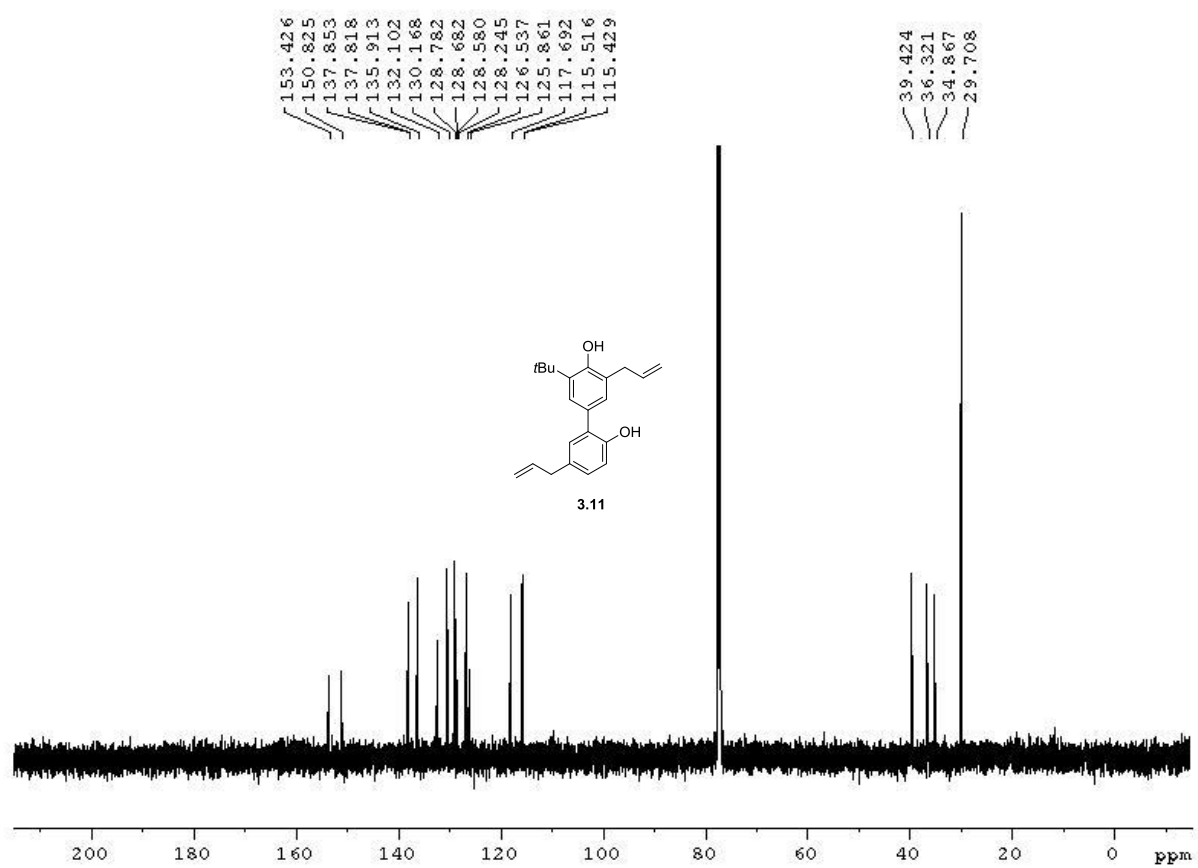
Figure A3.8 ^{13}C NMR spectrum of compound **3.11** (125 MHz, CDCl$_3$)

301
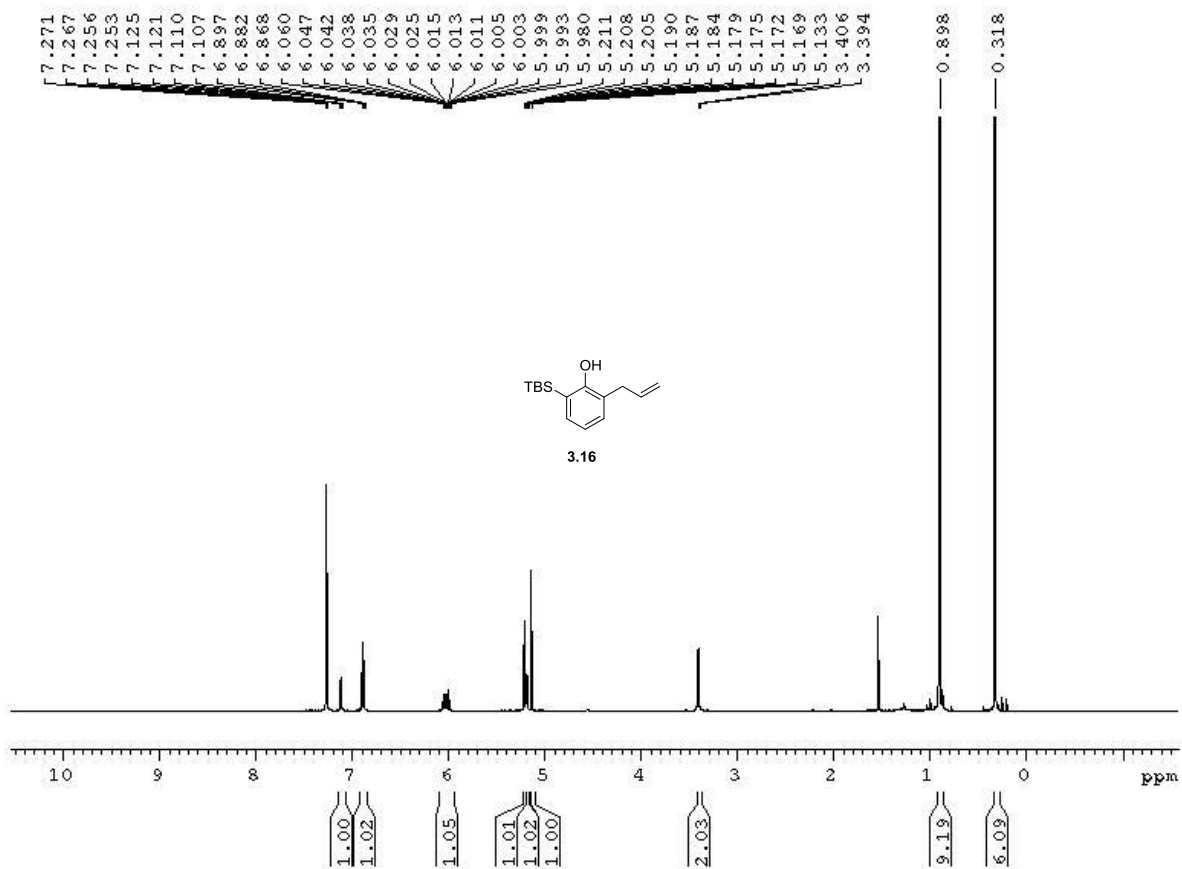
Figure A3.9 ^{1}H NMR spectrum of compound **3.16** (500 MHz, CDCl$_3$)
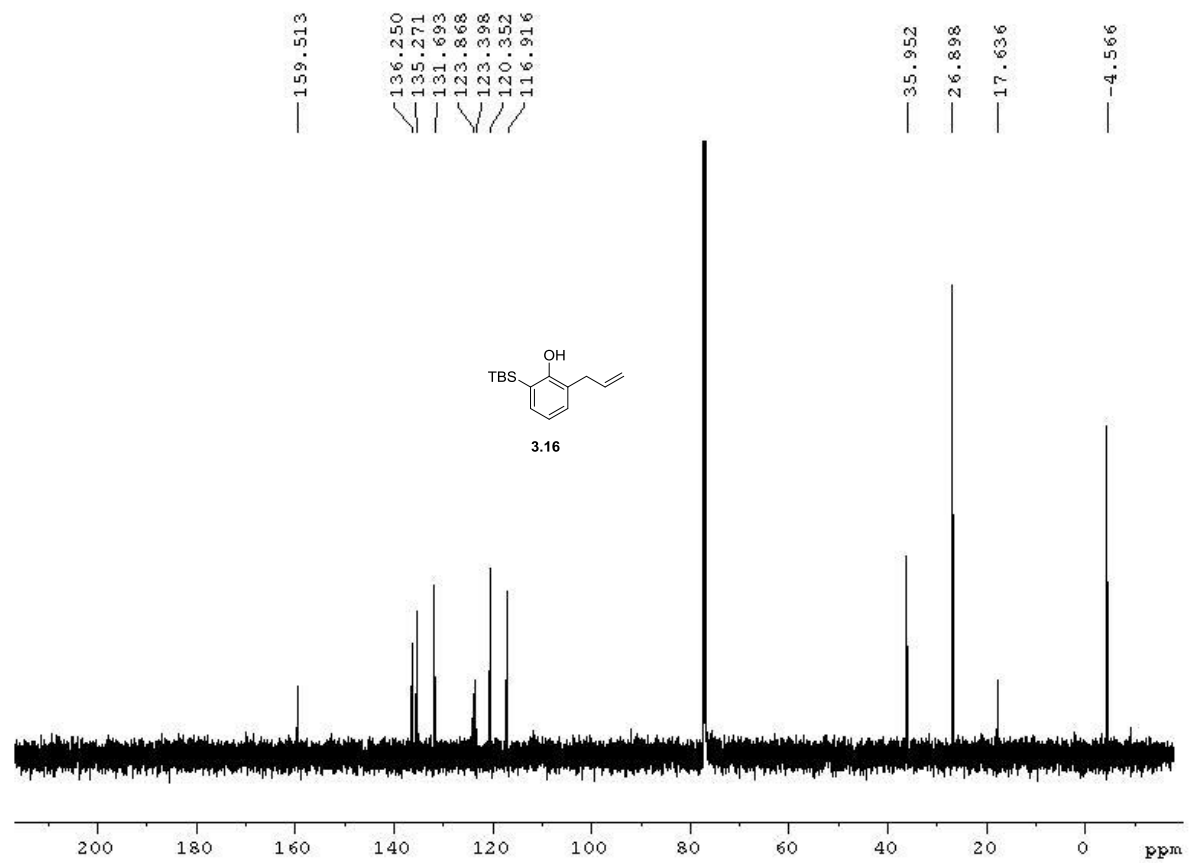
Figure A3.10 ^{13}C NMR spectrum of compound **3.16** (125 MHz, CDCl$_3$)
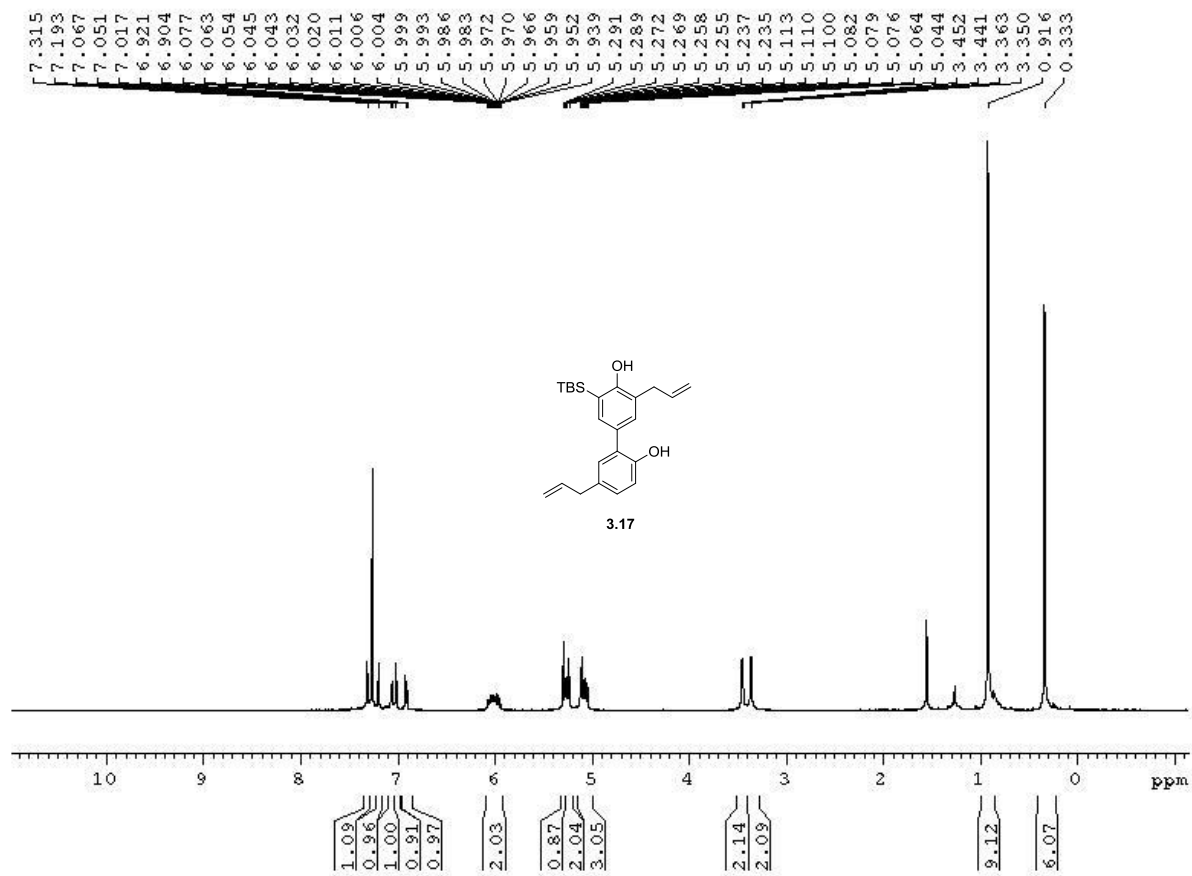
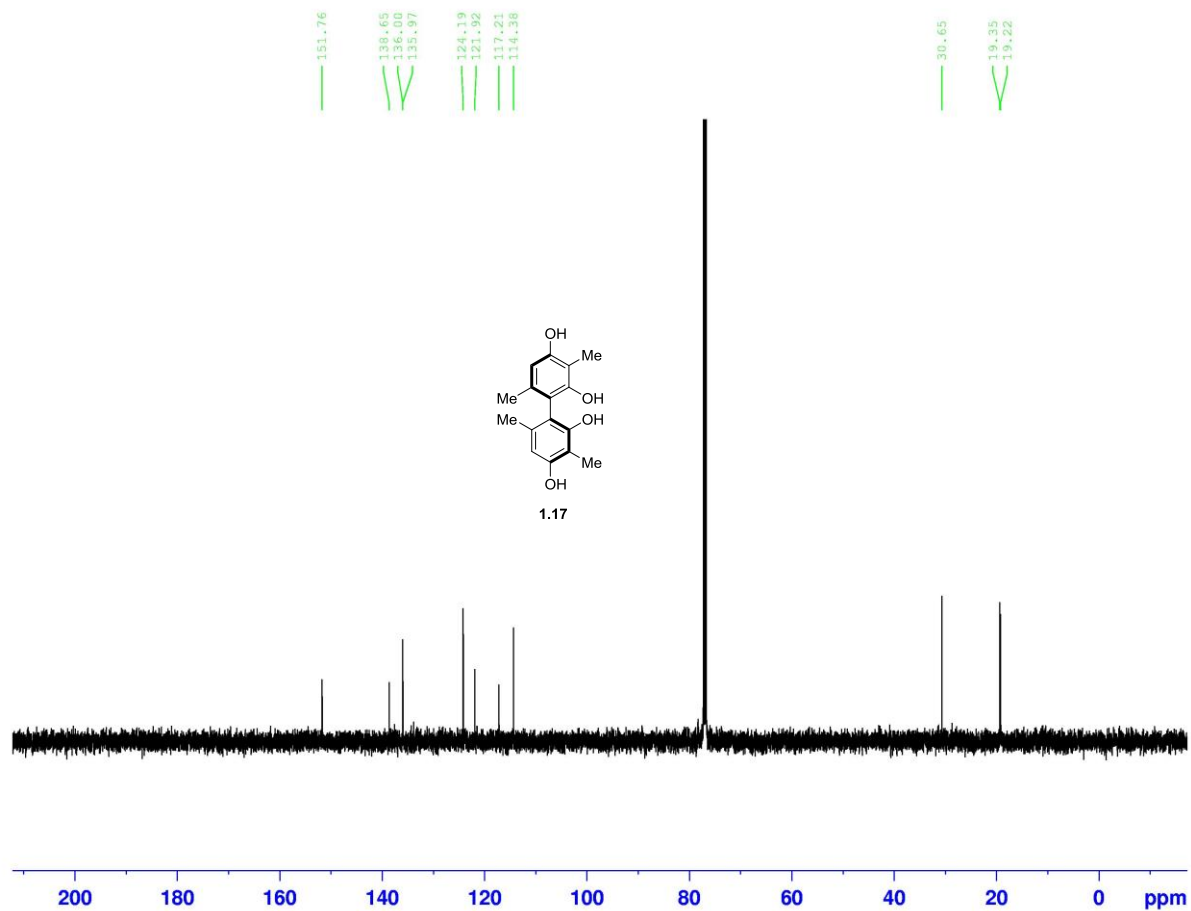**Figure A3.11** ^{1}H NMR spectrum of compound **3.17** (500 MHz, CDCl$_3$)
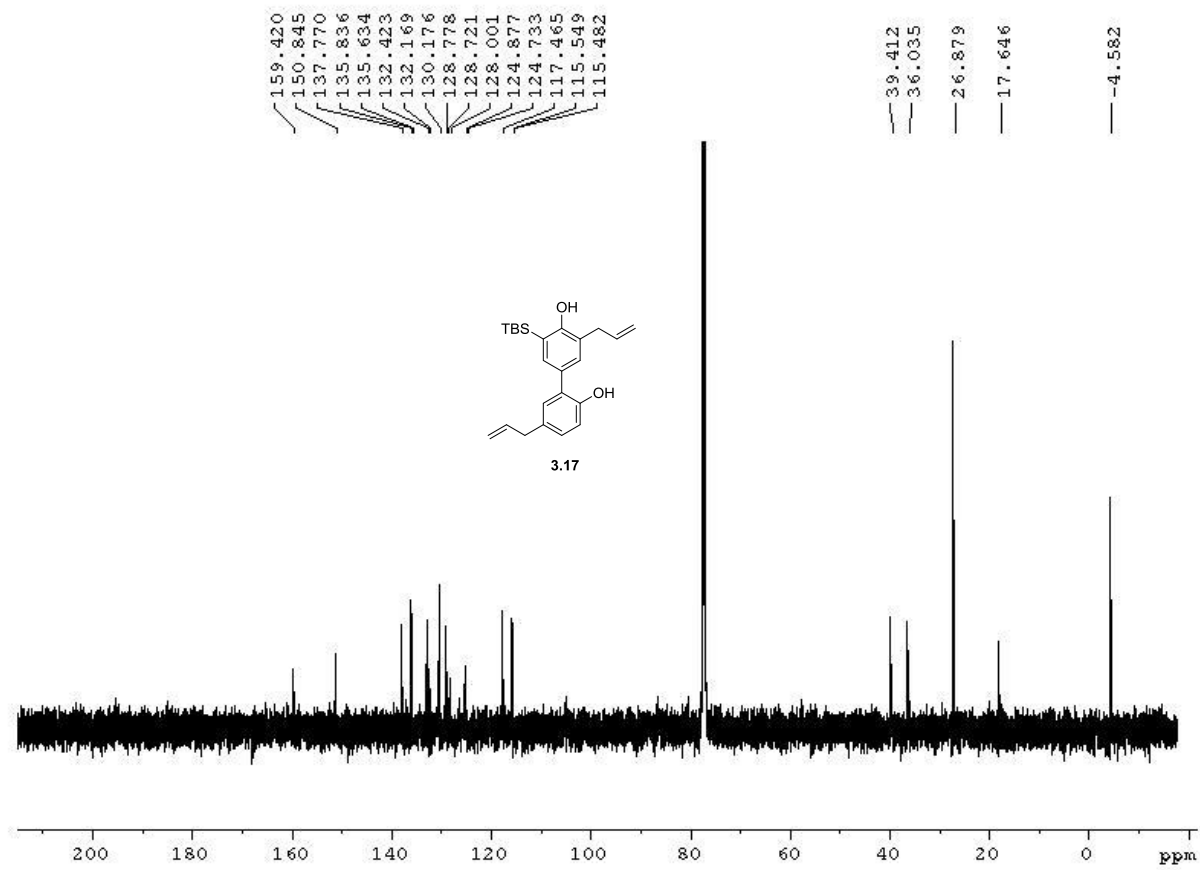
Figure A3.12 ^{13}C NMR spectrum of compound **3.17** (125 MHz, CDCl$_3$)
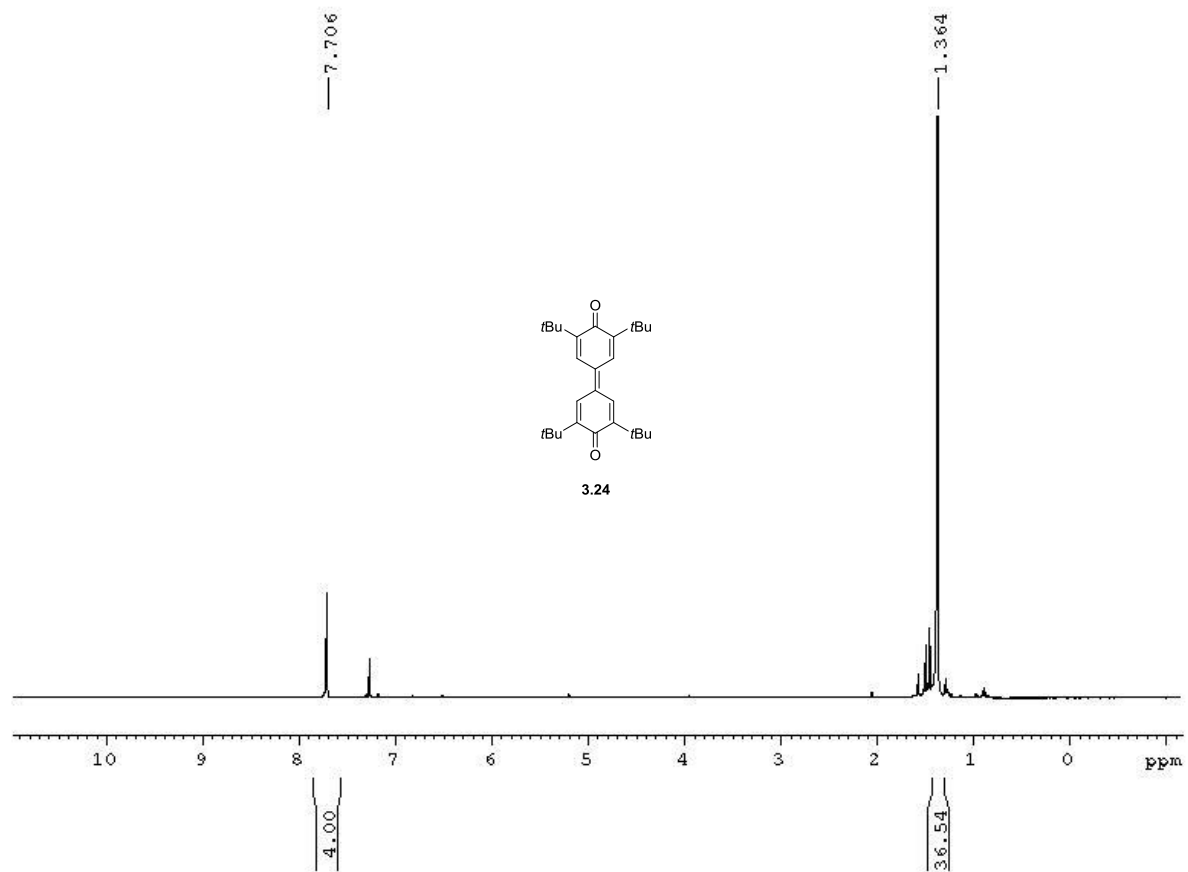
Figure A3.13 ^{1}H NMR spectrum of compound **3.24** (500 MHz, CDCl$_3$)
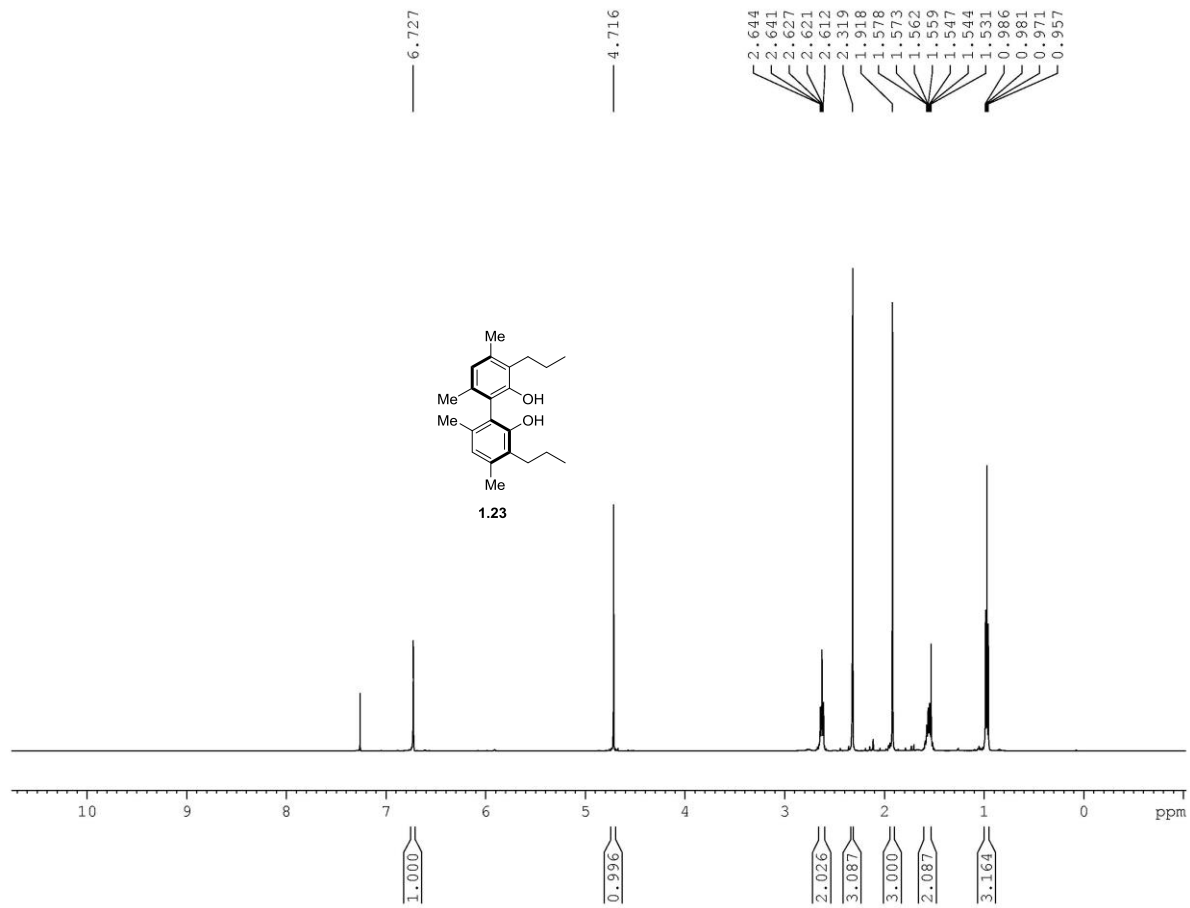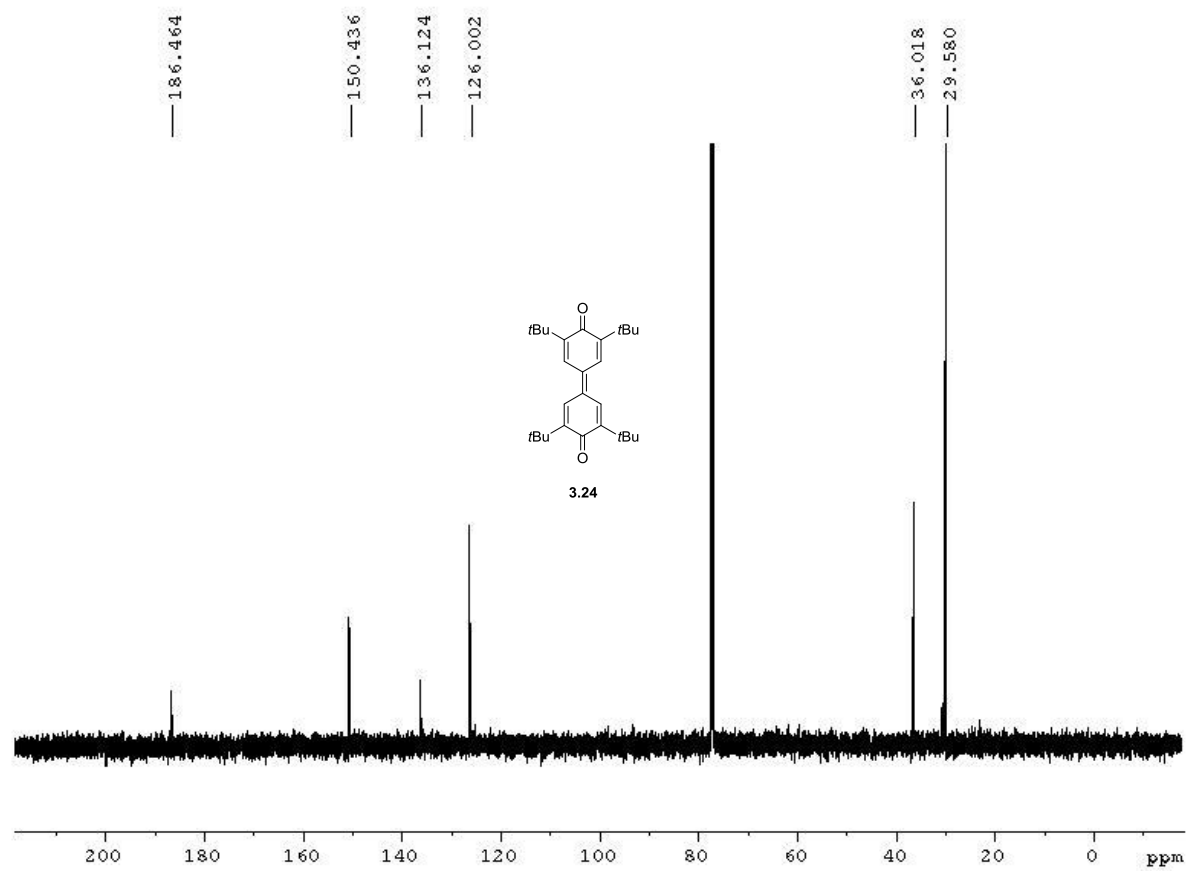
Figure A3.14 ^{13}C NMR spectrum of compound **3.24** (125 MHz, CDCl$_3$)
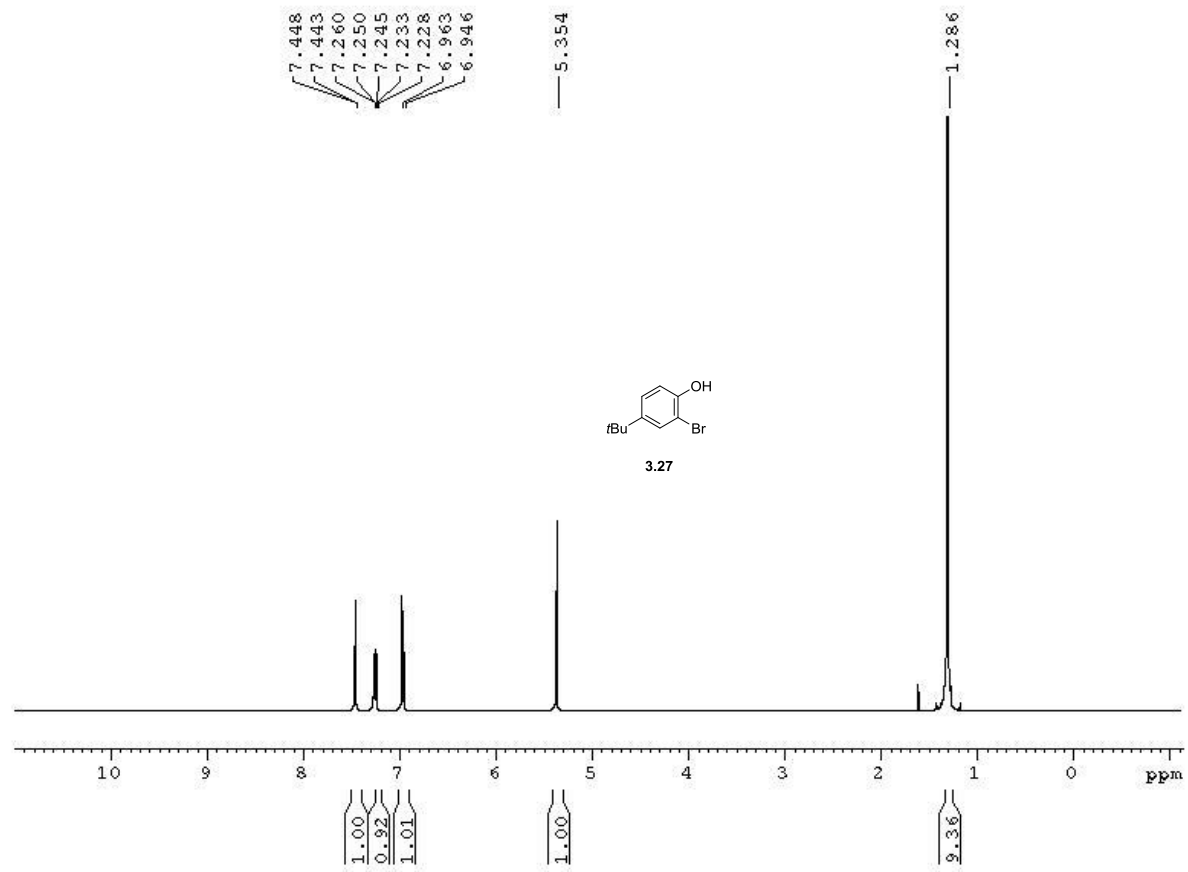
Figure A3.15 ^{1}H NMR spectrum of compound **3.27** (500 MHz, CDCl$_3$)

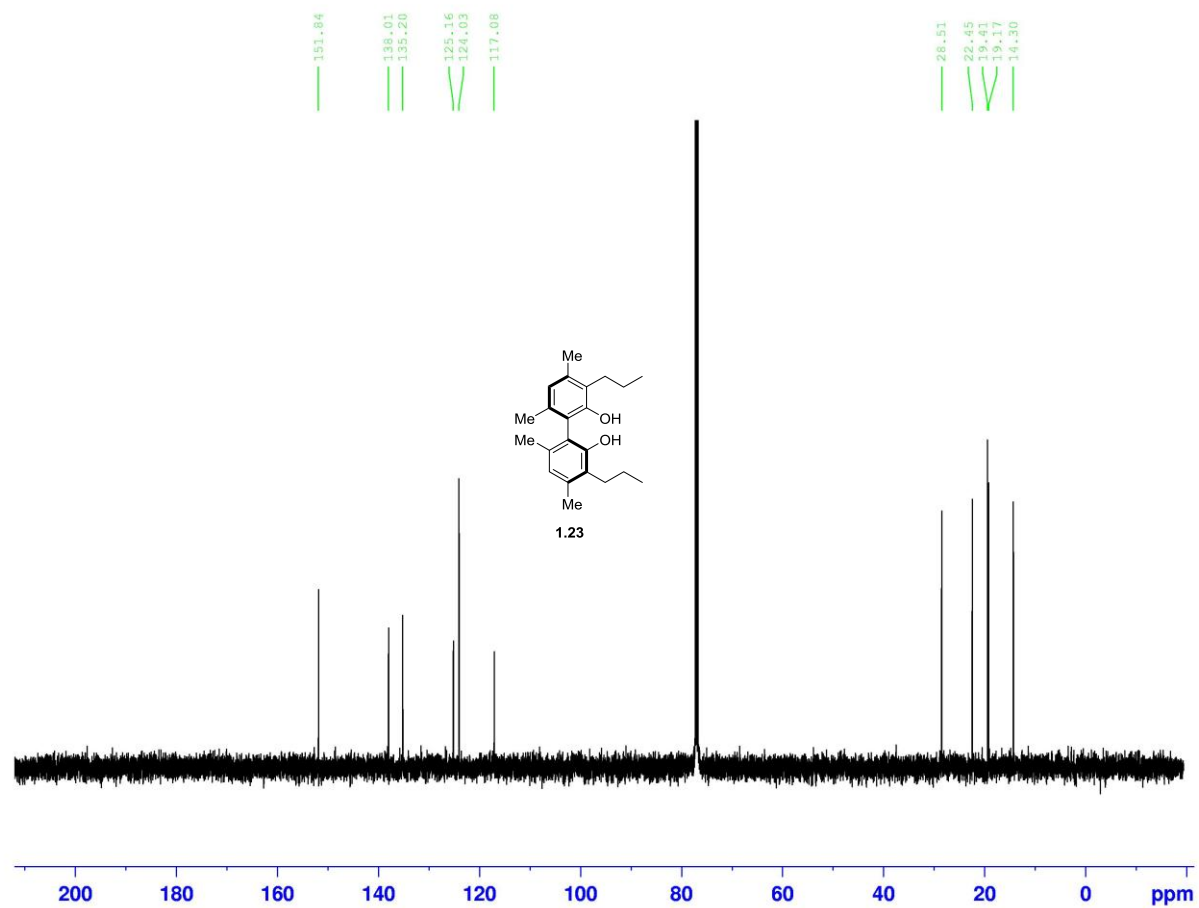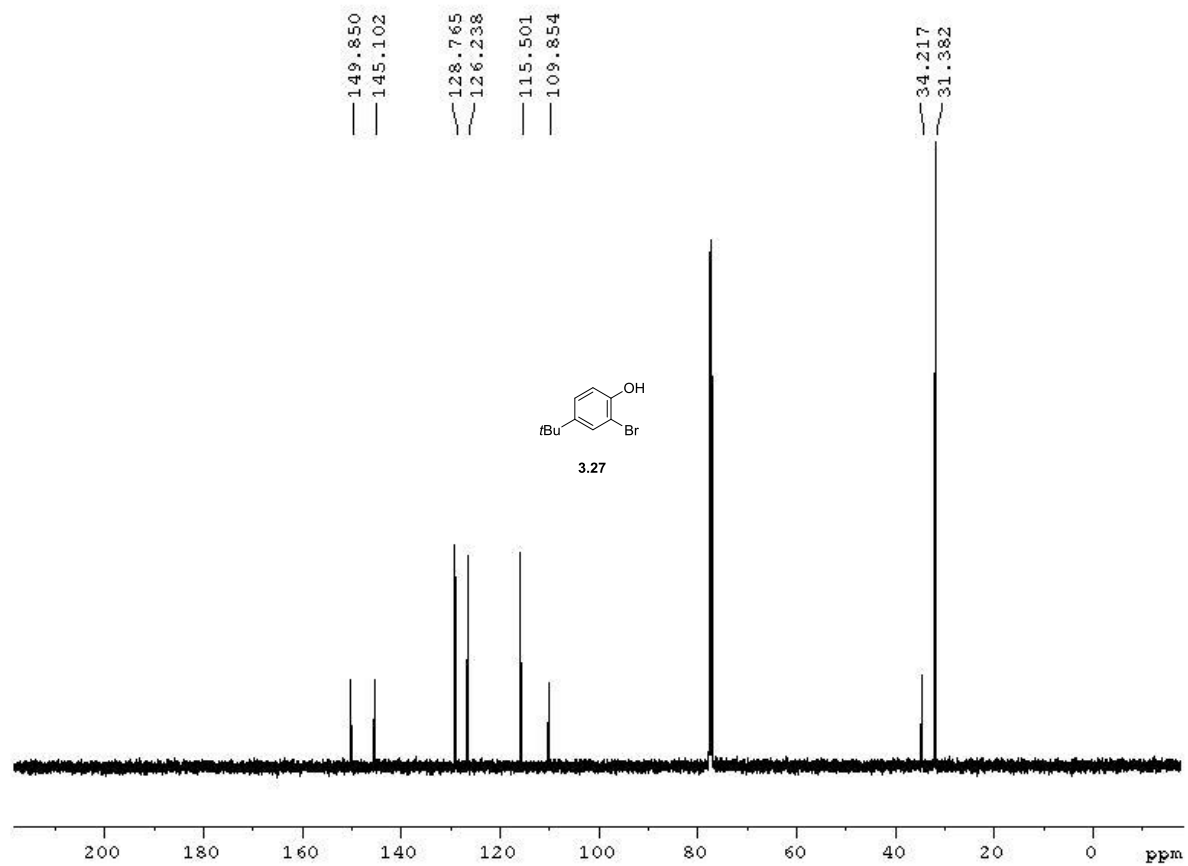**Figure A3.16** ^{13}C NMR spectrum of compound **3.27** (125 MHz, CDCl$_3$)
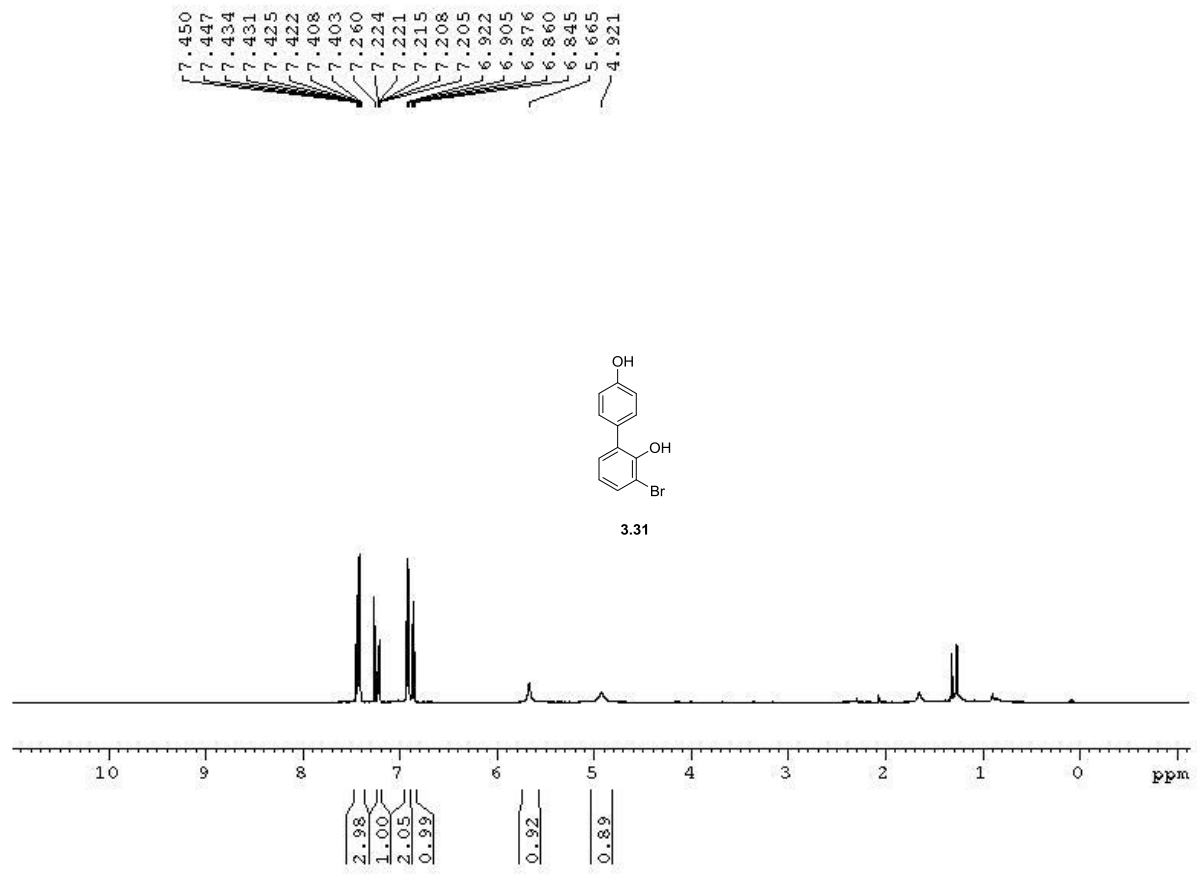
Figure A3.17 ^{1}H NMR spectrum of compound **3.31** (500 MHz, CDCl$_3$)
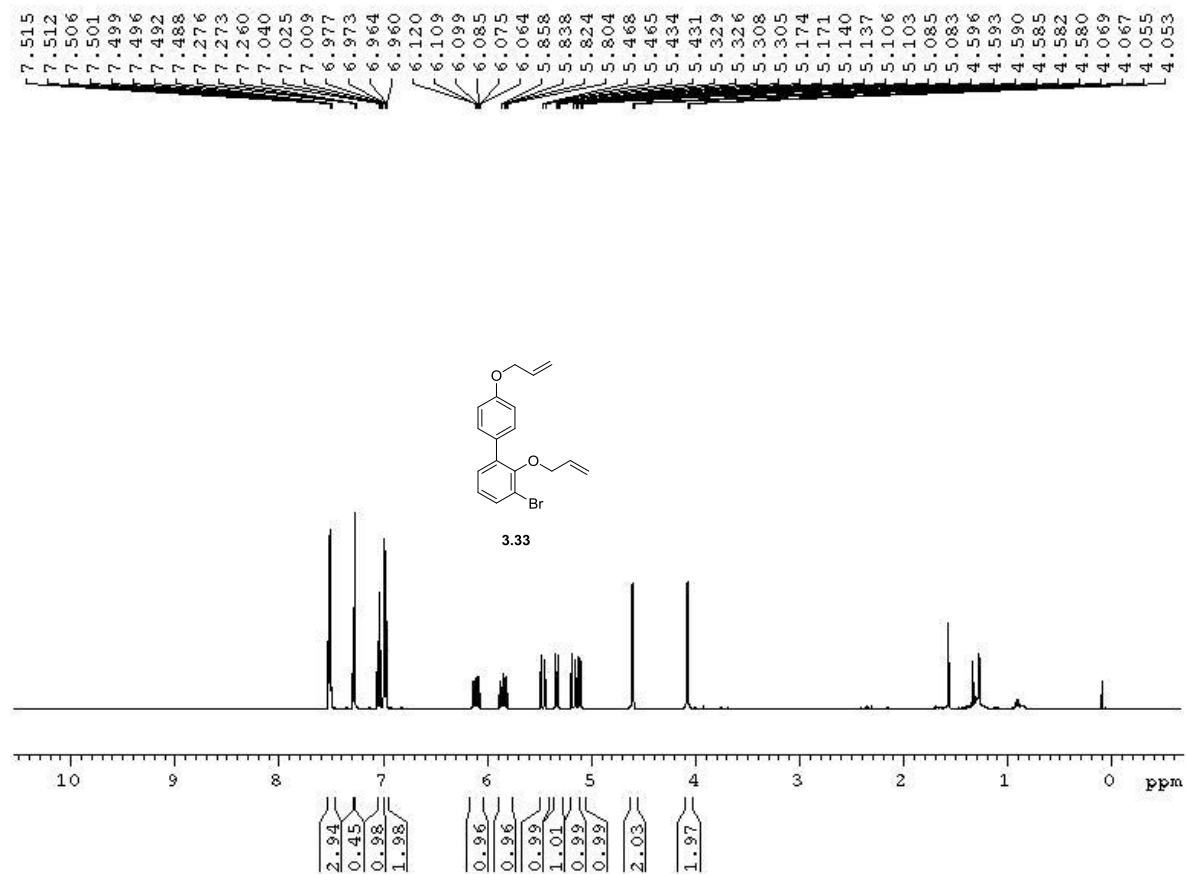
Figure A3.18 ^{1}H NMR spectrum of compound **3.33** (500 MHz, CDCl$_3$)
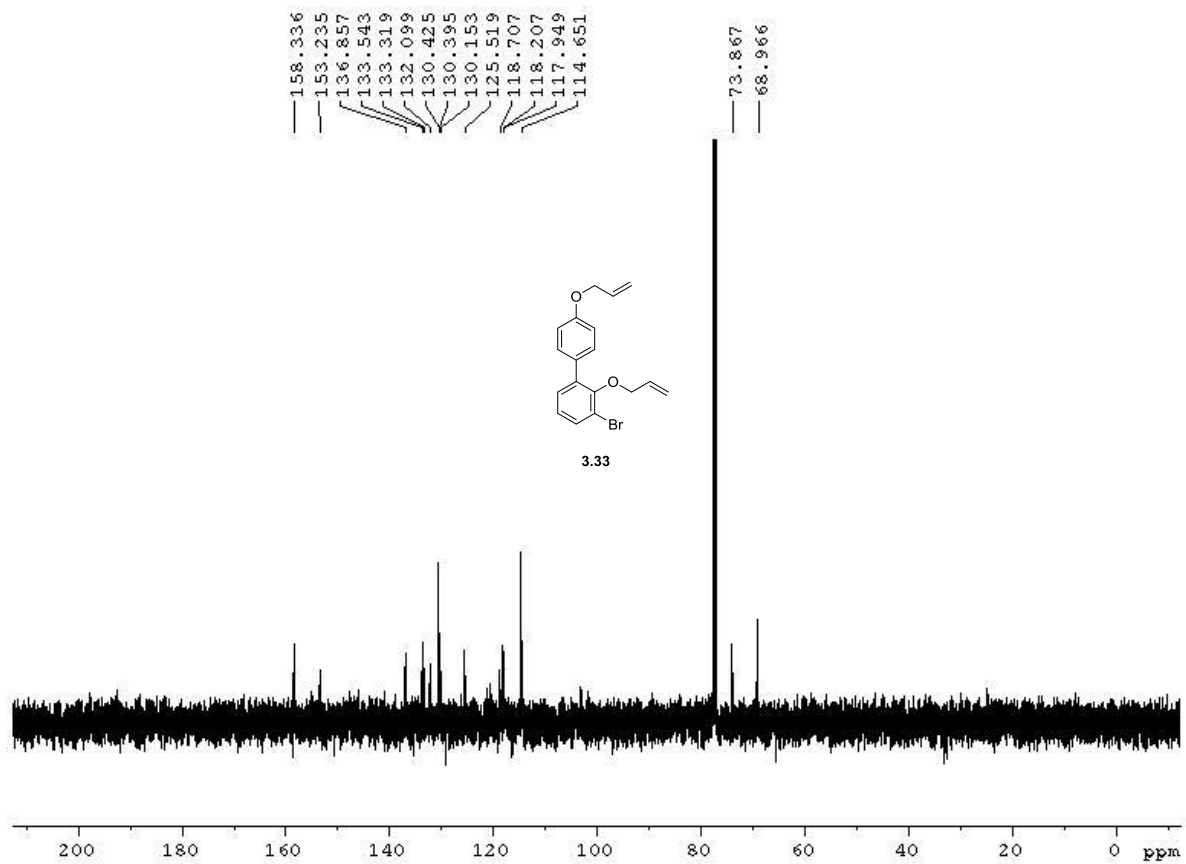
Figure A3.19 ^{13}C NMR spectrum of compound **3.33** (125 MHz, CDCl$_3$)
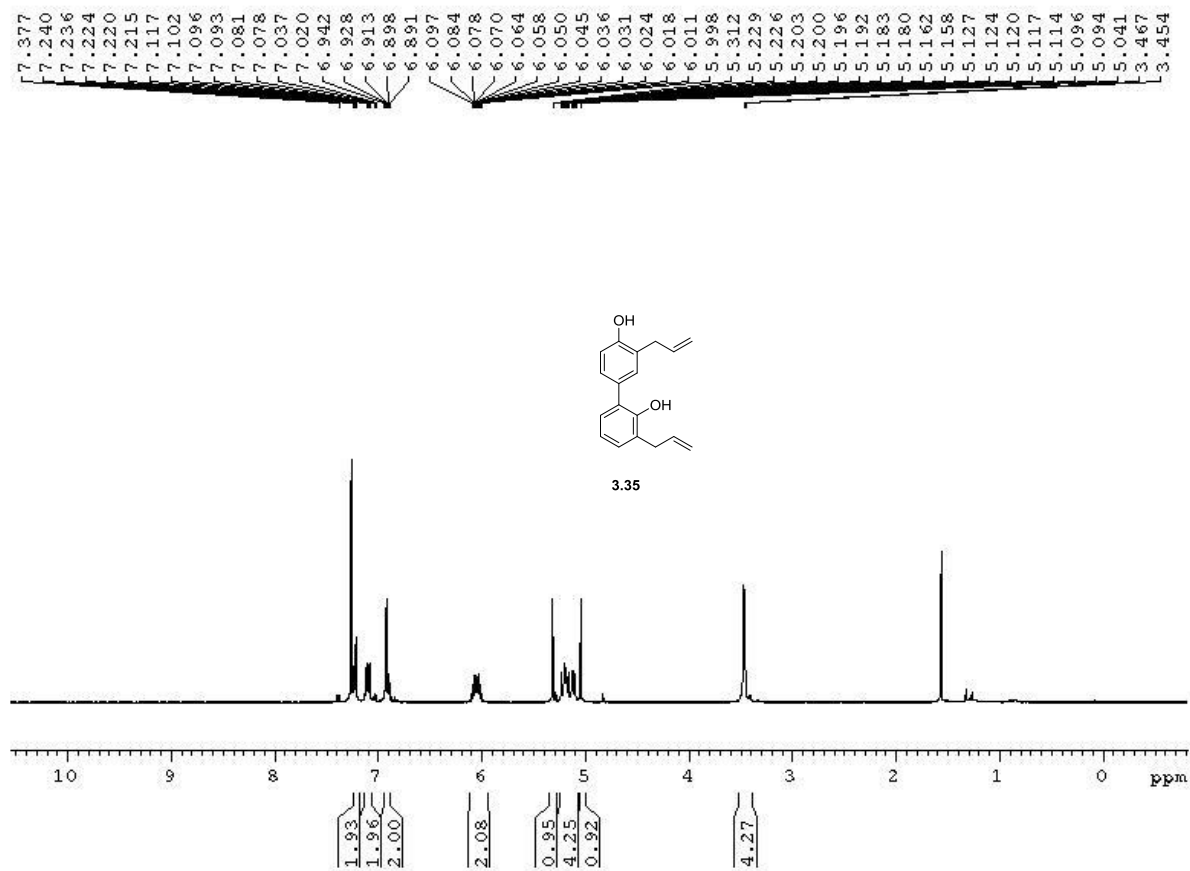
Figure A3.20 ^{1}H NMR spectrum of compound **3.35** (500 MHz, CDCl$_3$)
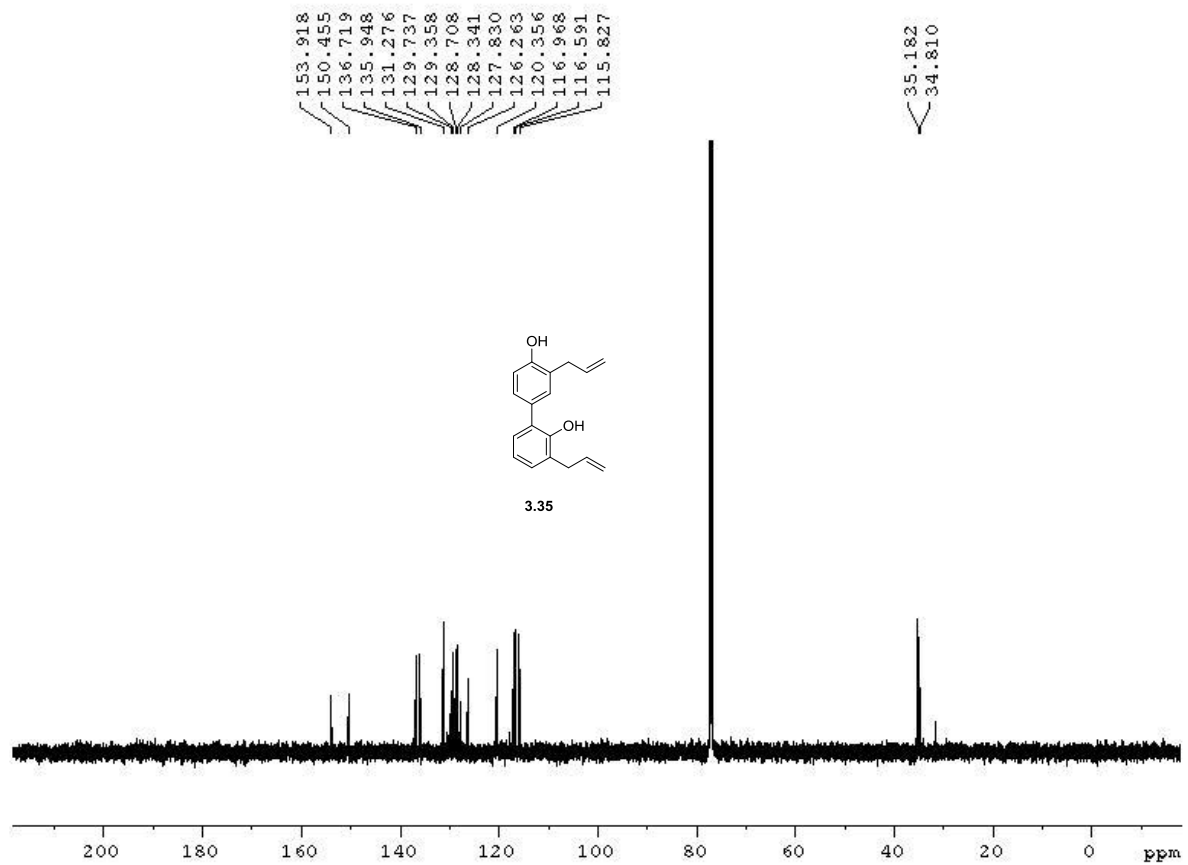
Figure A3.21 ^{13}C NMR spectrum of compound **3.35** (125 MHz, CDCl$_3$)

314
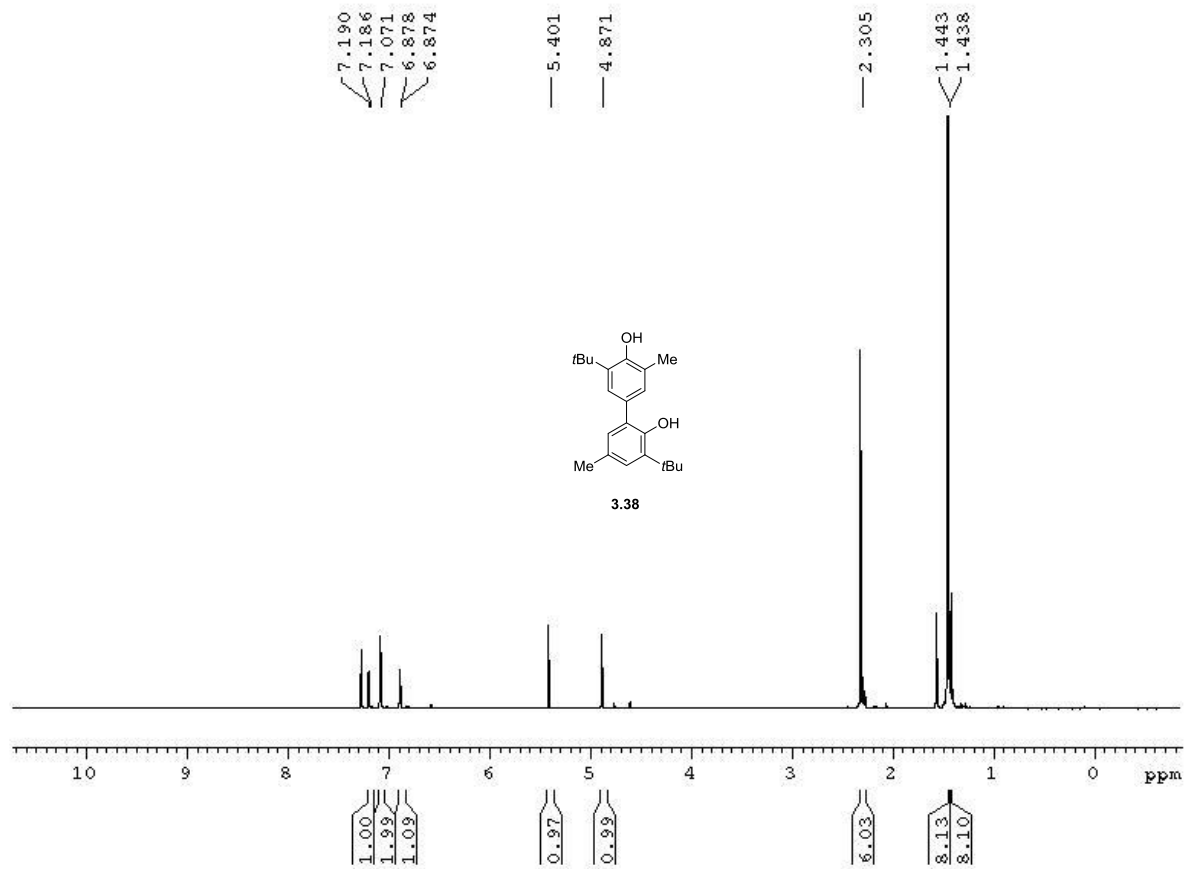
Figure A3.22 ^{1}H NMR spectrum of compound **3.38** (500 MHz, CDCl$_3$)
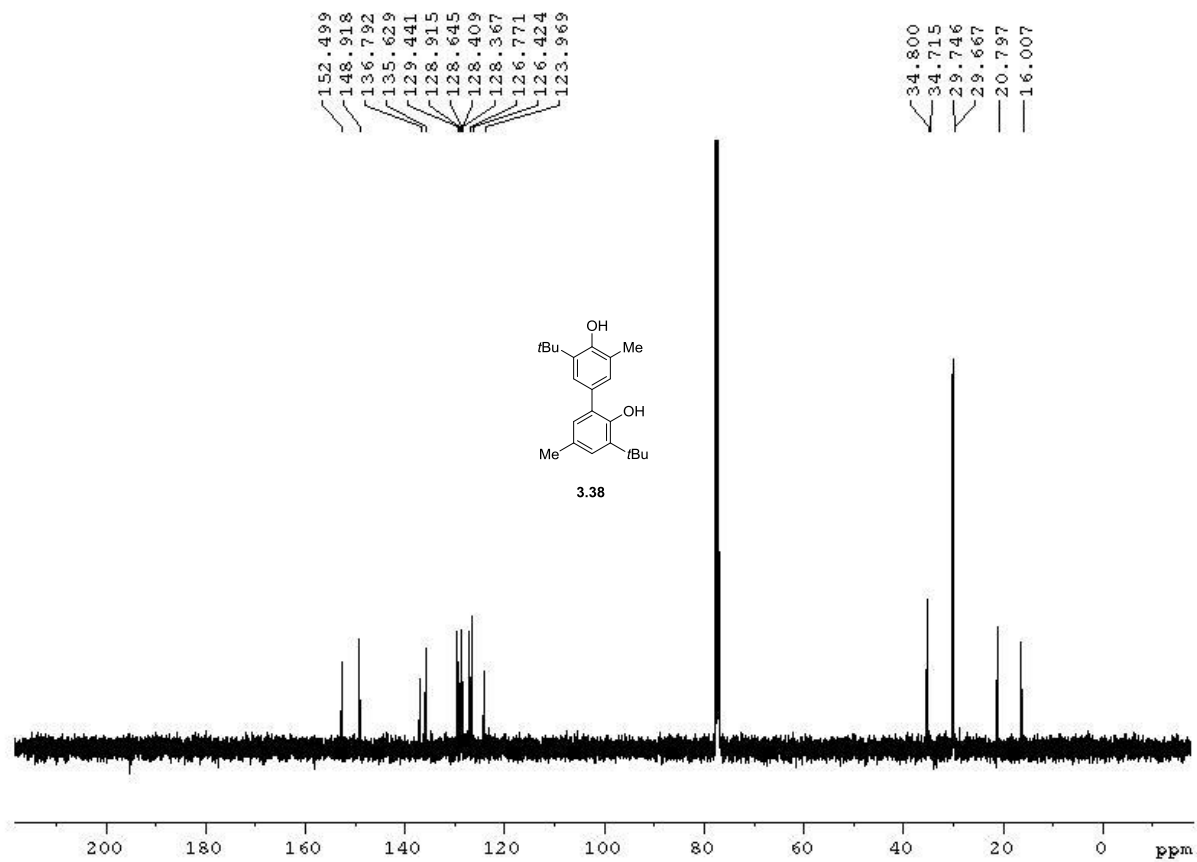
Figure A3.23 ^{13}C NMR spectrum of compound **3.38** (125 MHz, CDCl$_3$)
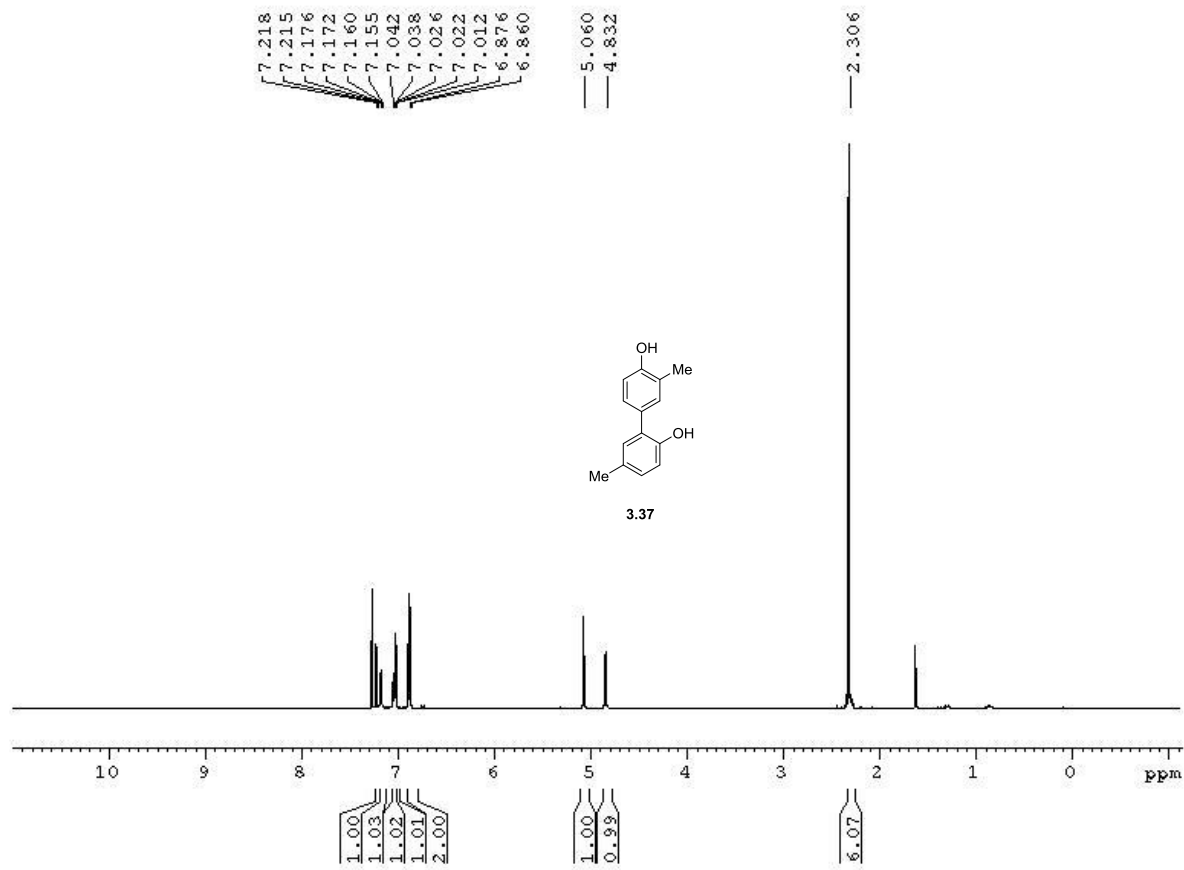
Figure A3.24 ^{1}H NMR spectrum of compound **3.37** (500 MHz, CDCl$_3$)
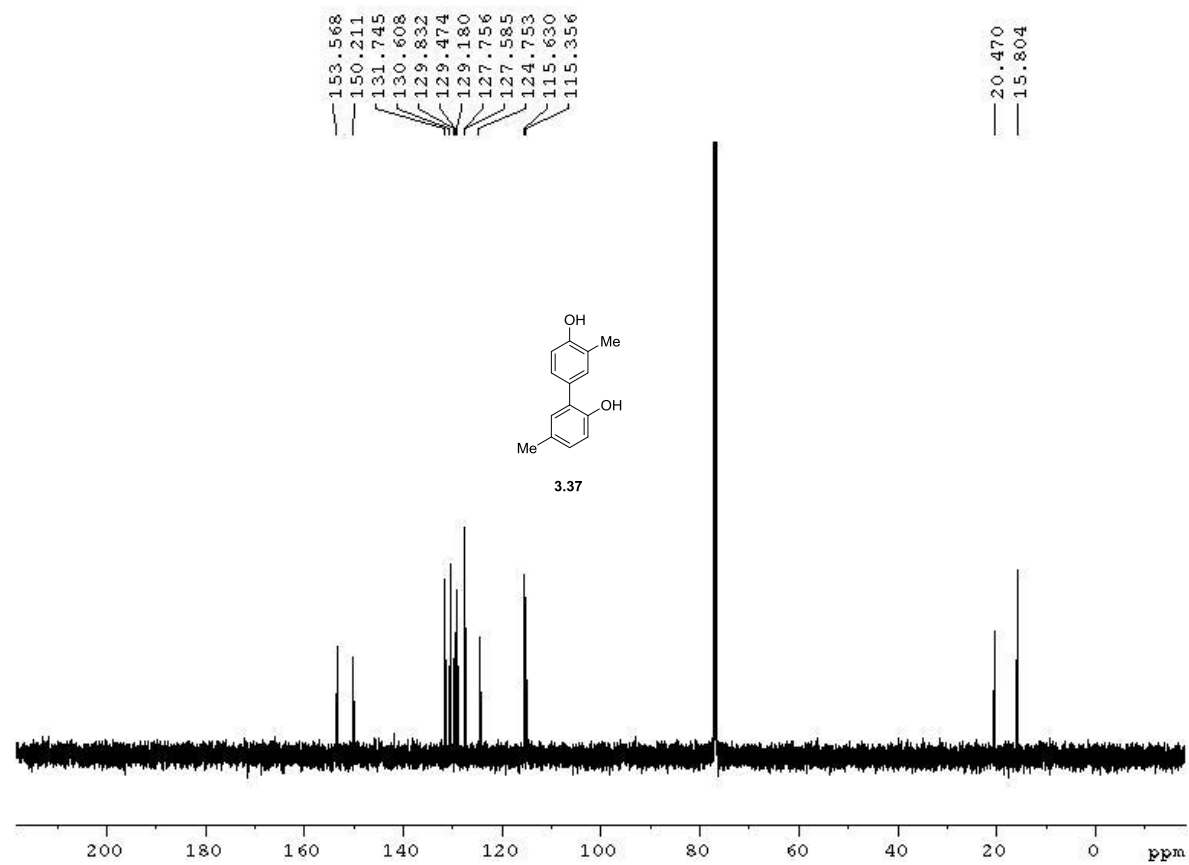
Figure A3.25 ^{13}C NMR spectrum of compound **3.37** (125 MHz, CDCl$_3$)
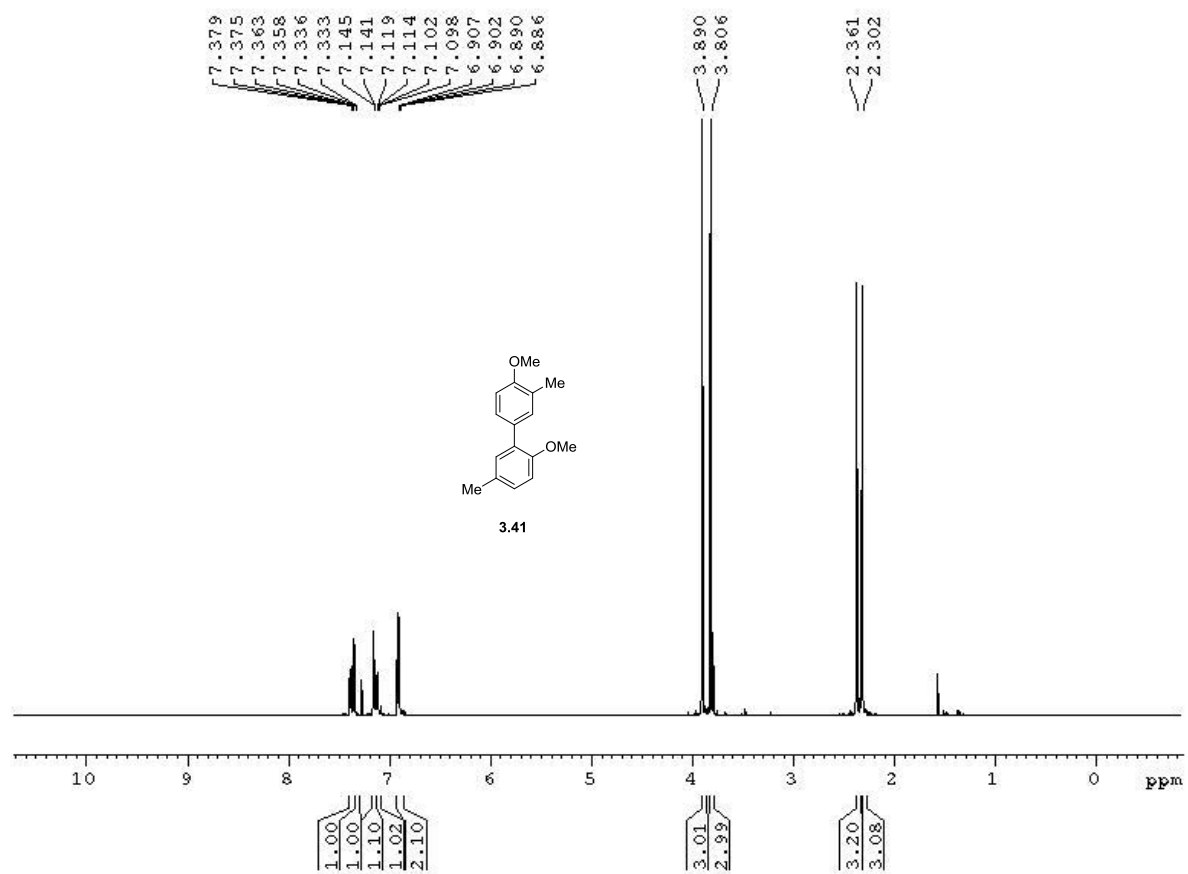
Figure A3.26 ^{1}H NMR spectrum of compound **3.41** (500 MHz, CDCl$_3$)
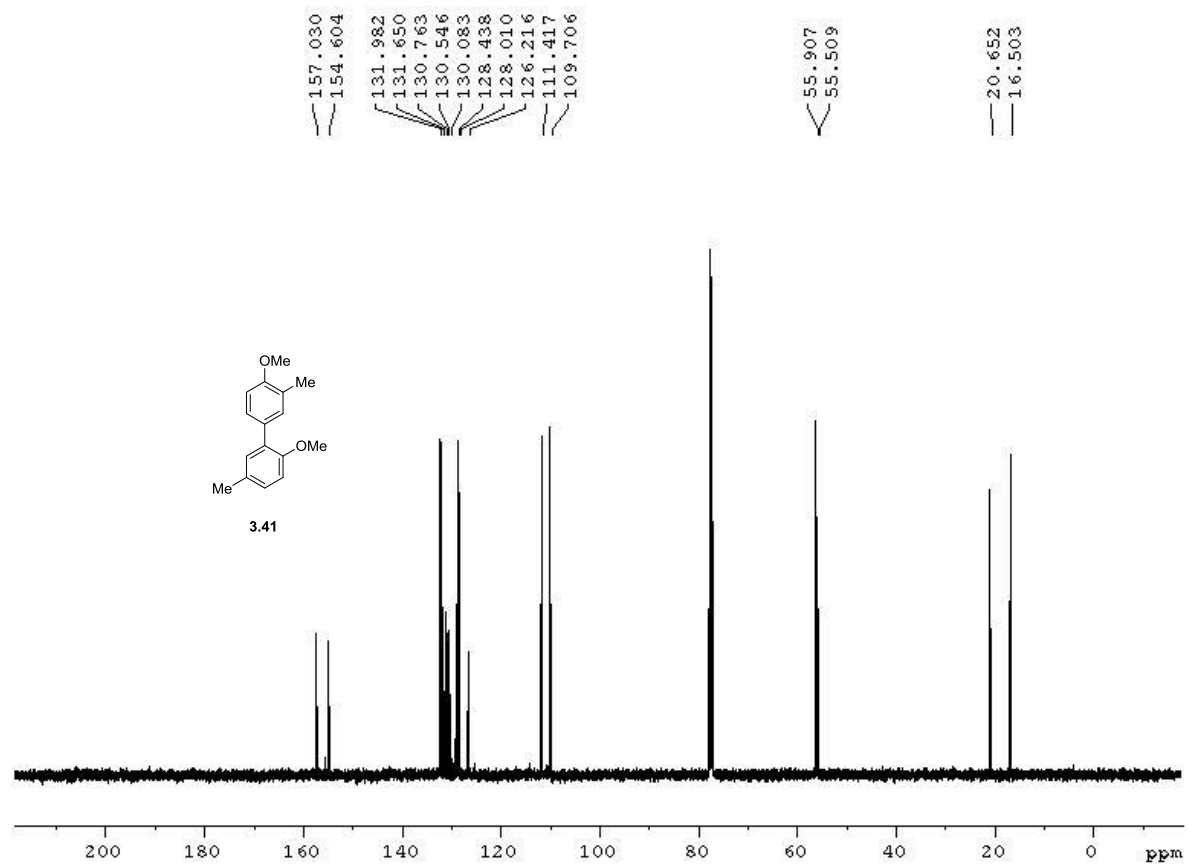
Figure A3.27 ^{13}C NMR spectrum of compound **3.41** (125 MHz, CDCl$_3$)

Figure A3.28 ^{1}H NMR spectrum of compound **3.42** (500 MHz, CDCl$_3$)
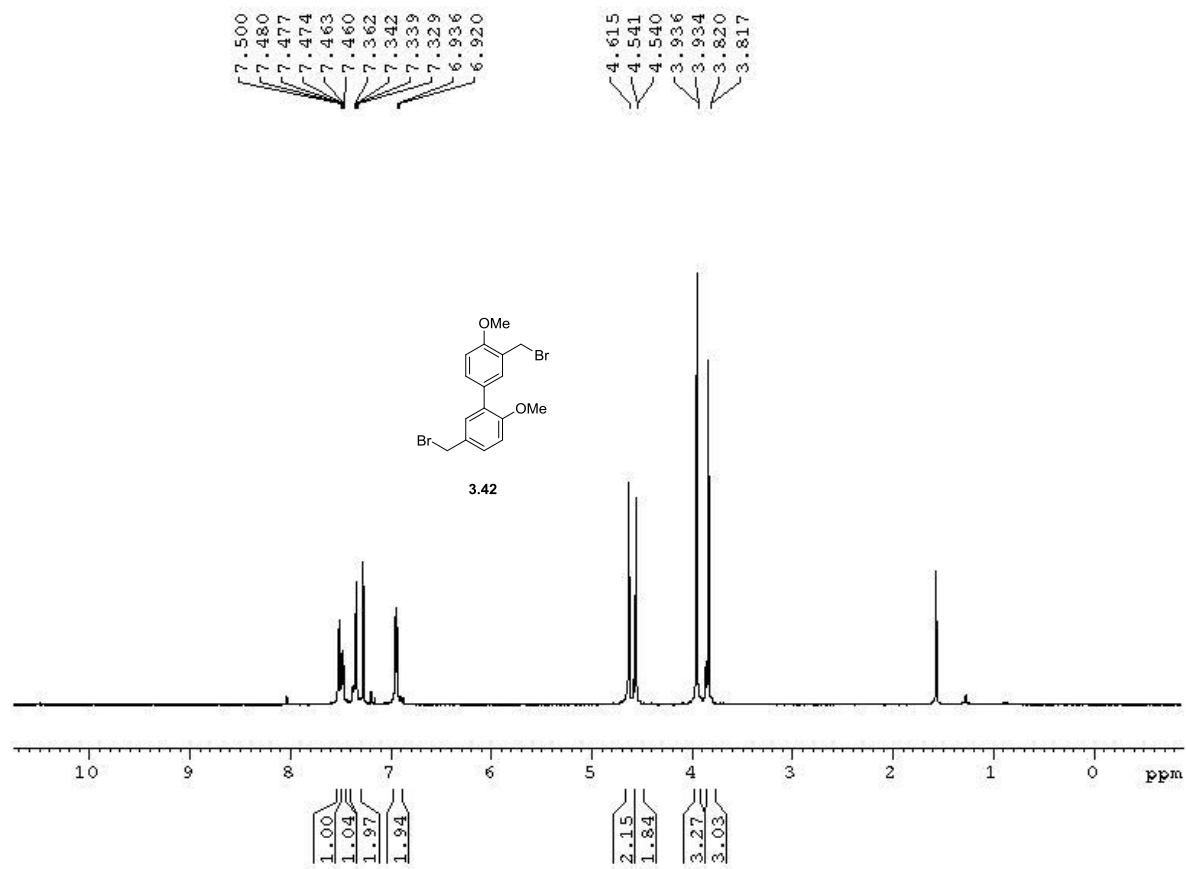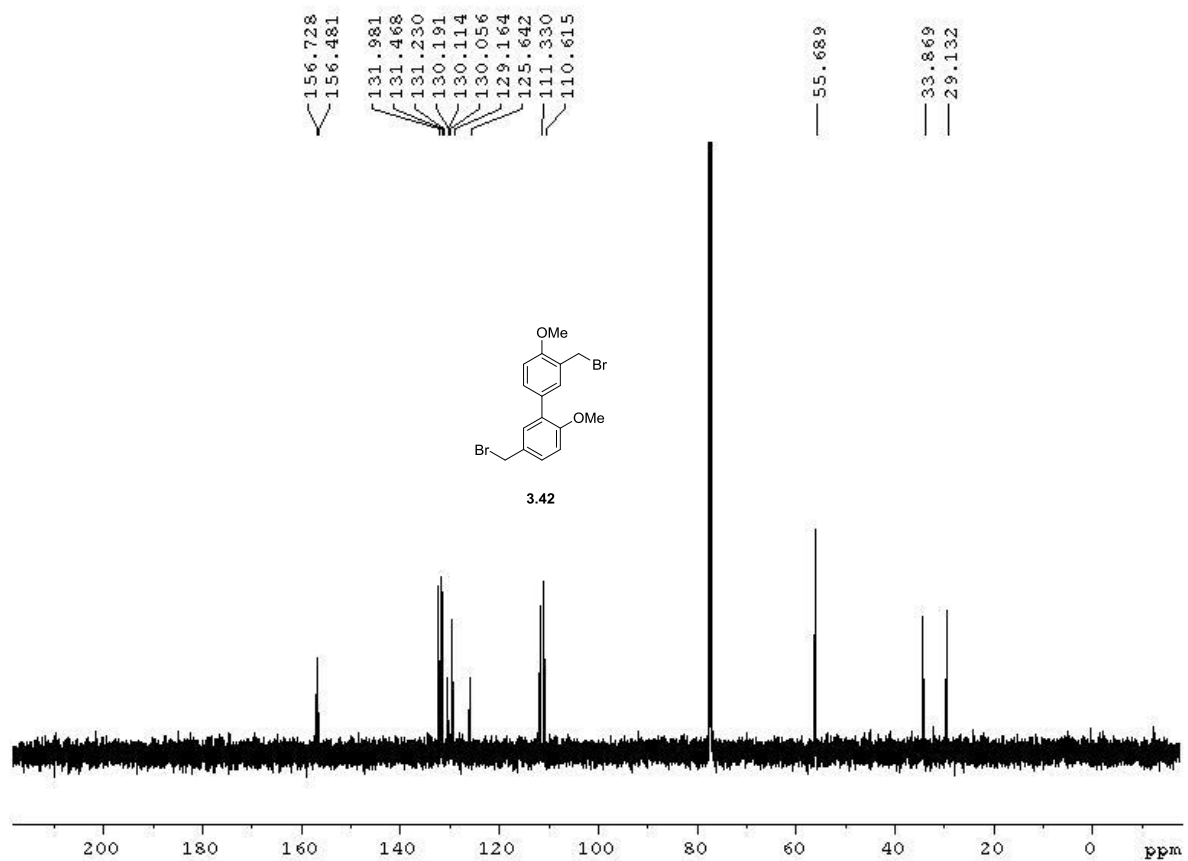
Figure A3.29 ^{13}C NMR spectrum of compound **3.42** (125 MHz, CDCl$_3$)
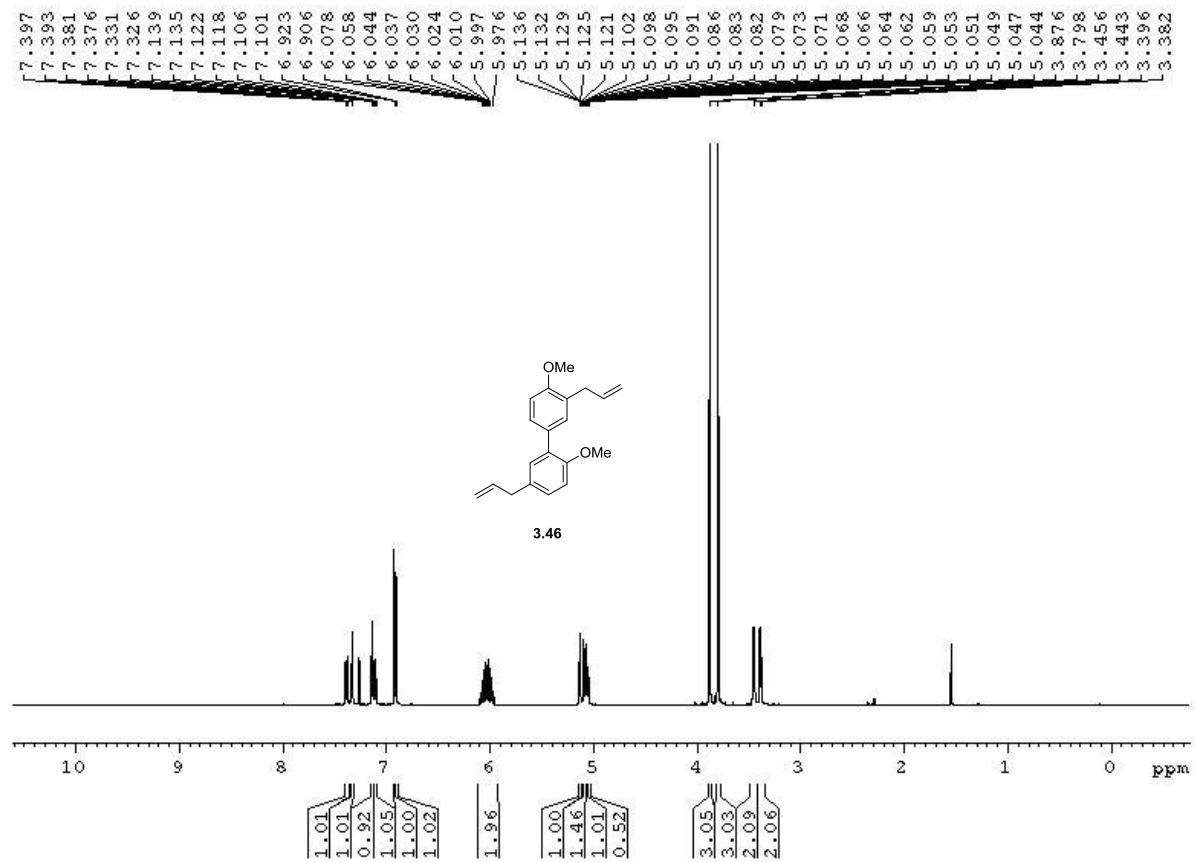
Figure A3.30 ^{1}H NMR spectrum of compound **3.46** (500 MHz, CDCl$_3$)

323
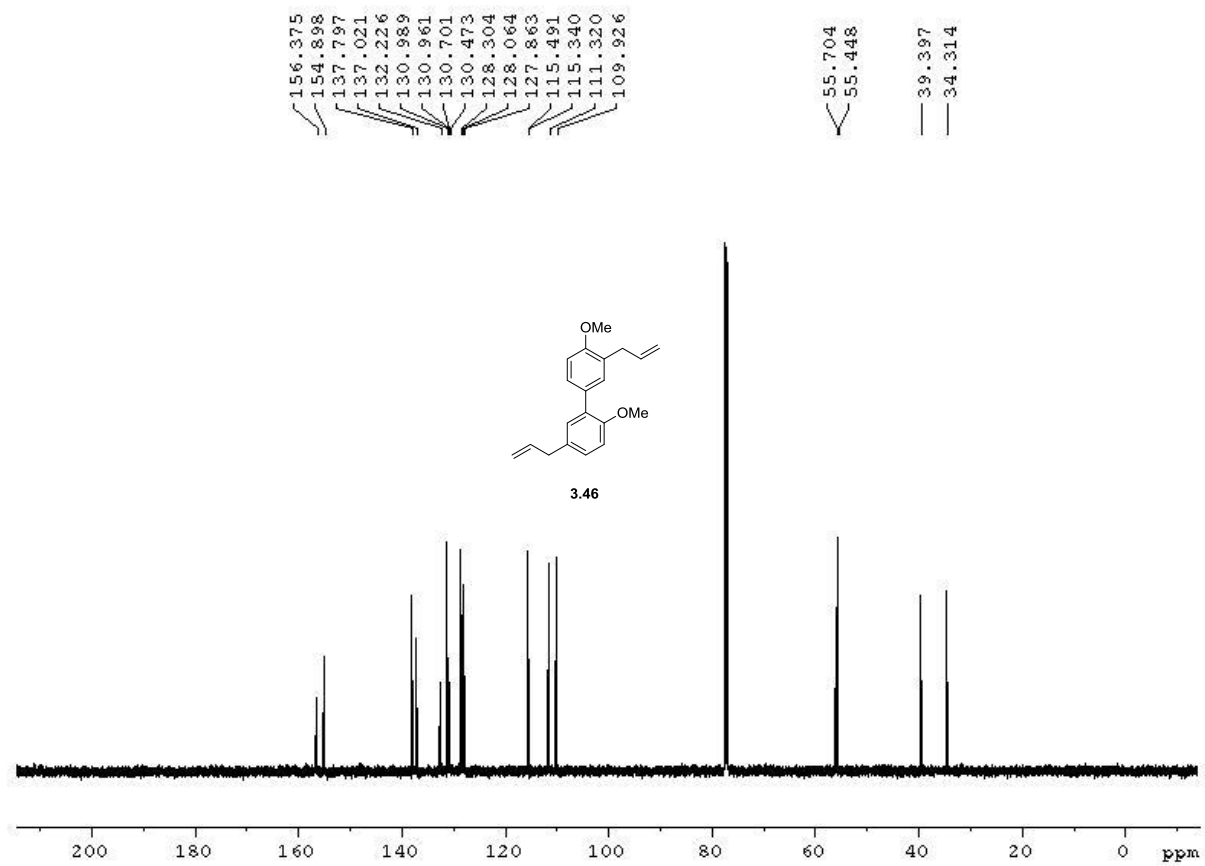
Figure A3.31 ^{13}C NMR spectrum of compound **3.46** (125 MHz, CDCl$_3$)

APPENDIX B: X-RAY CRYSTALLOGRAPHIC DATA[110]

B.1 X-Ray Structure Determination of Compound *(S)*-1.2
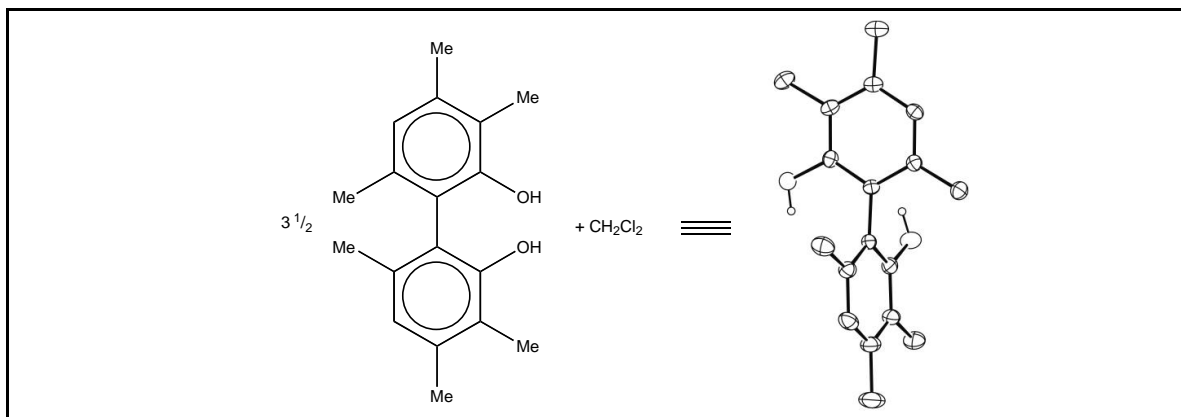
Compound *(S)*-1.2, $C_{64}H_{79}O_7Cl_2$, crystallizes in the orthorhombic space group $C222_1$(systematic absences hkl: h+k=odd) with a=18.667(2)Å, b=29.316(3)Å, c=21.428(3)Å, V=11726(2)Å^3, Z=8, and d_{calc}=1.168 g/cm^3 . X-ray intensity data were collected on a Bruker APEXII CCD area detector employing graphite-monochromated Mo-Kα radiation (λ=0.71073 Å) at a temperature of 143(1)K. Preliminary indexing was performed from a series of thirty-six 0.5° rotation frames with exposures of 10 seconds. A total of 2870 frames were collected with a crystal to detector distance of 37.605 mm, rotation widths of 0.5° and exposures of 30 seconds:

scan type	2θ	ω	φ	χ	frames

ϕ	-13.00	344.60	342.59	-39.24	739
ω	-5.50	321.57	133.99	70.63	71
ϕ	-23.00	315.83	87.00	28.88	589
ϕ	-20.50	342.55	321.55	-73.06	739
ϕ	-15.50	258.48	10.68	19.46	732

Rotation frames were integrated using SAINT [111], producing a listing of unaveraged F^2 and $\sigma(F^2)$ values which were then passed to the SHELXTL[112] program package for further processing and structure solution. A total of 154940 reflections were measured over the ranges $1.39 \leq \theta \leq 25.43°$, $-22 \leq h \leq 22$, $-35 \leq k \leq 35$, $-25 \leq l \leq 25$ yielding 10813 unique reflections (Rint = 0.0484). The intensity data were corrected for Lorentz and polarization effects and for absorption using SADABS[113] (minimum and maximum transmission 0.7143, 0.7452).

The structure was solved by direct methods (SHELXS-97[114]). The asymmetric unit consists of 3½ molecules of the title compound (one molecule lies on a crystallographic 2-fold axis at 1, y, ¾) plus a molecule of disordered dichloromethane. Refinement was by full-matrix least squares based on F^2 using SHELXL-97.[114] All reflections were used during refinement. The weighting scheme used was $w=1/[\sigma^2(F_o^2)+ (0.1094P)^2 + 8.8856P]$ where $P = (F_o^2 + 2F_c^2)/3$. Non-hydrogen atoms were refined anisotropically and hydrogen atoms were refined using a riding model. Refinement

(111) Bruker (2009) SAINT. Bruker AXS Inc., Madison, Wisconsin, USA.

(112) Bruker (2009) SHELXTL. Bruker AXS Inc., Madison, Wisconsin, USA.

(113) Sheldrick, G.M. (2007) SADABS. University of Gottingen, Germany.

(114) Sheldrick, G.M. (2008) Acta Cryst. A64,112-122.

converged to R1=0.0568 and wR2=0.1637 for 9109 observed reflections for which F > 4σ (F) and R1=0.0698 and wR2=0.1751 and GOF =1.043 for all 10813 unique, non-zero reflections and 712 variables. [115] The maximum Δ/σ in the final cycle of least squares was 0.008 and the two most prominent peaks in the final difference Fourier were +0.756 and -0.306 e/$\mathring{A}^3$.

Table B.1 lists cell information, data collection parameters, and refinement data. Final positional and equivalent isotropic thermal parameters are given in Tables B.2 and B.3. Anisotropic thermal parameters are in Table B.4. Tables B.5 and B.6 list bond distances and bond angles. Figures B.1 and B.2 are ORTEP[116] representations of the four molecules in the asymmetric unit with 30% probability thermal ellipsoids displayed.

---

(115) R1 = $\Sigma||F_o| - |F_c|| / \Sigma |F_o|$; wR2 = $[\Sigma w(F_o^2 - F_c^2)^2/\Sigma w(F_o^2)^2]^{1/2}$; GOF = $[\Sigma w(F_o^2 - F_c^2)^2/(n - p)]^{1/2}$ where n = the number of reflections and p = the number of parameters refined.

(116) "ORTEP-II: A Fortran Thermal Ellipsoid Plot Program for Crystal Structure Illustrations". C.K. Johnson (1976) ORNL-5138.
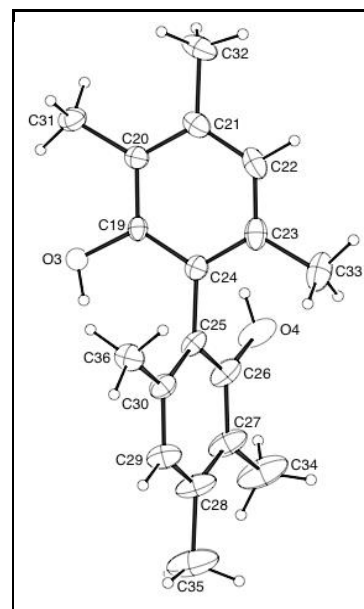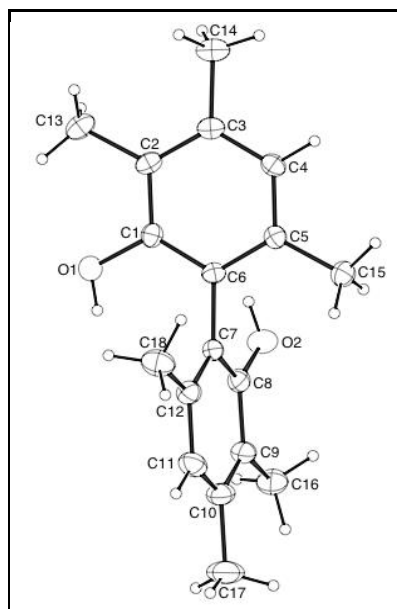
Figure B.1. ORTEP drawing of molecules no. 1 & 2 of the asymmetric unit with 30% probability thermal ellipsoids.
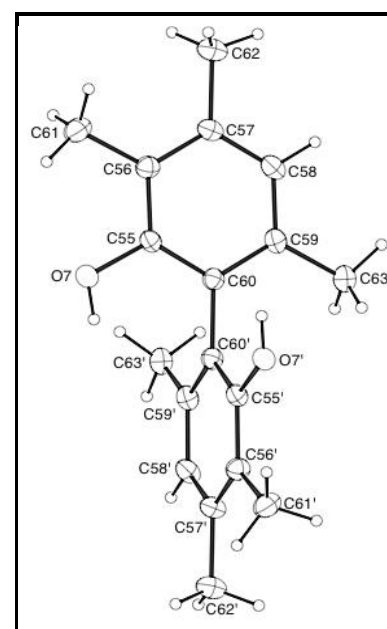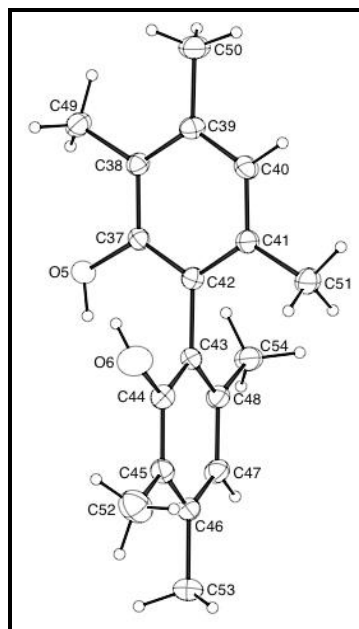
Figure B.2. ORTEP drawing of molecules no. 3 & 4 of the asymmetric unit with 30% probability thermal ellipsoids

328

Table B.1. Summary of Structure Determination of Compound (*S*)-**1.2**

Empirical formula	$C_{64}H_{79}O_7Cl_2$
Formula weight	1031.17
Temperature	143(1) K
Wavelength	0.71073 Å
Crystal system	orthorhombic
Space group	$C222_1$
Cell constants:	
a	18.667(2) Å
b	29.316(3) Å
c	21.428(3) Å
Volume	11726(2) Å^3
Z	8
Density (calculated)	1.168 Mg/m^3
Absorption coefficient	0.162 mm^{-1}
F(000)	4424
Crystal size	0.42 x 0.18 x 0.10 mm^3
Theta range for data collection	1.39 to 25.43°
Index ranges	$-22 \leq h \leq 22$, $-35 \leq k \leq 35$, $-25 \leq l \leq 25$
Reflections collected	154940
Independent reflections	10813 [R(int) = 0.0484]
Completeness to theta = 25.43°	99.9 %
Absorption correction	Semi-empirical from equivalents
Max. and min. transmission	0.7452 and 0.7143
Refinement method	Full-matrix least-squares on F^2
Data / restraints / parameters	10813 / 48 / 712
Goodness-of-fit on F^2	1.043
Final R indices [I>2sigma(I)]	R1 = 0.0568, wR2 = 0.1637
R indices (all data)	R1 = 0.0698, wR2 = 0.1751
Absolute structure parameter	0.07(16)
Largest diff. peak and hole	0.756 and -0.306 e.Å^{-3}

Table B.2. Refined Positional Parameters for (*S*)-**1.2**

Atom	x	y	z	U_{eq}, Å^2
C1	0.81286(15)	0.55693(9)	0.83239(12)	0.0325(6)
C2	0.88101(16)	0.57693(10)	0.83192(12)	0.0339(6)
C3	0.93511(15)	0.55479(10)	0.86464(13)	0.0349(6)
C4	0.92066(15)	0.51422(10)	0.89628(13)	0.0342(6)
C5	0.85228(15)	0.49517(9)	0.89718(13)	0.0319(6)
C6	0.79740(14)	0.51662(9)	0.86422(12)	0.0292(6)
C7	0.72352(14)	0.49694(9)	0.86152(13)	0.0319(6)
C8	0.70924(16)	0.46041(9)	0.82135(13)	0.0354(6)

C9	0.64235(16)	0.43874(11)	0.81936(15)	0.0417(7)
C10	0.58871(17)	0.45499(12)	0.85824(16)	0.0469(8)
C11	0.60143(18)	0.49208(13)	0.89649(16)	0.0479(8)
C12	0.66856(17)	0.51367(10)	0.89984(14)	0.0392(7)
C13	0.8931(2)	0.62005(11)	0.79540(15)	0.0465(8)
C14	1.01077(18)	0.57337(12)	0.86567(16)	0.0496(8)
C15	0.83947(18)	0.45248(10)	0.93386(14)	0.0407(7)
C16	0.6307(2)	0.39961(12)	0.77557(18)	0.0542(9)
C17	0.5154(2)	0.43246(16)	0.8588(2)	0.0709(11)
C18	0.67977(19)	0.55377(13)	0.94198(17)	0.0550(9)
O1	0.76077(12)	0.57884(8)	0.79833(11)	0.0455(5)
O2	0.76057(12)	0.44321(8)	0.78284(11)	0.0458(5)
C19	0.79726(14)	0.31105(9)	0.51919(13)	0.0309(6)
C20	0.82408(15)	0.31364(10)	0.57979(14)	0.0348(6)
C21	0.78958(18)	0.34289(11)	0.62145(15)	0.0438(7)
C22	0.73051(19)	0.36778(11)	0.60156(17)	0.0483(8)
C23	0.70360(17)	0.36488(10)	0.54160(18)	0.0456(8)
C24	0.73684(15)	0.33550(10)	0.49930(14)	0.0345(6)
C25	0.71014(16)	0.32899(9)	0.43441(15)	0.0377(7)
C26	0.65028(18)	0.30138(11)	0.42495(18)	0.0480(8)
C27	0.6202(2)	0.29480(13)	0.3661(2)	0.0614(10)
C28	0.6525(2)	0.31672(14)	0.31501(19)	0.0663(11)
C29	0.7122(2)	0.34433(12)	0.32409(17)	0.0549(9)
C30	0.74131(17)	0.35106(10)	0.38304(15)	0.0406(7)
C31	0.88803(17)	0.28575(12)	0.59801(15)	0.0456(7)
C32	0.8155(2)	0.34762(14)	0.68782(15)	0.0603(10)
C33	0.6410(2)	0.39333(14)	0.5234(2)	0.0678(11)
C34	0.5557(3)	0.26443(18)	0.3584(3)	0.0967(19)
C35	0.6252(3)	0.3094(2)	0.2488(3)	0.105(2)
C36	0.80491(19)	0.38244(12)	0.39093(16)	0.0486(8)
O3	0.83381(11)	0.28267(7)	0.47922(9)	0.0370(5)
O4	0.61769(14)	0.27993(10)	0.47377(13)	0.0643(8)
C37	0.53620(14)	0.20776(9)	0.56848(12)	0.0289(6)
C38	0.60401(15)	0.18840(9)	0.56143(13)	0.0313(6)
C39	0.66193(15)	0.20959(10)	0.59044(14)	0.0349(6)
C40	0.65020(16)	0.24896(10)	0.62618(15)	0.0378(7)
C41	0.58273(15)	0.26759(9)	0.63387(13)	0.0332(6)
C42	0.52439(14)	0.24686(9)	0.60442(13)	0.0301(6)
C43	0.45044(14)	0.26575(9)	0.61091(12)	0.0298(6)
C44	0.42887(15)	0.30223(9)	0.57328(13)	0.0326(6)
C45	0.36149(16)	0.32154(9)	0.57917(14)	0.0346(6)
C46	0.31292(16)	0.30356(10)	0.62211(13)	0.0345(6)
C47	0.33400(17)	0.26694(10)	0.65955(13)	0.0370(6)
C48	0.40177(16)	0.24793(10)	0.65417(13)	0.0344(6)
C49	0.61330(17)	0.14620(10)	0.52212(15)	0.0405(7)
C50	0.73675(18)	0.19147(13)	0.58401(19)	0.0517(8)
C51	0.57314(18)	0.30902(11)	0.67428(16)	0.0453(7)
C52	0.3455(2)	0.36194(14)	0.5402(2)	0.0662(11)
C53	0.23910(18)	0.32304(12)	0.62887(17)	0.0502(8)
C54	0.42265(19)	0.21030(13)	0.69459(14)	0.0506(8)
O5	0.48108(11)	0.18604(7)	0.53825(10)	0.0383(5)
O6	0.47488(14)	0.32025(8)	0.52956(12)	0.0563(6)
C55	0.92522(14)	0.45542(9)	0.70489(12)	0.0286(6)

C56	0.89243(15)	0.45694(9)	0.64656(13)	0.0319(6)
C57	0.92004(16)	0.42939(10)	0.59948(12)	0.0328(6)
C58	0.97859(16)	0.40168(10)	0.61212(13)	0.0356(6)
C59	1.01080(15)	0.40000(9)	0.67031(13)	0.0331(6)
C60	0.98407(13)	0.42768(9)	0.71796(12)	0.0278(5)
C61	0.82827(17)	0.48690(11)	0.63629(16)	0.0446(7)
C62	0.88834(19)	0.42920(12)	0.53475(13)	0.0436(7)
C63	1.07334(18)	0.36896(11)	0.68185(15)	0.0438(7)
O7	0.89552(11)	0.48242(7)	0.75092(9)	0.0360(4)
C64	0.5819(12)	0.5635(8)	0.6805(5)	0.149(6)
Cl1	0.5895(2)	0.5669(3)	0.7612(2)	0.170(2)
Cl2	0.6471(3)	0.5247(2)	0.6580(4)	0.199(3)
C64'	0.5964(13)	0.5555(6)	0.6545(4)	0.151(6)
Cl1'	0.6042(3)	0.5302(2)	0.7273(3)	0.167(3)
Cl2'	0.6301(4)	0.51870(19)	0.5990(3)	0.191(3)

$U_{eq}=^1/_3[U_{11}(aa^*)^2+U_{22}(bb^*)^2+U_{33}(cc^*)^2+2U_{12}aa^*bb^*\cos\gamma+2U_{13}aa^*cc^*\cos\beta+2U_{23}bb^*cc^*\cos\alpha]$

331

Table B.3. Positional Parameters for Hydrogens in Compound (*S*)-**1.2**

Atom	x	y	z	U_{iso}, Å^2
H4	0.9576	0.4995	0.9173	0.046
H11	0.5642	0.5032	0.9210	0.064
H13a	0.9232	0.6403	0.8189	0.070
H13b	0.8479	0.6346	0.7875	0.070
H13c	0.9158	0.6128	0.7564	0.070
H14a	1.0399	0.5548	0.8925	0.074
H14b	1.0102	0.6041	0.8810	0.074
H14c	1.0301	0.5730	0.8242	0.074
H15a	0.7956	0.4553	0.9569	0.061
H15b	0.8785	0.4477	0.9623	0.061
H15c	0.8361	0.4270	0.9059	0.061
H16a	0.5888	0.3830	0.7880	0.081
H16b	0.6716	0.3798	0.7767	0.081
H16c	0.6243	0.4110	0.7340	0.081
H17a	0.4860	0.4466	0.8900	0.106
H17b	0.5207	0.4006	0.8682	0.106
H17c	0.4934	0.4359	0.8186	0.106
H18a	0.7284	0.5540	0.9565	0.082
H18b	0.6479	0.5516	0.9770	0.082
H18c	0.6702	0.5814	0.9194	0.082
H1	0.7230	0.5647	0.8011	0.068
H2	0.7937	0.4615	0.7801	0.069
H22	0.7081	0.3872	0.6298	0.064
H29	0.7332	0.3586	0.2899	0.073
H31a	0.9288	0.3054	0.6030	0.068
H31b	0.8978	0.2636	0.5661	0.068
H31c	0.8785	0.2704	0.6367	0.068
H32a	0.8087	0.3193	0.7095	0.090
H32b	0.7889	0.3712	0.7084	0.090
H32c	0.8655	0.3553	0.6878	0.090
H33a	0.6536	0.4120	0.4882	0.102
H33b	0.6274	0.4125	0.5577	0.102
H33c	0.6016	0.3739	0.5123	0.102
H34a	0.5570	0.2406	0.3892	0.145
H34b	0.5560	0.2512	0.3175	0.145
H34c	0.5128	0.2821	0.3638	0.145
H35a	0.6546	0.3263	0.2201	0.157
H35b	0.5766	0.3198	0.2458	0.157
H35c	0.6273	0.2776	0.2386	0.157
H36a	0.7932	0.4060	0.4203	0.073
H36b	0.8167	0.3960	0.3514	0.073
H36c	0.8451	0.3653	0.4060	0.073
H3	0.8110	0.2798	0.4467	0.055

H4a	0.6445	0.2800	0.5041	0.097
H40	0.6891	0.2630	0.6453	0.050
H47	0.3020	0.2551	0.6886	0.049
H49a	0.6103	0.1542	0.4788	0.061
H49b	0.5762	0.1247	0.5320	0.061
H49c	0.6592	0.1328	0.5305	0.061
H50a	0.7385	0.1607	0.5991	0.078
H50b	0.7690	0.2101	0.6079	0.078
H50c	0.7506	0.1921	0.5409	0.078
H51a	0.6186	0.3179	0.6914	0.068
H51b	0.5405	0.3021	0.7076	0.068
H51c	0.5542	0.3336	0.6497	0.068
H52a	0.3638	0.3888	0.5601	0.099
H52b	0.2946	0.3648	0.5350	0.099
H52c	0.3678	0.3584	0.5000	0.099
H53a	0.2127	0.3182	0.5910	0.075
H53b	0.2424	0.3552	0.6371	0.075
H53c	0.2149	0.3082	0.6628	0.075
H54a	0.3814	0.1921	0.7041	0.076
H54b	0.4426	0.2222	0.7326	0.076
H54c	0.4578	0.1918	0.6738	0.076
H5	0.4437	0.2001	0.5442	0.057
H6	0.5001	0.2999	0.5152	0.084
H58	0.9969	0.3835	0.5803	0.047
H61a	0.7855	0.4688	0.6383	0.067
H61b	0.8316	0.5010	0.5960	0.067
H61c	0.8267	0.5100	0.6680	0.067
H62a	0.9102	0.4055	0.5105	0.065
H62b	0.8969	0.4581	0.5152	0.065
H62c	0.8377	0.4239	0.5374	0.065
H63a	1.0842	0.3524	0.6444	0.066
H63b	1.0616	0.3479	0.7146	0.066
H63c	1.1142	0.3868	0.6939	0.066
H7	0.9179	0.4790	0.7835	0.054
H64a	0.5346	0.5529	0.6686	0.199
H64b	0.5903	0.5930	0.6614	0.199
H64c	0.5465	0.5621	0.6457	0.201
H64d	0.6229	0.5839	0.6537	0.201

Table B.4. Refined Thermal Parameters (U's) for Compound (*S*)-1.2

Atom	U_{11}	U_{22}	U_{33}	U_{23}	U_{13}	U_{12}
C1	0.0381(15)	0.0323(13)	0.0271(13)	0.0018(11)	-0.0004(11)	0.0005(12)
C2	0.0386(15)	0.0348(14)	0.0284(13)	-0.0043(12)	0.0068(12)	-0.0084(12)
C3	0.0331(15)	0.0414(15)	0.0303(13)	-0.0069(12)	0.0040(12)	-0.0053(12)
C4	0.0308(14)	0.0402(15)	0.0317(14)	-0.0035(12)	-0.0041(12)	0.0013(12)
C5	0.0339(14)	0.0309(14)	0.0310(13)	-0.0028(11)	-0.0007(11)	0.0017(12)
C6	0.0301(14)	0.0318(13)	0.0259(12)	-0.0036(11)	-0.0005(10)	-0.0040(11)
C7	0.0280(13)	0.0334(14)	0.0345(14)	0.0080(11)	-0.0028(11)	-0.0008(11)
C8	0.0367(15)	0.0346(14)	0.0348(14)	0.0032(12)	-0.0068(12)	-0.0017(12)
C9	0.0328(15)	0.0443(16)	0.0481(17)	0.0073(14)	-0.0070(13)	-0.0065(13)
C10	0.0372(17)	0.0536(19)	0.0499(18)	0.0076(16)	-0.0075(14)	-0.0136(15)
C11	0.0334(16)	0.063(2)	0.0469(18)	0.0082(16)	0.0069(14)	0.0036(15)
C12	0.0372(16)	0.0416(16)	0.0388(16)	0.0052(13)	0.0006(13)	-0.0029(13)
C13	0.0525(19)	0.0454(17)	0.0415(17)	0.0036(14)	0.0107(15)	-0.0112(15)
C14	0.0384(17)	0.060(2)	0.0499(18)	-0.0109(17)	0.0061(15)	-0.0124(16)
C15	0.0434(17)	0.0412(16)	0.0375(15)	0.0047(13)	0.0005(13)	-0.0002(14)
C16	0.049(2)	0.053(2)	0.061(2)	-0.0064(16)	-0.0151(17)	-0.0137(16)
C17	0.0386(19)	0.086(3)	0.088(3)	0.003(3)	0.000(2)	-0.0198(19)
C18	0.0444(19)	0.067(2)	0.053(2)	-0.0111(17)	0.0072(16)	0.0002(17)
O1	0.0401(12)	0.0466(12)	0.0498(12)	0.0160(10)	-0.0059(10)	-0.0019(10)
O2	0.0411(12)	0.0461(12)	0.0501(12)	-0.0106(10)	0.0032(10)	-0.0080(10)
C19	0.0227(12)	0.0317(13)	0.0383(14)	-0.0009(11)	0.0040(11)	-0.0028(11)
C20	0.0316(14)	0.0392(15)	0.0336(14)	0.0006(12)	0.0015(11)	-0.0094(12)
C21	0.0450(17)	0.0472(17)	0.0391(16)	-0.0059(14)	0.0074(14)	-0.0146(15)
C22	0.0457(19)	0.0432(17)	0.056(2)	-0.0165(15)	0.0183(16)	-0.0094(14)
C23	0.0326(16)	0.0359(15)	0.068(2)	-0.0034(15)	0.0103(15)	-0.0029(13)
C24	0.0287(14)	0.0336(14)	0.0414(15)	0.0014(12)	0.0013(12)	-0.0079(11)
C25	0.0313(14)	0.0301(13)	0.0518(18)	0.0069(13)	-0.0106(13)	0.0000(12)
C26	0.0404(18)	0.0393(16)	0.064(2)	0.0172(16)	-0.0150(16)	-0.0078(14)
C27	0.057(2)	0.054(2)	0.073(2)	0.0208(19)	-0.032(2)	-0.0236(18)
C28	0.069(3)	0.069(2)	0.060(2)	0.014(2)	-0.036(2)	-0.023(2)
C29	0.064(2)	0.0525(19)	0.0483(19)	0.0114(16)	-0.0153(17)	-0.0108(17)
C30	0.0377(16)	0.0359(15)	0.0483(17)	0.0017(13)	-0.0085(14)	-0.0033(13)
C31	0.0390(17)	0.0570(19)	0.0410(16)	0.0054(15)	-0.0057(14)	-0.0084(15)
C32	0.078(3)	0.070(2)	0.0339(17)	-0.0109(16)	0.0057(17)	-0.023(2)
C33	0.044(2)	0.051(2)	0.108(3)	-0.010(2)	0.001(2)	0.0091(17)
C34	0.089(3)	0.086(3)	0.115(4)	0.032(3)	-0.059(3)	-0.053(3)
C35	0.112(4)	0.121(4)	0.081(3)	0.022(3)	-0.053(3)	-0.046(4)
C36	0.0482(19)	0.0515(18)	0.0461(18)	0.0019(15)	0.0034(15)	-0.0170(15)
O3	0.0328(10)	0.0447(11)	0.0334(10)	-0.0055(9)	-0.0009(8)	0.0035(9)
O4	0.0489(14)	0.0705(16)	0.0736(17)	0.0333(15)	-0.0247(13)	-0.0281(13)
C37	0.0275(13)	0.0321(13)	0.0272(13)	0.0013(11)	-0.0007(11)	-0.0021(11)
C38	0.0300(14)	0.0327(14)	0.0311(13)	-0.0008(11)	0.0028(11)	-0.0005(11)
C39	0.0292(14)	0.0367(15)	0.0389(15)	-0.0003(12)	0.0042(12)	0.0006(12)

334

C40	0.0283(14)	0.0398(15)	0.0452(16)	-0.0092(13)	-0.0067(12)	-0.0023(12)
C41	0.0312(14)	0.0325(14)	0.0360(14)	-0.0043(12)	-0.0009(12)	-0.0006(11)
C42	0.0302(14)	0.0291(13)	0.0308(13)	0.0000(11)	-0.0001(11)	-0.0001(11)
C43	0.0269(13)	0.0327(14)	0.0299(13)	-0.0040(11)	-0.0028(11)	0.0005(11)
C44	0.0341(15)	0.0285(13)	0.0351(14)	0.0001(11)	0.0026(12)	-0.0041(11)
C45	0.0389(16)	0.0287(14)	0.0361(15)	-0.0003(11)	-0.0053(12)	0.0028(12)
C46	0.0343(15)	0.0336(14)	0.0357(15)	-0.0061(12)	-0.0028(12)	0.0053(12)
C47	0.0382(16)	0.0403(15)	0.0324(14)	0.0019(12)	0.0059(12)	0.0044(13)
C48	0.0361(15)	0.0369(15)	0.0301(13)	0.0013(11)	0.0016(12)	0.0062(12)
C49	0.0376(16)	0.0404(16)	0.0436(16)	-0.0095(13)	0.0044(14)	0.0009(13)
C50	0.0327(16)	0.055(2)	0.068(2)	-0.0123(17)	0.0011(16)	0.0054(15)
C51	0.0412(17)	0.0417(16)	0.0531(18)	-0.0184(15)	-0.0032(15)	-0.0005(14)
C52	0.067(3)	0.057(2)	0.074(3)	0.007(2)	-0.013(2)	0.0057(19)
C53	0.0369(17)	0.057(2)	0.057(2)	-0.0049(16)	-0.0025(15)	0.0150(15)
C54	0.0462(18)	0.073(2)	0.0329(15)	0.0107(15)	0.0055(14)	0.0226(17)
O5	0.0308(10)	0.0382(10)	0.0459(12)	-0.0120(9)	-0.0061(9)	0.0013(8)
O6	0.0548(14)	0.0474(13)	0.0667(16)	0.0135(12)	0.0119(12)	-0.0021(11)
C55	0.0284(13)	0.0302(13)	0.0272(13)	-0.0025(11)	0.0038(11)	-0.0018(11)
C56	0.0304(14)	0.0339(14)	0.0314(14)	0.0011(11)	-0.0011(11)	-0.0035(11)
C57	0.0373(15)	0.0351(14)	0.0260(13)	-0.0008(11)	0.0001(11)	-0.0065(12)
C58	0.0390(16)	0.0384(15)	0.0294(14)	-0.0062(12)	0.0060(12)	-0.0050(12)
C59	0.0315(14)	0.0343(14)	0.0337(14)	-0.0025(11)	0.0057(12)	0.0000(12)
C60	0.0257(13)	0.0299(13)	0.0279(13)	0.0003(11)	0.0018(10)	-0.0027(11)
C61	0.0410(17)	0.0482(18)	0.0446(17)	0.0035(15)	-0.0089(14)	0.0065(14)
C62	0.0510(19)	0.0489(17)	0.0309(14)	-0.0025(13)	-0.0053(13)	-0.0067(15)
C63	0.0406(17)	0.0485(17)	0.0422(16)	-0.0058(14)	0.0024(14)	0.0124(14)
O7	0.0353(11)	0.0418(10)	0.0310(10)	-0.0080(9)	-0.0008(8)	0.0055(9)
C64	0.123(14)	0.177(15)	0.147(9)	0.007(14)	0.029(12)	-0.001(10)
Cl1	0.086(2)	0.288(7)	0.135(3)	0.071(4)	-0.031(2)	-0.061(4)
Cl2	0.097(3)	0.181(5)	0.320(9)	-0.008(7)	0.026(5)	0.013(3)
C64'	0.107(12)	0.187(15)	0.159(10)	0.069(10)	0.006(13)	0.050(11)
Cl1'	0.142(4)	0.188(5)	0.172(5)	0.091(4)	-0.079(4)	-0.065(4)
Cl2'	0.180(6)	0.118(3)	0.274(7)	0.062(4)	0.082(6)	-0.004(3)

The form of the anisotropic displacement parameter is:

$$\exp[-2\pi^2 \, (a^{*2}U_{11}h^2 + b^{*2}U_{22}k^2 + c^{*2}U_{33}l^2 + 2b^*c^*U_{23}kl + 2a^*c^*U_{13}hl + 2a^*b^*U_{12}hk)]$$

335

Table B.5. Bond Distances in Compound (*S*)-1.2, Å

C1-O1	1.375(3)	C1-C6	1.395(4)	C1-C2	1.401(4)
C2-C3	1.390(4)	C2-C13	1.504(4)	C3-C4	1.395(4)
C3-C14	1.514(4)	C4-C5	1.394(4)	C5-C6	1.394(4)
C5-C15	1.497(4)	C6-C7	1.496(4)	C7-C8	1.400(4)
C7-C12	1.403(4)	C8-O2	1.361(4)	C8-C9	1.402(4)
C9-C10	1.387(5)	C9-C16	1.498(5)	C10-C11	1.382(5)
C10-C17	1.519(5)	C11-C12	1.406(5)	C12-C18	1.497(5)
C19-O3	1.375(3)	C19-C20	1.394(4)	C19-C24	1.403(4)
C20-C21	1.395(4)	C20-C31	1.499(5)	C21-C22	1.389(5)
C21-C32	1.509(5)	C22-C23	1.382(5)	C23-C24	1.396(4)
C23-C33	1.488(5)	C24-C25	1.489(4)	C25-C26	1.394(4)
C25-C30	1.403(4)	C26-O4	1.364(4)	C26-C27	1.394(5)
C27-C28	1.405(6)	C27-C34	1.508(5)	C28-C29	1.392(5)
C28-C35	1.523(6)	C29-C30	1.389(5)	C30-C36	1.511(4)
C37-O5	1.373(3)	C37-C38	1.395(4)	C37-C42	1.398(4)
C38-C39	1.393(4)	C38-C49	1.507(4)	C39-C40	1.403(4)
C39-C50	1.501(4)	C40-C41	1.383(4)	C41-C42	1.398(4)
C41-C51	1.502(4)	C42-C43	1.494(4)	C43-C44	1.398(4)
C43-C48	1.399(4)	C44-O6	1.376(4)	C44-C45	1.385(4)
C45-C46	1.395(4)	C45-C52	1.480(5)	C46-C47	1.397(4)
C46-C53	1.499(4)	C47-C48	1.387(4)	C48-C54	1.456(4)
C55-O7	1.381(3)	C55-C56	1.393(4)	C55-C60	1.395(4)
C56-C57	1.391(4)	C56-C61	1.501(4)	C57-C58	1.389(4)
C57-C62	1.508(4)	C58-C59	1.385(4)	C59-C60	1.396(4)
C59-C63	1.501(4)	C60-C60#1	1.496(5)	C64-Cl2	1.736(9)
C64-Cl1	1.737(9)	C64'-Cl2'	1.724(10)	C64'-Cl1'	1.733(9)

Symmetry transformations used to generate equivalent atoms:

#1 -x+2,y,-z+3/2

Table B.6. Bond Angles in (*S*)-**1.2**, °

O1-C1-C6	120.6(2)	O1-C1-C2	116.3(2)	C6-C1-C2	123.1(3)
C3-C2-C1	117.4(2)	C3-C2-C13	123.1(3)	C1-C2-C13	119.4(3)
C2-C3-C4	120.2(3)	C2-C3-C14	121.1(3)	C4-C3-C14	118.7(3)
C5-C4-C3	121.7(3)	C4-C5-C6	119.0(3)	C4-C5-C15	119.2(3)
C6-C5-C15	121.7(3)	C5-C6-C1	118.6(3)	C5-C6-C7	121.5(2)
C1-C6-C7	119.9(2)	C8-C7-C12	119.2(3)	C8-C7-C6	119.6(2)
C12-C7-C6	121.1(3)	O2-C8-C7	121.5(3)	O2-C8-C9	116.2(3)
C7-C8-C9	122.4(3)	C10-C9-C8	118.0(3)	C10-C9-C16	122.3(3)
C8-C9-C16	119.7(3)	C11-C10-C9	120.1(3)	C11-C10-C17	119.5(3)
C9-C10-C17	120.4(3)	C10-C11-C12	122.5(3)	C7-C12-C11	117.7(3)
C7-C12-C18	121.7(3)	C11-C12-C18	120.6(3)	O3-C19-C20	115.8(2)
O3-C19-C24	121.3(2)	C20-C19-C24	123.0(3)	C19-C20-C21	117.6(3)
C19-C20-C31	119.9(3)	C21-C20-C31	122.4(3)	C22-C21-C20	119.5(3)
C22-C21-C32	119.7(3)	C20-C21-C32	120.7(3)	C23-C22-C21	122.8(3)
C22-C23-C24	118.7(3)	C22-C23-C33	119.7(3)	C24-C23-C33	121.6(3)
C23-C24-C19	118.4(3)	C23-C24-C25	122.4(3)	C19-C24-C25	119.2(3)
C26-C25-C30	119.1(3)	C26-C25-C24	118.6(3)	C30-C25-C24	122.3(3)
O4-C26-C27	116.8(3)	O4-C26-C25	120.9(3)	C27-C26-C25	122.3(3)
C26-C27-C28	118.0(3)	C26-C27-C34	120.1(4)	C28-C27-C34	121.9(4)
C29-C28-C27	120.0(3)	C29-C28-C35	118.7(4)	C27-C28-C35	121.3(4)
C30-C29-C28	121.5(3)	C29-C30-C25	119.1(3)	C29-C30-C36	119.7(3)
C25-C30-C36	121.2(3)	O5-C37-C38	116.1(2)	O5-C37-C42	121.5(2)
C38-C37-C42	122.4(2)	C39-C38-C37	118.3(2)	C39-C38-C49	121.7(3)
C37-C38-C49	119.9(2)	C38-C39-C40	119.3(3)	C38-C39-C50	121.6(3)
C40-C39-C50	119.1(3)	C41-C40-C39	122.2(3)	C40-C41-C42	119.0(2)
C40-C41-C51	119.8(3)	C42-C41-C51	121.3(3)	C41-C42-C37	118.8(2)
C41-C42-C43	121.1(2)	C37-C42-C43	120.1(2)	C44-C43-C48	118.7(3)
C44-C43-C42	119.7(2)	C48-C43-C42	121.5(2)	O6-C44-C45	118.2(3)
O6-C44-C43	120.4(3)	C45-C44-C43	121.4(3)	C44-C45-C46	119.7(3)
C44-C45-C52	117.3(3)	C46-C45-C52	123.0(3)	C45-C46-C47	119.1(3)
C45-C46-C53	121.2(3)	C47-C46-C53	119.8(3)	C48-C47-C46	121.2(3)
C47-C48-C43	119.8(3)	C47-C48-C54	120.0(3)	C43-C48-C54	120.2(3)
O7-C55-C56	116.5(2)	O7-C55-C60	120.5(2)	C56-C55-C60	123.0(2)
C57-C56-C55	118.0(3)	C57-C56-C61	121.9(3)	C55-C56-C61	120.1(3)
C58-C57-C56	119.3(2)	C58-C57-C62	119.1(3)	C56-C57-C62	121.6(3)
C59-C58-C57	122.5(3)	C58-C59-C60	118.9(3)	C58-C59-C63	120.5(3)
C60-C59-C63	120.7(3)	C55-C60-C59	118.3(2)	C55-C60-C60#1	119.8(2)
C59-C60-C60#1	121.9(2)	Cl2-C64-Cl1	104.9(7)	Cl2'-C64'-Cl1'	108.9(7)

Symmetry transformations used to generate equivalent atoms:

#1 -x+2,y,-z+3/2

B.2 X-Ray Structure Determination of Compound 2.44 dimer
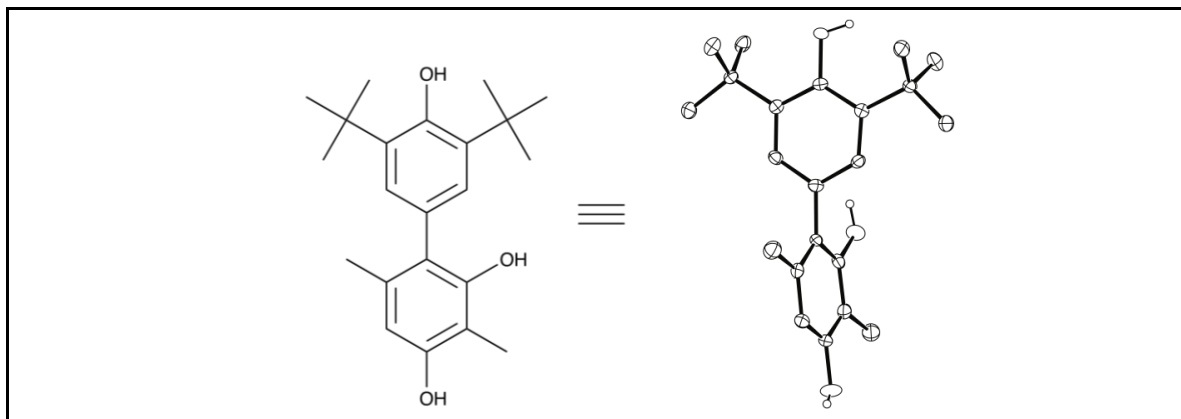
Compound **2.44 dimer**, $C_{22}H_{30}O_3$, crystallizes in the monoclinic space group $P2_1/c$ (systematic absences 0k0: k=odd and h0l: l=odd) with a=22.703(2)Å, b=5.6209(5)Å, c=31.063(3)Å, β=103.463(2)°, V=3855.1(6)Å^3, Z=8, and d_{calc}=1.180 g/cm^3 . X-ray intensity data were collected on a Bruker APEXII CCD area detector employing graphite-monochromated Mo-Kα radiation (λ=0.71073 Å) at a temperature of 100(1)K. Preliminary indexing was performed from a series of thirty-six 0.5° rotation frames with exposures of 10 seconds. A total of 1560 frames were collected with a crystal to detector distance of 44.9 mm, rotation widths of 0.5° and exposures of 10 seconds:

scan type	2θ	ω	φ	χ	frames
φ	-25.50	321.01	15.44	32.61	730
ω	-23.00	330.56	32.55	-99.10	91
φ	-28.00	327.36	13.34	30.75	739

Rotation frames were integrated using SAINT,[111] producing a listing of unaveraged F^2 and σ (F^2) values which were then passed to the SHELXTL[112] program package for further processing and structure solution. A total of 39587 reflections were measured over the ranges 1.84 ≤ θ ≤ 25.37°, -27 ≤ h ≤ 27, -6 ≤ k ≤ 6, -37 ≤ l ≤ 37 yielding 7060 unique reflections (Rint = 0.0308). The intensity data were corrected for Lorentz and polarization effects and for absorption using SADABS[113] (minimum and

338

maximum transmission 0.7099, 0.7452).

The structure was solved by direct methods (SHELXS-97[114]). Refinement was by full-matrix least squares based on F^2 using SHELXL-97. All reflections were used during refinement. The weighting scheme used was $w = 1/[\sigma^2(F_o^2) + (0.0859P)^2 + 1.9383P]$ where $P = (F_o^2 + 2F_c^2)/3$. Non-hydrogen atoms were refined anisotropically and hydrogen atoms were refined using a riding model. Refinement converged to R1=0.0444 and wR2=0.1263 for 5462 observed reflections for which $F > 4\sigma$ (F) and R1=0.0640 and wR2=0.1528 and GOF =1.056 for all 7060 unique, non-zero reflections and 474 variables.[115] The maximum Δ/σ in the final cycle of least squares was 0.020 and the two most prominent peaks in the final difference Fourier were +0.337 and -0.399 e/Å^3.

Table B.8 lists cell information, data collection parameters, and refinement data. Final positional and equivalent isotropic thermal parameters are given in **Tables B.9** and **B.10**. Anisotropic thermal parameters are in Table B.11. Tables B.12 and B.13 list bond distances and bond angles. **Figures B.3** and **B.4** are ORTEP[116] representations of the molecule with 50% probability thermal ellipsoids displayed.
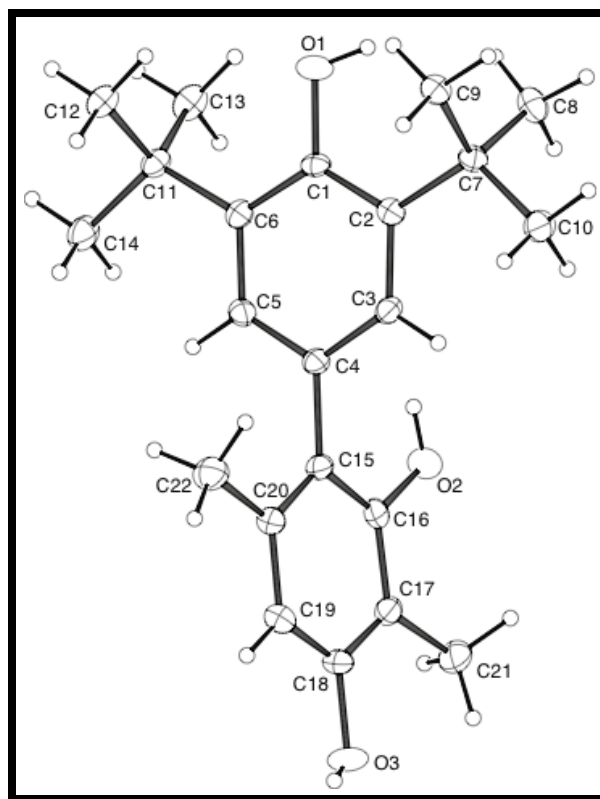
Figure B.3. ORTEP drawing of molecule no. 1 of the asymmetric unit with 50% probability thermal ellipsoids.
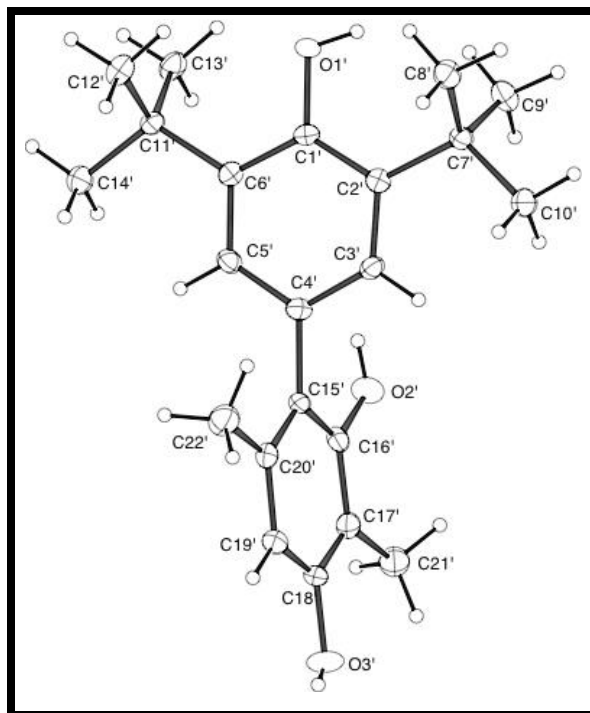
Figure B.4. ORTEP drawing of molecule no. 2 of the asymmetric unit with 50% probability thermal ellipsoids.

Table B.7. Summary of Structure Determination of Compound **2.44 dimer**

Empirical formula	$C_{22}H_{30}O_3$
Formula weight	342.46
Temperature	100(1) K
Wavelength	0.71073 Å
Crystal system	monoclinic
Space group	$P2_1/c$
Cell constants:	
a	22.703(2) Å
b	5.6209(5) Å
c	31.063(3) Å
β	103.463(2)°
Volume	3855.1(6) Å^3
Z	8
Density (calculated)	1.180 Mg/m^3
Absorption coefficient	0.077 mm^{-1}
F(000)	1488
Crystal size	0.42 x 0.16 x 0.06 mm^3
Theta range for data collection	1.84 to 25.37°
Index ranges	$-27 \leq h \leq 27$, $-6 \leq k \leq 6$, $-37 \leq l \leq 37$
Reflections collected	39587
Independent reflections	7060 [R(int) = 0.0308]
Completeness to theta = 25.37°	99.7 %
Absorption correction	Semi-empirical from equivalents
Max. and min. transmission	0.7452 and 0.7099
Refinement method	Full-matrix least-squares on F^2
Data / restraints / parameters	7060 / 0 / 474
Goodness-of-fit on F^2	1.056
Final R indices [I>2sigma(I)]	R1 = 0.0444, wR2 = 0.1263
R indices (all data)	R1 = 0.0640, wR2 = 0.1528
Largest diff. peak and hole	0.337 and -0.399 e.Å^{-3}

Table B.8. Refined Positional Parameters for Compound **2.44 dimer**

Atom	x	y	z	U_{eq}, Å^2
C1	0.54649(8)	0.1057(3)	0.09101(6)	0.0142(4)
C2	0.60330(8)	0.2196(3)	0.10266(6)	0.0149(4)
C3	0.63238(8)	0.2215(3)	0.14753(6)	0.0161(4)
C4	0.60702(8)	0.1212(3)	0.17980(6)	0.0154(4)
C5	0.55030(8)	0.0165(3)	0.16702(6)	0.0161(4)
C6	0.51834(8)	0.0046(3)	0.12279(6)	0.0152(4)
C7	0.63337(8)	0.3379(3)	0.06834(6)	0.0164(4)
C8	0.65043(9)	0.1501(3)	0.03725(6)	0.0219(4)
C9	0.59157(8)	0.5291(3)	0.04127(6)	0.0178(4)
C10	0.69175(9)	0.4685(4)	0.09049(6)	0.0233(4)
C11	0.45552(8)	-0.1152(3)	0.11024(6)	0.0171(4)
C12	0.40678(8)	0.0645(3)	0.08850(6)	0.0204(4)
C13	0.45598(9)	-0.3277(3)	0.07920(7)	0.0226(4)
C14	0.43610(9)	-0.2126(4)	0.15105(7)	0.0249(4)
C15	0.64148(8)	0.1259(3)	0.22723(6)	0.0173(4)
C16	0.68753(8)	-0.0410(3)	0.24164(6)	0.0190(4)
C17	0.72419(8)	-0.0421(4)	0.28431(6)	0.0210(4)
C18	0.71175(8)	0.1298(4)	0.31319(6)	0.0236(4)
C19	0.66597(9)	0.2952(4)	0.30041(6)	0.0238(4)
C20	0.63078(8)	0.2970(3)	0.25719(6)	0.0193(4)
C21	0.77565(9)	-0.2171(4)	0.29724(7)	0.0279(5)
C22	0.58267(9)	0.4817(4)	0.24276(7)	0.0264(5)
O1	0.51606(6)	0.0922(2)	0.04721(4)	0.0222(3)
O2	0.69923(6)	-0.2129(3)	0.21342(4)	0.0249(3)
O3	0.74713(7)	0.1286(3)	0.35607(4)	0.0349(4)
C1'	0.95300(8)	0.7716(3)	0.65809(6)	0.0143(4)
C2'	0.89497(8)	0.8761(3)	0.64483(6)	0.0147(4)
C3'	0.86645(8)	0.8601(3)	0.60005(6)	0.0160(4)
C4'	0.89331(8)	0.7500(3)	0.56918(6)	0.0162(4)
C5'	0.95102(8)	0.6549(3)	0.58377(6)	0.0167(4)
C6'	0.98236(8)	0.6628(3)	0.62798(6)	0.0149(4)
C7'	0.86260(8)	0.9971(3)	0.67761(6)	0.0155(4)
C8'	0.90181(9)	1.1927(3)	0.70487(6)	0.0219(4)
C9'	0.84403(9)	0.8112(3)	0.70832(6)	0.0223(4)
C10'	0.80419(8)	1.1223(4)	0.65330(6)	0.0222(4)
C11'	1.04615(8)	0.5522(3)	0.64277(6)	0.0162(4)
C12'	1.09275(8)	0.7473(3)	0.66166(7)	0.0226(4)
C13'	1.04709(8)	0.3574(3)	0.67747(6)	0.0204(4)
C14'	1.06668(9)	0.4360(4)	0.60415(6)	0.0245(4)
C15'	0.85782(8)	0.7270(3)	0.52225(6)	0.0156(4)
C16'	0.81407(8)	0.5478(3)	0.51248(6)	0.0184(4)
C17'	0.77511(8)	0.5206(4)	0.47106(6)	0.0216(4)
C18'	0.78280(8)	0.6777(4)	0.43834(6)	0.0229(4)

	0.82696(8)	0.8527(4)	0.44652(6)	0.0224(4)
C19'	0.82696(8)	0.8527(4)	0.44652(6)	0.0224(4)
C20'	0.86471(8)	0.8813(3)	0.48851(6)	0.0187(4)
C21'	0.72637(9)	0.3340(4)	0.46264(7)	0.0282(5)
C22'	0.91161(9)	1.0755(4)	0.49680(7)	0.0264(4)
O1'	0.98382(6)	0.7716(2)	0.70210(4)	0.0181(3)
O2'	0.80751(6)	0.3863(2)	0.54416(4)	0.0243(3)
O3'	0.74451(7)	0.6513(3)	0.39686(4)	0.0357(4)

$$U_{eq}={}^1/_3[U_{11}(aa^*)^2+U_{22}(bb^*)^2+U_{33}(cc^*)^2+2U_{12}aa^*bb^*\cos\gamma+2U_{13}aa^*cc^*\cos\beta+2U_{23}bb^*cc^*\cos\alpha]$$

Table B.9. Positional Parameters for Hydrogens in Compound **2.44 dimer**

Atom	x	y	z	U_{iso}, Å^2
H3	0.6703	0.2930	0.1561	0.021
H5	0.5329	-0.0482	0.1887	0.021
H8a	0.6720	0.2252	0.0178	0.033
H8b	0.6143	0.0773	0.0201	0.033
H8c	0.6756	0.0307	0.0545	0.033
H9a	0.6108	0.5964	0.0196	0.027
H9b	0.5842	0.6522	0.0608	0.027
H9c	0.5538	0.4576	0.0266	0.027
H10a	0.7205	0.3567	0.1067	0.035
H10b	0.6829	0.5869	0.1104	0.035
H10c	0.7084	0.5438	0.0682	0.035
H12a	0.3683	-0.0143	0.0802	0.031
H12b	0.4169	0.1304	0.0626	0.031
H12c	0.4046	0.1898	0.1091	0.031
H13a	0.4164	-0.3979	0.0715	0.034
H13b	0.4847	-0.4438	0.0939	0.034
H13c	0.4671	-0.2742	0.0528	0.034
H14a	0.4349	-0.0850	0.1714	0.037
H14b	0.4646	-0.3307	0.1653	0.037
H14c	0.3966	-0.2831	0.1420	0.037
H19	0.6586	0.4060	0.3208	0.032
H21a	0.7602	-0.3675	0.3043	0.042
H21b	0.8046	-0.1582	0.3226	0.042
H21c	0.7949	-0.2372	0.2730	0.042
H22a	0.5863	0.5494	0.2151	0.040
H22b	0.5873	0.6045	0.2648	0.040
H22c	0.5435	0.4095	0.2391	0.040
H1	0.5395	0.1224	0.0314	0.033
H2	0.6755	-0.1986	0.1892	0.037
H3a	0.7463	0.2607	0.3671	0.052
H3'	0.8280	0.9254	0.5904	0.021
H5'	0.9694	0.5833	0.5633	0.022
H8a'	0.8801	1.2644	0.7246	0.033

H8b'	0.9111	1.3116	0.6853	0.033
H8c'	0.9387	1.1241	0.7218	0.033
H9a'	0.8796	0.7360	0.7258	0.033
H9b'	0.8185	0.6935	0.6908	0.033
H9c'	0.8223	0.8882	0.7275	0.033
H10a'	0.7862	1.2017	0.6744	0.033
H10b'	0.7763	1.0067	0.6373	0.033
H10c'	0.8135	1.2368	0.6329	0.033
H12a'	1.0822	0.8199	0.6868	0.034
H12b'	1.0927	0.8658	0.6394	0.034
H12c'	1.1324	0.6778	0.6705	0.034
H13a'	1.0188	0.2347	0.6651	0.031
H13b'	1.0361	0.4247	0.7029	0.031
H13c'	1.0870	0.2908	0.6861	0.031
H14a'	1.1066	0.3718	0.6145	0.037
H14b'	1.0671	0.5530	0.5817	0.037
H14c'	1.0392	0.3105	0.5920	0.037
H19'	0.8315	0.9526	0.4236	0.030
H21a'	0.7431	0.1853	0.4559	0.042
H21b'	0.6944	0.3815	0.4381	0.042
H21c'	0.7105	0.3158	0.4885	0.042
H22a'	0.9187	1.1261	0.5271	0.040
H22b'	0.8974	1.2078	0.4777	0.040
H22c'	0.9487	1.0165	0.4909	0.040
H1'	0.9602	0.8031	0.7177	0.027
H2'	0.8328	0.4130	0.5672	0.036
H3a'	0.7450	0.7732	0.3824	0.054

Table B.10. Refined Thermal Parameters (U's) for Compound **2.44 dimer**

Atom	U_{11}	U_{22}	U_{33}	U_{23}	U_{13}	U_{12}
C1	0.0163(9)	0.0127(8)	0.0122(8)	0.0006(7)	0.0005(7)	0.0037(7)
C2	0.0172(9)	0.0126(8)	0.0149(9)	0.0006(7)	0.0041(7)	0.0020(7)
C3	0.0131(8)	0.0175(9)	0.0168(9)	0.0012(7)	0.0017(7)	0.0003(7)
C4	0.0149(9)	0.0165(9)	0.0144(9)	0.0017(7)	0.0023(7)	0.0033(7)
C5	0.0167(9)	0.0169(9)	0.0150(9)	0.0038(7)	0.0046(7)	0.0033(7)
C6	0.0145(9)	0.0126(8)	0.0180(9)	0.0013(7)	0.0027(7)	0.0027(7)
C7	0.0183(9)	0.0165(9)	0.0143(9)	0.0033(7)	0.0037(7)	0.0006(7)
C8	0.0255(10)	0.0198(10)	0.0231(10)	0.0034(8)	0.0113(8)	0.0026(8)
C9	0.0212(9)	0.0147(9)	0.0180(9)	0.0033(7)	0.0054(7)	-0.0002(7)
C10	0.0202(10)	0.0278(10)	0.0214(10)	0.0061(8)	0.0042(8)	-0.0055(8)
C11	0.0153(9)	0.0157(9)	0.0192(9)	0.0024(7)	0.0014(7)	0.0002(7)
C12	0.0166(9)	0.0188(9)	0.0240(10)	0.0009(8)	0.0011(7)	0.0003(8)
C13	0.0207(10)	0.0154(9)	0.0300(11)	-0.0002(8)	0.0025(8)	-0.0029(8)
C14	0.0188(10)	0.0283(11)	0.0269(11)	0.0071(9)	0.0040(8)	-0.0049(8)
C15	0.0139(9)	0.0230(10)	0.0142(9)	0.0038(7)	0.0015(7)	-0.0014(7)

345

C16	0.0164(9)	0.0249(10)	0.0174(9)	0.0031(8)	0.0074(7)	-0.0004(8)
C17	0.0143(9)	0.0299(10)	0.0184(9)	0.0070(8)	0.0030(7)	-0.0001(8)
C18	0.0188(10)	0.0381(11)	0.0127(9)	0.0031(8)	0.0012(7)	-0.0025(8)
C19	0.0230(10)	0.0327(11)	0.0162(9)	-0.0028(8)	0.0057(8)	-0.0011(9)
C20	0.0170(9)	0.0252(10)	0.0156(9)	0.0014(8)	0.0035(7)	-0.0008(8)
C21	0.0204(10)	0.0380(12)	0.0241(10)	0.0105(9)	0.0028(8)	0.0066(9)
C22	0.0251(10)	0.0286(11)	0.0244(10)	-0.0013(9)	0.0032(8)	0.0065(9)
O1	0.0266(7)	0.0245(7)	0.0132(6)	0.0001(5)	-0.0002(5)	0.0015(6)
O2	0.0258(8)	0.0294(8)	0.0194(7)	0.0002(6)	0.0046(6)	0.0079(6)
O3	0.0282(8)	0.0573(10)	0.0144(7)	-0.0003(7)	-0.0043(6)	0.0032(8)
C1'	0.0152(9)	0.0138(8)	0.0125(8)	0.0003(7)	0.0005(7)	-0.0012(7)
C2'	0.0164(9)	0.0122(8)	0.0155(9)	-0.0003(7)	0.0037(7)	-0.0007(7)
C3'	0.0135(8)	0.0177(9)	0.0156(9)	0.0007(7)	0.0008(7)	0.0019(7)
C4'	0.0178(9)	0.0170(9)	0.0127(9)	0.0008(7)	0.0017(7)	0.0006(7)
C5'	0.0193(9)	0.0172(9)	0.0140(9)	-0.0021(7)	0.0049(7)	0.0017(7)
C6'	0.0150(9)	0.0131(8)	0.0163(9)	0.0005(7)	0.0027(7)	0.0002(7)
C7'	0.0161(9)	0.0164(9)	0.0136(8)	-0.0014(7)	0.0029(7)	0.0013(7)
C8'	0.0215(10)	0.0209(10)	0.0233(10)	-0.0080(8)	0.0051(8)	0.0011(8)
C9'	0.0270(10)	0.0209(10)	0.0216(10)	0.0002(8)	0.0113(8)	0.0029(8)
C10'	0.0203(9)	0.0257(10)	0.0207(10)	-0.0026(8)	0.0047(8)	0.0065(8)
C11'	0.0150(9)	0.0182(9)	0.0145(9)	0.0014(7)	0.0017(7)	0.0036(7)
C12'	0.0169(9)	0.0220(10)	0.0277(10)	0.0017(8)	0.0030(8)	0.0009(8)
C13'	0.0174(9)	0.0195(9)	0.0233(10)	0.0052(8)	0.0026(7)	0.0054(8)
C14'	0.0213(10)	0.0308(11)	0.0214(10)	0.0009(9)	0.0048(8)	0.0105(9)
C15'	0.0142(9)	0.0213(9)	0.0110(9)	-0.0022(7)	0.0023(7)	0.0050(7)
C16'	0.0183(9)	0.0237(10)	0.0147(9)	-0.0004(7)	0.0069(7)	0.0044(8)
C17'	0.0155(9)	0.0300(11)	0.0193(10)	-0.0063(8)	0.0039(7)	0.0014(8)
C18'	0.0162(9)	0.0404(12)	0.0112(9)	-0.0044(8)	0.0013(7)	0.0052(8)
C19'	0.0193(9)	0.0344(11)	0.0139(9)	0.0049(8)	0.0048(7)	0.0045(8)
C20'	0.0148(9)	0.0248(10)	0.0170(9)	0.0004(8)	0.0046(7)	0.0048(8)
C21'	0.0226(10)	0.0361(12)	0.0252(11)	-0.0108(9)	0.0043(8)	-0.0042(9)
C22'	0.0231(10)	0.0292(11)	0.0265(10)	0.0056(9)	0.0052(8)	0.0000(9)
O1'	0.0177(6)	0.0253(7)	0.0100(6)	-0.0020(5)	0.0006(5)	0.0043(6)
O2'	0.0270(7)	0.0280(7)	0.0174(7)	0.0024(6)	0.0039(6)	-0.0035(6)
O3'	0.0273(8)	0.0607(11)	0.0148(7)	0.0009(7)	-0.0042(6)	-0.0039(8)

The form of the anisotropic displacement parameter is:

$\exp[-2\pi^2 (a^{*2}U_{11}h^2+b^{*2}U_{22}k^2+c^{*2}U_{33}l^2+2b^*c^*U_{23}kl+2a^*c^*U_{13}hl+2a^*b^*U_{12}hk)]$

Table B.11. Bond Distances in Compound **2.11 dimer**, Å

C1-O1	1.377(2)	C1-C2	1.410(2)	C1-C6	1.414(2)
C2-C3	1.396(2)	C2-C7	1.544(2)	C3-C4	1.387(3)
C4-C5	1.387(3)	C4-C15	1.499(2)	C5-C6	1.398(2)
C6-C11	1.543(2)	C7-C10	1.531(3)	C7-C8	1.540(3)
C7-C9	1.547(2)	C11-C12	1.534(2)	C11-C14	1.537(3)
C11-C13	1.537(3)	C15-C16	1.398(3)	C15-C20	1.398(3)
C16-O2	1.371(2)	C16-C17	1.391(3)	C17-C18	1.391(3)
C17-C21	1.509(3)	C18-C19	1.382(3)	C18-O3	1.386(2)
C19-C20	1.393(3)	C20-C22	1.498(3)	C1'-O1'	1.383(2)
C1'-C6'	1.408(2)	C1'-C2'	1.413(2)	C2'-C3'	1.394(2)
C2'-C7'	1.545(2)	C3'-C4'	1.395(3)	C4'-C5'	1.390(3)
C4'-C15'	1.498(2)	C5'-C6'	1.393(2)	C6'-C11'	1.544(2)
C7'-C10'	1.536(2)	C7'-C9'	1.538(3)	C7'-C8'	1.539(2)
C11'-C14'	1.531(3)	C11'-C13'	1.533(2)	C11'-C12'	1.542(3)
C15'-C16'	1.397(3)	C15'-C20'	1.397(3)	C16'-O2'	1.373(2)
C16'-C17'	1.390(3)	C17'-C18'	1.388(3)	C17'-C21'	1.503(3)
C18'-O3'	1.384(2)	C18'-C19'	1.386(3)	C19'-C20'	1.393(3)
C20'-C22'	1.505(3)				

Table B.12. Bond Angles in Compound **2.44 dimer**, °

O1-C1-C2	119.82(15)	O1-C1-C6	117.60(15)	C2-C1-C6	122.58(15)
C3-C2-C1	116.83(16)	C3-C2-C7	120.25(15)	C1-C2-C7	122.92(15)
C4-C3-C2	122.62(16)	C5-C4-C3	118.64(16)	C5-C4-C15	121.75(16)
C3-C4-C15	119.61(15)	C4-C5-C6	122.46(16)	C5-C6-C1	116.82(16)
C5-C6-C11	120.47(16)	C1-C6-C11	122.71(15)	C10-C7-C8	107.02(15)
C10-C7-C2	111.82(14)	C8-C7-C2	110.75(14)	C10-C7-C9	105.56(14)
C8-C7-C9	110.34(14)	C2-C7-C9	111.15(14)	C12-C11-C14	106.38(15)
C12-C11-C13	110.19(15)	C14-C11-C13	106.60(15)	C12-C11-C6	110.70(14)
C14-C11-C6	111.90(15)	C13-C11-C6	110.90(15)	C16-C15-C20	118.76(16)
C16-C15-C4	118.89(16)	C20-C15-C4	122.30(16)	O2-C16-C17	116.36(16)
O2-C16-C15	120.63(16)	C17-C16-C15	123.00(17)	C18-C17-C16	116.43(17)
C18-C17-C21	122.84(17)	C16-C17-C21	120.71(18)	C19-C18-O3	120.53(18)
C19-C18-C17	122.27(17)	O3-C18-C17	117.20(17)	C18-C19-C20	120.38(18)
C19-C20-C15	119.13(17)	C19-C20-C22	120.52(17)	C15-C20-C22	120.34(16)
O1'-C1'-C6'	116.58(15)	O1'-C1'-C2'	120.72(15)	C6'-C1'-C2'	122.69(16)
C3'-C2'-C1'	116.69(16)	C3'-C2'-C7'	120.28(15)	C1'-C2'-C7'	123.01(15)
C2'-C3'-C4'	122.58(16)	C5'-C4'-C3'	118.45(16)	C5'-C4'-C15'	122.45(16)
C3'-C4'-C15'	119.01(15)	C4'-C5'-C6'	122.38(16)	C5'-C6'-C1'	117.17(16)
C5'-C6'-C11'	120.58(15)	C1'-C6'-C11'	122.24(15)	C10'-C7'-C9'	106.63(15)
C10'-C7'-C8'	105.40(15)	C9'-C7'-C8'	110.56(15)	C10'-C7'-C2'	111.50(14)
C9'-C7'-C2'	110.54(14)	C8'-C7'-C2'	111.97(15)	C14'-C11'-C13'	106.83(15)
C14'-C11'-C12'	107.12(15)	C13'-C11'-C12'	110.14(15)	C14'-C11'-C6'	111.98(14)

C13'-C11'-C6'	110.81(15)	C12'-C11'-C6'	109.85(14)	C16'-C15'-C20'	118.85(16)
C16'-C15'-C4'	117.89(16)	C20'-C15'-C4'	123.20(16)	O2'-C16'-C17'	116.04(17)
O2'-C16'-C15'	120.76(16)	C17'-C16'-C15'	123.20(17)	C18'-C17'-C16'	116.52(18)
C18'-C17'-21'	121.98(17)	C16-C17'-C21'	121.48(18)	O3'-C18'-C19'	121.16(18)
O3'-C18'-C17'	117.06(18)	C19'-C18'-C17'	121.77(17)	C18'-C19'-C20'	120.99(18)
C19'-C20'-C15'	118.60(17)	C19'-C20'-C22'	120.04(17)	C15'-C20'-C22'	121.36(16)

B.3 X-Ray Structure Determination of Compound 2.44 trimer
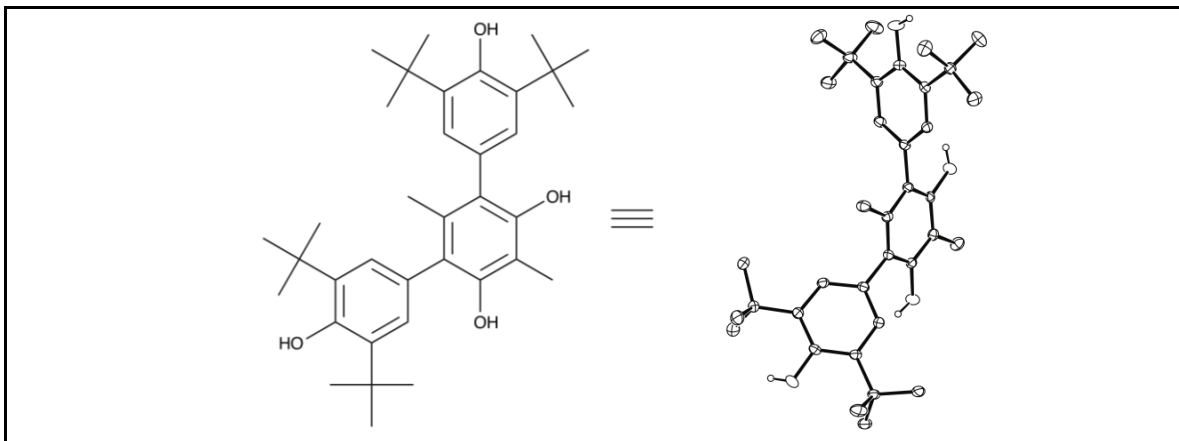
Compound 8039, $C_{36}H_{50}O_4$, crystallizes in the monoclinic space group $P2_1/n$ (systematic absences 0k0: k=odd and h0l: h+l=odd) with a=13.9613(6)Å, b=16.2398(7)Å, c=13.9786(6)Å, β=95.349(2)°, V=3155.5(2)Å^3, Z=4, and d_{calc}=1.151 g/cm^3 . X-ray intensity data were collected on a Bruker APEXII CCD area detector employing graphite-monochromated Mo-Kα radiation (λ=0.71073 Å) at a temperature of 100(1)K. Preliminary indexing was performed from a series of thirty-six 0.5° rotation frames with exposures of 10 seconds. A total of 3106 frames were collected with a crystal to detector distance of 37.5 mm, rotation widths of 0.5° and exposures of 10 seconds:

scan type	2θ	ω	φ	χ	frames
φ	-15.50	258.48	8.28	19.46	739
ω	-18.00	246.32	310.97	36.30	201
ω	-20.50	354.79	178.64	-31.86	160
φ	-23.00	328.34	44.17	79.39	528
φ	-23.00	334.21	38.95	73.66	739
φ	19.50	59.55	348.71	026.26	739

Rotation frames were integrated using SAINT[111], producing a listing of unaveraged F^2 and σ (F^2) values which were then passed to the SHELXTL[112] program package for further processing and structure solution. A total of 93926 reflections were measured over the ranges 1.93 ≤ θ ≤ 27.54°, -18 ≤ h ≤ 18, -21 ≤ k ≤ 19, -18 ≤ l ≤ 18

yielding 7263 unique reflections (Rint = 0.0316). The intensity data were corrected for Lorentz and polarization effects and for absorption using SADABS[113] (minimum and maximum transmission 0.7107, 0.7456).

The structure was solved by direct methods (SHELXS-97[114]). Refinement was by full-matrix least squares based on F^2 using SHELXL-97.[114] All reflections were used during refinement. The weighting scheme used was $w=1/[\sigma^2(F_o^2) + (0.0536P)^2 + 1.5851P]$ where $P = (F_o^2 + 2F_c^2)/3$. Non-hydrogen atoms were refined anisotropically and hydrogen atoms were refined using a riding model. Refinement converged to R1=0.0417 and wR2=0.1056 for 6029 observed reflections for which $F > 4\sigma(F)$ and R1=0.0525 and wR2=0.1125 and GOF =1.023 for all 7263 unique, non-zero reflections and 380 variables.[115] The maximum Δ/σ in the final cycle of least squares was 0.000 and the two most prominent peaks in the final difference Fourier were +0.371 and -0.310 e/Å^3.

Table B.13 lists cell information, data collection parameters, and refinement data. Final positional and equivalent isotropic thermal parameters are given in **Tables B.14** and **B.15**. Anisotropic thermal parameters are in **Table B.16**. **Tables B.17** and **B.18** list bond distances and bond angles. **Figure B.5** is an ORTEP[116] representation of the molecule with 50% probability thermal ellipsoids displayed.
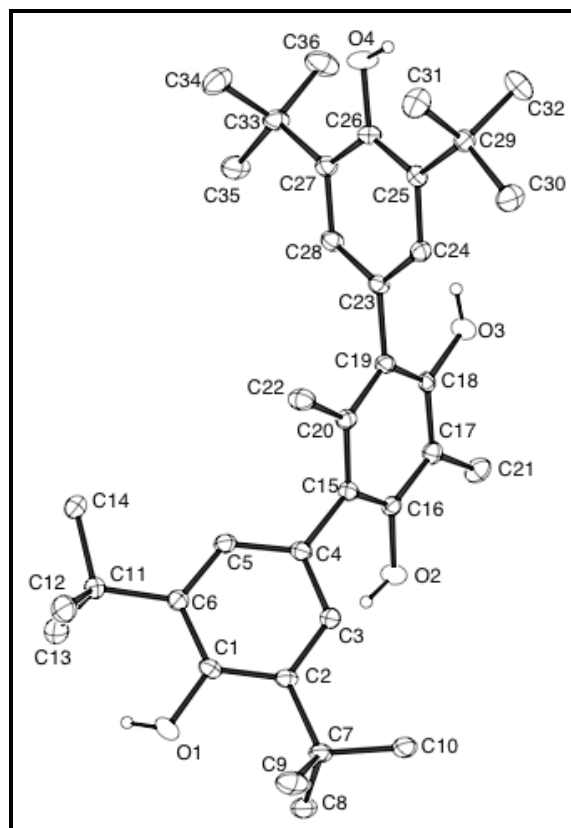
Figure B.5. ORTEP drawing of the title compound with 50% probability thermal

ellipsoids

Table B.13. Summary of Structure Determination of Compound **2.44 trimer**

Empirical formula	$C_{36}H_{50}O_4$
Formula weight	546.76
Temperature	100(1) K
Wavelength	0.71073 Å
Crystal system	monoclinic
Space group	$P2_1/n$
Cell constants:	
a	13.9613(6) Å
b	16.2398(7) Å
c	13.9786(6) Å
β	95.349(2)°
Volume	3155.5(2) Å^3
Z	4
Density (calculated)	1.151 Mg/m^3
Absorption coefficient	0.073 mm^{-1}
F(000)	1192
Crystal size	0.42 x 0.15 x 0.10 mm^3
Theta range for data collection	1.93 to 27.54°
Index ranges	$-18 \leq h \leq 18$, $-21 \leq k \leq 19$, $-18 \leq l \leq 18$
Reflections collected	93926
Independent reflections	7263 [R(int) = 0.0316]
Completeness to theta = 27.54°	99.9 %
Absorption correction	Semi-empirical from equivalents
Max. and min. transmission	0.7456 and 0.7107
Refinement method	Full-matrix least-squares on F^2
Data / restraints / parameters	7263 / 0 / 380
Goodness-of-fit on F^2	1.023
Final R indices [I>2sigma(I)]	R1 = 0.0417, wR2 = 0.1056
R indices (all data)	R1 = 0.0525, wR2 = 0.1125
Largest diff. peak and hole	0.371 and -0.310 e.Å^{-3}

Table B.14. Refined Positional Parameters for Compound **2.44 trimer**

Atom	x	y	z	U_{eq}, Å^2
C1	0.71333(9)	0.71338(7)	0.34968(9)	0.0163(2)
C2	0.67249(8)	0.73317(7)	0.25661(9)	0.0146(2)
C3	0.62591(9)	0.66981(7)	0.20304(9)	0.0153(2)
C4	0.62066(9)	0.58955(7)	0.23784(9)	0.0150(2)
C5	0.65802(9)	0.57454(7)	0.33220(9)	0.0160(2)
C6	0.70246(9)	0.63503(7)	0.39089(9)	0.0156(2)
C7	0.68226(9)	0.81984(7)	0.21333(9)	0.0170(2)
C8	0.78835(9)	0.83676(8)	0.19969(10)	0.0209(3)
C9	0.64485(10)	0.88729(8)	0.27741(11)	0.0258(3)
C10	0.62511(10)	0.82684(8)	0.11415(10)	0.0248(3)
C11	0.73935(9)	0.61553(8)	0.49588(9)	0.0187(3)
C12	0.69426(11)	0.67560(9)	0.56477(10)	0.0272(3)
C13	0.84990(10)	0.61867(9)	0.51002(10)	0.0276(3)
C14	0.70978(10)	0.52835(8)	0.52456(9)	0.0218(3)
C15	0.58476(8)	0.51975(7)	0.17451(8)	0.0142(2)
C16	0.63220(8)	0.50376(7)	0.09197(8)	0.0144(2)
C17	0.61055(8)	0.43631(7)	0.03258(8)	0.0148(2)
C18	0.54115(8)	0.38218(7)	0.06072(8)	0.0130(2)
C19	0.49174(8)	0.39485(7)	0.14160(8)	0.0140(2)
C20	0.51299(8)	0.46488(7)	0.19833(8)	0.0144(2)
C21	0.66280(10)	0.42021(8)	-0.05498(9)	0.0210(3)
C22	0.45826(10)	0.47889(8)	0.28535(9)	0.0205(3)
C23	0.42489(9)	0.32789(7)	0.16790(8)	0.0149(2)
C24	0.32603(9)	0.33032(7)	0.14485(8)	0.0155(2)
C25	0.26594(8)	0.26482(7)	0.16528(8)	0.0145(2)
C26	0.31019(9)	0.19477(7)	0.20937(9)	0.0158(2)
C27	0.41018(9)	0.18928(7)	0.23325(9)	0.0161(2)
C28	0.46504(9)	0.25698(7)	0.21181(9)	0.0166(2)
C29	0.15633(9)	0.26931(8)	0.13845(9)	0.0168(2)
C30	0.12689(10)	0.35265(9)	0.09338(11)	0.0264(3)
C31	0.10056(10)	0.26079(9)	0.22807(10)	0.0259(3)
C32	0.12378(10)	0.20261(9)	0.06386(11)	0.0284(3)
C33	0.45826(9)	0.11159(7)	0.27908(10)	0.0197(3)
C34	0.42030(11)	0.09379(9)	0.37685(11)	0.0298(3)
C35	0.56784(9)	0.12147(8)	0.29751(11)	0.0245(3)
C36	0.43883(11)	0.03766(8)	0.21096(12)	0.0296(3)
O1	0.76452(7)	0.77388(6)	0.40030(7)	0.0252(2)
O2	0.70572(6)	0.55301(6)	0.06655(7)	0.0203(2)
O3	0.52500(7)	0.31255(5)	0.00498(6)	0.0204(2)
O4	0.25746(6)	0.12657(5)	0.23092(7)	0.0234(2)

$U_{eq}=\frac{1}{3}[U_{11}(aa^*)^2+U_{22}(bb^*)^2+U_{33}(cc^*)^2+2U_{12}aa^*bb^*\cos\gamma+2U_{13}aa^*cc^*\cos\beta+2U_{23}bb^*cc^*\cos\alpha]$

Table B.15. Positional Parameters for Hydrogens in Compound **2.44 trimer**

Atom	x	y	z	U_{iso}, Å^2
H3	0.5973	0.6816	0.1418	0.020
H5	0.6530	0.5217	0.3569	0.021
H8a	0.7935	0.8875	0.1654	0.031
H8b	0.8134	0.7926	0.1638	0.031
H8c	0.8245	0.8408	0.2614	0.031
H9a	0.6807	0.8860	0.3394	0.039
H9b	0.5780	0.8779	0.2845	0.039
H9c	0.6525	0.9401	0.2483	0.039
H10a	0.6298	0.8821	0.0905	0.037
H10b	0.5588	0.8136	0.1197	0.037
H10c	0.6511	0.7892	0.0703	0.037
H12a	0.7145	0.6608	0.6300	0.041
H12b	0.6254	0.6725	0.5544	0.041
H12c	0.7148	0.7307	0.5527	0.041
H13a	0.8714	0.6018	0.5742	0.041
H13b	0.8712	0.6739	0.4997	0.041
H13c	0.8760	0.5823	0.4649	0.041
H14a	0.7398	0.4885	0.4863	0.033
H14b	0.6411	0.5229	0.5140	0.033
H14c	0.7299	0.5193	0.5913	0.033
H21a	0.6777	0.4716	-0.0840	0.031
H21b	0.6227	0.3879	-0.1002	0.031
H21c	0.7213	0.3908	-0.0366	0.031
H22a	0.3909	0.4695	0.2683	0.031
H22b	0.4679	0.5345	0.3074	0.031
H22c	0.4812	0.4415	0.3355	0.031
H24	0.2988	0.3770	0.1149	0.021
H28	0.5312	0.2551	0.2273	0.022
H30a	0.1457	0.3960	0.1379	0.040
H30b	0.0584	0.3540	0.0783	0.040
H30c	0.1581	0.3602	0.0356	0.040
H31a	0.1162	0.3062	0.2707	0.039
H31b	0.1181	0.2101	0.2604	0.039
H31c	0.0327	0.2608	0.2089	0.039
H32a	0.0557	0.2070	0.0474	0.043
H32b	0.1386	0.1491	0.0905	0.043
H32c	0.1568	0.2102	0.0073	0.043
H34a	0.4542	0.0476	0.4065	0.045
H34b	0.3528	0.0814	0.3675	0.045
H34c	0.4302	0.1412	0.4175	0.045
H35a	0.5946	0.1310	0.2377	0.037
H35b	0.5951	0.0722	0.3267	0.037
H35c	0.5823	0.1674	0.3397	0.037

H36a	0.4631	0.0494	0.1504	0.044		
H36b	0.3708	0.0278	0.2011	0.044		
H36c	0.4704	-0.0103	0.2389	0.044		
H1	0.8024	0.7528	0.4415	0.038		
H2	0.7164	0.5893	0.1069	0.030		
H3a	0.4848	0.2835	0.0278	0.031		
H4	0.2000	0.1358	0.2175	0.035		

Table B.16. Refined Thermal Parameters (U's) for Compound **2.44 trimer**

Atom	U_{11}	U_{22}	U_{33}	U_{23}	U_{13}	U_{12}
C1	0.0177(6)	0.0132(5)	0.0179(6)	-0.0032(4)	0.0003(5)	-0.0026(4)
C2	0.0135(5)	0.0113(5)	0.0190(6)	0.0006(4)	0.0014(4)	-0.0005(4)
C3	0.0154(6)	0.0148(5)	0.0153(5)	0.0011(4)	-0.0001(4)	-0.0005(4)
C4	0.0155(6)	0.0136(5)	0.0160(6)	-0.0015(4)	0.0019(4)	-0.0027(4)
C5	0.0200(6)	0.0117(5)	0.0164(6)	0.0005(4)	0.0025(5)	-0.0020(4)
C6	0.0179(6)	0.0144(5)	0.0146(5)	-0.0008(4)	0.0012(4)	-0.0005(4)
C7	0.0157(6)	0.0111(5)	0.0234(6)	0.0025(4)	-0.0021(5)	-0.0015(4)
C8	0.0180(6)	0.0171(6)	0.0273(7)	0.0042(5)	-0.0003(5)	-0.0032(5)
C9	0.0241(7)	0.0135(6)	0.0396(8)	-0.0007(5)	0.0022(6)	0.0021(5)
C10	0.0250(7)	0.0168(6)	0.0303(7)	0.0084(5)	-0.0088(6)	-0.0055(5)
C11	0.0242(6)	0.0171(6)	0.0143(6)	0.0003(4)	-0.0005(5)	-0.0035(5)
C12	0.0412(8)	0.0231(7)	0.0175(6)	-0.0040(5)	0.0034(6)	-0.0030(6)
C13	0.0263(7)	0.0311(7)	0.0243(7)	0.0068(6)	-0.0037(5)	-0.0065(6)
C14	0.0290(7)	0.0197(6)	0.0162(6)	0.0033(5)	0.0001(5)	-0.0039(5)
C15	0.0160(6)	0.0119(5)	0.0143(5)	-0.0001(4)	-0.0006(4)	-0.0008(4)
C16	0.0139(5)	0.0140(5)	0.0150(5)	0.0029(4)	-0.0003(4)	-0.0010(4)
C17	0.0155(6)	0.0147(5)	0.0143(5)	0.0008(4)	0.0009(4)	0.0030(4)
C18	0.0142(5)	0.0113(5)	0.0126(5)	0.0002(4)	-0.0034(4)	0.0017(4)
C19	0.0134(5)	0.0118(5)	0.0164(6)	0.0016(4)	-0.0009(4)	-0.0002(4)
C20	0.0150(6)	0.0131(5)	0.0152(5)	0.0011(4)	0.0013(4)	0.0005(4)
C21	0.0245(7)	0.0196(6)	0.0199(6)	0.0016(5)	0.0074(5)	0.0021(5)
C22	0.0234(6)	0.0188(6)	0.0204(6)	-0.0036(5)	0.0082(5)	-0.0049(5)
C23	0.0171(6)	0.0124(5)	0.0151(5)	-0.0017(4)	0.0011(4)	-0.0023(4)
C24	0.0174(6)	0.0136(5)	0.0154(6)	0.0008(4)	0.0008(4)	0.0005(4)
C25	0.0134(5)	0.0155(5)	0.0145(5)	-0.0014(4)	0.0010(4)	-0.0002(4)
C26	0.0157(6)	0.0131(5)	0.0187(6)	0.0000(4)	0.0027(4)	-0.0024(4)
C27	0.0170(6)	0.0132(5)	0.0179(6)	0.0002(4)	0.0005(5)	-0.0001(4)
C28	0.0136(6)	0.0158(5)	0.0201(6)	-0.0006(5)	-0.0004(4)	-0.0014(4)
C29	0.0131(6)	0.0189(6)	0.0183(6)	0.0008(5)	0.0001(4)	-0.0002(4)
C30	0.0166(6)	0.0271(7)	0.0345(8)	0.0100(6)	-0.0022(5)	0.0020(5)
C31	0.0185(6)	0.0338(7)	0.0264(7)	0.0047(6)	0.0069(5)	0.0037(5)
C32	0.0211(7)	0.0327(7)	0.0303(7)	-0.0077(6)	-0.0037(6)	-0.0040(6)
C33	0.0158(6)	0.0136(5)	0.0292(7)	0.0029(5)	-0.0007(5)	0.0002(4)
C34	0.0258(7)	0.0275(7)	0.0358(8)	0.0140(6)	0.0016(6)	0.0018(6)
C35	0.0183(6)	0.0178(6)	0.0363(8)	0.0052(5)	-0.0032(5)	0.0010(5)

355

C36	0.0242(7)	0.0156(6)	0.0476(9)	-0.0040(6)	-0.0038(6)	0.0018(5)
O1	0.0308(5)	0.0162(4)	0.0263(5)	-0.0031(4)	-0.0102(4)	-0.0055(4)
O2	0.0210(5)	0.0202(4)	0.0205(5)	-0.0020(3)	0.0059(4)	-0.0073(4)
O3	0.0272(5)	0.0152(4)	0.0189(4)	-0.0051(3)	0.0028(4)	-0.0043(3)
O4	0.0144(4)	0.0162(4)	0.0395(6)	0.0068(4)	0.0014(4)	-0.0037(3)

The form of the anisotropic displacement parameter is:

$$\exp[-2\pi^2\,(a^{*2}U_{11}h^2+b^{*2}U_{22}k^2+c^{*2}U_{33}l^2+2b^*c^*U_{23}kl+2a^*c^*U_{13}hl+2a^*b^*U_{12}hk)]$$

Table B.17. Bond Distances in Compound **2.44 trimer**, Å

C1-O1	1.3721(14)	C1-C2	1.4082(17)	C1-C6	1.4107(16)
C2-C3	1.3970(16)	C2-C7	1.5430(16)	C3-C4	1.3954(16)
C4-C5	1.3940(17)	C4-C15	1.4957(16)	C5-C6	1.3885(16)
C6-C11	1.5423(17)	C7-C8	1.5357(17)	C7-C9	1.5369(18)
C7-C10	1.5380(18)	C11-C13	1.5384(19)	C11-C14	1.5384(17)
C11-C12	1.5452(18)	C15-C20	1.4039(16)	C15-C16	1.4072(17)
C16-O2	1.3739(14)	C16-C17	1.3905(16)	C17-C18	1.3919(16)
C17-C21	1.5049(17)	C18-O3	1.3799(14)	C18-C19	1.3935(17)
C19-C20	1.4024(16)	C19-C23	1.5009(16)	C20-C22	1.5127(16)
C23-C24	1.3883(17)	C23-C28	1.3974(17)	C24-C25	1.4005(16)
C25-C26	1.4089(16)	C25-C29	1.5430(16)	C26-O4	1.3787(14)
C26-C27	1.4075(17)	C27-C28	1.3885(16)	C27-C33	1.5404(16)
C29-C30	1.5327(18)	C29-C31	1.5416(18)	C29-C32	1.5422(18)
C33-C35	1.5360(18)	C33-C34	1.539(2)	C33-C36	1.5407(18)

Table B.18. Bond Angles in Compound **2.44 trimer**, °

O1-C1-C2	117.36(10)	O1-C1-C6	120.40(11)	C2-C1-C6	122.23(11)
C3-C2-C1	117.08(10)	C3-C2-C7	121.03(11)	C1-C2-C7	121.83(10)
C4-C3-C2	122.55(11)	C5-C4-C3	117.78(11)	C5-C4-C15	120.17(10)
C3-C4-C15	121.81(11)	C6-C5-C4	122.85(11)	C5-C6-C1	117.14(11)
C5-C6-C11	120.54(10)	C1-C6-C11	122.31(10)	C8-C7-C9	109.21(10)
C8-C7-C10	107.47(11)	C9-C7-C10	107.26(11)	C8-C7-C2	109.48(10)
C9-C7-C2	111.99(10)	C10-C7-C2	111.31(10)	C13-C11-C14	106.70(11)
C13-C11-C6	110.94(10)	C14-C11-C6	111.28(10)	C13-C11-C12	111.17(11)
C14-C11-C12	106.48(11)	C6-C11-C12	110.13(11)	C20-C15-C16	118.57(10)
C20-C15-C4	123.22(11)	C16-C15-C4	117.89(10)	O2-C16-C17	115.49(10)
O2-C16-C15	121.65(10)	C17-C16-C15	122.84(11)	C16-C17-C18	116.55(11)
C16-C17-C21	121.84(11)	C18-C17-C21	121.54(11)	O3-C18-C17	116.06(10)
O3-C18-C19	120.79(10)	C17-C18-C19	123.12(11)	C18-C19-C20	118.94(11)
C18-C19-C23	117.26(10)	C20-C19-C23	123.55(11)	C19-C20-C15	119.91(11)
C19-C20-C22	118.72(10)	C15-C20-C22	121.36(11)	C24-C23-C28	118.35(11)
C24-C23-C19	123.37(10)	C28-C23-C19	118.13(11)	C23-C24-C25	122.18(11)
C24-C25-C26	117.12(11)	C24-C25-C29	120.93(10)	C26-C25-C29	121.94(10)

O4-C26-C27	115.81(10)	O4-C26-C25	121.53(11)	C27-C26-C25	122.66(11)
C28-C27-C26	116.97(11)	C28-C27-C33	120.70(11)	C26-C27-C33	122.31(10)
C27-C28-C23	122.71(11)	C30-C29-C31	106.07(11)	C30-C29-C32	106.94(11)
C31-C29-C32	110.31(11)	C30-C29-C25	111.31(10)	C31-C29-C25	111.28(10)
C32-C29-C25	110.74(10)	C35-C33-C34	106.91(11)	C35-C33-C27	111.89(10)
C34-C33-C27	110.52(11)	C35-C33-C36	107.47(11)	C34-C33-C36	110.32(11)
C27-C33-C36	109.66(11)				

357

B.4 X-Ray Structure Determination of Compound 2.51
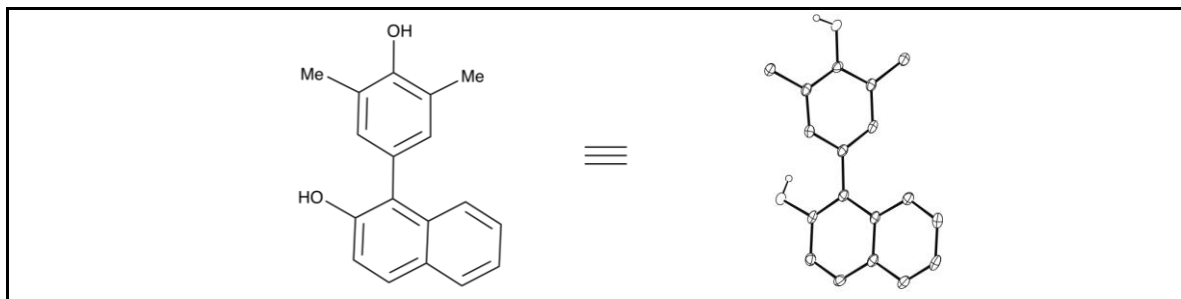
Compound 8035, $C_{18}H_{16}O_2$, crystallizes in the orthorhombic space group Pbca (systematic absences hk0: h=odd, 0kl: k=odd, and h0l: l=odd) with a=11.3975(3)Å, b=8.0182(2)Å, c=28.4322(8)Å, V=2598.35(12)Å^3, Z=8, and d_{calc}=1.351 g/cm^3 . X-ray intensity data were collected on a Bruker APEXII CCD area detector employing graphite-monochromated Mo-Kα radiation (λ=0.71073 Å) at a temperature of 100(1)K. Preliminary indexing was performed from a series of thirty-six 0.5° rotation frames with exposures of 10 seconds. A total of 2522 frames were collected with a crystal to detector distance of 46.8 mm, rotation widths of 0.5° and exposures of 5 seconds:

scan type	2θ	ω	φ	χ	frames
φ	-18.00	326.91	14.40	32.61	727
ω	-28.00	323.98	127.55	-99.10	113
φ	17.00	7.21	5.42	-71.55	262
φ	22.00	341.63	35.87	25.13	681
φ	24.50	357.68	31.84	64.29	739

Rotation frames were integrated using SAINT[111], producing a listing of unaveraged F^2 and σ(F^2) values which were then passed to the SHELXTL[112] program package for further processing and structure solution. A total of 38341 reflections were measured over the ranges 1.43 ≤ θ ≤ 25.42°, -13 ≤ h ≤ 13, -9 ≤ k ≤ 9, -34 ≤ l ≤ 34 yielding 2390 unique reflections (Rint = 0.0329). The intensity data were corrected for Lorentz and polarization effects and for absorption using SADABS[113] (minimum and

358

maximum transmission 0.6571, 0.7452).

The structure was solved by direct methods (SHELXS-97[114]). Refinement was by full-matrix least squares based on F^2 using SHELXL-97. [114] All reflections were used during refinement. The weighting scheme used was w=1/[σ^2(F_o^2)+ (0.0464P)^2 + 1.4305P] where P = (F_o^2 + 2F_c^2)/3. Non-hydrogen atoms were refined anisotropically and hydrogen atoms were refined using a riding model. Refinement converged to R1=0.0340 and wR2=0.0874 for 2115 observed reflections for which F > 4σ(F) and R1=0.0400 and wR2=0.0933 and GOF =1.050 for all 2390 unique, non-zero reflections and 186 variables.[115] The maximum Δ/σ in the final cycle of least squares was 0.000 and the two most prominent peaks in the final difference Fourier were +0.197 and -0.207 e/Å^3.

Table B.19 lists cell information, data collection parameters, and refinement data. Final positional and equivalent isotropic thermal parameters are given in Tables B.20 and B.21. Anisotropic thermal parameters are in Table B.22. Tables B.23 and B.24 list bond distances and bond angles. Figure B.6 is an ORTEP[116] representation of the molecule with 50% probability thermal ellipsoids displayed.
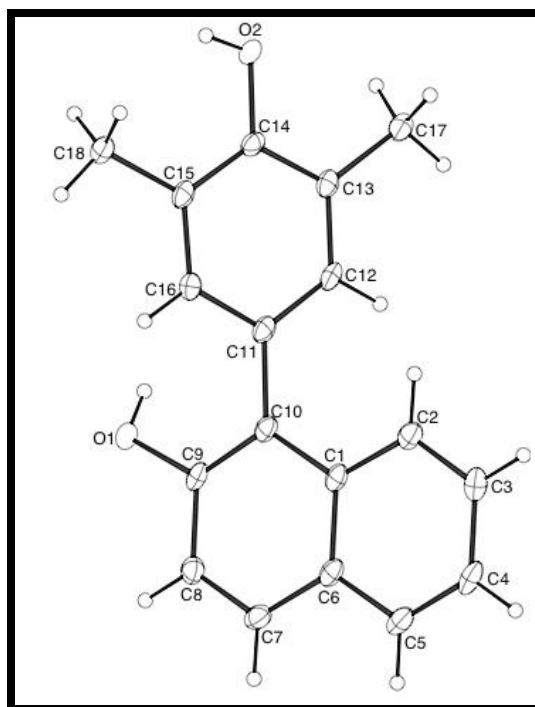
Figure B.6. ORTEP drawing of the title compound with 50% probability thermal
ellipsoids

Table B.19. Summary of Structure Determination of Compound **2.51**

Empirical formula	$C_{18}H_{16}O_2$
Formula weight	264.31
Temperature	100(1) K
Wavelength	0.71073 Å
Crystal system	orthorhombic
Space group	Pbca
Cell constants:	
a	11.3975(3) Å
b	8.0182(2) Å
c	28.4322(8) Å
Volume	2598.35(12) Å^3
Z	8
Density (calculated)	1.351 Mg/m^3
Absorption coefficient	0.087 mm^{-1}
F(000)	1120
Crystal size	0.42 x 0.28 x 0.04 mm^3
Theta range for data collection	1.43 to 25.42°
Index ranges	$-13 \leq h \leq 13$, $-9 \leq k \leq 9$, $-34 \leq l \leq 34$
Reflections collected	38341
Independent reflections	2390 [R(int) = 0.0329]
Completeness to theta = 25.42°	99.8 %
Absorption correction	Semi-empirical from equivalents
Max. and min. transmission	0.7452 and 0.6571
Refinement method	Full-matrix least-squares on F^2
Data / restraints / parameters	2390 / 0 / 186
Goodness-of-fit on F^2	1.050
Final R indices [I>2sigma(I)]	R1 = 0.0340, wR2 = 0.0874
R indices (all data)	R1 = 0.0400, wR2 = 0.0933
Largest diff. peak and hole	0.197 and -0.207 e.Å^{-3}

Table B.20. Refined Positional Parameters for Compound **2.51**

Atom	x	y	z	U_{eq}, Å^2
C1	0.56206(11)	0.31207(16)	0.17142(4)	0.0145(3)
C2	0.48677(12)	0.20921(16)	0.19844(4)	0.0169(3)
C3	0.51792(12)	0.15542(17)	0.24259(4)	0.0198(3)
C4	0.62668(12)	0.20076(17)	0.26214(4)	0.0203(3)
C5	0.70231(12)	0.29854(17)	0.23704(4)	0.0183(3)
C6	0.67278(11)	0.35601(16)	0.19131(4)	0.0153(3)
C7	0.75195(12)	0.45478(16)	0.16514(4)	0.0169(3)
C8	0.72254(11)	0.51109(16)	0.12147(4)	0.0164(3)
C9	0.61345(11)	0.46739(16)	0.10154(4)	0.0146(3)
C10	0.53322(11)	0.36876(16)	0.12489(4)	0.0140(3)
C11	0.42298(11)	0.31571(16)	0.10081(4)	0.0144(3)
C12	0.31094(11)	0.34590(16)	0.11850(4)	0.0151(3)
C13	0.20999(11)	0.29254(16)	0.09539(4)	0.0148(3)
C14	0.22391(11)	0.20691(16)	0.05278(4)	0.0142(3)
C15	0.33406(11)	0.17806(15)	0.03328(4)	0.0148(3)
C16	0.43192(11)	0.23211(16)	0.05787(4)	0.0148(3)
C17	0.08952(11)	0.32431(17)	0.11499(4)	0.0182(3)
C18	0.34590(11)	0.09156(17)	-0.01346(4)	0.0174(3)
O1	0.59374(8)	0.52945(11)	0.05685(3)	0.0161(2)
O2	0.12306(8)	0.15473(11)	0.03020(3)	0.0168(2)

$U_{eq}=^1/_3[U_{11}(aa^*)^2+U_{22}(bb^*)^2+U_{33}(cc^*)^2+2U_{12}aa^*bb^*\cos\gamma+2U_{13}aa^*cc^*\cos\beta+2U_{23}bb^*cc^*\cos\alpha]$

Table B.21. Positional Parameters for Hydrogens in Compound **2.51**

Atom	x	y	z	U_{iso}, Å^2
H2	0.4147	0.1774	0.1860	0.022
H3	0.4667	0.0885	0.2597	0.026
H4	0.6471	0.1643	0.2921	0.027
H5	0.7742	0.3279	0.2501	0.024
H7	0.8248	0.4816	0.1778	0.022
H8	0.7744	0.5783	0.1048	0.022
H12	0.3033	0.4037	0.1467	0.020
H16	0.5060	0.2120	0.0454	0.020
H17a	0.0956	0.3941	0.1423	0.027
H17b	0.0538	0.2202	0.1235	0.027
H17c	0.0423	0.3789	0.0917	0.027
H18a	0.4274	0.0827	-0.0216	0.026
H18b	0.3056	0.1547	-0.0371	0.026
H18c	0.3123	-0.0180	-0.0114	0.026
H1	0.5237	0.5495	0.0536	0.024
H2a	0.1407	0.1007	0.0068	0.025

Table B.22. Refined Thermal Parameters (U's) for Compound **2.51**

Atom	U_{11}	U_{22}	U_{33}	U_{23}	U_{13}	U_{12}
C1	0.0184(6)	0.0144(6)	0.0106(6)	-0.0030(5)	0.0009(5)	0.0032(5)
C2	0.0192(6)	0.0186(7)	0.0128(6)	-0.0020(5)	-0.0002(5)	0.0012(5)
C3	0.0242(7)	0.0216(7)	0.0137(6)	0.0017(5)	0.0043(5)	0.0026(6)
C4	0.0292(7)	0.0229(7)	0.0087(6)	0.0005(5)	-0.0014(5)	0.0057(6)
C5	0.0214(7)	0.0213(7)	0.0121(6)	-0.0030(5)	-0.0034(5)	0.0040(5)
C6	0.0199(6)	0.0149(6)	0.0112(6)	-0.0038(5)	-0.0005(5)	0.0037(5)
C7	0.0173(6)	0.0190(7)	0.0144(6)	-0.0042(5)	-0.0024(5)	0.0004(5)
C8	0.0184(7)	0.0172(6)	0.0135(6)	-0.0017(5)	0.0023(5)	-0.0008(5)
C9	0.0200(6)	0.0155(6)	0.0082(6)	-0.0015(5)	0.0003(5)	0.0036(5)
C10	0.0164(6)	0.0150(6)	0.0107(6)	-0.0027(5)	0.0002(5)	0.0027(5)
C11	0.0193(7)	0.0140(6)	0.0099(6)	0.0028(5)	-0.0013(5)	-0.0003(5)
C12	0.0218(7)	0.0155(6)	0.0080(5)	0.0000(5)	-0.0001(5)	-0.0001(5)
C13	0.0193(6)	0.0145(6)	0.0107(6)	0.0029(5)	0.0003(5)	0.0000(5)
C14	0.0176(6)	0.0152(6)	0.0100(5)	0.0033(5)	-0.0028(5)	-0.0018(5)
C15	0.0208(6)	0.0136(6)	0.0100(6)	0.0026(5)	-0.0002(5)	-0.0007(5)
C16	0.0171(6)	0.0156(6)	0.0116(6)	0.0017(5)	0.0014(5)	0.0000(5)
C17	0.0194(7)	0.0229(7)	0.0122(6)	-0.0013(5)	-0.0003(5)	0.0005(5)
C18	0.0205(6)	0.0205(7)	0.0113(6)	-0.0015(5)	0.0000(5)	-0.0013(5)
O1	0.0168(4)	0.0217(5)	0.0099(4)	0.0025(4)	-0.0001(3)	0.0010(4)
O2	0.0177(5)	0.0233(5)	0.0094(4)	-0.0022(4)	-0.0010(3)	-0.0023(4)

The form of the anisotropic displacement parameter is:

$\exp[-2\pi^2 (a^{*2}U_{11}h^2+b^{*2}U_{22}k^2+c^{*2}U_{33}l^2+2b^*c^*U_{23}kl+2a^*c^*U_{13}hl+2a^*b^*U_{12}hk)]$

Table B.23. Bond Distances in Compound **2.51**, Å

C1-C2	1.4167(18)	C1-C6	1.4270(18)	C1-C10	1.4369(17)
C2-C3	1.3741(18)	C3-C4	1.406(2)	C4-C5	1.3663(19)
C5-C6	1.4200(17)	C6-C7	1.4123(18)	C7-C8	1.3633(17)
C8-C9	1.4105(18)	C9-C10	1.3792(18)	C9-O1	1.3829(15)
C10-C11	1.4928(17)	C11-C12	1.3935(18)	C11-C16	1.3967(17)
C12-C13	1.3924(17)	C13-C14	1.4014(17)	C13-C17	1.5036(17)
C14-O2	1.3815(15)	C14-C15	1.3918(18)	C15-C16	1.3858(17)
C15-C18	1.5050(17)				

Table B.24. Bond Angles in Compound **2.51,** °

C2-C1-C6	117.68(11)	C2-C1-C10	123.02(12)	C6-C1-C10	119.28(11)
C3-C2-C1	121.45(12)	C2-C3-C4	120.51(12)	C5-C4-C3	119.87(12)
C4-C5-C6	120.99(12)	C7-C6-C5	120.85(12)	C7-C6-C1	119.65(11)
C5-C6-C1	119.50(12)	C8-C7-C6	120.56(12)	C7-C8-C9	120.02(12)
C10-C9-O1	122.75(11)	C10-C9-C8	122.24(11)	O1-C9-C8	115.01(11)
C9-C10-C1	118.22(11)	C9-C10-C11	120.04(11)	C1-C10-C11	121.64(11)
C12-C11-C16	117.75(11)	C12-C11-C10	123.80(11)	C16-C11-C10	118.44(11)
C13-C12-C11	122.25(11)	C12-C13-C14	117.70(11)	C12-C13-C17	121.85(11)
C14-C13-C17	120.45(11)	O2-C14-C15	121.00(11)	O2-C14-C13	117.12(11)
C15-C14-C13	121.87(11)	C16-C15-C14	118.22(11)	C16-C15-C18	121.16(11)
C14-C15-C18	120.62(11)	C15-C16-C11	122.17(12)		

B.5 X-Ray Structure Determination of Compound Cr-Salen-Cy
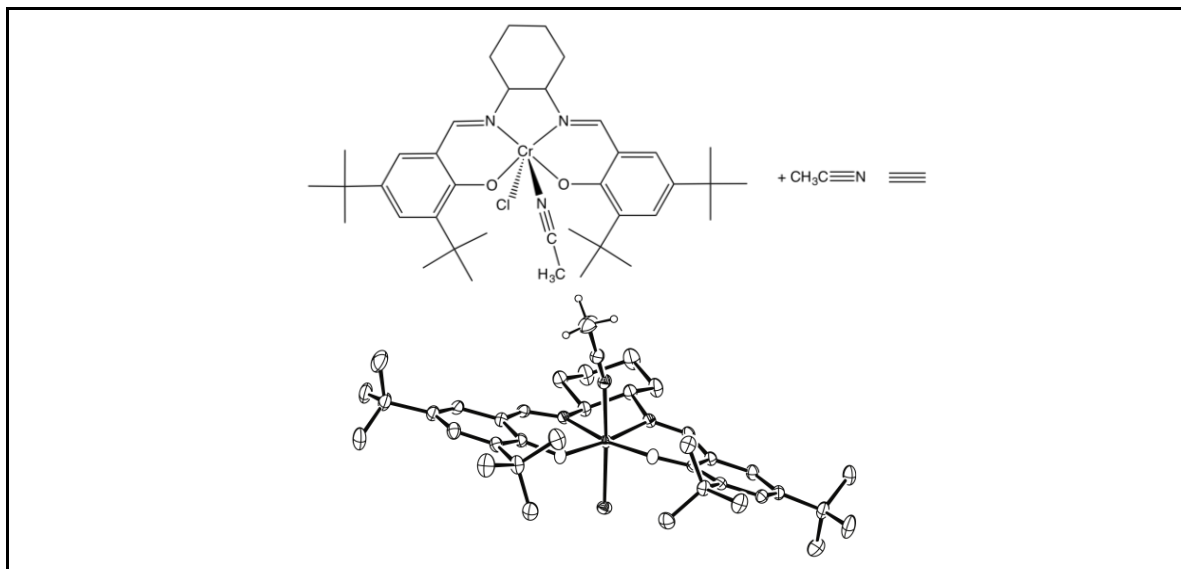
Compound Cr-Salen-Cy, $C_{80}H_{116}N_8O_4Cl_2Cr_2$, crystallizes in the monoclinic space group $P2_1/c$ (systematic absences 0k0: k=odd and h0l: l=odd) with a=19.9990(6)Å, b=15.4397(5)Å, c=27.2127(8)Å, β=106.446(2)°, V=8058.9(4)Å^3, Z=4, and d_{calc}=1.178 g/cm^3 . X-ray intensity data were collected on a Bruker APEXII CCD area detector employing graphite-monochromated Mo-Kα radiation (λ=0.71073 Å) at a temperature of 100(1)K. Preliminary indexing was performed from a series of thirty-six 0.5° rotation frames with exposures of 10 seconds. A total of 2767 frames were collected with a crystal to detector distance of 37.4 mm, rotation widths of 0.5° and exposures of 10 seconds:

scan type	2θ	ω	φ	χ	frames
φ	-23.00	315.83	12.48	28.88	739
ω	-15.50	340.80	341.11	-63.64	99
ω	24.50	14.22	11.23	-20.60	107
ω	27.00	276.67	5.00	57.63	227
φ	19.50	59.55	348.71	-26.26	739
φ	-23.00	334.21	38.95	73.66	739
ω	17.00	321.08	318.36	83.36	117

Rotation frames were integrated using SAINT[111], producing a listing of unaveraged F^2 and σ (F^2) values which were then passed to the SHELXTL[112] program

365

package for further processing and structure solution. A total of 213237 reflections were measured over the ranges $1.53 \leq \theta \leq 27.58°$, $-26 \leq h \leq 26$, $-20 \leq k \leq 20$, $-35 \leq l \leq 35$ yielding 18559 unique reflections (Rint = 0.0371). The intensity data were corrected for Lorentz and polarization effects and for absorption using SADABS[113] (minimum and maximum transmission 0.6640, 0.7456).

The structure was solved by direct methods (SHELXS-97[114]). Refinement was by full-matrix least squares based on F^2 using SHELXL-97.[114] All reflections were used during refinement. The weighting scheme used was $w = 1/[\sigma^2(F_o^2) + (0.0535P)^2 + 7.9203P]$ where $P = (F_o^2 + 2F_c^2)/3$. Non-hydrogen atoms were refined anisotropically and hydrogen atoms were refined using a riding model. Refinement converged to R1=0.0406 and wR2=0.1042 for 14928 observed reflections for which $F > 4\sigma$ (F) and R1=0.0557 and wR2=0.1166 and GOF =1.019 for all 18559 unique, non-zero reflections and 926 variables.[115] The maximum Δ/σ in the final cycle of least squares was 0.002 and the two most prominent peaks in the final difference Fourier were +1.538 and -0.767 e/Å^3.

Table B.25 lists cell information, data collection parameters, and refinement data. Final positional and equivalent isotropic thermal parameters are given in **Tables B.26** and **B.27**. Anisotropic thermal parameters are in **Table B.28**. **Tables B.29** and **B.30** list bond distances and bond angles. **Figures B.7** and **B.8** are ORTEP[116] representations of the molecule with 50% probability thermal ellipsoids displayed.
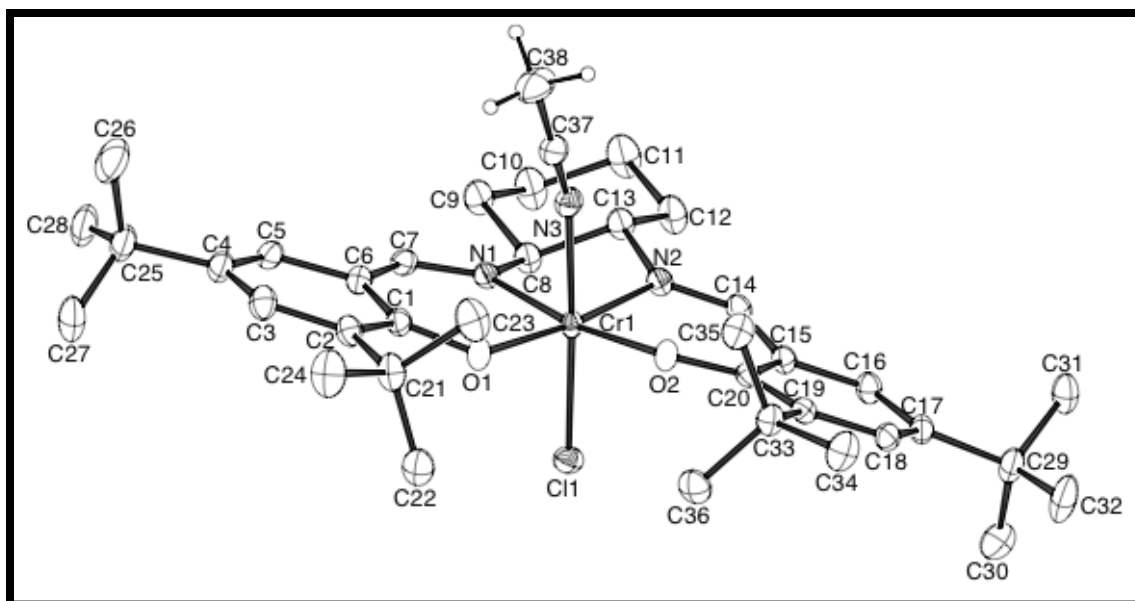
Figure B.7. ORTEP drawing of molecule no. 1 of the asymmetric unit with 50% probability thermal ellipsoids
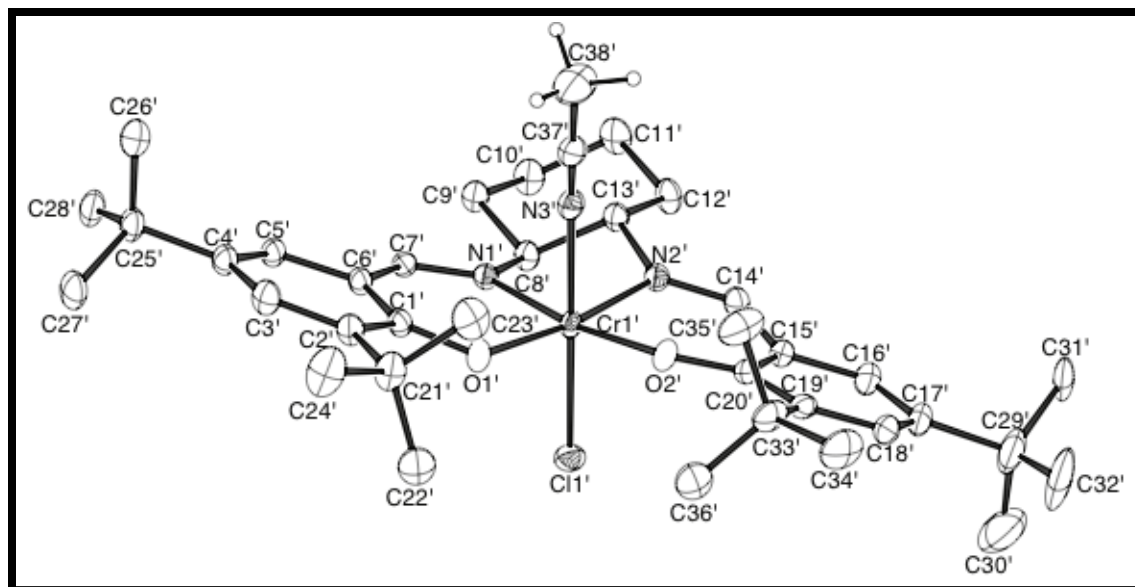
Figure B.8. ORTEP drawing of molecule no. 2 of the asymmetric unit with 50% probability thermal ellipsoids

367

Table B.25. Summary of Structure Determination of Compound **Cr-Salen-Cy**

Empirical formula	$C_{80}H_{116}N_8O_4Cl_2Cr_2$
Formula weight	1428.71
Temperature	100(1) K
Wavelength	0.71073 Å
Crystal system	monoclinic
Space group	$P2_1/c$
Cell constants:	
a	19.9990(6) Å
b	15.4397(5) Å
c	27.2127(8) Å
β	106.446(2)°
Volume	8058.9(4) Å^3
Z	4
Density (calculated)	1.178 Mg/m^3
Absorption coefficient	0.387 mm^{-1}
F(000)	3064
Crystal size	0.35 x 0.15 x 0.12 mm^3
Theta range for data collection	1.53 to 27.58°
Index ranges	$-26 \leq h \leq 26, -20 \leq k \leq 20, -35 \leq l \leq 35$
Reflections collected	213237
Independent reflections	18559 [R(int) = 0.0371]
Completeness to theta = 27.58°	99.4 %
Absorption correction	Semi-empirical from equivalents
Max. and min. transmission	0.7456 and 0.6640
Refinement method	Full-matrix least-squares on F^2
Data / restraints / parameters	18559 / 137 / 926
Goodness-of-fit on F^2	1.019
Final R indices [I>2sigma(I)]	R1 = 0.0406, wR2 = 0.1042
R indices (all data)	R1 = 0.0557, wR2 = 0.1166
Largest diff. peak and hole	1.538 and -0.767 e.Å^{-3}

Table B.26. Refined Positional Parameters for Compound **Cr-Salen-Cy**

Atom	x	y	z	U_{eq}, Å^2
Cr1	0.911864(14)	0.578376(19)	0.236883(10)	0.01432(7)
Cl1	0.91164(2)	0.42964(3)	0.225102(17)	0.02016(9)
O1	0.93019(6)	0.56848(9)	0.30945(5)	0.0193(3)
O2	1.00726(6)	0.59243(8)	0.23657(4)	0.0172(2)
N1	0.80851(7)	0.57821(10)	0.22736(5)	0.0165(3)
N2	0.88133(7)	0.59570(10)	0.16045(5)	0.0168(3)
N3	0.91049(8)	0.71233(11)	0.25062(6)	0.0209(3)
C1	0.88904(9)	0.58747(12)	0.33794(7)	0.0177(3)
C2	0.91891(9)	0.60228(12)	0.39160(7)	0.0193(4)
C3	0.87420(10)	0.61568(13)	0.42152(7)	0.0229(4)
C4	0.80099(10)	0.61465(13)	0.40270(7)	0.0221(4)
C5	0.77300(10)	0.60423(12)	0.35088(7)	0.0204(4)
C6	0.81558(9)	0.59266(12)	0.31778(7)	0.0183(3)
C7	0.77914(9)	0.58393(11)	0.26379(7)	0.0176(3)
C8	0.76822(9)	0.56721(13)	0.17292(7)	0.0194(4)
C9	0.69144(9)	0.59165(14)	0.15867(7)	0.0245(4)
C10	0.65849(10)	0.57473(16)	0.10120(8)	0.0316(5)
C11	0.69652(10)	0.62290(17)	0.06830(8)	0.0352(5)
C12	0.77404(10)	0.60117(15)	0.08355(7)	0.0264(4)
C13	0.80669(9)	0.61761(13)	0.14056(7)	0.0208(4)
C14	0.91994(9)	0.58024(12)	0.13105(6)	0.0175(3)
C15	0.99428(9)	0.56551(12)	0.14758(6)	0.0168(3)
C16	1.02611(9)	0.54405(12)	0.10943(7)	0.0195(4)
C17	1.09740(9)	0.53671(12)	0.11945(7)	0.0190(4)
C18	1.13730(9)	0.55735(12)	0.16957(7)	0.0179(3)
C19	1.10924(9)	0.57881(11)	0.20927(6)	0.0155(3)
C20	1.03535(9)	0.57853(11)	0.19919(6)	0.0145(3)
C21	0.99846(10)	0.60136(14)	0.41453(7)	0.0235(4)
C22	1.02782(10)	0.51204(14)	0.40721(7)	0.0273(4)
C23	1.03225(11)	0.67025(16)	0.38874(8)	0.0319(5)
C24	1.02037(12)	0.62118(17)	0.47218(8)	0.0350(5)
C25	0.75647(11)	0.62467(14)	0.43999(8)	0.0283(4)
C26	0.75996(15)	0.71897(17)	0.45830(10)	0.0443(6)
C27	0.78439(12)	0.56473(17)	0.48639(8)	0.0362(5)
C28	0.67991(11)	0.60089(17)	0.41437(8)	0.0339(5)
C29	1.12937(10)	0.50621(14)	0.07739(7)	0.0238(4)
C30	1.10856(13)	0.41142(15)	0.06426(9)	0.0378(5)
C31	1.10157(11)	0.56136(15)	0.02887(7)	0.0274(4)
C32	1.20877(11)	0.51269(19)	0.09406(8)	0.0375(6)
C33	1.15535(9)	0.60136(13)	0.26325(7)	0.0190(4)
C34	1.23305(10)	0.60668(15)	0.26555(8)	0.0276(4)
C35	1.13513(10)	0.68993(13)	0.28003(7)	0.0240(4)
C36	1.14716(10)	0.53185(14)	0.30161(7)	0.0259(4)

369

C37	0.91865(10)	0.77649(13)	0.27178(8)	0.0236(4)
C38	0.93133(13)	0.85793(14)	0.29974(10)	0.0381(5)
Cr1'	0.404130(14)	0.629097(19)	0.747023(10)	0.01493(7)
Cl1'	0.40295(2)	0.48115(3)	0.733106(18)	0.02259(10)
O1'	0.42331(6)	0.61763(9)	0.81994(5)	0.0207(3)
O2'	0.49913(7)	0.64286(9)	0.74604(5)	0.0203(3)
N1'	0.30097(7)	0.62777(10)	0.73774(5)	0.0155(3)
N2'	0.37249(8)	0.65065(10)	0.67111(5)	0.0171(3)
N3'	0.40540(8)	0.76222(11)	0.76014(6)	0.0199(3)
C1'	0.38214(9)	0.63771(12)	0.84820(6)	0.0176(3)
C2'	0.41154(9)	0.65446(13)	0.90173(7)	0.0210(4)
C3'	0.36650(10)	0.67200(14)	0.93092(7)	0.0234(4)
C4'	0.29324(10)	0.67290(13)	0.91172(7)	0.0212(4)
C5'	0.26592(9)	0.65811(12)	0.86039(7)	0.0186(4)
C6'	0.30857(9)	0.64262(12)	0.82791(6)	0.0171(3)
C7'	0.27191(9)	0.63286(11)	0.77416(6)	0.0158(3)
C8'	0.26003(9)	0.62016(12)	0.68326(6)	0.0173(3)
C9'	0.18316(9)	0.64393(13)	0.67066(6)	0.0193(4)
C10'	0.14960(10)	0.63791(14)	0.61261(7)	0.0237(4)
C11'	0.18733(10)	0.69624(14)	0.58413(7)	0.0257(4)
C12'	0.26419(10)	0.67147(14)	0.59578(7)	0.0226(4)
C13'	0.29844(9)	0.67611(12)	0.65335(6)	0.0178(3)
C14'	0.41031(10)	0.63764(12)	0.64070(7)	0.0204(4)
C15'	0.48442(10)	0.62154(12)	0.65646(7)	0.0216(4)
C16'	0.51565(12)	0.60263(15)	0.61727(8)	0.0309(5)
C17'	0.58665(12)	0.59573(16)	0.62704(9)	0.0365(5)
C18'	0.62729(11)	0.61393(14)	0.67720(9)	0.0314(5)
C19'	0.60034(10)	0.63286(12)	0.71766(8)	0.0231(4)
C20'	0.52606(9)	0.63173(12)	0.70793(7)	0.0193(4)
C21'	0.49088(10)	0.65322(15)	0.92575(7)	0.0265(4)
C22'	0.52087(11)	0.56399(16)	0.91903(8)	0.0328(5)
C23'	0.52528(11)	0.72288(16)	0.90051(9)	0.0344(5)
C24'	0.51068(12)	0.6728(2)	0.98335(8)	0.0414(6)
C25'	0.24811(10)	0.69493(14)	0.94704(7)	0.0238(4)
C26'	0.25267(12)	0.79270(15)	0.95706(8)	0.0331(5)
C27'	0.27370(11)	0.64561(15)	0.99806(7)	0.0296(5)
C28'	0.17162(10)	0.66993(15)	0.92240(7)	0.0278(4)
C29'	0.62237(12)	0.57191(17)	0.58627(8)	0.0503(7)
C30'	0.6063(3)	0.47567(17)	0.57337(19)	0.0686(18)
C31'	0.59296(18)	0.6270(3)	0.53784(12)	0.0323(10)
C32'	0.70177(12)	0.5849(4)	0.60612(15)	0.0653(16)
C30"	0.6614(2)	0.4904(2)	0.59639(16)	0.0515(12)
C31"	0.5583(2)	0.5501(3)	0.52902(16)	0.0557(13)
C32"	0.6581(2)	0.6479(2)	0.57231(19)	0.0572(13)
C33'	0.64651(10)	0.65498(14)	0.77138(9)	0.0284(4)
C34'	0.72449(11)	0.65826(17)	0.77406(11)	0.0428(6)

370

C35'	0.62725(11)	0.74496(15)	0.78699(10)	0.0386(6)
C36'	0.63781(11)	0.58709(16)	0.81043(9)	0.0333(5)
C37'	0.42004(10)	0.82991(13)	0.77506(8)	0.0243(4)
C38'	0.44045(15)	0.91601(16)	0.79436(13)	0.0499(7)
C39'	0.42858(15)	0.63935(16)	0.14399(9)	0.0420(6)
C40'	0.50361(15)	0.64456(18)	0.15708(13)	0.0560(8)
N4'	0.36915(15)	0.63571(17)	0.13473(12)	0.0655(7)
C39	0.9206(5)	0.8054(5)	0.1341(3)	0.064(2)
N4	0.8654(5)	0.8068(6)	0.1094(4)	0.132(5)
C39*	0.9503(4)	0.7855(4)	0.1109(3)	0.0618(18)
N4*	0.9169(5)	0.7729(4)	0.0708(3)	0.126(4)
C40	0.99328(15)	0.8007(2)	0.16344(10)	0.0530(7)

$U_{eq}=\frac{1}{3}[U_{11}(aa^*)^2+U_{22}(bb^*)^2+U_{33}(cc^*)^2+2U_{12}aa^*bb^*\cos\Box+2U_{13}aa^*cc^*\cos\Box+2U_{23}bb^*cc^*\cos\Box]$

Table B.27. Positional Parameters for Hydrogens in Compound **Cr-Salen-Cy**

Atom	x	y	z	U_{iso}, Å^2
H3	0.8938	0.6260	0.4563	0.030
H5	0.7248	0.6048	0.3371	0.027
H7	0.7307	0.5823	0.2547	0.023
H8	0.7706	0.5057	0.1646	0.026
H9a	0.6866	0.6524	0.1662	0.033
H9b	0.6678	0.5575	0.1786	0.033
H10a	0.6596	0.5131	0.0946	0.042
H10b	0.6101	0.5929	0.0917	0.042
H11a	0.6908	0.6848	0.0718	0.047
H11b	0.6760	0.6077	0.0326	0.047
H12a	0.7972	0.6365	0.0639	0.035
H12b	0.7802	0.5408	0.0759	0.035
H13	0.8017	0.6795	0.1468	0.028
H14	0.8982	0.5783	0.0960	0.023
H16	0.9981	0.5344	0.0762	0.026
H18	1.1856	0.5566	0.1766	0.024
H22a	1.0071	0.4688	0.4236	0.041
H22b	1.0774	0.5120	0.4221	0.041
H22c	1.0173	0.4994	0.3713	0.041
H23a	1.0204	0.6592	0.3526	0.048
H23b	1.0820	0.6682	0.4029	0.048
H23c	1.0155	0.7265	0.3946	0.048
H24a	1.0035	0.6774	0.4779	0.053
H24b	1.0703	0.6201	0.4850	0.053
H24c	1.0010	0.5784	0.4898	0.053
H26a	0.8073	0.7334	0.4763	0.067
H26b	0.7311	0.7259	0.4808	0.067
H26c	0.7437	0.7566	0.4293	0.067

H27a	0.7869	0.5065	0.4747	0.054
H27b	0.7537	0.5668	0.5078	0.054
H27c	0.8301	0.5835	0.5056	0.054
H28a	0.6607	0.6399	0.3865	0.051
H28b	0.6539	0.6053	0.4390	0.051
H28c	0.6773	0.5426	0.4016	0.051
H30a	1.1283	0.3757	0.0937	0.057
H30b	1.1257	0.3929	0.0364	0.057
H30c	1.0587	0.4064	0.0545	0.057
H31a	1.0518	0.5559	0.0168	0.041
H31b	1.1219	0.5417	0.0028	0.041
H31c	1.1137	0.6210	0.0367	0.041
H32a	1.2224	0.5716	0.1029	0.056
H32b	1.2266	0.4943	0.0665	0.056
H32c	1.2273	0.4762	0.1233	0.056
H34a	1.2487	0.5511	0.2574	0.041
H34b	1.2597	0.6234	0.2994	0.041
H34c	1.2392	0.6488	0.2413	0.041
H35a	1.1405	0.7334	0.2562	0.036
H35b	1.1648	0.7034	0.3136	0.036
H35c	1.0875	0.6885	0.2808	0.036
H36a	1.0989	0.5266	0.3003	0.039
H36b	1.1736	0.5483	0.3356	0.039
H36c	1.1639	0.4773	0.2929	0.039
H38a	0.9428	0.8466	0.3359	0.057
H38b	0.8902	0.8933	0.2897	0.057
H38c	0.9694	0.8877	0.2922	0.057
H3'	0.3859	0.6840	0.9655	0.031
H5'	0.2178	0.6583	0.8465	0.025
H7'	0.2235	0.6300	0.7652	0.021
H8'	0.2629	0.5598	0.6729	0.023
H9a'	0.1784	0.7024	0.6823	0.026
H9b'	0.1597	0.6048	0.6882	0.026
H10a'	0.1514	0.5785	0.6015	0.031
H10b'	0.1010	0.6550	0.6046	0.031
H11a'	0.1836	0.7560	0.5941	0.034
H11b'	0.1653	0.6916	0.5476	0.034
H12a'	0.2683	0.6132	0.5836	0.030
H12b'	0.2876	0.7107	0.5782	0.030
H13'	0.2954	0.7363	0.6638	0.024
H14'	0.3881	0.6387	0.6057	0.027
H16'	0.4874	0.5946	0.5840	0.041
H18'	0.6755	0.6132	0.6837	0.042
H22a'	0.5004	0.5209	0.9357	0.049
H22b'	0.5705	0.5646	0.9340	0.049
H22c'	0.5105	0.5507	0.8832	0.049

H23a'	0.5748	0.7225	0.9161	0.052
H23b'	0.5069	0.7787	0.9051	0.052
H23c'	0.5157	0.7108	0.8646	0.052
H24a'	0.4917	0.6289	1.0005	0.062
H24b'	0.4922	0.7283	0.9888	0.062
H24c'	0.5605	0.6736	0.9969	0.062
H26a'	0.3000	0.8082	0.9742	0.050
H26b'	0.2234	0.8080	0.9782	0.050
H26c'	0.2375	0.8231	0.9251	0.050
H27a'	0.2743	0.5846	0.9914	0.044
H27b'	0.2429	0.6569	1.0187	0.044
H27c'	0.3199	0.6645	1.0159	0.044
H28a'	0.1534	0.7030	0.8916	0.042
H28b'	0.1450	0.6819	0.9459	0.042
H28c'	0.1687	0.6093	0.9143	0.042
H30a'	0.6273	0.4582	0.5473	0.103
H30b'	0.5568	0.4675	0.5612	0.103
H30c'	0.6248	0.4413	0.6036	0.103
H31a'	0.6152	0.6108	0.5123	0.048
H31b'	0.6017	0.6872	0.5461	0.048
H31c'	0.5436	0.6175	0.5249	0.048
H32a'	0.7229	0.5694	0.5797	0.098
H32b'	0.7203	0.5489	0.6356	0.098
H32c'	0.7117	0.6445	0.6154	0.098
H30a"	0.6323	0.4458	0.6039	0.077
H30b"	0.7019	0.4977	0.6251	0.077
H30c"	0.6756	0.4743	0.5668	0.077
H31a"	0.5290	0.6000	0.5190	0.084
H31b"	0.5306	0.5018	0.5339	0.084
H31c"	0.5801	0.5365	0.5028	0.084
H32a"	0.6268	0.6964	0.5653	0.086
H32b"	0.6726	0.6347	0.5424	0.086
H32c"	0.6983	0.6619	0.6002	0.086
H34a'	0.7392	0.6023	0.7658	0.064
H34b'	0.7512	0.6742	0.8080	0.064
H34c'	0.7316	0.7003	0.7500	0.064
H35a'	0.6337	0.7872	0.7629	0.058
H35b'	0.6566	0.7589	0.8206	0.058
H35c'	0.5794	0.7451	0.7873	0.058
H36a'	0.5894	0.5824	0.8090	0.050
H36b'	0.6642	0.6044	0.8442	0.050
H36c'	0.6544	0.5320	0.8024	0.050
H38a'	0.4582	0.9141	0.8310	0.075
H38b'	0.4007	0.9537	0.7849	0.075
H38c'	0.4759	0.9374	0.7800	0.075
H40a	0.5199	0.6878	0.1831	0.084

Atom						
H40b	0.5174	0.6599	0.1272	0.084		
H40c	0.5234	0.5895	0.1697	0.084		
H40a	1.0010	0.7492	0.1841	0.079		
H40b	1.0051	0.8506	0.1852	0.079		
H40c	1.0219	0.7992	0.1405	0.079		
H40a*	1.0084	0.8600	0.1670	0.079		
H40b*	1.0332	0.7633	0.1709	0.079		
H40c*	0.9664	0.7889	0.1868	0.079		

Table B.28. Refined Thermal Parameters (U's) for Compound **Cr-Salen-Cy**

Atom	U_{11}	U_{22}	U_{33}	U_{23}	U_{13}	U_{12}
Cr1	0.01079(13)	0.01855(15)	0.01355(13)	0.00100(10)	0.00332(10)	-0.00033(10)
Cl1	0.0164(2)	0.0186(2)	0.0248(2)	0.00217(16)	0.00481(16)	0.00038(16)
O1	0.0144(6)	0.0290(7)	0.0150(6)	0.0016(5)	0.0051(5)	0.0007(5)
O2	0.0131(6)	0.0243(7)	0.0145(5)	-0.0012(5)	0.0046(5)	-0.0016(5)
N1	0.0140(7)	0.0184(7)	0.0166(7)	0.0025(6)	0.0036(5)	0.0004(6)
N2	0.0133(7)	0.0202(8)	0.0159(7)	0.0026(6)	0.0025(5)	-0.0008(6)
N3	0.0168(7)	0.0223(8)	0.0248(8)	0.0003(6)	0.0080(6)	0.0005(6)
C1	0.0182(8)	0.0177(9)	0.0188(8)	0.0000(7)	0.0078(7)	-0.0016(7)
C2	0.0198(9)	0.0206(9)	0.0177(8)	-0.0007(7)	0.0058(7)	-0.0038(7)
C3	0.0256(10)	0.0260(10)	0.0185(8)	-0.0040(7)	0.0085(7)	-0.0039(8)
C4	0.0250(9)	0.0217(9)	0.0235(9)	-0.0021(7)	0.0130(8)	-0.0001(7)
C5	0.0181(9)	0.0201(9)	0.0254(9)	-0.0001(7)	0.0102(7)	0.0017(7)
C6	0.0176(8)	0.0198(9)	0.0185(8)	-0.0004(7)	0.0071(7)	-0.0003(7)
C7	0.0123(8)	0.0176(9)	0.0228(8)	0.0018(7)	0.0050(7)	0.0007(6)
C8	0.0136(8)	0.0263(10)	0.0171(8)	0.0037(7)	0.0024(6)	0.0007(7)
C9	0.0131(8)	0.0355(11)	0.0238(9)	0.0078(8)	0.0032(7)	0.0014(8)
C10	0.0143(9)	0.0523(14)	0.0254(10)	0.0114(9)	0.0008(7)	-0.0004(9)
C11	0.0170(9)	0.0579(15)	0.0272(10)	0.0161(10)	0.0004(8)	0.0023(9)
C12	0.0163(9)	0.0432(12)	0.0178(8)	0.0091(8)	0.0015(7)	0.0006(8)
C13	0.0136(8)	0.0287(10)	0.0193(8)	0.0055(7)	0.0031(7)	0.0013(7)
C14	0.0161(8)	0.0216(9)	0.0137(7)	0.0024(6)	0.0025(6)	-0.0016(7)
C15	0.0152(8)	0.0194(9)	0.0159(8)	0.0016(6)	0.0048(6)	-0.0009(7)
C16	0.0186(9)	0.0253(10)	0.0143(8)	0.0012(7)	0.0042(7)	-0.0007(7)
C17	0.0184(8)	0.0228(9)	0.0177(8)	0.0027(7)	0.0080(7)	0.0014(7)
C18	0.0133(8)	0.0208(9)	0.0201(8)	0.0030(7)	0.0057(7)	0.0009(7)
C19	0.0142(8)	0.0158(8)	0.0157(7)	0.0013(6)	0.0030(6)	-0.0013(6)
C20	0.0147(8)	0.0129(8)	0.0162(8)	0.0010(6)	0.0050(6)	-0.0015(6)
C21	0.0200(9)	0.0331(11)	0.0168(8)	-0.0014(7)	0.0039(7)	-0.0059(8)
C22	0.0217(9)	0.0387(12)	0.0198(9)	0.0036(8)	0.0033(7)	0.0024(8)
C23	0.0248(10)	0.0401(13)	0.0292(10)	0.0003(9)	0.0048(8)	-0.0120(9)
C24	0.0291(11)	0.0531(15)	0.0204(9)	-0.0074(9)	0.0030(8)	-0.0089(10)
C25	0.0301(11)	0.0332(11)	0.0278(10)	-0.0031(8)	0.0183(8)	0.0013(9)
C26	0.0558(16)	0.0421(14)	0.0467(14)	-0.0143(11)	0.0333(12)	-0.0017(12)
C27	0.0357(12)	0.0529(15)	0.0258(10)	0.0013(10)	0.0181(9)	-0.0017(11)

C28	0.0292(11)	0.0461(14)	0.0336(11)	0.0011(10)	0.0206(9)	0.0031(10)
C29	0.0205(9)	0.0343(11)	0.0188(8)	0.0000(8)	0.0093(7)	0.0036(8)
C30	0.0481(14)	0.0349(13)	0.0366(12)	-0.0031(10)	0.0221(11)	0.0084(11)
C31	0.0246(10)	0.0415(12)	0.0175(8)	0.0006(8)	0.0085(7)	-0.0017(9)
C32	0.0214(10)	0.0701(17)	0.0237(10)	0.0020(10)	0.0109(8)	0.0099(10)
C33	0.0131(8)	0.0253(10)	0.0174(8)	-0.0011(7)	0.0022(6)	-0.0012(7)
C34	0.0150(9)	0.0410(12)	0.0250(9)	-0.0049(9)	0.0025(7)	-0.0018(8)
C35	0.0196(9)	0.0271(10)	0.0247(9)	-0.0067(8)	0.0052(7)	-0.0064(8)
C36	0.0247(10)	0.0316(11)	0.0189(8)	0.0054(8)	0.0021(7)	0.0019(8)
C37	0.0198(9)	0.0233(10)	0.0303(10)	0.0023(8)	0.0111(8)	0.0009(7)
C38	0.0403(13)	0.0225(11)	0.0570(15)	-0.0118(10)	0.0228(11)	-0.0033(9)
Cr1'	0.01143(13)	0.01978(15)	0.01420(13)	0.00070(10)	0.00465(10)	0.00076(10)
Cl1'	0.0182(2)	0.0192(2)	0.0309(2)	0.00290(17)	0.00778(17)	0.00207(16)
O1'	0.0141(6)	0.0322(8)	0.0164(6)	0.0030(5)	0.0054(5)	0.0030(5)
O2'	0.0148(6)	0.0264(7)	0.0217(6)	-0.0020(5)	0.0084(5)	0.0005(5)
N1'	0.0143(7)	0.0180(7)	0.0136(6)	0.0018(5)	0.0032(5)	0.0014(6)
N2'	0.0163(7)	0.0189(8)	0.0169(7)	0.0009(6)	0.0058(6)	0.0004(6)
N3'	0.0158(7)	0.0237(9)	0.0211(7)	-0.0002(6)	0.0067(6)	0.0001(6)
C1'	0.0150(8)	0.0219(9)	0.0163(8)	0.0042(7)	0.0049(6)	0.0016(7)
C2'	0.0159(8)	0.0288(10)	0.0170(8)	0.0038(7)	0.0028(7)	0.0015(7)
C3'	0.0217(9)	0.0339(11)	0.0131(8)	0.0012(7)	0.0025(7)	0.0015(8)
C4'	0.0201(9)	0.0273(10)	0.0171(8)	0.0040(7)	0.0071(7)	0.0042(7)
C5'	0.0141(8)	0.0245(9)	0.0178(8)	0.0042(7)	0.0055(6)	0.0035(7)
C6'	0.0155(8)	0.0217(9)	0.0147(8)	0.0035(6)	0.0051(6)	0.0018(7)
C7'	0.0120(8)	0.0178(8)	0.0178(8)	0.0032(6)	0.0043(6)	0.0021(6)
C8'	0.0156(8)	0.0227(9)	0.0127(7)	-0.0004(6)	0.0026(6)	0.0000(7)
C9'	0.0157(8)	0.0263(10)	0.0152(8)	0.0009(7)	0.0030(6)	0.0006(7)
C10'	0.0175(9)	0.0345(11)	0.0163(8)	-0.0001(7)	0.0003(7)	-0.0010(8)
C11'	0.0217(9)	0.0369(11)	0.0149(8)	0.0044(8)	-0.0005(7)	0.0013(8)
C12'	0.0213(9)	0.0323(11)	0.0137(8)	0.0029(7)	0.0041(7)	-0.0014(8)
C13'	0.0158(8)	0.0219(9)	0.0154(8)	0.0019(7)	0.0040(6)	0.0010(7)
C14'	0.0245(9)	0.0212(9)	0.0171(8)	0.0010(7)	0.0087(7)	0.0002(7)
C15'	0.0245(9)	0.0199(9)	0.0249(9)	0.0036(7)	0.0144(8)	0.0043(7)
C16'	0.0385(12)	0.0338(12)	0.0276(10)	0.0075(9)	0.0210(9)	0.0127(9)
C17'	0.0396(12)	0.0424(13)	0.0387(12)	0.0173(10)	0.0293(10)	0.0202(10)
C18'	0.0254(10)	0.0309(11)	0.0465(12)	0.0155(9)	0.0244(9)	0.0115(9)
C19'	0.0188(9)	0.0168(9)	0.0379(11)	0.0066(8)	0.0148(8)	0.0037(7)
C20'	0.0196(9)	0.0150(8)	0.0272(9)	0.0031(7)	0.0130(7)	0.0018(7)
C21'	0.0157(9)	0.0427(12)	0.0181(8)	0.0000(8)	0.0000(7)	0.0008(8)
C22'	0.0203(10)	0.0444(13)	0.0302(10)	0.0073(9)	0.0015(8)	0.0069(9)
C23'	0.0206(10)	0.0428(13)	0.0369(11)	0.0003(10)	0.0035(9)	-0.0069(9)
C24'	0.0221(10)	0.0738(18)	0.0223(10)	-0.0052(11)	-0.0037(8)	0.0049(11)
C25'	0.0235(9)	0.0342(11)	0.0160(8)	0.0038(7)	0.0092(7)	0.0051(8)
C26'	0.0410(12)	0.0355(12)	0.0285(10)	0.0005(9)	0.0192(9)	0.0034(10)
C27'	0.0303(11)	0.0436(13)	0.0169(9)	0.0053(8)	0.0099(8)	0.0044(9)
C28'	0.0237(10)	0.0412(12)	0.0223(9)	0.0049(8)	0.0126(8)	0.0073(9)

C29'	0.0482(14)	0.0734(18)	0.0421(13)	0.0145(12)	0.0335(11)	0.0273(13)
C30'	0.087(3)	0.075(3)	0.051(3)	0.001(3)	0.032(3)	0.043(3)
C31'	0.0183(18)	0.062(3)	0.0206(18)	0.0114(18)	0.0123(15)	0.0079(19)
C32'	0.034(2)	0.136(4)	0.034(2)	0.015(3)	0.023(2)	0.033(3)
C30"	0.071(3)	0.046(2)	0.051(2)	-0.0068(19)	0.038(2)	0.013(2)
C31"	0.061(3)	0.068(3)	0.046(2)	-0.003(2)	0.027(2)	0.007(2)
C32"	0.061(3)	0.062(3)	0.059(3)	0.004(2)	0.033(2)	-0.002(2)
C33'	0.0131(9)	0.0263(11)	0.0466(12)	-0.0012(9)	0.0099(8)	0.0011(8)
C34'	0.0172(10)	0.0415(14)	0.0712(17)	0.0008(12)	0.0147(11)	0.0005(9)
C35'	0.0213(10)	0.0305(12)	0.0621(15)	-0.0129(11)	0.0085(10)	-0.0029(9)
C36'	0.0200(10)	0.0417(13)	0.0365(11)	0.0053(10)	0.0050(9)	0.0053(9)
C37'	0.0196(9)	0.0245(11)	0.0321(10)	0.0023(8)	0.0123(8)	0.0017(8)
C38'	0.0506(16)	0.0242(12)	0.086(2)	-0.0140(13)	0.0375(15)	-0.0119(11)
C39'	0.0533(16)	0.0316(13)	0.0356(12)	-0.0059(10)	0.0035(11)	0.0098(11)
C40'	0.0490(16)	0.0333(14)	0.077(2)	0.0005(13)	0.0029(15)	0.0065(12)
N4'	0.0538(16)	0.0491(15)	0.088(2)	-0.0126(14)	0.0117(14)	0.0101(12)
C39	0.076(5)	0.042(4)	0.058(5)	0.029(3)	-0.010(4)	-0.028(4)
N4	0.090(6)	0.083(6)	0.162(9)	0.088(6)	-0.065(6)	-0.050(5)
C39*	0.061(4)	0.042(3)	0.059(4)	0.020(3)	-0.019(3)	-0.018(3)
N4*	0.143(7)	0.071(4)	0.098(5)	0.037(4)	-0.069(5)	-0.043(4)
C40	0.0568(17)	0.0549(17)	0.0429(14)	0.0096(12)	0.0071(13)	-0.0222(14)

The form of the anisotropic displacement parameter is:

$$\exp[-2\pi^2\,(a^{*2}U_{11}h^2+b^{*2}U_{22}k^2+c^{*2}U_{33}l^2+2b^*c^*U_{23}kl+2a^*c^*U_{13}hl+2a^*b^*U_{12}hk)]$$

Table B.29. Bond Distances in Compound **Cr-Salen-Cy,** Å

Cr1-O1	1.9097(12)	Cr1-O2	1.9224(12)	Cr1-N1	2.0091(15)
Cr1-N2	2.0129(14)	Cr1-N3	2.1033(17)	Cr1-Cl1	2.3186(5)
O1-C1	1.314(2)	O2-C20	1.312(2)	N1-C7	1.290(2)
N1-C8	1.482(2)	N2-C14	1.282(2)	N2-C13	1.476(2)
N3-C37	1.134(3)	C1-C6	1.418(2)	C1-C2	1.431(2)
C2-C3	1.385(3)	C2-C21	1.536(3)	C3-C4	1.408(3)
C4-C5	1.372(3)	C4-C25	1.536(3)	C5-C6	1.415(2)
C6-C7	1.450(2)	C8-C9	1.521(2)	C8-C13	1.535(2)
C9-C10	1.538(3)	C10-C11	1.523(3)	C11-C12	1.524(3)
C12-C13	1.524(2)	C14-C15	1.444(2)	C15-C16	1.402(2)
C15-C20	1.426(2)	C16-C17	1.378(2)	C17-C18	1.408(2)
C17-C29	1.535(2)	C18-C19	1.391(2)	C19-C20	1.425(2)
C19-C33	1.537(2)	C21-C23	1.533(3)	C21-C22	1.534(3)
C21-C24	1.535(3)	C25-C26	1.534(3)	C25-C28	1.536(3)
C25-C27	1.537(3)	C29-C32	1.526(3)	C29-C30	1.536(3)
C29-C31	1.537(3)	C33-C35	1.532(3)	C33-C36	1.538(3)
C33-C34	1.540(2)	C37-C38	1.454(3)	Cr1'-O2'	1.9195(13)
Cr1'-O1'	1.9196(12)	Cr1'-N1'	2.0063(15)	Cr1'-N2'	2.0095(15)
Cr1'-N3'	2.0850(17)	Cr1'-Cl1'	2.3145(5)	O1'-C1'	1.313(2)

O2'-C20'	1.308(2)	N1'-C7'	1.285(2)	N1'-C8'	1.482(2)
N2'-C14'	1.285(2)	N2'-C13'	1.475(2)	N3'-C37'	1.129(3)
C1'-C6'	1.420(2)	C1'-C2'	1.432(2)	C2'-C3'	1.386(3)
C2'-C21'	1.536(3)	C3'-C4'	1.409(3)	C4'-C5'	1.367(2)
C4'-C25'	1.531(2)	C5'-C6'	1.412(2)	C6'-C7'	1.446(2)
C8'-C9'	1.522(2)	C8'-C13'	1.534(2)	C9'-C10'	1.534(2)
C10'-C11'	1.521(3)	C11'-C12'	1.527(3)	C12'-C13'	1.523(2)
C14'-C15'	1.443(3)	C15'-C16'	1.411(3)	C15'-C20'	1.421(3)
C16'-C17'	1.373(3)	C17'-C18'	1.405(3)	C17'-C29'	1.525(3)
C18'-C19'	1.387(3)	C19'-C20'	1.433(2)	C19'-C33'	1.531(3)
C21'-C24'	1.534(3)	C21'-C22'	1.534(3)	C21'-C23'	1.539(3)
C25'-C26'	1.532(3)	C25'-C28'	1.535(3)	C25'-C27'	1.539(3)
C29'-C30"	1.465(4)	C29'-C32"	1.479(4)	C29'-C32'	1.5388
C29'-C31'	1.5388	C29'-C30'	1.5396	C29'-C31"	1.747(4)
C33'-C35'	1.534(3)	C33'-C36'	1.537(3)	C33'-C34'	1.541(3)
C37'-C38'	1.445(3)	C39'-N4'	1.144(4)	C39'-C40'	1.443(4)
C39-N4	1.117(10)	C39-C40	1.449(9)	C39*-N4*	1.122(8)
C39*-C40	1.465(7)				

Table B.30. Bond Angles in Compound **Cr-Salen-Cy,** °

O1-Cr1-O2	96.51(5)	O1-Cr1-N1	91.29(6)	O2-Cr1-N1	170.26(6)
O1-Cr1-N2	172.92(6)	O2-Cr1-N2	89.52(5)	N1-Cr1-N2	82.35(6)
O1-Cr1-N3	84.44(6)	O2-Cr1-N3	87.29(6)	N1-Cr1-N3	87.68(6)
N2-Cr1-N3	92.16(6)	O1-Cr1-Cl1	93.21(4)	O2-Cr1-Cl1	94.26(4)
N1-Cr1-Cl1	91.10(5)	N2-Cr1-Cl1	90.03(5)	N3-Cr1-Cl1	177.33(5)
C1-O1-Cr1	128.58(11)	C20-O2-Cr1	128.95(11)	C7-N1-C8	122.60(15)
C7-N1-Cr1	125.19(12)	C8-N1-Cr1	112.17(11)	C14-N2-C13	122.64(15)
C14-N2-Cr1	124.05(12)	C13-N2-Cr1	112.89(11)	C37-N3-Cr1	160.37(16)
O1-C1-C6	122.55(16)	O1-C1-C2	119.19(16)	C6-C1-C2	118.25(16)
C3-C2-C1	118.12(17)	C3-C2-C21	121.99(16)	C1-C2-C21	119.88(16)
C2-C3-C4	124.25(17)	C5-C4-C3	117.06(17)	C5-C4-C25	123.17(18)
C3-C4-C25	119.76(17)	C4-C5-C6	121.69(17)	C5-C6-C1	120.35(16)
C5-C6-C7	115.87(16)	C1-C6-C7	123.74(16)	N1-C7-C6	125.27(16)
N1-C8-C9	116.76(15)	N1-C8-C13	107.24(14)	C9-C8-C13	111.20(15)
C8-C9-C10	109.16(16)	C11-C10-C9	111.92(18)	C10-C11-C12	111.79(17)
C11-C12-C13	110.49(17)	N2-C13-C12	115.62(15)	N2-C13-C8	107.01(14)
C12-C13-C8	111.06(15)	N2-C14-C15	125.73(16)	C16-C15-C20	120.44(16)
C16-C15-C14	116.73(15)	C20-C15-C14	122.65(16)	C17-C16-C15	122.27(16)
C16-C17-C18	116.34(16)	C16-C17-C29	120.25(16)	C18-C17-C29	123.40(16)
C19-C18-C17	124.31(16)	C18-C19-C20	118.31(15)	C18-C19-C33	122.11(15)
C20-C19-C33	119.58(15)	O2-C20-C19	119.94(15)	O2-C20-C15	122.21(15)
C19-C20-C15	117.83(15)	C23-C21-C22	109.26(17)	C23-C21-C24	107.12(17)
C22-C21-C24	107.63(17)	C23-C21-C2	110.36(16)	C22-C21-C2	110.25(16)
C24-C21-C2	112.11(16)	C26-C25-C4	109.19(17)	C26-C25-C28	108.78(19)

C4-C25-C28	111.46(17)	C26-C25-C27	109.39(19)	C4-C25-C27	109.78(17)
C28-C25-C27	108.21(18)	C32-C29-C17	112.10(16)	C32-C29-C30	108.80(19)
C17-C29-C30	108.85(16)	C32-C29-C31	108.19(17)	C17-C29-C31	110.18(16)
C30-C29-C31	108.66(17)	C35-C33-C19	110.47(15)	C35-C33-C36	109.43(15)
C19-C33-C36	109.89(15)	C35-C33-C34	106.79(16)	C19-C33-C34	112.12(15)
C36-C33-C34	108.04(16)	N3-C37-C38	178.2(2)	O2'-Cr1'-O1'	96.65(5)
O2'-Cr1'-N1'	170.38(6)	O1'-Cr1'-N1'	91.53(6)	O2'-Cr1'-N2'	89.55(6)
O1'-Cr1'-N2'	172.09(6)	N1'-Cr1'-N2'	81.89(6)	O2'-Cr1'-N3'	85.93(6)
O1'-Cr1'-N3'	85.69(6)	N1'-Cr1'-N3'	89.65(6)	N2'-Cr1'-N3'	89.87(6)
O2'-Cr1'-Cl1'	94.09(4)	O1'-Cr1'-Cl1'	93.89(4)	N1'-Cr1'-Cl1'	90.39(5)
N2'-Cr1'-Cl1'	90.55(5)	N3'-Cr1'-Cl1'	179.58(4)	C1'-O1'-Cr1'	127.50(11)
C20'-O2'-Cr1'	128.89(12)	C7'-N1'-C8'	122.27(15)	C7'-N1'-Cr1'	125.13(12)
C8'-N1'-Cr1'	112.59(10)	C14'-N2'-C13'	123.35(15)	C14'-N2'-Cr1'	124.38(13)
C13'-N2'-Cr1'	112.08(10)	C37'-N3'-Cr1'	164.39(16)	O1'-C1'-C6'	122.51(16)
O1'-C1'-C2'	119.58(16)	C6'-C1'-C2'	117.90(16)	C3'-C2'-C1'	118.17(16)
C3'-C2'-C21'	121.30(16)	C1'-C2'-C21'	120.53(16)	C2'-C3'-C4'	124.44(17)
C5'-C4'-C3'	116.74(16)	C5'-C4'-C25'	122.83(17)	C3'-C4'-C25'	120.33(16)
C4'-C5'-C6'	122.04(16)	C5'-C6'-C1'	120.58(16)	C5'-C6'-C7'	115.33(15)
C1'-C6'-C7'	124.09(16)	N1'-C7'-C6'	125.15(16)	N1'-C8'-C9'	116.29(14)
N1'-C8'-C13'	105.57(14)	C9'-C8'-C13'	111.73(15)	C8'-C9'-C10'	109.67(15)
C11'-C10'-C9'	110.69(15)	C10'-C11'-C12'	111.18(16)	C13'-C12'-C11'	109.56(15)
N2'-C13'-C12'	116.23(15)	N2'-C13'-C8'	106.44(14)	C12'-C13'-C8'	111.85(15)
N2'-C14'-C15'	125.28(17)	C16'-C15'-C20'	120.44(18)	C16'-C15'-C14'	116.63(18)
C20'-C15'-C14'	122.68(16)	C17'-C16'-C15'	121.7(2)	C16'-C17'-C18'	117.03(19)
C16'-C17'-C29'	123.4(2)	C18'-C17'-C29'	119.6(2)	C19'-C18'-C17'	124.43(19)
C18'-C19'-C20'	117.78(19)	C18'-C19'-C33'	122.71(18)	C20'-C19'-C33'	119.51(17)
O2'-C20'-C15'	122.54(16)	O2'-C20'-C19'	119.32(17)	C15'-C20'-C19'	118.10(17)
C24'-C21'-C22'	107.60(18)	C24'-C21'-C2'	111.65(17)	C22'-C21'-C2'	110.63(17)
C24'-C21'-C23'	107.42(19)	C22'-C21'-C23'	109.58(18)	C2'-C21'-C23'	109.88(16)
C4'-C25'-C26'	108.34(16)	C4'-C25'-C28'	111.19(16)	C26'-C25'-C28'	109.10(17)
C4'-C25'-C27'	110.60(16)	C26'-C25'-C27'	109.83(17)	C28'-C25'-C27'	107.78(16)
C30"-C29'-C32"	117.3(2)	C30"-C29'-C17	113.9(2)	C32"-C29'-C17'	110.9(3)
C30"-C29'-C32'	66.6(3)	C32"-C29'-C32'	57.4(2)	C17'-C29'-C32'	111.3(2)
C30"-C29'-C31'	133.6(2)	C32"-C29'-C31'	55.7(2)	C17'-C29'-C31'	110.2(2)
C32'-C29'-C31'	109.6	C30"-C29'-C30'	43.9(2)	C32"-C29'-C30'	142.4(3)
C17'-C29'-C30'	106.8(2)	C32'-C29'-C30'	109.5	C31'-C29'-C30'	109.5
C30"-C29'-C31"	102.7(2)	C32"-C29'-C31"	102.1(2)	C17'-C29'-C31"	108.6(2)
C32'-C29'-C31"	139.6(2)	C31'-C29'-C31"	48.4(2)	C30'-C29'-C31"	63.7(2)
C19'-C33'-C35'	109.62(17)	C19'-C33'-C36'	110.63(17)	C35'-C33'-C36'	109.87(19)
C19'-C33'-C34'	112.40(19)	C35'-C33'-C34'	106.69(18)	C36'-C33'-C34'	107.51(18)
N3'-C37'-C38'	178.7(2)	N4'-C39'-C40'	178.4(3)	N4-C39-C40	176.3(14)
N4*-C39*-C40	179.0(8)	C39-C40-C39*	41.4(4)		

378

APPENDIX C: CHIRAL HPLC CHROMATOGRAMS
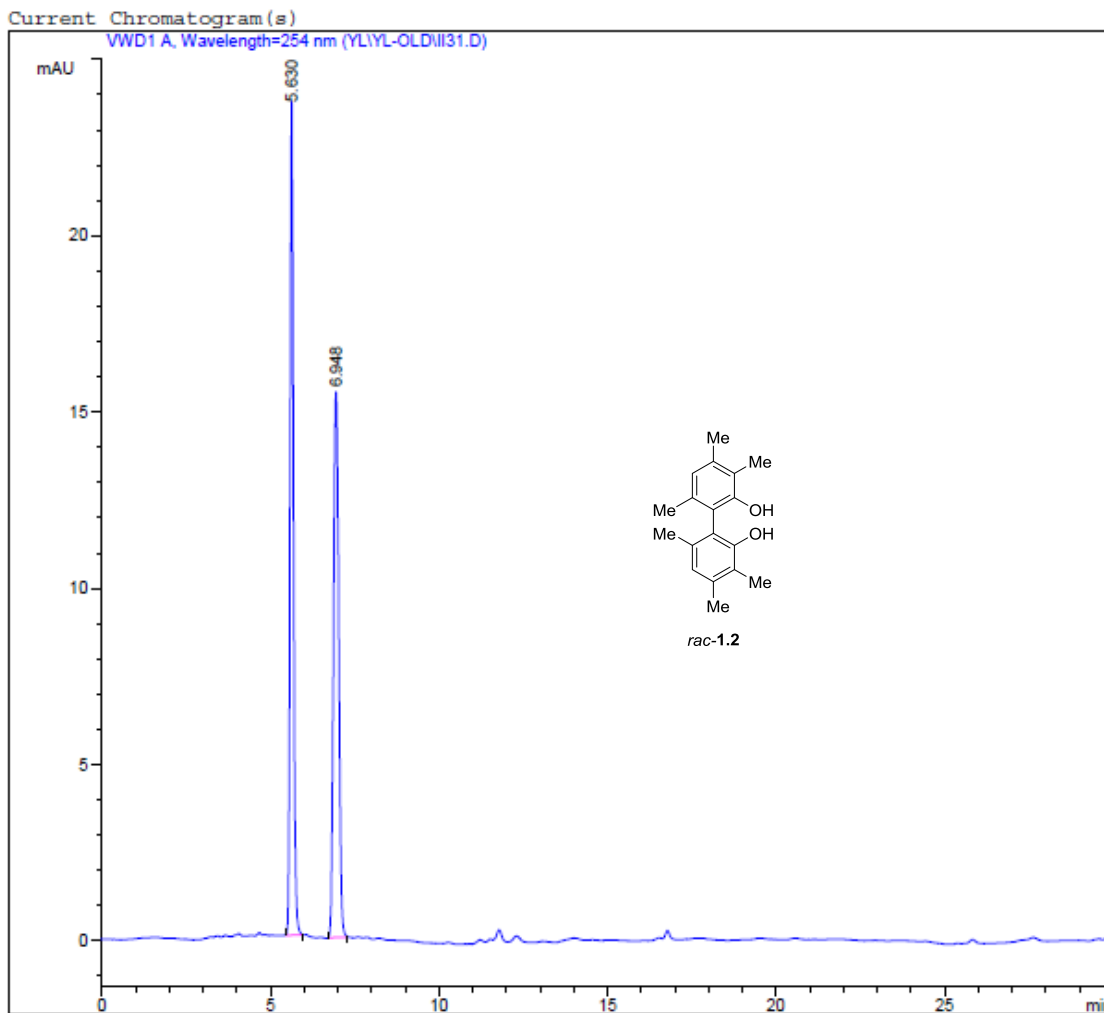

```
=================================================================
                      Integration Results
=================================================================

Signal 1: VWD1 A, Wavelength=254 nm
 Integrated with enhanced integrator!

Peak   Time    Type     Area       Height    Width    Start    End
  #    [min]           [mAU*s]     [mAU]     [min]    [min]    [min]
----|--------|----|-----------|------------|-------|--------|--------|
  1   5.630  BB    163.64006   23.65071   0.1069   5.470    5.940
  2   6.948  BB    167.38150   15.47991   0.1742   6.717    7.275

=================================================================
```

Figure C.1 HPLC chromatogram of compound *racemic* **1.2**

Figure C.2 HPLC chromatogram of compound (*S*)-**1.2**

Figure C.3 HPLC chromatogram of compound *racemic* **1.17**

Figure C.4 HPLC chromatogram of compound **1.17**

```
========================================================================
                         Integration Results
========================================================================

Signal 1: VWD1 A, Wavelength=254 nm
 Integrated with enhanced integrator!

Peak    Time    Type     Area         Height       Width     Start      End
  #     [min]          [mAU*s]        [mAU]        [min]     [min]      [min]
----|---------|----|------------|------------|-------|--------|--------|
   1    7.931  BB     598.33435     61.63962   0.1496    7.693    8.479
   2   15.077  BB     604.62708     29.79046   0.3110   14.667   15.841

========================================================================
```

Figure C.5 HPLC chromatogram of compound *racemic* **1.18**

```
Current Chromatogram(s)
      VWD1 A, Wavelength=254 nm (YL\YL-OLD\III200.D)
 mAU




 400




 300




 200




 100




   0


       0      2.5      5       7.5     10      12.5     15      17.5      min
```


1.18
82% ee

```
================================================================
                    Integration Results
================================================================

Signal 1: VWD1 A, Wavelength=254 nm
 Integrated with enhanced integrator!

Peak    Time    Type      Area        Height     Width    Start    End
  #    [min]           [mAU*s]       [mAU]      [min]    [min]    [min]
----|--------|----|-----------|-----------|-------|--------|--------|
   1    7.844 BB    5618.63379   470.15958   0.1802    7.571    8.721
   2   15.291 BB     541.60052    23.52526   0.3487   14.900   16.191

================================================================
```

Figure C.6 HPLC chromatogram of compound **1.18**
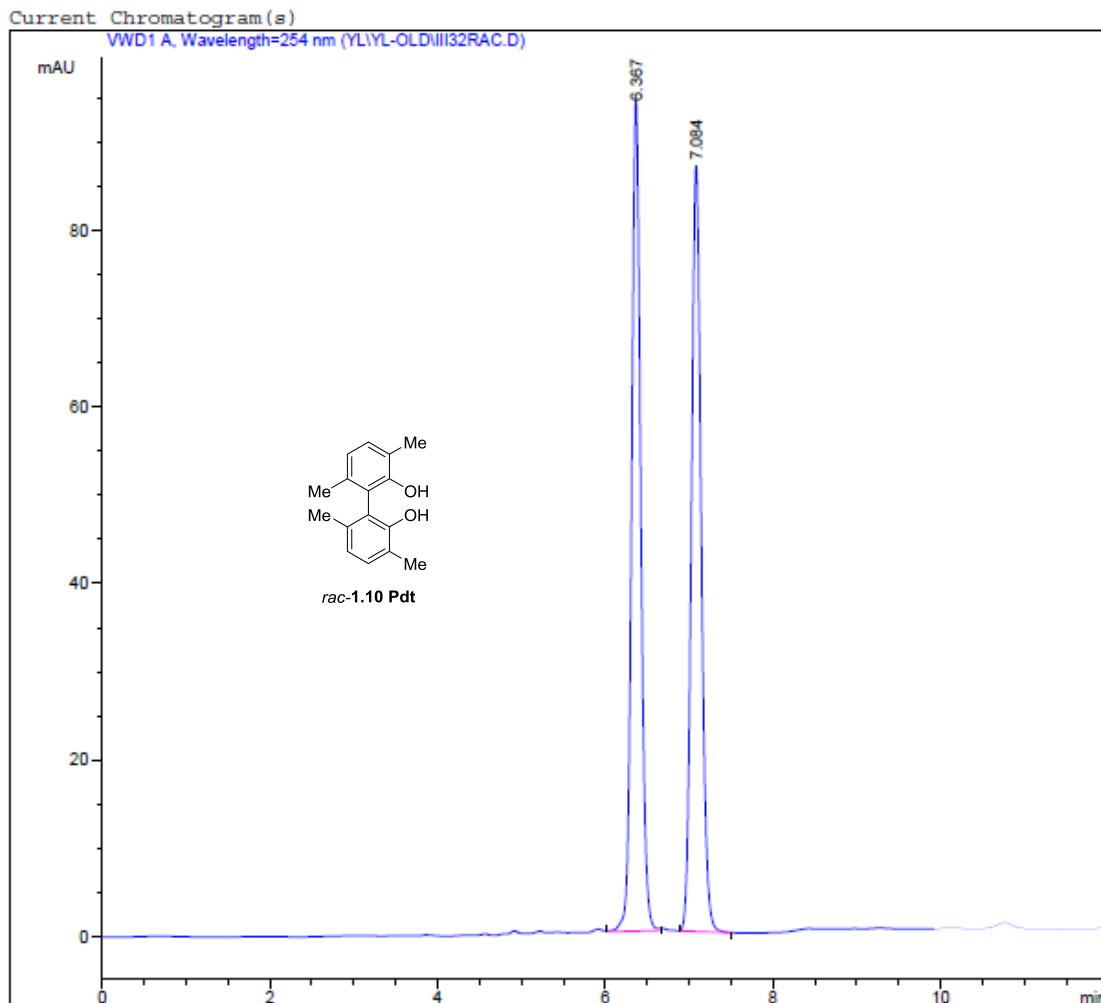
384

```
======================================================================
                        Integration Results
======================================================================

Signal 1: VWD1 A, Wavelength=254 nm
 Integrated with enhanced integrator!

Peak    Time    Type      Area          Height     Width      Start       End
 #      [min]            [mAU*s]        [mAU]      [min]      [min]      [min]
----|--------|----|------------|------------|-------|--------|--------|
  1     6.367  VB      710.34619     94.09510   0.1157     6.015      6.664
  2     7.084  PP      705.74231     86.77472   0.1240     6.887      7.513

======================================================================
```

Figure C.7 HPLC chromatogram of compound *racemic* **1.10 Pdt**

```
==================================================================
                      Integration Results
==================================================================

Signal 1: VWD1 A, Wavelength=254 nm
 Integrated with enhanced integrator!

Peak    Time    Type      Area        Height       Width     Start     End
  #    [min]           [mAU*s]        [mAU]        [min]     [min]     [min]
----|--------|----|-----------|------------|-------|--------|--------|
   1   6.376 BB       14.68403     1.95147  0.1140     6.249    6.581
   2   7.092 BP       74.84369     9.12863  0.1262     6.897    7.377

==================================================================
```

Figure C.8 HPLC chromatogram of compound **1.10 Pdt**

```
Current Chromatogram(s)
    VWD1 A, Wavelength=254 nm (YL\YL-OLD\YLV143_R.D)
mAU
100-


 80-


 60-


 40-


 20-


  0-

    0      2.5      5       7.5      10      12.5     15      17.5    min
```

rac-**1.22**

```
=====================================================================
                        Integration Results
=====================================================================

Signal 1: VWD1 A, Wavelength=254 nm
 Integrated with enhanced integrator!

Peak    Time    Type      Area          Height      Width     Start      End
  #     [min]          [mAU*s]          [mAU]       [min]     [min]      [min]
----|---------|----|------------|-------------|-------|--------|--------|
   1    3.808 VV       556.84216      99.14023   0.0859    3.666     3.978
   2    4.304 VB       530.03882      89.50958   0.0895    4.156     4.606

=====================================================================
```

Figure C.9 HPLC chromatogram of compound *racemic* **1.22**

387

```
Current Chromatogram(s)
       VWD1 A, Wavelength=254 nm (YL\YL-OLD\YLV-143.D)
  mAU
                       4.288

300

250

200

150

100

 50
                 3.802

  0

      0    2.5     5     7.5    10    12.5   15    17.5   min
```

==
                        Integration Results
==

Signal 1: VWD1 A, Wavelength=254 nm
 Integrated with enhanced integrator!

```
Peak   Time   Type    Area         Height       Width    Start     End
 #     [min]          [mAU*s]      [mAU]        [min]    [min]     [min]
----|--------|----|-----------|------------|-------|--------|--------|
  1   3.802  VV    265.26334    43.63847    0.0898   3.660    3.982
  2   4.288  VB   1939.18542   321.85019    0.0907   4.143    4.645
```

==

Figure C.10 HPLC chromatogram of compound **1.22**

388

```
==================================================================
                     Integration Results
==================================================================

Signal 1: VWD1 A, Wavelength=254 nm
 Integrated with enhanced integrator!

Peak    Time    Type     Area        Height    Width    Start    End
 #      [min]           [mAU*s]      [mAU]     [min]    [min]    [min]
----|--------|----|-----------|-----------|-------|--------|--------|
   1   4.291  VV    931.83197    82.49828  0.1696   4.151   4.551
   2   5.407  BV    836.43250    95.69226  0.1326   5.208   5.681

==================================================================
```
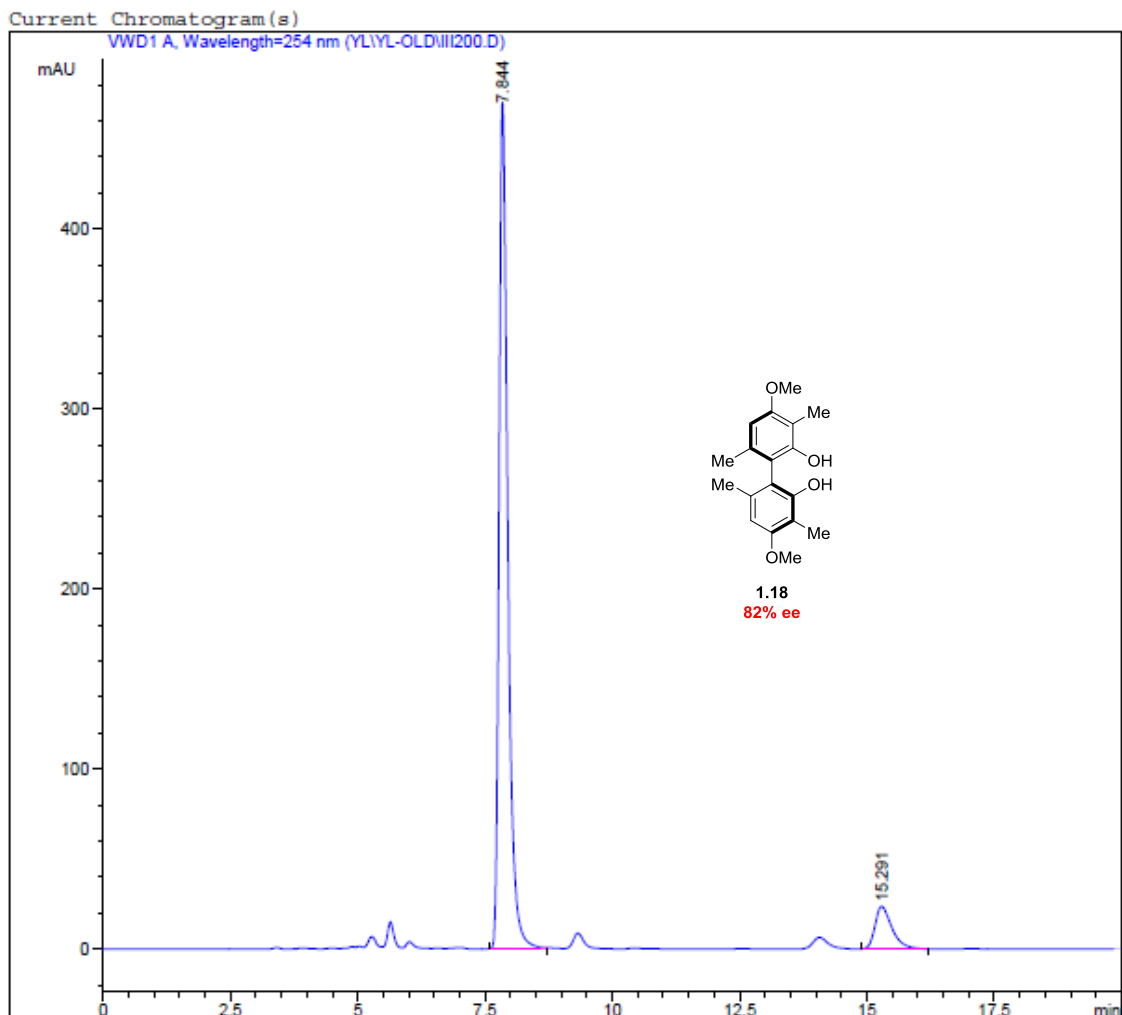
Figure C.11 HPLC chromatogram of compound *racemic* **1.23**

389

Figure C.12 HPLC chromatogram of compound **1.23**

Figure C.13 HPLC chromatogram of compound *racemic* **1.28**
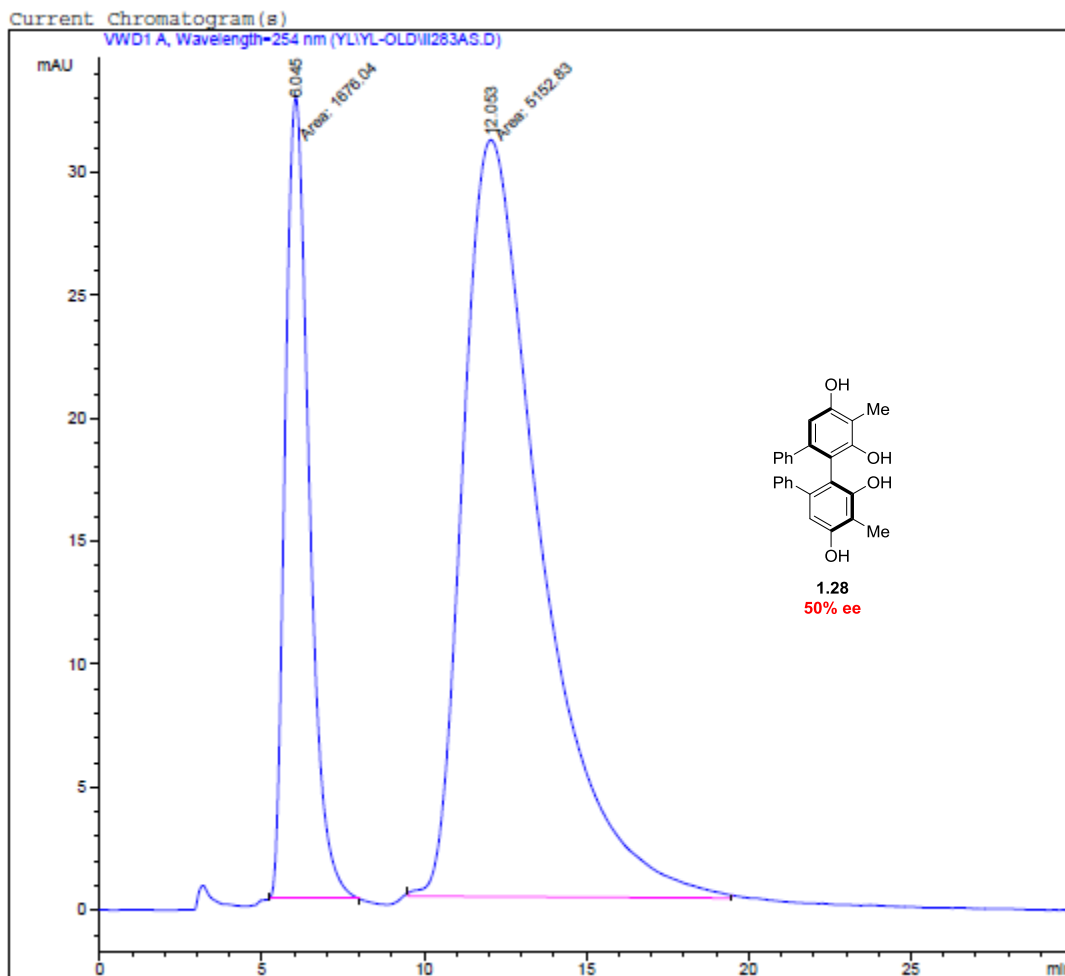
Figure C.14 HPLC chromatogram of compound **1.28**
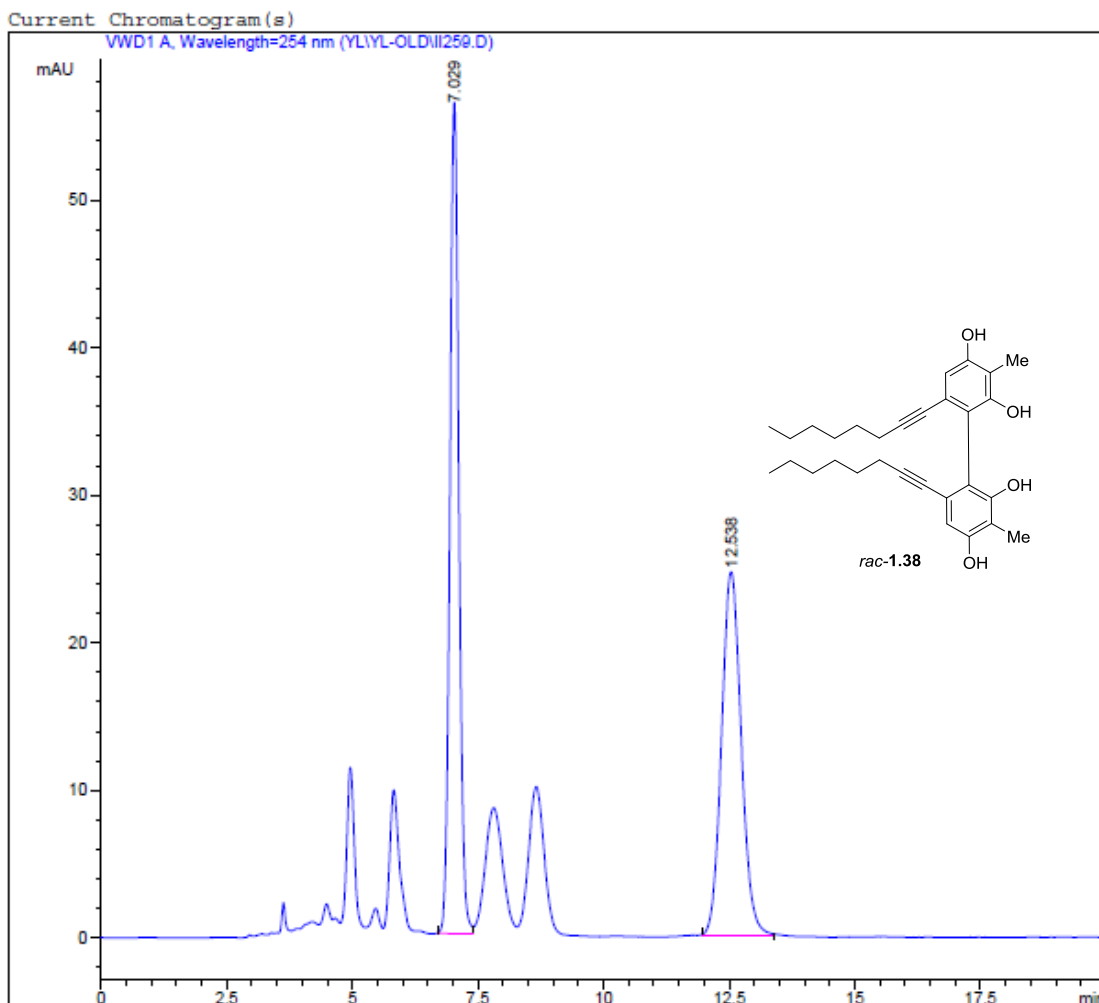
```
========================================================================
                        Integration Results
========================================================================

Signal 1: VWD1 A, Wavelength=254 nm
 Integrated with enhanced integrator!

Peak    Time    Type      Area          Height      Width     Start     End
  #     [min]           [mAU*s]         [mAU]       [min]     [min]     [min]
----|--------|----|------------|------------|-------|--------|--------|
   1    6.045 MM    1654.17041    32.43134    0.8501    5.157    7.573
   2   12.053 MM    4975.93945    30.53578    2.7159    9.963   18.164

========================================================================
```
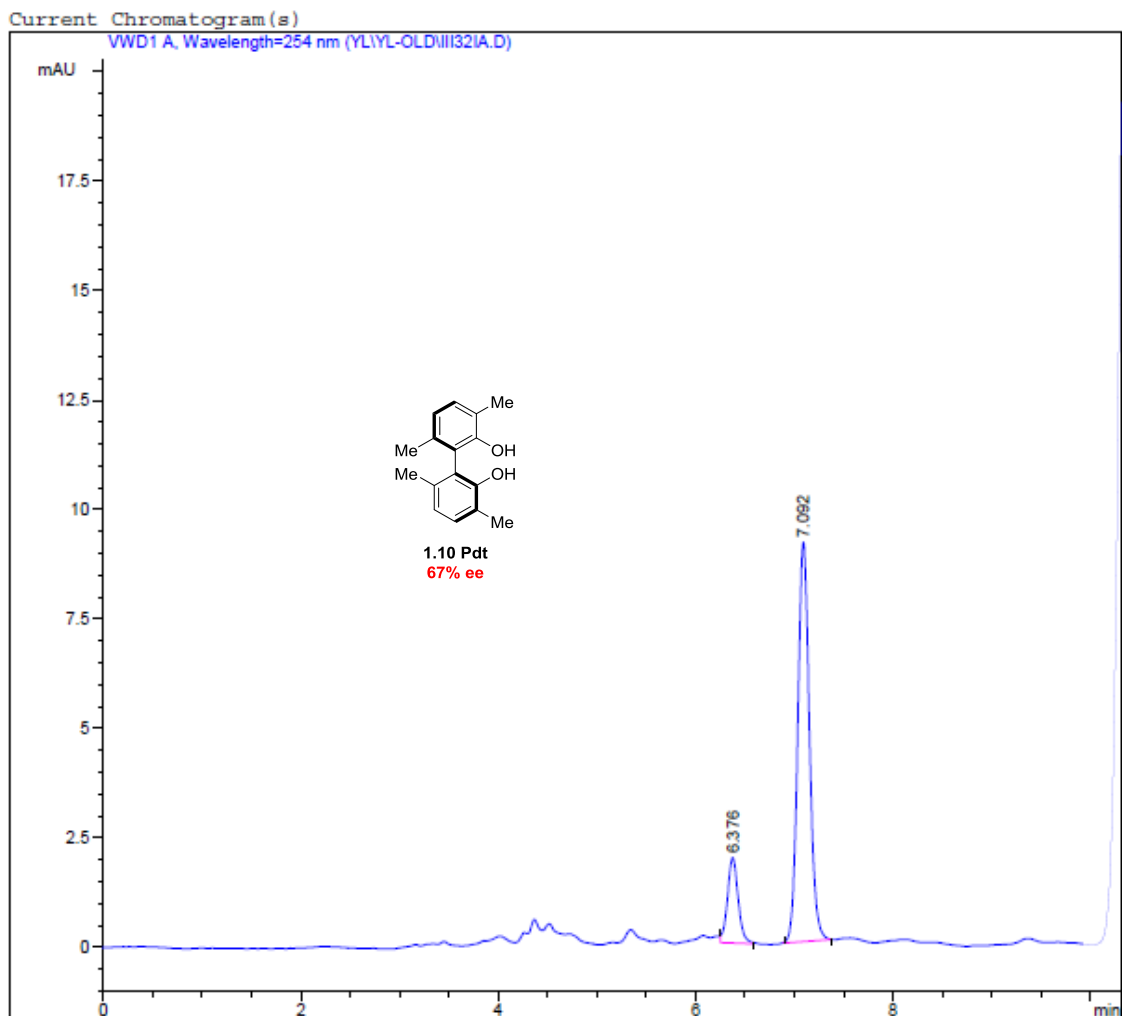
Figure C.15 HPLC chromatogram of compound *racemic* **1.38**
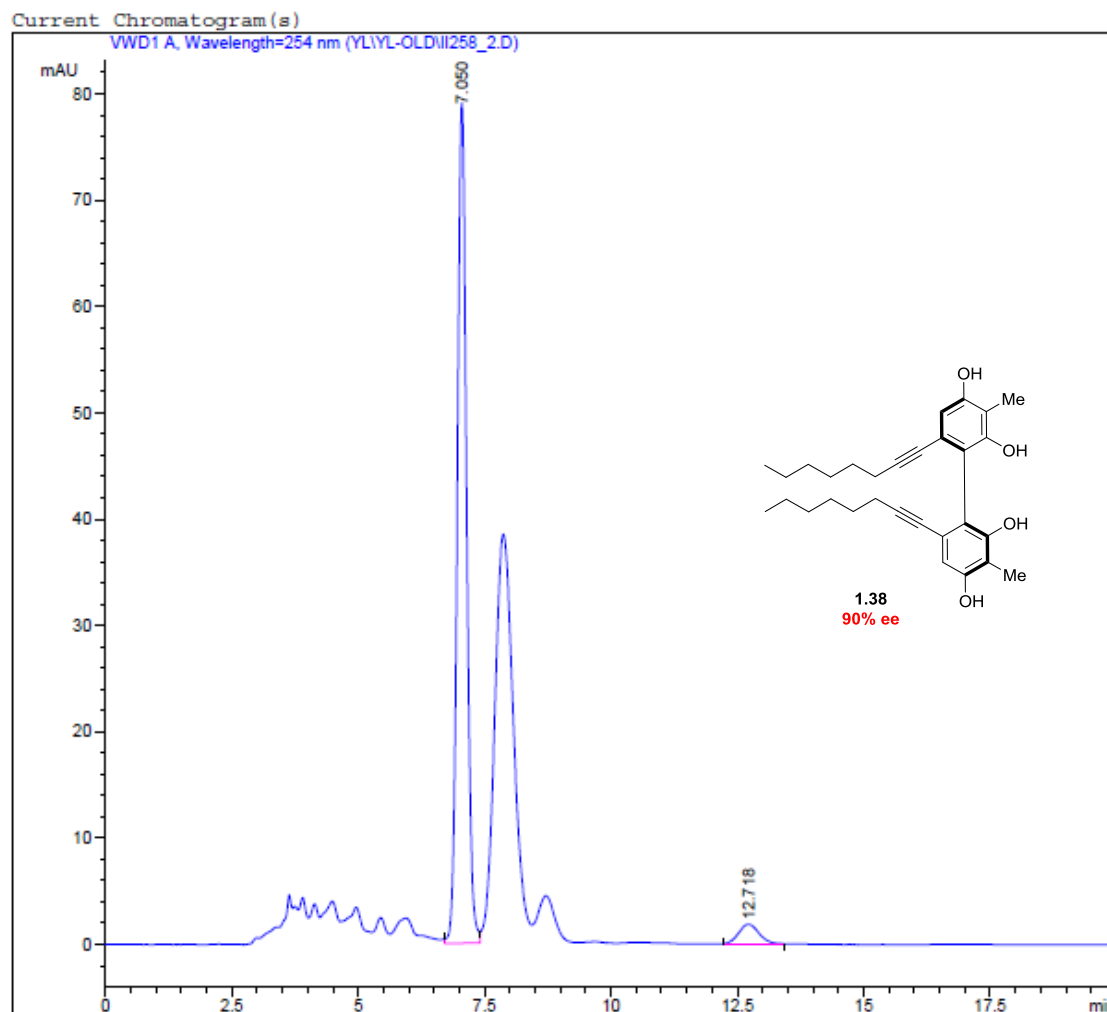
Current Chromatogram(s)
VWD1 A, Wavelength=254 nm (YL\YL-OLD\II258_2.D)

===
                        Integration Results
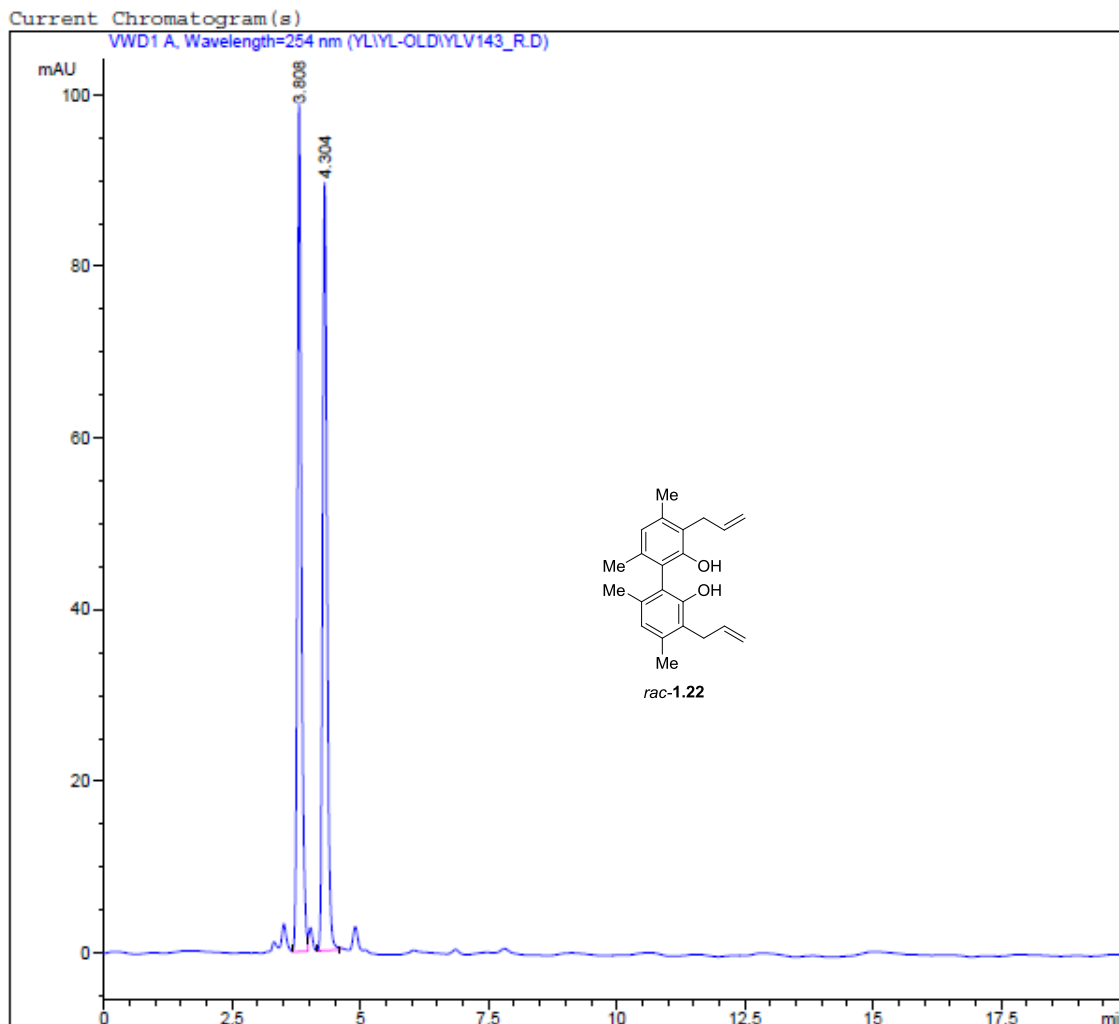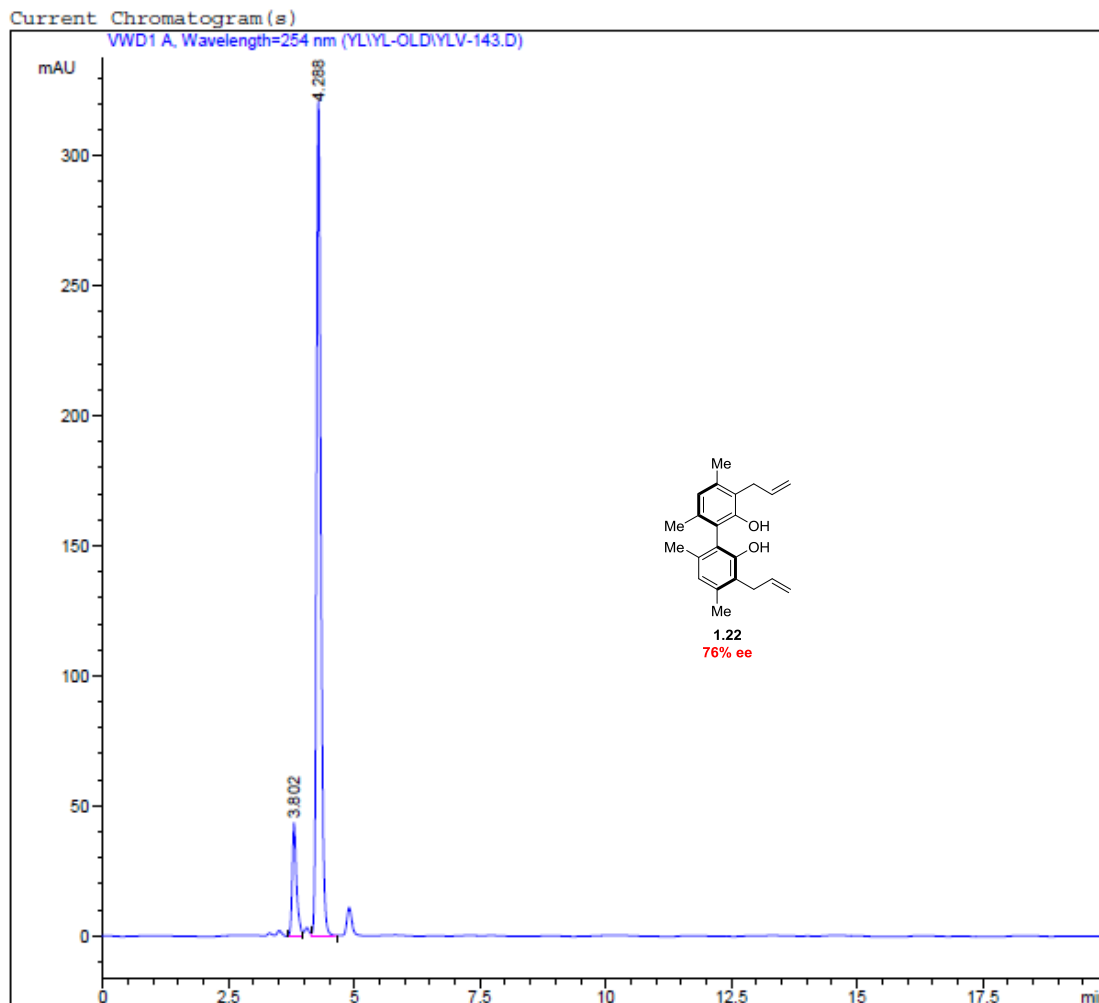===

Signal 1: VWD1 A, Wavelength=254 nm
 Integrated with enhanced integrator!

Peak #	Time [min]	Type	Area [mAU*s]	Height [mAU]	Width [min]	Start [min]	End [min]
1	7.050	BV	1007.29608	79.01242	0.1968	6.712	7.408
2	12.718	BB	51.32779	1.84031	0.4098	12.216	13.434

===

Figure C.16 HPLC chromatogram of compound **1.38**

394

BIBLIOGRAPHY

Adams, R.; Morris, R. C.; Butterbaugh, D. J.; Kirkpatrick, E. C. "Stucture of Gossypol" *J. Am. Chem. Soc.* **1938**, *60*, 2191–2193.

Alexander, J. B.; La, D. S.; Cefalo, D. R.; Hoveyda, A. H.; Schrock, R. R. "Catalytic Enantioselective Ring-Closing Metathesis by a Chiral Biphen-Mo Complex" *J. Am. Chem. Soc.* **1998**, *120*, 4041-4042.

Alexander, J. B.; Schrock, R. R.; Davis, W. M.; Hultzsch, K. C.; Hoveyda, A. H.; Houser, J. H. "Synthesis of Molybdenum Imido Alkylidene Complexes That Contain 3,3-Dialkyl-5,5,6,6-tetramethyl-1,1-biphenyl-2,2-diolates (Alkyl = *t*-Bu, Adamantyl). Catalysts for Enantioselective Olefin Metathesis Reactions" *Organometallics* **2000**, *19*, 3700-3715.

Amatore, M.; Gosmini, C. "Direct Method for Carbon-Carbon Bond Formation: The Functional Group Tolerant Cobalt-Catalyzed Alkylation of Aryl Halides" *Chem. Eur. J.* **2010**, *16*, 5848-5852.

Amblard, F.; Govindarajan, B.; Lefkove, B.; Rapp, K. L.; Detorio, M.; Arbiser, J. L.; Schinazi, R. F. "Synthesis, cytotoxicity, and antiviral activities of new neolignans related to honokiol and magnolol" *Bioorg. Med. Chem. Lett.* **2007**, *17*, 4428-4431.

Amstrong D. R.; Breckenridge, R. J.; Cameron C.; Nonhebel, D. C.; Pauson, P. L.; Perkins, P. G. "The Role of Stereoelectronic Factors in the Oxidation of Phenols" *Tetrahedron Lett.* **1983**, *24*, 1071-1074.

Arkley, V.; Dean, F. M.; Robertson, A.; Sidisunthorn, P. "451. Usnic Acid. Part XII. Pummerer's Ketone" *J. Chem. Soc.* **1956**, 2322–2328.

Armstrong, D. R.; Cameron, C.; Nonhebel, D. C.; Perkins, P. G. "Oxidative Coupling of Phenols. Part 10. The Role of Steric Effects in the Formation of C-O Coupled Products" *J. Chem. Soc.-Perkin Trans. 2* **1983**, 581-585.

Armstrong, D. R.; Cameron, C; Nonhebel, D. C.; Perkins, P. G. "Oxidative Coupling of Phenols. Part 6. A Study of the Role of Spin Density Factors on the Product Composition in the Oxidations of 3,5-Dimethylphenol and Phenol" *J. Chem. Soc. Perk. Trans. 2* **1983**, 563–568.

Aveniente, M.; Pinto, E. F.; Santos, L. S.; Rossi-Bergmann, B.; Barata, L. E. S. "Structure–Activity Relationship of Antileishmanials Neolignan Analogues" *Bioorg. Med. Chem.* **2007**, *15*, 7337–7343.

Barhate, N. B.; Chen, C.-T. "Catalytic Asymmetric Oxidative Couplings of 2-Naphthols by Tridentate *N*-Ketopinidene-Based Vanadyl Dicarboxylates" *Org. Lett.* **2002**, *4*, 2529-2532.

Baskin, R.; Gali, M.; Park, S. O.; Zhao, Z, J.; Keseru, G. M.; Bisht, K. S.; Sayeski, P. P. "Identification of novel SAR properties of the Jak2 small molecule inhibitor G6: Significance of the *para*-hydroxyl orientation" *Bioorg. Med. Chem. Lett.* **2012**, *22*, 1402-1407.

Bergbreiter, D.; Hobbs, C.; Hongfa, C. "Polyolefin-Supported Recoverable/Reusable Cr(III)-Salen Catalysts" *J. Org. Chem.* **2011***, 76,* 523–533.

Bigot, A.; Dau, M. E. T. H.; Zhu, J. "Total Synthesis of an Antitumor Agent RA-VII via an Efficient Preparation of Cycloisodityrosine" *J. Org. Chem.* **1999**, *64*, 6283-6296.

Bios-Choussy, M.; Cristau, P.; Zhu, J. "Total Synthesis of an Atropdiastereomer of RP-66453 and Determination of Its Absolute Configuration" *Angew. Chem., Int. Ed.* **2003**, *42*, 4238-4241.

Boger, D. L.; Patane, M. A.; Zhou, J. C. "Total Synthesis of Bouvardin, *O*-Methylbouvardin, and *O*-Methyl-*N^9*-desmethylbouvardin" *J. Am. Chem. Soc.* **1994**, *116*, 8544-8556.

Bordwell, F. G.; Cheng, J. P. "Substituent Effects on the Stabilities of Phenoxyl Radicals and the Acidities of Phenoxyl Radical Cations" *J. Am. Chem. Soc.* **1991**, *113*, 1736–1743.

Bringmann, G.; Gulder, T.; Gulder, T. M; Breuning, M. "Atroposelective Total Synthesis of Axially Chiral Biaryl Natural Products" *Chem. Rev.* **2011**, *111*, 563–639.

Bringmann, G.; Günther, C.; Ochse, M.; Schupp, O.; Tasler, S. "Biaryls in Nautre: A Multi-Facetted Class of Stereochemically, Biosynthetically, and Pharmacologically Intriguing Secondary Metaobolites" *Prog. Chem. Org. Nat. Prod.* **2001**, *82*, 1–249.

Bringmann, G.; Menche, D. "Stereoselective Total Synthesis of Axially Chiral Natural Products via Biaryl Lactones" *Acc. Chem. Res.* **2001**, *34*, 615–624.

Bringmann, G.; Mortimer, A. J. P.; Keller, P. A.; Gresser M. J.; Garner, J.; Breuning, M. "Atroposelective Synthesis of Axially Chiral Biaryl Compounds" *Angew. Chem. Int. Ed.* **2005**, *44*, 5384–5427.

Bringmann, G.; Scharl, H.; Maksimenka, K.; Radacki, K.; Braunschweig, H.; Wich, P.; Schmuck, C. "Atropodiastereoselective Cleavage of Configurationally Unstable Biaryl Lactones with Amino Acid Esters" *Eur. J. Org. Chem.* **2006**, 4349–4361.

396

Brown, C.;Krzystek, J.; Achey, R; Lita, A.; Fu, R.; Meulenberg, R. W.; Polinski, M.; Peek, N.; Wang, Y.; van de Burgt, L. J.; Profeta, Jr. S.; Stiegman, A. E.; Scott, S. L. "Mechanism of Initiation in the Phillips Ethylene Polymerization Catalyst: Redox Processes Leading to the Active Site" *ACS. Catal.* **2015**, *5*, 5574–5583.

Cao, T. "Part B: The Regioselective Oxidative Coupling of Phenols" *Dissertation.* **2013**, University of Pennsylvania, Philadelphia, PA

Chen, C.-M.; Liu, Y.-C. "A Concise Synthesis of Honokiol" *Tetrahedron Lett.* **2009**, *50*, 1151-1152.

Chen, C.-T.; Kao, J.-Q.; Salunke, S. B.; Lin, Y.-H. "Enantioselective Aerobic Oxidation of α-Hydroxy-Ketones Catalyzed by Oxovanadium(V) Methoxides Bearing Chiral, *N*-Salicylidene-*tert*-butylglycinates" *Org. Lett.*, **2011**, *13*, 26-29.

Chen, P.-Y.; Wu, Y.-H.; Hsu, M.-H.; Wang, T.-P.; Wang, E.-C. "Cerium Ammonium Nitrate-Mediated the Oxidative Dimerization of p-alkenylphenols: A New Synthesis of Substituted (±)-*trans*-dihydrobenzofurans" *Tetrahedron* 2013, *69*, 653–657

Chen, Y.–H.; Cheng, D.–J.; Zhang, J.; Wang, Y.; Liu, X.–Y.; Tan, B. "Atroposelective Synthesis of Axially Chiral Biaryldiols via Organocatalytic Arylation of 2-Naphthols" *J. Am. Chem. Soc.* **2015**, *137*, 15062–15065.

Chioccara, F.; Poli, S.; Rindone, B.; Pilati, T.; Brunow, G.; Pietikäinen, P.; Setälä, H. "Regio- and Diastereo-selective Synthesis of Dimeric Lignans Using Oxidative Coupling." *Acta Chem. Scand.* **1993**, *47*, 610–616.

Cho, J.; Woo, J.; Han, J. E.; Kubo, M.; Ogura, T.; Nam, W. "Chromium(V)-oxo and Chromium(III)-superoxo Complexes Bearing a Macrocyclic TMC Ligand in Hydrogen Atom Abstraction Reactions" *Chem. Sci.* **2011**, *2*, 2057.

Chu, C.-Y.; Hwang, D.-R.; Wang, S.-K.; Uang, B.-J. "Chiral Oxovanadium Complex Catalyzed Enantioselective Oxidative Coupling of 2-Naphthols" *Chem. Commun.* **2001**, 980–981.

Chu, C.-Y.; Uang, B.-J. "Catalytic Enatioselective Coupling of 2-Naphthols by New Chiral Oxovanadium Complexed Bearing a Self Accelerating Functional Group" *Tetrahedron:Asymmetry*, **2003**, *14*, 53-55.

Cocchietto, M.; Skert, N.; Nimis, P. L.; Sava, G. "A review on usnic acid, an interesting natural compound" *Naturwissenschaften* **2002**, *89*, 137–146.

Cozzi, P. G. "Metal–Salen Schiff base complexes in catalysis: practical aspects" *Chem. Soc. Rev.* **2004**, *33*, 410–421.

Dagne, E.; Steglich, W. "Knipholone: a Unique Anthraquinone Derivative from *Kniphofia Foliosa*" *Phytochemistry* **1984**, *23*, 1729-1731.

397

Daniels, R. N.; Fadeyi, O. O.; Lindsley, C. W. "A New Catalytic Cu(II)/Sparteine Oxidant System for β,β-Phenolic Couplings of Styrenyl Phenols: Synthesis of Carpanone and Unnatural Analogs" *Org. Lett.* **2008**, *10*, 4097–4100.

Davin, L. B.; Lewis, N. G. "Dirigent phenoxy radical coupling: advances and challenges" *Current Opinion in Biotechnology* **2005**, *16*, 398–406.

Davin, L. B.; Lewis, N. G. "Dirigent Proteins and Dirigent Sites Explain the Mystery of Specificity of Radical Precursor Coupling in Lignan and Lignin Biosynthesis" *Plant Physiology* **2000**, *123*, 453–461.

Decicco, C. P.; Song, Y.; Evans, D. A. "Intramolecular *O*-Arylation of Phenols with Phenylboronic Acids: Application to the Synthesis of Macrocyclic Metalloproteinase Inhibitors" *Org. Lett.* **2001**, *3*, 1029-1032.

Degnan, A. P.; Meyers, A. I. "Total Syntheses of (−)-Herbertenediol, (−)-Mastigophorene A, and (−)-Mastigophorene B. Combined Utility of Chiral Bicyclic Lactams and Chiral Aryl Oxazolines" *J. Am. Chem. Soc.* **1999**, *121*, 2762–2769.

Denton, R. M.; Scragg, J. T.; Galofre, A. M.; Gui, X.; Lewis, W. "A Concise Synthesis of Honokiol" *Tetrahedron* **2010**, *66*, 8029-8035.

Dreher, S. D.; Dormer, P. G.; Sandrock, D. L.; Molander, G. A. "Efficient Cross-Coupling of Secondary Alkyltrifluoroborates with Aryl Chlorides − Reaction Discovery Using Parallel Microscale Experimentation" *J. Am. Chem. Soc.* **2008,** *130,* 9257–9259.

Durandetti, M.; Nedelec, J.-Y.; Perichon, J. "Nickel-Catalyzed Direct Electrochemical Cross-Coupling between Aryl Halides and Activated Aryl Halides" *J. Org. Chem.* **1996**, *61*, 1748-1755.

Egami, H.; Matsumoto, K.; Oguma, T.; Kunisu, T.; Katsuki, T. "Enantioenriched Synthesis of C-1-Symmetric Binols: Iron-Catalyzed Cross-Coupling of 2-Naphthols and Some Mechanistic Insight" *J. Am. Chem. Soc.* **2010**, *132*, 13633-13635.

Elo, H.; Matikainen, J.; Pelttari, E. "Potent activity of the lichen antibiotic (+)-usnic acid against clinical isolates of vancomycin-resistant enterococci and methicillin-resistant Staphylococcus aureus" *Naturwissenschaften* **2007**, *94*, 465–468.

Elsler, B.; Schollmeyer, D.; Dyballa, K. M.; Franke, R.; Waldvogel, S. R. "Metal- and Reagent-Free Highly Selective Anodic Cross-Coupling Reaction of Phenols" *Angew. Chem., Int. Ed.* **2014**, *53*, 5210-5213.

Esguerra, K. V. N.; Fall, Y.; Petitjean, L.; Lumb, J.−P. "Controlling the Catalytic Aerobic Oxidation of Phenols" *J. Am. Chem. Soc.* **2014**, *136*, 7662−7668.

Esumi, T.; Makado, G.; Zhai, H.; Shimizu, Y.; Mitsumoto, Y.; Fukuyama, Y. "Efficient synthesis and structure–activity relationship of honokiol, a neurotrophic biphenyl-type neolignan" *Bioorg. Med. Chem. Lett.* **2004**, *14*, 2621-2625.

Feng, J.; Yang, X.-B.; Liang, S.; Zhang, J.; Yu, X.-Q. "An efficient oxidative coupling method for synthesis of novel diastereomeric biaryl diols derived from estrone" *Tetrahedron Lett.* **2013**, *54*, 355–357.

Fujita, M.; Itokawa, H.; Sashida, Y. "Honokiol, a new phenolic compound isolated from the bark of *Magnolia obovata Thunb*" *Chem. Pharm. Bull.* **1972***, 20,* 212–213.

Fukuyama, Y.; Asakawa, Y. "Novel Neurotrophic Isocuparane-type Sesquiterpene Dimers, Mastigophorenes A, B, C, and D, Isolated from the Liverwort Mastigophora Diclados" *J. Chem. Soc., Perkin Trans.1* **1991**, 2737–2741.

Fukuyama, Y.; Nakade, K.; Minoshima, Y.; Yokoyama, R.; Zhai, H.; Mitsumoto, Y. "Neurotrophic activity of honokiol on the cultures of fetal rat cortical neurons" *Bioorg. Med. Chem. Lett.* **2002**, *12*, 1163-1166.

Fukuyama, Y.; Otoshi, Y.; Miyoshi, K.; Nakamura, K.; Kodama, M.; Nagasawa, M.; Hasegawa, T.; Okazaki, H.; Sugawara, M. "Neurotrophic sesquiterpene-neolignans from *magnoliaobovata*: structure and neurotrophic activity" *Tetrahedron* **1992**, *48*, 377–392.

Garrison, J. M.; Ostovic, D.; Bruice, T. C. "Is a Linear Relationship Between the Free Energies of Activation and One-Electron Oxidation Potential Evidence for One-Electron Transfer Being Rate Determining? Intermediates in the Epoxidation of Alkenes by Cytochrome P-450 Models. 4. Epoxidation of a Series of Alkenes by Oxo(meso-tetrakis(2,6-dibromophenyl)porphinato)chromium(V)" *J. Am. Chem. Soc.* **1989**, *111*, 4960–4966.

Ge, H. M.; Zhang, W. Y.; Ding, G.; Saparpakorn, P.; Song, Y. C.; Hannongbua, S.; Tan, R. X. "Chaetoglobin A and B, Two Unusual Alkaloids from Endophytic Chaetomium Globosum Culture" *Chem. Commun.* **2008**, 5978–5980.

Gisch, N.; Balzarini, J.; Meier, C. "Enzymatically Activated *cyclo*Sal-d4T-monophosphates: The Third Generation of *cyclo*Sal-Pronucleotides" *J. Med. Chem.* **2007**, *50*, 1658-1667.

Grieco, P. A.; Nunes, J. J.; Gaul, M. D. "Dramatic Rate Accelerations of Diels-Alder Reactions in 5 M Lithium Perchlorate-Diethyl Ether: The Cantharidin Problem Reexamined" *J. Am. Chem. Soc.* **1990**, *112*, 4595-4596.

Guo, Q-X.; Wu, Z-J.; Luo, Z-B.; Liu, Q-Z.; Ye, J-L.; Luo, S-W.; Cun, L-F.; Gong, L-Z. "Highly enantioselective oxidative couplings of 2-naphthols catalyzed by chiral bimetallic oxovanadium complexes with either oxygen or air as oxidant" *J. Am. Chem. Soc.* **2007**, 129, 13927-13938.

Guo. F.; Konkol, L. C.; Thomson, R. J. "Enantioselective Synthesis of Biphenols from 1,4-Diketones by Traceless Central-to-Axial Chirality Exchange" *J. Am. Chem. Soc.* **2011**, *133*, 18–20.

Hansen, K. B.; Leighton, J. L.; Jacobsen, E. N. "On the Mechanism of Asymmetric Nucleophilic Ring-Opening of Epoxides Catalyzed by (Salen)Cr(III) Complexes" *J. Am. Chem. Soc.* **1996**, *118*, 10924-10925.

Harada, K.; Arioka, C.; Miyakita, A.; Kubo, M.; Fukuyama, Y. "Efficient Synthesis of Neurotrophic Honokiol Using Suzuki-Miyaura Reactions" *Tetrahedron Lett.* **2014**, *55*, 6001-6003

Hassan, J.; Sevignon, M.; Gozzi, C.; Schulz, E.; Lemair, M. "Aryl-Aryl Bond Formation One Century after the Discovery of the Ullmann Reaction" *Chem. Rev.* **2002**, *102*, 1359-1470.

Henschke, J. P.; Murk, M. J.; Malan, C. G.; Herzberg, D.; Peterson, J. A.; Wildsmith, A. J.; Cobley, C. J.; Casy, G. "Synthesis and Application of HexaPHEMP, a Novel Biary Diphosphine Ligand" *Adv. Synth. Catal.* **2003**, *345*, 300-307.

Hewgley, J. B.; Stahl, S. S.; Kozlowski, M. C. "Mechanistic Study of Asymmetric Oxidative Biaryl Coupling: Evidence for Self-Processing of the Copper Catalyst to Achieve Control of Oxidase vs. Oxygenase Activity" *J. Am. Chem. Soc.* **2008**, *130*, 12232–12233.

Hon, S.-W.; Li, C.-H.; Kuo, J.-H.; Barhate, N. B.; Liu, Y.-H.; Wang, Y.; Chen, C.-T. "Catalytic Asymmetric Coupling of 2-Naphthols by Chiral Tridentate Oxovanadium(IV) Complexes" *Org. Lett.* **2001**, *3,* 869–872.

Hwang, D.-R.; Chen, C.-P.; Uang, B.-J. "Aerobic Catalytic Oxidative Coupling of 2-Naphthols and Phenols by VO(acac)$_2$" *Chem. Commun.* **1999**, 1207-1208.

Ikeya, Y.; Taguchi, H.; Mitsuhashi, H.; Takeda, S.; Kase, Y.; Aburada, M. "A Lignan from Schizandra Chinesis" *Phytochemistry* **1988**, *27*, 569-573.

Iried, R.; Masutani, K.; Katsuki, T. "Asymmetric Aerobic Oxidative Coupling of 2-Naphthol Derivatives Catalyzed by Photo-Activated Chiral (NO)Ru(II)-Salen Complex" *Synlett* **2000**, 1433-1436.

Jiang, Q.; Sheng, W.; Tian, M.; Tang, J.; Guo, C. "Cobalt(II)–Porphyrin-Catalyzed Aerobic Oxidation: Oxidative Coupling of Phenols" *Eur. J. Org. Chem.* **2013**, 1861–1866.

Katsuki, T. "Unique asymmetric catalysis of cis-β metal complexes of salen and its related Schiff-base ligands" *Chem. Soc. Rev.* **2004**, *33*, 437–444.

Keseru, G. M.; Nogradi, M. "Natural Products by Oxidative Phenolic Coupling Phytochemistry, Biosynthesis and Synthesis" In *Studies in Natural Products*

Chemistry, Vol. 20: Structure and Chemistry (Part F) (Atta-ur-Rahman, Editor) Elsevier Science **1998**, p 263.

Kobayashi, S.; Higashimura, H. "Oxidative polymerization of phenols revisited" *Prog. Polym. Sci.* **2003**, *28*, 1015–1048.

Kong, Z.; Tzeng, S.; Liu, Y. Bioorg. "Cytotoxic neolignans: an SAR study" *Med. Chem. Lett.* **2005**, *15*, 163-166.

Konsler, R. G.; Karl, J.; Jacobsen, E. N. "Cooperative Asymmetric Catalysis Using Dimeric Salen Complexes" *J. Am. Chem. Soc*. **1998**, *120*, 10780–10781.

Kotani, H.; Kaida, S.; Ishizuka, T.; Sakaguchi, M.; Ogura, T.; Shiota, Y.; Yoshizawa, K.; Kojima, T. "Formation and Characterization of a Reactive Chromium(V)–Oxo Complex: Mechanistic Insight into Hydrogen-Atom Transfer reactions" *Chem. Sci.* **2015**, *6*, 945–955.

Kozlowski, M. C.; Morgan, B. J.; Linton, E. C.; "Total Synthesis of Chiral Biaryl Natural Products by Asymmetric Biaryl Coupling" *Chem. Soc. Rev.* **2009**, 38, 3193–3207.

Krenitsky, P. J.; Boger, D. L. "Synthesis of the (*S,S,S*)-diastereomer of the 15-membered biaryl ring system of RP 66453" *Tetrahedron Lett*. **2003**, *44*, 4019-4022.

Kurahashi, T.; Fujii, H. "One-Electron Oxidation of Electronically Diverse Manganese(III) and Nickel(II) Salen Complexes: Transition from Localized to Delocalized Mixed-Valence Ligand Radicals" *J. Am. Chem. Soc.* **2011***, 133,* 8307–8316.

Lee, Y. E.; Cao, T.; Torruellas, C.; Kozlowski, M. C. "Selective Oxidative Homo- and Cross-Coupling of Phenols with Aerobic Catalysts" *J. Am. Chem. Soc.* **2014**, *136*, 6782–6785.

Lee, Y. E.; Kozlowski, M. C. *et al*. "Improved Synthesis of Honokiol" *Provisional Patent.*

Li, X.; Hewgley, J. B.; Mulrooney, C. A.; Yang, J.; Kozlowski, M. C. "Enantioselective Oxidative Biaryl Coupling Reactions Catalyzed by 1,5-Diazadecalin Metal Complexes: Efficient Formation of Chiral Functionalized BINOL Derivatives" *J. Org. Chem.* **2003**, *68*, 5500-5511.

Li, X.; Yang, J.; Kozlowski, M. C. "Enantioselective Oxidative Biaryl Coupling Reactions Catalyzed by 1,5-Diazadecalin Metal Complexes" *Org. Lett.* **2001**, *3*, 1137-1140.

Li, Y.; Wang, Q.; Dong, L.; Guo, X.; Wang, W.; Xie, J.; Chang, J. "Asymmetric Synthesis of (+)- and (-)-Wuweizisu C Stereoisomers and Their Chemosensitizing Effects on Multidrug-Resistant Cancer Cells" *Synthesis* **2009**, *2009*, 3383–3390.

Libman, A.; Shalit, H.; Vainer, Y.; Narute, S.; Kozuch, S.; Pappo, D. "Synthetic and Predictive Approach to Unsymmetrical Biphenols by Iron-Catalyzed Chelated Radical−Anion Oxidative Coupling" *J. Am. Chem. Soc.* **2015**, *137*, 11453-11460.

Lide, D. R. *CRC Handbook of Chemistry and Physics* (86th Ed) **2005**.

Lindsley, C. W.; Chan, L. K.; Goess, B. C.; Joseph, R.; Shair, M. D. "Solid-Phase Biomimetic Synthesis of Carpanone-like Molecules" *J. Am. Chem. Soc.* **2000**, *122*, 422–423.

Liu, L.; Wu, X.; Fan, L.; Chen, X.; Hu, Z. "Separation and determination of honokiol and magnolol in herbal medicines by flow injection-capillary electrophoresis" *Anal. Bioanal. Chem.* **2006**, *384*, 1533-1539.

Liu, S.-Y.; Wang, G.-Q.; Liang, Z.-Y.; Wang, Q.-A. "Synthesis of Dihydrobenzofuran Neoligans Licarin A and Dihydrocarinatin as Well as Related Triazolylglycosides*" Chemical Research in Chinese Universities* **2013**, *29*, 1119–1124.

Lu, S.; Poh, S. B.; Zhao, Y. "Kinetic Resolution of 1,1'-Biaryl-2,2'-Diols and Amino Alcoholsthrough NHC-Catalyzed Atroposelective Acylation" *Angew. Chem., Int. Ed.* **2014**, *53*, 11041–11045.

Luo, Z. B.; Liu, Q. Z.; Gong, L. Z.; Cui, X.; Mi, A. Q.; Jiang, Y. Z. "Novel Achiral Biphenol-Derived Diastereomeric Oxovanadium(IV) Complexes for Highly Enantioselective Oxidative Coupling of 2-Naphthols" *Angew. Chem., Int. Ed.* **2002**, *41*, 4532-4535.

Luo, Z.; Liu, Q.; Gong, L.; Cui, X.; Mi, A.; Jiang, Y. "The Rational Design of Novel Chiral Oxovanadium(IV) Complexes for Highly Enantioselective Oxidative Coupling of 2-Naphthols" *Chem. Commun.* **2002**, 914–915.

Ma, G.; Deng, J.; Sibi, M.P. "Fluxionally Chiral DMAP Catalysts: Kinetic Resolution of AxiallyChiral Biaryl Compounds" *Angew. Chem., Int. Ed.* **2014**, *53*, 11818–11821.

Majumder, P. L.; Chakraborty, S.; Roychowdhury, M. "Catalytic aerobic oxidative coupling of some simple phenols and natural phenanthrols with CuCl(OH)· TMEDA" *J. Indian Chem. Soc.* **2000**, *77*, 389-393.

Malkowsky, I. M.; Rommel, C. E.; Fröhlich, R.; Griesbach, U.; Pütter, H.; Waldvogel, S. R. *Chem. Eur. J.* **2006**, *12*, 7482-7488.

Manley, D. W.; McBurney, R. T.; Miller, P.; Walton, J. C. "Titania-Promoted Carboxylic Acid Alkylations of Alkenes and Cascade Addition−Cyclizations" *J. Org. Chem.* **2014**, *79*, 1386−1398.

Martinez, L. E.; Leighton, J. L.; Carsten, D. H.; Jacobsen, E. N. "Highly Enantioselective Ring Opening of Epoxides Catalyzed by (salen)Cr(III) Complexes" *J. Am. Chem. Soc.* **1995**, *117*, 5897-589.

Martinez, L. E.; Leighton, J. L.; Carsten, D. H.; Jacobsen, E. N. *J. Am. Chem. Soc.* **1995**, *117*, 5897-5898

Matsuda, H.; Kageura, T.; Oda, M.; Morikawa, T.; Sakamoto, Y.; Yoshikawa, M. "Effects of Constituents from the Bark of Magnolia obovata on Nitric Oxide Production in Lipopolysaccharide-Activated Macrophages" *Chem. Pharm. Bull.* **2001**, *49*, 716-720.

Matsumoto, K.; Egami, H.; Oguma, T.; Katsuki, T. "What Factors Influence the Catalytic Activity of Iron-Salan Complexes for Aerobic Oxidative Coupling of 2-Naphthols?" *Chem. Commun.* **2012**, *48*, 5823-5825.

Mazet, C.; Jacobsen, E. N. "Dimeric (salen)Al Complexes Display Expanded Scope in the Conjugate Cyanation of α, β-Unsaturated Imides" *Angew. Chem. Int. Ed.* **2008**, *47*, 1762–1765.

McGarrigle, E. M.; Gilheany, D. G. "Chromium− and Manganese−salen Promoted Epoxidation of Alkenes" *Chem. Rev.* **2005**, *105*, 1563–1602.

More, N. Y.; Jeganmohan, M. "Oxidative Cross-Coupling of Two Different Phenols: An Efficient Route to Unsymmetrical Biphenols" *Org. Lett.* **2015**, *17*, 3042−3045.

Mori, K,; Ichikawa, Y.; Kobayashi, M.; Shibata, Y.; Yamanaka, M.; Akiyama, T. "Enantioselective Synthesis of Multisubstituted Biaryl Skeleton by Chiral Phosphoric Acid Catalyzed Desymmetrization/Kinetic Resolution Sequence" *J. Am. Chem. Soc.* **2013**, *135*, 3964–3970.

Morimoto, K.; Sakamoto, K.; Ohnishi, Y.; Miyamoto, T.; Ito, M.; Dohi, T. Kita, Y. "Metal-Free Oxidative para Cross-Coupling of Phenols" *Chem. Eur. J.* **2013**, *19*, 8726–8731.

Noshino, H.; Itoh, N.; Nagashima, M.; Kurosawa, K. "Choice of Manganese(III) Complexes for the Synthesis of 4,4′-Biphenyldiols and 4,4′-Diphenoquiones" *Bull. Chem. Soc. Jpn*. **1992**, *65*, 620–622.

O'Brien, E. M.; Li, J.; Carroll, P. J.; Kozlowski, M. C. "Synthesis of the Cores of Hypocrellin and Shiraiachrome: Diastereoselective 1,8-Diketone Aldol Cyclization" *J. Org. Chem.* **2010**, *75*, 69-73.

O'Brien, M. K.; Vanasse, B. *e-EROS Encyclopedia of Reagents for Organic Synthesis*, **2001**.

Pal, T.; Pal, A. "Oxidative Phenol Coupling: A Key Step for the Biomimetic Synthesis of Many Important Natural Products" *Curr. Sci.* **1996**, *71*, 106–109.

Pelish, H. E.; Westwood, N. J.; Feng, Y.; Kirchhausen, T.; Shair, M. D. "Use of Biomimetic Diversity-Oriented Synthesis to Discover Galanthamine-Like Molecules with Biological Properties beyond Those of the Natural Product" *J. Am. Chem. Soc.* **2001**, *123*, 6740–6741.

Pereira, A. C.; Magalhães, L. G.; Gonçalves, U. O.; Luz, P. P.; Moraes, A. C. G.; Rodrigues, V.; da Matta Guedes, P. M.; da Silva Filho, A. A.; Cunha, W. R.; Bastos, J. K.; Nanayakkara, N. P. D.; e Silva, M. L. A. "Schistosomicidal and trypanocidal structure–activity relationships for (±)-licarin A and its (−)- and (+)-enantiomers" *Phytochemistry* **2011**, *72*, 1424–1430.

Pickel, B.; Constantin, M.-A.; Pfannstiel, J.; Conrad, J.; Beifuss, U.; Schaller, A. "An Enantiocomplementary Dirigent Protein for the Enantioselective Laccase-Catalyzed Oxidative Coupling of Phenols" *Angew. Chem. Int. Ed.* **2010**, *49*, 202 – 204.

Premsingh, S.; Venkataramanan, N. S.; Rajagopal, S.; Mirza, S. P.; Vairamani, M.; Rao, P. S.; Velavan, K. "Electron Transfer Reaction of Oxo(salen)chromium(V) Ion with Anilines" *Inorg. Chem.* **2004**, *43*, 5744–5753.

Quideau, S.; Deffieux, D.; Douat-Casassus, C.; Pouységu, L. "Plant Polyphenols: Chemical Properties, Biological Activities, and Synthesis" *Angew. Chem. Int. Ed.* **2011**, *50*, 586–621.

Quideau, S.; Feldman, K. S., Eds. [Tetrahedron Vol. 57, Issue 2.] *Tetrahedron* **2001**, *57*, 265–424.

Ray, S.; Das, A. K.; Banerjee, A. "Smart oligopeptide gels: *in situ* formation and stabilization of gold andsilver nanoparticles within supramolecular organogel networks" *Chem.Commun.* **2006**, *26*, 2816-2818.

Reddy, B. V. S.; Rao, R. N.; Reddy, N. S. S.; Yadav, J. S.; Subramanyam, R. "A Short and Efficient Synthesis of Honokiol via Claisen Rearrangement" *Tetrahedron Lett.* **2014**, *55*, 1049-1051.

Reisman, S. E.; Cherney, A. H. "Nickel-Catalyzed Asymmetric Reductive Cross-Coupling Between Vinyl and Benzly Electrophile" *J. Am. Chem. Soc.* **2014**, *136*, 14365-14368.

Ruminski, R. R.; Healy, M. H.; Coleman, W. F. "Photoredox Processes in 254–nm Photochemistry of Chromium(III) Ammine" *Inorg. Chem.* **1989**, *28*, 1666–1669.

Saito, S.; Yamamoto, H. "Designer Lewis Acid Catalysts-Bulky Aluminium Reagents for Selective Organic Synthesis" *Chem. Comm.* **1997**, 1585-1592.

Schaus, S. E.; Brånalt, J. E.; Jacobsen, E. N. "Asymmetric Hetero-Diels–Alder Reactions Catalyzed by Chiral (salen)Chromium(III) Complexes" *J. Org. Chem.* **1998**, *63*, 403-405.

Schmidt, B.; Riemer, M. "Suzuki-Miyaura Coupling of Halophenols and Phenol Boronic Acids: Systematic Investigation of Positional Isomer Effects and Conclusions for the Synthesis of Phytoalexins from Pyrinae" *J. Org. Chem.* **2014**, *79*, 4104-4118.

Schmink, J. R.; Bellomo, A.; Berritt, S. "Scientist-Led High-Throughput Experimentation (HTE) and Its Utility in Academia and Industry" *Aldrichimica Acta* **2013**, *46*, 71–80.

Schuehly, W.; Voith, W.; Teppner, H.; Kunert, O. "Substituted Dineolignans from *Magnolia garrettii*" *J. Nat. Prod.* **2010**, *73*, 1381–1384.

Serna, P.; Corma, A. "A Residue-free Production of Biaryls Using Supported Gold Nanoparticles" *J. Catal.* **2014**, *315*, 41-47.

Sevvel, R.; Rajagopal, S.; Srinivasan, C.; Alhaji, N. I.; Chellamani, A. "Mechanism of Selective Oxidation of Organic Sulfides with Oxo(salen)chromium(V) Complexes" *J. Org. Chem.* **2000**, *65*, 3334-3340.

Sha, S.–C. "New Strategy in C-H Functionalizations with Bismetallic Catalysts" *Dissertation*, **2015**, University of Pennsylvania, Philadelphia, PA

Shimazaki, Y. "Recent Advances in X-Ray Structures of Metal-Phenoxyl Radical Complexes" *Advances in Materials Physics and Chemistry* **2013**, *3*, 60-71.

Sokolowski, A.; Bothe, E.; Bill, E.; Weyhermüller, T.; Wieghardt, K. "Phenoxyl radical complexes of Chromium(III)" *Chem. Commun.,* **1996**, 1671-1672.

Somei, H.; Asano, Y.; Yoshida, T.; Takizawa, S.; Yamataka, H.; Sasai, H. "Dual Activation in a Homolytic Coupling Reaction Promoted by an Enantioselective Dinuclear Vanadium(IV) Catalyst." *Tetrahedron Lett.* **2004**, *45*, 1841-1844.

Srinivas, J.; Singh, P. P.; Varma, Y. K.; Hyder, I.; Kumar, H. M. S. "Concise Total Synthesis of Honokiol via Kumada Cross Coupling" *Tetrahedron Lett.* **2014**, *55*, 4295-4297.

Sun, X.; Li, W.; Hou, G.; Zhou, L.; Zhang, X. "Axial Chirality Control by 2,4-Pentanediol for the Alternative Synthesis of C3*-TunePhos Chiral Diphosphine Ligands and Their Applications in Highly Enantioselective Ruthenium-Catalyzed Hydrogenation of β-Keto Esters" *Adv. Synth. Catal.* **2009**, *351*, 2553-2557.

Takeya, T.; Okubo, T.; Tobinaga, S. "Synthesis of unsymmetrical biphenyl lignans, honokiol and related coumpounds, utilizing quinol-acetates as reactive intermediates" *Chem. Pharm. Bull.* **1986**, *34*, 2066-2075.

405

Takizawa, S.; Grçger, H.; Sasai, H. "Vanadium in Asymmetric Synthesis: Emerging Concepts in Catalyst Design and Applications" *Chem. Eur. J*, **2015**, *21*, 8992 – 8997.

Takizawa, S.; Katayama, T.; Kameyama, C.; Onitsuka, K.; Suzuki, T.; Yanagida, T.; Kawai, T.; Sasai, H. "Chiral dinuclear vanadium(V) catalysts for oxidative coupling of 2-naphthols" *Chem. Commun.* **2008**, 1810-1812.

Takizawa, S.; Katayama, T.; Sasai, H. "Chiral Dinuclear Vanadium(V) Catalysts for Oxidative Coupling of 2-Naphthols" *Chem. Commun,* **2008**, 4113-4122.

Takizawa, S.; Katayama, T.; Somei, H.; Asano, Y.; Yoshida, T.; Kameyama, C.; Rajesh, D.; Onitsuka, K.; Suzuki, T.; Mikami, M.; Yamataka, H.; Jayaprakash, D.; Sasai, H. "Dual activation in oxidative coupling of 2-naphthols catalyzed by chiral dinuclear vanadium complexes" *Tetrahedron* **2008**, 64, 3361-3371.

Takizawa, S.; Rajesh, D.; Katayama, T.; Sasai, H. "One-Pot Preparation of Chiral Dinuclear Vanadium(V) Complex" *Synlett*, **2009**, *10*, 1667–1669.

Tonami, H.; Uyama, H.; Kobayashi, S.; Higashimura, H.; Oguchi, T. "Oxidative Polymerization of 2,6-Disubstituted Phenols Catalyzed by Iron-Salen Complex" *J. Macromol. Sci., Pure Appl. Chem.* **1999**, *A36*, 719-730.

Tripathi, S.; Chan, M.-H.; Chen, C. "An Expedient Synthesis of Honokiol and Its Analogues as Potential Neuropreventive Agents" *Bioorg. Med. Chem. Lett.* **2012**, *22*, 216-221.

Venkataramanan, N. S.; Kuppuraj, G.; Rajagopal, S. "Metal–salen Complexes as Efficient Catalysts for the Oxygenation of Heteroatom Containing Organic Compounds—Synthetic and Mechanistic Aspects" *Coord. Chem. Rev.* **2005**, *249*, 1249–1268.

Vonlanthen, D.; Rotzler, J.; Neuburger, M.; Mayor, M. "Synthesis of Rotationally Restricted and Modular Biphenyl Building Blocks" *Eur. J. Org. Chem. **2010**,* 120–133

Waldvogel, S. R.; Mirk, D. Handbook of CH-Transformations, Vol. 1 (Ed.: G. Dyker), Wiley-VCH,Weinheim, **2005**, pp. 251.

Wang, E.-C.; Wein, Y.-S.; Kuo, Y.-H.; "A Concise and Efficient Synthesis of Salvinal From Isoeugenol Via a Phenoxenium Ion Intermediate" *Tetrahedron Lett.* **2006**, *47*, 9195–9197.

Wang, S.; Qian, Q.; Gong, H. "Nickel-Catalyzed Reductive Cross-Coupling of Aryl Halides with Secondary Alkyl Bromides and Allylic Acetate" *Org. Lett.,* **2012**, *14*, 3352-3355.

Weiss, U.; Merlini, L.; Nasini, G. "Naturally Occurring Perylenequinones" *Prog. Chem. Org. Nat. Prod.* **1987**, *52*, 1–71.

Whiting, D. A. "Oxidative coupling of phenols and phenol ethers": Comprehensive Organic Synthesis, Vol. 3. (Eds.:B. M. Trost, I. Fleming, G. Pattenden), Pergamon, Oxford, **1991**, pp. 659.

Yan, C.–S.; Peng, Y.; Xu, X.–B.; Wang, Y.–W. "Nickel-Mediated Inter- and Intramolecular Reductive Cross-Coupling of Unactivated Alkyl Bromides and Aryl Iodide at Room Temperature" *Chem. Eur. J.* **2012**, *18*, 6039-6048.

Yan, P.; Sugiyama, Y.; Takahashi, Y.; Kinemuchi, H.; Temma, T.; Habaue, S. "Lewis acid-assisted oxidative cross-coupling of 2-naphthol derivatives with copper catalysts" *Tetrahedron* **2008**, *64*, 4325–4331.

Zhang, Y.; Sigman, M. S. "Palladium(II)-Catalyzed Enantioselective Aerobic Dialkoxylation of 2-Propenyl Phenols: A Pronounced Effect of Copper Additives on Enantioselectivity" *J. Am. Chem. Soc.* **2007**, *129*, 3076–3077.